Technical Report
TR-19-05
December 2019

Biosphere synthesis for the safety evaluation SE-SFL

SVENSK KÄRNBRÄNSLEHANTERING AB

SWEDISH NUCLEAR FUEL
AND WASTE MANAGEMENT CO

Box 3091, SE-169 03 Solna
Phone +46 8 459 84 00
skb.se

ISSN 1404-0344
SKB TR-19-05
ID 1877689
December 2019

Biosphere synthesis for the safety evaluation SE-SFL

Svensk Kärnbränslehantering AB

Preface

This report is one of the main references for the evaluation of post-closure safety for a proposed concept for the repository for long-lived waste (SFL) in Sweden. The report presents a synthesis of the biosphere assessment undertaken as an integral part of the safety evaluation.

Jenny Brandefelt has been the project leader for SE-SFL and is responsible for the safety evaluation. A number of authors have contributed to the various sections of this report, as listed in Section 1.4.

An informal review of this report was performed by Ari Ikonen (EnviroCase Ltd., Finland), Björn Söderbäck and Eva Andersson (SKB), Georg Lindgren (Kemakta konsult AB) and Michael Thorne (Mike Thorne and Associates Ltd., United Kingdom). A formal review of this report was performed by Jordi Bruno (Amphos21 Consulting S.L., Spain) and Michael Thorne (Mike Thorne and Associates Ltd., United Kingdom).

Solna, December 2019

Jenny Brandefelt
Project leader SE-SFL

Summary

SKB is planning to construct a repository for long-lived low- and intermediate-level radioactive waste, SFL. The present repository design proposes two waste vaults: BHA with a bentonite clay backfill for legacy waste, and BHK with a concrete backfill for reactor internal components. The safety evaluation for SFL (SE-SFL) is the first analysis of post-closure safety for the SFL repository concept proposed by Elfwing et al. (2013). Its purpose is to assess under what conditions, in the repository and its environs, that the proposed design concept has the potential to meet the regulatory requirements for post-closure safety, and to provide a basis for prioritizing areas in which the level of knowledge and adequacy of methods must be improved in order to perform a full safety assessment for SFL. This report is one of the main references for SE-SFL. It describes the biosphere analysis, which is an integral part of the radionuclide transport modelling and dose calculations (Chapter 1).

The biosphere assessment allows estimations of the annual effective dose for a representative individual in the most exposed group. In addition to the specific objectives of this safety evaluation, the biosphere assessment in SE-SFL contributes to the iterative development of SKB's biosphere assessment. This includes formulation of evaluation cases, identification and description of the biosphere, formulation of the assessment model for radionuclide transport and exposure, selection and application of data, verification of the model through detailed analysis, and presentation and interpretation of results for the overall safety evaluation (Chapter 2).

No site has yet been selected for SFL. Thus, in order to have a realistic and consistent description of a site for geological disposal of radioactive waste, Laxemar was used as an example of a coastal location (Chapter 3). The Laxemar landscape is characterised by relatively deep fissure valleys that overlie the major deformation zones in the bedrock. The valleys are filled with thick sediments of glacial and post-glacial origin, and organic soils have often been converted into agricultural land. Groundwater levels in the regolith are shallow. There are a few small and shallow lakes in the area and most streams are influenced by land improvement and drainage operations. The projected changes of ecosystems with time, due to large scale climate variation and natural succession, are described (Chapter 4). Potential discharge areas of deep groundwater are identified and described (Chapter 5). One of the areas likely to receive discharge of groundwater from the postulated repository position is an agricultural field. The present state of this area (Object 206) and its historical development, from a sea basin to an infilled lake, are also described.

Biosphere features, events and processes (FEPs) that can influence post-closure safety for the proposed repository concept for SFL are described and audited (Chapter 6). Overall, the relevant FEPs for the SE-SFL evaluation were similar to those previously identified for SR-PSU. However, one FEP (*intrusion by organisms)* was excluded from, and two FEPs (*movement by organisms* and *change of pressure*) were added to the SE-SFL FEP list. Following SKBs latest safety assessment for the SFR repository, SR-PSU, four exposed groups were used to assess potential doses from projected releases. These groups are considered to be sufficient as credible bounding cases for exposure with respect to all major pathways.

In SE-SFL, a set of evaluation cases were identified. The base case is based on the reference evolution and six additional evaluation cases are designed to evaluate the sensitivity of the release and dose results to different biosphere conditions (Main report). For ease of interpretation and straightforward comparisons, the base case is highly stylized, and assumes constant, present-day climatic and other external conditions throughout the full assessment period. In the additional evaluation cases, biosphere conditions and properties of the discharge area are altered as compared with present-day conditions (described in Chapter 7 and evaluated in Chapter 11–12).

In order to analyse the evaluation cases, a linked chain of mathematical models is used to represent radionuclide transport from the waste vaults to the dose of potentially exposed groups. The biosphere model for transport and exposure (BioTEx or biosphere model), is the last link in this model chain (Chapter 8). This model is in essence the same as the biosphere model used in SR-PSU. However, a new model for continuous cultivation and a new hydrological routine have been implemented in SE-SFL. In addition, several technical modifications and improvements of the original model are introduced. The model updates have a relatively limited impact on deterministic calculations of

environmental concentrations under temperate conditions in a lake-mire ecosystem (Chapter 9). Nevertheless, the model updates are well motivated and ensure that consistent and robust estimates can be obtained also under varying conditions.

The biosphere model relies on nearly 200 input parameters. These parameters cover landscape geometries, regolith properties, hydrology and water exchange, aquatic and terrestrial ecosystem properties, distribution coefficients (K_d), concentration ratios (CR), human characteristics, and radionuclide-specific properties. The biosphere analysis has, as far as possible, utilised site-specific data to describe the potential discharge areas. SKB's site investigation programs (as reported in SDM-Laxemar, SR-Site and SR-PSU) have been the primary sources for data in SE-SFL (Chapter 10).

The total annual dose from each waste vault in the *present-day evaluation case* (the base case) is within an order of magnitude of the annual dose corresponding to the regulatory risk criterion of 10^{-6}**.** Draining and cultivation of a mire is the land use variant that causes the highest dose. This is primarily because radionuclides can accumulate in peat over a long period of time prior to exposure, and because the dose-contributing radionuclides predominantly yield dose through ingestion of food. The dominating radionuclides are for both waste vaults Mo-93 and C-14, and for BHA also Cl-36, Tc-99 and the U-238 decay chain series. The temporal dynamics of radionuclide-specific doses is driven by the release from the geosphere, but individual radionuclide properties clearly influence environmental concentrations and the variation in the total annual dose for a given release may span more than three orders of magnitude. The mechanisms behind the radionuclide-specific behaviour in the biosphere system include retention and decay, accumulation in peat, leaching from cultivated soil, plant uptake, and radiotoxicity (Chapter 11).

The six additional evaluation cases are analysed to study the effect of altered site characteristics or changed climate (Chapter 12). The *alternative discharge area evaluation case* shows that the characteristics of the biosphere object, e.g. object size and regolith thickness, are important for both the total dose and the relative contribution of individual radionuclides. Discharge into the sea can result in doses that are orders of magnitude lower than if radionuclides are discharged to a mire. Variant calculations demonstrate that using a time-independent representation of ecosystems is a reasonable and sound simplification to representing developing ecosystems in a discharge area.

The *increased greenhouse effect evaluation case* shows that the combination of decreased groundwater discharge and increased plant water demand may increase the annual dose from some radionuclides. However, the changes in external conditions are unlikely to result in an annual dose that is substantially higher than that calculated for present-day conditions. The effects of a warmer climate on radionuclide accumulation are reversed if irrigation with surface water is assumed to cover the crop water deficit.

The *alternative regional climate evaluation case* shows that a climate associated with higher rates of groundwater recharge and discharge (i.e. a climate with higher precipitation and/or lower annual temperature) is likely to result in a lower annual dose than in the base case. However, the response to variations in regional climate is modest, and it is unlikely that selection of a location with a favourable climate within the borders of Sweden would reduce the annual dose from SFL significantly as compared with the base case.

In the *initially submerged conditions evaluation case* the effects of locating SFL under the sea are evaluated. The calculations show that an initial submerged period is likely to delay transport from the repository due to lower groundwater flows. The maximum release rates to the biosphere are then delayed by the time it takes for the discharge area to emerge from the sea. As short-lived radionuclides decay, this leads to a lower maximum dose of such radionuclides, e.g. Mo-93. However, the effect is not dramatic if the submerged period is limited to 10 000 years or less. Moreover, the radionuclide specific dose from C-14 resulting from a submerged repository position may even be higher than from a land location, as the uptake of C-14 (per unit mass of stable carbon) is higher in aquatic plants (and food webs) than in terrestrial ecosystems.

The *simplified glacial cycle evaluation case* illustrates the release of radionuclides and dose consequences due to the passage of an inland ice sheet and to shoreline migration. Groundwater flow is changed in synchrony along the model chain, from the repository to the surface, and the conditions and properties of the surface system are modified according to climatic conditions and the succession of the discharge area. Although the maximum annual release of several dose-contributing radio-

nuclides increases when the ice front passes the repository, the annual dose never exceeds the maximum levels recorded in the initial temperate period. This is because dose-contributing radionuclides like Mo-93 and C-14 have decayed significantly by the time that the ice approaches, and because the surface conditions associated with the maximum release, i.e. permafrost or submerged conditions, prevent both exposure through cultivation of mire peat and extraction of well water.

The *drilled well evaluation case* shows that a discharge from BHA can lead to significant exposure via extraction of drinking and irrigation water from the bedrock. The resulting dose exceeds 100 μSv after 200 000 years and continues to increase during the assessment period. Ra-226 and its decay products are the main contributors to dose, and the geosphere release of Ra-226 at late times originates from U-238 in the waste (and accumulation of uranium and thorium isotopes in the near-field and the geosphere). Although the annual effective dose from the drilled well is significantly higher than that from a drained mire for BHA, the number of people exposed to water extracted from a single well is limited, and the dose from the well is in the same order of magnitude as the dose corresponding to the risk criterion for a small group.

Three sensitivity cases were used to examine how uncertainties in the biosphere assumptions may affect environmental concentrations and potential doses (Chapter 13). In the *aged soil case* the effects of changed soil conditions due to long-term cultivation are examined. Loss of organic matter is expected to result in e.g. decrease soil respiration and weaker sorption. However, the effects on the annual dose from the shifts caused by long-term cultivation are limited. In the *alternative K_d and CR values case* generic K_d values from IAEA that tend to be lower than the site-specific values, especially in mineral regolith layers, are used. However, the annual dose is relatively insensitive to decreased retention. This is partly due to the relatively high dose contribution of mobile radionuclides (C-14 and Cl-36) for which uncertainty in retention properties has limited or no effect on transport. This sensitivity case also highlight that the IAEA data do not always span sorption properties under conditions that are relevant for discharge into a mire ecosystems (e.g. with respect to grain size, redox conditions and organic matter content of regolith layers). In the *alternative object geometries and groundwater flows case* the sensitivity of environmental concentrations and doses to variations in parameters driving (or modifying) groundwater fluxes are examined. By varying parameter values independently, individual effects of properties that are typically correlated in the landscape (e.g. object and basin area, and thickness of individual regolith layers) are separated. The object area explains most of the concentration variations in the lower regolith profile. Object area also explains a significant part of the variation in regolith layers closer to the surface, as do the area of the basin (or catchment) and the thickness of the lowest, strongly sorbing, regolith layer.

Chlorine, molybdenum and nickel are identified as potentially important radionuclides in an early stage of SE-SFL. In Chapter 14 a review of the environmental patterns of theses radionuclides, and the processes influencing these patterns, are summarized. For chlorine the review shows that the immobilisation in soil organic matter and plant uptake and release are key processes for cycling and retention of chlorine in terrestrial ecosystems. Moreover, the link between plant and soil chlorine concentrations is weak, and the type of vegetation is the most important factor for plant chlorine concentrations. The mobility and potential for accumulation of molybdenum and nickel is primarily determined by their chemical form in combination with environmental conditions. A careful examination of K_d values used in SE-SFL show that the parameter values used capture a significant part of the environmental variation in the mobility of Mo and Ni, and that this variation is consistent with the understanding of the underlying biogeochemical processes (including e.g. speciation, solubility and interactions with organic matter).

The safety evaluation relies on compartment models, where the spatial heterogeneity of the regolith system is greatly simplified. This simplification is examined using distributed numerical models with a finer spatial resolution and a more detailed representation of radionuclide transport (Chapter 15). The comparative analysis illustrates how insights from a distributed 3D model can be used to inform the selection of the structure and the selection of parameters for a stylized compartment model. Moreover, the results suggest that stylized models can be used to calculate average accumulated activity and concentrations at the scale of a biosphere object with reasonable accuracy, and that patterns of accumulation can be somewhat improved if parameters are derived from the primary area of radionuclide discharge.

The SE-SFL evaluation deals with consequences far into the future, and thus a balanced handling of sometimes large uncertainties are an integral part of the assessment. The results are discussed in the context of model uncertainties, scenario (or system) uncertainties and parameter uncertainties (Chapter 16). It has been SKBs intention to handle uncertainties in a transparent and credible way, so that the interpretations of results are reasonable and balanced. Taken together, the discussion builds confidence that the biosphere analysis in SE-SFL yields robust estimates of annual effective dose, which reflect process understanding and a relevant description of an example site. Thus, the results from the safety evaluation are considered to give an adequate representation of dose consequences for this step of the SFL programme.

Finally the most important developments in the biosphere analysis are summarized, and the potential benefits from the development in future safety analyses are high-lighted (Chapter 17). In order to perform a full safety assessment for SFL, the adequacy of the methods used to assess the fate of key radionuclides should be critically evaluated in the light of present process knowledge. The next step of the SFL repository programme involves selection of a site for the repository. For this step a detailed description of the biosphere at the considered site will be needed. Such a description includes the estimation of the geometric properties of potential discharge areas, associated groundwater flows, and key ecosystem parameters, under relevant conditions and associated natural variation and uncertainties.

Sammanfattning

SKB planerar att bygga ett slutförvar för långlivat låg- och medelaktivt radioaktivt avfall (SFL). Den föreslagna utformningen består av två förvarsdelar: BHA (bergssal för historiskt avfall) som återfylls med bentonitlera och BHK (bergssal för härdkomponenter) som återfylls med betong. Säkerhetsvärderingen för SFL (SE-SFL) är den första analysen av säkerhet efter förslutning för det förvarskoncept som föreslagits av Elfwing et al. (2013). Syftet är att utreda under vilka omständigheter, hos förvaret och dess omgivningar, som det föreslagna utformningskonceptet har potential att uppfylla myndighetskraven kopplade till säkerhet efter förslutning. Dessutom ska analysen ge ett underlag för att prioritera områden där kunskapsnivån och metoder måste förbättras inför en fullständig analys av säkerheten efter förslutning för SFL. Denna rapport är en av huvudreferenserna för SE-SFL och beskriver biosfärsanalysen, som är en integrerad del av radionuklidtransportmodelleringen och dosberäkningarna som redovisas i säkerhetsvärderingen (kapitel 1).

Biosfärsanalysen syftar till att beräkna den årliga effektiva stråldosen för en representativ individ i den mest exponerade gruppen. Förutom de specifika målen för säkerhetsvärderingen bidrar biosfärsanalysen i SE-SFL till den iterativa utvecklingen av SKBs säkerhetsanalysmetodik för biosfären. Denna utveckling omfattar: att formulera utvärderingsfall, att identifiera och beskriva relevanta ekosystem, att utveckla modellen för transport av och exponering från radionuklider, att välja och tillämpa lämplig data, att verifiera modellen genom detaljerade analyser, samt att presentera och tolka resultat för den övergripande säkerhetsvärderingen (kapitel 2).

En anläggningsplats för SFL har ännu inte valts. För att få en realistisk och konsekvent beskrivning av en plats för ett geologisk slutförvar av radioaktivt avfall har Laxemar använts som ett exempel på en möjlig kustnära lokalisering (kapitel 3). Landskapet i Laxemar- kännetecknas av relativt djupa sprickdalar som sammanfaller med geologiska deformationszoner. Dalbottnarna har mäktiga lager av glaciala och post-glaciala avlagringar, och de organiska jordarna i dalgångarna utnyttjas ofta för jordbruk. Grundvattennivåerna i jordlagren är i regel ytliga. Det finns några små och grunda sjöar i området och de flesta bäckar är påverkade av dränerings- och andra markförbättringsåtgärder. Till följd av storskaliga klimatvariationer och ekosystemsuccession förväntas landskapet att utvecklas över tiden (kaptiel 4). Potentiella utsrömningsområden av djupt grundvatten har identifieras och beskrivs (kapitel 5). Ett av de områden som troligen kommer att få utsläpp av grundvatten från den antagna förvarspositionen utgörs av en jordbruksmark. Det nuvarande tillståndet för detta område (objekt 206), liksom dess historiska utveckling från en sjöbassäng till en igenväxt sjö, beskrivs också.

Biosfärsstrukturer, händelser och processer (FEP) som kan påverka säkerheten efter förslutning för det föreslagna förvaringskonceptet beskrivs och granskas (kapitel 6). FEP:arna som identifierats som relevanta för SE-SFL är i stort sett överensstämmande med de som identifierades i den senaste säkerhetsanalysen för SFR-förvaret, SR-PSU. En FEP (*intrång av organismer*) ströks emellertid, och två FEP:ar (*rörelse av organismer* och *förändring av tryck*) lades till SE-SFL's FEP-lista. Liksom i SR-PSU användes fyra exponerade grupper för att bedöma doser från potentiella utsläpp. Dessa grupper anses tillsammans vara tillräckliga som övre begränsningsfall för exponering med avseende på alla relevanta exponeringsvägar.

I SE-SFL identifierades en uppsättning utvärderingsfall. Basfallet baseras på den beskrivna referensutvecklingen och i sex ytterligar fall utvärderas känsligheten av beräknade utsläpp och doser för olika antagna biosfärsförhållanden (Huvudrapporten). För att förenkla tolkning av och jämförelser mellan beräkningsfall, är basfallet starkt stiliserat. I detta fall (*present-day evaluation case*, avsnitt 5.2) antas ett konstant, nutida klimat, och andra yttre förhållanden antas också vara konstanta under hela utvärderingsperioden. I de övriga fallen förändras förhållandena på ytan och egenskaperna på utströmningsområdet jämfört med dagens förhållanden (beskrivs i kapitel 7 och utvärderas i kapitel 11-12).

För att analysera utvärderingsfallen används en tredelad kedja av matematiska modeller som beskriver radionuklidtransporten från förvarsdelarna till ytan och sedan beräknar dos för den mest exponerade gruppen. Biosfärsmodellen för transport och exponering (BioTEx eller biosfärsmodellen) är den sista länken i denna modellkedja (kapitel 8). Modellen är i huvudsak densamma som i den tidigare säkerhetsanalysen SR-PSU. En ny modell för kontinuerlig odling och en ny rutin för att beräkna grundvatten flöden har emellertid introducerats i SE-SFL. Dessutom har flera tekniska förändringar införts i den ursprungliga modellen. De introducerade uppdateringarna har en relativt begränsad

inverkan på deterministiska beräkningar av miljökoncentrationer under tempererade förhållanden i sjö-/myr-ekosystem (kapitel 9). Trots den ringa effekten på modellresultaten är uppdateringarna väl motiverade och säkerställer att konsekventa och robusta uppskattningar erhålls även under varierande förutsättningar.

Biosfärmodellen bygger på mer än 200 ingångsparametrar. Dessa parametrar täcker landskapsgeometrier, regolitegenskaper, hydrologi och vattenutbyte, akvatiska och terrestra ekosystemegenskaper, fördelningskoefficienter (K_d), koncentrationsförhållanden (CR), mänskliga egenskaper och radionuklidspecifika egenskaper. Biosfärsanalysen har så långt som möjligt använt platsspecifik data för att beskriva det potentiella utströmningsområdet. SKB:s tidigare platsundersökningsprogram (som rapporterats i t.ex. SDM-Laxemar, SR-Site och SR-PSU) har varit de primära källorna för data som använts i SE-SFL (kapitel 10).

I basutvärderingsfallet (*present-day evaluation case*) beräknas den totala årliga dosen från var och en av de två förvarsdelarna att ligga inom en storleksordning av den årsdos som motsvarar det förskrivna riskkriteriet (10^{-6}). Uppodling av en dränerad myr är den markanvändningsvariant som orsakar högst dos. Detta beror främst på att radionuklider kan ackumulera i torv under en lång tidsperiod före exponeringstillfället, samt på att de radionuklider som dominerar dosen når de övre jordlagren och främst exponerar via intag av föda. De dominerande radionukliderna är Mo-93 och C-14 för både förvarsdelarna, samt Cl-36, Tc-99 och U-238 inklusive sönderfallskedja för BHA. Den temporära dynamiken i nuklidspecifika doser drivs av utsläppshastigheten från geosfären, men enskilda radionukliders egenskaper har en stark påverkan på miljökoncentrationerna. För ett givet utsläpp kan den totala årsdosen spänna över mer än tre storleksordningar mellan olika radionuklider. Mekanismerna bakom denna spridning kan förklaras av att radionuklidernas egenskaper i biosfären varierar med avseende på fördröjning och sönderfall i djupare jordlager, ackumulation i torv, urlakning från odlad jord, växtupptag och slutligen även radiotoxicitet (kapitel 11).

De övriga sex utvärderingsfallen utvärderas för att studera effekten av ändrade platsegenskaper eller ett förändrat klimat (kapitel 12). Utvärderingsfallet för alternativa utströmningsområden (*alternative discharge area*) visar att egenskaperna hos recipienten för utsläppet (t.ex. områdets storlek och jordlagrens djup) har en stark påverkan på så väl den totala dosen som på det relativa bidraget från enskilda radionuklider. Utsläpp till ett område som ligger under havet resulterar i doser som kan vara flera storleksordningar lägre än doserna från ett utsläpp till land. Beräkningsvarianter visar också att användning av en tidsoberoende modellrepresentation är en rimlig och robust förenkling av ekosystem som genomgår en naturlig succession i utsläppsområdet.

En ökad effekt av växthusgaser (*increased greenhouse effect*) kan höja den årliga dosen från vissa radionuklider. Detta beror på de kombinerade effekterna av en minskad grundvattenbildning och ett ökat vattenunderskott under odlingssäsongen. Men förändringen i yttre förhållanden som ett varmare klimat innebär kommer sannolikt inte att resultera i en dos som är väsentligt högre än den som beräknats för dagens förhållanden. Om vattenunderskottet för grödor däremot täcks av bevattning från en ytvattentäkt kan ett varmare klimat emellertid resultera i lägre doser än de som beräknats för dagens förhållanden.

I fallet alternativa regionala klimat (*alternative regional climate*) undersöks om en måttlig variation i klimatet kan påverka dosen från SFL. Fallet visar att ett klimat med högre nederbörd och/eller lägre årstemperatur sannolikt kommer att resultera i en lägre årlig dos än i basfallet. Detta beror på en ökad grundvattenbildning. Responsen på dos är emellertid blygsam, och det är inte sannolikt att ett platsval med avseende på ett gynnsamt klimat inom Sveriges gränser skulle ha någon betydande effekt på den årliga dosen från SFL jämfört med basfallet.

I fallet med inledande havstäckta förhållanden (*initially submerged conditions)* utvärderas effekterna av att lokalisera SFL under havet. Beräkningarna visar att en inledande havsperiod kommer att fördröja transporten från förvaret på grund av lägre grundvattenflöden. De maximala utsläppshastigheterna till biosfären försenas då med den tid det tar för utströmningsområdet att höjas upp ur havet. Då kortlivade radionuklider hinner sönderfalla, leder detta även till lägre maximala doser av dessa radionuklider, tex. Mo-93. Sänkningen av utsläpp under landperioden är dock inte dramatisk om havsperioden är kortare än 10 000 år. Dessutom kan den radionuklidspecifika dosen från C-14 från ett förvar som förläggs under havet, men nära strandlinjen, bli högre än vad som förväntas från en lokalisering högre upp på land. Anledning till detta är att upptaget av C-14 (per massa av stabilt kol) är högre i vattenväxter (och övriga näringskedjan) än i ett ekosystem på land.

I det förenklade glaciationsfallet (*simplified glacial cycle*) undersöks hur passagen av en inlandsis och efterföljande havstäckta förhållanden kan påverka utsläpp från SFL och potentiella doskonsekvenser. I fallet ändras grundvattenflödet synkront i modellkedjan, från förvaret upp till ytan, och förhållandena i ytsystemet ändras enligt klimatförhållanden och successionen av ekosystem i utströmningsområdet. Även om maximala utsläpp av flera dosbidragande radionuklider ökar när isfronten passerar förvaret, överskrider dosen i detta fall aldrig de högsta nivåerna som förekommer under den inledande tempererade perioden. Detta beror delvis på att aktiviteten av dosdominerande radionuklider som Mo-93 och C-14 minskat avsevärt vid tidpunkten då isen närmar sig. Dessutom råder det permafrost eller havstäckta förhållanden på ytan vid tidpunkterna för de maximala utsläppen, vilket förhindrar exponering från både uppodling av myrtorv och från brunnsvatten.

Fallet med en borrad brunn (*drilled well*) visar att ett utsläpp från BHA kan leda till en betydande exponeringen via dricks- och bevattningsvatten från berggrunden. Den resulterande dosen överskrider 100 μSv efter ca 200 000 år, och fortsätter att öka under bedömningsperioden. Ra-226 och dess sönderfallsprodukter är de viktigaste bidragande radionukliderna. Vid dessa sena tider är ursprunget till den resulterande dosen U-238 i historiska avfallet (vilket via sönderfall leder till en ansamling av uran- och torium-isotoper både i närfält och berggrund). Även om den årliga effektiva dosen från en borrade brunnen är betydligt högre än den från en dränerad myr för BHA, är antalet personer som exponeras från en enda brunn begränsat, och dosen från brunnen är i samma storleksordning som den dos som motsvarar riskkriteriet för en liten grupp.

Tre känslighetsfall användes för att undersöka hur osäkerheter i antagandet om ytsystemet påverkar miljökoncentrationer och potentiella doser (kapitel 13). I fallet med en åldrande jord (*aged soil*) undersöks hur förändrade markförhållanden på grund av långvarig odling påverkar ackumulation av radionuklider och dos från SFL. Förlusten av organiskt material (pga oxidering) förväntas resultera i bl.a. en minskad markrespiration och en svagare fastläggning av radionuklider. Beräkningarna visar emellertid att effekterna av långvarig odling på den årliga dosen är begränsade. I fallet med alternativa K_d- och *CR*-värden (*alternative K_d and CR values*) tenderar de platsspecifika K_d-värden som använts att vara högre än generiska K_d-värden från IAEA, särskilt i mineralrika regolitskikt. Den årliga dosen är emellertid relativt okänslig för en minskad retention. Detta beror delvis på det relativt höga dosbidraget från mobila radionuklider (C-14 och Cl-36) vars ackumulation och upptag inte påverkas av retentionsegenskaper i någon större grad. Beräkningsfallet belyser också att generiska parametervärden från IAEA inte alltid täcker in sorptionsegenskaper för förhållanden som är relevanta för utströmning i t.ex. ett myrekosystem (t.ex. med avseende på kornstorlek, redoxförhållanden och innehållet av organiskt material). Det sista känslighetsfallet (*alternative object geometries and groundwater flows)* undersökter hur alternativa geometrier och grundvattenflöden påverkar beräknade miljökoncentrationer och dos. I fallet varieras parametervärden för kopplade egenskaper (t.ex. objekt- och bassängområdets storlek och tjockleken på enskilda regolitskikt) oberoende av varandra, vilket gör att effekterna av individuella egenskaper går att särskilja. Storleken på utströmningsområdet var den faktor som kunde förklarade den största delen av koncentrationsvariationen i de undre regolitlagren. Storleken på området kunde också förklara en betydande del av variationen i ytligare markskikt. Radionuklidkoncentrationen i dessa skikt påverkades också av storleken av avrinningsområdet och tjockleken hos det understa, starkt sorberande, regolitskiktet.

Klor, molybden och nickel identifierades som potentiellt viktiga radionuklider i ett tidigt skede av SE-SFL. I kapitel 14 sammanfattas två litteratursammanställningar vilka beskriver dessa elements mönster i miljön och de processer som ligger bakom dessa mönster. Immobiliseringen i organiskt material i marken, liksom växtupptag och -frisättning, identifierades som nyckelprocesser för klorets kretslopp i terrestra ekosystem. Sammanställningen visar även att kopplingen mellan koncentrationen av klor i växter och mark är svag, men att halten av klor kan variera kraftigt mellan olika vegetationstyper. Rörligheten av och potentialen för ackumulation av molybden och nickel bestäms i huvudsak av ämnenas kemiska form och lokala miljöförhållanden. En noggrann undersökning av de K_d-värden som används i SE-SFL visade att dessa fångar upp en betydande del av den förväntade variationen i rörlighet för Mo och Ni, samt att de mönster som speglas av den använda parameteruppsättningen överensstämmer väl med den befintliga förståelsen för de bakomliggande biogeokemiska processerna (t.ex. kemisk speciering, löslighet och organisk komplexbildning).

Säkerhetsutvärderingen av SE-SFL förlitar sig på boxmodellering där den rumsliga heterogeniteten hos regolitlagren är mycket förenklad. Denna förenkling granskas med hjälp av distribuerade numeriska modeller med en finare rumslig upplösning och en mer detaljerad representation av radionuklidtransport

(kapitel 15). Den jämförande analysen illustrerar hur insikter från en distribuerad 3D-modell kan användas för att motivera valet av modellstruktur och parametrar för en stiliserad boxmodell. Dessutom tyder resultaten på att stiliserade modeller lämpar sig för att beräkna genomsnittlig ackumulerad aktivitet och koncentrationer på en skala av ett utströmningsområde med en acceptabel noggrannhet, samt att ackumulationsmönstret kan förbättras något om parametrar härleds från det primära området för utströmning av radionuklider.

SE-SFL-utvärderingen behandlar konsekvenser långt in i framtiden, och därför har en balanserad hantering av ibland stora osäkerheter varit en integrerad del av bedömningen. Resultaten diskuteras i ljuset av modellosäkerheter, scenario- (eller system-) osäkerheter och parameterosäkerheten (kapitel 16). Det har varit SKB:s avsikt att hantera osäkerheter på ett tydligt och trovärdigt sätt, så att tolkningen av resultaten blir rimlig och balanserad. Sammantaget stärker denna diskussion förtroende för att biosfärsanalysen i SE-SFL ger robusta uppskattningar av den årliga effektiva dosen, återspeglar processförståelse och ger en relevant beskrivning av en exempelplats. Således bedöms resultaten från säkerhetvärderingen ge en adekvat representation av doskonsekvenserna för detta steg i SFL-programmet.

Slutligen sammanfattas de viktigaste framstegen i biosfärsanalysen som gjorts i SE-SFL, och den möjliga nyttan av dessa för framtida säkerhetsanalyser poängteras (kapitel 17). Vidare bedöms det lämpligt att granska metodiken för att beskriva transport och ackumulation av radionuklider inför en fullständig säkerhetsanlys av SFL, så att denna speglar aktuell processförståelse för de mest dosbidragande radionukliderna på ett ändamålsenligt sätt. Nästa steg i SFL-programmet innebär val av en anläggningsplats. För detta steg krävs en detaljerad beskrivning av ytsystemet på den aktuella platsen. En sådan beskrivning bör omfatta geometriska egenskaper för potentiella utströmningsområden, grundvattenflöden i jordlager samt en rad ekosystemegenskaper för relevanta förhållanden, med tillhörande variation och osäkerhet.

Contents

1 Introduction

This report constitutes one of the main references supporting the safety evaluation for a proposed concept for the repository for long-lived waste (SFL) in Sweden. The purpose of the SFL safety evaluation (SE-SFL) is to provide input to the subsequent, consecutive steps in the development of SFL. This chapter gives the background to the project and an overview of the safety evaluation. Moreover, the role of this report is described in the context of the evaluation.

1.1 Background

The Swedish power industry has been generating electricity by means of nuclear power for more than 40 years. The Swedish system for managing and disposal of the waste from operation of the reactors has been developed over that period. When finalised, this system will comprise three repositories: the repository for short-lived radioactive waste (SFR), the repository for long-lived waste (SFL), and the Spent Fuel Repository.

The system for managing radioactive waste is schematically depicted in Figure 1-1. SKB currently operates SFR at Forsmark in Östhammar municipality to dispose of low- and intermediate-level waste produced during operation of the various nuclear power plants, as well as to dispose waste generated during applications of radioisotopes in medicine, industry, and research. Further, SFR is planned to be extended to permit the disposal of waste from decommissioning of nuclear facilities in Sweden. The spent nuclear fuel is presently stored in the interim storage facility for spent nuclear fuel (Clab) in Oskarshamn municipality. Clab is planned to be complemented by the Encapsulation Plant, together forming Clink. SKB has also applied to construct, possess and operate the Spent Fuel Repository at Forsmark in Östhammar municipality. The current Swedish radioactive waste management system also includes a ship and different types of casks for transport of spent nuclear fuel and other radioactive waste.

SFL will be used for disposal of the Swedish long-lived low- and intermediate-level waste. This comprises long-lived waste from the operation and decommissioning of the Swedish nuclear power plants, from early research in the Swedish nuclear programmes (legacy waste), from medicine, industry, and from research which includes the European Spallation Source (ESS) research facility. The long-lived low- and intermediate-level waste from the nuclear power plants consists of neutron-activated components and control rods and constitutes about one third of the waste planned for SFL. The rest originates mainly from the Studsvik site, where Studsvik Nuclear AB and Cyclife Sweden AB both produce and manage radioactive waste from medicine, industry and research. The legacy waste to be disposed of in SFL is currently managed by the company AB SVAFO.

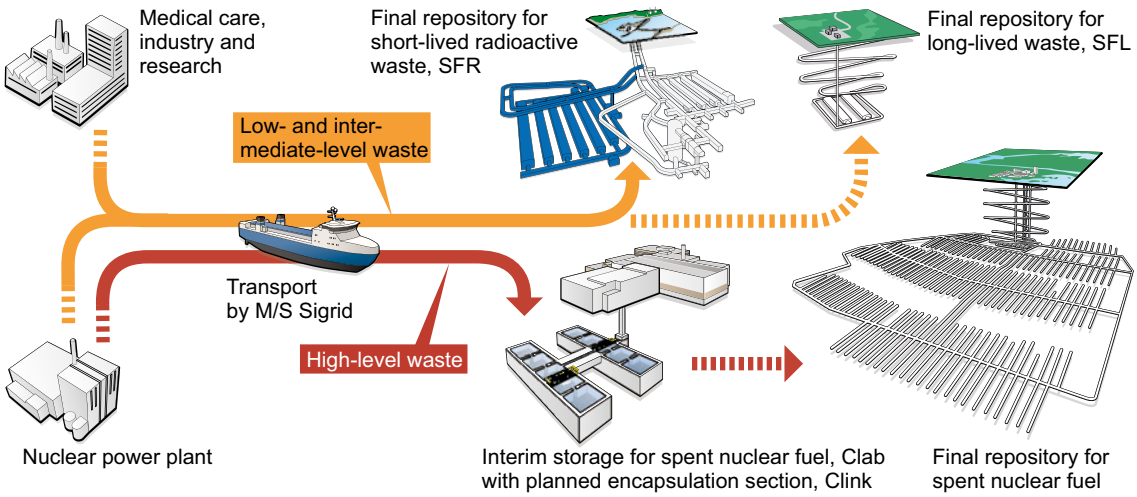

Figure 1-1. *The Swedish system for radioactive-waste management. Dashed arrows indicate future waste streams to facilities planned* ***for construction.***

In 1999, a preliminary safety assessment for SFL was presented (SKB 1999). The objective was to investigate the capacity of the facility to act as a barrier to the release of radionuclides and the importance of the repository location. The assessment was reviewed by the authorities (SKI/SSI 2001). One of the main comments was a lack of a clear account of the basis for the selection of the design and that no design alternatives had been considered. Reflecting the comments from the authorities on the preliminary safety assessment, possible solutions for management and disposal of the Swedish long-lived low- and intermediate-level waste were examined in the SFL concept study (Elfwing et al. 2013). After a first screening, four waste vault concepts were evaluated with respect to two evaluation factors; post-closure safety and robustness of the barrier safety functions (Evins 2013). Based on the evaluation, a system was proposed as a basis for further assessment of post-closure safety. According to this system, SFL is designed as a deep geological repository with two different sections:

- one waste vault, designed with a concrete barrier, BHK, for metallic waste from the nuclear power plants, and
- one waste vault, designed with a bentonite barrier, BHA, for the waste from Studsvik Nuclear AB, Cyclife Sweden AB and AB SVAFO.

A schematic illustration of the proposed facility layout and waste vault concepts for SFL is displayed in Figure 1-2. BHK is approximately 135 m long and BHA is approximately 170 m long. Both vaults have a cross sectional area of approximately 20×20 m^2. It is assumed that the waste vaults are located at 500 m below the surface and that this depth is sufficient to avoid adverse effects by permafrost during future glacial cycles, i.e. at a depth sufficient to exclude the possibility of freezing of the repository.

1.2 The SE-SFL safety evaluation

The purpose of SE-SFL is to provide input to the subsequent, consecutive steps in the development of SFL. These consecutive steps include further development of the design of the engineered barriers and the site-selection process for SFL. More specifically, there are two main objectives for SE-SFL. The first is to evaluate conditions in the waste, the barriers, and the repository environs under which the repository concept has the potential to fulfil the regulatory requirements for post-closure safety. The second is to provide SKB with a basis for prioritising areas in which the level of knowledge and adequacy of methods must be improved in order to perform a full safety assessment for SFL. This is in line with the iterative safety analysis process that the SFL repository programme follows, in which the results from post-closure safety analyses and related activities (e.g. information from a site selection process and development of numerical methods) are used to successively inform and improve the analysis. In accordance with the Nuclear Activities Act (1984:3), important research needs for the SFL programme that emerge as a result of SE-SFL will be reported in the research, development and demonstration (RD&D) programme. An important aspect of this is to ensure that the industry has well founded information to support long-term planning.

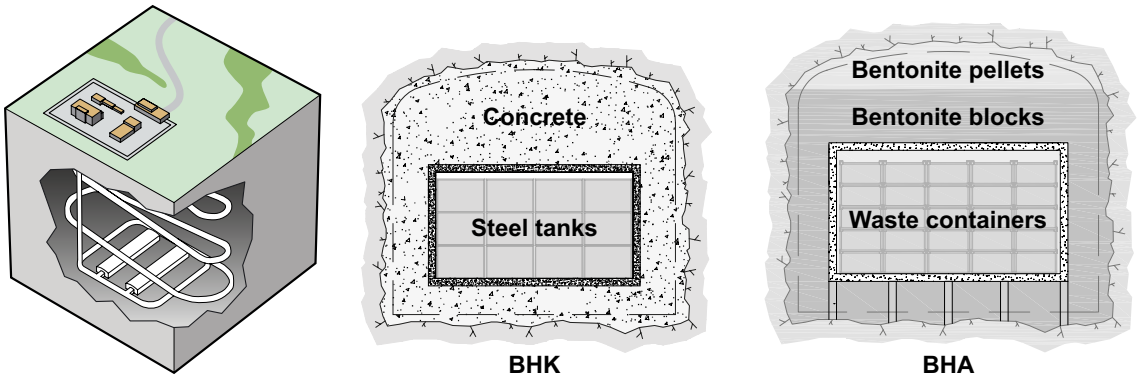

Figure 1-2. *Preliminary facility layout and the proposed repository concept for SFL (left), with one waste vault for metallic waste from the nuclear power plants (BHK, centre) and one waste vault for waste from Studsvik Nuclear AB, Cyclife Sweden AB and AB SVAFO (BHA, right).*

To reflect its status as a preliminary analysis the present analysis is denoted *safety evaluation*. The safety analysis methodology as applied in SE-SFL is a first evaluation of post-closure safety for the repository concept proposed by Elfwing et al. (2013) and is not part of a licence application. As such, the methodology follows the methodology established by SKB for the most recent safety assessments for the extended SFR (SR-PSU; SKB 2015a) and for the Spent Fuel repository (SR-Site; SKB 2011a) but is adapted in view of the objectives of SE-SFL. The adaption of the methodology for the purposes of SE-SFL is described in Section 2.5 of the **Main report**.

To the extent applicable, SE-SFL builds on knowledge from SR-PSU and SR-Site. There are commonalities regarding the waste, engineered barriers, bedrock, surface ecosystems and external conditions relevant to post-closure safety. For instance, SE-SFL and SR-Site both address timescales of one million years (see Section 2.3 of the **Main report**). A further similarity is the proposed depth of 300–500 m. There are similarities between SFR and SFL regarding the waste and waste packaging and the proposed engineered barriers.

No site has yet been selected for SFL and therefore data from SKB's site investigation programmes for the Spent Fuel Repository and for the extension of SFR have been utilised in SE-SFL. In order to have a realistic and consistent description of a site for geological disposal of radioactive waste, data from the Laxemar site in Oskarshamn municipality (see Figure 1-3), for which a detailed and coherent dataset exists, are used. Based on an initial hydrogeological analysis for SE-SFL, the location for the SFL repository was selected to be a part of the rock volume that was earlier found most suitable for a potential Spent Fuel Repository within the Laxemar site (SKB 2011b). Data from Forsmark are included in the analysis to extend the ranges of situations and parameter values addressed, while preserving the overall context defined for Laxemar.

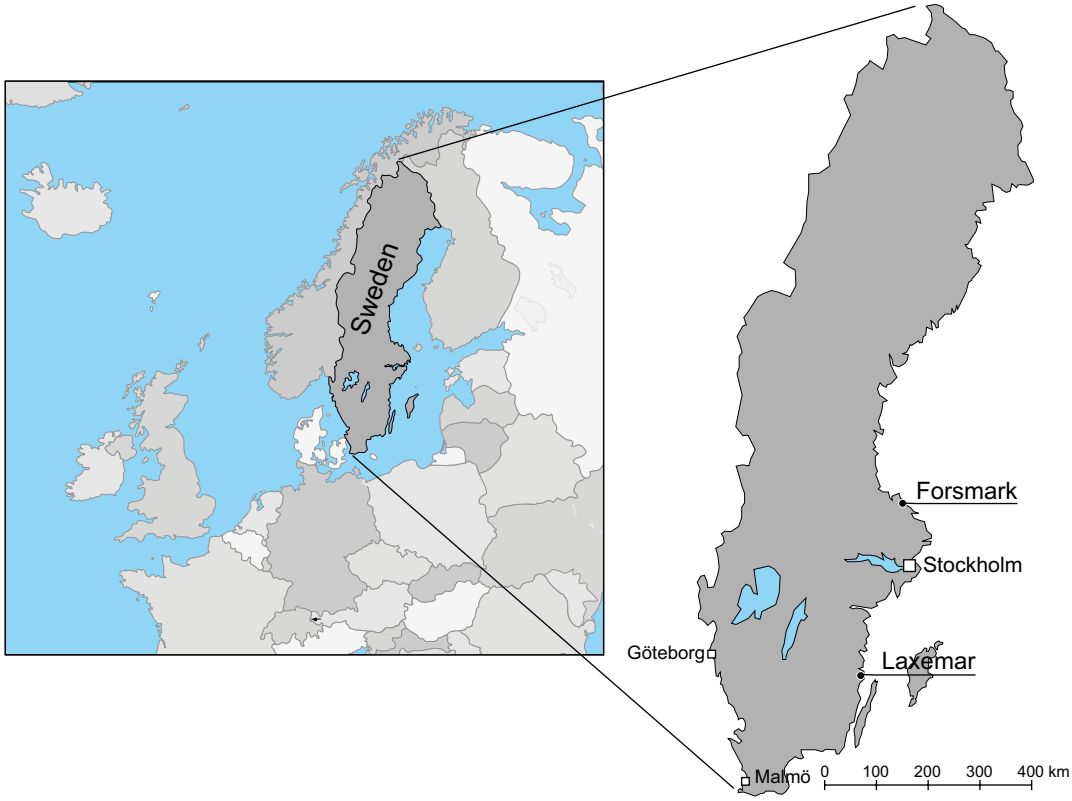

Figure 1-3. *Map showing the location of Laxemar and Forsmark. Data from the site investigations in Laxemar, along with the data from the SR-Site and SR-PSU assessments from Forsmark, are used in SE-SFL in order to have a realistic and consistent description of a site for geological disposal of radioactive waste, for which a detailed and coherent dataset exists.*

SE-SFL is further developed in comparison to the previous assessment (SKB 1999). Important improvements are an updated inventory and a more comprehensive and detailed account of internal and external processes. Moreover, in SE-SFL the description of biosphere has focused on vertical transport from the geosphere and accumulation in discharge areas (including ecosystem conversion), as compared with the stylised modules in SFL 3–5, which primarily described the upper parts of ecosystems. Moreover, the availability of data from the SR-Site and SR-PSU site investigations also allows for a more detailed representation of the biosphere (and the geosphere).

1.2.1 The SE-SFL report hierarchy

The **Main report** and main references in SE-SFL are listed in Table 1-1, also including the abbreviations by which they are identified in the text (abbreviated names in bold text). It can be noted that there are no dedicated process reports for the different systems in SE-SFL but there is a FEP-report. The SFR and SFL waste and repository concepts have many similarities, for instance the use of similar barrier materials and thus similar process interactions with the surrounding bedrock environment (Section 2.5.4 in the **Main report**). Therefore, the descriptions of internal processes for the waste (SKB 2014a) and the barriers (SKB 2014b) in SR-PSU are used in SE-SFL. For the bedrock system, the descriptions of internal processes for the geosphere in SR-Site (SKB 2010a) and SR-PSU (SKB 2014c) are used. There are also additional references, which include documents compiled within SE-SFL, for instance input data reports for the radionuclide transport and dose calculations (Shahkarami 2019, Grolander and Jaeschke 2019). In addition, SE-SFL also relies on references to documents that have been compiled outside of the project, either by SKB or other similar organisations, or are available in the scientific literature. In Figure 1-4, the hierarchy of the **Main report**, main references and additional references within SE-SFL is shown.

Table 1-1. Main references in SE-SFL and the abbreviations by which they are identified in the text, shown in bold.

Abbreviation used when referenced in this report	Text in reference list
Main report	**Main report, 2019.** Post-closure safety for a proposed repository concept for SFL. Main report for the safety evaluation SE-SFL. SKB TR-19-01, Svensk Kärnbränslehantering AB.
Biosphere synthesis	**Biosphere synthesis, 2019.** Biosphere synthesis for the safety evaluation SE-SFL. SKB TR-19-05, Svensk Kärnbränslehantering AB.
Climate report	**Climate report, 2019.** Climate and climate-related issues for the safety evaluation SE-SFL. SKB TR-19-04, Svensk Kärnbränslehantering AB.
FEP report	**FEP report, 2019.** Features, events and processes for the safety evaluation SE-SFL. SKB TR-19-02, Svensk Kärnbränslehantering AB.
Initial state report	**Initial state report, 2019.** Initial state for the repository for the safety evaluation SE-SFL. SKB TR-19-03, Svensk Kärnbränslehantering AB.
Radionuclide transport report	**Radionuclide transport report, 2019.** Radionuclide transport and dose calculations for the safety evaluation SE-SFL. SKB TR-19-06, Svensk Kärnbränslehantering AB.

1.3 The role of this report in SE-SFL

This report documents the biosphere assessment performed as an integral part of the safety evaluation of SFL. The main purpose of the biosphere assessment within SE-SFL is to allow the evaluation of the conditions under which the repository concept has the potential to fulfil the regulatory requirements for post-closure safety. To this end, the biosphere assessment allows estimations of the annual effective dose for a representative individual in the most exposed group that reflect a robust description of the biosphere and a credible handling of associated uncertainties. In addition to the specific objectives of the safety evaluation, the biosphere assessment in SE-SFL contributes to the iterative development of SKB's biosphere assessment and provides input to SKB's RD&D-program as further indicated in Section 1.4 and Chapter 2.

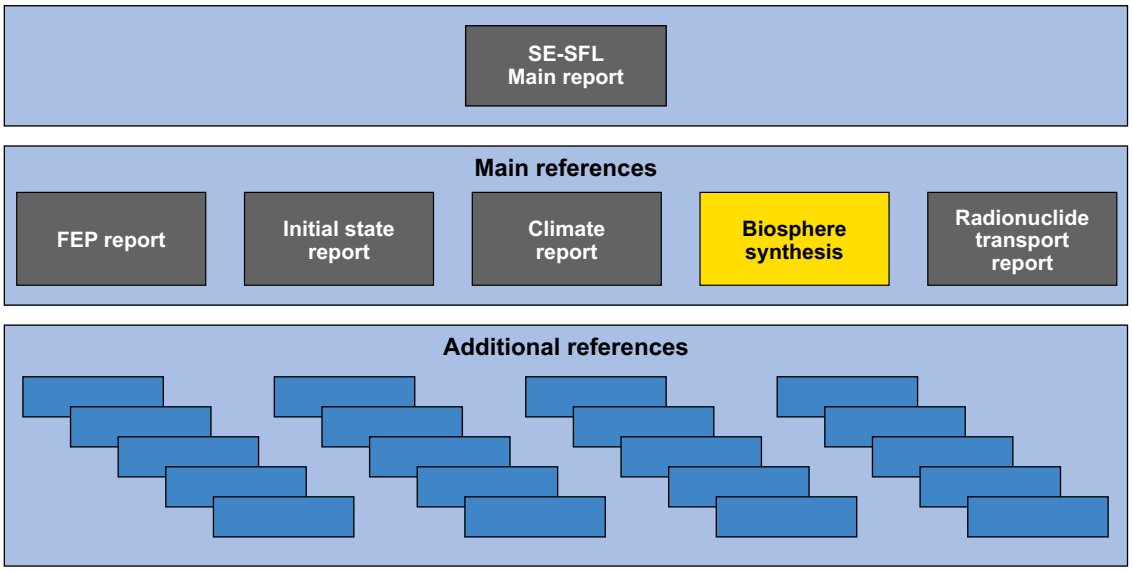

Figure 1-4. *The hierarchy of the Main report, main references and additional references in the safety evaluation of post-closure safety SE-SFL. The additional references either support the Main report or one or more of the main references.*

1.4 Structure of this report

The structure of this report was chosen to be similar to the structure of SKB's most recent Biosphere synthesis for SR-PSU (SKB 2014d). The background to the SE-SFL project and an overview of the safety evaluation is given in the present chapter. Chapter 2 gives a summary of the methodology used and the assessment context of the biosphere part of SE-SFL. This chapter also describes the integration of the biosphere assessment and the overall assessment of the SE-SFL.

The definition of the initial state for the safety evaluation is based on the principal characteristics of the biosphere at the present day at the example site Laxemar are presented in Chapter 3. The description includes a general outline of the site, as well as more specific descriptions of the context from which parameter values have been selected to underpin the SE-SFL. The projected changes of ecosystems with time, due to large scale climate variation and natural succession, are described in Chapter 4. Further, identification and detailed descriptions of individual discharge areas in the Laxemar area is given in Chapter 5.

As a basis for the safety evaluation, features, events and processes (FEPs) that can influence post-closure safety for the proposed repository concept for SFL are identified in the biosphere, as described in Chapter 6. These biosphere FEPs are considered in the selection of *evaluation cases* for SE-SFL. The evaluation cases are defined in order to facilitate assessment of conditions under which the proposed repository concept has the potential to meet applicable criteria on radiation protection after closure. Chapter 7 describes the biosphere conditions in the base evaluation case, assuming constant, present-day climatic and other external conditions throughout the full assessment period. Further, the six evaluation cases in which biosphere conditions are altered as compared with present-day conditions, are described.

In order to analyse the evaluation cases, an integrated conceptual model and a linked chain of mathematical models is used to represent radionuclide transport from the waste vaults to the dose of potentially exposed groups (Figure 1-5). The biosphere model for transport and exposure (BioTEx or biosphere model) used in SE-SFL, described in Chapter 8, is in essence the same as the one developed in the previous safety assessment SR-PSU. However, a few technical modifications and improvements were introduced, partly as a response to SSM's reviews on previous SKB assessment. The performance of the updated model is evaluated in Chapter 9, by comparisons with the original SR-PSU model. The biosphere model has, as far as possible, utilised site-specific data from the example site both for describing parameters and populating parameter values. The data selection processes used in SE-SFL and the parameters required by the biosphere model are described in Chapter 10.

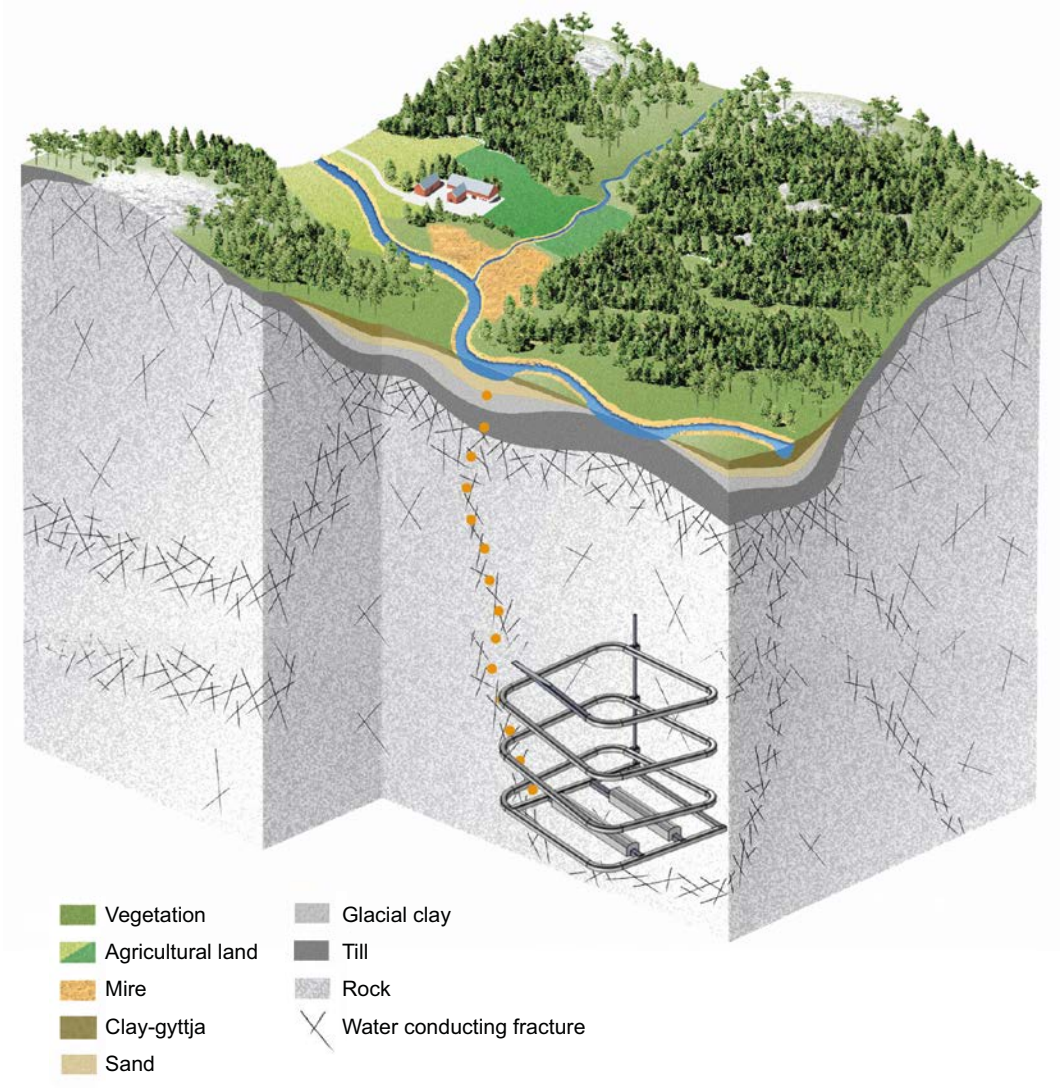

Figure 1-5. *Conceptual model of radionuclide transport in SE-SFL. The orange dotted line represents the path taken by radionuclides released from the deposited waste to surface ecosystems. The model chain consists of three mathematical models, representing the repository near-field (including the waste, waste packaging, concrete structure and concrete/bentonite backfill), the geosphere, and the biosphere (see Figure 2-4).*

In Chapter 11 the results from the base case are examined in detail. The chapter covers in-depth analyses of the annual effective dose (henceforth effective dose is simply written as dose, where there is no ambiguity) to different potentially exposed groups, contributions of exposure pathways and the dynamics of radionuclide transport and accumulation throughout the regolith profile. The results with respect to annual doses for the six evaluation cases in which biosphere conditions are altered as compared with present-day conditions are summarised in Chapter 12. In addition, Chapter 13 describes results from three sensitivity cases that examine how uncertainties in the biosphere assumptions may affect environmental concentrations and potential doses.

One of the objectives of SE-SFL is to provide SKB with a basis for prioritising areas in which the level of knowledge and adequacy of methods must be improved in order to perform a full safety assessment for SFL (Section 1.2). In support of this objective, two additional studies were performed. These include an examination of the environmental properties of three potentially important elements, namely chlorine (as chloride), molybdenum and nickel (Chapter 14). Further, patterns of radionuclide accumulation were studied using distributed numerical models with a greater spatial resolution and a more detailed representation of transport and chemical reactivity, as described in Chapter 15.

The results and analyses presented in this report are discussed, in the light of the main objectives of SE-SFL (Section 1.2), in Chapter 16. Finally, the developments made in the biosphere assessment within the safety evaluation SE-SFL are summarised in Chapter 17.

Terms and acronyms that are either rarely used outside SKB, or can be regarded as specialised terminology, are explained in Appendix A.

1.4.1 Contributors to the SE-SFL biosphere assessment

The work done in SE-SFL is based on the experience from SKB's previous safety assessments SR-Site and in particular SR-PSU and several persons that have contributed to the SE-SFL biosphere assessment have experience from these previous safety assessments. Ben Jaeschke (AFRY) was the editor of this report, and the authors are listed in Table 1.2. This report has been significantly improved at different stages by adjustments in accordance with comments provided by informal reviewers; Eva Andersson (SKB), Georg Lindgren (Kemakta konsult AB) and Björn Söderbäck (SKB); and external factual reviewers; Jordi Bruno (Amphos 21), Ari Ikonen (EnviroCase, Ltd.) and Mike Thorne (Mike Thorne and Associates Limited).

Table 1-2. Name and affiliation of persons who have contributed to the SE-SFL Biosphere synthesis. Each author's contributions are briefly described and references are given to the chapters of the report.

Name(s), affiliation	Contribution to the SE-SFL biosphere synthesis report	Chapter of this report
Jenny Brandefelt, SKB	Introduction, assessment context	1, 2
Ulrik Kautsky, SKB	Leading and coordinating the biosphere assessment	2
Jens-Ove Näslund & Johan Liakka, SKB	Climate description	3, 4
Gustav Sohlenius, Sveriges Geologiska Undersökning (SGU)	Regolith and land use	3, 4
Mårten Strömgren, Umeå University	GIS analysis, landscape development	Most figures based on maps
Mats Tröjbom, MTK AB	Chemistry	3, 4
Emma Lindborg, SKB	Hydrology	3, 4
Mona Sassner, DHI Sverige AB	Hydrology	5, 8
Anders Löfgren, EcoAnalytica in Scandinavia AB	Terrestrial ecosystems	1, 3–7, 10
Sara Grolander, Kemakta konsult AB	Element specific parameters and data quality	10
Per-Anders Ekström, Kvot AB	Model development, model and results evaluation	8, 9, 11–13
Thomas Grabs, SKB	Hydrology, transport and review of elements	8, 14, 15
Olle Hjerne, SKB	Aquatic ecosystems, data evaluation, synthesis	11–13
Teresia Svensson, Linköping University	Review and analysis of chlorine	14
Fredrik Lidman, Swedish University of Agricultural Sciences (SLU), Umeå	Review and analysis of molybdenum and nickel	14
Elena Abarca, Alvaro Sáinz-García, David García, Jorge Molinero and Diego Sampietro, Amphos 21	Distributed and reactive transport modelling, model evaluation	15
Peter Saetre, SKB	Model development, model, data and results evaluation, synthesis	2, 5–13, 15–17

2 Methodology and assessment context

2.1 Introduction

The methodology for assessment of radiological effects on humans and the environment from a repository for radioactive waste has developed continuously during the last few decades and SKB has been extensively involved in this development. Several biosphere assessments have been performed by SKB during this time, and the development has been reported in the RD&D Programme, most recently in SKB (2019). An extensive summary of earlier SKB work and key achievements were presented in the Biosphere syntheses of SR-Site (SKB 2010b) and SR-PSU (SKB 2014d). Both of these assessments were reviewed by the authorities, and the outcome of the reviews has provided important guidance for SKB's development of the biosphere assessment methodology. Most of the development of the biosphere model that has been introduced in SE-SFL is connected to issues raised in the two previous assessments, and thus the SE-SFL work is an important milestone also for the iterative safety analysis processes for SFR and the Spent Fuel Repository.

This chapter aims to give a brief overview of the assessment methodology used in the biosphere part of SE-SFL, illustrated in Figure 2-1. The biosphere work is an integrated part of the overall safety evaluation and consequently follows the overall methodology for SE-SFL. This methodology, as applied in the biosphere, is compatible with the IAEA BIOMASS methodology (IAEA 2003, Lindborg 2018), which provides guidance on the treatment of the biosphere in post-closure safety assessments for solid radioactive waste disposal. The sections of this chapter, which broadly follows that of the structure of the BIOMASS methodology, give a short description of each step of the methodology with references to chapters and sections in this report where the details are presented.

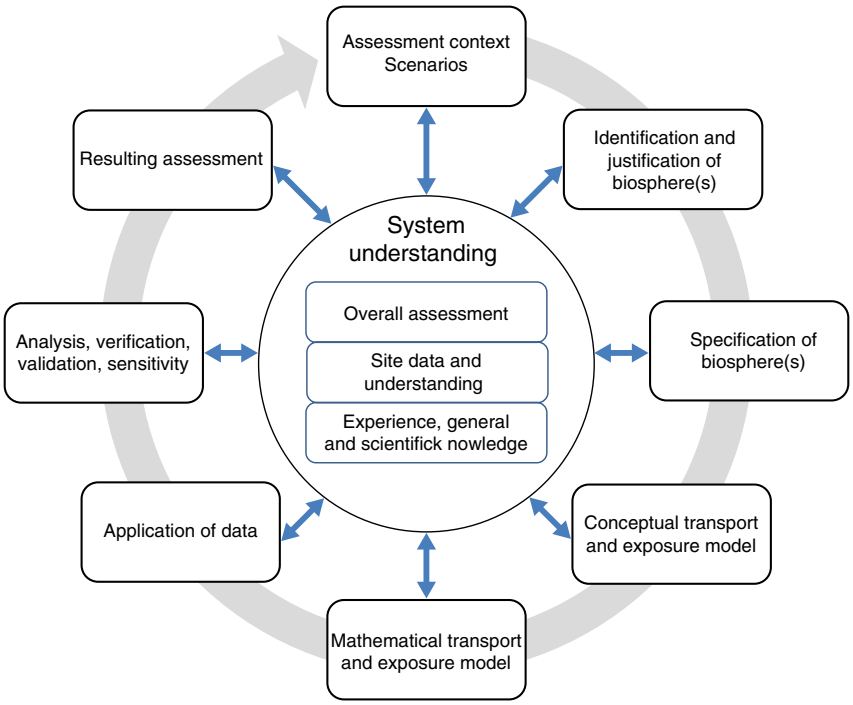

Figure 2-1. *Schematic illustration of SKB's biosphere methodology. The circle and two headed arrows indicate that the methodology is essentially iterative in nature. Understanding of the system, including the repository and the bedrock surrounding the repository, plays a central role in the assessment methodology. Knowledge of the overall assessment is an integrated part of the system understanding and the assessment context is considered at the start of the cycle. The figure is based on the ongoing work on updating the methodological guidance on undertaking post-closure biosphere assessments*[1].

[1] The work to update the BIOMASS methodology is the output of Working Group 6 of the second phase of the IAEA project Modelling and Data for Radiological Impact Assessment (MODARIA II), working in collaboration with the international BIOPROTA forum.

2.2 Overall methodology

The safety analysis methodology as applied in SE-SFL is a first evaluation of post-closure safety for the repository concept proposed by Elfwing et al. (2013) and is not part of a licence application. As such, the methodology follows the methodology established by SKB for the most recent safety assessments for the extended SFR (SR-PSU; SKB 2015a) and for the Spent Fuel repository (SR-Site; SKB 2011a) but is adapted in view of the objectives of SE-SFL. The adaption of the methodology for the purposes of SE-SFL is described in Section 2.5 of the **Main report**.

The safety evaluation SE-SFL consists of ten main steps that are partly carried out concurrently and partly consecutively. The biosphere assessment contributes to most of the steps of the safety evaluation (Figure 2-2 and **Main report**, Section 2.5): Thus, *features, events and processes* (FEPs) that can influence post-closure safety for the proposed repository concept for SFL are identified in the biosphere, and the expected state of the biosphere at closure is described as a part of *the initial state*. The influence of climate on biosphere conditions and potential exposure are explicitly considered when reference *external conditions* are chosen. The biosphere is an integral part of the analysed system, and thus relevant surface system FEPs are described as *internal processes*, and *input data* for radionuclide transport and dose calculations in surface systems are selected using a structured process. Given the long timescales considered in the assessment, the surface system is expected to go through significant changes, and this development is captured in the description of *the reference evolution*.

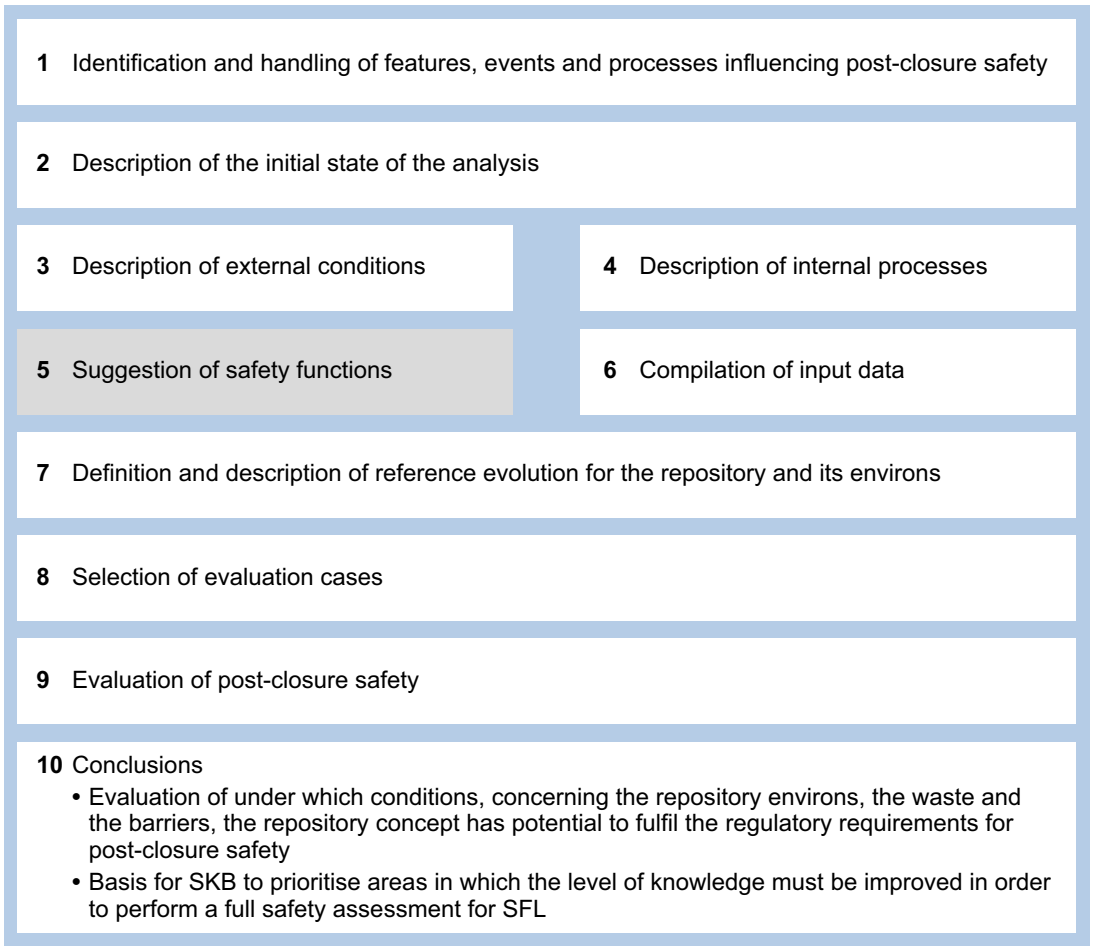

Figure 2-2. *Overview of the methodology applied for the evaluation of post-closure safety for the proposed repository concept for SFL. White background colour indicates that the work within the biosphere analysis contributes to and/or is an integral part of the step.*

Finally, biosphere FEPs are considered in the selection of *evaluation cases*, and *post-closure safety is evaluated* by analysing results from the integrated model chain, from the release from the waste vaults to the dose representative members of potentially exposed groups. Although the *conclusions* from overall evaluation of the repository concept are not drawn within the biosphere assessment, results from the biosphere are utilised in the discussion and in the identification of areas where knowledge and performance need to be improved for future steps.

2.3 System understanding

Understanding of the disposal system and its environment plays a central role in the biosphere assessment methodology (Figure 2-1). It includes both general understanding of the aims and components of the overall assessment, and detailed knowledge of the surface system. In SE-SFL understanding of the overall assessment has been facilitated by integrating biosphere aspects in most of the steps of SKB's assessment methodology (Figure 2-1, see also Section 2.10). Detailed knowledge of the surface system and how this knowledge can be applied to post-closure safety assessments comes from; 1) detailed descriptions of two extensively investigated potential Swedish sites for geological disposal of radioactive waste, namely Laxemar and Forsmark (e.g. SKB 2009, Lindborg 2008), 2) comprehensive descriptions of terrestrial and aquatic ecosystems that are potential recipients of groundwater discharge at a Swedish Baltic coastal site (Löfgren 2010, Andersson 2010, Aquilonius 2010), and 3) the experience from previous SKB safety assessments, primarily the SR-Site and SR-PSU assessments (SKB 2010b, 2014d). The understanding from SKB's RD&D program (e.g. SKB 2019) is continuously used to inform the iterative safety analysis processes, as is the shared experience from international collaboration forums that seek to address key uncertainties in the assessment of environmental and human health impacts (e.g. IAEA MODARIA II and BIOPROTA[2]).

Identification and handling of biosphere FEPs, relevant for post-closure safety for geological repositories for radioactive waste, is an integral part of the development of the current knowledge of the surface system. Lists of FEPs provide a structured way to check that potentially important aspects of the safety assessment have not been overlooked, and a comprehensive analysis of the biosphere interaction matrix facilitates understanding of radionuclide migration and accumulation in surface ecosystems (SKB 2013a). SKB has long experience of identifying and handling biosphere FEPs (e.g. SKB 2014d, 2015b), and in SE-SFL SKB's generic biosphere FEP list has been re-evaluated inorder to identify additional FEPs relevant to coastal sites in Sweden (Chapter 6).

2.4 Assessment context and evaluation cases

The context of the overall assessment of SE-SFL includes the objectives of the safety evaluation, basic knowledge on the radioactive waste, the proposed repository concept and the choice of an example site (see Sections 1.1–1.2). SE-SFL is conducted within the same regulatory regime as SKB's previous safety assessments. However, since there is no intention in SE-SFL to evaluate regulatory compliance in full, the evaluation focuses on certain parts of the requirements for a full application (see Section 2.2 in the **Main report** for details).

2.4.1 Endpoints of the assessment

The safety evaluation SE-SFL focuses on the protection of human health, as defined by the risk for harmful effects of ionising radiation for a representative individual in the group exposed to the greatest risk. According to the Swedish regulation (SSM 2008a) the factor to be used for conversion of effective dose to risk is 7.3 % Sievert^{-1}. Thus, for a scenario with the probability of one, a risk of 10^{-6} corresponds to an annual dose of 14 μSv.

[2] www.bioprota.org.

The term annual dose is defined as the mean annual effective dose over a lifetime for an individual living in the area with the highest concentration of radionuclides. Furthermore, adults are considered to provide a sufficiently good approximation of the average exposure during a lifetime. This is in line with the ICRP recommendations for long-lived solid waste (ICRP 2000, 2006). To estimate annual exposure during the lifetime of an individual, projected doses have been averaged over a period of 50 years, which is the integration period used by ICRP in the derivation of dose coefficients for adults. The dose coefficients used in the dose calculations take into account retention of radionuclides in the human body and exposure from radioactive progeny, as well as the different radiation sensitivities of various tissues and organs. Doses calculated using these coefficients are committed effective doses, which are appropriate for calculating the probability of harmful effects of ionising radiation using the dose to risk factors given in the Swedish regulation (SSM 2008a).

As SE-SFL is a first evaluation of post-closure safety for the proposed repository concept (and is not part of a licence application), the collective dose and potential effects on the environment are not evaluated at this step in the process.

2.4.2 Assessment approach and management of uncertainties

As in the previous safety assessments, SKB has aimed to make the transport model of natural ecosystems (Chapter 8) as comprehensive and realistic as possible, with respect to model structure, primary transport pathways, landscape development and the associated parameters. However, the uncertainties with respect to the characteristics of future human inhabitants of the area are large and essentially irreducible. Thus, potentially exposed groups are to be interpreted as credible bounding cases with respect to the identified exposure pathways (see below and Section 6.3).

To assess the potential for the proposed repository concept to meet applicable criteria on radiation protection after closure, a set of evaluation cases was defined in SE-SFL (Section 2.4.7). A few of these cases illustrate uncertainty in the external conditions and their evolution with potential implications for transport and exposure in the biosphere. These evaluation cases can be seen to address different types of *scenario uncertainties*. Moreover, to quantify the potential influence of changed soil conditions, due to ageing of organic soils, an additional sensitivity case was added to the biosphere analysis (Section 13.2). In addition, different aspects of *model uncertainties* were addressed by comparing results from alternative models (Chapters 9 and 15). A comprehensive sensitivity analysis of the effects of *parameter uncertainties* was outside the scope of the biosphere analysis in this early stage of the SFL safety analysis process. However, to cast some light on how sensitive the biosphere calculations are to the selected values of parameters, sensitivity calculations with respect to discharge area properties and K_d and *CR* values were also performed (Sections 12.2, 13.4 and 13.3). In Chapter 16 the results with respect to scenario, model and parameter uncertainties are summarised and discussed.

2.4.3 Disposal system and example site context

The radionuclide inventory for the waste planned for disposal in SFL is an important component of the overall assessment context. The radiotoxicity of the radionuclide inventory evaluated in SE-SFL stemming from the reactor internals decreases to less than 0.01 percent due to decay during the analysis period of one million years (Figure 2-3, details in Section 5.2 in the **Radionuclide transport report**). The radiotoxicity of the legacy waste decreases to a couple of percent of its initial value at closure during that period. For comparison, it can be noted that the total radiotoxicity at closure is about 10 times the corresponding value for the extended SFR and less than the value for a single copper canister in the Spent Fuel Repository.

No location has yet been selected for SFL, but Laxemar has been selected as an *example site* for the SE-SFL (Section 1.2). Laxemar is located on the coast of the Baltic Sea in south-eastern Sweden. The area, which is typical of this part of eastern Sweden, is characterised by a relatively flat topography in a fissure valley landscape. The landscape is a mosaic of coniferous forests, shallow lakes and wetlands, interlaced with patches of agricultural land (the latter primarily concentrated in the valleys). SKB conducted extensive site investigations at Laxemar during the period 2002 to 2007 with the objective of finding a potentially suitable site for the Spent Fuel Repository. An adequate description of the

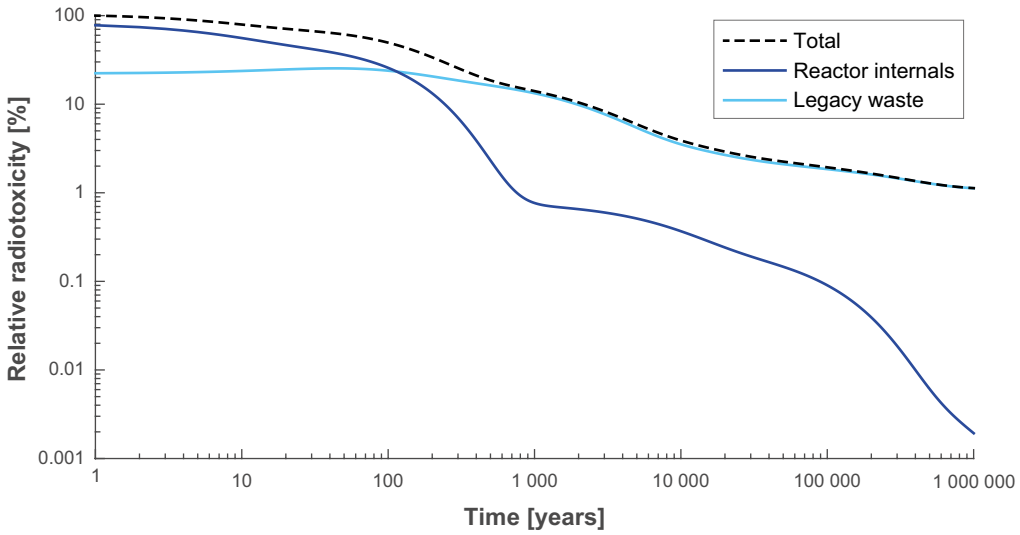

Figure 2-3. *Time dependency of the radiotoxicity of the radionuclide inventory evaluated in SE-SFL. The dashed black line shows the total inventory, the light blue line the inventory of the legacy waste (BHA), and the dark blue line the inventory for the reactor internals (BHK) (figure from* ***Main report****).*

repository environs, i.e. the bedrock surrounding the repository and the surface systems in the repository area, is an important part of the overall assessment. To this end, Chapter 3 provides a description of the present-day conditions for the surface system at the Laxemar example site. This description has an important role in the overall assessment, as part of the description of the initial state of the repository and its environs.

2.4.4 Source term and geosphere biosphere interface

Radionuclide transport and dose modelling in SE-SFL is performed with a set of models representing the waste vaults (near-field), the bedrock surrounding the repository (geosphere), and the surface systems in the repository area (biosphere) (Figure 2-4). The chain starts with the near-field model that describes the transport and retention of radionuclides in the waste domain and the engineered barriers, and the release to the bedrock. The geosphere model describes the subsequent transport and retention of radionuclides in and through the bedrock towards the surface. The output of the model is a time-dependent annual release of radionuclides from the bedrock to the regolith, which is the source term for transport and dose calculations in the biosphere. The radionuclide transport calculations are carried out as dynamic simulations, where the output from one model, in terms of the annual activity release for each radionuclide, is used as input for the next (Chapter 2 in the **Radionuclide transport report**).

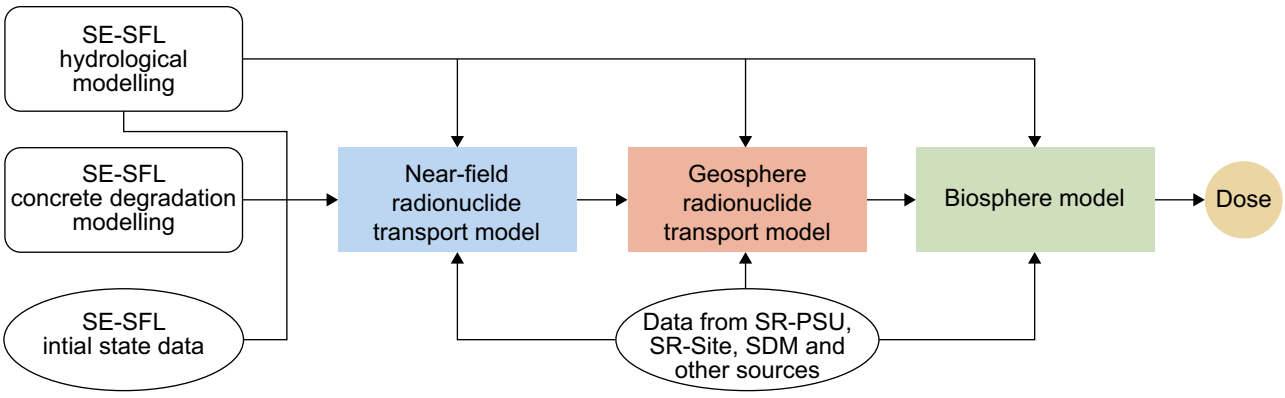

Figure 2-4. *Schematic representation of the SE-SFL radionuclide transport model chain and main sources of input for the respective models (figure from* ***Main report****).*

Hydrogeological simulations suggest that particles released from the postulated repository position will be discharged in topographically low-lying areas in the Laxemar landscape (Joyce et al. 2019). These results agree with SKB's general understanding and results from previous safety assessments, and consequently radionuclides from the geosphere are assumed to reach the lowermost regolith layers in local discharge areas in SE-SFL. The identification, delimitation and modelling of such discharge areas, i.e. biosphere objects, are described in Chapter 5. Potential dose consequences from extracting water for drinking and small-scale irrigation from a well drilled into the bedrock are also evaluated as a part of the biosphere analysis (Section 12.8). However, the description and parameterisation of the well is part of the geosphere description (Chapter 5 in Joyce et al. 2019).

2.4.5 Time frames

In accordance with the regulations and general advice, the timescale for the SE-SFL post-closure safety evaluation is one million years (Section 2.3.2 in the **Main report**).

2.4.6 Assumptions with respect to potentially exposed groups

Predictions of future human behaviour are inherently uncertain, especially on the time scales of thousands to tens and hundreds of thousands of years relevant for post-closure safety assessments. Thus, in the previous safety assessment SR-PSU, SKB reviewed exposure pathways of relevance within ecosystems of interest. Land-use variants, which resulted in relatively high exposure, and the associated potentially exposed groups (PEGs), were then identified from historically self-sustainable communities (SKB 2015b). The use of such groups is considered to ensure that the most exposed group is evaluated in the calculations of SE-SFL. This exposure pathway analysis and the potentially exposed groups are described in Section 6.3.

2.4.7 The base case and other evaluation cases

In SE-SFL fourteen evaluation cases have been defined to assess the conditions under which the repository concept has the potential to fulfil regulatory criteria with respect to radiological safety or to assess the sensitivity of assessment endpoints to selected uncertainties (Figure 2.5, **Main report**, Section 2.5.8). The term evaluation case is chosen instead of scenario, since a broader approach is applied in the selection of the cases than proposed in SSM's recommendations for scenario selection (i.e. some cases illustrates alternative repository designs and aspects of siting).

For ease of interpretation and straightforward comparison with the evaluation cases based on alternative assumptions or temporal evolutions, a base case is defined in SE-SFL. The base case assumes constant, present-day climatic and other external conditions throughout the full assessment period (Section 7.2 and **Main report**, Section 6.2). The assumed base case also addresses the regulatory requirement that the assessment of the repository's protective capability shall include a case based on the assumption that the biosphere conditions prevailing at the time when an application for a licence to construct the repository is submitted will not change (SSM 2008a, Chapter 10).

The base case is complemented by a set of cases that evaluate the sensitivity of the resulting activity release and dose to specific assumptions made with respect to conditions in the repository and its environs. These cases were chosen to illustrate conditions in the repository and the repository environs that are likely to improve the repository performance in comparison with the base case. Cases that illustrate the effects of uncertainties in bedrock properties, discharge area and the effect of a drilled well, as well as uncertainties relating to the regional climate and the future climate evolution, were also included in the evaluation (Figure 2-5, Section 8.2 in the **Main report**).

In six evaluation cases biosphere conditions are altered as compared with present-day conditions. The biosphere conditions of these cases, and the base case, are described in Chapter 7, and assessed annual doses are evaluated in Chapters 11–13. A full description of the evaluation cases and integrated interpretations of results (including the responses of the near-field and geosphere releases) can be found in the **Radionuclide transport report** (Chapters 5–7).

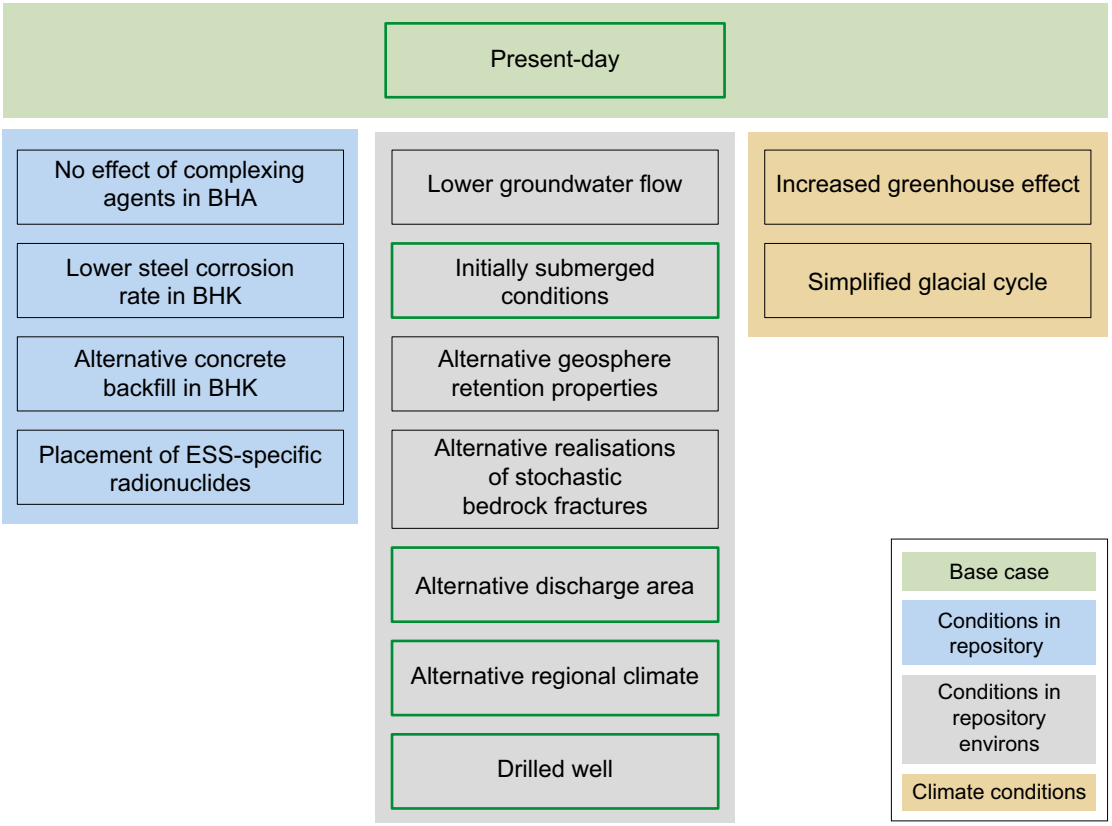

Figure 2-5. *Evaluation cases included in the evaluation of the potential for the proposed repository concept to meet applicable regulatory criteria after closure, grouped and colour-coded according to type of scenario driver (repository, environs or large-scale climate conditions). Cases outlined in green are described and evaluated in the present report (figure from* ***Main report****).*

2.5 Representation of the biosphere

This step of the methodology refers to identifying and describing (or specifying) the set of biosphere systems that are needed to support the safety assessment (Figure 2-1). Given that the waste vaults are postulated to be located in a coastal landscape, and that the evaluation period covers hundreds of thousands of years, deep groundwater discharge can be expected to occur both above and below the present sea level.

Based on previous SKB work, coastal sea basins, lakes and wetlands are the three natural ecosystems that are likely to occur in areas where deep groundwater is discharged (e.g. SKB 2010b, 2014d). In addition, two versions of agricultural land use have been used in previous assessments to evaluate effects from draining and cultivating natural ecosystem, and from using wetlands for hay-making. SKB has also used a garden plot system to assess consequences from exposure routes considered to be relevant on a smaller scale (e.g. irrigation and fertilisation with algae or ash). However, as many of the potential discharge areas in Laxemar are cultivated, an agricultural model for continuous cultivation is also required to represent present-day conditions, as prescribed in the base evaluation case.

This set of ecosystems is deemed to be sufficient to support all the evaluation cases identified in the overall assessment (Chapter 7) and covers all relevant exposure pathways (Section 6.3). The principal characteristics of the biosphere at the present day are presented in Chapter 3. In calculation cases that capture the transition of a discharge area from a coastal sea basin through a lake stage, to a mire, the transition between the ecosystems also needs to be described and handled (i.e. in the *initially submerged* and the *simplified glacial cycle* evaluation cases). The projected changes of ecosystems with time, due to large-scale climate variation and natural succession, are described in Chapter 4.

The identification and detailed description of individual discharge areas in the Laxemar area is given in Chapter 5. The quantitative description of these objects is facilitated by detailed supportive modelling of the example site, including a digital elevation map (DEM), a regolith depth model (RDM), a description of the surface hydrology (with MIKE SHE) and a coupled Regolith-Lake Development Model (RLDM).

2.6 Biosphere assessment model

In order to simulate radionuclide transport, accumulation and potential exposure in the biosphere, conceptual and numerical models of identified ecosystems needs to be developed. The biosphere model for transport and exposure (BioTEx or biosphere model) used in SE-SFL is in essence the same as the one developed in the previous safety assessment SR-PSU (Saetre et al. 2013a). The SR-PSU model handles coupled terrestrial and aquatic ecosystems and their temporal development. It has been verified by code comparisons, and part of the models has been validated (SKB 2013b). Moreover, it has proven to be useful through experience (SKB 2014d) and has been judged to give a good description of the biosphere system and to yield reasonable results (e.g. SSM 2019).

The structure of the SR-PSU model was based on biosphere FEPs (and a biosphere interaction matrix) that include FEPs that have been found to be important in safety assessments for radioactive waste disposal (SKB 2011a, 2013a), previously established conceptual models of aquatic and terrestrial ecosystem (Aquilonius 2010, Andersson 2010, Löfgren 2010), a conceptual landscape model (Lindborg 2010), and potentially exposed groups identified through a comprehensive exposure pathway analysis (SKB 2014d). The SR-PSU biosphere model handles coupled terrestrial and aquatic ecosystems and their temporal development (including changes in the sea level).

The re-evaluation of FEPs for the example site did not reveal any cause for model updates (Section 6.2.2). However, a few technical modifications and improvements were introduced (Table 8-1), partly as a response to SSM's reviews of previous SKB assessments. The requirements to evaluate present-day conditions motivated the development of a model of continuously cultivated land, as described in the previous step (Section 2.5). Finally, lack of a relevant hydrological description for ecosystem stages in the identified discharge areas drove the development of a new routine for derivation of hydrological parameters. In practice, these two updates were carried out in parallel, and iterations were needed to capture the main features of a drained and cultivated discharge area.

In SE-SFL the biosphere model is implemented in the Ecolego 6 compartment modelling software. As the base evaluation case in SE-SFL reflects constant external conditions, simplified models for stationary (or time-independent) conditions are introduced in SFL. This type of stand-alone version of the individual ecosystem models also facilitates comparisons between discharge areas and ecosystem types (Section 12.2). The biosphere model is implemented as an integrated component in the model chain (Figure 2-4), and a time-dependent geosphere release is used as the radionuclide input in all evaluation cases. Further, in the sensitivity cases a unit release rate is used in parallel, to simplify the interpretations of results. The BioTEx model is described in Chapter 8, and the performance of the updated model is evaluated in Chapter 9, by comparisons with the original SR-PSU model.

2.7 Application of data

The biosphere model has, as far as possible, utilised site-specific data both for describing parameters and populating parameter values. The primary source of data has been the quality assured dataset used in the previous safety assessment SR-PSU. This dataset includes a large number of site-specific parameters, based on the site investigations in Forsmark (Grolander 2013), as well as parameters that do not depend on the location of the repository, e.g. effective dose coefficients and characteristics of potentially exposed groups.

The selected example site, Laxemar, differs from Forsmark with respect to, for example, topography, rate of relative sea-level change, and soil and water chemistry. Parameters that describe specific discharge areas had to be extracted from supporting models underpinning the site descriptive model of Laxemar (Chapter 5). All other site-dependent parameters were evaluated to determine if the dif-

ference between typical values from the two sites were substantial. If that was the case the SR-PSU parameter value was disregarded, and a value better reflecting the surface conditions on the example site was chosen. In general uncertainty and natural variation of selected parameter values have not been considered in SE-SFL (see Section 16.4).

In addition, the modifications of the biosphere model introduced in SE-SFL occasionally required new parameters. When new parameters described the composite outcome of several processes (such as plant translocation), the choice of the mathematical description was conditioned on the availability and quality of data, that required a few iterations between the two steps in the methodology. The data selection processes used in SE-SFL and the parameters required by the biosphere model are described in Chapter 10.

Controlled handling of data and workflow is crucial to guarantee the quality of data and model results. The biosphere analysis in SE-SFL followed the quality plan for the safety evaluation project (Section 2.6 in the **Main report**). In addition, a QA process has been developed to assure that data are complete and correct, and that the usage, sources, review, and storage of data are traceable (Chapter 10).

2.8 Analysis, verification, validation and sensitivity analysis

The SR-PSU biosphere model has previously been verified and validated in parts. The effects of model updates introduced in SE-SFL were quantified by model comparisons with the original biosphere model, and differences in model results were in line with a-priori expectations, building confidence that the model modifications had been implemented as intended.

In Chapter 11 the results from the base or *present-day evaluation case* are examined in detail. The chapter covers in-depth analyses of the annual dose to different potentially exposed groups, contributions of exposure pathways and the dynamics of radionuclide transport and accumulation throughout the regolith profile. The fate of accumulated radionuclides upon draining and cultivation of a mire is also analysed. Patterns in annual doses are deduced from the geosphere release, radionuclide properties and mechanisms such as dilution, retention, retardation, radioactive decay and the formation of decay products. In this way, key radionuclides are identified, and their main exposure pathways, transport mechanisms and timescales are characterised.

This step demonstrates SKB's understanding of the BioTEx model and helps build confidence that the model results are reliable. Sense-checks and comparisons of model outputs with results and understanding from analytical solutions for steady-state conditions are also used to assure that the model performs as intended and that results are reasonable. In SKB's experience this type of high-level verification has proved to be very efficient for identifying inconsistencies in the data and/or problems with the mathematical implementations of the model that have clear effects on the model outcome.

In addition, sensitivity cases are used to build confidence in the results from the biosphere model (Chapter 13). For example, the *alternative hydrology case* confirms that the model response to changes in hydrology is reasonable across a large range of conditions spanning different object and watershed properties. Sensitivity cases are also used to examine potential effects of long-term cultivation and alternative choices of key parameter values.

2.9 Results for evaluation of safety

As a part of the SE-SFL radionuclide transport model chain, the biosphere model is applied to all evaluation cases in the overall assessment. As compared with previous safety assessments SR-Site and SR-PSU, more time and effort have been allocated to interpretation and communication of results. This is partly motivated by the aim to allow for an effective transfer of knowledge to the other ongoing safety analysis processes, and partly by the expected long-term gains of a better integrated overall assessment (see next section).

In Chapter 11 the six evaluation cases with biosphere conditions that differ from the base case are evaluated with respect to the annual dose. The plausibility of the results is confirmed by tracing back the dose response to the imposed change in environmental conditions and geosphere release (as compared with the base case). As mentioned in the previous section, the examination of results involves identification of key radionuclides and their exposure pathways, and annual doses are explained in terms of radionuclide properties and mechanisms for transport and accumulation in the biosphere.

The future location of SFL and the areas where groundwater from the repository will reach the surface are unknown. Thus, the *alternative discharge area evaluation case* is designed to study how total and nuclide-specific annual doses are affected by properties of the discharge area (Section 8.5.2 in the **Main report**). As the case utilises a large number of biosphere objects, and includes the effects of landscape development, the analysis of this case is expanded in the present report (Section 12.2), as compared with the analysis in Section 7.6 of the **Radionuclide transport report**. Thus, in this report the case is used to demonstrate SKB's understanding of the biosphere model with respect to variations in object properties and the effects of landscape development, and the case clearly puts the results from the base case in a broader context.

The *present-day* and the *alternative discharge area* cases are used to communicate how the properties of radionuclides and biosphere objects influence the outcome of the safety evaluation. As the results are intended to be shared with a wider audience, the presentation aims at building understanding by including all steps, from deep groundwater discharge to exposure and dose. However, when it comes to the presentation of the other evaluation cases, the focus is to clearly present the potential effects with respect to the factor or conditions that motivated the selection of the specific evaluation case.

2.10 Integration with the overall assessment

One of the aims in SE-SFL has been to strive for a seamless integration of the biosphere analysis with the overall safety evaluation. Hence, in SE-SFL, members of the biosphere team have worked with experts from other disciplines as a part of the radionuclide transport team. The integration has been facilitated by, for example, comprehensive descriptions of the initial state and of the evolution of the repository environs. Discussions and iterations between identification and definition of evaluation cases and the interpretation of results have improved the internal consistency of evaluation cases and made simplifications within the different domains (e.g. climate, near-field, geosphere and biosphere) properly balanced. An integrated analysis has allowed for a comprehensive and insightful interpretation of results, from the waste vaults to the surface ecosystems. The approach has also minimised the risk for misunderstandings or loss of focus on elaborated non-essential details that could otherwise have obscured the interpretations of results (see Chapter 17).

3 The Laxemar example site – present-day conditions

3.1 Introduction

No site has been selected for the SFL repository. However, in order to have a realistic and consistent description of a site for geological disposal of radioactive waste, data from the Laxemar site in Oskarshamn municipality (Figure 3-1) are used, for which a detailed and coherent dataset exists. Based on an initial hydrogeological analysis for SE-SFL, the example location for the SFL repository was selected to be a part of the rock volume that was earlier found suitable for a potential Spent Fuel Repository within the Laxemar site (SKB 2011b). A main assumption in the SE-SFL safety evaluation for the bedrock and surface systems is that the initial state conditions at repository closure at 2075 AD are present-day conditions.

This chapter describes the present conditions of the selected example site Laxemar both regarding a general outline of the site, but also more specifically to describe the context from which parameter values have been selected to underpin the SE-SFL. The following initial state descriptions are based on results from the site investigations conducted at Laxemar during the period 2002 to 2007 with the objective of finding a potentially suitable site for the Spent Fuel Repository. Results from the site investigations were compiled in a site description for the Laxemar-Simpevarp area (SKB 2009) and the Laxemar area can be regarded as typical for areas situated along the Baltic coast in this part of southern Sweden.

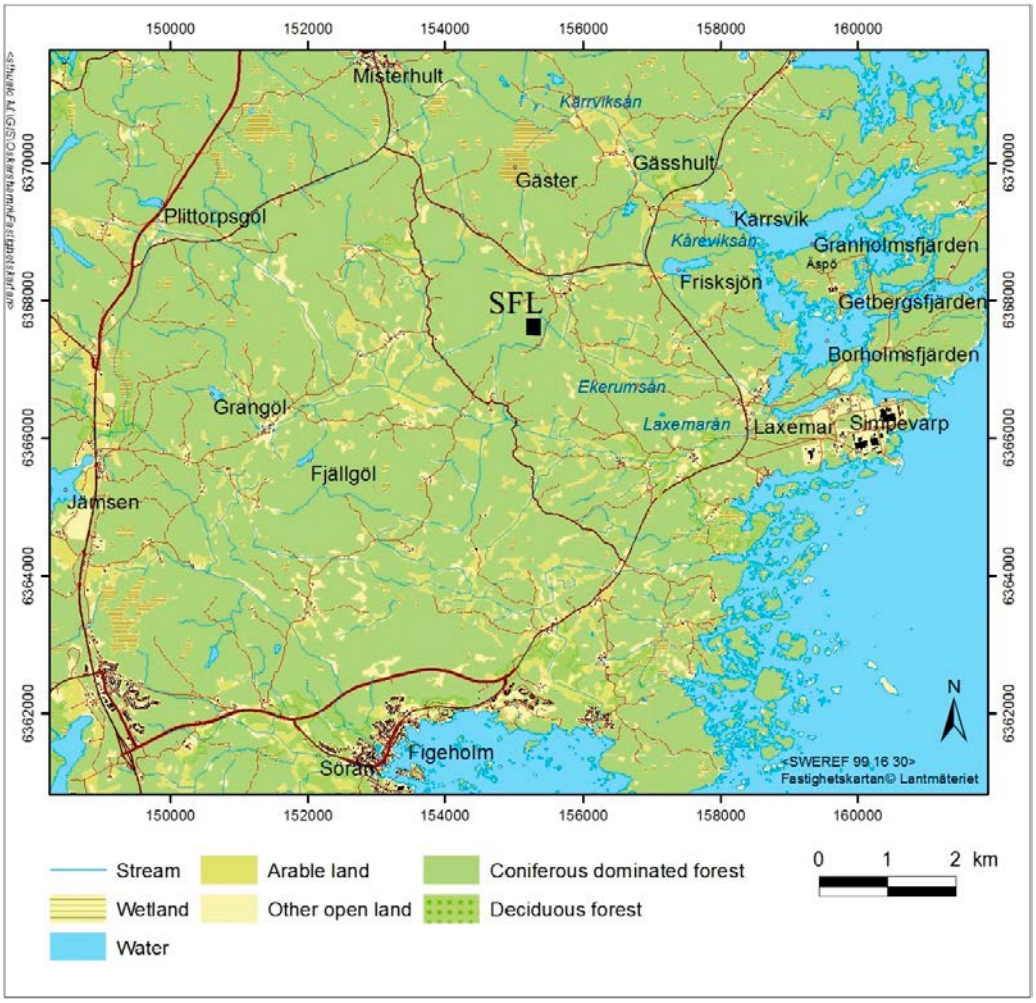

Figure 3-1. *The Laxemar area in the southeast of Sweden. This area corresponds to the regional model area that has been used for studies characterising this site. The example location for the SFL repository is indicated with a black square.*

3.2 Climate

Precipitation demonstrates a near-coastal gradient, with less precipitation at the coast compared with areas further inland. Based on long-term meteorological data from surrounding stations, the Swedish Meteorological and Hydrological Institute (SMHI) have estimated the 30-year (1961–1990) annual average precipitation to be 553 mm for the Äspö station (on the coast) and 630 mm for the Plittorp station (further inland). A more recent estimate of the mean annual precipitation in the Laxemar area has been estimated to be around 600 mm (Werner 2009).

The mean annual temperature in the Laxemar area is 6–7 °C. The mean temperature in January is –2 °C and mean temperature in July is 16–17 °C. Approximately 17 % of the accumulated precipitation during the period 9th September 2003 to 31st December 2007 fell in the form of snow, and based on biweekly measurements during this period a snow cover could be present between December/January and March/April (Werner 2009). During the 30-year period 1961–1990 the ground was covered by snow for on average about 75 days a year, with an average yearly maximum snow depth of 35–40 cm (Larsson-McCann et al. 2002).

For the three years 2005–2007, for which data are available from all discharge-gauging stations in the Laxemar area, the site-average specific discharge can be estimated to be ~165 mm y^{-1} (or ~ 5.2 L s^{-1} km^{-2}), which is within the interval of the regional long-term average for 40 to 45 years estimated by Larsson-McCann et al. (2002). During the same period (2005–2007), annual average precipitation was ~ 580 mm on Äspö and ~ 620 mm at Plittorp, whereas potential evapotranspiration was ~ 540 and 530 mm y^{-1}, respectively. Based on available site investigation data, the site-average water balance for the years 2005–2007 can thereby be estimated to be P = 600 mm y^{-1}, ET (actual evapotranspiration) = 435 mm y^{-1} and R (specific discharge) = 165 mm y^{-1} (Werner 2009).

3.3 Landscape, topography and regolith

The Laxemar area is part of the sub-Cambrian unconformity (peneplain) and is relatively flat with a gentle dip towards the east. The area is characterised by a relatively flat topography at low altitude, but with marked both short and longer valleys/topographical depressions (Figure 3-2). The most elevated areas are located at ~ 50 metres above the current sea level. The south-western and central parts of the Laxemar area are characterised by hummocky moraine and a smaller-scale topography (Sohlenius and Hedenström 2008). The whole area is located below the highest coastline associated with the latest glaciation, and the area has emerged from the Baltic Sea during the last 11 000 years. At the deglaciation around 12 000 BC, the central parts of the area were situated 50–100 m below the sea level, and the first islands emerged from the sea around 9 400 BC. The shoreline regression has subsequently prevailed and the rate of land uplift during the past 100 years has been ~ 1 mm $year^{-1}$. Sea bottoms are continuously transformed to new terrestrial areas or freshwater lakes, and lakes and wetlands will successively be covered by peat.

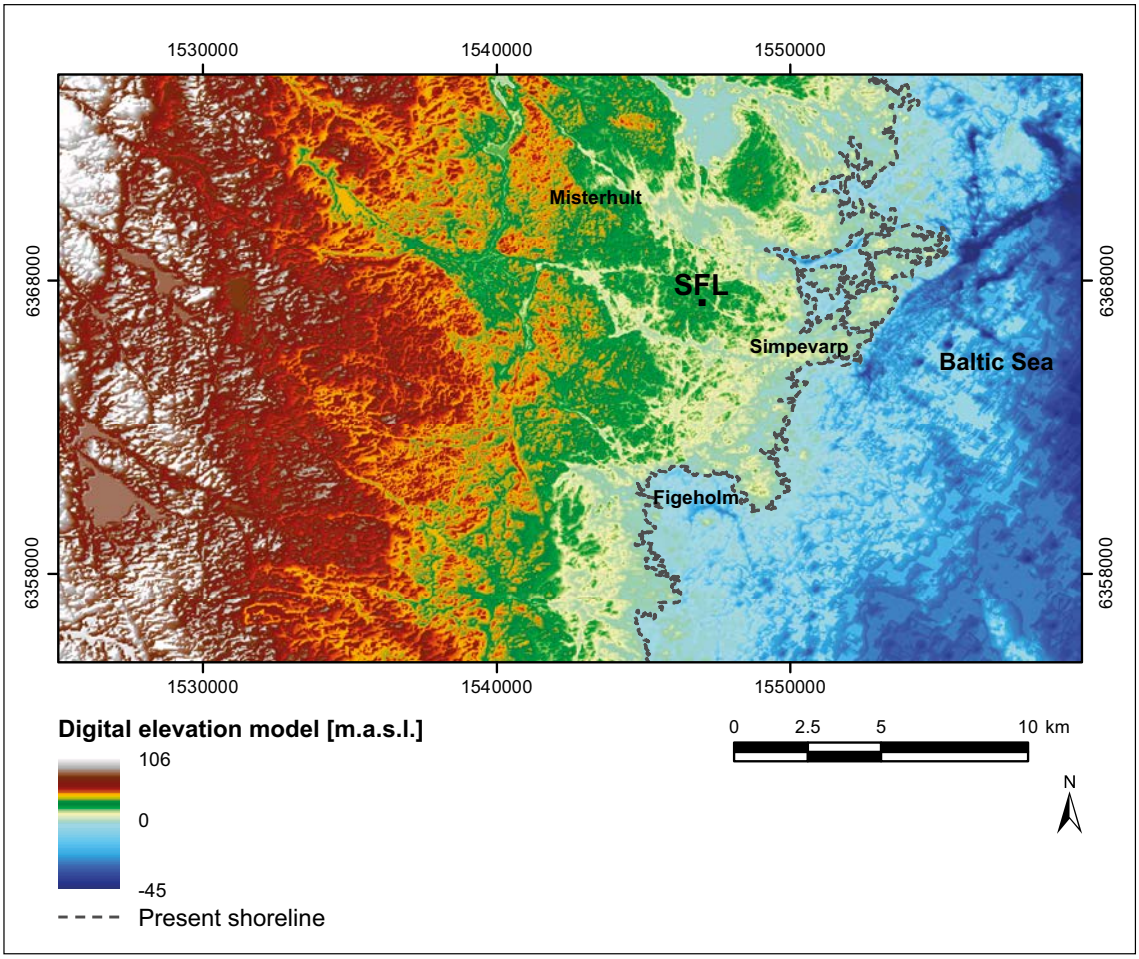

Figure 3-2. *DEM (Digital Elevation Model) of the Laxemar area, including the bathymetry of the lakes and the sea (Strömgren and Brydsten 2008). The DEM has a horizontal resolution of 20 m. The map shows the present shoreline and the example location for the SFL repository is indicated with a black square.*

3.3.1 Regolith

The predominantly thin regolith is mainly located in topographical depressions and valleys, whereas the high-altitude areas are dominated by exposed bedrock or thin layers of till and peat (Figure 3-3) (Sohlenius and Hedenström 2008). Glacial till is the most common Quaternary deposit and covers half of the terrestrial part of the regional model area. Sandy-gravelly till overlies the bedrock in the whole area, also in most areas with exposed/shallow rock (which may have a regolith depth of up to ~ 0.5 m) with the exception of some exposed/shallow rock areas where organic soil and a thin vegetation layer directly overlie the rock. In the valleys, the till is often overlain by glacial clay, which in turn is overlain by a thin layer of sand followed by clay gyttja and peat. The depth of the Quaternary deposits in the fissure valleys often exceeds 10 m. A Regolith Depth Model (RDM) visualises the stratigraphical distribution of the regolith in the Laxemar area (Figure 3-4) (Nyman et al. 2008). The model covers 280 km^2 including both terrestrial and marine areas. The stratigraphy is represented by six layers that correspond to different types of regolith (Figure 3-4).

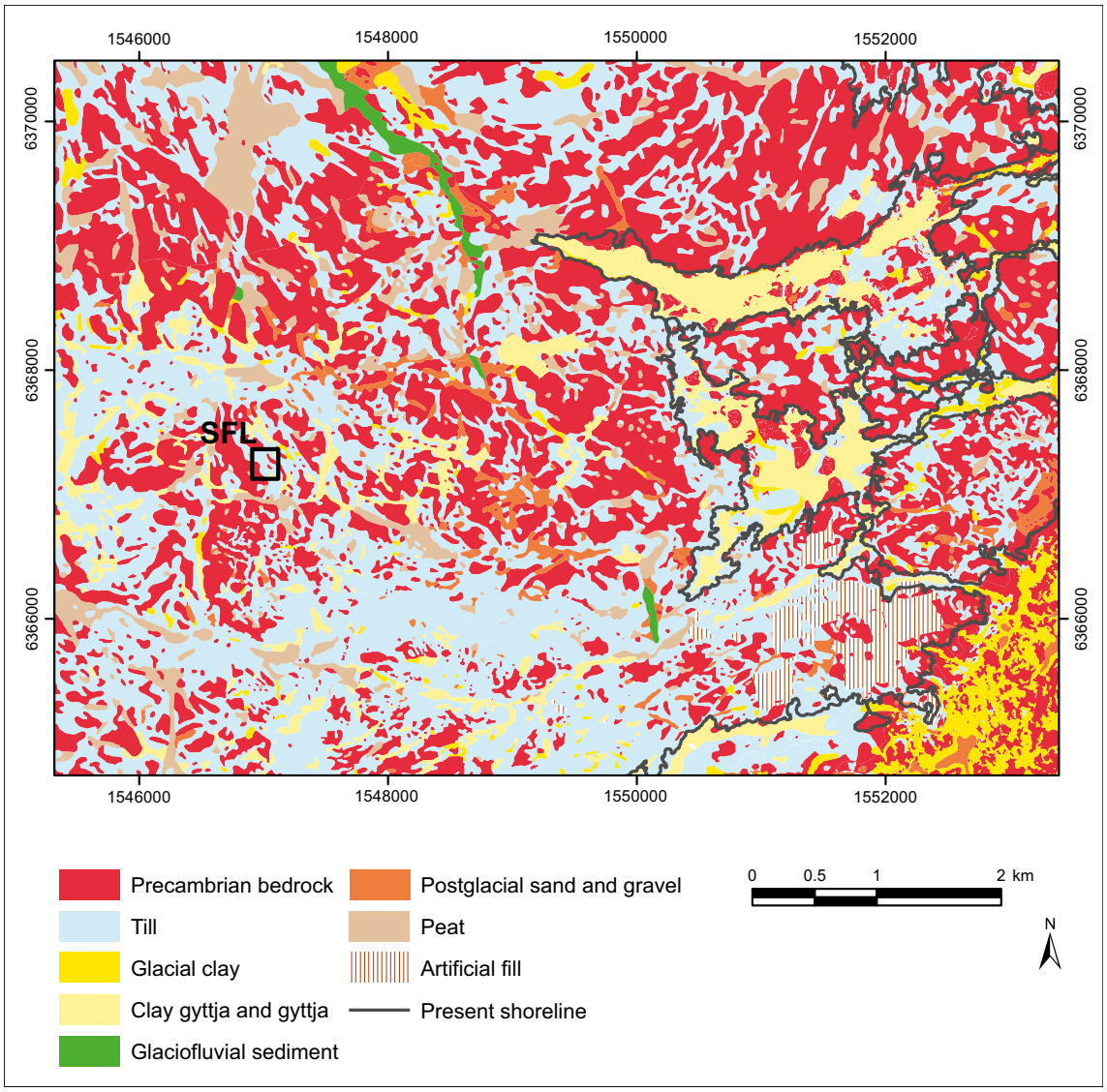

Figure 3-3. *Surface distribution (at a depth of 0.5 m) of regolith and areas with exposed bedrock in the Laxemar area. Note that lakes and the sea are shown without surface water and that the present shoreline is indicated in the map. The example location for the SFL repository is indicated with a square.*

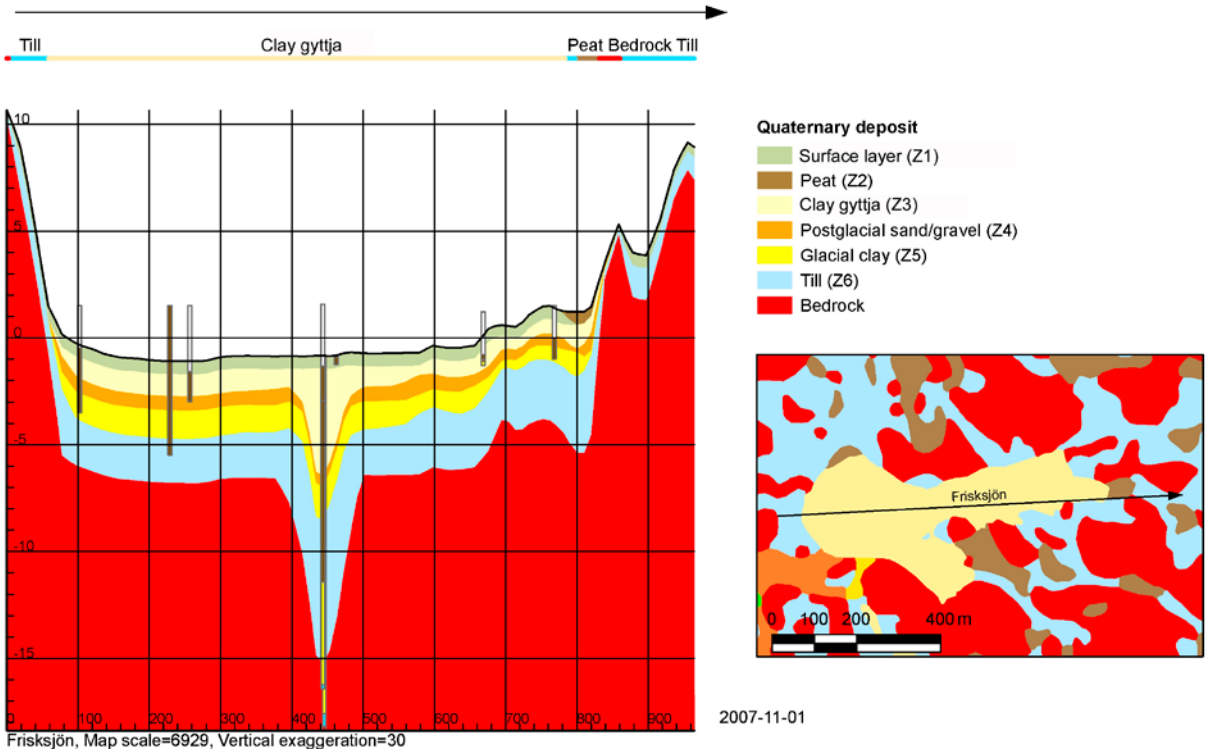

Figure 3-4. *The Regolith Depth Model (RDM) showing a vertical profile with stratigraphy and total regolith depth along a profile across Lake Frisksjön (see Figure 3-1 for location). The uppermost layer, Z1, is influenced by the impact from surface processes, e.g. roots and biological activity. The next layer (Z2) consists of peat. After that follows layer Z3, which is characterised by clay gyttja, followed by layer Z4 that consist of sand/gravel, glaciofluvial sediment or artificial fill. Layer Z5 correspond to glacial clay and the bottom layer Z6 correspond to till (figure from Nyman et al. 2008).*

3.3.2 Development during the Quaternary

The character of the current surface system is strongly influenced by the climate development during the Quaternary period. The climate during this period has been characterised by large and sometimes rapid changes in global temperature, and during which the Laxemar area was covered by an ice sheet at least three (but probably more) times. Preserved information older than the latest glacial phase is rare in Sweden in general, and consequently the duration and extent of early Quaternary glaciations is poorly known (See **Climate report** for further description). It is suggested that all known unconsolidated deposits in the Laxemar area were deposited either during the last phase of the latest glaciation or during and after the subsequent deglaciation (Söderbäck 2008, cf. Chapter 4 therein). However, the possible occurrence of older deposits cannot be excluded and there are indications of older deposits in adjacent areas outside the Laxemar area.

During the latest glaciation the ice sheet in the area moved from the north-west and deposited the glacial till. There are several glaciofluvial deposits, generally with a northerly strike, in the area. These deposits were formed when stones, gravel and sand were transported by the melt water within tunnels under the ice sheet. During continued retreat of the ice, glacial clay was deposited at the floor of the fissure valleys which are characteristic of the Laxemar area (Sohlenius and Hedenström 2008).

Relative sea-level change was fastest during the first few thousand years after the deglaciation and has subsequently decreased to the present rate of 1 mm year^{-1} (see also Figure 4-1). This continuous sea-level change has strongly influenced the development of the Baltic Sea. The interaction between isostatic recovery of the Earth's crust and eustatic sea-level variations has caused a varying depth of the straits connecting the Baltic Sea with the Atlantic Ocean by way of the North Sea, which in turn has caused varying salinity throughout the postglacial Holocene epoch. Between 4500 and 3000 BC, during the middle of the Littorina Sea stage, the salinity of the Baltic Basin offshore from Laxemar was almost twice that of today's Baltic.

The continuous shoreline regression since 6000 BC has also had a significant impact on the distribution and redeposition of fine-grained Quaternary deposits (Figures 3-3, 4-1). The most exposed areas have been subjected to wave washing and currents. Consequently, sand and gravel have been eroded from older deposits, and have been transported and redeposited at more sheltered locations. Periods of erosion have occurred also at sheltered locations, which have resulted in the erosion of fine-grained deposits such as glacial clay. In the coastal areas of Laxemar, clay gyttja has been deposited in the long and narrow valleys when these were shallow bays (Sohlenius and Hedenström 2008).

The relative sea-level transgression continuously transforms seafloors to new terrestrial areas or to freshwater lakes. Newly formed areas are successively, and also currently, exposed to erosion, whereas sheltered bays with conditions favourable for deposition of clay gyttja have formed in other areas. Lakes and wetlands are successively covered by fen peat, which at some locations is then covered by bog peat. Today's cultivated soils along the valleys in Laxemar have a high organic content. The regolith stratigraphy suggests that these areas have gone through both a sea bay phase and a lake phase, before developing into mires, which were then drained. Generally, remnants of peat are found in the cultivated soil, and below the drained soil there are thick layers of clay gyttja, typically with a high organic content (Sohlenius and Hedenström 2008).

3.4 Hydrology

The sandy-gravelly till that dominates in the area is characterised by a relatively high hydraulic conductivity (estimated to $\sim 4 \times 10^{-5}$ m s^{-1}). Furthermore, there are indications that the hydraulic conductivity of the quaternary deposits overlying the rock in the deepest parts of the large (i.e. wide and deep) valleys is about one order of magnitude higher than that of till in other parts of the area (Söderbäck and Lindborg 2009). Groundwater levels in the regolith are shallow; according to monitoring data, the average depth to the groundwater table is less than 1 m for at least half of the year. The depth to the groundwater table tends to be larger in high-elevation areas than in low-elevation areas, but this difference is small compared with the local spatial variation that follows the surface topography. This in turn implies that topography has a strong influence on near-surface patterns of groundwater recharge and discharge (Figure 4-4).

There are a few small and shallow lakes in the area. Average lake depths are in the range 1–4 m and maximum depths in the range 2–11 m. Wetlands cover in total ~ 3 % of the delineated catchment areas (Brunberg et al. 2004). Most streams in the area are influenced by land improvement and drainage operations. The flow in the streams shows strong seasonal variability, and in particular the smaller streams are dry during large parts of the year. Of the monitored streams, permanent waterflow occurs in the streams Laxemarån, Kåreviksån downstream from Lake Friskjön and Kärrviksån (Figure 3-1). The stream Ekerumsån is dry only during the summer, whereas the other monitored streams are dry for approximately half of the year. Except for some minor wetlands, the surface waters (lakes/ponds streams and wetlands) are located in low-altitude areas. These surface waters are mainly underlain by glacial and post-glacial sediments (see above).

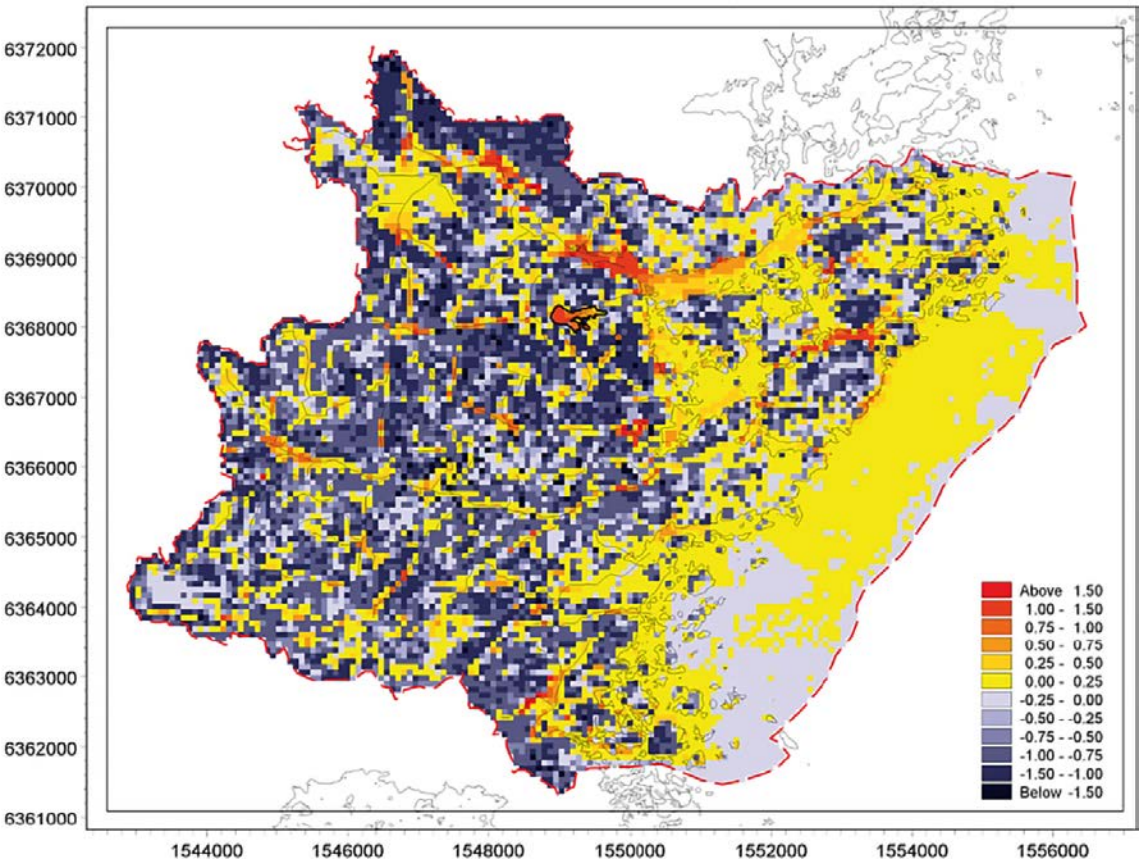

Figure 3-5. *Recharge and discharge areas in the Laxemar area. The colour indicates the mean hydraulic head differences between the two top layers, i.e. Positive values (yellow to red) indicate discharge conditions (i.e. upward flow of groundwater). Data from the year 2000 AD in the MIKE SHE model for SR-Site (Sassner et al. 2011).*

3.5 Hydrogeochemical characteristics of the surface system

Marine remnants in the Quaternary deposits influence the hydrochemistry at low elevation close to the coast, whereas higher-lying areas are mostly influenced by atmospheric deposition and weathering processes. The gradual isolation of former brackish bays has resulted in a succession from brackish water to freshwater, followed by formation of wetlands. In modern time, fertile soils such as wetlands have often been converted into agricultural land by ditching and drainage, further altering the hydrochemical conditions (Tröjbom et al. 2008). Chemical analyses of till samples indicate that the elemental composition of till from the area is relatively normal in a Swedish context (Tröjbom and Söderbäck 2006a).

Most fresh surface waters in the area are strongly coloured due to high concentrations of humic substances, leading to very high concentrations of dissolved organic carbon (DOC). The lakes are also relatively rich in nitrogen and phosphorus compared with the general conditions in Sweden. The total amount of dissolved ions measured as the electrical conductivity, is somewhat elevated compared with most Swedish lakes. The pH values of lakes and streams in the Laxemar area are close to neutral. A few streams show acid conditions and low alkalinity, indicating the presence of acidified waters with low buffering capacity. The shallow groundwater in the Laxemar area is characterised by neutral or slightly acid pH values, and, in a Swedish perspective, a typical content of major constituents and alkalinity. As mentioned, marine relicts influence groundwater at low elevation in the area, resulting in elevated concentrations of e.g. chloride and sulphate (Tröjbom and Söderbäck 2006a, Andersson 2010).

3.6 Ecosystems

The location of the Laxemar area close to the Baltic Sea means that the seashore is a characteristic feature in the east, together with coniferous forests, shallow lakes, various types of wetland with interlaced patches of agricultural land, the latter primarily concentrated in the valleys (Figure 3-1). Agricultural areas are primarily found along the valleys where fine-graded sediments such as glacial clay or clay gyttja are found. Typically, these areas have streams or ditches, which often are affected by human encroachments in order to drain the soils and enable cultivation. There are wetlands present in the landscape, but in many ways these have been affected by earlier draining activities.

3.6.1 Marine ecosystems

The marine area in Laxemar is separated from the open sea in the east by the large island of Öland, forming a funnel-like strait with its wide end to the north and the narrow end southwards. The sea bottom along the Laxemar coast slopes gradually downward in the offshore direction. The maximum depth recorded in the regional area is ~ 45 m and the range in mean depth among sea basins are between 0.1 m and 16 m (see below).

The sea floor in the Laxemar area can be divided into three marine subareas with distinct characteristics regarding ecosystem structuring factors, such as wave exposure, light penetration and substrate type. These subareas are; secluded bays (e.g. Borholmsfjärden and Granholmsfjärden), shallow exposed archipelago (in the southeast), and deep, exposed areas (the coast and the open sea in the eastern parts of the regional area) (Aquilonius 2010).

The local freshwater discharge to the Laxemar coastal area comes mainly from small streams entering the bays, and there is no larger river. The salinity in the outer, exposed parts of the regional model area is 6.8‰, which is similar to that in the Baltic Proper, whereas the salinity at sampling stations in the inner bays is lower (mean values between 5.5 and 6.3‰) and varies strongly over time due to the influence of freshwater input from land (Aquilonius 2010).

The offshore study area was divided into 19 sub-basins based on the current bathymetry and projected future drainage areas. For modelling purposes, the water exchange was estimated for each of the individual basins and presented as the Average Age of a water parcel (AvA). The average age varies from less than one day in the outer basins to 7–29 days in the sheltered inner bays.

The average light penetration depth (Secchi depth) in coastal water in the Laxemar area is 5.5 m, which is low compared with the value at the national monitoring station located further out in the Baltic Proper (8.7 m). However, the light penetration varies within the area, and the sheltered inner bays have Secchi depths of only 2–3 m. Nevertheless, large parts of the coastal area are shallow enough for light to reach the bottoms. Accordingly, the marine primary producers in the regional model area are dominated by benthic primary producers.

On soft bottoms situated within the photic zone, green algae, stonewort and yellow-green algae dominate. On hard substrates, i.e. till or bedrock, bladderwrack dominates in the shallow areas, whereas red algae dominate in the deeper areas. Three species dominate the benthic fauna, namely the bay mussel, the Baltic macoma and a small amphipod. Perch, roach and white bream have consistently dominated the catches in the inner bays of the area. In the more offshore areas, the marine cold-water species Baltic herring dominates the fish community. In the open sea, the zooplankton community is dominated by meso-zooplankton, especially copepods. However, in the summer a more diverse zooplankton community with cladocerans, rotifers and larvae of some benthic macroinvertebrates occurs. The littoral zone is highly diverse as a habitat and it is important for a large number of non-breeding waterfowl. However, the distribution of wintering waterfowl in the near-coastal zone and around islands, e.g. long-tailed duck (non-breeding), tufted duck, mute swan, Canada goose and herring gull, do not support the main concentrations of any waterfowl in the Baltic Sea during normal winters, but are found further out on the offshore banks.

The mean total biomass of producers and consumers (on an annual basis) varies between the different basins, from just below 35 gC m^{-2} to over 150 gC m^{-2}, with an average for the whole marine area of 91 gC m^{-2}. A comprehensive compilation of all data from the marine ecosystem in the Laxemar area is presented by Aquilonius (2010).

3.6.2 Limnic ecosystems

A larger area around Laxemar (referred to as the regional model area in SKB 2009) includes 26 catchments, 5 lakes and several streams. As mentioned above, the lakes are small with relatively shallow depths. The only lake situated near the analysed position for SFL is Lake Frisksjön (cf. Figure 3-1), which has a lake area of 0.13 km^2, a mean depth of 1.7 m and a maximum depth of 2.8 m. The lakes are characterised as mesotrophic brown-water, i.e. with moderate nutrient concentrations and with brown water colour. The water colour is caused by high inputs of organic matter from the surrounding catchments, and the concentration of organic carbon is very high in comparison with most Swedish lakes (Tröjbom and Söderbäck 2006a). Because of the brownish water, light penetration is poor, and the depth of the photic zone is generally small. As a result, macrophyte coverage is small and the biota is dominated by heterotrophic organisms, particularly bacteria. Perch is the dominant fish species, in numbers as well as in mass, and other common species are roach, bream and pike (Andersson 2010). Most lakes in the area are affected by human activities. The naming of some wetlands and minor fields indicates that several previous lakes have disappeared during the last few centuries due to draining for arable land.

Most of the streams in the Laxemar area are small with mostly calm or slowly flowing water, and as said before there are only three streams in the area with permanent waterflow throughout the year. As with the lakes, the streams are characterised as mesotrophic brown-water systems. In the largest stream, Laxemarån (Figure 3-1), five fish species have been noted: ide, roach, burbot, pike and ruffe, and there are indications that the stream is an important spawning site for both ide and roach. The streams are to a great extent influenced by human activities, which have altered their channels by various technical encroachments. A comprehensive compilation of data from the limnic ecosystems in the Laxemar area is presented in Andersson (2010).

3.6.3 Terrestrial ecosystems

The terrestrial vegetation in the area is strongly influenced by the characteristics of the regolith and by human land use. Below follows a brief description of three major vegetation types (forest, wetlands, and arable land) and the fauna within the investigation area. A comprehensive compilation of data from terrestrial ecosystems in the Laxemar area is presented in Löfgren (2010).

Forests cover approximately 73 % of the land area of the main catchments around Laxemar. These forests are dominated by Scots pine and Norway spruce. Scots pine dominates on bedrock and in areas with a shallow soil layer, whereas Norway spruce becomes more abundant in areas with a deeper soil cover in combination with mesic-moist conditions. Deciduous tree species, mainly pedunculate oak, but also hazel, rowan, Swedish whitebeam and Norway maple, are more common near the coast, making the mixed forest the second most common forest type.

The predominant humus form in the Scots pine and Norway spruce forests is moder-humus, and the predominant soil type is regosol. In areas where there is a deeper soil cover, podzols become more common. The occurrence of mull-like humus increases with the occurrence of deciduous trees (Lundin et al. 2005), and in this type of forest, the soil types regosol and umbrisol are found.

Wetlands are less frequent and cover today only a few percent of the area in the main catchments. The wetlands consist of both coniferous/deciduous forest swamps and open mires. Although not numerous, bogs are also present in the inland. In the northern part of the area where bedrock outcrops are common, small peat-accumulating, nutrient-poor wetlands are found in the depressions. Other important, but less common wetland types are the freshwater shores (wet meadows or marshes) and riparian wetlands along streams. The latter are inundated by water at least once a year and affected by overbank sedimentation.

Agricultural land (arable land and grasslands) covers 8.5 % of the land area of the main catchments and is mainly located along the valleys. Only 21 % of the arable area is used for grain production, which provides food for humans directly. The rest of the area is used for fodder and silage production for animals (Löfgren 2010). The average production of barley, including threshing loss and straw yield, was 190 gC m^{-2} $year^{-1}$ during the period 2000–2007.

The fauna of large mammals is dominated by roe deer, mountain hare, European hare and moose. Chaffinch, willow warbler and robin are the most common birds in the area. This composition of common mammalian and bird species is representative of a large part of southern Sweden. One top predator that is quite common in the area is the white-tailed eagle.

3.7 Wells and water-resources management

Morosini and Hultgren (2003) described more than 200 private wells in the area. Two thirds of the wells were shallow (~ 3 m) dug wells with a short distance to the groundwater (~ 1.5 m). The rest of the wells were drilled to considerable depth (~ 45 m) in areas with a greater depth to the groundwater level (~ 4.5 m). Shallow ditches constructed for drainage purposes are common in the forests, and the lake outlet from Lake Frisksjön has previously been changed and lowered in order to lower the level of the lake to gain more arable land. As described above, there are also many examples of drainage ditches in areas used for agriculture.

3.8 Human population and land use in a historic perspective

With archaeological methods, it is possible to identify traces of some 300–400 generations that have lived in the Laxemar area since the last deglaciation. There is a rich occurrence of prehistoric remains in the region, some of them indicating that the area was already exploited during the Early Stone Age (9000–4000 BC). Following the arrival of the first humans to the region, it has been characterised by its forest- and archipelago settlements. The main occupation since the colonisation of the area has been a combination of agriculture, forestry and fishing activities (Lundqvist 2006).

The settlement structure in the region during the medieval period (1100–1550 AD) was characterised by single farms, in contrast to, for example, Forsmark, where settlements were organised in small villages. The farms were later subdivided into several smaller farms when the population increased. Following a nationwide decline in the population during the middle of the medieval period, there was a strong population expansion. The strong population growth continued until the late 19th century, as did the areal extent of arable land, and even more so of meadows. Much of the new agricultural land was gained by the ditching of wetlands. At the turn of the century. The increase ceased and during the latter part of the 20th century the rural population, and people involved in agriculture, decreased. Agriculture still exists in the area, but most pastures have been abandoned, and some cultivated areas have been turned into woodlands.

The forests in the region have been used for many different purposes; pastures, firewood, fencing material, subsistence needs, slash-and-burn cultivation (Soininen 1959), as well as for production of charcoal, tar and potash. In addition to sawmill activities, production of charcoal, tar and potash, were in many cases an important part of the economy of the individual household. Trading in timber was advantageous at coastal locations since the timber was easily transported with rivers to coastal areas.

The present-day population density within the Laxemar area (7.4 inhabitants km^{-2}) is about one third of the average population density of the County of Kalmar (to which the area belongs) and less than half the population density of Sweden on average. One out of five properties in the region is a vacation house. The land use is dominated by forestry, and moose hunting is popular in the Misterhult parish. Besides hunting, the area is as well used for leisure activities such as hiking, canoeing, fishing and boating (Ottosson 2006).

4 Site development – future conditions and ecosystems

4.1 Introduction

This chapter gives an overview of the projected future development of the Laxemar site. Together with the description of present-day conditions presented in the previous chapter this information was used to describe how external conditions will affect site properties. The information was used to constrain the potential external conditions in a future landscape, to underpin the formulation of different evaluation cases (Chapter 7) and to parameterise these evaluation cases.

The long-term development of the Laxemar area is dependent on two main and partly interdependent factors: climate and relative sea-level change. These two factors in combination strongly affect various processes, which in turn determine the development of ecosystems and future conditions of importance for radionuclide transport, exposure and resulting doses and risks. Examples of such processes are fluvial erosion and sedimentation, groundwater recharge and discharge, soil formation, primary production, and decomposition of organic matter.

4.2 Climate and climate-related processes

In SE-SFL there are three reference external conditions or climate cases, present-day conditions, *increased greenhouse effect* and *Glaciation* (Chapter 2 in the **Main report**). Present-day external conditions are described in the previous chapter and the other two external conditions are described in detail in the **Climate report** and are briefly outlined below.

The *Increased greenhouse effect* and the *Glaciation* climate cases were defined based on the last (Weichselian) glacial cycle and future projections of anthropogenic climate change. The climate cases are highly simplified as compared with the ones used in full safety assessments such as SR-Site (SKB 2010c, 2011a) and SR-PSU (SKB 2014e). The strategy for selection and description of climate cases in SE-SFL was to identify and describe the range within which climate and climate-related processes may vary over these long timescales. However, since SE-SFL constitutes a first evaluation of post-closure safety for a proposed repository concept, located at an example site, the future climate developments chosen are intentionally simplified and limited in number as compared with the ones presented and used in a full safety assessment (e.g. SR-Site). This also means that the stylised climate development is representative for Sweden in general.

The climate cases were designed to cover the warmer and colder ends of possible future climate developments, respectively, but for simplicity they were characterised by the same reconstruction of the relative sea-level change. The three climate cases were put together using different climate domains representing characteristic climate-related conditions of importance for repository safety. Three relevant climate domains have previously been identified for Swedish Baltic Sea coastal sites SKB (2010c):

- The temperate climate domain (today).
- The periglacial climate domain.
- The glacial climate domain (site covered by an ice sheet or glacier).

Reconstructed changes in the relative sea-level at the Laxemar site are discussed in Section 4.2.1, and the simplified climate cases are reviewed in more detail in Sections 4.2.2 and 4.2.3.

4.2.1 Relative sea-level development

Relative sea-level is the net result of isostatic changes (vertical crustal movements, at present typically dominated by post-glacial uplift in Fennoscandia) and eustatic changes (global and regional sea-level changes) (Section 3.2, **Climate report**). To analyse and illustrate the development of the landscape after the last deglaciation in the Laxemar area, the time frame for development from a marine stage to a mire stage covers the period from 10 000 BC to 20 000 AD. In SE-SFL, the relative sea-level was modelled over this period using SKB's relative sea-level equations with site-specific parameters for Oskarshamn (Figure 4-1). This curve is used to describe water depths in the sea stage and when relevant areas emerge from sea. To facilitate the mathematical handling of the curve in the modelling of historical and future landscape development, it was decided to use a simplified curve excluding the historic Ancylus transgression (Figure 4-1). The Ancylus transgression influenced the Laxemar area only very early in the landscape development, during a period that did not affect the analysed location of SFL, justifying the assumption of not implementing it in the simplified SE-SFL calculations.

4.2.2 Increased greenhouse effect climate case

The *increased greenhouse effect climate case* assumed temperate climate conditions for the complete evaluation period of one million years, with a considerably warmer climate than at present during the first 23 000 years of the period (Figure 4-2). This climate case covers the uncertainty associated with the projected climate change due to human activities (see e.g. SKB 2010c, 2015a and references therein) and it facilitates evaluation of the importance of potential effects of warmer temperate condition for post-closure safety.

The increases in temperature and precipitation that occur as a result of the increased greenhouse effect were implemented as a simplified step-function (Figure 4-2). The conditions during the warmer period are chosen based on climate projections for 2100 AD for the intermediate emission scenario RCP4.5 (Meinshausen et al. 2011). Thus, from repository closure (2075 AD) to 25 075 AD, the annual near-surface air temperature and precipitation were assumed to be 2.6 °C and 12 % higher than at the present-day, respectively (Table 4-1 and Figure 4-2). After 25 075 AD, and for the remaining part of the analysis period of one million years, present-day temperate climate conditions are assumed.

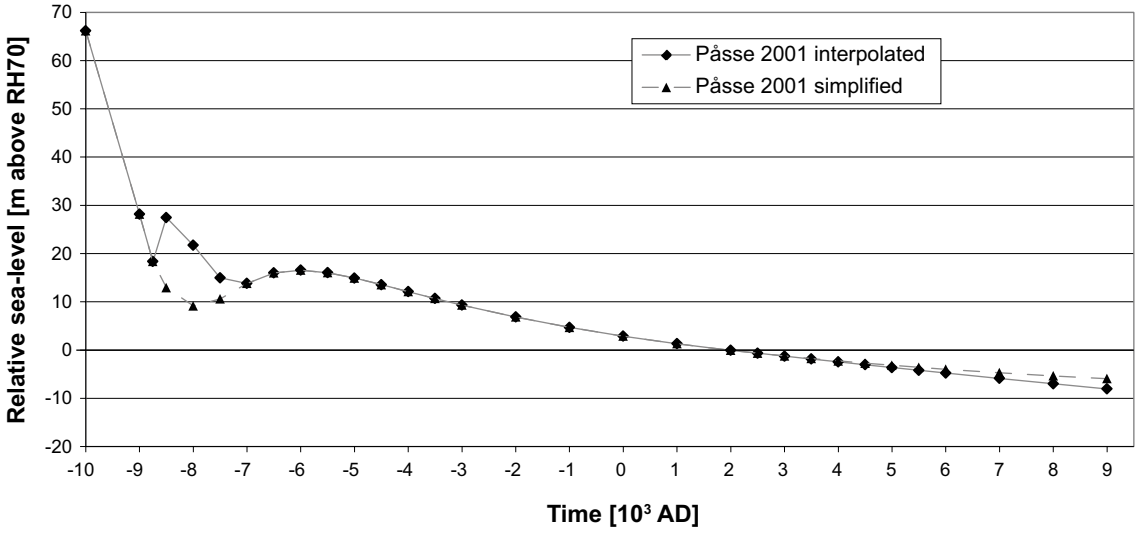

Figure 4-1. *Relative sea-level development at Laxemar during the Holocene, based on Påsse (2001). The solid line ("Påsse 2001 interpolated") includes the Ancylus transgression at around 8000 BC and also an adaptation (lowering of the last part of the curve) to data from Glacial Isostatic Adjustment (GIA) modelling used further into the future (see Climate report). The dashed line ("Påsse 2001 simplified") describes a simplified sea-level development used for the description of the development of the landscape (excluding the Ancylus transgression and the interpolation with GIA data).*

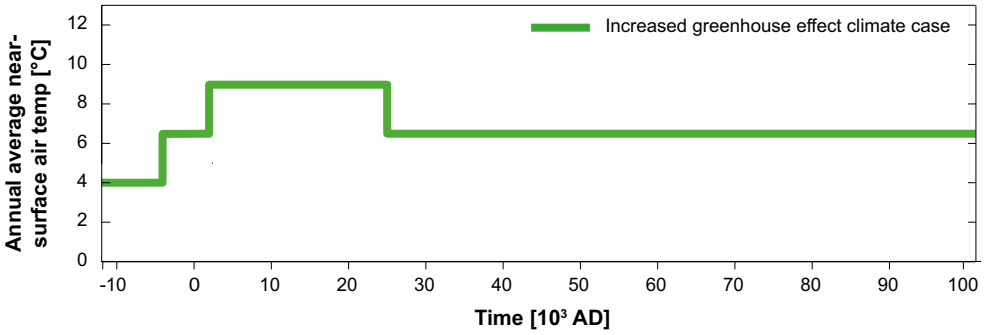

Figure 4-2. *Development of annual average air temperature from the last deglaciation and for the first 100 000 years after repository closure in the increased greenhouse effect climate case of the SE-SFL (from the* ***Climate report****).*

Table 4-1. Timing and duration of climate domains and the associated air temperatures at the Laxemar example site, from the last deglaciation and for first 100 000 years after repository closure of the SE-SFL in the *increased greenhouse effect climate case*. See also Figure 4-2. For a description of the estimates of the increase in air temperature after repository closure, see SKB (2014e). For the initial period dominated by anthropogenic warming, the estimated temperature increase has been added to the present-day Laxemar near surface air temperature (+6.4 °C; see Climate report). The submerged period is given both for the area above the repository and for the lower-lying landscape (the latter within brackets), see the text.

Time AD (years)	Climate domain	Annual near-surface air temperature (°C)	Source of temperature information
−12 000 to −8 800 (−12 000 to −4 100)	Submerged	+4	Estimated water temperature
−8 800 to 2 075 (−4 100 to 2 075)	Temperate	+6.4	Present-day near-surface air temperature Laxemar
2 075 to 25 075	Temperate	+9.0	Estimate of increase in air temperature (see SKB 2014e) added to the present-day Laxemar air temperature
25 075 to 102 000	Temperate	+6.4	Present-day near-surface air temperature Laxemar

4.2.3 Glaciation climate case

The *glaciation climate case* assumes that an early period of periglacial climate domain, with permafrost at the site, occurs ~ 17 000 years after repository closure. A second period of periglacial conditions starts ~ 50 000 years after repository closure and is followed by a period with the glacial climate domain, with an ice sheet covering the repository site (Table 4-2). The *glaciation climate case* covers the colder end of the range within which future climate may vary, and it facilitates evaluation of the importance of potential effects of periglacial, glacial, and submerged conditions, and the transitions between these states, for post-closure safety.

In the *glaciation climate case*, the changes in annual mean temperature are implemented as a simplified step-function (Figure 4-3). The simplistic stepwise climate description matches the simplistic assumptions regarding near-surface air temperature and precipitation that are made in the calculations of landscape development (see Section 4.3). In the evaluation of post-closure safety, the development from 2000 AD to 102 000 AD in the *glaciation climate case* is repeated every 100 000 years until one million years after repository closure to represent the effects of repeated Late Quaternary glacial-interglacial cycles.

Table 4-2. Timing and duration of periods with different climate domains, as well as air temperatures, from the last deglaciation and for the first 100 000 years after repository closure of the *glaciation climate case*. The time for the submerged period is given for the area receiving groundwater discharge from the repository.

Time AD (years)	Climate domain	Annual air temperature[1] (°C)	Source of temperature information
2000 to 17 500	Temperate	+6.4	Present-day near-surface air temperature Laxemar
17 500 to 20 500	Periglacial	–1	From Early periglacial climate case SR-PSU Forsmark
20 500 to 52 000	Temperate	+6.4	Present-day near-surface air temperature Laxemar
52 000 to 57 000	Periglacial	–4	Simplified from early periglacial climate case SR-PSU Forsmark
57 000 to 70 000	Glacial (cold-based conditions during the first 100 years, then warm-based until deglaciation)	–1	Approximate basal ice temperature (pressure melting point temperature based on an approximate 1 700 m average ice thickness over Laxemar)
70 000 to 78 700	Submerged	+4	Reference glacial cycle SR-Site Forsmark
78 700 to 102 000	Temperate	+6.4	Present-day near-surface air temperature Laxemar

[1] Near-surface air temperature during temperate conditions, water temperature during submerged conditions and basal ice temperature during glacial conditions.

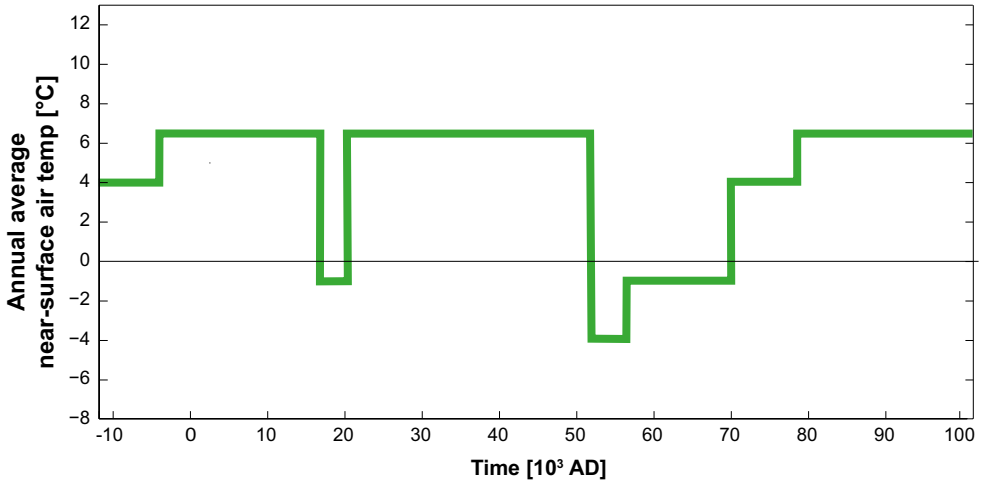

Figure 4-3. *Development of annual average air temperature from the last deglaciation and for the first 100 000 years after repository closure of the SE-SFL glaciation climate case (from the* ***Climate report****).*

4.3 Landscape development

At the end of the last deglaciation the Laxemar area was deglaciated around 12 000 BC (Chapter 3 in Söderbäck 2008). Thereafter, the isostatic rebound has been continuous and slowly declining in rate. The rate of rebound in Laxemar has decreased to a present rate of ~ 0.15 m (100 years)$^{-1}$, and it is predicted to decrease further. The present regressive relative sea-level development will continuously bring new areas of the sea floor above the wave base. This will expose sediments to wave erosion, and resuspended fine-grained particles will be transported out of the area into the Bothnian Sea or re-settle on deeper bottoms within the study area (Brydsten and Strömgren 2010, 2013). Accordingly, the relocation of sediments may have implications for transport and accumulation of radionuclides potentially originating from a future repository. The relative sea-level change will cause a continuing and predictable change in the abiotic environment, e.g. in water depth, soil profile, nutrient availability, but there are large uncertainties concerning the effect of greenhouse-induced warming on global and regional sea levels (eustatic change, see above Section 4.2.1). The location of the SE-SFL repository is, however, located at an average elevation of 21.5 m and is not expected to be affected by a potential negative shoreline migration during an increased greenhouse effect climate case (Section 4.2.2 and **Climate report**).

According to results from previous hydrogeological modelling of the Laxemar and Forsmark sites (e.g. Sassner et al. 2011 for Laxemar and Odén et al. 2014 for Forsmark), discharge of deep groundwater will almost exclusively take place at low points in the landscape, i.e. in lakes, wetlands, and streams, and in near-shore areas of the sea (see also Figure 5-1). Thus, the present description of landscape development is focused on these areas, as this is where accumulation of potentially released radionuclides may occur. To be able to evaluate the importance of landscape development on post-closure safety, the origin and succession of major ecosystems (at locations identified as potential discharge areas for deep groundwater, see Chapter 5) are described in relation to the development of the relative sea-level.

As the sea gets shallower, near-coastal erosion will occur on wave-exposed bottoms. Some sheltered areas inside a developing, denser archipelago will show accumulation for a short period (Brydsten 2009). Agriculture in the Laxemar area is typically concentrated along valleys with fine sediments, and on top of these fine sediments traces of peat are often found (Figure 3-3) (Sohlenius and Hedenström 2008). This pattern is the result of the isolation of a sea bay into a lake and its development into a wetland (Figure 4-4). Both the sea bay and the lake accumulate sediment and organic matter due to sedimentation and vegetation growth, and eventually most lakes are transformed to wetlands, except those of a considerable depth and size (not applicable to the Laxemar area) or those used as water reservoirs. The terrestrialised areas have during the last centuries often been ditched and transformed into agricultural land.

The future emerging land will follow the same pattern in terms of sediment deposition and the two large narrow sea basins surrounding the island Äspö today will gradually be transformed into large lakes. Due to their difference in depth it will happen around 2500 AD and 5100 AD, respectively (Chapter 5). Newly isolated lakes will occasionally be affected by flooding with brackish water from the Baltic Sea during periods of high sea level, in the same way as can be seen in low-elevation present-day lakes in other areas (e.g. Forsmark, Johansson 2008). The frequency of such events will decrease with time and will cease once the lake threshold has emerged above the reach of high sea levels. The rate of sedimentation in lakes is dependent on lake volume (Brydsten 2004), whereas the colonisation by littoral plants requires shallow water (< 2 metres). Thus, the rate of lake infilling is mainly dependent on lake depth and lake area (Brydsten and Strömgren 2010, Grolander and Jaeschke 2019). The only lake present in the vicinity of the analysed example site for SFL is the small and shallow Lake Frisksjön, and this lake is likely to be fully transformed into a wetland within 8000 years (Grolander and Jaeschke 2019).

Human land-use is a factor that could have a large impact on landscape development. Apart from ditching and cultivation of food and fodder crops, forestry and livestock grazing may have large consequences for the future vegetation distribution in Laxemar (Figure 4-4, Löfgren 2010).

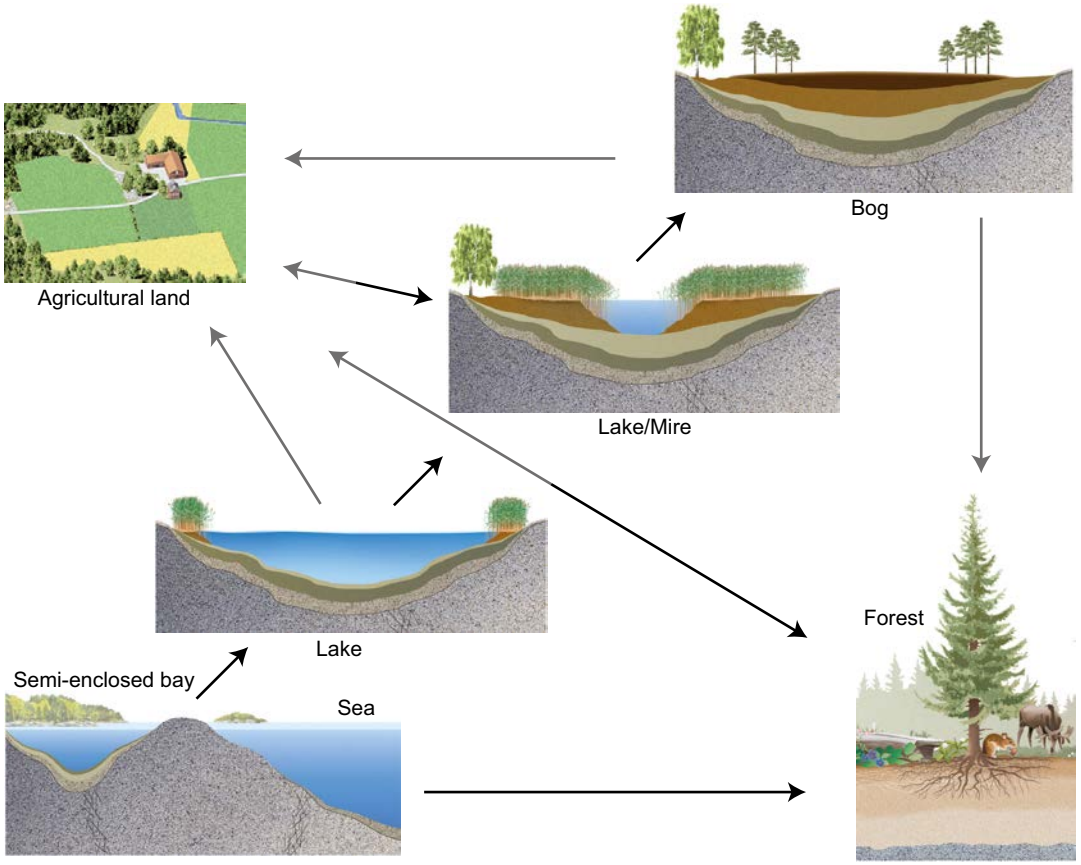

Figure 4-4. *A schematic illustration of the major ecosystems that may be found at certain points during a temporal sequence, in which the original sea bottom slowly becomes land due to relative sea-level decrease. Black arrows indicate natural succession, whereas grey arrows indicate human-induced changes to provide new agricultural land or improved forestry. Agricultural land may be abandoned and will then develop into forest or, if the hydrological conditions are suitable, into a fen. A forest may be "slashed and burned" and used as agricultural land.*

The potential for sustainable human exploitation of food resources in the area over the next few thousand years is not expected to differ much from the situation today. Similarly, the potential water supply for humans is expected to be roughly unaltered during this period. The present stream stretches are likely to extend themselves as relative sea-level falls (see Chapter 3 in Grolander and Jaeschke 2019). The deep lakes developing around Äspö will have the potential to be used as freshwater reservoirs when the salinity decreases in the future. Wells may be dug in the regolith in the area which is land today, but construction of wells and cultivation of new land is unlikely to occur before the land has emerged at least 1 m above sea level, making salt water intrusions at high sea level unlikely (see Chapter 5 in SKB 2014d).

The description above, which involves relative sea-level change and succession resulting in new land areas outside the present shoreline, is considered directly applicable in some of the SE-SFL evaluation cases (see *Alternative discharge area evaluation case* in Section 7.3).

4.4 Hydrological development

Hydrological processes play a substantial role in the development of surface systems, primarily by regulating the availability of water for biomass production, by regulating the rate of decomposition and by the role of water as a medium for transport of dissolved substances and particles. Based on the hydrological modelling performed within the framework of SDM-Site Laxemar, conceptual and numerical hydrological models describing the present and future hydrology in Laxemar were

developed and presented in Sassner et al. (2011). MIKE SHE water flow models were created for describing the hydrological conditions at 2000 AD, 5000 AD and 10 000 AD under temperate climate conditions.

The main difference between the external conditions at the three time points was the location of the coastline, which affects the distance to the sea and determines the proportions of land and water within the model area. The same soil depth model and meteorological data for a one-year period (measured between August 2004 and July 2005 in Laxemar) were used as input data in all simulations. This selected year had an accumulated precipitation of 550 mm, which is close to the annual average for the reference normal period (1961–1990) and is also close to the locally measured annual average for the period 2003–2007 (Sassner et al. 2011, Werner et al. 2008).

According to the MIKE SHE modelling, the overall water balance does not change dramatically due to landscape development. A comparison between the water balances extracted from the three different models shows that the variation in the overall water balance is small. The total runoff and the total evapotranspiration remain almost the same; the changes are within 10 % regardless of the time or the land area studied. The depth to the groundwater table is also similar in the three models. For the 2000 AD model, the median represents a depth to the groundwater table of approximately 2.5 metres below ground, whereas for the 5000 AD and 10 000 AD models the median corresponds to a depth of ~ 2.7 metres (Figure 4-5). Thus, the main changes occur when going from 2000 AD to 5000 AD because during this time the change in relative sea-level is larger than during the period 5000 AD to 10 000 AD. The results are consistent with studies from the Forsmark site, showing that the overall water balance is in principle unchanged if the climate is unchanged in a changing landscape (Bosson et al. 2012).

The variations of intra-annual hydrological conditions were analysed in the 2000 AD model and it was concluded that the depth to the groundwater table is highly dependent on the meteorological situation. During periods of wet weather conditions, the mean groundwater table is located at a depth of approximately 1 m below ground, whereas under dry weather conditions the mean depth is at ~ 3.5 m below ground.

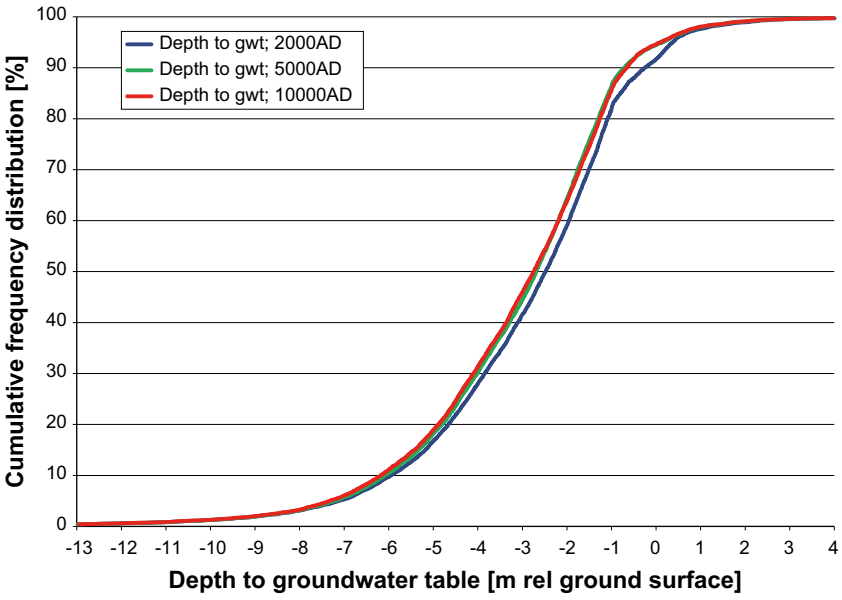

Figure 4-5. *Cumulative frequency of the depth to the groundwater table for the models at 2000 AD, 5000 AD, and 10 000 AD. The curves are based on the annual mean values for the area constituting land at 2000 AD (from Sassner et al. 2011).*

As illustrated in Figure 4-6, the hydrology of periglacial environments is influenced by ice, snow and frozen ground. In particular, frozen ground in the form of permafrost is a typical feature of periglacial systems that controls the distribution and routing of water across the landscape. In an unfrozen landscape, the topographical gradient together with the physical properties of soil and bedrock influence the interactions between surface water and deep and shallow groundwaters. In a permafrost landscape, the topographical influence on the hydraulic gradient of the deep sub-permafrost groundwater is dampened due to low hydraulic permeability of the frozen ground. Two hydrological systems can be defined in permafrost environments; one in the active layer above the permafrost that thaws and freezes seasonally, and one in the continuously unfrozen system below the permafrost. The two systems may be connected via through taliks. Taliks are unfrozen areas, often occurring under lakes or rivers in the permafrost region (see Hartikainen et al. 2010). Through taliks, which are unfrozen throughout the entire permafrost layer, are the only spots in the periglacial landscape where radionuclides from the repository can be transported up to the biosphere (see Figure 4-6). Given that lakes and streams often are locations for human settlement and land use, through taliks can potentially be locations where humans are exposed to radionuclides during periods of periglacial conditions. However, the generally low productivity in the permafrost region (see Section 4.7.3) requires utilisation of a larger area to supply the resources needed by even a small community, which means that radionuclide discharge through a talik may affect a comparatively small part of the food consumed by humans living in the talik area.

For the Laxemar site, no simulations with periglacial climate and permafrost were performed. Results from site investigations and modelling studies of the Two Boat Lake site in western Greenland, and modelling studies of the Forsmark site, indicate that the runoff generation during periglacial conditions is controlled by temperature rather than saturation (Johansson 2016). A large part of the snowmelt occurs when the active layer is still frozen, hence preventing infiltration. Moreover, once the active layer is thawed it is quickly saturated, which promotes ground-surface storage, ponding and surface-water runoff. Permafrost also delays groundwater discharge to streams, because the active layer must thaw before near-surface groundwater flow is initiated. Johansson (2016) showed that altitude differences between taliks controls recharge and discharge through those taliks and hence the exchange of deep and shallow groundwater. Permafrost may change the general direction of groundwater flow relative to unfrozen conditions, implying that discharge areas under temperate climate conditions may turn into recharge areas for groundwater under periglacial conditions. However, results from numerical simulations as well as data analysis from the Two Boat Lake site in Greenland indicate that although groundwater flows in and through taliks do exist, they are small compared with other water balance components, such as precipitation, evapotranspiration and runoff (Johansson 2016).

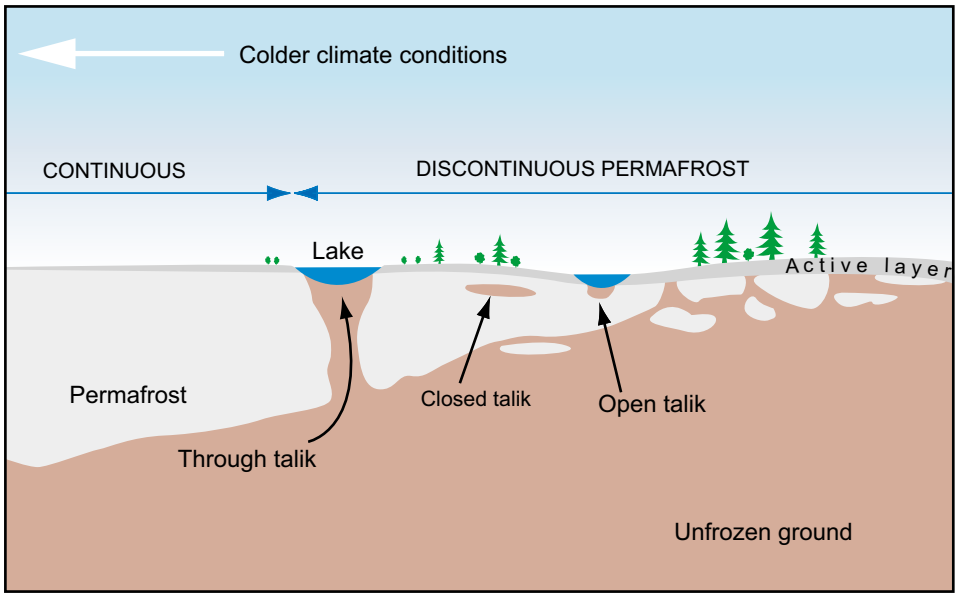

Figure 4-6. *A schematic profile through a permafrost area with an active layer and different types of taliks (Bosson et al. 2010).*

4.5 Hydrogeochemical development

The hydrogeochemical conditions observed in the Laxemar area today are a consequence of past landscape development, past and present land use, and anthropogenic inputs. The ongoing shoreline migration creates a spatial gradient from coast to inland, representing a time span from 0 to 12 000 years since the withdrawal of the sea, with the highest areas emerging earliest and areas at the present coastline emerging very recently (Figure 4-1). The present conditions in the Laxemar area can therefore be translated into a succession of future chemical conditions.

Several factors will influence the future development of the chemical environment of the Laxemar landscape. External abiotic factors, such as land uplift, climate and atmospheric deposition, set the overall limits, whereas internal factors, such as primary production and land use, may have a profound influence via feedback mechanisms. In the long term, the chemical environment characterised by parameters such as pH, major ions and organic content, determines speciation and transport properties of naturally occurring trace elements and radionuclides potentially originating from nuclear waste.

The future chemical conditions in Laxemar will, to a large extent, resemble present conditions. Due to the ongoing shoreline migration, marine influences will characterise surface water and shallow groundwater in the newly formed land areas, but these influences will diminish in gradually higher located areas. Concentrations of nutrients, major ions and organic matter will probably stay relatively constant compared with present conditions in the future, presumably mesotrophic brown-water, lake and stream systems, which implies that speciation and transport properties for radionuclides will remain relatively unchanged.

4.6 Marine ecosystems

4.6.1 Development under temperate conditions

The future temperate marine ecosystems at Laxemar are assumed be similar to those existing at present (Aquilonius 2010). The major change will occur when deeper offshore areas, as a result of the uplift of the sea-floor, shift from being dominated by pelagic primary producers to benthic primary producers. The primary production in these shifting habitats will most probably be of similar magnitude to that in today's shallow coastal areas. At present, the whole marine area is net autotrophic, due to the high primary production in the shallow areas, and it is likely that the marine ecosystem will continue to be net autotrophic also in the long-term future.

4.6.2 Effects of global warming

Under global warming conditions, increases in precipitation do not necessarily mean an increased runoff because an increased temperature also means a higher evapotranspiration, especially during the vegetation period. Here, it is assumed that the runoff will decrease (Chapter 5 in Grolander and Jaeschke 2019). Therefore, the load of nutrients and particulate matter will not greatly change in the marine areas of the Swedish east and south coasts. Decreased duration and extent of sea ice, increased water temperature, and changes in wind stress will affect the rate of nutrient supply through their effect on vertical mixing and upwelling. Changes in vertical mixing and upwelling will affect the timing, location, and species composition of phytoplankton blooms, which in turn will affect the zooplankton community and the productivity of fish. Since bacterial respiration is temperature-dependent, the increased temperature will most likely be associated with increased bacterial respiration in the pelagic and benthic marine ecosystem (The BACC Author Team 2008).

In addition, a higher respiration rate at the bottoms, induced by higher temperature and increased primary production, may lead to an increase in anoxic bottoms, which in turn will affect the reproduction of many fish species that are dependent on oxygen-rich bottoms for reproduction. Another negative effect for fish dependent on the spring bloom for successful reproduction is that the earlier start of the season might shift the start of the spring bloom, causing a mismatch between primary producers and consumers, which will have effects along the food chain that reduce fish productivity. For other fish species, the higher temperature will mean a higher growth rate and a longer growth season, and for these species production is expected to be higher (The BACC Author Team 2008).

It is likely that the thermocline in most coastal areas will become established at greater depth during the summer. As a result, the warm-water species will extend their habitats at the expense of the cold-water species. A similar spread of freshwater species at the expense of species with higher salinity optima is also likely to occur if there is a decrease in salinity. The range and biomass of marine species may decrease, at the same time as the range and biomass of freshwater species will increase. In the case of marine mammals, a reduction in the extent of ice cover during the winter will lead to reduced reproduction of seals, since they need ice to breed their pups (The BACC Author Team 2008).

Overall, the changes in temperature predicted in a global warming case are not expected to have large implications on essential processes and properties of marine ecosystems and therefore the same parameter values are mainly used as under temperate conditions in the SE-SFL (see Chapter 7, Chapter 7 in Grolander and Jaeschke 2019, Aquilonius 2010).

4.6.3 Periglacial conditions

In a future periglacial climate, the primary production could, due to the altered nutrient conditions, be higher, lower or similar to that in present conditions. However, it is likely that it will be within the range of estimates for the Laxemar area today (Aquilonius 2010). In addition, a likely development is that rates of respiration will decrease along with temperature. As the environment becomes colder, some temperate species presently at the site, may be limited by their cold-tolerance and will become rarer or absent at the site, whereas polar (Arctic) species may extend into the area, with present cold-water species becoming more abundant and new species entering the site. For marine areas in the Baltic Sea, the same types of higher organisms are expected as present today, although species abundance and composition may be altered. With lower temperatures, the growing season of marine mammals will be shorter. On the other hand, the ice will provide the mammals an increased habitat for breeding, and they may therefore increase in abundance. The bird fauna population has been very stable in the Baltic during the recent interglacial (The BACC Author Team 2008) and will probably be similar in the future. Overall, periglacial conditions are assumed to have small implications on important processes and properties of marine ecosystems and therefore the same parameter values are mainly used as under temperate conditions in the SE-SFL (see Chapter 7, Chapter 7 in Grolander and Jaeschke 2019, Aquilonius 2010).

4.7 Limnic ecosystems

4.7.1 Development under temperate conditions

The lake ecosystem gradually matures in an ontogenetic process that includes sedimentation and deposition of substances originating from the surrounding catchment or produced within the lake. Hence, the long-term fate for most lakes is an inevitable filling-up and transformation to a wetland, as further discussed in Chapter 8 in Andersson (2010) and in the summary description in Lindborg (2010). The lakes forming in the future from the coastal bays Borholmsfjärden and Granholmsfjärden, due to the shoreline regression, will be much larger and deeper than the present Lake Frisksjön. It is assumed that these lakes will be similar in terms of thermal stratification, and relation between Secchi depth and net primary production as in more shallow lakes. In these two future deep lakes, a large part of the pelagic production may be utilised directly in the pelagic habitat by zooplankton, but losses through the outlet will probably be large due to large catchment areas and associated short retention times for these deep and low-lying future lakes. It is also possible that such lakes, due to inflow of matter from the large upstream catchment, will become dystrophic, i.e. with brown water and dominated by respiration of allochthonous material produced in the surrounding terrestrial catchment. The larger inflow of uncontaminated organic material produced in the surrounding catchment would most probably act as dilution to potentially contaminated organic carbon produced in the lake. Therefore, such a change, in which the lakes becomes net heterotrophic, instead of net autotrophic as today, has not been accounted for in calculations of effects on dose to humans under prolonged landscape development (Chapter 7).

4.7.2 Effects of global warming

Lakes are affected by global warming and lake ecosystems have been proposed to serve as sentinels of climate change due to their rapid and observable responses (Adrian et al. 2009). However, the response of lakes to global warming is individual and affected by catchment characteristics, lake morphometry and food web interactions, Generally, the effect on abiotic parameters is relatively easily foreseen, whereas effects on biotic parameters are difficult to predict. Increased air temperature will lead to a longer stratification period in summer and shorter periods with ice coverage. Since the winter temperature in the global warming scenario will be somewhat higher than today, periods of ice coverage will likely be shorter and interrupted by open water periods. This also has implications for other abiotic and biotic parameters in the lakes, such as mixing, light conditions, biomass and production. Based on modelling, it is also assumed that runoff during warmer conditions will decrease on a yearly basis (Chapter 5 in Grolander and Jaeschke 2019). This will increase the retention time of water in lakes. Processes within the lake, such as mixing and anoxia, may influence the future nutrient concentrations in the water column. In most lakes, dissolved organic carbon (DOC) is expected to increase due to global warming.

There may be a shift in occurrence of anoxia from winter to summer. At present, anoxia occurs during winter in the whole water column of the shallow Lake Frisksjön. A shortened period with ice coverage reduces the risk of anoxia in winter. On the other hand, increased production in summer can lead to increased amounts of degradable matter, resulting in increased respiration (eutrophication) and increased anoxia during summer stratification. The effects of higher temperature on biotic components in lakes are difficult to foresee and there may, for example, be an increase or decrease in phytoplankton biomass. Therefore, the same parameter values are used as for temperate conditions are applied for a warmer climate. For a more comprehensive discussion on possible effects of global warming on lakes, readers are referred to Andersson (2010).

4.7.3 Periglacial conditions

As the environment becomes colder, some temperate species occurring at the site today may be limited by their cold-tolerance and will become rarer or absent at the site, whereas polar (Arctic) species may increase in the area, with present cold-water species becoming more abundant and new species entering the site. A large difference between Lake Frisksjön in Laxemar and future periglacial lakes is that there will be no reed surrounding the periglacial lakes (Andersson 2010). The reed belts surrounding Lake Frisksjön may be important for the functioning of the lake by influencing the composition of water entering the lake from the sub-catchment. Moreover, the reed belts may function as sheltered breeding areas for aquatic organisms. In periglacial regions, lakes may instead be surrounded by other vascular plants or bryophytes.

A useful approach to describe the potential species present in Sweden under different climate conditions is to gather information on the biota composition in areas with the relevant climate today. For the periglacial climate domain this has been done using the information gained in the SKB assessment for the Greenland Analogue Surface Project (GRASP, see Clarhäll 2011). No amphibian or mammal species were identified in the limnic reference ecosystems at the Greenland site, and these organism types are expected to be absent also in lakes in Laxemar under periglacial conditions. Otherwise, organism types are expected to be similar to those at present although the abundance and composition of species may be altered.

In addition to existing lakes defined by bedrock depressions, there will be thermokarst lakes (thaw lakes) in a periglacial system. Thermokarst lakes develop in a cyclic pattern where permafrost freezes and thaws, forming temporary water-filled depressions with a lifespan of a couple of hundred years. Thermokarst lakes are usually small and shallow. From an ecological point of view, they may be important for the landscape, as they may be hotspots of biological activity in tundra regions with abundant microbial activity, primary production, benthic communities and birds. However, thermokarst lakes do not have connection to the deep groundwater system and are therefore not important in our context.

In colder climates, lake ice coverage will be thicker and persist longer during the winter. This leads to less light penetration, affecting the primary producers beneath the ice as well as the mixing and transport of nutrients. Nutrient concentrations may be lower due to a shorter runoff season, altered

weathering, production and retention in the ground surrounding the lake, as well as to altered internal circulation of nutrients. There is an increased risk of oxygen depletion during the winter due to longer periods with ice cover.

Despite a shorter growing season, the biomass of primary producers is not necessarily lower under periglacial conditions than in temperate regions. Species composition may change, but biomass and production of benthic primary producers under periglacial conditions are assumed to closely resemble the biomass and production under temperate conditions, which is supported by investigations reviewed in Andersson (2010). Even if primary production is similar in periglacial and temperate climate domains, biomass and production of fish will probably decrease under periglacial conditions, which is also assumed in the evaluation case for periglacial conditions (Section 7.3.6, for further details see Andersson 2010).

4.8 Terrestrial ecosystems

4.8.1 Development under temperate conditions

Based on hydrological modelling, the mire has been identified as the terrestrial ecosystem type that most likely could be affected by an inflow of radionuclide-containing groundwater from the repository, due to its location in the low-lying parts of the landscape (see Section 4.3 and Chapter 5). Most wetlands constitute discharge areas, however, the raised bog, with rain-fed production on the bog plane, has a restricted or non-existent connection to the groundwater table and is of less interest in a safety assessment in which radionuclides enter the ecosystem from below (Löfgren 2010). Consequently, the focus here is on fen-type mire ecosystems and their potential use as agricultural land after drainage.

Simply put, mires are formed through three different processes: terrestrialisation, paludification and primary mire formation (Kellner 2003). Terrestrialisation is the filling-in of shallow lakes by sedimentation and establishment of vegetation. Paludification, which is the dominant process of mire formation in Sweden, is peat formation on somewhat less water-permeable soils, mainly as a consequence of changed hydrological conditions or arising from expanding mires. Primary mire formation is when peat is developed directly on fresh soils after emergence from water or ice. In Laxemar, terrestrialisation and paludification seem to be dominating (e.g. Kellner 2003). However, terrestrialisation probably represents the largest areas of peatland development in the investigation area today. This pattern, in which reed is the dominating pioneer during terrestrialisation, is also seen in the peat archives of bogs further inland (for Laxemar see Nilsson 2004, Svensson 1988), but is probably also a function of nutrient conditions in the surrounding drainage area.

One of the largest impacts on mire ecosystems is drainage, which historically has been pursued to create arable land or to improve the forestry yield (Löfgren 2010). Land suitable for cultivation is often situated in the low-lying parts of the terrain and often occurs in small irregular pockets in the surrounding boulder-rich valleys with water-laid sediments. From the middle of the 19th century, larger wetland areas in the woodlands were drained and cultivated as arable land (Eliasson 1992).

4.8.2 Effects of global warming

A warmer climate usually means potentially increased biomass and net primary production (NPP), as well as reduced carbon storage in the short term, depending on the magnitude of the climate change (Chapin et al. 2002, The BACC Author Team 2008). Most properties of the mire and the agricultural ecosystems are expected to be marginally affected by a moderate change in regional climate (Chapter 11, Löfgren 2010). The expected responses in plant- and crop-related parameters due to a warmer climate (e.g. increased biomass, NPP, transpiration and leaf area index), are assumed to have only minor effects on radionuclide transport and accumulation. Modelling of the vegetation with the dynamic vegetation model LPJ-GUESS (Sitch et al. 2003) generated data to describe the vegetation under global warming climate conditions. The modelling results suggested that Laxemar would be dominated by broad-leaved trees, with a larger biomass than today but with similar NPP (Kjellström et al. 2009).

Other modelling approaches, e.g. The BACC Author Team (2008), highlight the uncertainties concerning the carbon dynamics in wetlands. Increased temperature, resulting in increased evapotranspiration, will likely lower the groundwater table and increase heterotrophic respiration. This can initially be balanced by increased plant production in the mire, which is enhanced by drying. Strack et al. (2008) suggested that dry peatland areas such as bog hummocks and ridges will act as smaller sinks than today or even sources, of CO_2, whereas wet zones will likely become greater sinks. For agricultural land on drained mires, a warmer climate, where precipitation does not compensate for higher evapotranspiration during the vegetation period, means that the plant-water deficit will increase. The increased demand for water by the cultivated crops can either be supplied by increased groundwater uptake through capillary rise or it can be supplied by irrigation. Consequently, by increasing the total plant water uptake and also adding a potential pathway for radionuclide transport, irrigation, not considered relevant under present-day conditions, radionuclide transport and accumulation may be different from present-day conditions (See Chapter 4 in SKB 2015b). The effect of this added pathway is evaluated in SE-SFL (Chapter 7).

4.8.3 Periglacial conditions

In a periglacial climate, the terrestrial vegetation consists of sedges, herbs and shrubs. At more exposed and drier localities, lichens dominate, whereas wet ground is dominated by bryophytes. The precipitation will likely be lower than during temperate conditions, due to the limited evapotranspiration transporting water to the atmosphere (Kjellström et al. 2009). The low evapotranspiration means that wet ground is prevalent, because surplus water is unable to infiltrate into the ground (Section 4.4, Bosson et al. 2010, French 2007). This may result in larger areas of wetlands compared with a temperate climate but, on the other hand, the peat formation rate is slower, partly because the terrestrial plant productivity is low.

A sufficiently reduced temperature will eventually change a temperate or boreal environment to a more tundra-like environment. This will lower biomass and NPP in both forested taiga and tundra peatlands. Such a change might also increase relative carbon storage in relation to NPP, whereas the actual amount that is stored, e.g. as peat, is likely to be lower than under present conditions, even though the mineralisation also is slowed down by the temperature decrease. The specific conditions found in a permafrost landscape will dramatically change the potential for cultivation to the extent that no considerable crop production occurs under periglacial conditions e.g. it is difficult to ditch a mire surrounded by frozen ground. For a detailed discussion on terrestrial ecosystems and how they are expected to change under different climate conditions, the reader is referred to Löfgren (2010).

As the environment becomes colder, the geographical ranges of organisms will move south. Some temperate species presently at the site may be limited by their cold-tolerance and will become rarer or absent at the site, whereas polar (Arctic) species may extend into the area with present polar species becoming more abundant and new species entering the site. The species potentially present in the assessment area under different climate conditions can be described using information on the biota composition in areas with the relevant climate today. For the periglacial climate domain this has been done using the information gained in the SKB assessment for the Greenland Analogue Surface Project (GRASP, see SKB 2013b). There, large trees, gastropods, amphibians and reptiles are absent, and these organism types are also expected to be absent throughout parts of Sweden under periglacial conditions. Otherwise, organism types are expected to be similar to those occurring presently, although the abundance and composition of species may be altered.

5 Identification and characterisation of biosphere objects in the landscape

5.1 Introduction

A central part of a safety evaluation is to identify areas that potentially could be affected by release from a planned repository. Hydrogeological simulations suggest that particles released from a repository will be discharged in topographically low-lying areas in the landscape (e.g. Joyce et al. 2019). In SKB's safety assessments these areas are called biosphere objects. A biosphere object is an area that potentially, at any time during the considered assessment period, could receive a discharge of radionuclide-containing groundwater associated with the repository. That means that secondary discharge from upstream biosphere objects is not included in the identification process described below and this is a consequence of an evaluation made by SKB (2014d. The biosphere objects are the unit of modelling in the radionuclide transport model for the biosphere (described in Chapter 8) and serve as the basis for extraction of site-specific parameter values (Chapter 10).

In this chapter, biosphere objects at the Laxemar example site are identified in the landscape based on hydrological modelling of deep groundwater. The biosphere object areas are outlined mainly based on the present landscape and site conditions (Chapter 3). The historical and future development were modelled for certain biosphere objects, based on processes identified in Chapter 4, using the coupled Regolith-Lake Development Model (RLDM). A simplified model for predicting ingrowth in historical lakes was also developed in SE-SFL and is briefly described here. The approach to the identification, delimitation and modelling of biosphere objects follows the same methodology as was used in SR-Site (Lindborg 2010) and SR-PSU (SKB 2014d). The present chapter describes the biosphere objects that were used in the base case (Present-day) and in the other different evaluation cases (described in Chapter 7) using Laxemar as an example site in the SE-SFL.

5.2 General landscape discharge patterns in Laxemar

5.2.1 Hydrological modelling of potential discharge areas

In earlier safety assessments, e.g. SR-Site and SR-PSU, discharge of deep groundwater from a repository were identified based on a specific geographical position of the repository (SKB 2010b, 2014d). As the location of a future repository has not been determined for SFL, the identification of biosphere objects was made in two steps, where the first step was focused on the identification of discharge areas in general terms within a larger scale of the landscape, whereas the second step was based on release from a hypothetical repository position.

The identification of biosphere objects in the landscape was made as a part of the SR-Site evaluation of the Laxemar site. Werner et al. (2006) analysed the discharge patterns of deep groundwater in the Laxemar area, and the study area was expanded in a later analysis by Sassner et al. (2011) (see also Section 4.4). Using particle tracking in the modelling tool MIKE SHE, particles were uniformly released over the modelled area, starting from depths of 40 m and 150 m below the present sea level (m.b.s.l.), respectively. The starting depths are in the bedrock, well below the deepest regolith layer, and therefore are considered relevant for describing the discharge into the regolith. The resulting discharge patterns were similar in the two studies, with particles being discharged to the only lake in the area, Lake Frisksjön, to the mire Gästern, and to several agricultural land areas, along streams and the coastline, and in coastal bays (Figure 5-1). In the later study, modelling of the discharge was done for three different time points (2000 AD, 5000 AD and 10 000 AD) using a 5000-year simulation period and the results are very similar. Differences exist in connection to the sea only, which is due to the relative sea-level change and the associated creation of new land areas. In new land areas, formed as a result of the shoreline regression, the modelled pattern of groundwater recharge and discharge areas in the regolith is similar to that observed in present land areas. This indicates that near-surface hydraulic gradients and flow directions, given constant climate conditions, are more dependent on topography than on the distance to the shoreline. The number of particles left in the model volume at the end of simulation decreases from the 2000 AD model to the 5000 AD and

10 000 AD models. This was noted also for the Forsmark site in the Forsmark SR-Site study (Bosson et al. 2010), and the reason is that the part of the model domain covered by sea decreases with time. The low gradients below the sea cause very low flow velocities, and therefore many particles that are released below the sea remain in the model at the end of the simulation.

The exit locations of particles reaching the ground surface (discharge area) are concentrated along the streams, in lakes and along lakesides, and along the coastline (Figure 5-1). Based on these simulations, nine discharge areas, representing four different ecosystem types were identified. These included the two semi-enclosed sea bays Inre Granholmsfjärden (201) and Borholmsfjärden (208), Lake Frisksjön (207) and the Gästern mire (203) (Figure 5-2). Moreover, as deep groundwater tends to be discharged into streams situated in valleys (Figure 5-1), where agricultural land today is dominating, five agricultural land areas were selected (Figure 5-2). These were selected to represent arable land at different locations in the landscape, from smaller objects in the uppermost catchment of a stream network (204 and 206) to larger areas along the banks of the relatively large stream Laxemarån (212, 213) (Table 5-1).

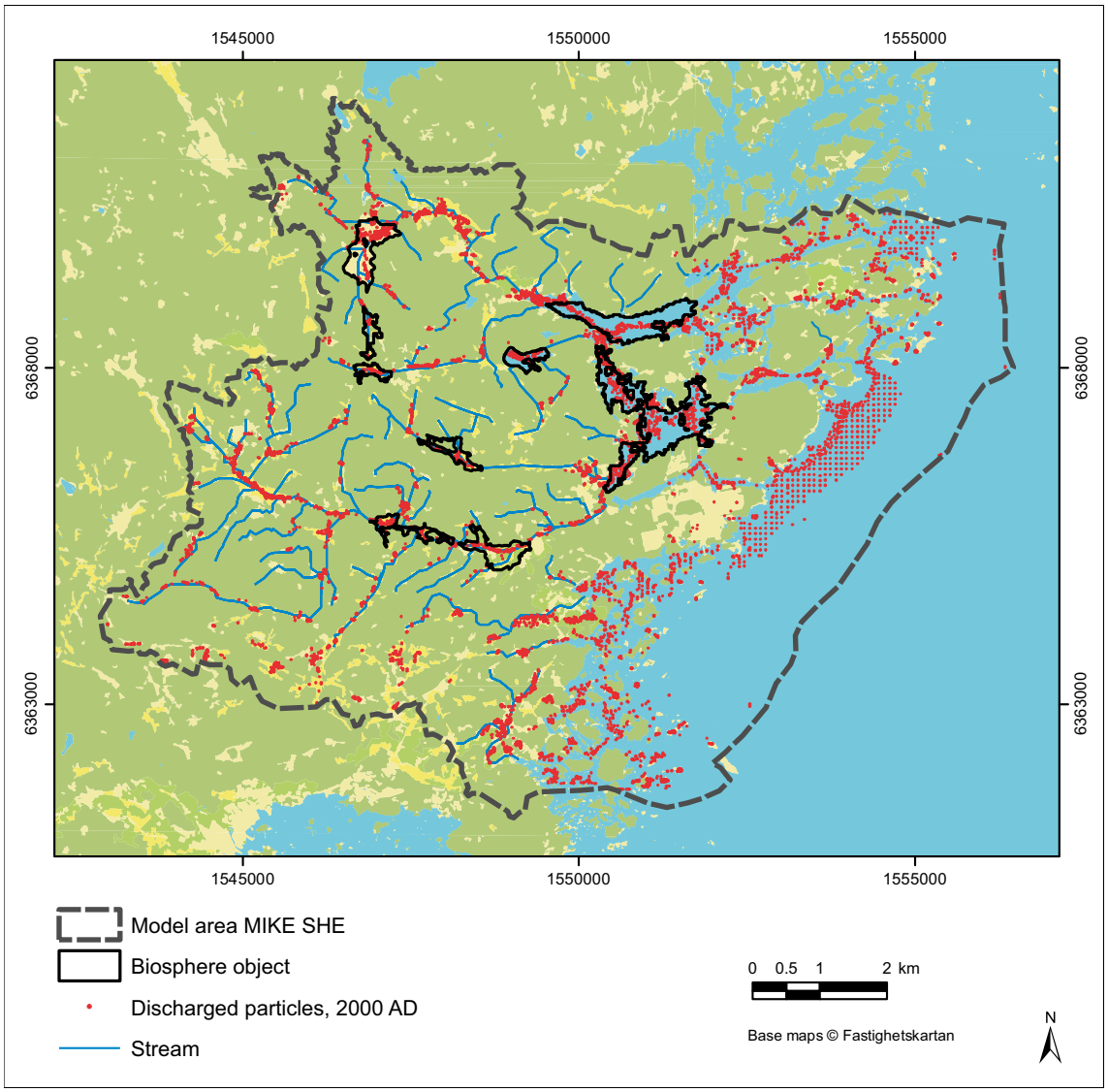

Figure 5-1. *The location at the surface of discharge particles released at a depth of 150 m below sea level in the bedrock. The MIKE SHE simulation was run for 5 000 years using present conditions (2000 AD). Redrawn from Sassner et al. (2011). The selected biosphere objects are indicated by black contour lines in the figure.*

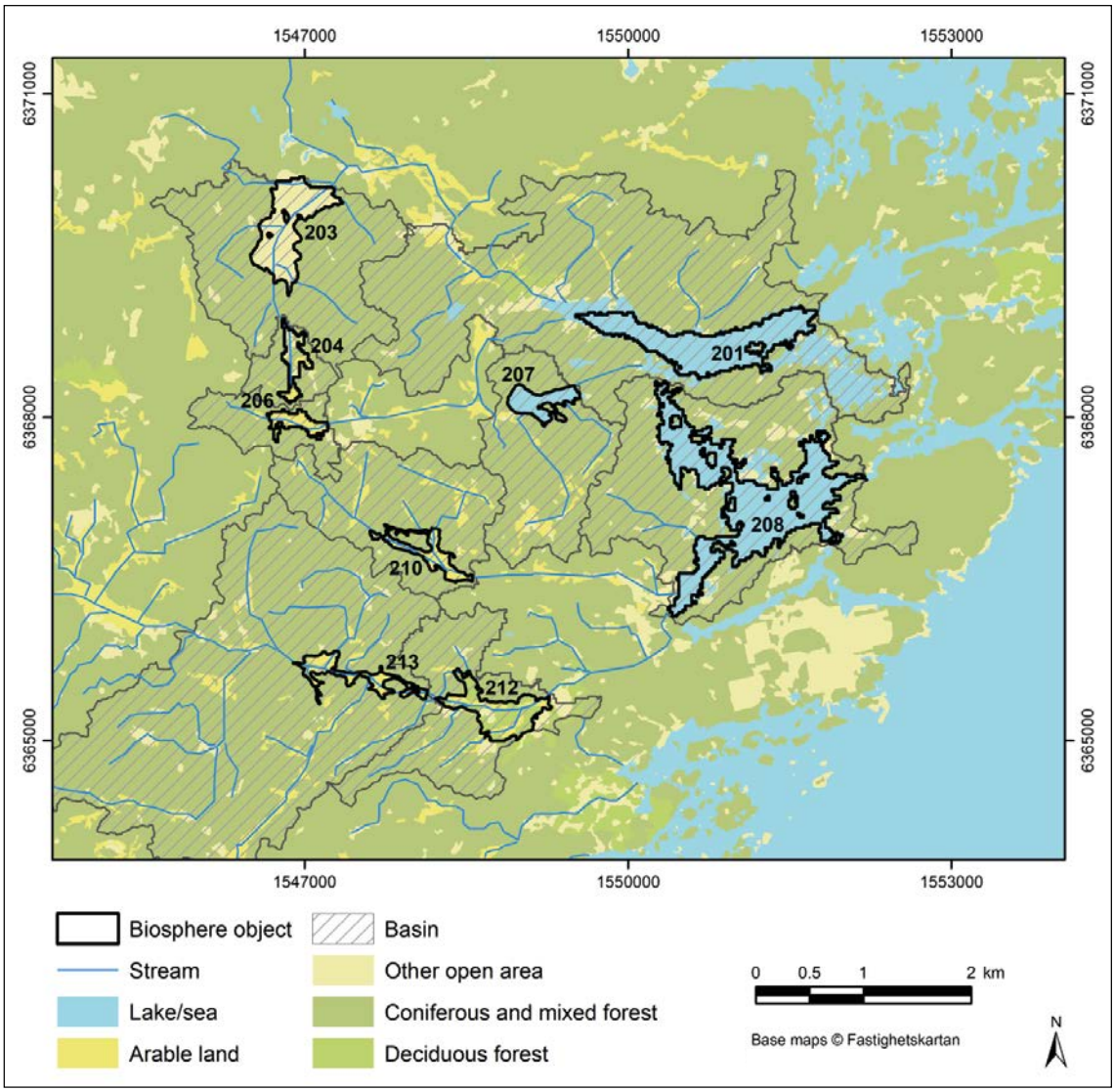

Figure 5-2. *The nine biosphere objects analysed in SE-SFL, projected onto the present land-use map in the Laxemar area. The objects represent different ecosystems and locations in the landscape, and deep groundwater is expected to potentially be discharged in all of them. The hatched areas represents the former sea basin associated with the biosphere objects. The areas of biosphere objects 201 and 208 correspond to the future lake basin and are, therefore, somewhat smaller than the present sea basins (see also Figure 3-1).*

5.2.2 Outlining the biosphere objects in the landscape of today

The spatial delimitation of the biosphere objects was made in accordance with earlier safety assessments (SKB 2014d, Lindborg 2010). That is, the biosphere objects were outlined based on topography to represent clearly defined ecosystems, reflecting reasonably homogenous biotic properties (e.g. type of vegetation, and rates of primary production and decomposition) and abiotic characteristics (e.g. regolith stratification and groundwater hydrology). In contrast to previous assessments, most of the biosphere objects in Laxemar are above the present sea level, such as agricultural land, mires and lakes. There are also two semi-enclosed sea basins, where the sea basins set the boundary for the aquatic part of the biosphere object today, but their future lake basins are also shown in Figure 5-2 within the delineated area.

The areal extents of the biosphere objects situated above the sea level approximately reflect a historical lake basin. For the two sea objects (201 and 208), the size of the future lake basin was determined from the digital elevation model (Strömgren and Brydsten 2008), accounting for

the bathymetry of the basin and the vertical position of the lake threshold (Sassner et al. 2011). Accumulation of sediments primarily occurs in the central deeper parts of the sea basin, and this part of the biosphere object was used to assess accumulation of radionuclides in regolith layers throughout the sea basin stage. Following the SR-PSU methodology, the size of the central sea basin that accumulates radionuclides was set to the size of the future lake (i.e. the lake basin). As the biosphere object emerges from the sea, the area, depth and volume of open water are continuously reduced until the sea bay finally becomes isolated. At this point the biosphere object turns into a lake-mire complex, and the total areal extent of such objects does not change (i.e. it equals that of the lake basin at all times). However, the lake/wetland ratio within the biosphere object will change continuously due to ingrowth of wetland vegetation. There is one lake in the investigation area today, namely Lake Frisksjön (207 in Figure 5-2). This lake has been lowered in one or several drainage enterprises, but the successional development (with the RLDM, see below) was modelled for the original lake. For simplicity, the original areal extent of the lake basin is used to outline this biosphere object through the assessment (rather than the extent of the present lake).

There is one large mire present in the area today (Gästern, 203 in Figure 5-2) and the corresponding biosphere object was outlined based on the areal extent of the present mire (which approximates the earlier lake basin). Also, biosphere objects representing agricultural ecosystems were outlined based on the present areal extent of cultivated land (204, 206, 210, 212 and 213 in Figure 5-2). In some cases, the object areas were expanded to include adjacent areas within the same elevation, based on the digital elevation model (DEM). Consequently, biosphere object 212 includes deciduous forest bordering the presently cultivated area, and the outlined object can be interpreted as a coherent area reflecting earlier land use. The topsoils in the outlined agricultural objects show high organic content (histosols), and below the peaty soil layer there is lacustrine gyttja (Sohlenius and Hedenström 2008, Morosini et al. 2007), indicating that these areas were preceded by a lake-mire stage. Thus, it is reasonable to assume that the outlined agricultural biosphere objects also represent the basins of historic lakes.

The identified and delimited biosphere objects are shown in Table 5-1, together with their estimated lake basin areas, the total area that generates discharge into the biosphere object (watershed area, Figure 1-2) and the sub-catchment that generates diffusive discharge to the biosphere object. This is further described in Grolander and Jaeschke (2019, Sections 3.2.1, 5.3 and Figure 5-3).

Table 5-1. A representative set of biosphere objects in the Laxemar area. The selection is based on their ability to attract deep groundwater discharge, size, location in a landscape context and ecosystem type. Note that the geometric entities are hierarchically arranged so that the lake basin is included in the sub-catchment, and the sub-catchment is included in the watershed. Watershed is the total area generating water flow to the biosphere object. The sub-catchment is defined as the catchment of the outlet of a lake/wetland minus the catchment of the inlet of the same lake/wetland i.e. the area that generates horisontal groundwater inflow into the biosphere object. The lake basin area outlines the biosphere object after it has been isolated from the sea.

ID	Name	Ecosystem	Watershed[1] (m^2)	Sub-catch[2] (m^2)	Lake basin[3] (m^2)
201	Inre Granholmsfjärden	Sea Bay	15 372 000	4 257 900	511 000
203	Gästern	Mire	3 114 800	2 303 200	368 000
204	Brandegöl	Cultivated	449 600	418 900	94 000
206	Marstrand	Cultivated	615 200	414 600	78 000
207	Frisksjön	Lake	1 738 800	846 200	174 000
208	Borholmsfjärden	Sea Bay	22 995 600	3 947 000	803 000
210	Skettkärret	Cultivated	1 915 600	1 245 700	116 000
212	Bredängen	Cultivated	14 792 800	1 678 200	253 000
213	Klotängen	Cultivated	13 053 200	3 173 400	136 000

1 = Including lake area, from RLDM (stored at svn://svn.skb.se/projekt/SFLsurface/Indata/Landscape geometries/SFL_parameters_TS_all_basins, last time step),

2 = From the previous description and assessment of Laxemar (JASP; SKB 2010d; stored at svn://svn.skb.se/projekt/SrSite-Bio/Forsmark/Landscape/Parameters_SS/sub_catch.xls),

3 = Stored at svn://svn.skb.se/projekt/SrSite-Bio/Forsmark/Indata/Landscape_geometries/Calculation_landscape_parameters_Laxemar.xlsm (First sheet)

5.3 Repository-specific discharge patterns in Laxemar

To derive biosphere data that are coherent with the description of transport in the safety evaluation, surface discharge patterns for particles released from the postulated repository location were also studied (Figure 5-3). The SFL repository is located below a local hill in the landscape, and the surface above the repository is located approximately 21.5 m above present sea level.

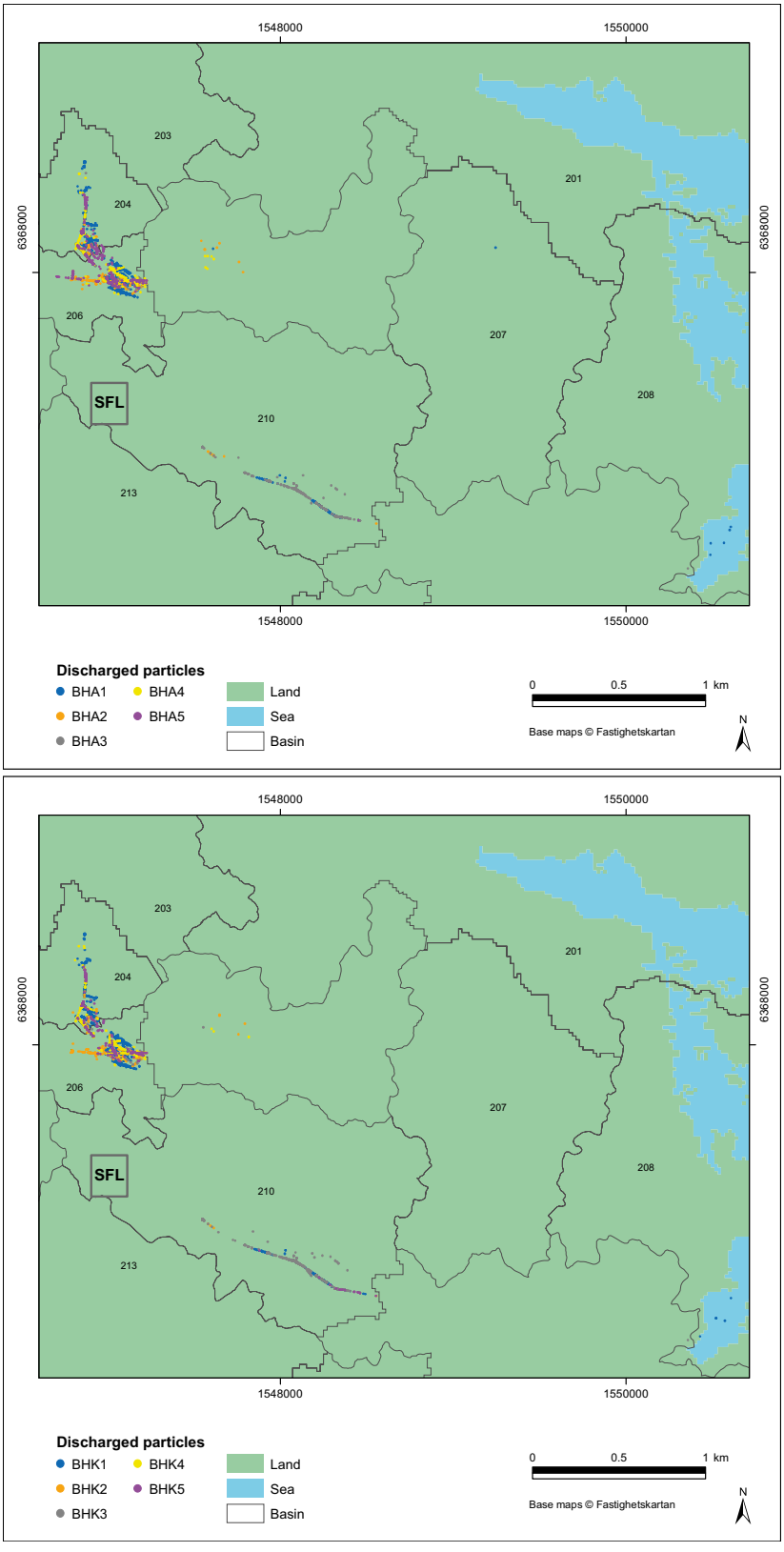

Figure 5-3. *Distribution of potential discharge from a hypothetical repository in Laxemar. The discharge is based on particle tracking from the two waste vaults BHA (above) and BHK (below) in five different realisations of the stochastic fracture networks. Locations of particles are on the surface of the bedrock before entering the regolith. This is from where the transport starts in the biosphere assessment. The outlined areas correspond to the former sea basins of the biosphere objects. Note that for objects 204, 206 and 210 (which are the first objects along three different streams) the area of the basin coincides with area of the watershed for the lake. The example location for the SFL repository is indicated with a square.*

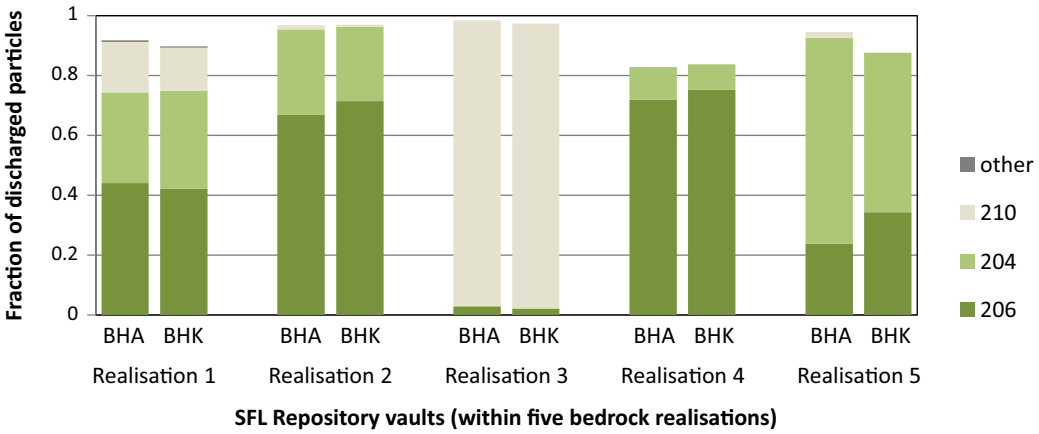

Figure 5-4. *The distribution of particles among biosphere objects discharged from two waste vaults (BHA and BHK) which are hypothetically located in Laxemar. The results are based on five realisations of the stochastic fracture networks (see also Figures 5-2 and 5-3).*

The results of a set of modelling realisations of groundwater flow in the bedrock surrounding the repository in Laxemar show that basins 204, 206 and 210 are the targets for discharge of deep groundwater from the hypothetical position of the SFL repository (Section 4.6 in Joyce et al. 2019, Figure 5-4). Moreover, the pattern is similar for releases from the two different vaults BHA and BHK. An analysis of the abundance of the released particles among biosphere objects indicate that most of the total potential release (> 60 %) from SFL would typically end up underneath (or close to) one of three biosphere objects (Figure 5-4). In three of five realisations of the stochastic fracture networks, biosphere object 206 received most discharge from the repository. This exercise supported the previous general approach used to identify areas which may potentially receive discharge from a geological repository, and highlights object 206 as especially relevant for coherent modelling of transport and accumulation in SE-SFL.

5.4 Properties of biosphere objects today

5.4.1 Regolith stratigraphy and depths

For the biosphere objects that were evaluated under present conditions, the regolith stratigraphy and depths were assigned based on the Regolith Depth Model for Laxemar (Nyman et al. 2008, RDM is described in Chapter 3, Figure 5-5). The different regolith layers for the six terrestrial biosphere objects in Figure 5-5 correspond to those that were used in the model for the calculation of transport and exposure to radionuclides (see Section 8.3, Figure 8.1). Five of these biosphere objects are today agricultural land, whereas biosphere object 206 is a mire.

5.4.2 Water balances

Water balance components for the identified biosphere objects were mainly extracted based on simulations made with the distributed hydrological MIKE SHE model (Bosson et al. 2009), see also the description in Section 5.3 in Grolander and Jaeschke 2019). The water-balances included components of horizontal water flows into and out from each object, and across the boundary of mire and lake/stream parts of the objects. The water balances also described the vertical water fluxes between surface water and regolith, between the bedrock and the regolith, and between calculation layers within the regolith (Figure 5-6).

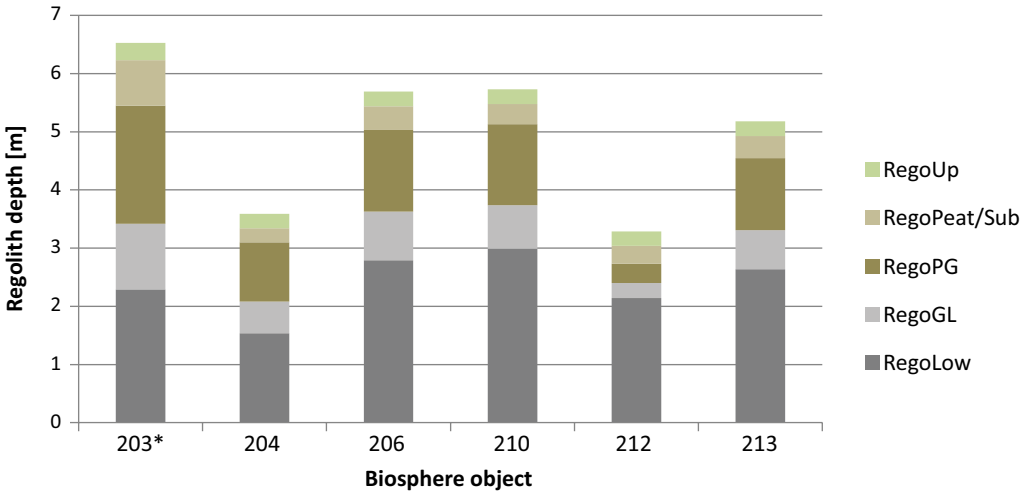

Figure 5-5. *Thickness of regolith compartments for six terrestrial biosphere objects based on the regolith depth model (RDM) describing the present conditions at Laxemar. RegoUp represents the biologically active layer with a high rate of decomposition and root uptake. RegoPeat represents peat in the mire or organic soil in agricultural land. RegoPG is post-glacial clay, the RegoGL is glacial clay and RegoLow is till. * mire ecosystem (other objects are agricultural ecosystems). Figure is from Grolander and Jaeschke (2019).*

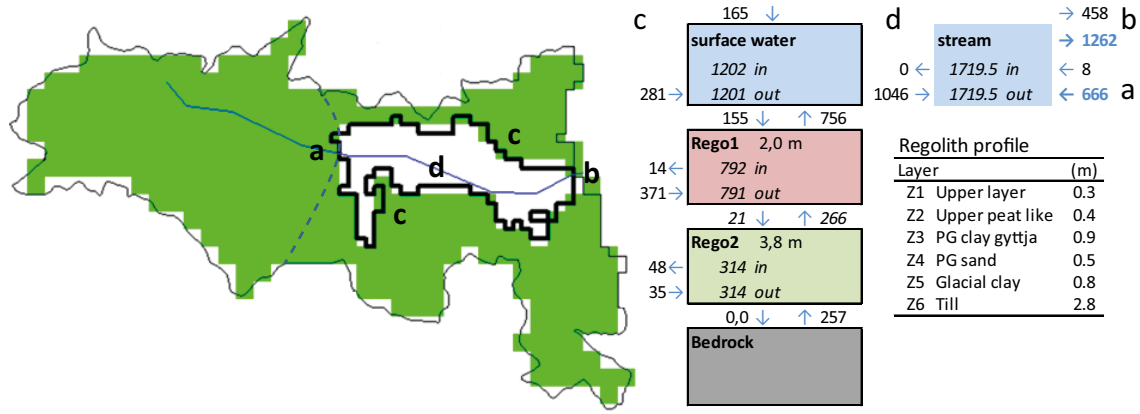

Figure 5-6. *Water balances for present conditions of biosphere object 206 in Laxemar. Map of the biosphere object and its catchment. The thin black line outlines the borders of the basin. The green and the white areas represent the watershed and the object within the basin, respectively. The blue line represents a stream, and the dotted line approximately subdivides the basin into the catchments of the inlet and outlet of the stream, where the area to the right of the line corresponds to the sub-catchment. Right) Stacked boxes represent Mike SHE calculation layers within the object and arrows represent water fluxes across object or regolith layer boundaries. Numbers in the boxes show net in- and outflow of water. Blue numbers indicate streamflow (from Mike11). All units are in 10^{-3} m^3 m^{-2} $year^{-1}$ (normalised to the area of the object). Average regolith depth for the calculation layers are given in the boxes, and the average depth of geological layers are listed in the table. For details on the methodology see Section 5.3 in Grolander and Jaeschke (2019). Letters are used to link components in the left and right panels.*

5.5 Temporal development of biosphere objects

The landscape relief in the Laxemar area is determined mainly by the bedrock topography. The small-scale undulations of the bedrock surface are smoothed by glacial and post-glacial deposits, which, to a limited extent, are redistributed by wave erosion when the shoreline regresses over the area (Brydsten and Strömgren 2013). The properties of the biosphere objects change continuously, e.g. due to the withdrawal of the sea, erosion, sedimentation, lake infilling and ecosystem succession (see Chapter 4).

5.5.1 The coupled Regolith-Lake Developmental Model

The successional development of sea basins (all objects) and lake basins (objects 201, 207 and 208) was described with the coupled Regolith-Lake Developmental Model (RLDM, Brydsten and Strömgren 2010) as a part of the comparative analysis of safety related site characteristics (SKB 2010d). The RLDM describes the development of regolith stratigraphy, and layer thickness over time during the period considered in the safety assessment. The RLDM is divided into two modules: a marine module that predicts the sediment dynamics caused by wind waves and a lake module that predicts the lake infill processes. The RLDM marine module starts at the time when the area has recently been deglaciated and all regolith materials are of glacial origin. These conditions are generated using the Regolith Depth and stratigraphy Model (RDM) for Laxemar (Nyman et al. 2008). In the marine sediment modelling, postglacial sediment is added or removed in each raster cell based on the sediment dynamic environment for that time. These sediment dynamic data are output from the sediment dynamic model as presented by Brydsten (2009). In a cell where erosion is the predominant process, all postglacial sediments are resuspended and transported out of the cell. For each time step, the RLDM marine module outputs are raster maps of Quaternary surface geology, thickness of marine postglacial sediments (RDM), and sea-bottom elevation (i.e. a new Digital Elevation Model, DEM, is made for each time-step).

The development of lakes is described with a separate module within the RLDM based on expressions for net sedimentation rate and vegetation colonisation (Brydsten and Strömgren 2013). Each lake is modelled separately. The DEM and the thickness of the marine postglacial sediment from the time step before lake isolation is used as input to the module. The lake module runs in 100-year time steps until the lake is completely infilled. Raster maps of the thickness of the marine and limnic postglacial sediment (gyttja clay and clay gyttja), and the thickness of the peat are outputs from the lake module for each time step. In a post-processing routine, the outputs from the marine and lake modules are merged into single raster maps for Quaternary surface geology, DEM, and RDM. The combined data describes the development of the biosphere object.

The historical and projected development of the present lake Frisksjön (207) served as an example to illustrate the outcome of the RLDM (Figure 5-7 left panel). For the illustration, four characteristics are displayed; the area of open water, the average depth of the open water, the thickness of post-glacial sediments in the object and the peat thickness in the mire. The description of the object starts at −10 000 AD when the latest inland ice had withdrawn and the landscape was covered by more than 50 m of water. During the first 2000 years, the relative land rise (Figure 4-1) reduces the average water depth of the object, but no other properties were affected. This is because the basin was still fully submerged, and because the bottoms of the basin were characterised as transport bottoms (i.e. neither sedimentation nor erosion was dominating sediment transport).

Around −8000 AD, parts of the basin emerged from the sea (Figure 5-7 left panel). Islands emerging north-east of the bay sheltered it from wind, and post-glacial sediments started to accumulate in parts of the basin. The area of open water and average water depth diminished as the combined result of sea-level changes, sediment accumulation and the bathymetry of the submerged part of the basin. The net sea-level was steadily decreasing, but there was a period (of approximately 2000 years) when the rise in sea-level was larger than the post-glacial uplift, and consequently the water depth (and the area of open water) increased in this period. As lake isolation started, the water depth again increased. This was because of ingrowth of vegetation and terrestrialisation of the shallow sea bottom at the bay margins, and only the deeper parts remained as open lake surface area. Vegetation continued to expand into the lake, and the peat filled the lake volume in the colonised areas. Net sedimentation occurred in the open lake areas, and the rate of accumulation decreased as the water volume decreased. The lake was fully colonised by vegetation approximately 10 000 years after isolation.

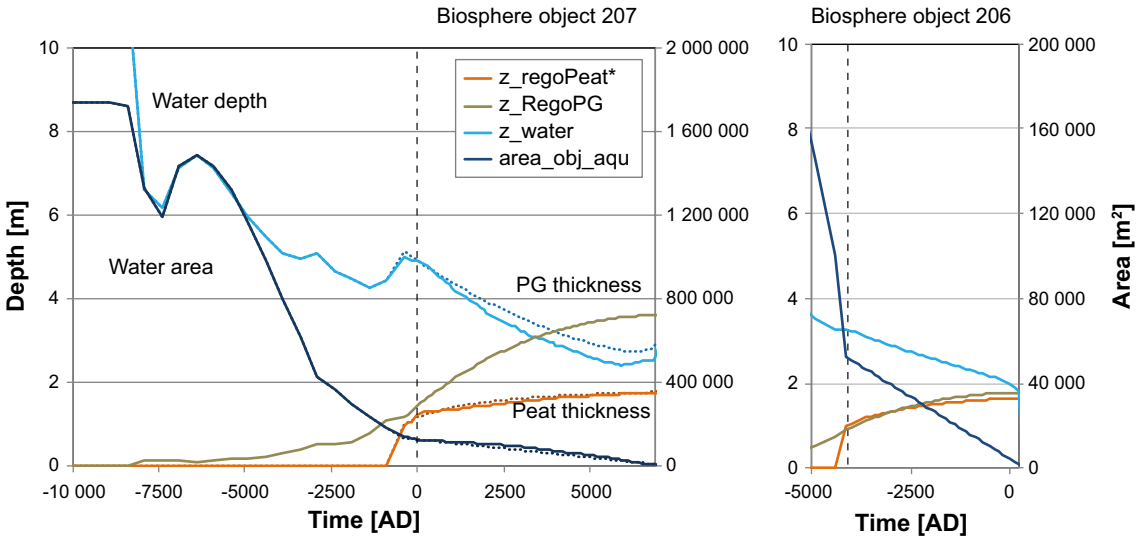

Figure 5-7. *Development of biosphere objects according to the RLDM and a simplified version describing lake infilling. Left panel: Development of Lake Frisksjön (207). Solid lines represent lake area (dark blue, area_obj_aqu), water depth (light blue, z_water), peat thickness (orange, z_regoPeat*) and the average depth of post-glacial fine sediments in the object (brown, z_regoPG). Dotted lines represent the same properties calculated with the simplified model. Lake isolation occurs at year 0 AD (dashed vertical line). Right panel: Developmen of biosphere object 206. Lake isolation occurs 4100 BC, and the properties after isolation is described by the simplified model.*

As a description of the development of historic lakes in areas that are presently cultivated was lacking in the comparative analysis of site characteristics (SKB 2010d), a simplified description of the mire ingrowth has been developed in SE-SFL (Chapter 3 in Grolander and Jaeschke 2019). The overall patterns of a steadily increasing mire area, and a steadily decreasing water depth, are well captured with the simple calculations. Moreover, the development of the average thickness of peat and post-glacial fine sediments closely match the output of the RLDM (Figure 5-7, left panel).

5.5.2 The example of biosphere object 206

The development of certain properties of the historic lake object 206 (as predicted by the simplified model) is shown in Figure 5-7 (right panel). This development from a sea to a mire for a potential discharge area can also be exemplified as a sequence of important stages (Figure 5-8). Different ecological characteristics of the different stages can be assigned based on descriptions from the present area (Chapter 3):

- Sea stage (Figure 5-8a). In this stage the biosphere object is an aquatic ecosystem. As the landscape emerges from the sea, the sea basin is reduced in size as the relative sea-level is lowered. The thickness of post-glacial sediments typically increases due to sedimentation but may decrease in periods of wave erosion. Pelagic and benthic primary production respond to the changes in water depth and bathymetry. During the beginning of this period there is no emergent vegetation in the central deep parts (i.e. the lake basin), but this area becomes vegetated as the bay gets shallower. The fauna is typical for brackish water conditions. The stage ends when the lake threshold reaches sea level at extreme low water.
- Transitional stage (Figure 5-8b): This stage describes the isolation of the sea bay. At the present rate of land-rise, the stage spans approximately 300 years. However, as the rate of land-rise decreases with time, the period is considerably longer for objects in lower terrain (e.g. 500 years for object 207) and will be much longer when the present sea bays are isolated (~ 1 000 years). During this period occasional brackish water flooding will successively become more unusual, and the aquatic biota will change from brackish to freshwater communities.
- Lake-Mire stage (Figure 5-8c): In this stage, the lake threshold has emerged above the sea level at extreme high water. The lake ecosystem (aquatic) is surrounded by a mire ecosystem (terrestrial), and the aquatic biota is typical for freshwater conditions. The aquatic sediments build up, the

surrounding wetland expands into the lake, and peat gradually covers the aquatic sediments. The lake stage ends when the lake has been fully transformed into a mire. The length of this stage varies with the initial size and morphometry of the lake. For small objects (like object 206), it is projected to be sustained for approximately 4 000 years, whereas the lakes to be formed in the present sea bay are projected to be sustained for a much longer period (10 000 to 20 000 years).

- Mire stage (Figure 5-8d): In this stage, a mire ecosystem covers the lake basin and a central stream is the only aquatic ecosystem remaining in the object. The fen may gradually be transformed to a raised bog which is disconnected from discharging groundwater. However, this succession is not accounted for in this assessment. Thus, in the context of this assessment, the mire stage is the end-stage of succession, and the stage is assumed to be stable in temperate and periglacial conditions.

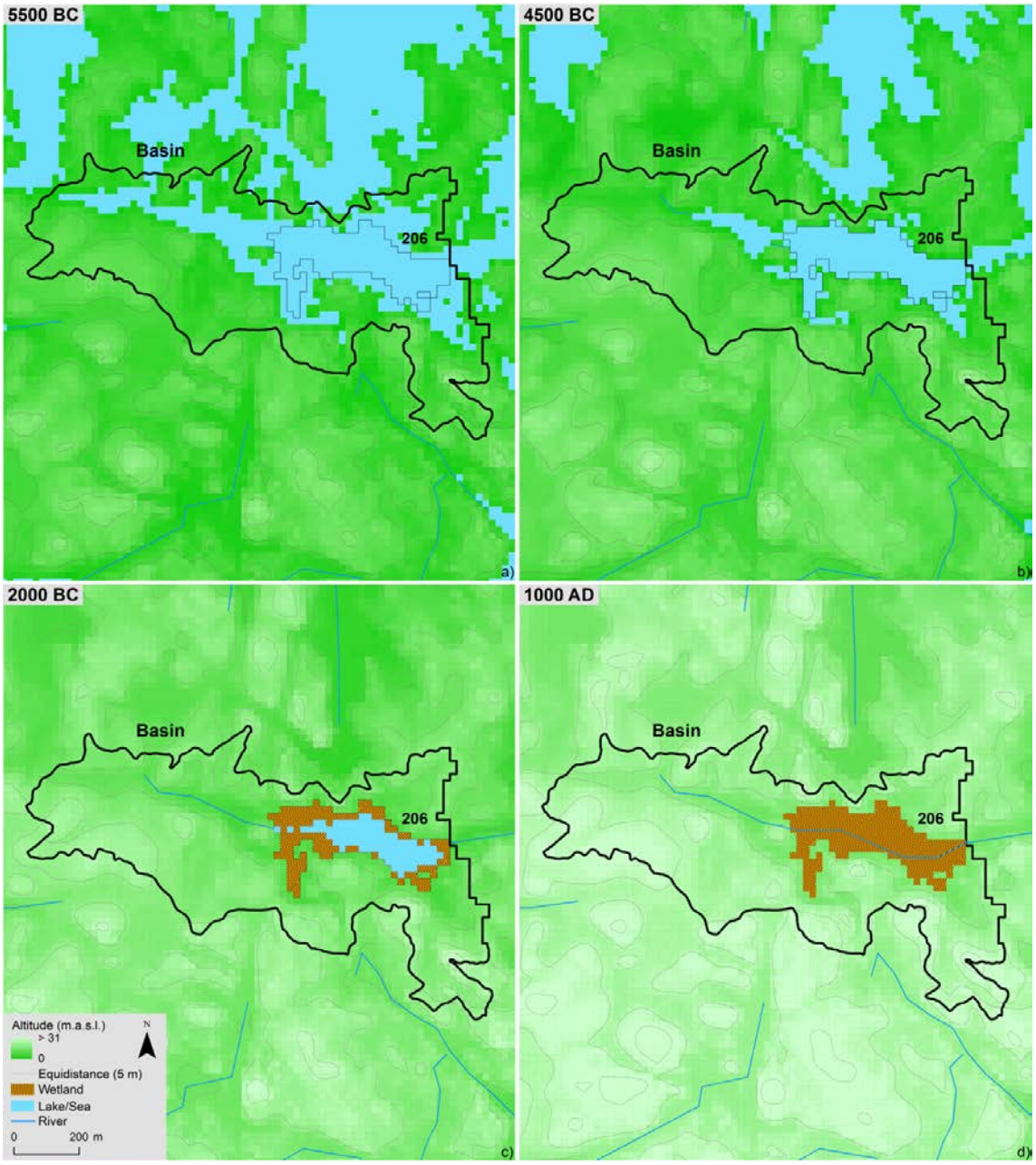

Figure 5-8. *Illustration of the development of biosphere object 206, (a) from a sea basin just before the start of lake isolation, (b) at lake isolation, (c) into a lake, and finally into (d) a mire. The biosphere object is presently agricultural land (Figure 5-2) with the delimitation identical to the mire seen in (d). The black line outlines the original sea basin, which coincides with the watershed for this object. Grey contour lines follow constant elevation, with a five meter difference between lines.*

5.6 Additional biosphere objects

No site has been selected for SFL and Laxemar has been used as an example site in this assessment. In order to extend the analysis to a site with other characteristics than Laxemar, six biosphere objects from the Forsmark site, with a flatter topography and a faster rate of relative sea-level change than the example site Laxemar, were also included (Figure 5-9, see Section 3.6 in Grolander and Jaeschke 2019). The development of these objects (from sea basins to mires) was modelled as part of the SR-PSU safety assessment using the RLDM as described above (Brydsten and Strömgren 2013). How the Forsmark biosphere objects was used in SE-SFL is described in Section 7.3.

The development of biosphere objects in Laxemar described so far can be used in an evaluation of dose at a near-coast location with shoreline regression, where the sea bay and the lake stages are transient. Thus, to evaluate a situation where radionuclides are directly released into the sea for a long period of time, or a situation where radionuclides reach a large freshwater body in a mature terrestrial landscape (e.g. as a consequence of human damming activities), two objects in a permanent sea and three in a permanent lake stage were included in the assessment. In other words, these biosphere objects were modelled using time-independent parameter values. The properties of these biosphere objects were based on the two present sea basins (201 and 208) and Lake Frisksjön (207) (see Section 3.4 in Grolander and Jaeschke 2019 for details).

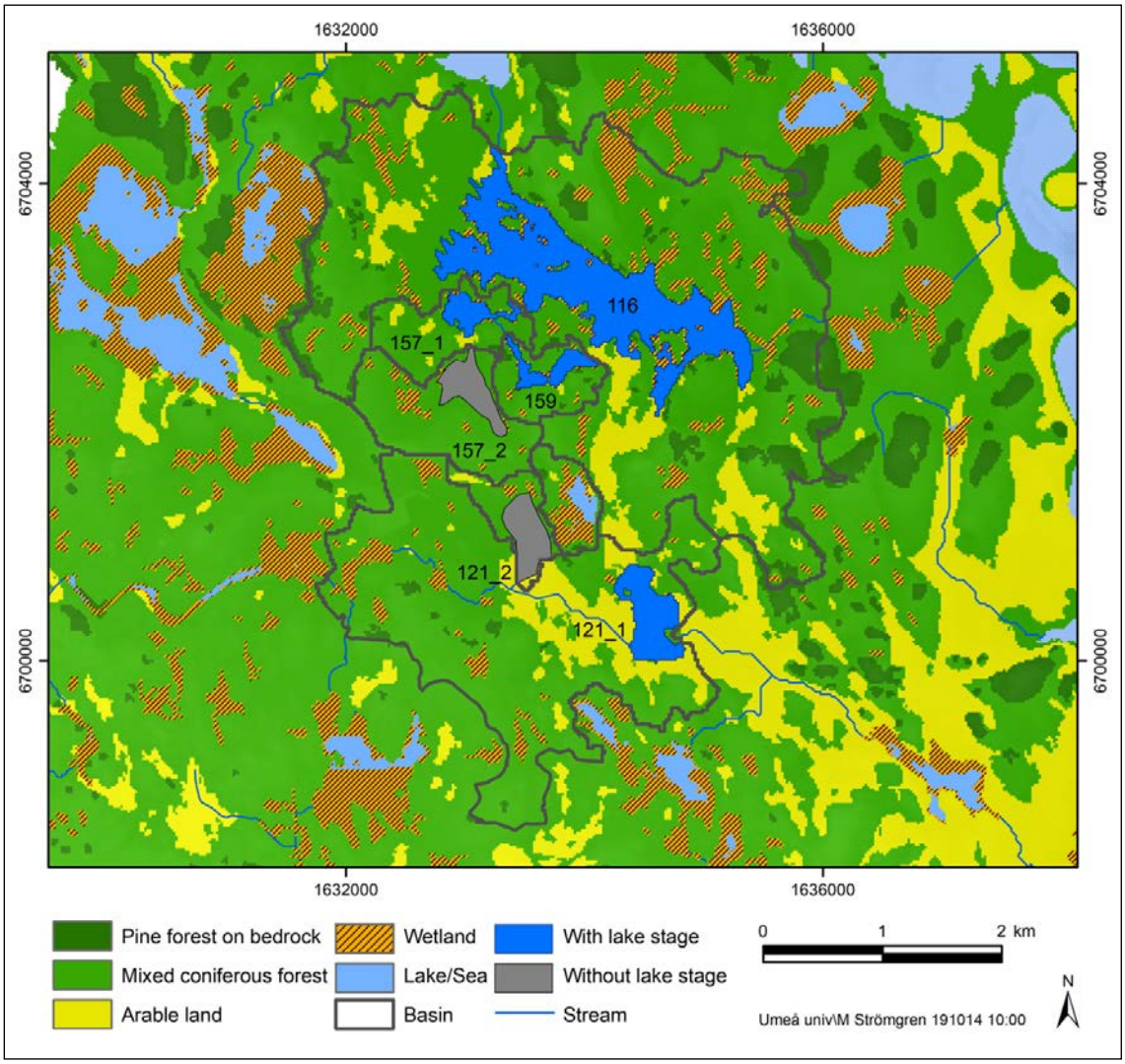

Figure 5-9. *The six biosphere objects in the Forsmark area included in SE-SFL at 4500 AD. All of the objects are presently located under the seabed. Grey biosphere objects will develop into mires when they emerge from the sea, whereas blue objects will go through a lake stage before being infilled with a mire.*

6 FEP handling, exposure pathway analysis, and description of evaluation cases

6.1 Introduction

In this chapter, SKB's work with identifying features, events and processes (FEPs) important for transport and accumulation of radionuclides are described in Section 6.2.1. The incorporation of these FEPs in different parts of the biosphere modelling is also described in Section 6.2.2. Section 6.3 summarises the analysis of (human) exposure pathways and briefly describes the different potentially exposed groups used in the safety evaluation.

6.2 FEP handling

A FEP is a feature, event or process, or other factor, that needs to be considered in an assessment of repository safety or performance. This includes physical features, events and processes that could directly or indirectly influence the release and transport of radionuclides from the repository or subsequent radiation exposure to humans and other organisms (IAEA 2004)[3]. In this section the attention is on the identification and handling of FEPs that are of significance for transport and accumulation of radionuclides in the surface environment.

Ecosystems are dynamic systems that continuously evolve as a result of a complex interplay of internal and external factors linked to each other through many interacting processes. Thus, a systematic approach is needed to identify and analyse the ecosystems likely to receive discharges of deep groundwater, their internal components (where radionuclides may accumulate) as well as the internal and external processes that affect the transport, accumulation and exposure to radionuclides of organisms and humans that live in or utilise the ecosystem. For the time frame of a safety assessment for a geological repository, the effects of landscape development and ecosystem succession on transport, accumulation and exposure also need to be considered, as well as the effects of large-scale climate change. The former two are handled as biosphere FEPs, but the effects of large-scale climate change are handled in separate calculation cases (Sections 7.3 and 7.4).

In the SR-PSU assessment a major effort on the identification and handling of biosphere FEPs was carried out (SKB 2014d, 2015b) and that is largely replicated in this section. The previous evaluation focused on the identification of FEPs relevant to the Forsmark site. Thus, in the present assessment, which has a broader context, the generic biosphere FEP list (SKB 2013a) has been re-evaluated in order to potentially identify additional FEPs relevant to coastal sites in Sweden. To improve the traceability in this chapter, identifiers in SKB's FEP database are given in parentheses when applicable. Thus, biosphere components are identified as CompBio*nn*, processes are identified as Bio*nn*, and variables (or internal conditions) are identified as VarBio*nn* (where *nn* is the number of the FEP).

6.2.1 Identification of components, processes and conditions important for transport and accumulation of radionuclides in the biosphere

An interaction matrix (IM) is a practical tool to display identified components and pathways that may potentially affect radionuclide transport, accumulation and exposure. When constructing an IM, the major components of the system (in the case of the biosphere, an ecosystem), are listed along the lead diagonal of the matrix. The dynamics of the system are then described in terms of processes acting between the major components. Processes are displayed as off-diagonal elements in the matrix and represent direct interactions between two components that will result in a change in at least one

[3] In a broader sense the term can also be used for other factors, e.g. regulatory requirements or modelling issues, which constrain or focus the analysis. In SE-SFL these broader considerations are primarily taken to be a part of the assessment context (Section 2.4).

of the components[4]. Thus, an IM is a transparent and consistent way to identify processes that may be important to consider in a safety assessment. The identified features and processes can then be listed and checked for their potential importance in a specific safety assessment, and FEPs of little or no relevance can be dismissed (Avila and Moberg 1999, Velasco et al. 2006, Harrison and Hudson 2006). The derived FEP list can also be useful when checking how the relevant FEPs have been taken into account in the biosphere assessment (IAEA 2003).

SKB has been working with IMs to describe the effects of a potential release of radionuclides from deep repositories since the early 1990s (Eng et al. 1994, Skagius et al. 1995, Pers et al. 1999). An early version of the IM for the biosphere was presented in 2001 (Kautsky 2001, SKB 2001). SKB produced the IM for the biosphere with the aid of experts from several scientific disciplines including geology, oceanography, hydrology, soil science, chemistry, physiology and ecology. This initial IM has been further developed and updated to reflect the current understanding of ecosystem processes and radionuclide behaviour at the investigated site and to transparently illustrate the dynamics of the biosphere system, based on interactions between physical and biological components (SKB 2013a) The understanding reflected in the IMs has been used to assist the planning of site investigations, the modelling of the site and its development, and the development of the radionuclide transport and exposure model.

In SKB's biosphere IM, ten physical components, two boundary components (geosphere and external conditions), and 50 processes were identified (SKB 2013a). The physical components include four different environmental media namely: regolith (CompBio02), soil water (CompBio03), surface water (CompBio04), and atmosphere (CompBio05). Six organism groups were also identified as being exposed, directly or indirectly, through these media, namely primary producers (CompBio06), decomposers (CompBio07), filter feeders (CompBio08), herbivores (CompBio09), carnivores (CompBio10), and humans (CompBio10).

Not all processes between the components in the IM are expected to be important for transport and accumulation of radionuclides from a repository in the rock, and some processes are traditionally handled outside the biosphere assessment. Thus, of the 50 initially identified processes, 46 were considered relevant and sufficient for assessing the safety of human health and the environment in SE-SFL (Table 7-1). The four processes that were deemed to either have a negligible influence on the assessment results, or were outside the context of the SFL evaluation, were: loading, radiolysis, irradiation and intrusion into the repository (see Section 6.1.2).

To illustrate the nature of these processes, they have been grouped into six broad categories, namely 1) biological processes, 2) processes related to human behaviour, 3) chemical, mechanical and physical processes, 4) transport processes, 5) radiological and thermal processes and 6) landscape development processes. In the text below, these process categories are defined, and key processes are briefly described. In addition, internal conditions (variables) that affect biosphere components and/or processes are also briefly described. A detailed description of all components, processes and conditions is given in SKB (2013a). The rationale for why some of the initially identified biosphere processes are not relevant for a safety assessment for a repository situated in the rock are also given in that report.

Biological processes

Biological processes are those that are dependent on organisms. One pathway of exposure to radionuclides is via intake of water and food, and thus the distribution of biota and food-web interactions are important. In addition, biota may influence the distribution of radionuclides in abiotic pools by, for example, disturbing sediment or affecting water composition. The biotic processes are general and may involve both humans and other organisms. Processes that are strictly related to humans are categorised as processes related to human behaviour (see below). Consumption (Bio02), decomposition (Bio04), excretion (Bio05), food supply (Bio06), growth (Bio07), habitat supply (Bio08), primary production (Bio13), stimulation/ inhibition (Bio14), and uptake (Bio15) are biotic processes that

[4] The matrix is read clockwise, so the off-diagonal elements represent one-directional interactions. To represent the bi-directional effects of a process, it needs to be entered in the two complementary off-diagonal elements on opposite sides of the lead diagonal.

influence the distribution of radionuclides in biota and the transport of radionuclides in food webs. The processes of bioturbation (Bio01) and particle release/trapping (Bio12) are biotic processes that influence the abiotic compartment of the environment. Bioturbation influences the properties of the regolith and thereby affects the accumulation of radionuclides in the regolith. Particle release and trapping influence the amounts of particles in water and air, which is important for the transport of radionuclides adhering to particles.

Processes related to human behaviour

Human behaviour may have a large effect on the biosphere, e.g. by introducing species of biota, elements or radionuclides. Water use (e.g. irrigation) (Bio19), anthropogenic release (e.g. fertilisation) (Bio16), and species introduction/extermination (e.g. cultivation of a drained mire) (Bio18) are important processes related to human behaviour that should be considered in a safety assessment.

Chemical, mechanical and physical processes

Chemical, mechanical and physical processes can influence the state of elements and compounds, which can be important for the transport of radionuclides. For example, in some oxidation states elements are tightly bound to particles, whereas in other conditions they may be easily dissolved and transported by water. Chemical, mechanical and physical processes that should be considered in the safety assessment are, for example, element supply (Bio22), phase transitions (Bio24) and sorption/desorption (Bio27). Element supply is the amount of an element available for use by biota and a low element supply may limit biotic production. The process of phase transition is important, among others, for transport of C-14 from water to air (i.e. degassing). The process sorption/desorption determines whether radionuclides are bound to surfaces or dissolved in water and is crucial to consider when determining the transport and biological availability of radionuclides, and sorption/desorption properties are typically affected by properties of the local environment such as pH and Eh.

Transport processes

Transport processes are those whereby elements and other substances are transported from one point to another in a system. The processes assigned to this category include: convection (Bio32), resuspension (Bio39), relocation (Bio38), deposition (Bio34), import (Bio36) and water saturation (Bio40). The latter two are not transport processes per se but are included in the category because they are the result of, or affect, transport.

Convection concerns the transport of a substance (e.g. water) or a conserved property (e.g. temperature) in a liquid or gas. The process includes advection/dispersion through surface- and groundwater flows, as well as water-mediated element transport (e.g. diffusion and transport through capillary rise). Deep groundwater discharge is especially important for the transport upwards from a repository to the surface environment. Surface water flow is also important for relocation of radionuclides, since relatively fast transport through the landscape can take place in surface waters (as compared with groundwater) and may affect the retention time and dilution of radionuclides in surface water bodies. Advection and diffusion of gas are important for the transport and dilution of C-14.

The processes resuspension, relocation and deposition are important for the transport from sediment to the water column and vice versa. Deposition relates, in addition to sedimentation, also to meteorological precipitation, which is important for water balances and water flows. Import and water saturation are not transport processes that occur within the biosphere system. However, import has been assigned to this category as it is, by definition, the result of transport into the biosphere system (SKB 2013a). Water saturation is strictly speaking storage of soil water (and thus an internal state). However, as it is the result of water transport, and as it affects both advective and diffusive transport of elements, it has been included in the transport category for convenience.

Radiological and thermal processes

Radiological and thermal processes are those processes that concern radionuclides, solar insolation and temperature. Processes that are important to consider in a safety assessment includes: radionuclide release (Bio47), radioactive decay (Bio41), exposure (Bio42), light-related processes (Bio45) and heat-storage (Bio43). Radionuclide release refers to the hypothetical amounts of radionuclides, originating from a repository, that are released from the geosphere to the biosphere per unit time. This is strictly speaking not an internal process of the biosphere system, but it is included as it is a fundamental pre-requisite for the safety analysis. Radioactive decay is a removal mechanism for the released activity and a source for decay products. As the activity resulting from a potential release from a geological repository is expected to be too low for significant detrimental effects on the environment, exposure and the resulting dose are endpoints from dose calculations, rather than internal processes of relevance for transport and accumulation in the biosphere. The handling of exposure is described in Section 6.2. Heat storage has a strong influence on both biotic and abiotic components of aquatic ecosystems, and influences, for example, the distribution of biota, mixing of the water column, and occurrence of ice cover (which in turn limits exchange across the air-water interface). Light-related processes include insolation, light absorption, light reflection and light scattering, which influence primary production in both aquatic and terrestrial ecosystems.

Landscape development processes

For the time frame of a safety assessment for a geological repository the effects of landscape development need to be considered in the safety assessment. The processes included in this category include the following: change in rock-surface location, sea level change and thresholding. The combined effect of the first two processes determines the rate of relative sea-level change and the resulting development of the shoreline. The occurrence and location of topographical thresholds that delimit water bodies (thresholding) is also important. This is because the threshold typically limits the exchange of water for coastal basins and because the position of the threshold, in relation to sea-level, determines when a sea basin is isolated (and becomes a lake).

Internal conditions

The variables representing internal conditions of the biosphere system may have a significant influence on biosphere components and their interactions, and thus their effects on transport and accumulation should be considered (Table 6-1). The geometry (VarBio01) of the landscape and of individual biosphere components affects both transport rates and the potential for accumulation of radionuclides in the environment. It includes, for example, topography and bathymetry, the size of the biosphere object, the thickness of regolith layers and the shape of organisms. Material and water composition (VarBio02, 06) includes chemical composition (e.g. salinity and the concentrations of minerals and nutrients) as well as physical features (such as grain size and porosity). These conditions, together with temperature (VarBio03), strongly influence biogeochemical processes and process rates. The successional stage of a biosphere object (VarBio04) determines the type of ecosystem that occurs at a given time and thereby affects the processes at the site. In addition to natural successional stages (e.g., sea basin, lake or mire) it is also important to consider stages resulting from human activities e.g. agricultural land that originates from draining activities. Radionuclide inventory (Varbio03) is the amounts of radionuclides stored within a physical component. However, in most instances the concentration of radionuclides resulting from a release from a geological repository is expected to be too small to influence processes and reactions in the biosphere (SKB 2013a).

6.2.2 Handling of potentially safety relevant FEPs in the biosphere assessment of SFL

In SKB's previous evaluation of biosphere FEPs 45 (out of 50 examined) processes and variables were identified as relevant and sufficient to consider for a safety assessment of a geological repository (SKB 2013a). The identification of relevant FEPs and model development has been going on in parallel at SKB for the last 20 years and knowledge of important FEPs has been considered in the development and improvements of the radionuclide model for the biosphere. Consequently, many relevant FEPs are included as components and/or processes in the dynamic model (Appendix E in Saetre et al. 2013b). However, most of the FEPs are not explicitly included in the model but are used in the derivation of parameters for the model. To check that the relevant FEPs have been included/represented in an appropriate manner in the assessment, the FEPs were mapped to different modelling activities in the previous safety assessment (SR-PSU, SKB 2015b). This audit has been updated as appropriate for SE-SFL, and the results are summarised in Table 6-1. A check against internationally identified FEPs related to the biosphere was reported in the FEP report for SR-PSU (SKB 2014f) and the re-evaluation of the earlier non-significant FEPs is reported in the **FEP report**.

Overall, the set of biosphere-related FEPs that is listed for the SFL evaluation is very similar to the one used in SR-PSU (SKB 2014f). However, three FEPs were re-evaluated in the present assessment. First, *intrusion by organisms* (Bio09) was excluded, since intrusion of non-human organisms at depths of several 100 m was considered irrelevant. Moreover, intrusion by humans was considered a case of potential future human action (FHA) which is not included in the context of SE-SFL (**Main report**). On the other hand, *movement by organisms* (Bio11) was considered a relevant FEP. This is because filter feeders are present along the Swedish West coast and can dominate the benthic biomass in the central and southern parts of the Baltic Sea (including the example site, Chapter 2). *Change of pressure* (Bio20) was also considered a relevant FEP, as it may have a significant effect on the sea level which in turn influences the rate of water exchange of coastal basins (Engqvist 2010).

The rationale for excluding the other three biosphere processes in the present SE-SFL evaluation is the same as the rationale detailed in SKB (2013a). Briefly, *loading* (Bio23) was excluded as the effect of the weight of regolith layers on the underlying rock was deemed insignificant and the mechanical stress from ice-sheet loading was handled outside the biosphere assessment. *Irradiation* (Bio44) was excluded as the activity concentrations caused by a release of radionuclides from a repository were expected to be too small (resulting in dose rates at least an order of magnitude below those from background radiation) to have significant effects on the mineralogy of the regolith. Similarly, disintegration of molecules (caused by activity from the waste) was not expected to have any significant effects on the water composition in aquatic ecosystems or in regolith. Consequently, *radiolysis* (Bio46) was not considered a relevant FEP for a geological repository. The rationale for excluding these three FEPs is deemed to be appropriate also for the present evaluation.

Table 6-1. Handling of biosphere processes (Bio*nn*) and internal conditions (VarBio*nn*) in the different model activities of the SFL safety evaluation. Aqua, Mire, and Agri represents the three ecosystem types included in the modelling, i.e. aquatic, mire, and agricultural land. K_d/CR represents sorption/desorption parameter values and concentration ratios. X indicates that the process is included in the model. Biosphere system components and external conditions are not included in the table. Processes that were excluded in SR-PSU (Forsmark) but are considered relevant in SE-SFL are listed in *italic*. 1 = The potential movement of water generated by filter feeders is implicitly included in the aquatic part of the biosphere radionuclide model by assuming that the water compartment is well mixed. 2 = The effects of changes in atmospheric pressure on water exchange are accounted for in the oceanographic model, which underpins the parameter describing the water residence time of coastal basins.

Process and Variables		Radionuclide model				Supporting activity						
		Transport modelling			Dose calculations	Landscape modelling	Hydrological modelling	Ecosystem-specific parameters				
FEP ID	Name	Aqua	Mire	Agri	Humans			Aqua	Mire	Agri	K_d/CR	Human
Biological processes												
Bio01	Bioturbation	X		X				X		X		
Bio02	Consumption	X	X		X	X		X	X	X		X
Bio03	Death	X	X			X		X	X			
Bio04	Decomposition	X	X	X		X		X	X	X		
Bio05	Excretion	X	X					X	X	X	X	
Bio06	Food supply				X			X	X	X		
Bio07	Growth					X				X		
Bio08	Habitat supply				X	X		X	X	X		X
Bio10	Material supply				X	X		X	X	X		X
Bio11	*Movement*	X[1)]										
Bio12	Particle release/ trapping	X	X					X	X	X		
Bio13	Primary production	X	X			X		X	X	X		
Bio14	Stimulation/ inhibition					X		X	X	X		
Bio15	Uptake	X	X		X			X	X	X	X	X
Processes related to human behaviour												
Bio16	Anthropogenic release			X	X					X		X
Bio17	Material use			X	X					X		X
Bio18	Species introduction/ extermination				X			X		X		
Bio19	Water use			X	X							X
Chemical, mechanical and physical processes												
Bio20	*Change of pressure*						X[2)]					
Bio21	Consolidation			X						X		
Bio22	Element supply					X		X	X	X	X	
Bio24	Phase transitions	X	X	X			X	X	X	X		
Bio25	Physical properties change	X	X	X			X	X	X	X		
Bio26	Reactions	X	X	X				X	X	X	X	
Bio27	Sorption/ desorption	X	X	X	X						X	
Bio28	Water supply				X	X	X					X
Bio29	Weathering							X	X	X	X	
Bio30	Wind stress					X		X	X	X		

Process and Variables		Radionuclide model				Supporting activity						
		Transport modelling			Dose calculations	Landscape modelling	Hydrological modelling	Ecosystem-specific parameters				
FEP ID	Name	Aqua	Mire	Agri	Humans			Aqua	Mire	Agri	K_d/CR	Human
Transport processes												
Bio31	Acceleration						X					
Bio32	Convection	X	X	X			X	X	X	X		
Bio33	Covering	X	X			X	X	X	X			
Bio34	Deposition	X	X			X	X	X	X			
Bio35	Export	X	X	X		X	X					
Bio36	Import	X	X	X		X	X					
Bio37	Interception			X			X			X		
Bio38	Relocation			X		X				X		
Bio39	Resuspension	X			X	X		X				
Bio40	Water saturation					X	X			X		
Radiological and thermal processes												
Bio41	Radioactive decay	X	X	X	X							X
Bio42	Exposure				X							X
Bio43	Heat storage							X	X			
Bio45	Light related processes							X	X	X		
Bio47	Radionuclide release	X	X	X								
Landscape development processes												
Bio48	Change in rock surface location					X	X					
Bio49	Sea level change					X	X					
Bio50	Thresholding					X	X					
Variables (Internal conditions)												
VarBio01	Geometry	X	X	X	X	X	X	X	X	X		X
VarBio02	Material composition	X	X	X		X	X	X	X	X	X	
VarBio03	Radionuclide inventory	X	X	X	X							
VarBio04	Stage of succession	X	X	X	X	X	X	X	X	X		X
VarBio05	Temperature	X	X	X	X	X	X	X	X	X		
VarBio06	Water composition	X	X	X	X			X	X	X	X	

6.3 Exposure pathway analysis and potentially exposed groups

A comprehensive exposure pathway analysis has been conducted for SR-PSU (SKB 2015b). In that analysis, the approach covered sustainable land use that has been typical for Northern Europe. This exposure pathway analysis is considered valid also for SE-SFL and should be applicable to all potential locations along the Swedish coast.

In the SR-PSU analysis, potential exposure pathways relevant for the long-term safety of a geological disposal facility, focusing on human exposure, were identified (Figure 6-1). The potential exposure pathways were further assessed to determine key pathways to include in an assessment of long-term safety. The methodology applied was based upon the exposure pathway evaluation presented in ATSDR (2005). For a geological disposal facility at the site, terrestrial environments (such as agricultural land and mires) and aquatic environments (such as lakes, rivers and the sea) may receive repository-derived radionuclides. Environmental media in these environments considered in the analysis were atmosphere (indoor or outdoor), regolith, water (well and surface waters) and biota. Three modes of exposure were identified as relevant to be included in a safety assessment – ingestion, inhalation and external irradiation.

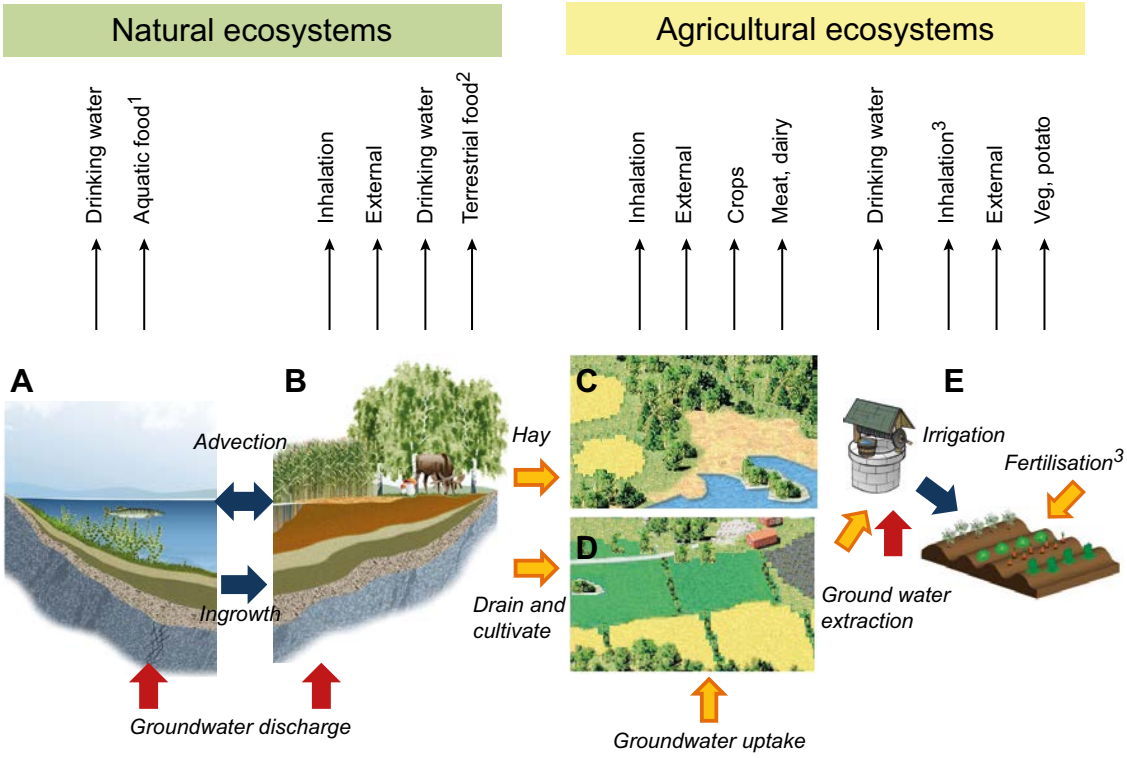

Figure 6-1. *Exposure pathways included in the dose calculations for potentially exposed groups using natural resources and/or living in biosphere objects. Hunter-gatherers use natural aquatic (A) and mire (B) ecosystems. The other three potentially exposed groups represent different uses of arable land, namely infield-outland agriculture (C), draining and cultivating the mire (D) and small-scale horticulture on a garden-plot (E). Bold arrows represent input of radionuclides from the bedrock (red), from natural ecosystems or deep regolith deposits (orange), or water-bound transfer of radionuclides within the biosphere (blue). The thin arrows (top) represent exposure routes: 1 = fish and crayfish, 2 = game, berries and mushroom, 3 = Combustion of biofuel results in exposure of radionuclides from inhalation and fertilisation. The exposed groups are described in Section 6.3.*

The modes of exposure were combined with the receptors in the environment to establish a comprehensive set of cases (exposure route cases) considered potentially relevant to safety (SKB 2015b). In total, 22 exposure route cases were identified and mapped to one (or more) exposed groups (Table 6-2). Of these exposure routes, four (external exposure from outdoor vegetation, external exposure from sediment, and ingestion of inorganic and organic soil, respectively) were evaluated with assessment-specific data in SR-PSU (Section 10.10 in SKB 2014d) and showed to give only insignificant contributions to dose. In SE-SFL these exposure routes were re-evaluated (analysis described, and results reported Appendix B). It was shown that none of them was quantitatively important for radionuclides that contribute to the dose from the two waste vaults, and consequently these pathways were also excluded in SE-SFL.

Table 6-2. Potentially important exposure route cases and the corresponding potentially exposed groups (HG = hunter-gatherers, IO = infield-outland farmers, DM = drained-mire farmers, GP = garden-plot households). 1 = Indirect exposure routes are those that can lead to transfer of radionuclides from one environmental medium to another as a result of human activities. 2 = relative importance determined to be insignificant, and route excluded from assessment (see Appendix B).

Environmental medium	Exposure route case	Potentially exposed group	Comment
Atmosphere – outdoor	Inhalation of gases during breathing	HG, IO, DM, GP	Occurs during all outdoor activities.
	Inhalation of dust during breathing	HG, IO, DM, GP	Occurs during all outdoor activities.
Regolith – soil (inorganic)	Inadvertent soil ingestion[2]	GP	Occurs as a consequence of outdoor activities.
	External irradiation from the ground when staying outdoors	IO, GP	Occurs during all outdoor activities where there is soil.
	External irradiation from sediments[2]	HG	Occurs during outdoor activities such as fishingor bathing.
Regolith – peat	Inadvertent peat ingestion[2]	DM	Occurs as a consequence of outdoor activities.
	External irradiation from the ground when staying outdoors	HG, IO, DM	Occurs during all outdoor activities where there are peat soils.
	Indirect[1] – contamination of the environment	GP	Inhalation of gas and dust originating from the burning of peat as biofuel.
	Indirect[1] – contamination of soil	GP	Burning of peat as biofuel, and depositing ashes as fertilisers.
Well water	Ingestion of well water	IO, DM, GP	Drinking water from a dug well or a bedrock well.
	Indirect[1] – contamination of crops and soils	GP	Irrigation of small-scale horticulture.
	Indirect[1] – contamination of fauna that drinks water	IO, DM	Drinking water for livestock.
Surface water	Ingestion of water	HG, IO, DM, GP	Drinking water from a stream or a lake.
	Indirect[1] – contamination of crops and soils	GP	Use of surface water for irrigation.
	Indirect[1] – contamination of fauna that drinks water	IO, DM	Livestock drink or are watered with surface water.
Flora	Ingestion of crops, berries, mushrooms	HG, IO, DM, GP	Fundamental source of foodstuffs.
	External irradiation outdoors from vegetation[2]	HG	Exposure to radionuclides in the standing vegetation.
	Indirect[1] – contamination of the environment from burning wood fuel	GP	Inhalation of gas and dust originating from the burning of wood as biofuel.
	Indirect[1] – contamination of the environment by ash and manure	IO, GP	Burning of wood as biofuel, and depositing ashes as fertilisers. Depositing manure as fertiliser.
	Indirect[1] – contamination of soils by fertilisation with aquatic flora	GP	Fertilisation with seaweed.
Fauna	Ingestion of terrestrial food	HG, IO, DM	Fundamental source of foodstuffs.
	Ingestion of aquatic food	HG	Eating fish.

Four potential potentially exposed groups were included in the analysis. These groups were considered credible to use as bounding cases for the most exposed groups with respect to exposure through all major exposure pathways in SR-PSU (SKB 2015b). When characterising the most exposed groups, physical and biological characteristics of the biosphere objects, human requirements for energy and nutrients, and habits from historical and present societies were considered (Saetre et al. 2013a). The four potentially exposed groups identified were the following:

Hunter-gatherers (HG) – A hunter and gatherer community using the undisturbed biosphere for living space and food. The major exposure pathways are from foraging discharge areas in the landscape (fishing, hunting, and collecting berries and mushrooms), and from drinking water from surface water (streams or lakes). Land use and habits of a typical hunter-gatherer community have been extracted from historical records, and the group is assumed to be made up of 30 individuals that forage an area of approximately 200 km^2.

Infield-outland farmers (IO) – Self-sustained agriculture in which infield farming of crops is dependent on nutrients from mires (outland). Radionuclides in wetland hay reach the cultivated soil through fertilisation with manure. The major exposure pathways are from growing food and raising livestock, and from drinking water from a dug well (or from surface water). A self-sufficient community of infield-outland farmers is assumed to be made up of 10 persons. A wetland area of 0.1 km^2 (10 ha) is needed to supply winter fodder to the herd of livestock corresponding to the amount of manure needed to support infield crop production for this group.

Family farmers (DM/Agri) – Self-sustained agriculture on a former lake or wetland, where both crops and fodder are cultivated on organic soils. This exposed group is considered for two periods; DM refers to conditions directly after draining, whereas Agri refers to conditions after prolonged cultivation. The radionuclides reach the cultivated soil through groundwater uptake. For early cultivation (DM) radionuclides that have accumulated for an extended time prior to drainage is also accounted for. The major exposure pathways are from growing food and raising livestock, and from drinking water from a dug well (or from surface water). A self-sufficient community of drained-mire farmers is assumed to be made up of 10 persons. A wetland area of 6 ha is needed to support food production for this group, assuming a level of technology similar to that from the turn of the nineteenth century.

Garden-plot households (GP) – A household that is self-sustained with respect to vegetables and root crops produced through small-scale horticulture. Radionuclides reach the cultivated soil through fertilisation (with algae or biomass ash) and irrigation. The major exposure pathways are from growing food and from drinking water from a dug well (or from surface water). A garden-plot household is assumed to be made up of five persons and a 140 m^2 area garden plot is assumed to be sufficient to support the family with vegetables and root crops. The productivity and diet for this group have been determined from present habits.

The HG community uses undisturbed ecosystems, whereas the other three groups actively cultivate the land. For HG and DM/Agri exposure occurs within the boundaries of the biosphere object. However, for the IO and GP groups, exposure occurs due to utilising resources from the biosphere object (e.g. organic fertilisers, biofuel or irrigation water) and the location of the exposed area is not constrained by the boundaries of the biosphere object.

During marine conditions, natural ecosystems can be used for food gathering and as a source for organic fertilisers, but no cultivation of the biosphere object is possible. The possibility to use the biosphere object for agriculture and water supply increases when the shoreline has passed. Hay and surface waters can be used when an object has been isolated from the sea. Wells can be dug, and mires can be drained when the risk of salt water intrusion has been reduced, which is assumed to occur when the land is at least 1 m above sea level. For all groups the annual dose from exposure are calculated as an average over a period of 50 years (Section 2.4.1). Doses are evaluated continuously over the assessment period, but for the DM group doses arise from an event (the draining and cultivation of a natural wetland). This event is cautiously evaluated for all times when cultivation is feasible (discussed in 16.3.4).

It follows from the description above that the four potentially exposed groups represent four different types of future land use. In the remaining of the report, especially in the description of modelling results in Chapter 9, the groups are therefore frequently referred to as “land use variants”. However, for the present discussion of exposure and the definition of calculation cases, the nomenclature of the potentially exposed group is retained.

7 Description of the biosphere in selected evaluation cases

7.1 Introduction

In SE-SFL evaluation cases were defined to assess the conditions under which the repository concept has the potential to fulfil regulatory criteria with respect to radiological safety or to assess the sensitivity of assessment endpoints to selected uncertainties (Section 2.4.7 in this report and Section 2.5.8 in the **Main report**). An evaluation case in the SE-SFL safety analysis methodology loosely corresponds to a scenario in a full safety assessment. In SE-SFL a broader approach to the selection of calculations was applied, as the objective of SE-SFL also includes inputs to the further development of the repository concept and the site-selection process. It can also be noted that the evaluation cases are not directly related to the scenario categories (main scenario, less probable scenarios and residual scenarios) defined in the SSM guidance.

In total, fourteen evaluation cases were selected in SE-SFL. Three evaluation cases were linked to the reference evolution, namely the *present-day*, the *increased greenhouse effect* and *the simplified glacial cycle* evaluation cases. The *present-day* evaluation case constitutes the base case for the transport and dose calculations in SE-SFL. It is highly stylised and thus allows for a straight-forward evaluation of the repository performance given postulated or perturbed conditions in the waste vaults and the geosphere. In the other two reference cases, effects of altered climate conditions and large-scale landscape evolution were evaluated.

Three cases were designed to examine the effects of conditions affected by the repository location, namely: the *alternative regional climate*, the *alternative discharge area*, and the *initially submerged conditions* evaluation cases. In addition, one case evaluated the potential dose resulting from extracting water from a *drilled well*. Four of the seven remaining cases examined the effects of alternative assumptions with respect to repository characteristics, and the last three evaluated effects of alternative geosphere conditions. More detailed information on the selection of the evaluation cases can be found in the SE-SFL **Main report** (Section 2.5.8), whereas technical information with respect to assumptions and technical handling of the calculations are described in the **Radionuclide transport report** (Sections 5, 6 and 7).

In total there were six evaluation cases where biosphere conditions were altered as compared with present-day conditions (Table 7-1). This chapter describes the biosphere conditions postulated in these cases, and in the base case. The present conditions of discharge areas in Laxemar (and their expected development under temperate conditions) are described in Chapter 5, and the data selection process for present conditions is described in detail in Chapter 10.

Table 7-1. Short description of biosphere conditions in SE-SFL evaluation cases. Biosphere object refers to the area where the release was discharged to the surface, Ecosystem to the state or states of the area during the simulation and Hydrology indicates if groundwater flows have been modified in the calculations (as compared with the *present-day* evaluation case). Succession indicates whether the ecosystems states were modelled in sequence (if not, ecosystem properties are time-independent). Abbreviations of potentially exposed groups are the same as in Table 6-2. Lx and Fm refers to Laxemar and Forsmark, respectively. Note that most ecosystem parameter values were the same in all evaluation cases (e.g. K_d and *CR* values). However, some ecosystem parameters were adjusted for a warmer climate (1) and some were adjusted for colder conditions (2) (see text for details).

Evaluation case	Short description	Geosphere release	Biosphere object	Ecosystem	Hydrology	Succession	Pot. exp.group
Present-day	Present-day conditions	Base case	206	Mire, Agri	Present day	No	HG, IO, DM, GP
Alternative discharge area							
Without landscape development	Effects of ecosystem type, and object properties	Base case	Nine in Lx, Six in Fm	Sea, Lake, Mire, Agri	Present day (object specific)	No	HG, IO, DM, GP
With landscape development	Effects of relative sea-level change and succession	Base case	Three in Lx, Six in Fm	Sea, Lake, Mire	Function of sea depth (object specific)	Yes	HG, IO, DM, GP
Increased greenhouse effect	Effects of global warmingand irrigation	Base case	206	Mire[1], Agri[1]	Global warming ± irrigation	No	HG, IO, DM, GP
Alternative regional climate	Effects of different regional cli-mate	Base case	206	Mire, Agri	Regional variation	No	HG, IO, DM, GP
Initially submerged conditions	Effects of initially submerged conditions	Function of sea depth	206	Sea, Lake, Mire	Function of sea depth	Yes	HG, IO, DM, GP
Simplified glacial cycle	Effects of perma-frost and passage of inland ice	Function of ice-front and sea depth	206, 207, 201	Sea, Lake[2], Mire[2]	Talik, function of ice-front and sea depth	Yes	HG, IO, DM, GP
Drilled well	Drilled well for drinking and small-scale irrigation	Base case	geosphere well	Kitchen garden	Present day Lx	No	GP

7.2 Present-day (base case)

The *present-day evaluation case* constituted the base case for the radionuclide transport and dose calculations in SE-SFL (**Main report**, Section 7.4). It assumes constant external conditions prevail during the entire analysis period of 1 million years after repository closure. In this section the detailed assumptions behind this calculation case are listed with respect to external conditions, the link between the geosphere and the biosphere, landscape geometries, surface hydrology, ecosystem parameters and potentially exposed groups.

7.2.1 Climate conditions

Present-day climate conditions were assumed to prevail during the entire analysis period (see **Climate report** for a detailed description). The present-day climate was represented by the 30-year average for the normal period (1961–1990). This means that the annual average temperature was 6.4 °C and the annual average precipitation was 553 mm (Chapter 3 in the **Climate report**).

7.2.2 Geosphere-biosphere link

The results of a set of modelling realisations of groundwater flow in the bedrock surrounding the repository in Laxemar (Joyce et al. 2019) indicate that the majority of the total potential release (> 60 %) from SFL would typically end up underneath (or close to) one of three biosphere objects (204, 206 or 210, see Section 5.3). Object 206 was the object that received the largest fraction of particles discharged from the repository (43–74 %) in three of five realisations of the stochastic fracture networks, and, therefore, as a simplification the full radionuclide release from SFL was assumed to be discharged into biosphere object 206. The importance of this assumption was evaluated in the *alternative discharge area evaluation case*.

7.2.3 Landscape geometries and regolith properties

As the release was directed to a terrestrial ecosystem clearly located above the sea level, the ongoing shoreline migration and landscape development were not considered in this evaluation case. That is, the physical and biological properties of the ecosystems were assumed to be constant during the entire analysis period of 1 million years after repository closure. Consequently, the present regolith depth was used for the agricultural ecosystem throughout the simulations (Chapter 5, and details in Nyman et al. 2008).

An alternative state of the discharge area was also evaluated in the base case, namely a mire ecosystem that could have developed in the lake basin of 206 without human intervention. The regolith stratigraphy of this mire ecosystem was set to reflect the state of mature fen. As the area is presently cultivated, successional development of the lake that historically occupied object 206 was simulated and the end stage was used to characterise the mature fen (Chapter 5, and details in Grolander and Jaeschke 2019).

7.2.4 Surface hydrology

The groundwater flows are the main driver of radionuclide transport, and these were derived from a water balance representing the present conditions in object 206 (Chapter 5). Separate conceptual water-balance models and descriptions of the regolith profile were used for the agricultural field and the mire, respectively (Figure 8-3). Thus, the upper layers of cultivated soil were assumed to be unsaturated and drained by ditches surrounding the arable land. In the mire ecosystem, the upper peat layer was assumed to be saturated and excess ground and surface water was discharged into a central stream. Effects of the ecosystem state on groundwater discharge from the bedrock and local catchment were assumed to be small and were not explicitly considered. However, the vertical discharge profile was assumed to be affected by local watershed characteristics and regolith depth (which differs between the two ecosystem states) and percolation was described by different functions in the agricultural and mire systems (Chapter 5 in Grolander and Jaeschke 2019).

7.2.5 Ecosystem properties

In the recent safety assessment of the SFR repository and its extension (SR-PSU), ecosystem properties reflected the present and future conditions of Forsmark. The difference in regional climate between Laxemar and Forsmark is limited. (For example, Laxemar is characterised by a 1.4 °C warmer average annual temperature and receive only 53 mm more annual precipitation as compared with Forsmark, Chapter 3 in the **Climate report**). Thus, most parameter values derived for terrestrial ecosystems in Forsmark were also judged relevant for the SFL safety evaluation. However, a few terrestrial ecosystem and element-specific properties were updated in SE-SFL to reflect the conditions in Laxemar. In addition, a few new parameters were introduced in SE-SFL due to model-updates (Chapter 10).

7.2.6 Potentially exposed groups

The land-use and productivity of a family farm was assumed for continuous cultivation of the object (Agri). Three land-use variants were assessed for potential exposure from a mire ecosystem, namely hunter and gatherers (HG), infield-outland farmers (IO), and a household with a garden-plot (GP). Potential exposure from draining and cultivating the mire for 50 years was also assessed (DM) with the land-use of a family farm. Exposure routes included; ingestion of food and drinking water, inhalation from breathing air and direct external radiation (see Section 6.3 for details).

7.3 Alternative discharge area

The main objective of the *alternative discharge area evaluation case* was to examine how annual doses are affected by properties of the discharge area and landscape development, and to what extent the simplifications made in the *present-day evaluation case* influence the projected doses (**Main report**, Section 8.5.2). The case considered multiple types of ecosystems and their succession in response to relative sea-level change and shoreline migration. The selected biosphere objects also varied with respect to geometrical characteristics, regolith stratigraphy, and associated groundwater flows. In the discharge area evaluation case, a main objective was to analyse how doses are influenced by object properties for possible biosphere objects at a coastal site in Sweden.

For ease of presentation, the evaluation case was divided into two variants. In the first variant, biosphere objects with a time-independent (or stationary) ecosystem state (i.e. sea bay, lake, mire or agricultural land) were used for the evaluation. In the second variant, the effects of landscape development and succession were examined by describing development from sea bays, through isolation of lakes and development of mires. The effects of landscape developments on doses in biosphere object 206 were also analysed in the *glaciation* and the *initially submerged* evaluation cases.

For this evaluation case, biosphere objects from both Laxemar and Forsmark were used. All the Laxemar biosphere objects were likely discharge areas for deep groundwater, and thus the between-object variation to some extent illustrates the potential effect of alternative locations of the SFL repository within the Laxemar area (or uncertainties in the transport pathways from the repository to the surface system). The topography is flatter in Forsmark, and the rate of relative sea-level change is faster. By including biosphere objects from Forsmark potential effects of landscape relief can be examined (Figure 5-9).

7.3.1 Climate conditions

In the *alternative discharge area evaluation case* the same climate conditions as in the *present-day evaluation case* were assumed.

7.3.2 Geosphere – biosphere link

The size and temporal pattern of the radionuclide release from the geosphere into the lowest regolith layer (till) in each of the investigated biosphere objects (see next section) were the same as in the release into object 206 in the *present-day evaluation case*.

7.3.3 Landscape geometry and regolith properties

Time independent ecosystems

As in the *present-day evaluation case*, the ongoing shoreline displacement and landscape development was not addressed in the simulation of the time-independent ecosystems. That is, constant conditions were assumed for the entire assessment period of 1 million years.

Nine potential discharge areas of deep groundwater (i.e. biosphere objects) in Laxemar and six areas in Forsmark were used in the analysis. The selected biosphere objects vary with respect to geometrical properties (object and watershed surface area), the depths of water, the regolith stratigraphy, and associated groundwater flows (see Section 7.3.4).

The Laxemar biosphere objects were five present agricultural ecosystems (objects 204, 206, 210, 212 and 213), one mire (203), one lake (207), and two coastal bays (208 and 201, Figure 5-2). The five agricultural objects and the three aquatic objects were also described as mire ecosystems (that could have or will develop in the absence of human intervention). The coastal bays were selected to illustrate consequences of a continuous release to the sea. To broaden the variation, object 201 was described in an earlier successional stage (9500 BC), representing a more open sea basin with a higher rate of water exchange.

Moreover, to evaluate a situation where radionuclides reach a freshwater body in a mature terrestrial landscape, projected lakes at isolation of objects 201 and 208 were also used as time-independent ecosystems. This represent artificial lakes (or reservoirs) created by future inhabitants for water management, water supply and/or amenity and ensures that peak doses in aquatic ecosystems would not be missed if lakes were only included in the early period of landscape development simulations. The parameters for water depth, water volume, rates of sedimentation and resuspension for the time-independent aquatic ecosystems were taken from the Regolith Landscape Development Model (RLDM) for the specified time slice (Chapter 3 in Grolander and Jaeschke 2019).

Biosphere objects with landscape development

The effect of landscape development on potential dose was examined by assessment of three Laxemar objects and six Forsmark objects. The succession of discharge areas from a sea basin, through a lake-mire system to a mature mire was described with the RLDM (see Chapter 3 in Grolander and Jaeschke 2019 and references therein for details and methods). Properties that change in response to shoreline regression and ecosystem succession include the areas of the aquatic and terrestrial parts of the object, depth of the waterbody and surface water turnover time, thickness of regolith layers and groundwater flows.

The simulation of the Laxemar objects starts with present conditions (objects 201, 207 and 208, Figure 5-2). The Forsmark objects are presently submerged. To represent potential discharge areas for a repository located on land, the projected shoreline for year 4400 AD was used at the start of the assessment. At this time, the biosphere objects are just about to be isolated from the sea (object 157_1 and 116) or have recently become isolated lakes (121_1, 159) (Figure 5-9). Two of the mires develop on a hill slope, rather than in a lake basin, and are mires at the start of the simulation (121_2 and 157_2).

7.3.4 Surface hydrology

The estimated residence time of water in coastal basins (or the average age) was calculated with the CouBa model (Engqvist 2010), and water residence times for past and future open coasts were estimated from present day open coastal conditions. Thus, for each sea basin, the water residence time was expressed as a time series given the historic and future projected changes in relative sea-level (Section 5.2 in Grolander and Jaeschke 2019).

The surface hydrology in biosphere objects is influenced by local topography, by thicknesses and hydraulic properties of regolith layers, and by precipitation/evapotranspiration. Groundwater flows at Forsmark and Laxemar have previously been simulated with the MIKE-SHE tool, and the results summarised as water balances at the level of individual biosphere objects (Chapter 5 and Werner et al. 2013).

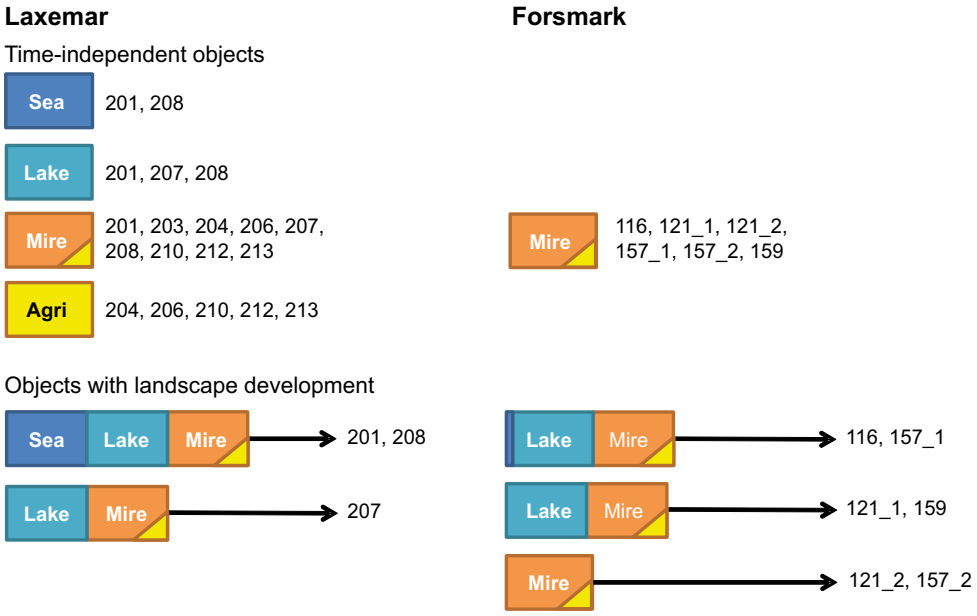

Figure 7-1. *Overview of Laxemar (left side) and Forsmark (right side) biosphere objects included in the two variants of the alternative discharge area evaluation case. Twenty-five combinations of biosphere objects and ecosystem types were used in the time independent variant of the assessment, whereas landscape development was explicitly modelled for nine objects. In the variant with landscape development, the lake stage describes a developing lake-mire system, and the endpoint of this stage was reached when mire ingrowth was complete. The yellow triangle indicates that the consequences of draining and cultivating the lake-mire system were also evaluated. The numbers are the identifiers of the biosphere objects.*

MIKE SHE water balances in Laxemar were available only for present conditions. Therefore, to extrapolate ground and surface water fluxes for all successional stages, stylised water balance models were developed and applied in SE-SFL (Section 8.4.2 and detailed descriptions in Chapter 5 of Grolander and Jaeschke 2019). For consistency, hydrological flows for all objects and ecosystem stages in Laxemar were calculated with this method.

For Forsmark, MIKE SHE water balances were available for each of the three natural successional stages (sea, lake-mire and mire) for all six biosphere objects (Werner et al. 2013), and consequently the parameters previously derived in SR-PSU (Werner et al. 2013, Grolander 2013) were also used in this evaluation. In the landscape development variant, linear interpolation was used to describe the surface hydrology in the period between the sea and lake stages.

7.3.5 Ecosystem properties

Parameters for terrestrial ecosystems from the *present-day evaluation case* were used for all objects in the *alternative discharge area calculation case*. Most SR-PSU parameter values derived for aquatic ecosystems in Forsmark (Grolander 2013) were judged to be relevant for the SFL safety evaluation. However, the values for a few aquatic ecosystem and element specific parameters were updated in SE-SFL to reflect the conditions in Laxemar (Section 10.3.5). Due a change in the description of release of chloride upon mineralisation (Section 8.4.1), one new aquatic parameter was also introduced in SE-SFL (Section 10.3.5).

7.3.6 Potentially exposed groups

The land-use variants from the *present-day evaluation case* were used also in this evaluation case. That is, a family farm was used to evaluate exposure from the continuously cultivated land (Agri). The potential exposures from a mire ecosystem were evaluated for the exposed groups: hunter and gatherers (HG), infield-outland farmers (IO), a household with a garden-plot (GP), and a family farm cultivating the drained mire (DM). Time-independent aquatic ecosystems (sea bays and lakes) were evaluated for hunters and gathers only. In the variant with landscape development, all the land-use variants above were evaluated available (see Section 6.3).

7.4 Increased greenhouse effect

The *increased greenhouse effect evaluation case* was designed to illustrate the potential effects of warmer climate conditions on post-closure safety (**Main report**, Section 8.6.1). Climate conditions due to an increased greenhouse effect were derived from temperature and precipitation changes expected according to IPCC's intermediate emissions scenario RCP4.5. Two variants were evaluated; in the first, crop water deficit was covered by an increased uptake of groundwater through capillary rise (variant A), whereas in the second variant it was covered by irrigation with surface water (variant B).

7.4.1 Climate conditions

In this case, temperate climate conditions with a considerably warmer and somewhat wetter climate than at present were assumed during the first 23 000 years after repository closure. After this initial period the climate returned (instantaneously) to present-day conditions, which prevailed for the remaining part of the assessment period (one million years). The warmer climate case corresponds to the IPCC intermediate emissions scenario RCP4.5 in which the atmospheric CO_2 concentration stabilises at 543 ppm. This elevated CO_2 level corresponded to a mean annual temperature and an annual precipitation that are 2.6 °C and 12 % higher than present conditions. Taking the projected change in near-surface temperature and precipitation during the central vegetation season (June to August) for RCP4.5, western Poland was identified as a reasonable regional analogue to Laxemar (Appendix C in the **Climate report**).

7.4.2 Geosphere – Biosphere link

Radionuclides from the repository were discharged to the same biosphere object as in the main calculation case, namely biosphere object 206. The near-field and geosphere conditions were not expected to be significantly affected by the increased greenhouse effect (Section 5.3.2 in the **Radionuclide transport report**). Thus, the size and temporal pattern of the geosphere release into the lowest regolith layer (till) was the same as in the release into object 206 in the *present-day evaluation case*.

7.4.3 Landscape geometries and regolith properties

As in the *present-day evaluation case*, landscape development was not considered. That is, the geometry and stratigraphy of the discharge area did not change, and no biological succession was accounted for during the entire assessment period of 1 million years. Dose consequences were examined in two variants of the biosphere object, namely a continuously cultivated field and a mire ecosystem, both located in the original lake basin.

7.4.4 Surface hydrology

The combined effect of increased temperature and temperature is expected to result in a decrease of groundwater discharge from the bedrock (−8.3 %), and in a lower runoff (−20 %) (Losjö et al. 1999, Grolander and Jaeschke 2019). In the evaluation case, these changes were projected to propagate through the regolith profile. Thus, the discharge through the lower regolith profile (RegoLow, RegoGL and RegoPG) was expected to decrease by approximately 10 %, whereas the reduction of discharge in the upper peat of the mire was expected to be similar to that of the net precipitation and runoff, i.e. −18 % (Figure 7-2, details in Grolander and Jaeschke 2019).

7.4.5 Ecosystem properties

Most properties of mires and agricultural ecosystems were expected to be only marginally affected by a moderately warmer climate. However, in a warmer climate where increased precipitation does not compensate for higher evapotranspiration, the plant water deficit during the vegetation period was expected to increase. An increased demand for water could either fully or partly be supplied by an increased groundwater uptake through capillary rise, and/or it could be covered by irrigation. Using western Poland and a dry year in southern Sweden as reasonable climate analogues, the water deficit was projected to increase by 30 % (Grolander and Jaeschke 2019). Moreover, it was cautiously assumed that the deficit was fully compensated by radionuclide-containing water, either from groundwater (variant A) or from irrigation with surface water (variant B) (Figure 7-2).

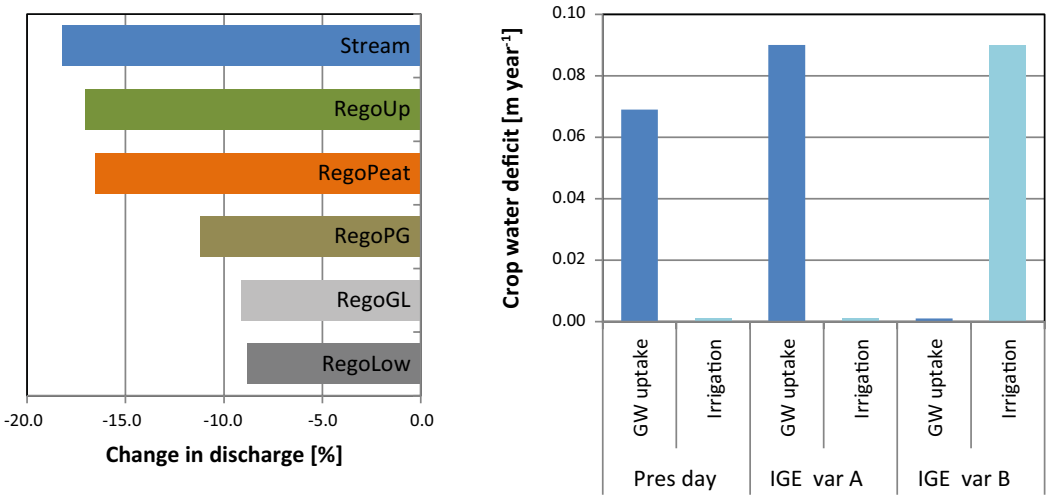

Figure 7-2. *Parameters describing hydrology and water uptake in the increased greenhouse effect evaluation case (IGE). Left: Change in groundwater discharge in the undisturbed mire ecosystem relative to present-day conditions. Right: Water deficit of crops (cereal, potato and fodder) and type of water sources covering the deficit in present-day conditions, and in the two variants of warmer climate. Short bars represent a value of zero.*

Large-scale irrigation of cereal and fodder production is not practiced in Laxemar under present climatic conditions. Adding large-scale irrigation as an exposure pathway to family farming (DM and Agri) thus required definition of new parameters describing this practice (Grolander and Jaeschke 2019). Moreover, the processes for accumulation on edible parts of crop (cereals), element translocation (potatoes) and leaf weathering (fodder) were added to the models describing agriculture in warmer conditions (Section 8.4.1). The concentration of stable CO_2 in the atmosphere was expected to be elevated (543 ppm) in both variants, and finally, the amounts and frequency of irrigation of a garden plot (GP) were adjusted to reflect warmer conditions (Grolander and Jaeschke 2019).

7.4.6 Potentially exposed groups

The land-use variants from the *present-day evaluation case* were used also in this evaluation case. That is, a family farm was used to evaluate exposure from the continuously cultivated land (Agri). The potential exposures from a mire ecosystem were evaluated for the exposed groups: hunter and gatherers (HG), infield-outland farmers (IO), a household with a garden-plot (GP), and a family farm cultivating the drained mire (DM).

7.5 Alternative regional climate

The *alternative regional climate evaluation case* was designed to illustrate to what extent the external conditions driven by the regional climate at the repository site may affect the calculated dose (**Main report**, Section 8.4.4). In this evaluation case three additional locations along the Swedish coast were used to exemplify alternative temperature and precipitation regimes for the site of the repository (Figure 7-3).

7.5.1 Climate conditions

The North and Central regional climate variants correspond to additional locations along the Baltic coast, and the Southwest climate corresponds to a location facing the Swedish west coast (i.e. on the shores of Kattegatt/Skagerrak) (Figure 7-3, Table 7-2). As in the *present-day evaluation case*, the variant climatic conditions were assumed to prevail during the entire analysis period of 1 million years (after repository closure).

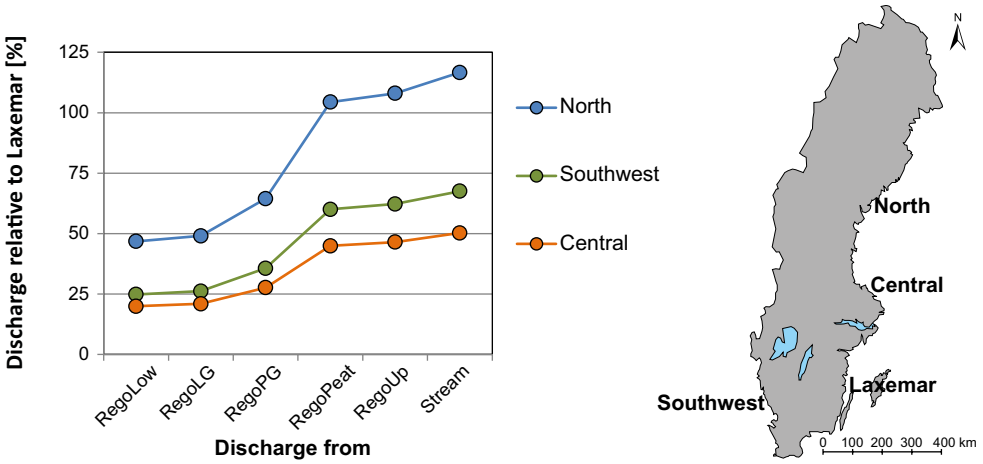

Figure 7-3. Groundwater discharge pattern as a function of regolith layer and regional climate. The rates were calculated for a time-independent mire (object 206) and were expressed relative to those in Laxemar. The regional climate variants were selected as examples along the Swedish coast. Annual precipitation values and mean annual air temperatures for all locations are given in Table 7-2.

Table 7-2. Present-day climate conditions for Laxemar and three other sites along the Swedish coast chosen to represent different regional climate along the Swedish coast. The locations of the sites are shown in Figure 7-3. All values are for the reference period 1961–1990 (Alexandersson and Eggertsson Karlström 2001) (table modified from the Climate report).

Climate- or climate-dependent parameter	North	Central (Forsmark)	Laxemar	Southwest
Mean annual air temperature (°C)	2.6	5.0	6.4	7.3
Annual precipitation (mm)	654	606	553	738

7.5.2 Geosphere – biosphere link

Radionuclides from the repository were discharged to the same biosphere object as in the main calculation case, namely biosphere object 206. The near-field and geosphere conditions were not expected to be significantly affected by changes in the regional climate (Section 7.7.2 in the **Radionuclide transport report**). Thus, the size and temporal pattern of the geosphere release into the lowest regolith layer (till) was the same as in the release into object 206 in the *present-day evaluation case*.

7.5.3 Landscape geometries and regolith properties

As in the *present-day evaluation case*, landscape development was not considered. That is, the geometry and stratigraphy of the discharge area did not change, and no biological succession was accounted for during the entire assessment period of 1 million years. Dose consequences were examined in two variants of the biosphere object, namely a continuously cultivated field and a mire ecosystem, both located in the original lake basin.

7.5.4 Surface hydrology

Groundwater flow for the alternative regional climate variants was derived by assuming that deep groundwater discharge and surface runoff follow a simple temperature and precipitation response previously predicted for the Äspö area (Losjö et al. 1999, Grolander and Jaeschke 2019). The response in runoff and bedrock discharge was then translated into groundwater flow rates through the regolith profile (Grolander and Jaeschke 2019). Thus, a high precipitation and cold Northern climate was expected to yield approximately 40 % more discharge from the bedrock and more than twice as much surface runoff as presently observed in Laxemar. Warm and high precipitation conditions (as in the Southwest) and slightly colder and higher precipitation conditions than in Laxemar (as in Central Sweden) were also expected to yield more discharge, but at levels that were intermediate between those expected in the North and in the Laxemar region (Figure 7-3).

7.5.5 Ecosystem properties

Most properties of mires and agricultural ecosystems were expected to be only marginally affected by a moderate change in regional climate, and most parameters were given values from the present-day evaluation case. However, precipitation and temperature were expected to influence evapotranspiration and plant-water deficit in cultivated soils. Thus, the groundwater uptake in cultivated soil, and the amount of irrigation water required by a kitchen garden, were adjusted to lower rates in a Northern climate (~ 35 % reduction), to somewhat lower rates in the Central climate, and to somewhat higher rates in a Southwest climate. Similarly, the yearly percolation from cultivated soil was assumed to follow the patterns of runoff with the highest rates in the North and Southwest regions, and the lowest rate in the Laxemar region. For details see Grolander and Jaeschke (2019).

7.5.6 Potentially exposed groups

The land-use variants from the *present-day evaluation case* were used also in this evaluation case. That is, a family farm was used to evaluate exposure from the continuously cultivated land (Agri). The potential exposures from a mire ecosystem were evaluated for the exposed groups: hunter and gatherers (HG), infield-outland farmers (IO), a household with a garden-plot (GP), and a family farm cultivating the drained mire (DM).

7.6 Initially submerged conditions

The *initially submerged conditions evaluation case* was designed to illustrate the effect of siting the repository just off the coast, in a location with a relatively steep coast and slow shoreline migration (**Main report**, Section 8.4.2).

Three variants, with varying durations of sea cover were considered. In the first variant the repository was assumed to be located under the seabed, but relatively close to the coast. That is at a position where the groundwater discharge starts to be influenced by the land emerging out of the sea at the time of repository closure. In the second variant the period from repository closure until the discharge starts to be influenced by the emerging land was set at 5 000 years, whereas the corresponding period was 10 000 years in the third variant.

7.6.1 Climate conditions

In the *initially submerged conditions evaluation case,* the same climate conditions as in the *present-day evaluation case* were assumed.

7.6.2 Geosphere-biosphere link

The groundwater flow in the near-field and geosphere was assumed to respond to large-scale changes in the relative sea-level (Section 7.3.2 in the **Radionuclide transport report**). The timing of changes in groundwater flow through the repository and the geosphere was changed in synchrony with the shift in groundwater flow to the biosphere (see below). The shifts in groundwater flow caused shifts in the near-field and the geosphere release, and thus the release to the biosphere varied between the three variants (Section 7.3.4 in the **Radionuclide transport report**). Radionuclides from the repository were discharged to the same biosphere object as in the main calculation case, namely biosphere object 206. During submerged conditions, the discharge was restricted to the central area of the sea basin, which develops into a lake-mire complex.

7.6.3 Landscape geometries and regolith properties

The development of the landscape in the *initially submerged evaluation case* is described based on the reconstructed shoreline displacement from the last glacial maximum 20 000 years ago (Section 4.2.1).

The potential impacts of a radionuclide release were only evaluated for the undisturbed development states of the biosphere object (i.e., from sea basin to lake-mire ecosystem states). The biosphere object started as a sea basin in all variants of this evaluation case. The first variant started when the average water depth was 6 m (8400 BC). Variants two and three started 5 000 and 10 000 years earlier (corresponding to 13 400 BC and 18 400 BC in the reconstruction). As the description of the landscape development does not cover the period before 10 000 BC it was assumed the conditions at 10 000 BC (i.e. an average water depth of 50 m and a water residence time of 4 days) were also characteristic of the preceding submerged period.

As land rises, the sea basin will develop into a bay, which finally gets isolated from the sea. The development of the object, i.e. the change in bathymetry and the accumulation of post-glacial sediments during the submerged period was described with the coupled regolith-lake development model (Section 5.4). The volume of the original lake was estimated from the surface area of the biosphere object and the present regolith stratigraphy, accounting for assumed soil compaction and the loss of a peat associated with cultivation (Section 3.4 in Grolander and Jaeschke 2019).

Given the present elevation of the lake threshold, and the reconstructed shoreline displacement, the isolation of the former lake was projected to have occurred at 4100 BC. If this lake had been undisturbed it may have persisted for several thousand years, during which the mire parts would have expanded until the lake basin was filled with peat. The historic infilling of this lake was described as a function of vegetation ingrowth and net sediment accumulation, and, according to this projection, the mire ingrowth was completed around year 0 AD (Section 3.4 in Grolander and Jaeschke 2019).

7.6.4 Ecosystem properties

Properties of aquatic ecosystems were assumed to be the same as used in the *alternative discharge area evaluation case*, and biomass and net primary production were calculated for each time step of the sea and lake stages accordingly. Properties for the mire ecosystems were assumed to be the same as the ones used in the *present-day evaluation case*.

7.6.5 Surface hydrology

None of the states that the discharge area goes through in this evaluation case can be observed in Laxemar at present. Thus, as in the *alternative discharge area evaluation case*, conceptual water balance models (Section 8.4.2) in combination with discharge information from the local catchment were used to calculate groundwater flux rates for object 206 for all stages (sea, lake, mire).

For the description of the hydrology two distinct periods were acknowledged (the sea and the land periods). It was assumed that the groundwater regime in the sea basin starts to become influenced by the surrounding terrestrial landscape when the average water depth is 6 m. Moreover, when the lake threshold was above the sea level the influence from meteoric water was assumed to be fully realised, resulting in discharge from the local catchment and a ten times higher discharge from the bedrock. Linear interpolation was used to describe the surface hydrology in the period between the sea and land period (Figure 7-4, Sections 5.5.3 and 5.8 in Grolander and Jaeschke 2019).

7.6.6 Potentially exposed groups

All exposed groups for natural ecosystems (sea, lake and mire) were included in this evaluation case. Hunters and gatherers (HG) were assumed to forage the area in all conditions. A garden plot household (GP) was assumed to be exposed in both submerged (fertilisation with algae) and terrestrial (fertilisation with ash and irrigation) conditions. Infield-outland farming (IO) depends on availability of hay from the terrestrial part of the object, which was assumed to occur after lake isolation. Consequences of converting the lake-mire complex into an agricultural ecosystem (by draining, DM) were evaluated (at all times) when the biosphere object was sufficiently elevated above the sea level (Section 6.3).

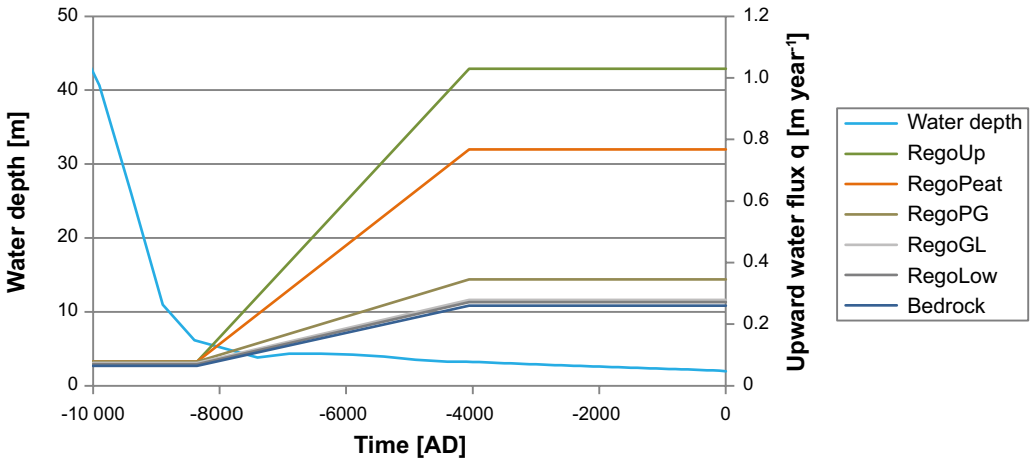

Figure 7-4. *Handling of groundwater flow parameters in response to landscape development. The graph shows how the upward fluxes from the bedrock through the regolith column changed as a function of time for the mire part in object 206. The end of the sea stage occurred when the average water depth was 6 m (~ 8400 BC) and the start of the land stage occurred when the lake threshold was at sea level (~ 4100 BC). Note that the change in upward flux increased towards the surface of the regolith stack, reflecting an increasing influence of discharge from the local catchment.*

7.7 Simplified glacial cycle

The *simplified glacial cycle evaluation case* (**Main report**, Section 8.6.2) was designed to analyse post-closure safety for the simplified glacial cycle variant of the SE-SFL reference evolution (Section 6.4 in the **Main report**). The evaluation case covered the colder end of the range within which future climate may vary and facilitated the evaluation of the importance for post-closure safety of periglacial, glacial, and submerged conditions. During each cycle the area that received discharge of deep groundwater from the repository, and the conditions within this area, were assumed to vary with the postulated shifts in climatic conditions.

7.7.1 Climate conditions

The development of external conditions was based on the *simplified glacial cycle climate case* (Section 4.3 in the **Climate report**). This case was based on the overall climate development in the reconstruction of the last glacial-interglacial cycle. It includes an early periglacial period at around 19 000 AD in combination with a simplified glacial cycle. The sequence of events considered is illustrated in Figure 7-5. To evaluate the effects of repeated Late Quaternary glacial-interglacial cycles on repository performance, this sequence was repeated every 100 000 years until one million years AD.

Permafrost was assumed to develop from non-existing to a continuous cover at the repository site during the first 100 years of each of the periglacial periods. Similarly, the transition from the periglacial to the temperate climate domain at 20 500 AD was assumed to occur during the last 100 years of the periglacial period. For the second periglacial period that ends at 57 000 AD, the permafrost was assumed to decay during the initial 100 years of the period of glacial climate domain.

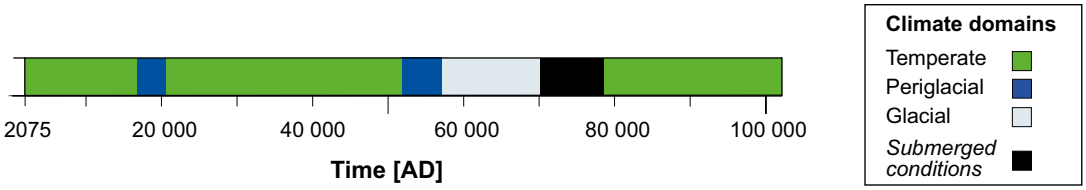

Figure 7-5. *The climate development at Laxemar in the first 100 000 years of the simplified glacial cycle climate case, shown as a succession of climate domains and submerged periods (from Figure 5-27 in the* ***Radionuclide transport report****).*

7.7.2 Geosphere – biosphere link

In accordance with the main assumptions of SE-SFL (**Climate report**, Section 1.1), the repository was postulated to be located below the maximum permafrost depth. However, the groundwater flow in the near-field and geosphere was assumed to respond to the advance and retreat of an inland-ice, as well as to changes in the relative sea-level (Section 5.4.2 in the **Radionuclide transport report**). The shifts in groundwater flow caused significant changes in the near-field and the geosphere release as compared with the releases in *the present-day evaluation case* (Section 5.4.4 in the **Radionuclide transport report**).

In periods of temperate conditions, radionuclides from the repository were discharged to the same biosphere object as in the *present-day evaluation case*, namely biosphere object 206. During periods of periglacial climate, the mire in object 206 was assumed to be frozen, and consequently not connected to deep flowing groundwater. During this period the geosphere release was instead assumed to reach a lake via a through-talik. When the site was covered by inland ice (glacial conditions) radionuclides from the geosphere were assumed to be discharged to a sea basin in front of the ice margin.

No explicit analyses of discharge during periglacial and glacial conditions have been made in SE-SFL. Instead, Lake Frisksjön (at isolation) was used as an example of a possible permafrost lake. A through-talik was assumed to form and prevail beneath the waterbody during the complete periglacial period. Given the surface area and average water depth of this lake (190 m radius and 4 m, respectively) it is plausible that a through-talik may form beneath the waterbody, even when permafrost reaches a depth down to 300 m (Hartikainen et al.. 2010, Claesson Liljedahl et al. 2016).

The location of the ice margin was expected to vary, possibly being located far away from the repository for much of a glacial period. Instead of a detailed description of the fate of radionuclides during this period, a simplifying assumption was used in the biosphere calculations. This assumption was justified as isostatic depression may give submerged conditions beyond the ice margin. Thus, the release was assumed to reach sea basin 208 during the complete period of glacial conditions. The water turnover time in an offshore basin was expected to be short. However, it cannot be excluded that radionuclides may at times discharge to a coastal location, and thus the present semi-enclosed coastal basin (with a residence time of 1 month) was cautiously selected to represent the recipient under glacial conditions.

In transition periods (typically 100 years) the fraction of the release discharged into one of the three objects changed linearly. For example, in the first transition to periglacial conditions, the fraction of the release to object 206 decreased from one to zero over a period of 100 years, and simultaneously release reaching the talik lake increased from zero to one.

To examine whether repetition of the last glacial-interglacial cycle affected the performance of the repository the glacial cycle was repeated ten times. When the ice sheet retreats most loose regolith layers on top of the till were expected to be removed by glacial erosion. Moreover, the remaining regolith was assumed to be flushed out by large quantities of surface water when the ice sheet melts. Thus, the radionuclide inventory in all regolith layers was assumed to be negligible at the start of the submerged period in each interglacial-glacial cycle.

7.7.3 Landscape geometries and regolith properties

Object 206 started as mire in this calculation case. After glaciation, the area will be submerged, and it was assumed that the groundwater flows during the submerged period will reach the central parts of the basin (which will later become the lake basin). As the land rises, the sea basin is expected to develop into a bay, which finally would get isolated from the sea. The development of the object, i.e. the change in bathymetry and the accumulation of post-glacial sediments during the submerged period was described with the coupled regolith-lake development model (see Section 7.6.3). Mire ingrowth was expected to be complete approximately 4000 years after isolation (Figure 5-7). For details on the landscape development see Chapter 3 in Grolander and Jaeschke (2019). The biosphere objects used to assess consequences of a release during permafrost (207) and submerged conditions (208) did not change for this simulation.

7.7.4 Surface hydrology

This evaluation case includes several discharge areas that are in states that cannot be observed in Laxemar today. Thus, conceptual water-balance models in combination with empirically derived rules for percolation and discharge from the surrounding local catchment were used to calculate groundwater flows which were object and state specific. The procedure used is described in detail in Section 5.9 in Grolander and Jaeschke (2019) and is briefly outlined below.

For temperate conditions, groundwater flows for the submerged stage of object 206 were calculated from the projected regolith stratigraphy (at 10 000 BC) and a reduced rate of deep groundwater discharge (by a factor of 0.1[5]). This period was assumed to prevail for as long as the average water depth exceeds 6 m. Water flows for the lake and mire parts of the object were calculated using boundary conditions from the available water balance for terrestrial conditions. Groundwater flows for coastal conditions were calculated by linear interpolation in the period between the sea stage (water depth > 6 m) and the start of the land stage (i.e. at lake isolation).

For periglacial conditions, net precipitation and runoff was assumed to increase by approximately 20 %, whereas the discharge from bedrock was assumed to be unaffected by permafrost. All groundwater flows and solute diffusion were halted by permafrost in the mire that fully covers the lake basin in object 206, except for the active layer which was represented by the upper regolith. Groundwater from the bedrock was instead assumed to reach the unfrozen lake part of object 207. In the transition periods between temperate and periglacial domains, the runoff and bedrock discharge into object 206 was calculated by linear interpolation.

When glacial conditions persist, the discharge was assumed to reach the semi-enclosed bay that was object 208, and constant vertical and lateral water flows from permanent aquatic conditions were used in the calculations (as described in the *alternative discharge area evaluation case)*. The location of biosphere objects 206, 207 and 208 are shown in Figure 5-2.

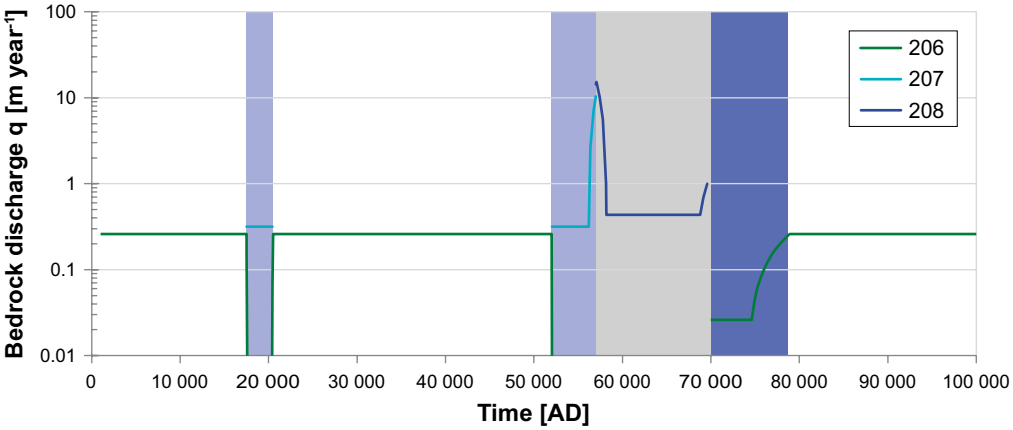

Figure 7-6. *Bedrock discharge as a function of biosphere object (Table 5-1 in Grolander and Jaeschke 2019) and the climate development at Laxemar in the first 100 000 years of the simplified glacial cycle climate case shown as a succession of climate domains and submerged periods. In the simulations, the object-specific discharge (m year^{-1}) was scaled by a flow factor (between 0 and 35) depending on the climate domain (temperate or periglacial), the position of the ice front (end of second periglacial period and glacial), or the water depth (during the submerged domain). Background colour represents climate domains, i.e. surface condition where lavender = periglacial, grey = glacial, blue=submerged, and white = temperate. The vertical black line indicates the start of the second interglacial-glacial cycle.*

[5] This value corresponds to the change in groundwater discharge for an object between fully submerged conditions (covered by 5.7 m of water, and with 98 % of the catchment below water) and emerged conditions (Section 5.5 in Grolander and Jaeschke 2019).

7.7.5 Ecosystem properties

The properties of terrestrial and aquatic ecosystems were the same as the ones used for temperate conditions in the *present-day calculation case* and the *alternative discharge area evaluation case*, except for a few properties in periods of permafrost. These include biological properties like biomass, net primary production and mineralisation in the mire, and the production of fish and crayfish in the lake. A few additional chemical and physical properties e.g. CO_2 concentration in the atmosphere, the solubility of CO_2 in water and the coefficient for gas exchange, were also altered in the periglacial periods (Section 10.5 in Grolander and Jaeschke 2019). For periods between temperate and periglacial domains, properties were assumed to change linearly over time.

7.7.6 Potentially exposed groups

All exposed groups for natural ecosystems (sea, lake and mire) were included in this evaluation case. Hunters and gatherers (HG) were assumed to forage the area in all conditions. A garden plot household (GP) was assumed to be exposed in both submerged (fertilisation with algae) and terrestrial (fertilisation with ash and irrigation) conditions. Infield-outland farming (IO) depends on availability of hay from the terrestrial part of the object, which was assumed to occur after lake isolation. Consequences of converting the lake-mire complex into an agricultural ecosystem (by draining, DM) were evaluated (at all times) when the biosphere object was sufficiently elevated above the sea level (Section 6.3).

7.8 Drilled well

In the *drilled well evaluation case,* the effect of using drinking water from a well drilled into the bedrock was analysed (**Main report**, Section 8.5.3). To facilitate the interpretation of results, the exposure from other sources were excluded from this evaluation case.

7.8.1 Climate conditions

In the *drilled well evaluation case* the same climate conditions as in the *present-day evaluation case* were assumed.

7.8.2 Location of wells

Five hypothetical drilled wells were positioned in the areas north and east of the repository where discharge from the repository occurs (Figure 7-7 and Joyce et al. 2019). In five realisations of the stochastic fracture network, the discharge from the waste vaults primarily reached biosphere objects 204 and 206 and, in one realisation, also biosphere object 210 (Chapter 5, Joyce et al. 2019). Therefore, two wells were positioned close to each of objects 204 and 206, and one well was positioned close to object 210.

The exact position of the drilled well was determined accounting for three separate criteria: First, to ensure drinking water quality, a well should be protected from inflowing surface water and, therefore, low areas in the landscape, such as wetlands and agricultural land, were avoided. Second, to avoid an unnecessarily deep well, high locations in the terrains were avoided. Third, to ensure adequate yield, the well needed to intersect at least one fracture in the flowing fracture network.

7.8.3 Geosphere – biosphere link

With the postulated withdrawal rate only one of the five wells received simulated particles from the repository. The properties from this single well were used to assess the potential dose in this evaluation case. The effect of the well on the geosphere transport properties was found to be small in the hydrogeological study (Joyce et al. 2019) and, therefore, the releases from the geosphere to the well were estimated by multiplying the base case releases from the geosphere by the fraction of particle tracks that end up in the well (3.1 % for BHA and 2.1 % for BHK).

The amount of water extracted from the well was assumed to be 700 L day^{-1} (255 m^3 $year^{-1}$, Grolander 2013). This is higher than the water use expected from a tap in a yard, and somewhat lower than present-day levels when connected to a public water supply (either of these could correspond to a garden-plot household, Werner et al. 2013). The water concentration was calculated by dividing the geosphere release that reaches the well by the water extraction rate.

7.8.4 Landscape development

As in the *present-day evaluation case*, landscape development was not taken into account in this calculation case.

7.8.5 Surface hydrology

Following the SR-PSU methodology, a highly stylised surface hydrology was used for the *garden plot* in SE-SFL (Saetre et al. 2013b, Grolander 2013).

7.8.6 Ecosystem properties

The effects of a potential release to a discharge area were not evaluated in this case, as they were already evaluated in the *present-day evaluation case*.

7.8.7 Exposed population

The dose from exposure to radionuclides in well water was evaluated using a garden plot household of five individuals. The members of the group were exposed through drinking water, and by ingestion of vegetables and potatoes from an irrigated kitchen garden. There were no a *priori* assumptions on the physical location of the household. In accordance with the guidance in the regulations (SSM 2008a), the family household utilising a well was viewed as a small group. Consequently, the calculated dose was evaluated against an annual committed effective dose criterion of 140 μSv (which corresponds to an annual risk criterion of approximately 10^{-5}).

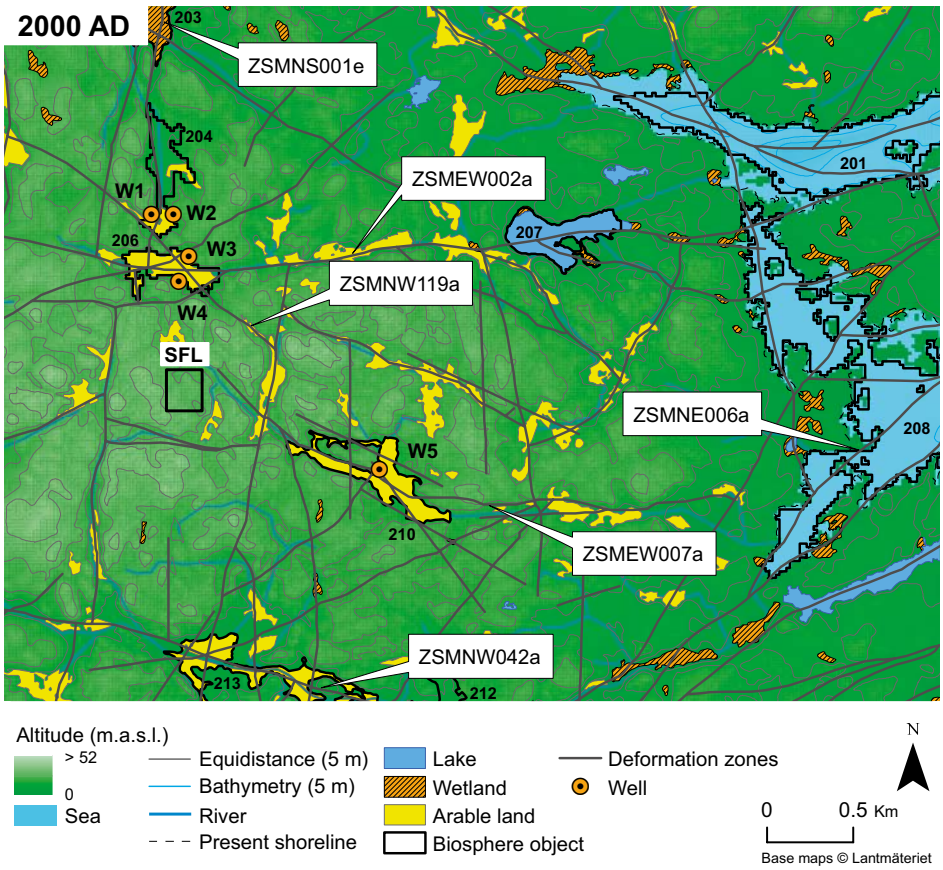

Figure 7-7. *Potential well locations (orange, labelled W1 to W5) in the present Laxemar landscape. Biosphere objects are identified by numbers (e.g. 204, 206 and 210) and the names of deformation zones are given in white squares (ZSM). The spatial location and extent of deformation zones is for a depth of 20 m below sea level. The example location for the SFL repository is indicated with a square. Grey contour lines follow constant elevation, with a difference of 5 m between lines. Figure modified from Joyce et al. (2019).*

8 The biosphere transport and exposure model

8.1 Introduction

The biosphere transport and exposure model (BioTEx) is the last link in a chain of models used to simulate radionuclide transport from a deep repository to the surface. The BioTEx model aims at describing radionuclide accumulation in surface-near ecosystems and to calculate potential doses to humans. The other two models in the chain focus on transport pathways across repository barriers or in the bedrock (Shahkarami 2019, **Radionuclide transport report**).

Given the requirements of the SFL safety evaluation (Chapter 2), the biosphere model needs to handle relevant features, events and processes for transport and accumulation of radionuclides, and cover important exposure pathways (Chapter 6). As the waste vaults are postulated to be located in a coastal landscape, and because the evaluation period covers hundreds of thousands years, the model must have the capabilities to handle both terrestrial and aquatic ecosystems and their temporal development, which is mainly driven by changes in climate and relative sea-level. Moreover, the model needs to handle transport, accumulation and decay of radionuclides (including in-growth of decay products) with different biogeochemical behaviour.

The biosphere model developed in the previous safety assessment of the final repository for short-lived low- and intermediate-level radioactive waste (SFR), and its planned extension, has the above-mentioned capabilities (Saetre et al. 2013b). In the SR-PSU assessment, the model was primarily applied to a single discharge area and its downstream connected areas. The model simulated transport and accumulation of radionuclides in two hydrologically connected ecosystems (i.e. an aquatic and a mire ecosystem), and transitions between ecosystems (i.e. lake isolation and lake ingrowth) were handled in a continuous manner.

This chapter summarises the structure of the ecosystem models that are part of the BioTEx model for SE-SFL. The model compartments and the processes that transfer radionuclides are outlined for each ecosystem (Sections 8.3 and 8.4). For details on approaches, assumptions and the mathematical representation the reader is referred to the original model report (Saetre et al. 2013b). Advective transport by groundwater and surface water is an important part of the model, and therefore the application of flow modelling results in SE-SFL is summarised in Section 8.4.2. Calculations of exposure and the resulting doses from ingestion, inhalation and external radiation are then described in Section 8.5. Model updates introduced since SR-PSU are described in the relevant context. In Chapter 9 the effects of model updates are evaluated by comparison of results with those from the SR-PSU model. Modelling aspects that are related to the implementation in specific evaluation cases are described in Chapter 7 (Sections 7.3 to 7.8).

8.2 Model approach and overview

The mathematical approach used in the biosphere model is that of compartment modelling. This approach has been described in detail by Saetre et al. (2013b). It assumes that a system can be adequately represented by a limited number of compartments or pools, each of which is homogeneous and connected to other compartments. Discharge of radionuclides into the biosphere is evaluated over thousands of years. The discharge area is considered at the scale of a coastal basin, a lake mire complex, or an agricultural field, and the annual average dose is calculated over an adult lifetime of 50 years for future inhabitants (Section 2.4.1). At these scales, it is assumed that most biogeochemical interactions can be approximated by equilibrium or steady-state conditions. Thus, ecosystem states are represented by average conditions, and fluxes of water, solid matter and gas are typically described as functions of aggregated empirical parameters that are assumed to capture the outcome of the underlying processes.

In the evaluation cases of SE-SFL, radionuclides released from the repository enter the surface system through deep groundwater discharge and then reach soil, sediments, water and air. Two types of ecosystems are simulated, namely aquatic (sea, lake and stream ecosystems) and terrestrial types (mire and agricultural ecosystems). In the compartment models used in the transport and dose calculations,

each compartment represents a radionuclide inventory associated with a physical (or biological) component in the surface ecosystems (Figure 8-1). The dynamic change in each compartment is the result of radionuclide flows, which are associated with either mass flows of water, solids (including organic matter) or gas, or with the transition between inorganic and organic forms.

The endpoints of the radionuclide transport model are the concentrations of radionuclides in environmental surface media in discharge areas, and the identification of potential areas reached by radionuclides (i.e. biosphere objects; Chapter 5) is a prerequisite for the modelling. Parameters describing the properties of biosphere objects (and their changes over time) were derived from site investigations and modelling of the development of the Laxemar and Forsmark areas (Chapter 5). The final step in the biosphere modelling consists of calculating doses to humans that are exposed to radionuclides in the environment. These calculations depend on the environmental concentrations and exposure pathways and habits identified as relevant for a safety assessment of a geological repository (Section 6.3; also, Chapter 6 in SKB 2014d).

As a result of SSM's reviews of SR-Site and SR-PSU (e.g. SSM 2017, 2018, Walke et al. 2017), the biosphere models have been somewhat modified in SE-SFL. These updates include a higher spatial discretisation of the two deepest regolith layers and the introduction of a hydrological-sub routine. Other updates have been introduced to improve consistency and transparency. For example, several model parameters are replaced with functions in the model code, including the dynamic development of peat thickness. Moreover, the specific activity approach is applied to model plant uptake of radionuclides behaving similarly to macronutrients in all terrestrial ecosystems. These and other model updates are listed under appropriate headings in the description below and they are summarised in Table 8-1.

The BioTEx model is implemented in the Ecolego 6 compartment modelling software[6]. As the base calculation case in SE-SFL is fixed to reflect present conditions in Laxemar, a simplified agricultural model for stationary (or time-independent) conditions is introduced in SE-SFL. Moreover, to broaden the ensemble of examined conditions in potential discharge areas, stand-alone versions of the biosphere ecosystem sub-models are also used to calculate dose separately in mire and aquatic ecosystems under stationary conditions.

[6] When the model was migrated to Ecolego 6, the enhanced functionality in the tool was utilised. For example, in the present version of the model linear interpolation in transition periods is done with inbuilt interpolation routines, rather than by user-defined functions (as was done in SR-PSU, appendix G in Saetre et al. 2013).

Table 8-1. Overview of updates to the biosphere transport and exposure model (BioTEx). The first column indicate if the update affects state variables, processes or dose calculations, and which ecosystem models are affected by the modification.

Type/Sub-model	Update	Short description	Rationale
State variables			
Aqua, Mire, Agri	Vertical discretisation*	RegoLow and RegoGL represented by five sub-compartments each.	Adjust numerical dispersion within these layers to be more similar to physical dispersion.
Mire	Peat thickness*	Time-dependent parameter replaced with explicit modelling of the amount of organic carbon in the peat layer using a separate compartment.	Increased consistency between C-12 and C-14 calculations, particularly in probabilistic simulations.
Agriculture			
All	Plant retention	Adjustment for plant retention excluded by removing parameter *f_crop*.	Model simplification (process not important to the assessment endpoint with present parameter values).
infield-outland	Numeric simulation*	Steady-state solution replaced by numeric simulation.	Improved representation of historic accumulation. Exact handling of contribution from decay products.
Garden plot	Atmospheric concentrations	Repeated calculations replaced with scaling factors.	Improved computational efficiency.
Agri	New model	Multi-regolith layer model representing continuous cultivation of agricultural land.	Model reflects present conditions in Laxemar (*present-day evaluation case*).
Processes			
Plant uptake	Uptake of C-14*	Parameter for DIC concentration (*Conc_DIC*) in terrestrial ecosystems replaced by a function.	Increased consistency between C-12 and C-14 calculations, particularly in probabilistic simulations.
	Uptake of plant nutrients	Root uptake of Cl-36, Ca-41 and K-40 described as plant-regulated in terrestrial ecosystems.	Increased consistency and realism.
	Leaf uptake*	Plant uptake through translocation of intercepted irrigation water.	Completeness of transport pathways.
Litter release	Fraction released*	Parameter (*df_decomp* for Cl-36) replaced with a function.	Parameter inter-dependency explicitly expressed.
Groundwater uptake	Origin of water	Concentration of water taken from first undisturbed regolith layer below ditching depth.	Increased realism and consistency between ecosystem (Mire) and exposure sub-models (DM).
Gas exchange	Diffusion from unsaturated soil	Parameter for diffusivity (*D_CO2_soil*) replaced with a function.	Parameter inter-dependency explicitly expressed.
	Exchange within unsaturated soil	Explicit functions for diffusive gas transport between RegoUp and RegoSub included in agricultural model	Completeness of transport pathways given increased discretisation.
Vertical advection	Groundwater flux parameters*	New routine for derivation of hydrological parameters.	Allows for a systematic and transparent extrapolation to conditions lacking water balance data.
Dose calculations			
Inhalation	Dose from combustion	Aggregated dose coefficients replaced by explicit (two step) calculations.	Consistency with dose calculations of inhalation of radionuclides from other sources (i.e. dust and $^{14}CO_2$).

* Indicates that the model updates address issues raised by SSM, or their external experts, in the two previous safety assessments (i.e. SR-Site and SR-PSU).

8.3 Model compartments

Model compartments in the BioTEx models were designed based on previously established (i) conceptual ecosystem understanding (Aquilonius 2010, Andersson 2010, Löfgren 2010), (ii) landscape and landscape development understanding (Lindborg 2010, Lindborg et al. 2013, Chapter 4 of this report), as well as on (iii) previously identified biosphere components that have been found to be important in safety assessments for radioactive waste disposal by SKB (SKB 2010a, 2014d).

In practice, identified biosphere components (Section 6.2.1) were considered in the context of discharge areas potentially affected by deep groundwater from the repository. The aim was to translate biosphere components into model compartments that allowed a meaningful representation of radionuclide transport and accumulation processes at an appropriate spatial scale given the underlying assumption of homogeneity with respect to physical, chemical and biological properties. This was ensured by carrying out a preliminary model analysis which led to the decision to split several, initially highly aggregated biosphere components into smaller parts. For instance, the regolith component was split into several compartments to better represent different geological deposits (and their inorganic and organic fractions). On the other hand, components that were considered to have small or insignificant radionuclide inventories were excluded (e.g. consumers). Compartments with a fast turnover of radionuclides, (e.g. liquid phases), were, in many cases, combined with compartments having slower dynamics (e.g. solid phases), assuming that equilibrium would be approached within each time step of the simulation. The final set of compartments is described in Table 8-2, and the conceptual model of the coupled lake and mire ecosystem is presented in Figure 8-1.

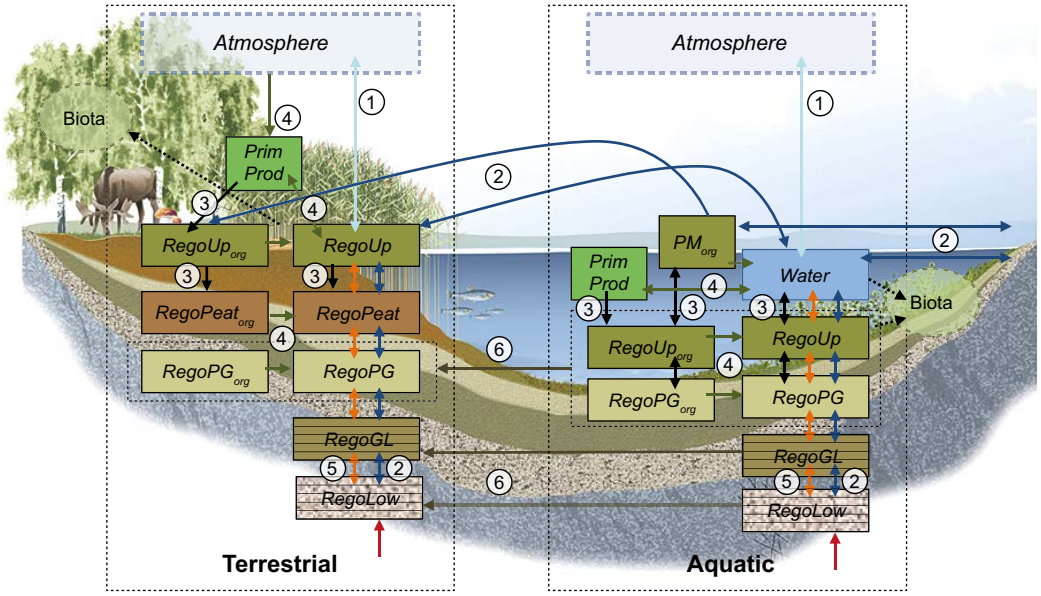

Figure 8-1. *Conceptual model corresponding to the BioTEx model used to simulate transport and accumulation in a discharge area with two natural ecosystems (delimited by thin dotted black lines). Each box in the two ecosystems corresponds to a radionuclide inventory associated with a physical or biological compartment. Note that in SE-SFL the two lowermost regolith layers are represented by five compartments each. Arrows represent flows of radionuclide between compartments and flows into and out of the system. Radionuclide flows are linked to mass flows of gas (1, light blue), water (2, dark blue) and solid matter (3, black), to transitions between inorganic and organic forms of radionuclides (4, green), to diffusion in soil pore water (5, red), and to ingrowth of wetland vegetation (6). The red arrow indicates that the geosphere release enters the biosphere via groundwater discharge to the till. Dotted boxes (atmosphere and biota) are assumed to be in equilibrium with the corresponding environmental media, and the uptake of radionuclides into biota (dotted arrow) is not included in the mass balance of the BioTEx model.*

Table 8-2. Description of compartments representing radionuclide inventories in the BioTEx model (see also Figure 8-1); note that the PM_{org} compartment is also referred to as $Water_{org}$ in the technical description (Saetre et al. 2013b). The agricultural ecosystem has been included in SE-SFL to describe the present conditions of several potential discharge areas.

Ecosystem/Name	Description
Aquatic	
Water	Radionuclides in open water of sea basins, lakes and streams, including radionuclides dissolved in water and adsorbed to particulate matter.
PM_{org}	Radionuclides stored in refractory organic particulate matter suspended in the water column.
PrimProd	Radionuclides stored in aquatic primary producers, including radionuclides in pelagic, microbenthic and macrobenthic primary producers.
RegoUp	Radionuclides in the upper oxic and biologically active layer of aquatic sediments, including radionuclides in pore water and adsorbed on sediment particles.
$RegoUp_{org}$	Radionuclides incorporated into organic particulate matter in the upper aerobic and biological active layer of aquatic sediments.
RegoPG	Radionuclides in post-glacial aquatic sediments (clay gyttja) below the biologically active layer, including radionuclides in pore water and adsorbed on sediment particles.
$RegoPG_{org}$	Radionuclides incorporated into organic particulate matter in post-glacial aquatic sediments (clay gyttja) below the biologically active layer.
RegoGL	Radionuclides in glacial clay (typically overlaid by post-glacial deposits), including radionuclides in pore water and adsorbed on sediment particles.
RegoLow	Radionuclides in till (typically overlaid by glacial clay), including radionuclides in pore water and adsorbed on sediment particles.
Mire	
PrimProd	Radionuclides stored in mire vegetation biomass, including both above- and below-ground biomass of bryophytes, vascular plants, dwarf shrubs and trees.
RegoUp	Radionuclides in the upper oxic and biologically active layer of peat (acrotelm peat), including radionuclides in pore water and adsorbed on peat.
$RegoUp_{org}$	Radionuclides incorporated into organic matter in the upper aerobic and biologically active layer of peat (acrotelm peat).
RegoPeat	Radionuclides in deep, permanently anoxic, peat (catotelm peat), including radionuclides in pore water and adsorbed on peat.
$RegoPeat_{org}$	Radionuclides incorporated into organic matter in the deep, permanently anoxic peat (catotelm peat).
RegoPG	Radionuclides in post-glacial sediments (clay gyttja) overlaid by peat, including radionuclides in pore water and adsorbed on sediment particles.
$RegoPG_{org}$	Radionuclides incorporated into particulate organic matter in post-glacial sediments (clay gyttja) overlaid by peat.
RegoGL	Radionuclides in glacial clay buried under peat and typically overlaid by post-glacial deposits. Inventory includes radionuclides in pore water and adsorbed on sediment particles.
RegoLow	Radionuclides in till, buried under peat and typically overlaid by glacial clay. Inventory includes radionuclides in pore water and adsorbed on sediment particles.
Agricultural	
RegoUp	Radionuclides in the upper (ploughed) unsaturated soil layer of cultivated land, including radionuclides in pore water and adsorbed on peat.
RegoSub	Radionuclides in the unsaturated sub-soil layer of cultivated land (below the ploughed layer), including radionuclides in pore water and adsorbed on peat.
RegoPG	Radionuclides in post-glacial sediments (clay gyttja) overlaid by cultivated soil, including radionuclides in pore water and adsorbed on sediment particles.
RegoGL	Radionuclides in glacial clay buried under cultivated soil and typically overlaid by post-glacial deposits. Inventory includes radionuclides in pore water and adsorbed on sediment particles.
RegoLow	Radionuclides in till, buried under cultivated soil and typically overlaid by glacial clay. Inventory includes radionuclides in pore water and adsorbed on sediment particles.

In response to the regulatory review of the SR-Site assessment, SKB has increased the discretisation of the two deepest regolith layers. The lower-most layer, till (RegoLow), typically represents the major part of the regolith stack, and the groundwater flux rates are relatively low. With these conditions, the numerical dispersion within one compartment is likely to considerably exceed the physical dispersion rate, and thus result in an underestimate of the solute transport time through the layer. For transport in one dimension, it can be shown that five compartments will yield a numerical dispersion that equals a physical dispersivity corresponding to a tenth of the transport length, which is considered typical for field-scale dispersion[7]. Moreover, as radionuclide distribution (i.e. the K_d value) is normally an order of magnitude larger in the glacial clay (RegoGL) than in the till (Tröjbom et al. 2013), the numerical dispersion of one compartment leads to a similar underestimation of the breakthrough time for many radionuclides also in this layer. Consequently, both the RegoLow and RegoGL layers were each represented with five stacked compartments in the SE-SFL model.

8.3.1 Aquatic ecosystems

Two major types of aquatic ecosystems are recognised, namely marine (Aquilonius 2010) and limnic ecosystems (Andersson 2010). For the purpose of the present biosphere evaluation, these two systems have been regarded as structurally and functionally similar, and consequently a common set of physical compartments was identified for all aquatic ecosystems by Saetre et al. (2013b). Based on Saetre et al. (2013b) and the references therein (especially Andersson 2010, Aquilonius 2010, SKB 2013c), the main considerations and assumptions underlying the modelling of aquatic ecosystems at Forsmark are summarised as follows.

All aquatic organism compartments identified in SKB (2013c) were considered to have fast dynamics, and the amounts of elements in consumers were considered small in relation to inventories in sediment and water. Consequently, filter feeders, herbivores, carnivores and decomposers were not included as dynamic model compartments. For a few elements, e.g. Mn in the sea (Aquilonius 2010), the inventory in primary producers made up a substantial fraction of that in water. Primary production is also the main source of organic carbon (and C-14) in sediments, and thus SKB found it appropriate to explicitly include aquatic primary producers (PrimProd, cf. Figure 7-1) as separate model compartment.

To represent the radionuclide fluxes associated with sedimentation, radionuclide concentrations on suspended particulate matter needed to be estimated. Due to the temporal resolution of the model, it was considered reasonable to represent dissolved and adsorbed radionuclides within one compartment (Water) and by partitioning radionuclides within the inventory by assuming equilibrium. However, the radionuclide concentrations in refractory particulate organic matter are not necessarily in equilibrium with those in surface water. Therefore, a compartment representing radionuclides stored in refractory particulate organic matter in the water column was added as a model compartment (PM_{org}).

For the modelling of radiocarbon (C-14), a single compartment was deemed not to be sufficient to represent storage (and subsequent release) of radionuclides in aquatic sediments. Compartments representing radionuclides stored in organic matter were identified as essential in order to describe the accumulation in aquatic sediments. The storage of carbon in sediments is a function of organic matter input and mineralisation. Mineralisation rates are highly dependent on oxygen, and in oxygen-depleted environments even decomposable (labile) organic matter will accumulate. This implied a need for a vertical stratification of the aquatic sediments into oxygenated top sediments and oxygen-depleted deep sediments. It was assumed that radionuclides in pore water are in equilibrium with radionuclides adsorbed on solids, and consequently each layer was described with one compartment and a layer specific distribution coefficient (K_d).

The oxygenated top sediments were represented by two sub-compartments, one representing radionuclides adsorbed on solids/dissolved in pore water (RegoUp), and one representing radionuclides in organic matter ($RegoUp_{org}$). The sum of these two inventories reflects the total radionuclide contents in the biologically active aquatic sediment, wherein fauna can be exposed to ionising radiation.

[7] Based on data from the 1974 review of data on field-scale dispersion (Gelhar et al. 1992), the rule of thumb that the macro-dispersivity typically scales to one tenth of the transport length has been recommended for use in calculations of groundwater solute transport (e.g. Spitz and Moreno 1996).

Below the oxygenated layer, decomposition rates slow down and organic matter builds up in aquatic sediments. These regolith layers correspond to marine or lacustrine gyttja, and the build-up of these sediments started after the last glaciation (i.e. they are post-glacial sediments). As with the oxygenated layer (see above), radionuclides stored in post-glacial sediments are represented with two sub-compartments, i.e. one that represents radionuclides adsorbed on solids/dissolved in pore water (RegoPG) and one that represents radionuclides in organic matter ($RegoPG_{org}$).

The older sediments buried under post-glacial gyttja are depleted of organic matter and the amount of radionuclides stored in organic matter in these layers was considered quantitatively insignificant. Older deposits at the site consist primarily of two classes, till and glacial clay. The ontogeny and physical properties are different for these two geological layers, and thus minerogenic old sediments were split into two compartments, glacial clay (RegoGL) and till (RegoLow). Both compartments account for radionuclides adsorbed on solids and radionuclides dissolved in pore water.

The last physical biosphere component identified in SKB (2013c) is the atmosphere. As part of the SR-PSU safety assessment, SKB developed a new conceptual and numerical model of the atmosphere, which allows a separation between near-surface and higher layers (Saetre et al. 2013b). The dynamics in the atmosphere are fast (hours) compared with the dynamics in water (weeks/months) and regolith (years or more), and the transport times in the upper atmospheric layers are much faster compared to the transport times in the surface water. Thus, in SE-SFL (as in SR-PSU) the atmosphere was treated as a dynamic equilibrium in the radionuclide transport model, and concentrations of volatile radionuclides (i.e. C-14) were calculated using a steady-state solution (Section 8.2 in Saetre et al. 2013b).

8.3.2 Mire ecosystems

Two major types of terrestrial ecosystems are likely to be affected by radionuclides from a geological repository, namely mire ecosystems and agricultural ecosystems (Löfgren 2010). SKB has previously identified several biosphere components that should be considered in a safety assessment of a geological repository (SKB 2013c). Considerations and assumptions related to the modelling of the terrestrial ecosystems are summarised in the following. The main underlying references given in Saetre et al. (2013b) are the SR-Site terrestrial ecosystems (Löfgren 2010) and landscape modelling (Lindborg 2010) reports. Model compartments of the mire ecosystem are illustrated in Figure 8-1.

Site and literature data indicate that inclusion or exclusion of organism compartments is not likely to affect simulated dynamics and concentrations of radionuclide inventories in regolith layers. Consequently, terrestrial herbivores (incl. humans and livestock), carnivores (incl. humans) and decomposers were not included as separate model compartments in the radionuclide transport model. For a few elements (e.g. non-metals like Br and Cl) the inventory in primary producers in wetlands is substantial as compared to that in soils in natural terrestrial ecosystems (Löfgren 2010). Primary production is also the main source of organic carbon in peat formed in wetlands, and thus it was found appropriate to include terrestrial primary producers (PrimProd) as an explicit model compartment in the sub-model of the mire ecosystem.

With the modelling of radiocarbon (C-14) in mind, the need for separate compartments reflecting storage (and release) of radionuclides in organic matter was identified. The accumulation of carbon in peat is a function of organic matter input and mineralisation. Mire peat is usually characterised by strong vertical gradients with respect to oxygen content, hydraulic conductivity and organic matter quality, and thus a need for separate compartments in an oxygenated top layer and an oxygen-depleted deep layer of peat was identified. Radionuclides in pore water and radionuclides adsorbed on solids were assumed to be in equilibrium, and thus the two inventories were described with one compartment and an equilibrium partition coefficient (K_d).

The oxygenated surface peat was modelled using two sub-compartments, one representing radionuclides adsorbed on solids/dissolved in pore water (RegoUp), and one representing radionuclides in organic matter ($RegoUp_{org}$). The sum of these two inventories reflects radionuclides in the biologically active peat, where roots take up elements and mire-dwelling organisms can be exposed to ionising radiation. Below the oxygenated layer, decomposition rates slow down and organic matter accumulates in peat that may grow to a thickness of several metres below the groundwater table, given sufficient time. Radionuclides in deep peat are also modelled using two sub-compartments, one for radionuclides adsorbed on solids/dissolved in pore water (RegoPeat), and one for those in organic matter ($RegoPeat_{org}$).

Mire peat develops on top of layers that were deposited when the discharge area was covered by water (i.e. when the area was a sea basin or a lake). To also account for radionuclides that accumulated in earlier successional stages or those accumulated during transport through these layers, we recognised the need for representing radionuclides stored in organic matter of marine and lacustrine sediments ($RegoPG_{org}$) and radionuclides adsorbed on solids/dissolved in pore water of the same layer (RegoPG), and the underlying minerogenic layers of glacial clay (RegoGL) and till (RegoLow).

In SE-SFL, the development of peat thickness was calculated by explicit modelling of the amount of solid organic carbon in the peat layer using a separate compartment within Ecolego (Section 4.4.9 in Grolander 2013). While this update has no effect for deterministic calculations, it will ensure consistency in the behaviour of stable carbon (i.e. peat) and radionuclides in probabilistic calculations[8].

As in the SR-PSU assessment, the atmosphere was treated also here as a dynamic equilibrium in mire ecosystems, and the concentrations of volatile radionuclides in the canopy atmosphere (and layers above) were calculated using a steady-state solution (Section 8.1 in Saetre et al. 2013b).

8.3.3 Agricultural ecosystems

Agricultural ecosystems are simulated in order to calculate the potential exposure of future human inhabitants. In SE-SFL, the three stylised agricultural land use variants developed in SR-PSU are used to assess dose to future human inhabitants. These are: draining and cultivating a mire (DM) over a human lifetime (50 years), irrigating and fertilising a garden plot over a human lifetime (GP), and long-term fertilisation of a cultivated minerogenic soil due to infield-outland agriculture (IO) (see Saetre et al. 2013b and Section 6.3). In the first variant, radionuclide accumulation in lake and mire regolith layers is included in the initial conditions for agricultural soil, and radionuclides also reached the cultivated soil through groundwater uptake. In the other two variants, radionuclides reach cultivated soil from above. Thus, for dose calculations it is considered sufficient to represent the dynamics of radionuclides in the soil-plant system with regolith compartments, representing radionuclides in the upper biologically active soil layers of cultivated soil.

As in SR-PSU, the analytical solutions to the model are used to calculate activity concentrations in agricultural soil for the DM and GP systems. However, as the infield-outland agriculture evaluates long-term input of radionuclides (through organic fertilisation), the input of radionuclides is modelled as a continuous input (from mire vegetation) in SE-SFL, and soil concentrations are calculated through numerical simulations. This approach gives a more realistic representation of radionuclide accumulation over time, particularly because it allows a direct and exact handling of the contributions of decay products in the dose calculations[9].

Elemental pools in decomposers and consumers (herbivores and carnivores) are expected to be small in relation to the pools in the uppermost layers of cultivated soil. The turnover of soil animals and microbiota is typically very fast. Also, the majority of plant biomass is expected to have a relatively fast turnover, as annual crops (cereals, root crops and vegetables) were considered. For simplicity, organism components were therefore not included as separate compartments in the agricultural ecosystem sub-models, and consequently radionuclide concentrations in crop, and livestock and dairy products were calculated assuming they were in equilibrium with soil and fodder concentrations, respectively.

[8] The importance of consistency in the calculations of stable and radioactive carbon in probabilistic calculations has been pointed out by SSM's external reviewer of SR -PSU (Walke et al. 2017).

[9] The advantage of including decay products explicitly in the calculations has been pointed out by Walke et al. (2017).

In SR-PSU, the effect of plant storage on radionuclide transport was accounted for by a scaling factor (f_{crop}). However, with the parameter values (i.e. *CR* values and plant concentrations of macronutrients) that are used for crops in SE-SFL, the fraction of radionuclides immobilised in biomass is small (< 1 %)[10], and the effect on radionuclide retention in the plant–soil system is marginal. Consequently, the calculations of activity concentrations in the regolith in agricultural systems were simplified in SE-SFL, by not deducting the fraction retained in plants.

The oxygenated and unsaturated layer of cultivated soil was represented by two sub-compartments, one representing radionuclides adsorbed on solids, dissolved in pore water or bound in crop (RegoUp), and one representing radionuclides in soil organic matter ($RegoUp_{org}$). The sum of these inventories reflects radionuclides in the biologically active layer of cultivated soil, where roots take up elements.

As in the SR-PSU assessment, the atmosphere was treated as being in dynamic equilibrium in agricultural ecosystems, and the concentrations of volatile radionuclides in the canopy atmosphere (and layers above) were calculated using a steady-state solution (Section 8.1 in Saetre et al. 2013b). To improve computational efficiency in SE-SFL, atmospheric calculations for the garden plot were solved for a normalised release, and canopy concentrations were calculated by scaling with the release from the appropriate combinations of source terms (from algae or ash fertilisation and irrigation).

The base calculation case in SE-SFL reflects present conditions in Laxemar (Chapter 7). As many of the potential discharge areas are presently cultivated, an agricultural model for continuous cultivation is introduced in SFL (Figure 8-2). This model does not account for radionuclides in organic matter, as long-term accumulation of organic matter is expected to be limited in agricultural ecosystems. Following radio-ecological practice, the upper soil layer was set to a relatively shallow depth, corresponding to the ploughing depth (IAEA 2010). To complete the regolith profile of cultivated land in Laxemar, a compartment representing unsaturated soil conditions below this depth was added to the model (RegoSub). This compartment represents radionuclides adsorbed on solids and radionuclides dissolved in pore water.

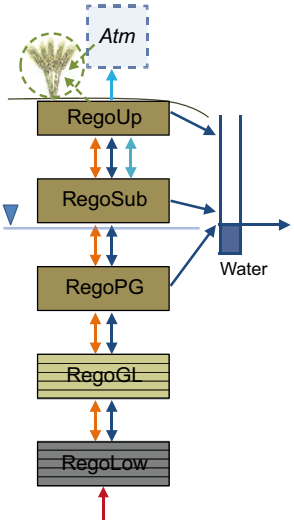

Figure 8-2. *Conceptual model corresponding to the radionuclide transport model (BioTEx) used for continuously cultivated agricultural ecosystems. Each large box corresponds to a radionuclide inventory associated with a regolith layer. Note that the two lowermost regolith compartments are represented by five sub-compartments each. Solid arrows represent radionuclide fluxes between compartments and fluxes out of the system. Radionuclide fluxes are linked to diffusion of gas (light blue) and solutes (orange), and to mass fluxes of water (dark blue). The water from the three uppermost compartments is drained to a ditch (marked 'Water' in the figure). The red arrow indicates that the geosphere release enters the biosphere via groundwater discharge to the till. The activity concentrations in the atmosphere and in the crops are calculated assuming equilibrium conditions.*

[10] This statement is also true for Cl-36, for which the activity concentration in plants is calculated by a specific activity approach.

8.4 Transport processes

8.4.1 Process identification

In SR-PSU, SKB identified processes important for transport and accumulation of radionuclides in natural and agricultural ecosystems by considering conceptual models for the landscape and for the aquatic and terrestrial ecosystems. In all ecosystems, flows of radionuclides were associated with mass flows (of water, solid matter and gas), or with transitions between inorganic and organic forms of radionuclides (i.e. primary production and mineralisation of organic matter). The exchange of radionuclides between solid and liquid states was also highlighted as a key process for radionuclide transfer in all types of ecosystems (Saetre et al. 2013b).

In the next step, it was assessed which of these processes may be of quantitative importance for the flow of radionuclides between the identified model compartments, and the identified processes were checked against the processes in the SKB FEP list (SKB 2013a, Chapter 6). The processes identified in SR-PSU were considered valid also for evaluations of other coastal sites. Below is a brief description of the processes that are represented by a flow of radionuclides in the transport model (see also Table 8-3 for an overview).

Bioturbation

Bioturbation refers to translocation of radionuclides by mixing of sediment and soil particles in aquatic and terrestrial regolith layers. Mixing of aquatic sediments by, for example, infauna organisms, leads to improved oxygenation. When the depth of the upper sediment layer is reduced during episodes of resuspension, bioturbation causes the oxygen front to penetrate the underlying sediments, resulting in an apparent translocation of radionuclides from anoxic regolith layers to the upper, biologically active, sediment layer. The combined effect of ploughing and soil fauna activity (e.g. earthworm burrowing) mixes cultivated soil. When drained mire and lacustrine sediments are cultivated, radionuclides from deeper regolith layers are redistributed and mixed with radionuclides in the upper soil horizon.

Plant uptake

Plant uptake is fixation of inorganic radiocarbon and other radionuclides into plant biomass, as a result of primary production. In aquatic ecosystems, plants take up dissolved radionuclides from the surrounding water. In terrestrial (mire and agricultural) ecosystems, plants take up radionuclides from the upper soil layers through root uptake, and from the canopy atmosphere through atmospheric fixation (C-14 only).

Plant root uptake of C-14 is regulated by the concentration of stable carbon dissolved in the pore water. In SE-SFL, this parameter has been replaced by model calculations. The calculations are based on soil respiration (a well-known and measured soil property) and the rate of degassing (calculated on the same principles as used for C-14) (Saetre and Ekström 2017a). This model update makes transport calculations of C-12 and C-14 consistent and ensures that this consistency is retained in probabilistic simulations.

For consistency, in SE-SFL, uptakes of macronutrients (e.g. Cl) are assumed to be regulated in all terrestrial plants, i.e. the concentrations of essential elements are assumed to be a plant-type specific property which is independent of soil concentration (Tuovinen et al. 2011, 2016). Thus, uptake (or crop concentrations) of for example Cl-36 are calculated as being proportional to the stable chloride concentration in the plant, and the ratio of Cl-36 and stable chloride dissolved in pore water[11]. This approach is referred to as a specific activity approach, and the model update makes the assumptions behind the mechanisms of plant uptake (and retention) of macronutrients more biologically plausible. Describing plant uptake in this way also makes independent sampling of plant and soil parameters in probabilistic simulations more informative compared with a conceptualisation based on the two strongly correlated radio-ecological parameters K_d and CR (see e.g. Sheppard et al. 2011).

[11] In SR-PSU this approach was used as an upper limit for plant uptake in the mire ecosystem (section 6.2.1 in Saetre et al. 2013a).

Table 8-3. Overview of radionuclide flows (processes) included in the BioTEx model (see Figure 8-1). The processes have been categorised with respect to the underlying mechanism, namely mass-flow of solids (MS), water (MW) or gas (MG), diffusion in water (DW) or in gas (DG), or incorporation into or release from organic matter due to photosynthesis (PP) or mineralisation (Min). "Y" indicates that the process is included as a dynamic flow between compartments in the aquatic, mire or agricultural sub-model. * indicates that only the steady-state outcome of the process is accounted for. Subscripts indicate that flows can occur between ecosystems (BTW), that the initial inventory in agricultural soil is conditioned on environmental concentrations in natural ecosystems (INIT), or the system(s) of cultivation including the process; drained mire (DM), continuous cultivation (Agri), infield-outland agriculture (IO) or a garden plot (GP).

Process	Related FEP in Chapter 6	Type	Radionuclide flux		
			Aqua	Mire	Agriculture
Biological					
Bioturbation	Bioturbation	MS	Y		Y^{DM}
Plant uptake	Uptake, Primary production	PP	Y	Y	*
Leaf retention/translocation	Uptake, Primary production	PP			$*^{Agri,GP}$
Litter respiration/release	Primary production, Decomposition	Min	Y	Y	Y^{IO}
Litter production	Excretion, Particle release/trapping	PP	Y	Y	
Regolith mineralisation	Decomposition	Min	Y	Y	$Y^{DM,IO,GP}$
Vegetation ingrowth^{BTW}	Primary production, Covering, Terrestrialisation	MS	Y	Y	
Water bound					
Horizontal advection^{BTW}	Convection	MW	Y	Y	
Vertical advection	Convection	MW	Y	Y	Y
Vertical diffusion	Convection	DW	Y	Y	
Groundwater uptake	Convection	MW			$Y^{DM,Agri}$
Solid liquid phase partition	Reactions, Sorption/desorption		*	*	*
Sediment dynamics					
Sedimentation	Deposition	MS	Y		
Resuspension	Resuspension	MS	Y		
Burial	Deposition, Resuspension, Decomposition	MS	Y	Y	
Gas transport/transition					
Degassing	Phase transition, Convection	MG	Y	Y	Y
Gas uptake	Phase transition	MG	Y	Y	
Gas exchange within unsaturated soil	Convection	MG			Y^{Agri}
Human behaviour					
Drain/cultivate$^{BTW, INIT}$	Stage of succession	MS			Y^{DM}
Fertilise^{BTW}	Anthropogenic release	MS			$Y^{IO,GP}$
Irrigate	Anthropogenic release	MW			Y^{GP}
Radiological					
Radionuclide decay/ingrowth	Decay		Y	Y	Y

In SE-SFL, plant uptake of radionuclides intercepted on leaves, and subsequent translocation to edible parts, is included for agricultural land-use variants with irrigation. The crops considered are potatoes (in the garden plot land-use variant), and cereals (agricultural land use variants in increased greenhouse-effect climate). Interception of radionuclides in irrigation water is calculated from the activity concentration in the irrigation water, the leaf area index and the leaf storage capacity (Saetre et al. 2013b)[12]. The translocation of radionuclides is then represented by an empirical translocation factor that describes the fraction of an intercepted radionuclide that ends up in the edible part of the crop (IAEA 2010).

[12] The amount of intercepted radionuclides corresponds to the leaf retention at the time for irrigation (t=0) in Equation 7-55 in Saetre et al. (2013a).

Leaf retention

Leaf retention refers to the temporary retention of radionuclides in intercepted irrigation water on the surface of crop leaves. The resulting activity concentration is added to the internal activity concentration of the edible parts of crops to calculate the dose from ingestion. In SR-PSU, leaf retention was only accounted for with respect to vegetables grown in a kitchen garden. In SE-SFL, large-scale irrigation is considered as an option to cover crop water deficiency in a warmer climate (due to increased greenhouse effect) and consequently leaf retention is also accounted for with respect to fodder (consumed by cattle)[13].

Litter respiration/release

When organic matter is metabolised by decomposers and grazers, labile organic carbon is transformed to inorganic carbon. Litter respiration/release thus refers to the release of radionuclides from fast (within a year) decomposition of aquatic and wetland net primary production. Through this process, radionuclides stored in plant biomass are released to the water column and to the upper peat layer in aquatic and mire ecosystems, respectively.

In SE-SFL, the fraction of radionuclides in litter that is released through mineralisation of labile organic matter (df_{decomp}) is calculated within Ecolego as a function of the refractory organic material in litter and the inorganic fraction of the plant's element inventory[14]. This modification was done to avoid parameter combinations that are not physically possible[15], and to preserve the dependence of litter release on the content of refractory litter, also in probabilistic simulations.

Litter production

Most of the biomass produced annually is metabolised by grazers and decomposers (see litter respiration above). However, a part of the biomass production is made up of refractory organic matter. This decomposes much more slowly, and consequently a fraction of the biomass production will contribute to the build-up of organic matter in the upper regolith layer. Litter production thus represents the transfer of radionuclides stored in plant biomass to the upper regolith layers in aquatic and mire ecosystems, respectively.

Regolith mineralisation

When refractory organic matter is metabolised by decomposers, organic carbon is transformed to inorganic carbon. Regolith mineralisation refers to the release of radionuclides from slow decomposition of organic matter in soil and sediments. Through this process, radionuclides stored in organic regolith layers are released to the pore water of the corresponding regolith layer in aquatic, mire and agricultural ecosystems, respectively.

Vegetation ingrowth

Wetland vegetation will colonise shores and bottoms of the sea and lakes. The establishment of mosses, emergent and floating-leaved vegetation is associated with soft bottoms, where organic matter from refractory litter accumulates, ultimately forming a peat layer that will cover the aquatic sediments. The process, vegetation ingrowth[16], thus represents the translocation of radionuclides in aquatic regolith layers to the corresponding mire regolith layer, caused by peatland succession.

[13] Radionuclides intercepted (and retained) by cereal grain are considered to be included in the empirical factor that describes translocation.

[14] Function described in Section 9.6.3 in Grolander (2013).

[15] This problem was pointed of for the SR-PSU parametrisation of microalgae and plankton by Walke et al. (2017).

[16] Vegetation ingrowth is also referred to as rate of infill in older SKB literature (e.g. Brydsten and Strömgren 2010).

Horizontal advection

This process represents advective transport of radionuclides by lateral bulk movement of water. In the submerged period, horizontal transport of radionuclides by advection occurs through water exchange between adjacent sea basins. In the land period, it occurs through diffuse groundwater flow or through streamflow (see Section 8.4.2).

Vertical advection

This process represents transport of radionuclides by vertical bulk movement of water and is the quantitatively most important mechanism for vertical transport of radionuclides between pore water in adjacent regolith layers and between aquatic sediments and the above water column (see Section 8.4.2).

Groundwater uptake

During dry periods of the year, capillary rise can cause an upward flow of groundwater to unsaturated soil layers. In areas receiving deep groundwater discharge, water uptake thus has the potential to transport water containing radionuclides from saturated soil layers to the overlying cultivated and biologically active layer, where it can be taken up by fodder and food crops.In SR-PSU, it was cautiously assumed that the radionuclide concentration in the water from the saturated zone was that of glacial clay (unless this layer was entirely incorporated into the cultivated layer). In SE-SFL, the concentration of this water is explicitly calculated for the model of the continuously cultivated agricultural land (Figure 8-2). For consistency (and increased realism) the concentration in this water for the drained mire agriculture is taken from the uppermost regolith layer which is undisturbed by the ditching (see Section 7.2.1 in Saetre et al. 2013b). Mires formed in lake basins typically have a thick peat layer, and consequently the post-glacial gyttja (rather than glacial clay) will typically be the uppermost saturated layer which is undisturbed by ditching.

Vertical diffusion

Diffusion refers to the transport of radionuclides due to Brownian movement of molecules in solution and/or gas. The rate of diffusion is strongly dependent on distance; diffusion is only considered to be a quantitatively important at scales of less than one metre. Consequently, this process is considered relevant for vertical transport of radionuclides between adjacent regolith layers, and between the sediment surface and water. Diffusion of radionuclides in gas is included in the process degassing, see below.

Solid liquid phase partition

In regolith layers, and in the water column, there is an exchange of elements (including radionuclides) between the solid state (the soil/sediment matrix and suspended particulate matter), and the liquid state (pore water or the water column). The exchange of radionuclides between the solid and liquid state is considered to be fast (occurring in days) as compared with the model resolution (years), and thus this process is described by an equilibrium-partitioning coefficient (K_d), rather than by dynamic fluxes (see Saetre et al. 2013b and Tröjbom et al. 2013).

Sedimentation

Particles suspended in the water column will be pulled downwards by gravity, and ultimately settle on the top of the uppermost sediment layer in aquatic ecosystems. Thus, the process, sedimentation, refers to the flux of radionuclides associated with the surface structure of suspended particulate matter, or stored in suspended particulate organic matter, to the corresponding inventory in the upper aquatic sediments.

Burial

If the rate of sedimentation of particulate matter is larger than the rate of resuspension, or if the rate of production of litter is larger than the rate of mineralisation, there is a net accumulation of sediments, and the total thickness of the regolith layer will grow. As the depth of the upper biological active zone is limited by oxygen supply from above, the deeper layer of this zone will become anoxic because of burial. Radionuclides associated with buried sediments will consequently be translocated from the upper sediments to the oxygen-depleted sediment layers below.

Degassing

There will be an exchange of gas between the open-water and soil (soil pore water) surfaces and the overlying atmosphere. Degassing refers to the radionuclide flux caused by this exchange of dissolved gas from the water column (for aquatic ecosystems), or from the soil pore water (for terrestrial ecosystems), to the atmosphere. For saturated soils, degassing is limited by the phase transition, whereas for well drained agricultural ecosystems it is limited by gas diffusion through air-filled soil pores.

In SR-PSU, the diffusivity of CO_2 in unsaturated soil (*D_CO2_soil*) was calculated for typical values of porosity and soil saturation for three soil types, and the uncertainties of these parameters were quantified by probabilistic simulations (Section 5.4.5 in Grolander 2013). In SE-SFL, the calculation of the diffusivity is incorporated as a function in the model (Saetre and Ekström 2017a). This update makes the interdependency of model parameter values more transparent in the model code and ensures that the dependency is maintained in probabilistic simulations.

Gas diffusion is also expected to be a fast process distributing C-14 within unsaturated soil layers (as compared with solute transport). Consequently, this process has been included in SE-SFL in the model for the continuously cultivated land, operating between the two unsaturated soil layers (RegoSub and RegoUp in Figure 8-2).[17]

Gas uptake

There will be an exchange of gas between the surfaces of open water and soil pore water, and the overlying atmosphere. Gas uptake refers to the radionuclide flux caused by the gross exchange of gas from the atmosphere (source) to gas dissolved in the water column, or in the soil pore water of surface peat, for aquatic and mire ecosystems, respectively.

Drain/cultivate

Draining lakes and wetlands will lower the groundwater table, and organic regolith layers above the water table will subside due to compaction and decomposition. In the model, the process ‘drain/cultivate’ thus refers to the transfer of radionuclides from wetland regolith layers to the unsaturated layer of cultivated soil in an agricultural ecosystem. This transfer of radionuclides controls initial radionuclide inventories in the cultivated soil, but it does not affect radionuclide inventories in natural ecosystems.

Fertilise

The key principle behind the agrarian infield-outland system is to fertilise arable land with nutrients from meadows and pastures, using animal manure as organic fertiliser. The process fertilise thus represents the input of radionuclides originally stored in vegetation to cultivated soil. In the infield-outland land use variant, the radionuclides are originally stored in wetland vegetation, and this is also true for fertilisation with ash from combustion of wood in one garden-plot variant. However, the garden plot also considers peat ash and marine macro algae as relevant sources for fertilisation.

Irrigate

Radionuclides in water can be transferred to soil and vegetation through irrigation of arable land. Under the current climatic conditions, irrigation of soil for growing potatoes and vegetables in the open is plausible in the Laxemar area. Thus, irrigation refers to the input of radionuclides from irrigation water to cultivated soil on the scale of a household garden-plot. In SR-PSU, irrigation was only considered relevant for a kitchen garden. However, in SE-SFL, large-scale irrigation is considered as an option to cover crop water deficiency in a warmer climate and thus irrigation is also considered relevant for cultivation of a drained mire, when temperatures are elevated due to, for instance, global warming caused by increased greenhouse-gas emissions.

[17] As with molecular diffusion in water of saturated soil layers, the net gas diffusion between unsaturated soil layers is described by two flows (back and forth) against zero concentration (Section 4.4 in Saetre et al. 2013a).

Radionuclide decay/ingrowth

Radioactive decay is the process by which a nucleus of an unstable atom loses energy by emitting particles (e.g. alpha or beta) or gamma rays of ionising radiation. Radioactive decay is treated as a removal mechanism in all model compartments. For decay that results in a radioactive progeny nuclide, the radioactive decay is matched by a source term representing ingrowth for the decay product.

8.4.2 Hydrology and advective transport

Detailed hydrological flow modelling contributes to the modelling of transport and accumulation of radionuclides in the biosphere in several ways. The underpinning flow modelling comprised several distinct components: the exchange of water between individual sea basins and the coastal zone was estimated (Engqvist 2010), discharge areas for groundwater potentially carrying radionuclides from the repository were identified (Werner et al. 2006, Sassner et al. 2011), the network of present and future streams was described (Bosson et al. 2009, Sassner et al. 2011), and ground- and surface-water flows were modelled (Bosson et al. 2009, Sassner et al. 2011).

In SE-SFL, the MIKE SHE flow models were used to derive water balances for biosphere objects, and parameters for the BioTEx model were calculated from these (Werner et al. 2013). However, water balances were only available for the present conditions of the Laxemar landscape. Thus, to allow calculation of water flows given future and past conditions, stylised water balance models have been developed in SE-SFL. These water balance models include three natural successional stages (sea, lake and mire) (Figure 8-3), and an agricultural land (including unsaturated regolith layers and ditches). Using these stylised models, in combination with empirically derived rules for percolation and object-specific boundary conditions, the discharge profiles have been calculated for multiple successional stages and climate conditions that are significantly different from present conditions (Chapter 5 in Grolander and Jaeschke 2019).

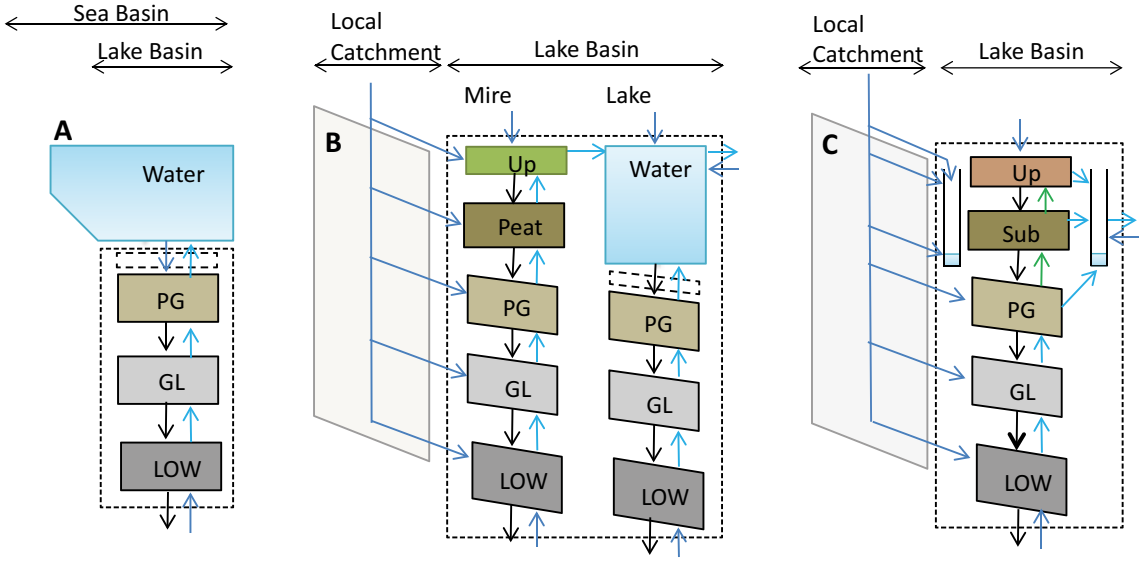

Figure 8-3. *Stylised water balance models for biosphere objects in three successional stages: A) sea basin, B) lake-mire complex and C) continuously cultivated land. Boxes represent regolith layers or surface water, and arrows represent flows of water. Dark blue arrows indicate water discharged into the object across its boundary. Black arrows indicate percolating water. Light blue arrows represent discharging groundwater within the object. Green arrows represent groundwater uptake driven by plants. Arrows towards the right-hand side represent the stream inlet (dark blue) and outlet (light blue). Dashed compartment indicates that the upper part of aquatic sediments (RegoUp) is regarded as having little hydraulic resistance and the flows through this compartment are assumed to be the same as at the top of the consolidated sediments (RegoPG). When the biosphere object is cultivated (panel C), all discharge from the upper part of the local catchment (i.e. above the groundwater table), and from the stream inlet, is drained into the ditch surrounding the cultivated area. The local catchment (i.e. the area of the sub-catchment less the area of the biosphere object) is indicated in light grey.*

Flows of surface water during transitions between successional stages have been handled in a similar way as in SR-PSU (Appendix G, Saetre et al. 2013b). However, due to the lack of data only one mire stage was used in the simulations in SE-SFL. Moreover, the transition between sea and lake conditions was assumed to start when the local catchment begins to emerge from the sea, which was approximated to occur when the average water depth of a basin falls below 6 m (Chapter 5 in Grolander and Jaeschke 2019).

8.5 Calculating future exposure to humans

The doses to humans resulting from a potential release of radionuclides from an existing or hypothetical repository for long-lived waste need to be evaluated over hundreds of thousands of years. The evaluation involves estimating activity concentrations of radionuclides in the environment (air, soil and water, see previous sections), and in plants and animals that may serve as foodstuffs for human inhabitants. Assumptions on properties and habits of the humans that will live in or utilise the biosphere objects are required to estimate external exposure and intakes of contaminated foods. As in previous SKB safety assessments, assumptions on human habits are derived from historically sustainable land-uses which would result in relatively high exposures. The land-uses are formalised into a number of potentially exposed groups (PEGs), and the use of these groups ensures that the most exposed group is evaluated in the calculations of SE-SFL (Section 6.3).

Radionuclides in the environment may lead to both external and internal exposure. In this safety evaluation, the total dose from exposure to radionuclides in the environment is the sum of exposure through ingestion, inhalation and from external radiation. The internal exposure from ingestion is the product of the activity concentration in the contaminated food (or water) and the amount of contaminated food (or water) consumed. The resulting dose is calculated by multiplication with the appropriate dose conversion factor for ingestion which accounts for retention in the human body and exposure from decay products.

Both radionuclides in gaseous form and radionuclides adsorbed to dust particles contribute to the activity concentration in air. This means that the internal exposure from inhalation of contaminated air depends on the activity concentration in air from particles and from radionuclides in gaseous form, the inhalation rate, and the time spent in contact with contaminated air. The dose from inhalation can then be calculated by multiplying exposure with an appropriate dose coefficient.

In SR-PSU, aggregated dose coefficients were used to convert activity concentrations in combusted fuel directly to dose from inhalation of particles. For increased transparency and consistency, these calculations are now made in two steps in SE-SFL. First the activity concentration in the air is calculated from the activity concentration in the combusted fuel[18], and then the dose from inhalation is calculated as described above.

External exposure through the environment is calculated from the activity concentrations in environmental media and the time spent in contact with or close to the media. In this safety evaluation, only exposure from the soil is considered, since this is the only medium expected to be associated with both high activity concentrations and long exposure times (in contrast to direct irradiation from water or air). The exposure pathways considered in SE-SFL are summarised in Chapter 6. A more detailed description, including the mathematical models, is given in Saetre et al. (2013a, b).

[18] In SE-SFL, the concentration in air is calculated by multiplying the activity concentration in the combusted fuel (per dry weight) with the fraction that ends up in fly ash and exhaust gas after the combustion (as described in Equation 7-66 in Saetre et al. 2013a), and then applying a conversion factor accounting for the fuel combustion rate and atmospheric dispersal (Stenberg and Rensfeldt 2015, Grolander and Jaeschke 2019).

9 Comparison between the SE-SFL and SR-PSU biosphere models

9.1 Introduction

As a result of SSM's reviews of SR-Site and SR-PSU (e.g. SSM 2017, 2018, Walke et al. 2017), and from SKB's own development and research programs the BioTEx model has been somewhat modified in SE-SFL (Table 8-1). The most important update is a higher spatial discretisation of the two deepest regolith layers. Additionally, for improved consistency and transparency, several model parameters have been replaced with functions in the model code, including the dynamic development of peat thickness and calculations of the pore water dissolved inorganic carbon (DIC) concentration. Moreover, the specific activity approach is applied to model plant uptake of radionuclides behaving similarly to macronutrients (e.g. Cl-36 relative to stable chlorine) in all terrestrial ecosystems. In addition, a new multi-layer model for continuous agriculture is introduced. To evaluate the effects of model updates, model inter-comparison is performed, as described in this chapter.

The model comparisons were focused on natural ecosystems, since long-term accumulation in a mire (followed by drainage and cultivation) is expected to be the pathway leading to the highest exposure of future human inhabitants (see for example SKB 2010b and SKB 2014d, and Section 11.2 in this report). Moreover, to simplify the comparisons and interpretations, a unit release rate is used as a geosphere release and environmental concentrations are selected as the endpoint for comparisons. Model differences in radionuclide specific dose per unit release rate (i.e. LDF values) are expected be proportional to differences in these concentrations in the water and peat for the aquatic and terrestrial ecosystems, respectively.

This chapter starts by describing the increased discretisation that is introduced in the SE-SFL model in some detail (Section 9.2). Next, the methods for making the comparisons are described (Section 9.3). The model comparisons are first made for a biosphere object that develops continuously from a sea basin, through a lake stage, to a mire (Section 9.4). As the effects of the model updates depend on the properties of the biosphere object, the comparison is then expanded to include an object with a relatively high rate of area-specific groundwater discharge (Section 9.5). In a separate section (9.6), the results from the new (and more finely discretised) model for continuously cultivated soil are compared with results from the simplified model used to evaluate dose from cultivation of a drained mire. The chapter ends with a summary of the results (Section 9.7) and it is concluded that these well-motivated model updates are likely to have a relatively limited impact on deterministic calculations in many situations.

9.2 Vertical discretisation

The increased discretisation of the till (RegoLow) and glacial clay (RegoGL) compartments have the potential to affect both the time to reach equilibrium (in all regolith layers) and the equilibrium concentrations of radionuclides (primarily in till and glacial clay). This is because a higher vertical resolution decreases the numerical dispersion (delaying and prolonging the break-through of sorbing radionuclides). Moreover, the more finely discretised model captures the depth-dependent change in upward flow within the two regolith layers (if such a gradient exists). This may result in a modelled upward groundwater flow through each layer that, on average, is less in the discretised model than in the original model, where the flow across the upper boundary is used to represent the flow through the layer (Figure 9-1A). Thus, for conditions where the transport rate is low (e.g. due to limited groundwater flux and/or strong sorption), the more finely discretised model may lead to a significant retardation of radionuclides in the lower regolith layers. Moreover, when transport is slower, the relative importance of radioactive decay will increase. Consequently, a more finely discretised model may predict lower activities in upper regolith layers, particularly in the case of relatively short-lived radionuclides.

There are several differences between the simplified model of the drained soil and the continuously cultivated soil (Figure 9-1B). The most important difference, from a dose perspective, is that the drained mire includes an initial inventory of radionuclides (resulting from long-term accumulation in the preceding natural-state mire peat) that is lacking in the model of the continuously cultivated soil.

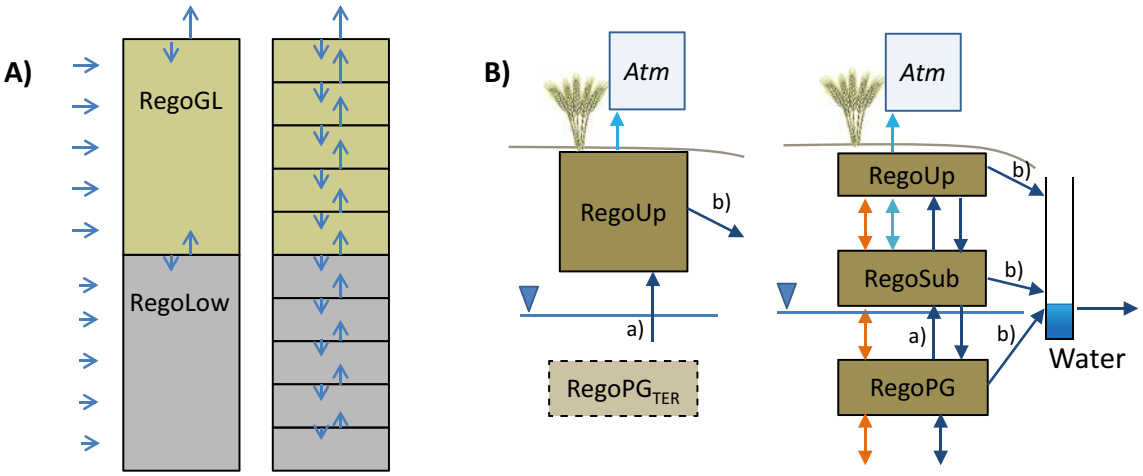

Figure 9-1. *Schematic pictures of models compared. A) Simple and discretised representation of till (RegoLow) and glacial clay (RegoGL). Longer blue arrows indicate higher groundwater flows and vice versa. Note that in the simpler model the upward groundwater flow at the upper boundary has been used to represent the flow conditions throughout the compartment. B) Simplified and discretised representations of the unsaturated layer of agricultural soil. Saturated layers are located below the groundwater table, which is illustrated as a horizontal blue line. Arrows represent radionuclide fluxes associated with groundwater advection (dark blue), gas diffusion (light blue), and solute diffusion (orange); a) = groundwater uptake, b) = runoff. Note that the source of the deep groundwater in the drained mire is that of an undisturbed regolith layer below the ditching depth (RegoPG$_{TER}$ in the example).*

Due to simplifying (and cautious) assumptions, the activity concentration of the groundwater that reaches the unsaturated soil in the drained mire is higher than in the continuously cultivated soil, as the deep groundwater in the drained mire is drawn from a deeper regolith layer. However, the present model comparison focuses on structural differences in the representation of the unsaturated layer, i.e. how the predictions from a simplified one-compartment model differ from those of a more complex two-compartment model. Thus, the comparison excludes the effects of how the earlier accumulation and radionuclide concentrations in deep groundwater affect the model endpoints.

9.3 Methods

Four relatively long-lived radionuclides that were expected to have a significant impact on the final dose consequences in the SE-SFL safety evaluation were selected to examine the model performance; namely C-14, Cl-36, Mo-93 and Ni-59. The first radionuclide, C-14, is unusual in many ways; it adsorbs very weakly to soil particles or suspended material, in some chemical forms it is highly volatile and will degas when in contact with the atmosphere, and its long-term accumulation occurs through plant fixation and subsequent storage of organic matter in deep peat. The second radionuclide is Cl-36. This radionuclide has weak sorption properties, and as a plant nutrient it accumulates in plant biomass. However, as Cl-36 is primarily stored in inorganic forms in organisms, most of it is readily released upon plant senescence. The third radionuclide, Mo-93, has highly variable sorption properties; molybdenum is relatively mobile in inorganic regolith layers, but adsorbs strongly to sediments that are rich in organic matter, including peat and post-glacial clay gyttja. The last radionuclide here, Ni-59, is relatively immobile, especially in deep regolith layers. Thus, Ni-59 may accumulate in deeper regolith layers for thousands of years before reaching the surface environment.

The comparisons of models were done based on a unit release rate (1 Bq year^{-1}). The activity concentrations in regolith pore water and surface water were chosen as the primary endpoints. The solute concentration allows for a direct assessment of dilution, and as the solid state is linearly related to the pore water concentration (through the K_d value) it can also be straightforwardly used to compare radionuclide accumulation in different regolith layers.

To evaluate the effects of an increased discretisation of the lower regolith layers, the SR-PSU and the SE-SFL models were run to equilibrium (1 million years). In the model inter-comparison, radionuclides were released to the future lake 116 in Forsmark starting 2000 years before the present. During the simulation, the object transforms through natural succession from a coastal basin into a mire (including a 5000-year-long lake phase). The parameter values for SE-SFL were used in the comparison (see Chapter 10), but the time scale for the development of the object was selected to be that of the original location in Forsmark (to allow for a substantial sea period). That is, in the simulation lake isolation occurs around 4500 AD, and a mire covers the lake basin at 9900 AD. To facilitate results interpretation, a third version of the biosphere model was run in parallel. In this model, all modifications introduced in SE-SFL were implemented except the increased discretisation.

The specific groundwater flow from the bedrock into object 116 is relatively limited even during the terrestrial stage (~10 mm year^{-1}). Under such conditions, the transport of sorbing radionuclides can be slow, and the effect of radioactive decay may be substantial. A limited discharge rate at the bedrock boundary also leads to a steeper groundwater flux gradient towards the surface of the object. To broaden the scope of the model comparison, we also evaluated the case of a permanent mire object (206), subject to an order of magnitude larger area-specific discharge of deep groundwater (260 mm year^{-1}).

The comparison of agricultural models is focused on the potential impact of model structure on accumulation of radionuclides during cultivation. The initial inventory of radionuclides in the drained mire was set to zero (no earlier accumulation was accounted for). Moreover, the same values were used in both models for groundwater uptake (0.04 m year^{-1}), total rate of runoff/percolation from the unsaturated zone (0.2 m year^{-1}), thickness of the unsaturated zone (0.5 m) and other soil properties (i.e. density, porosity and soil saturation for cultivated clay gyttja). The models were solved for steady state conditions, and for ease of presentation the response (i.e. the activity concentration in pore water) was normalised with that in the regolith below the cultivated soil (i.e. RegoPG, which is the source for groundwater uptake).

9.4 Model comparisons of a developing object

In this section, a model comparison is reported for an object that develops from sea to a mire (through a lake stage) and has a relatively low area specific discharge of groundwater from the geosphere (i.e. object 116 from Forsmark).

9.4.1 Carbon-14

C-14 adsorption on regolith was considered negligible ($K_d = 0$), and the transport and accumulation of this radionuclide is marginally affected by radioactive decay. The effects of the SE-SFL model updates on C-14 resulted in an increase in the pore water concentration in the two lowest regolith layers (RegoLow and RegoGL), and a slightly increased period until equilibrium was reached in all regolith layers (in the initial submerged period). In the mire of object 116, a moderate (1.6-fold) concentration gradient between the lowest and the topmost layer of the till remains at the end of the simulation (Figure 9-2). However, the average concentration in the till is only 35 % larger in the more discretised model compared with the original model. The pattern in the glacial clay layer is similar, and the average concentration in this layer is 20 % higher in the more discretised model. The effects of the discretisation are larger in the lake part of object 116, and the average concentration in the till and glacial clay layers is two times and 30 % larger, respectively, in the updated model (Figure 9-3). However, equilibrium concentrations in all regolith layers above glacial clay were unaffected by the model updates introduced in SE-SFL.

The delay to reach equilibrium is primarily caused by a decrease in the numerical dispersion, whereas the increased equilibrium concentrations in the lower regolith layers can be explained by a lower (and more representative) upward flow of groundwater in the more discretised model (see discussion above). The differential response in the terrestrial and aquatic parts of object 116 (during the terrestrial stage) is caused by differences in the groundwater flow patterns between the two ecosystems. That is, in the mire, the net flux is clearly directed upwards, whereas in the lake/stream the downward flux almost balances out the upward flow, which leads to an increased circulation of groundwater

within regolith layers. By comparing the original SR-PSU model with an updated model without an increased discretisation, we conclude that the other model updates listed in Table 8-1 have marginal effect on concentrations of C-14 in all regolith layers of the natural ecosystems (data not shown).

9.4.2 Chlorine-36

Cl-36 is mobile and has a long half-life. Therefore, the transport and accumulation of this radionuclide is only marginally affected by radioactive decay. For Cl-36 the effects of model updates on environmental concentrations are very similar to those for C-14 (Figures 9-2 and 9-3). That is, also for Cl-36 the increased discretisation resulted in an increased concentration in the two lowest regolith layers (RegoLow and RegoGL)[19], and the time to reach equilibrium increased. The initial transport delay is more pronounced for Cl-36 than for C-14, as Cl-36 has, in contrast to C-14, a non-zero K_d value in all layers. As with C-14, equilibrium pore water concentrations in all regolith layers above the glacial clay are unaffected by the model discretisation, and other model updates listed in Table 8-1 have an insignificant effect on water concentrations (data not shown).

In SE-SFL the fraction of Cl-36 released during mineralisation is expressed as a function of the inorganic fraction of the plant inventory. This model formulation thereby corrects a previous inconsistency of the parameterisation of litter release in aquatic ecosystems, and the updated model predicts a significantly larger accumulation of Cl-36 in the organic compartment of aquatic sediments (data not shown). Thus, the total activity concentration in the surface sediments (RegoUp + RegoUporg) of the lake has increased by approximately a factor of two in the SE-SFL model compared with the SR-PSU model. However, only a fraction of this effect propagates to the aquatic post-glacial sediments (~10 % increase in RegoPG + RegoPGorg), and the transfer of an increased Cl-36 activity in organic sediments to terrestrial regolith (through mire ingrowth) does not have any noticeable effect (< 1 %) on the inventory in the terrestrial post-glacial regolith.

9.4.3 Molybdenum-93

Mo-93 has a low to moderate K_d value in lower regolith layers, and high K_d values in regolith layers containing organic matter. In combination with a relatively short half-life (4 000 years) and low groundwater velocities, this may lead to a substantial reduction of activity because of radioactive decay during transport through several regolith layers[20]. The effects of the SE-SFL model updates on Mo-93 can be seen as an increase in the concentration in till (RegoLow), and a concentration decrease in the layers above it. Moreover, for regolith layers above the till and glacial clay, the reduction in numerical dispersion leads to a 20 % delay in the time to reach equilibrium in peat (RegoPeat), and this time is extended by ~ 5 000 years[21] (Figure 9-2).

Increasing losses through radioactive decay lead to a steeper concentration gradient within the till layer, resulting in a 4.5-fold difference between the bottom and top sub-compartments. The cumulative effect of radioactive decay results in a 40 % reduction in the net upward release from the till layer (as compared with the release from a less finely discretised model) at steady-state in the mire (Figure 9-3). The increased discretisation also leads to a 36 % increase in average Mo-93 concentration within the till layer. This increase is similar to that of radionuclides that are less affected by decay such as C-14 and Cl-36.

[19] The increase of the Cl-36 concentrations in till (RegoLow) and glacial clay (RegoGL) were 30 % and 15 % in the mire part of the object, whereas the corresponding increases in the lake/stream part were 90 % and 45 %.

[20] In object 116, the residence times of Mo in the three lower-most regolith layers (RegoLow, RegGL and RegoPG) are considerably longer than the half-life of Mo-93, and in peat (RegoPeat) the residence times is similar to the half-life.

[21] The time to reach 95 % of equilibrium concentration in peat is approximately 30 000 years in the more discretised SE-SFL model as compared with 25 000 years for the original SR-PSU model.

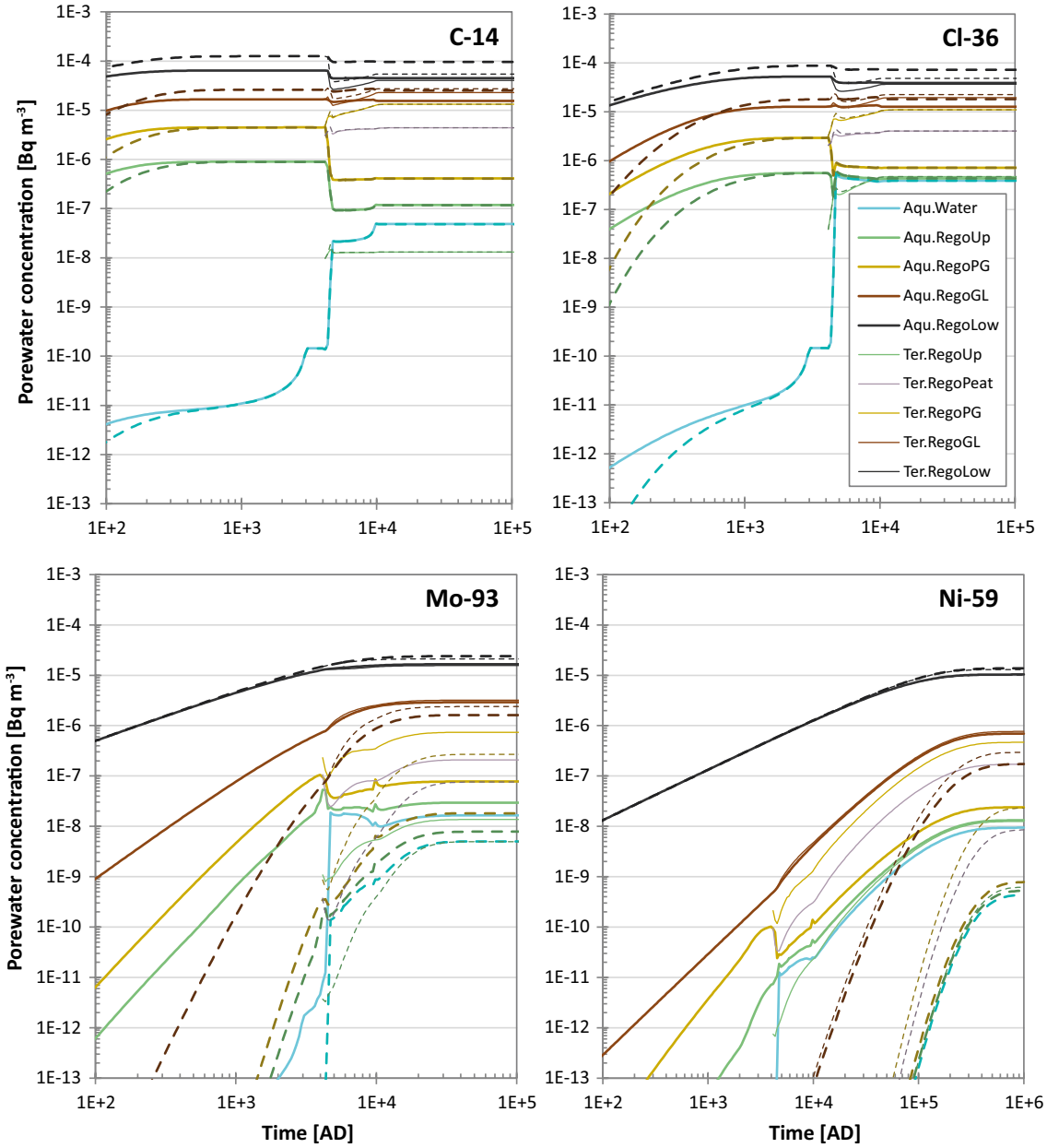

Figure 9-2. *Model comparison of pore water concentration of four radionuclides in object 116. Solid lines represent calculation with the original SR-PSU model, whereas dashed lines represent calculation with the updated SE-SFL model. The bold lines represent concentrations in aquatic ecosystems (sea or lake/stream), whereas the thin lines correspond to concentrations in the mire ecosystem. Calculations are based on a unit release rate (1 Bq year^{-1}). Note that the evaluation time corresponds to 10^{6} years for Ni-59 but only 10^{5} years for the other three radionuclides.*

The discretised model returns a similar 4.5-fold gradient between the bottom and top of the sub-compartments for the glacial clay in the mire (Figure 9-3). However, in contrast to the results for C-14 and Cl-36, the increased discretisation of the glacial clay (RegoGL) and till (RegoLow) model compartments did not result in an increased concentration in the glacial clay layer Instead, the average concentration of the glacial clay is 25 % lower in the discretised model compared with the original model (Figure 9-4). The main reason for this decrease is the 40 % decrease in the net release of radionuclides from the till to the glacial clay layer.

The cumulative effect of the increased discretisation on radioactive decay causes a reduction of the net release from the glacial clay to the above soil column by 60 % as compared with the SR-PSU model. This reduction in release is propagated to the above regolith layers (RegoPG, RegoPeat

and RegoUp) and the concentrations in those layers are consequently 60 % lower than those in the SR-PSU model. Finally, it is observed that other model updates listed in Table 8-1 have an insignificant effect on the activity concentrations of regolith layers in natural ecosystems (data not shown).

9.4.4 Nickel-59

Ni-59 is a radionuclide that has a high K_d value in several regolith layers and a relatively long half-life, which leads to a substantial influence of radioactive decay on transport and accumulation in several regolith layers[22]. The effects of the SE-SFL model updates on Ni-59 are similar to those for Mo-93, as the concentration in the lowest regolith (RegoLow) increases whereas concentrations in more superficial layers decrease. The reduction in numerical dispersion leads to a 75 % increase in the time required to reach equilibrium in layers above the till and glacial clay (Figure 9-2). However, as Ni-59 has a larger K_d value than Mo-93 (in the lower regolith layers), the increase in absolute time is extended to more than 10^5 years (Figure 9-2).

Radioactive decay in combination with high sorption leads to a steeper concentration gradient within the till layer as compared with Mo-93 (resulting in a 10-fold difference between the bottom and top sub-compartments), and causes a 60 % reduction in the net release to the glacial clay layer (as compared to the release from a less discretised model) (Figure 9-3). However, the effect of increased discretisation on the average concentration within the till layer itself is similar to that of the other investigated radionuclides; the average concentration of Ni-59 in till increases by 30 %.

In the glacial clay, the effect of radioactive decay is larger and the discretised model returns an even steeper concentration gradient (20-fold difference between the bottom and top sub-compartments), with the average concentration in this layer being 60 % lower in the discretised model than in the original model (Figure 9-3). The cumulative effect of the increased discretisation on the loss of activity through radioactive decay, causes a reduction of the net release from the glacial clay to the above-soil column by more than 90 % as compared with the SR-PSU model (Figure 9-3). This reduction in release is propagated to the overlying regolith layers (RegoPG, RegoPeat and RegoUp)[23] and the concentrations in these layers are an order of magnitude lower in the more discretised model than in the SR-PSU model. Finally, it is observed that other model updates listed in Table 8-1 have an insignificant effect on the activity concentrations of regolith layers in the natural ecosystems (data not shown).

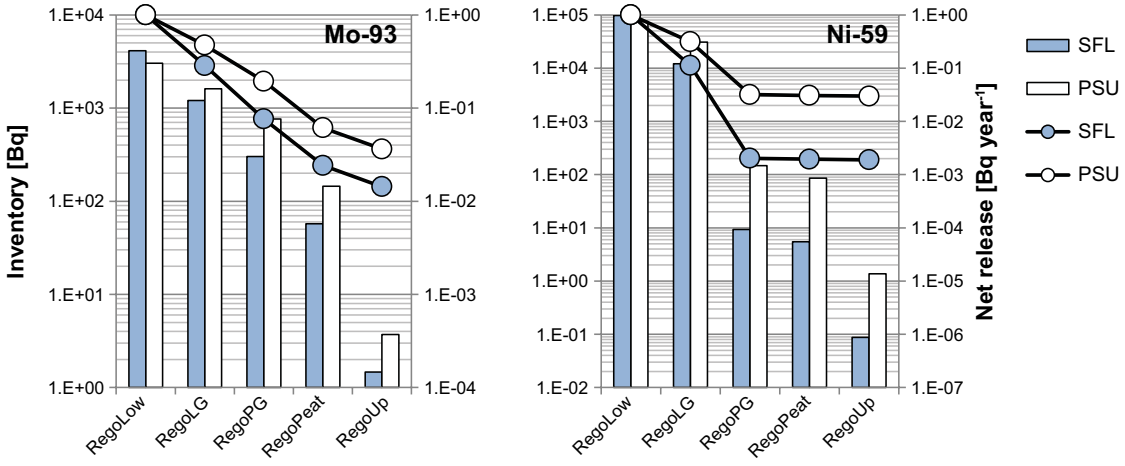

Figure 9-3. *Model comparison of steady-state inventory and net release to the overlying regolith layer (or stream) in the mire ecosystem in object 116. Bars represent inventory (Bq) and circles net release with groundwater from below (Bq year^{-1}). White bars/symbols represent results from the original SR-PSU model, whereas blue bars/symbols represent results from the updated SE-SFL model. Calculations are based on a unit geosphere release rate (1 Bq year^{-1}).*

[22] In object 116, the residence time of Ni in the two lower-most regolith layers (RegoLow and RegGL) is significantly longer than the half-life of Ni-59.

[23] Less than 0.2 % of the unit release reaches the soil layers above the glacial clay layer in the more discretised SE-SFL model.

9.5 Model comparisons – impact of groundwater discharge rate

In this section, the sensitivity of the model response to differences in object properties is illustrated by including an object with a relatively high area-specific groundwater discharge. The comparison is only carried out for the end stage, which is most relevant for exposure from most radionuclides.

The area-specific discharge of deep groundwater from the bedrock (m year^{-1}) into object 206 is an order of magnitude larger than that into object 116 (see Section 9.3), and the inflow of water from the local catchment has virtually no effect on the groundwater flow in the lower part of the regolith profile of object 206. This leads to a groundwater flux pattern where the upward flow is approximately constant (and much larger than percolation) in the deeper parts of the regolith profile. Moreover, the average thickness of the glacial clay layer in 206 is only half of that in object 116. The combined effects of the increased bedrock discharge and the difference in thickness of regolith layers, is water residence times that are 20 times shorter in the till layer, and 30 times shorter in the glacial clay layer in object 206, as compared with object 116. For Mo-93 and Ni-59, this translates into a decrease in the effect of radioactive decay on the accumulation of activity in the deeper parts of the regolith profile (Figure 9-4).

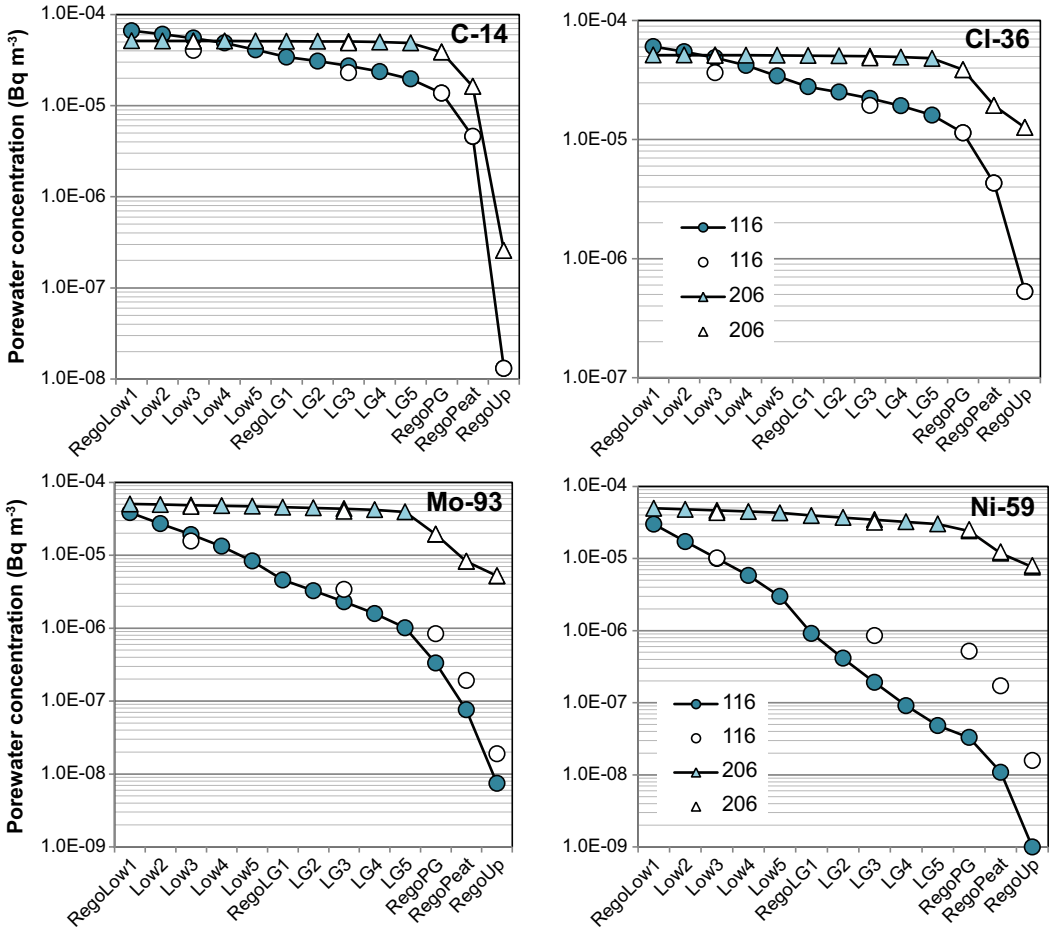

Figure 9-4. *Model comparison of steady-state pore water concentrations of four radionuclides in the mire of two biosphere objects. Circles represent concentrations in object 116, and triangles represents concentrations in object 206. White symbols represent the original SR-PSU model, and connected blue symbols represents the more finely discretised model used in SE-SFL. For simplicity, the concentration of RegoLow and RegoGL from the SR-PSU model has been plotted with the central layer (Low3, GL3) in the graph. Calculations are based on a unit release rate to each object (1 Bq year^{-1}).*

The differences in object properties result in a groundwater concentration gradient in object 206 that is quite different from that in object 116 (Figure 9-4). Due to the short residence times, very small amounts of C-14 and Cl-36 are lost through radioactive decay which leads to quasi-constant concentrations in the till and glacial clay layers. Moreover, as the change in upward flow throughout the deeper parts of the regolith column is limited, there is virtually no effect of the increased discretisation on the concentration in the regolith layers in object 206. This stands in contrast to the limited (but noticeable and expected) effect of an increased discretisation on the concentration of C-14 and Cl-36 in object 116 (as seen in Figure 9-4 and discussed in Section 9.3)

For Mo-93 (and Ni-59) the fast turnover rate of groundwater in object 206 reduces the loss of activity due to decay by more than an order of magnitude, as compared with object 116. In the more finely discretised model, the cumulative loss of activity in the till and glacial clay equals only 8 % and 15 % for Mo-59 in object 206 (as compared with 71 % and 92 % in object 116).The marginal effect of decay give rise to a weak concentration gradient through the deepest part of the regolith profile (Figure 9-4). The corresponding losses in the till and glacial clay for Ni-59 are 15 % and 40 % in object 206, (as compared to 89 % and 99.8 % in object 116). Given the relatively weak effects of radioactive decay in object 206, it is not surprising that the increased discretisation has a marginal effect on regolith activity concentrations. Thus, the average concentrations in the till and glacial clay layers of the more finely discretised model exceed those predicted by the original SR-PSU model by less than 10 % while the concentration in the groundwater leaving the glacial clay layer is nearly identical in the two models (Figure 9-4).

9.6 Discretisation of the unsaturated soil layer in the agricultural model

In both the original representation and the SE-SFL representations of continuously cultivated soil, the activity concentration in the unsaturated soil is consistently lower than in the saturated soil (Figure 9-5). For non-volatile radionuclides[24] (Cl-36, Mo-93, Ni-59) the concentration gradient is primarily due to drainage of groundwater and dilution by meteoric water towards the surface. The resulting concentration gradient is weak, so the difference between the three layers (RegoPG, RegoSub and RegoUp) is less than an order of magnitude.

The concentration of C-14 decrease much more dramatically in the unsaturated soil, and the pore water concentration of C-14 in upper regolith (RegoUp) is almost three orders of magnitude lower than in the saturated soil. The concentration drop is due to degassing from the topmost layer. Gas diffusion is also effective in mixing C-14 in the unsaturated soil, and the concentration in the subsoil (RegoSub) resembles that of the upper layer (rather than that of the saturated soil). Thus, for C-14 one well-mixed compartment appears to be a conceptually reasonable approximation to the unsaturated soil profile.

In the two-compartment model, the concentrations of Cl-36, Mo-93 and Ni-59 in the uppermost layer are less than 50 % of that in the subsoil (Figure 9-5). Consequently, one could expect that the concentrations in the unsaturated soil in the one-compartment model (which includes the sub-soil) would be higher than in the top layer of the two-compartment model. However, the upward flux of groundwater from the saturated zone (and through the unsaturated soil) is relatively low (< 0.1 m year^{-1}) and thus solute diffusion (a process that is not included in the simple model) contributes to the upward transport in the two-compartment model. Thus, the cautious assumption of mixing in the simple model is completely (Cl-36) or partially (Mo-93 and Ni-59) compensated for by having overlooked the contribution from diffusion of radionuclides from the saturated layer. The net effect is that the simple model returns similar, or somewhat cautious, estimates of the activity concentration in the uppermost regolith layer (where root uptake is assumed to occur). At steady state, the Cl-36 concentrations simulated by the one-compartment model differ only by a few percent (2 %) compared with those predicted by the two-compartment model. However, concentrations of Mo-93, C-14 and Ni-59 are 13 %, 21 % and 69 % higher in the one-compartment model than in the two-compartment model.

[24] Cl-36 has some capability for volatilisation, but in the model it is assumed to be non-volatile.

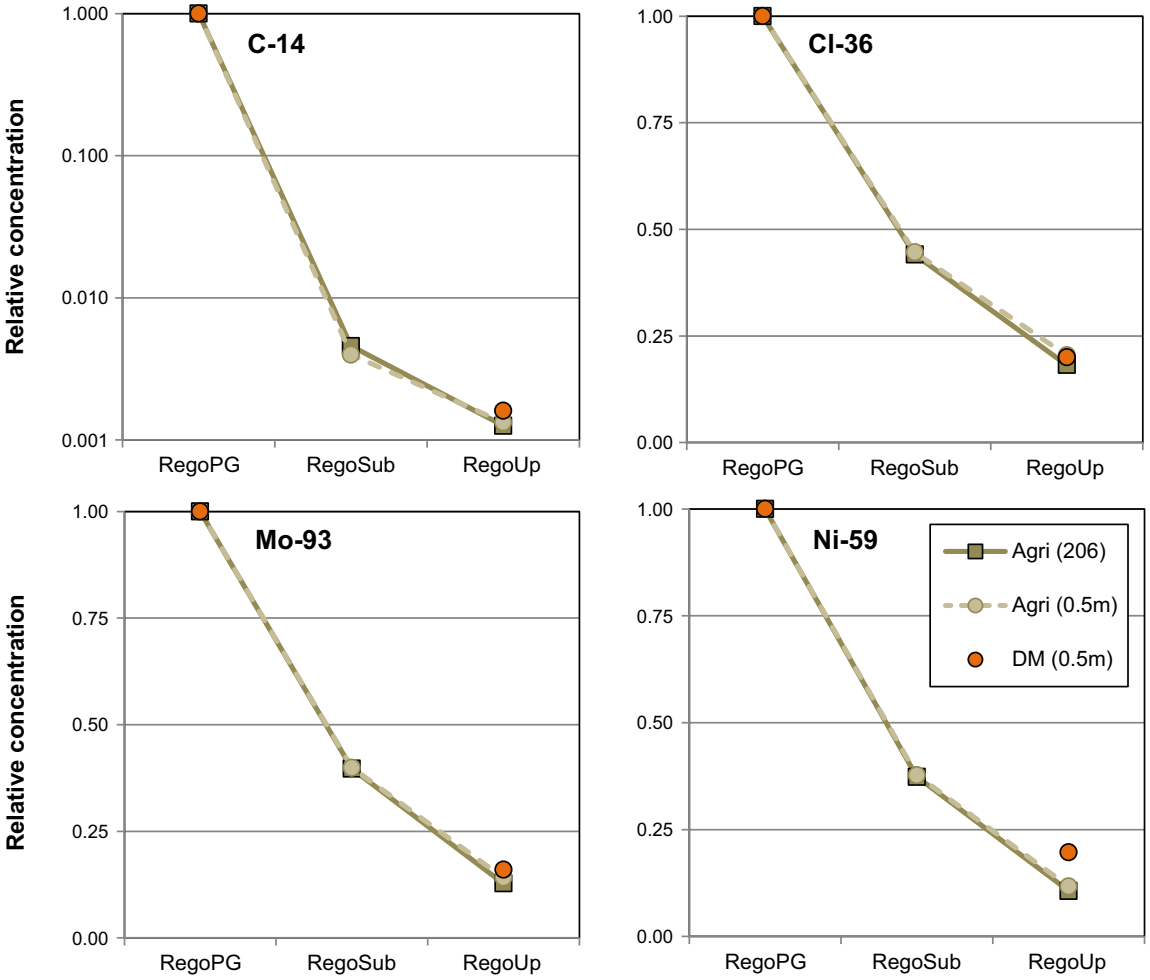

Figure 9-5. *Model comparison of steady-state pore water concentration of four radionuclides in the unsaturated layer of cultivated soil. Orange circles represents the concentration in the simple one compartment model (DM 0.5m), whereas light brown circles (Agri 0.5m) represents the concentrations from the two-compartment model. For reference, the results from the regolith depth of object 206 are included (dark brown squares, Agri 206). For C-14 (upper left) the scale of the activity concentration is logarithmic. Note that all activity concentrations are expressed in relation to that of the saturated layer (RegoPG).*

9.7 Concluding remarks on the model comparison

Several modifications to the biosphere model were introduced in SE-SFL, and the effects of model updates have been evaluated this chapter. The increased vertical discretisation of the two deepest regolith layers clearly has the potential to affect environmental concentrations (and the time to reach equilibrium concentrations). However, the effect of an increased discretisation strongly depends on the properties of the considered biosphere object and radionuclide, and the effects of the model update vary throughout the regolith profile. For example, our model comparison shows that in an area with a high bedrock discharge (260 mm year^{-1}), and a limited change in the upward flow with regolith depth, the vertical discretisation will have little or no effect on the steady-state groundwater concentration.

On the other hand, in an area with a limited discharge from the bedrock (10 mm year^{-1}), the residence times of Mo-93 and Ni-59 in glacial clay are similar to, or exceed, the half-life for radioactive decay. Thus, a notable reduction of activity occurs in this layer, and less activity reaches the layers above it. An increased discretisation prolongs the residence time in glacial clay, and for Ni-59 the cumulative reduction may be an order of magnitude larger in the more finely discretised model. Finally, for mobile radionuclides (i.e. C-14 and Cl-36) the effect of a more finely discretised model is relatively limited. That is, as the activity concentrations of these radionuclides are only marginally affected by radioactive decay, an increased fineness of discretisation will only result in a short delay of the

breakthrough, and thus effects on steady-state concentrations in the lower regolith do not propagate to the upper layers. Even with a pronounced vertical flow gradient (as in object 116), the radionuclide concentrations in the till layer (important for dose assessment assuming that groundwater is extracted) simulated by the more finely discretised model exceeded the concentrations estimated by the less-finely discretised model by less than a factor two.

In SE-SFL, a model describing continuous cultivation in the discharge area has been introduced to facilitate the assessment under present-day conditions. The description of the unsaturated layer is more detailed than in the model used to assess dose consequences from early cultivation of a mire. A model comparison shows that the original stylised model gives similar estimates of the activity concentrations of Cl-36, C-14 and Mo-93 in the soil layer where plant uptake occurs to those resulting from the more detailed model, but that the original model estimates for Ni-59 are somewhat cautious (though still within a factor of two, Figure 9-5).

In summary, the model updates introduced in SE-SFL have had a relatively limited impact on calculations of environmental concentrations in many situations, as compared with those obtained with the original SR-PSU model. However, in cases where the residence time is similar to (or longer than) the radioactive half-life, the reduction of activity along the transport pathway will be larger in a more finely discretised model. Nevertheless, the model updates are well motivated and ensure that robust model estimates can also be obtained under varying conditions. Hence, the model robustness in future probabilistic calculations is expected to be improved by the model updates (both in terms of internal consistency and representation of dependencies). In addition, the more detailed model of an agricultural ecosystem introduced in SE-SFL confirms that the output from the stylised models (used to assess consequences after drainage) is reasonable.

10 Data used in the biosphere assessment

10.1 Introduction

The biosphere (BioTEx) model relies on a large number of input parameters. The ambition in SE-SFL has been to, as far as possible, use site-specific data from the example site Laxemar and from Forsmark for describing parameters and populating parameter values. The primary source of data has been the quality assured dataset used in the previous safety assessment SR-PSU. This dataset includes a large number of parameters derived from the site investigations in Forsmark (Grolander 2013), as well as parameters that do not depend on the location of the repository (e.g. effective dose coefficients and characteristics for potentially exposed groups).

This chapter focuses on the choice of parameter values for the present temperate conditions of the example site Laxemar (as utilised in the base case and most other evaluation cases). For the rationale and choice of parameter values for other conditions (as postulated for a warmer or colder climate) the reader is referred to Grolander and Jaeschke (2019). In Chapter 5 the concept of discharge area specific properties is introduced, and in Chapter 12 several object specific parameters are exemplified. The detailed description of individual parameter values can be found in Grolander (2013), Tröjbom et al. (2013) or Grolander and Jaeschke (2019).

This chapter describes how data have been selected in SE-SFL (Section 10.2) and to give an overview of the types of parameters that are used in this safety evaluation (Section 10.3). In the text, special attention is given to parameters 1) where values different from those used in SR-PSU were selected, and 2) that were introduced in SE-SFL, due to updates of the BioTEx model (Table 8-1). The last section of this chapter (Section 10.4) briefly describes the QA process that has been developed to assure that data are complete, correct and traceable.

10.2 Parameter evaluation and selection

The procedure for data selection in SE-SFL is described in detail in Chapter 1 in Grolander and Jaeschke (2019). In this section, a summary is provided (Figure 10-1).

For parameters with properties that were considered not to depend on the location of the repository, the values from the SR-PSU assessment were primarily used (Grolander 2013). These parameters include half-life of the radionuclide, dose coefficients and characteristics of humans. Parameters used to characterise land-use and characteristics of livestock are based on present and historic records that are considered to relevant for any location along the Swedish coast. Other examples of parameters considered as generic are the concentration of carbon in the atmosphere, the diffusivity of elements in water and gas, the density of liquids, and the atmospheric drag coefficient.

In the SR-PSU assessment, many parameter values reflected present and future conditions at Forsmark (Grolander 2013). The difference in regional climate between Laxemar and Forsmark is limited. Laxemar was characterised by 1.4 °C warmer average annual temperature and received 53 mm more average annual precipitation compared with Forsmark (Chapter 3 in the **Climate report**) and thus many parameter values derived for Forsmark are also relevant for the SE-SFL (Grolander and Jaeschke 2019). However, Laxemar and Forsmark differ in some aspects, such as shoreline displacement, topography and soil chemistry. For parameters that could potentially be affected by local conditions, the parameter value from SR-PSU was compared with a corresponding value for Laxemar. The value for Laxemar was primarily taken from SKB's site investigations, as applied in SKB's comparative analysis of site characteristics related to long-term safety for the Spent Fuel Repository (SKB 2010d). If relevant site data from Laxemar were missing in SKB's databases, candidate values were derived from the literature. A difference of less than 10 % between the parameter values representing Forsmark and Laxemar, respectively, was considered negligible. When this was the case the value from the quality-assured SR-PSU data was used to represent Laxemar. In all other cases, values from an alternative source were selected to represent Laxemar in SE-SFL. In the next section, these parameters are highlighted, whereas the rationale and numeric values used are presented in Grolander and Jaeschke (2019). Examples of updated parameter values are found among the categories terrestrial and aquatic ecosystem parameters, and element specific parameters (Section 10.3).

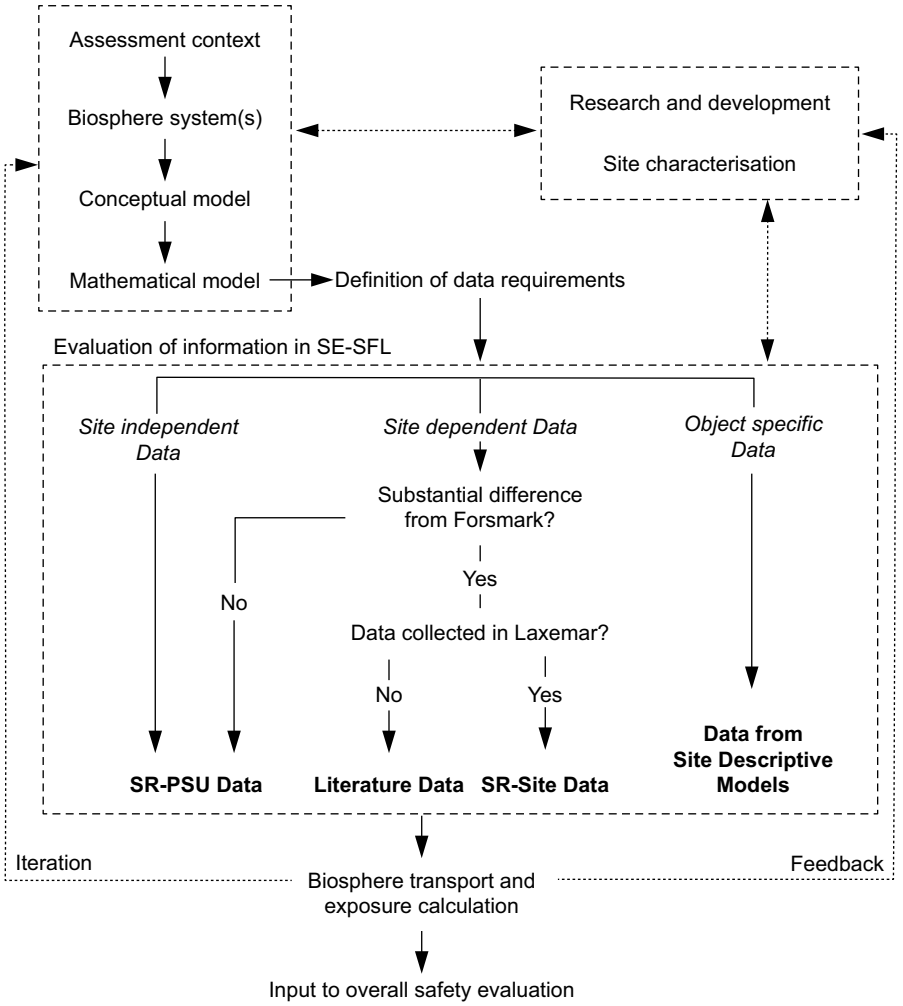

Figure 10-1. *The main pathways for data selection in the SE-SFL assessment context. Data types are written in italic and selected data sources in bold text. Figure modified from Lindborg (2018).*

As SKB's methodology of defining discharge areas is geographically anchored in the landscape, properties of the identified discharge areas are, by definition, site specific. Values for these landscape geometry parameters were derived from the site-specific modelling (SDM) for Laxemar as described in Chapter 5. However, some development was needed to project regolith depth for past stages of lakes and, and to extract hydrological parameters from the hydrological models. In addition, the modification of the BioTEx model in SE-SFL occasionally required new parameters.

10.3 Description of parameters

The biosphere transport and exposure model (BioTEx) relies on nearly 600 input parameters, of which one third represent radionuclide- or element-specific properties (Table 10-1). These parameters can be divided into eight categories: Landscape geometries, Regolith properties, Hydrology and water exchange, Terrestrial ecosystem properties, Aquatic ecosystem properties, Distribution coefficients (K_d) and Concentration ratios (CR), Human characteristics, and Radionuclide-specific properties. For each parameter, a best estimate was derived from site or literature data, and these were used for deterministic calculations of human exposure. The parameters used in the radionuclide model reflect important processes related to transport and accumulation of, and exposure to, radionuclides.

Table 10-1. The eight parameter categories used in the biosphere (BioTEx) model and the number of parameters (N) in each category.

Category	N
Landscape geometries	27
Regolith properties	26
Hydrological parameters	33
Terrestrial ecosystem	110
Aquatic ecosystem	40
Element-specific K_d and CR[1]	$29 \times N_e$
Human characteristics	22
Radionuclide specific properties[2]	$7 \times N_r$

1) CR (18) and K_d (11) parameters are given for each analysed element (N_e)
2) Half-life, dose coefficients and the effect of ingrowth (during cultivation) are given for each analysed radionuclide (N_r)

10.3.1 Landscape geometries

The geometric parameters describe the spatial extents of the biosphere objects, such as surface areas, water and regolith depths, and the areas of their catchments, in the present and future landscape. The spatial delineation of biosphere objects is described in Section 5.2.2. Briefly, the areas of biosphere objects that are presently above the sea correspond to the boundaries of the lake phase, and the boundaries of the original sea basins set upper limits to the areas of the sub-catchments. The regolith thicknesses for present terrestrial conditions were derived from the regolith depth model whereas the regolith thickness and water depths for all other conditions were calculated with the Regolith-Lake Development Model (Sections 5.4 and 5.5).

10.3.2 Regolith properties

Regolith properties include physical soil properties such as porosity, bulk density and water saturation, but also the soil compaction that occurs when organic soils are drained and cultivated. In SE-SFL, separate parameter values for porosity and bulk density are given for five regolith types in mires (till, glacial clay, post-glacial clay-gyttja, deep peat and surface peat), for two agricultural soils (peat like and clay-gyttja like), and two aquatic sediment types (sea and lake). Site data were available from both Forsmark and Laxemar, but as the differences in properties between the two sites were small, the previously quality-assured SR-PSU data were used also in SE-SFL.

Parameter values for soil saturation and degree of compaction (of agricultural soils) were derived from both site-specific and literature data but were not considered to differ between Forsmark and Laxemar. However, it was noted that postglacial clay-gyttja dominated the present agricultural land in Laxemar, and therefore this regolith type was assigned to both the infield-outland and garden plot land-use variants (as opposed to glacial clay which was selected in SR-PSU)[25].

10.3.3 Hydrological parameters

Hydrological parameters describe water exchange for sea basins, and surface and groundwater flows for discharge areas on land. All hydrological parameters used in the biosphere assessment were derived within the SE-SFL project, from previous site descriptive models.

The residence times of water in coastal basins in the Laxemar area were estimated for the time period 3000 BC through 9000 AD by the average age of water parcels (Engqvist 2010). Surface water flows through sea basins, approximating the dilution of discharging radionuclides, were estimated by dividing the water volume of a basin (see above) by the residence time of the water. Thus, for each sea basin, the water residence time was expressed as a time series given the past and future projected changes in relative sea level (Section 5.2 in Grolander and Jaeschke 2019).

[25] This also include the distribution coefficient (K_d).

Hydrological parameters for biosphere objects above the shoreline were based on water balances derived from the SDM-Site and SR-Site MIKE SHE models. However, water balances were only available for the present conditions of the Laxemar landscape. Therefore, stylised water balance models for the sea and the land stages (Figure 8-3) were developed to estimate water flows under conditions differing from those for which water balance were originally derived (Section 8.4.2 and detailed descriptions in Chapter 5 in Grolander and Jaeschke 2019). For consistency, hydrological flows for all objects and ecosystem stages in Laxemar were calculated with this method (Figure 10-2). The approach also allowed for a coherent derivation of hydrological parameters for other evaluation cases with a different climate (Section 5.9 in Grolander and Jaeschke 2019).

10.3.4 Terrestrial ecosystem

Terrestrial ecosystems include both mire and agricultural ecosystems. Ecosystem properties that are used as parameters in the BioTEx model include, for example, biomass, leaf area index, net primary production, mineralisation, soil respiration and sustainable production of berries, mushrooms and game meat. Similar properties were also used to characterise different agricultural ecosystems (including a garden plot). However, to assess a broad array of exposure pathways, additional parameters influencing radionuclide transfers associated with meat and dairy production and/or irrigation, fertilisation, leaf interception and plant translocation were also required (Chapter 8 in Grolander and Jaeschke 2019).

Some parameter values were changed for terrestrial ecosystems, due to differences found during site investigations between the example site Laxemar and Forsmark: the fraction of dissolved CO_2 in the total pool of dissolved inorganic carbon in peat pore water, the length of the season when a garden plot is irrigated, and the wind velocity at 10 m (Chapter 8 in Grolander and Jaeschke 2019). Due to model updates, a few new parameters were introduced in SE-SFL. These included, the soil respiration, the fraction of inorganic chlorine in primary producers, and the concentrations of some macronutrients[26] in mire vegetation, fungi and crops and the corresponding concentrations in pore water of soils.

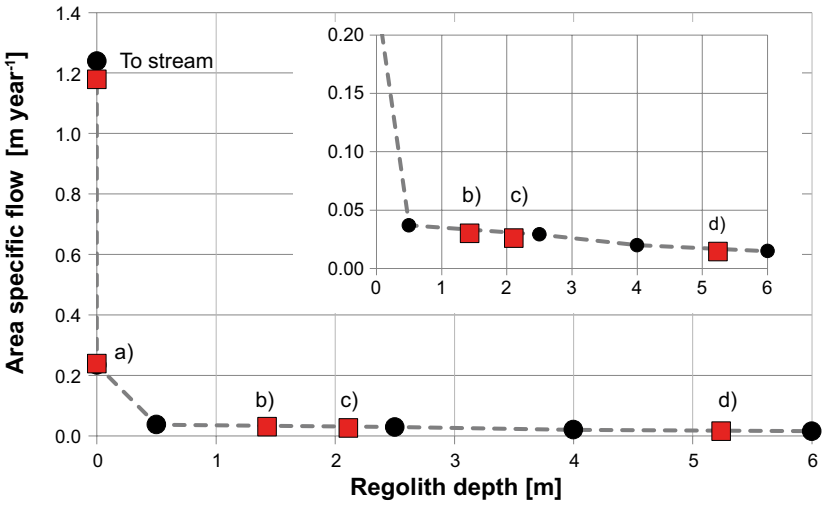

Figure 10-2. *Discharge within and out of a mire biosphere object. Calculated upward specific groundwater flows across regolith boundaries, and out of the object via stream discharge (red squares), are superimposed on the flows from the MIKE SHE water balance for object 157_1 at 11 000 AD (black circles connected by grey dashed line). Letters indicate vertical boundaries between regolith layers; a) RegoUp (or overland water) and RegoPeat, b) RegoPeat and RegoPG , c) RegoPG and RegoGL, and, d) RegoGL and RegoLow (figure from Grolander and Jaeschke 2019).*

[26] Soil and plant concentrations of Cl, Ca and K are used to calculate tissue concentration of Cl-36, Ca-41 and K-40 in plant and fungi, and thus these parameters replace the CRs for these elements in terrestrial plants and fungi.

10.3.5 Aquatic ecosystem

Aquatic ecosystems describe both limnic and marine environments. Ecosystem properties that are used as parameters in the BioTEx model include for example biomass and production of aquatic primary producers, mineralisation rates in water and sediments, and the concentrations of inorganic carbon and particulate matter. In addition, the amount of edible food produced within the aquatic objects (fish and crayfish) is needed to evaluate exposure from consumption of aquatic food.

Most aquatic ecosystem properties were deemed to be similar in Forsmark and Laxemar. However, a few parameter values were updated in SE-SFL to better reflect the conditions in Laxemar. These were: the concentration of particulate matter in sea and lake water, the dissolved inorganic carbon concentrations in sea and lake water, the fraction of dissolved CO_2 in the total pool of dissolved inorganic carbon in lake water, the production of edible fish in lakes, the depth of lakes in which crayfish may be found, and the thickness of the oxygenated zone of lake sediments (Chapter 7 in Grolander and Jaeschke 2019).

Biomass and net primary production are dependent on the photic depth (which is less in brown-water lakes than in clear-water lakes) and the area and average basin depth of aquatic objects. Thus, these parameters will vary over time, and consequently object-specific time series of these variables were calculated for past, present and future aquatic ecosystems in Laxemar. These object-specific time series included the variables: biomass and net primary production for benthic macro vegetation in the sea and lakes, benthic micro vegetation in sea and lakes, and phytoplankton in sea and lakes (Chapter 7 in Grolander and Jaeschke 2019). In addition, the fraction of inorganic chlorine in aquatic primary producers was introduced as a parameter in SE-SFL, to give a more reasonable description of Cl-36 released from litter (Section 8.4.1 Litter respiration/release).

10.3.6 Element-specific parameters

Element-specific parameters in SE-SFL refers to the distribution coefficients (K_d) that were used to calculate the sorption of elements onto soils and particulate matter, and the concentration ratios (*CR*) that were used to calculate uptake of radionuclides in biota (Table 10-2). In SE-SFL, parameters for 41 elements were selected. Most of these elements were also included in SR-PSU (Tröjbom et. al. 2013). However, eight new elements (Be, Gd, La, K, Re, Si, Tb, and Ti) were included in SE-SFL, and element analogues were used to assign parameter values for these elements (Chapter 6 in the Grolander and Jaeschke 2019).

Table 10-2. Origin of concentration ratios and distribution coefficients used in SE-SFL. L=Laxemar, F=Forsmark.

Description	Site	Name	Description	Site	Name
Concentration ratio (*CR*) between			**Distribution coefficient (K_d) for**		
soil and mushrooms	F	cR_ter_mush	particulate matter in lake water	L	kD_PM_lake
soil and mire primary producers	L	cR_ter_pp	particulate matter in sea water	L	kD_PM_sea
soil and cereal	F	cR_agri_cereal	upper layer of aquatic sediments	L	kD_regoUp_aqu
soil and fodder	F	cR_agri_fodder	surface peat	F	kD_regoUp_ter
soil and potatoes	F	cR_agri_tuber	deep peat	F	kD_regoPeat
soil and vegetables	F	cR_agri_veg	post-glacial sediments (e.g. clay-gyttja)	F	kD_regoPG
herbivores and their diet	L	cR_food_herbiv			
lake water and crayfish	F	cR_lake_cray	glacial clay	F	kD_regoGL
lake water and fish	L	cR_lake_fish	lower regolith (till)	F	kD_regoLow
lake water and macrophytes	L	cR_lake_pp_macro	soil in Garden plot, drained mire and infield outland agricultural systems	F	kD_regoUp
lake water and microphytobenthos	L	cR_lake_pp_micro			
lake water and plankton	L	cR_lake_pp_plank			
sea water and fish	L	cR_sea_fish			
sea water and macrophytes	L	cR_sea_pp_macro			
sea water and microphytobenthos	L	cR_sea_pp_micro			
sea water and plankton	L	cR_sea_pp_plank			

K_d values depend on the local biogeochemical environment in the regolith or water compartment. In SE-SFL, separate K_d values were given for the five mire regolith types, two agricultural soils (see Section 10.3.2), and one aquatic sediment. In addition, K_d values were also provided for sorption on particulate matter in lake and sea water respectively. As in SR-PSU, *CR* values were given for seven terrestrial organism groups (mire vegetation, fungi, food for herbivores, cereals, fodder, tubers, vegetables) and nine aquatic groups (macroalgae, microalgae, plankton, fish from lakes and the sea, and crayfish for lake only).

As the geochemical properties of the two sites differ, values for element-specific parameters in SE-SFL were based on data from Laxemar when available. However, data to calculate site-specific distribution coefficients were only available for aquatic conditions (i.e. K_d for particulate matter and sediments, Table 10-2). For terrestrial conditions, all K_d values were taken from SR-PSU (Section 5.4.2 in Grolander and Jaeschke 2019). There were more data available with respect to animal and plant concentrations from Laxemar, and thus it was possible to update *CR* values for two thirds of the organism groups. Thus, for terrestrial ecosystems, *CR* values for herbivores and mire vegetation were given site-specific values, and for aquatic ecosystems the *CR* values for fish and aquatic primary producers were updated (Table 10-3).

10.3.7 Human characteristics

Parameters related to the characteristics of humans are based upon literature values. This category comprises basic parameters such as yearly demands for water and energy, inhalation rate and parameters related to different land-use types, e.g. garden plot and drained mire, and the diet of the most exposed groups. Parameters that describe the fractions of the yearly energy demand that are fulfilled by consumption of different food items, fraction of arable land used for cultivation of cereals, tubers and fodder, exposure time, and number of individuals in the exposed group, have been derived using historical records and official Swedish statistics (Grolander 2013, Saetre et al. 2013a). These parameters do not change between sites or evaluation cases, but different exposed groups may be used in different evaluation cases (see Chapter 7).

10.3.8 Radionuclide-specific properties

Radionuclide-specific dose coefficients were used for converting the activity concentrations in environmental media (in Bq kgC^{-1} or m^{-3}) to annual doses (in Sv)[27]. Three kinds dose coefficients were used, namely for ingestion, for inhalation and for external exposure from the ground. The doses obtained with these coefficients are the annual effective committed doses to members of the public that are classified as adults. The selected dose coefficients and motivations for their selection are presented in Grolander (2013). Dose coefficient values for radionuclides not included in the SR-PSU assessment are described in Grolander and Jaeschke (2019).

The dose coefficients in the source documentation include the contribution from decay products that grow in after a radionuclide is ingested or inhaled (e.g. ICRP 1996). However they do not include the contribution from decay products in the environment. The contribution of these are either explicitly accounted for with the BioTEx model (e.g. Pb-210 and Po-210), or they are accounted for by including them in augmented dose coefficients that assume that they are present in secular equilibrium (Section 2.2 in Grolander and Jaeschke 2019). The dose coefficients are assumed to be generic (i.e. independent of the environment) and do not change between evaluation cases.

Half-lives were primarily taken from Grolander (2013). However half-lives that were previously based on ICRP recommendations were updated in SE-SFL in accordance with ICRP (2008) (Section 2.3 in Grolander and Jaeschke 2019).

[27] To obtain the annual exposure the environmental concentrations were multiplied by rates of intake, rates of breathing or time in contact with medium causing external exposure.

Table 10-3. Ratio of geometric mean of *CR* or K_d values for Laxemar to those for Forsmark, for elements and parameters that were added/updated in SE-SFL. Most of the ratios are within one order of magnitude (i.e. between −1 and 1 in the table) and some parameters were not changed (white). In some cases, the Laxemar *CR* or K_d values were more than one order of magnitude lower than the Forsmark value (marked in deep blue) and in a few cases the Laxemar value was one order of magnitude higher than for Forsmark (marked in bright yellow). Note that the same parameter value was used for all three groups of aquatic primary producers (macrophytes, microphytes and plankton), and that ratios in the table are given on a logarithmic scale.

	cR_Lake_Fish	cR_Lake_pp	cR_Sea_Fish	cR_Sea_pp	cR_Ter_pp	cR_foodToHerb.	kD_Aqu_regoUp	kD_Lake_PM	kD_Sea_PM
Ac									
Ag							-0.7		
Am									
Ba	-0.4	0.0	1.0	0.6	-0.1	0.1	-0.1	-0.5	2.4
Be		1.4					0.1	-0.1	0.6
Ca	-0.7	0.0	1.5	-0.3	-0.8	0.7	-0.1	-0.2	1.3
Cd		0.6	0.3	0.2	0.0	0.5	-0.7	0.3	0.8
Cl	-0.1	-1.4	-0.1	0.1		-0.1	0.4		
Cm									
Co	0.4	0.3	0.8	1.0	-0.5	0.9	0.1	-0.2	0.7
Cs	-0.8	-0.1	-0.1	1.1	0.3	-0.3	0.3	-0.3	1.0
Eu		1.3		-1.2			0.4	-0.3	0.1
Gd		1.4		-1.2	-0.3		0.1	-0.1	0.5
Ho		1.3		-1.2			0.3	-0.3	0.4
I	0.2	0.4	0.2	0.2			0.1	0.3	0.0
K	-0.3	-2.0	-0.1	0.0	0.2	0.1	-0.3	0.3	1.1
La	0.6	1.3			-0.7	1.2	0.5	0.2	0.5
Mo	0.1	-0.3	0.4	0.4	0.2	0.0	-0.4	-0.1	1.2
Nb	0.2	1.2			0.0	0.4	0.3	-0.5	0.8
Ni		0.6	0.1	0.5	-0.3	1.3	0.1	0.3	0.1
Np									
Pa									
Pb		1.1	-0.5	0.2	0.0	0.9	-0.2	0.1	-0.3
Pd									
Po									
Pu									
Ra						1.2			
Re								0.5	0.0
Se	-0.5	0.0	0.1	-0.1			0.0	-0.1	-0.3
Si	0.1	0.8	0.6	1.5	-2.7	0.2	-0.7	-0.1	1.4
Sm		1.2		-1.3	-0.2	0.8	0.4	-0.1	0.4
Sn					0.0	-0.2	0.0		
Sr	-0.4	0.4			-0.3	0.8	-0.2	-0.3	0.0
Tb	-0.3	1.2		-1.0			0.3	-0.3	0.5
Tc									
Th		0.8	0.4	1.6			0.4	-0.2	0.9
Ti	0.9	1.5	1.3	1.6		-0.1	0.3	0.0	1.0
U	-1.2	0.2			-0.2	0.0	-0.2	-1.5	0.3
Zr	0.5	0.7	0.1	1.3	-0.2	0.2	0.1	-0.3	0.8

10.4 Quality assurance procedure

Controlled handling of data and workflow is crucial to guarantee the quality of data and model results. The biosphere analysis in SE-SFL has followed the quality plan for the safety evaluation project (Section 2.6 in the **Main report**). According to this plan all reports go through a traceable factual review by experts and a quality review step. In addition, a QA process has been developed to assure that data are complete and correct, and that the usage, sources, review, and storage of data are traceable.

The QA process includes a factual review of all selected parameter values and a quality control of delivery. Data files for the selected parameter group are stored on the Subversion, SVN, server, ensuring full version handling and traceability. Briefly, the QA process includes the roles of a data deliverer, a data reviewer and a QA coordinator. Each delivery file contains a macro-controlled review system and all additions, changes and deletions to the data entries are logged. The QA process will make sure that information on the following questions is available:

- Which values were finally selected to be used in the assessment?
- How has the data point been derived (reference to source report)?
- How has the data point been reviewed (methods for reviewing, side calculations)?
- Who (data deliverer, data reviewer and QA coordinator) has done what, and when?
- Where are the files stored?

Data used for Forsmark, taken from the previous assessment SR-PSU, were not included in the present factual review and QA procedure; these data are considered to be already quality assured within the SR-PSU assessment (Grolander 2013).

11 Analysis of the present-day evaluation case

11.1 Introduction

In the *present-day evaluation case* (the *base case*), the time-dependent geosphere radionuclide release resulting from the near-field and geosphere simulations (Section 5.2.9 in the **Radionuclide transport report**) is all assumed to be discharged into the till in biosphere object 206. Constant present-day climate and other conditions in Laxemar persist for the entire analysis period of 1 million years after repository closure. Thus, the ongoing shoreline displacement and landscape development are not taken into account, and the physical and biological properties of the ecosystem are assumed to be constant throughout the simulation. An alternative state of the discharge area is also evaluated, namely a mire ecosystem that could have developed in the lake basin of object 206 in the absence of human intervention. The assumptions of present-day conditions and lack of landscape development are such that this is not a realistic future scenario. However, it makes straightforward comparisons between radionuclides and evaluation cases easier (Sections 7.2 and Grolander and Jaeschke 2019 for more details).

The objective of this chapter is to present and analyse the results from the biosphere transport and exposure model (BioTEx) for this *base case*. The results cover the in-depth analyses of the annual dose to different potentially exposed groups, contributions of exposure pathways and the dynamics of radionuclide transport and accumulation throughout the regolith profile. The fate of accumulated radionuclides upon draining and cultivation of a mire is also analysed. A main purpose is to explore how the main patterns in environmental activity concentrations and annual doses are deduced from the geosphere release, radionuclide properties and mechanisms such as dilution, retention, retardation, radioactive decay and the formation of decay products. The focus is on differences in behaviour and resulting doses among the radionuclides making the largest contributions to dose and to provide a general understanding to facilitate the analysis and interpretation of the *other evaluation cases* (Chapter 12) and *sensitivity cases* (Chapter 13).

This step demonstrates SKB's understanding of the BioTEx model and helps in building confidence that the model results are reliable. Sense checks and comparisons of model outputs with results and understanding from analytical solutions of steady-state conditions are also used to assure that the model performs as intended and that results are reasonable. In SKB's experience this type of high-level verification has proved to be very efficient for identifying inconsistencies in the data and/or problems with the mathematical implementation of the model that have clear effects on the model outcome.

11.2 Annual doses and exposure pathways

In *the present-day evaluation case*, effective doses to humans are estimated separately for radionuclide releases from the two waste vaults, BHA and BHK. Annual doses are calculated accounting for radionuclide transport through the regolith layers and continous cultivation in an agricultural ecosystem (Agri, similar to present conditions) or through the regolith in an undisturbed mire ecosystem that could have developed in the lake basin of object 206 in the absence of human intervention.

Mire doses are estimated for family farmers on a drained mire (DM), infield-outland farmers (IO), garden-plot households (GP) and hunter and gatherers (HG, see Section 6.3) to identify the most exposed group of possible future inhabitants. Doses to farmers (IO, DM and Agri) include doses arising from the use of water from a dug well, but doses excluding use of a well are also presented to illustrate the well contribution.

Modelled annual doses from BHA releases into the continuously cultivated agricultural land (Agri) increase shortly after the repository closure, peak just before year 10 000 AD and decrease slowly until the end of the simulation (Figure 11-1, upper left panel). Agricultural doses from BHK releases are also highest before year 10 000 AD at a slightly lower level than BHA doses and decrease rapidly after year 20 000 AD (Figure 11-1, upper right panel). Doses from the drained mire farming (DM)

generally exceed doses from other land-use variants (GP, IO, HG) in the mire ecosystem as well as continuously cultivated land (Agri, Figure 11-1). The highest drained mire doses from BHK releases (around 18 000 AD) are somewhat lower and drop earlier and faster than for BHA releases. Doses to hunters and gatherers (HG) are more than one order of magnitude smaller than for farmers on the drained mire (DM), whereas doses for infield-outland farmers (IO) and garden-plot households (GP) are in between.

Since drained mire farmers (DM) is the most exposed group in the *present-day evaluation case*, the following presentation and interpretation of the results is focused on this group. In this land-use variant, radionuclides accumulate continuously in the mire ecosystem up to the point of drainage. The average annual dose from early cultivation (50 years following drainage, approximately corresponding to a human lifetime of the most exposed generation) is evaluated for each point in time, cautiously assuming that the mire has not been disturbed prior to the point of drainage.

The main pathway for exposure of drained mire farmers (DM) from BHA releases is ingestion of crops from the cultivated soil (Figure 11-2). The contribution from well water accounts for about 4 % of the dose at the time of maximum dose from BHA and increases with time (as the activity of Tc-99 and decay products from the U-238 chain reach the biosphere, Sections 11.3, 11.5 and 11. 6) up to 30 % at the end of the simulation period. The contribution of well water to the dose from BHK is small for all land-use variants and times. This is because the primary dose-contributing radionuclides (C-14 and Mo-93, Sections 11.3 and 11.5) are poorly retained in the lower regolith layers and are easily taken up by plants. Drinking water could contribute considerably to the dose from BHA for other land-use variants (Agri, GP, IO), but the contribution never exceeds that from ingestion of crops at the times when the dose reaches maximum levels. The contributions from inhalation and external exposure are insignificant for both BHA and BHK releases.

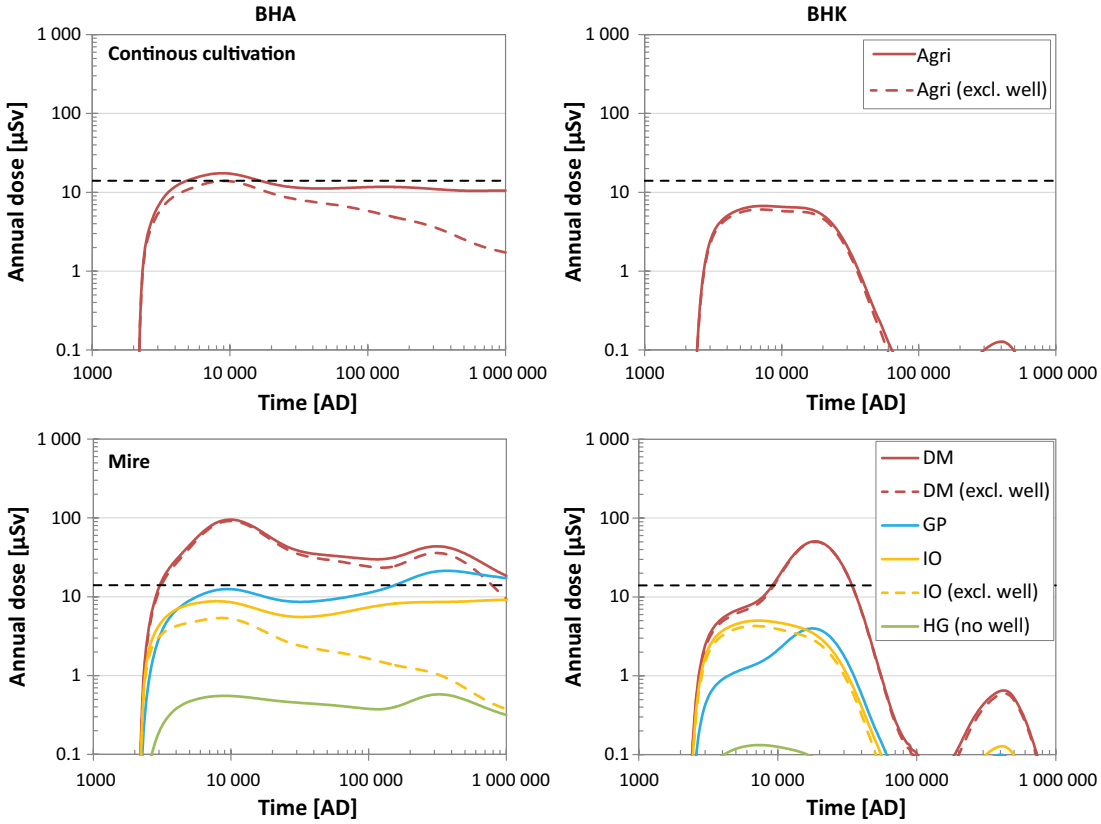

Figure 11-1. *Annual effective doses during the simulation period originating from releases from BHA (left panels) and BHK (right panels) for continuously cultivated agricultural soil (upper panels) and different land use variants of a mire ecosystem (lower panels) in biosphere object 206. The dose contribution from well water is illustrated by replacing exposure from well water with exposure from stream water (dashed coloured lines). Dashed black lines show the effective dose corresponding to the regulatory risk criterion (14 µSv).*

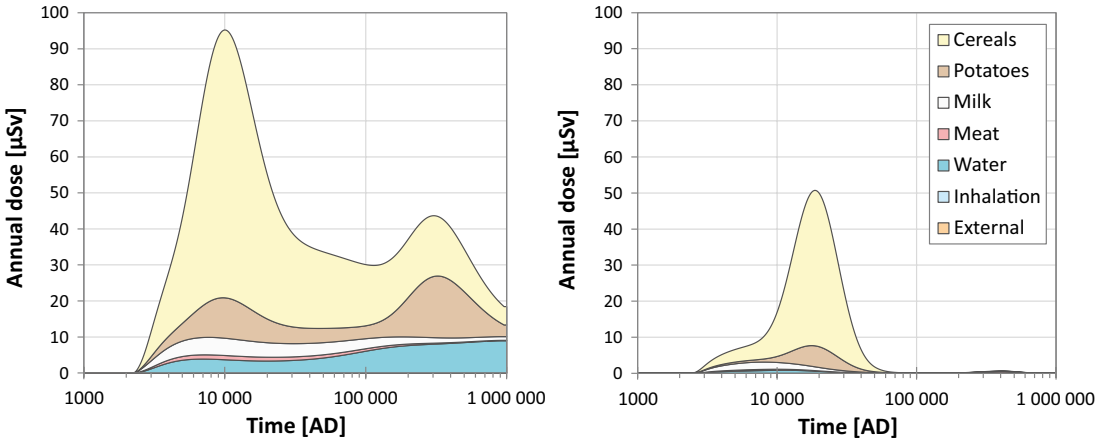

Figure 11-2. *Exposure pathways for drained mire farmers (DM) from BHA (left panel) and BHK (right) releases give doses that mainly derive from ingestion of different types of food (cereals, potatoes, milk, meat) produced on a farm. Exposure through food intake dominates, but for BHA releases, drinking water from a dug well contributes significantly, especially at the end of the simulation period. Observe that the annual effective doses summed over exposure pathways are identical to the dose curves in Figure 11-1, but look different due to the different scales (arithmetic vs logarithmic).*

11.3 Radionuclide-specific annual doses

The release of several radionuclides from both waste vaults yield DM-doses in the base case that are of the same order of magnitude as the regulatory risk criterion for a final repository for radioactive waste (Figure 11-3, upper panels). C-14 dominates the very early doses and Mo-93 is the main contributing radionuclide to maximum total annual doses from both BHA (around 10 000 AD) and BHK (around 18 000 AD). Cl-36 contributes significantly to the dose from BHA for the first 200 000 years and dominates the total dose for a significant period. Tc-99 contributes significantly for the last 900 000 years of the simulation period, and U-238, including its decay products (e.g. U-234, Th-230, Ra-226, Pb-210 and Po-210), contribute to the dose from BHA at the end of the assessment period. These results and an analysis of relationships between the doses and releases from the U-238 decay chain are presented and discussed in Section 11.6. Ni-59 dominates the dose from BHK in the latter part of the assessment period, and Ca-41 has a similarly high dose peak around 35 000 AD, but their maximum doses are almost two orders of magnitude below the maximum annual Mo-93 dose. The total contribution of all other radionuclides is small in comparison with the radionuclides mentioned above (and separately plotted in Figure 11-3), and the total dose contribution from these other radionuclides is 50 times smaller than the maximum annual doses from BHA and they make an even smaller contribution from BHK.

The development of radionuclide-specific annual doses over time depends on the radionuclide release rate (Bq year^{-1}) from the geosphere (Figure 11-3). However, radionuclide properties that influence their transport and accumulation in the biosphere (half-life and distribution coefficient, K_d), plant uptake and radio-toxicity (as measured by the associated dose coefficient, *DC*) explain differences in temporal patterns and relationships between the magnitudes of geosphere releases and doses arising from the various radionuclides.

To illustrate and understand how radionuclide properties influence model results, the *present-day evaluation case* primarily focuses on the radionuclides that contribute most to the drained mire doses from the BHA releases and also represent a wide range of radionuclide properties (Table 11-1). C-14 is non-sorbing and Cl-36 is weakly sorbing, whereas Mo-93 sorbs to organic fractions of the upper soil layers (post-glacial sediments and peat) and Tc-99 is strongly sorbing, especially to the glacial clay. The half-lives of Mo-93 and C-14 are 4000 and 5730 years, respectively, whereas Cl-36 and Tc-99 decay more slowly (half-lives of 301 000 and 211 100 years, respectively). C-14 differs from the other radionuclides since it may exist in the gas phase (carbon dioxide or methane) in the upper regolith and degassing is a more important removal mechanism of C-14 than surface-water transport. Plant uptake is modelled either by using plant- and element-specific concentration ratios (*CR*, e.g. Mo-93, Tc-99) or by a specific activity approach (e.g. C-14, Cl-36, Section 8.4.1), but both methods imply that plant concentrations are proportional to the radionuclide environmental concentration (in soil, pore water or, for C-14, air).

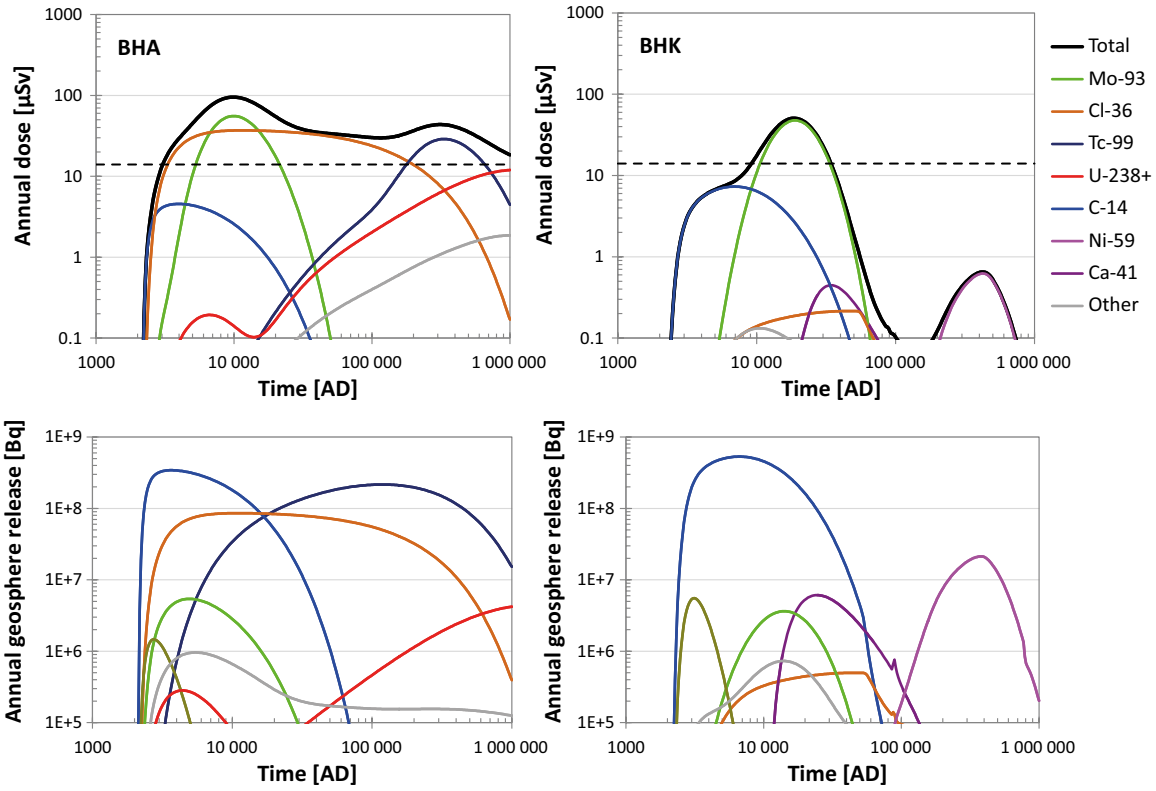

Figure 11-3. *Annual dose (upper panels) in the drained mire case from BHA (left panels) and BHK (right panels) respectively and annual geosphere releases (lower panels) for the radionuclides contributing most to total dose. For comparison, the annual dose (14 µSv) corresponding to the regulatory risk criterion is indicated by the black hatched horizontal line in the upper panels. Doses and releases of radionuclides in the U-238 decay chain (U-238+) are analysed in Section 11.2.5.*

The radiotoxicity to humans from ingestion of individual radionuclides depends on the type of decay (mainly alpha, beta, gamma), the yield and energy of their emissions, and the degree to which they are taken up and accumulated in various tissues and organs of humans (ICRP 2012). Mo-93 is approximately three times more radiotoxic than Cl-36 and five times more toxic than C-14 and Tc-99 (Table 11-1).

Table 11-1. Properties of radionuclides that contribute significantly to the dose from BHA. K_d is the distribution coefficient, *CR* the soil-to-plant concentration ratio and *DC* the dose coefficient for ingestion.

Parameter	Unit	Specification	Cl-36	C-14	Mo-93	Tc-99
Half-life	years		301 000	5 730	4 000	211 100
K_d	$m^3\ kg_{DW}^{-1}$	regoUp (Agri)	0.021	0	0.74	0.067
		regoUp (Mire)	0.021	0	4.4	0.41
		regoPeat	0.027	0	3.9	2.6
		regoPG	0.0084	0	3.4	4.1
		regoGL	0.0051	0	0.22	54
		regoLow	0.00054	0	0.021	3.6
CR	$m^3\ kg_{DW}^{-1}$	cereals	-	-	1.2	0.064
		tubers (potatoes)	-	-	0.90	0.56
DC	$Sv\ Bq^{-1}$	ingestion	9.3×10^{-10}	5.8×10^{-10}	3.1×10^{-09}	6.4×10^{-10}

The results addressed here initially focus on Cl-36, whose properties (long-lived and weakly sorbing) make it behave much like a tracer of the groundwater flow and is therefore relatively easy to understand (Section 11.4). Successively more complexity is introduced when the Cl-36 results are compared with those for C-14 and by accounting for the effects of retention and decay in the regolith of the more strongly sorbing Mo-93 and Tc-99 (Section 11.5). Further complexity is added when the effects of ingrowth of decay products with different properties than from their parent are accounted for in the U-238 decay chain (Section 11.6).

11.4 Chlorine-36 (Cl-36) results

The release of Cl-36 from the geosphere to the till increases shortly after closure, peaks around 10 000 AD, and decreases slowly for several hundred thousand years (Figure 11-4). The sorption of Cl-36 is weak in all regolith layers (Table 11-1) and most of the Cl-36 released from the geosphere is transported to the upper regolith and exported out of the biosphere object with the surface water to downstream objects. Only a minor fraction (not even visible in Figure 11-4 but shown in Figure 11-5) is retained within the regolith layers. On average, Cl-36 is retained in the surface system for about 50 years, which is short a time in relation to its half-life (301 000 years).

The small fraction of Cl-36 in the regolith layers is nevertheless large enough to make a significant dose contribution. Thus, it is important to understand how environmental concentrations of Cl-36 contribute to human exposure and the mechanisms influencing environmental concentrations in the surface system. Radionuclide releases with the deep groundwater are diluted by groundwater flows, and thus the pore water concentration in the regolith layers will always decrease towards the surface with increasing groundwater flows (Figure 11-5). The decrease in the concentration of Cl-36 towards the surface is only marginally influenced by radioactive decay due to its long half-life. Thus, Cl-36 behaves like a tracer of groundwater transport. The situation is different for more short-lived or more sorbing radionuclides, for which the decay can further decrease pore water concentrations towards the surface (see e.g. Mo-93 and Tc-99, Section 11.5).

The inventory of the radionuclides within a regolith layer is positively related to the pore water concentration, the distribution coefficient (K_d), and the regolith layer thickness. Moreover, the inventory in the pore water is proportional to the porosity. This is most important for non-sorbing radionuclides whereas the inventory for sorbing radionuclides is positively related to the soil density.

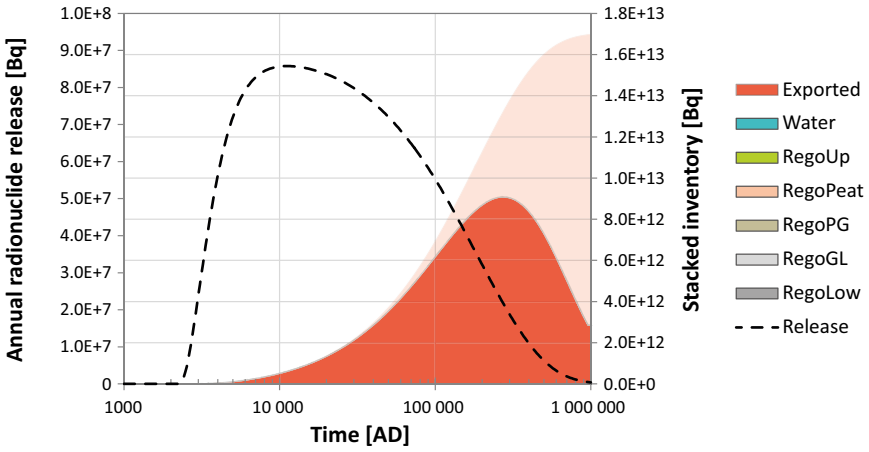

Figure 11-4. *The release of Cl-36 from the bedrock to the regolith over time (the dashed black line, left hand vertical axis) and the inventory of the released radionuclide (coloured areas, right hand vertical axis) as a function of time. The inventory of Cl-36 in regolith layers is insignificant in relation to the proportion exported (red) and the proportion decayed after export (semi-transparent red) and is therefore not visible in the plot but is further analysed in Figure 11-5.*

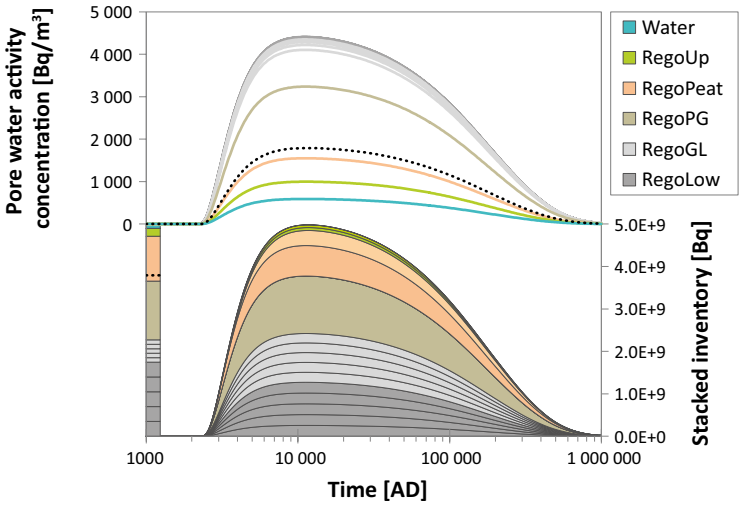

Figure 11-5. *Pore water concentration (upper panel) and inventory (lower panel) of Cl-36 in regolith layers in the mire as a function of time. The dotted black line in the upper panel is the average pore water activity concentration of Cl-36 in the cultivated soil (RegoUp) during the first 50 years after draining. The lighter shades of RegoPeat and RegoUp in the lower panel indicate the inventory in the organic fraction. The bar to the left in the lower panel shows the relative regolith layer thickness and the dotted black line within the peat layer (RegoPeat) in this bar is the lower depth of the cultivated soil after draining the mire in biosphere object 206.*

Despite lower pore water concentrations (and soil densities), the proportion of the Cl-36 regolith inventory in the upper regolith layers (RegoPG, RegoPeat and RegoUp) is relatively large due to the higher sorption in the upper layers (Figure 11-5 and K_d values in Table 11-1). Most of the inventory is sorbed to the solid phase, but due to the relatively low sorption for Cl-36, the dissolved fraction in the pore water is not insignificant. In the upper regolith layers, there is also a fraction of Cl-36 stored in organic matter, originating from incompletely decomposed plant material (see Section 8.3).

The dose from Cl-36 to humans in the drained mire case occur partly due to drinking water from a dug well (Figure 11-6) and this is proportional to the pore water concentration in the till (RegoLow in Figure 11-5). The largest dose contribution (~ 80 %) however, is due to ingestion of various food items originating from plant root uptake of contaminated water from the cultivated soil (Figure 11-6). The modelled plant root uptake of Cl-36 is proportional to the concentration of Cl-36 relative to that of stable chlorine in pore water of the cultivated soil (see specific activity uptake in Section 8.4.1). The pore water concentration of stable chlorine was assumed constant and the dose of Cl-36 is therefore proportional to the average pore water activity concentration available for plant root uptake during the first 50 years after draining of the mire (black dotted line in the upper panel of Figure 11-5). This pore water activity concentration, in turn, depends on both the activity concentration in the pore water that enters the cultivated soil from below (through groundwater uptake during the growing season), and on the stored inventory that has accumulated in the mire (RegoUp and the part of RegoPeat above the black dotted line in the bar to the left in the lower panel of Figure 11-5) before draining. To avoid underestimation, the incoming pore water activity concentration from below is taken from the layer below the origin of the cultivated soil. In object 206, the groundwater uptake is thus from the post-glacial clay-gyttja layer (RegoPG, see upper panel in Figure 11-5). In the case of Cl-36, the contribution from the accumulated inventory is similar to that resulting from groundwater uptake from below and originates mainly from desorption of sorbed Cl-36 and to a lesser extent from mineralisation of organically bound chlorine (Figure 11-7).

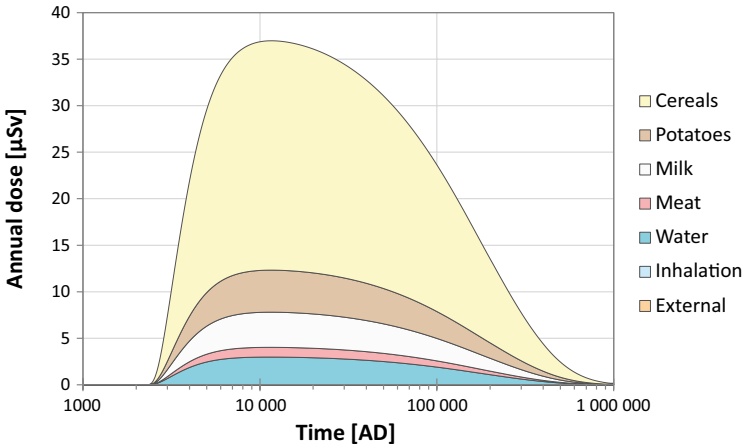

Figure 11-6. *Exposure routes of Cl-36 in the drained mire (DM) land use variant. Ingestion of various food items dominates exposure. Drinking water from a dug well also contributes, whereas inhalation and external radiation are insignificant (not visible from the line widths).*

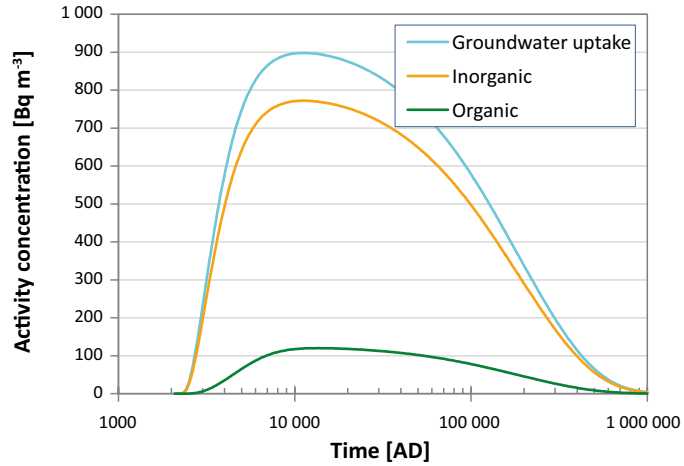

Figure 11-7. *Sources of Cl-36 contributing to the pore water activity concentration of the upper cultivated soil during the first 50 years of cultivation of the drained mire as a function of time. The contribution from the groundwater uptake is similar to the contribution from the accumulated inventory before draining that originates mainly from desorption of sorbed Cl-36 (inorganic) and to a lesser extent from mineralisation of organically bound chlorine (organic).*

There is a temporal development of the contribution by the different source terms to the pore water concentration during the 50 years after draining (Figure 11-8). Leaching from the accumulated inventory of Cl-36 sorbed to the inorganic soil before draining dominates initially, but levels off as the storage successively becomes depleted. The contribution from the groundwater uptake is low initially since most of the Cl-36 sorbs to the cultivated soil, but increases until equilibrium is reached, and becomes the most important source after 20 years. The contribution from mineralisation of the organically bounded Cl-36 is limited throughout the 50-year cultivation period. This contribution is, similar to the contribution from groundwater uptake, low initially due to sorption and increases as equilibrium establishes but would eventually (later than 50 years after draining) level off as the pool of organic matter decreases due to decomposition.

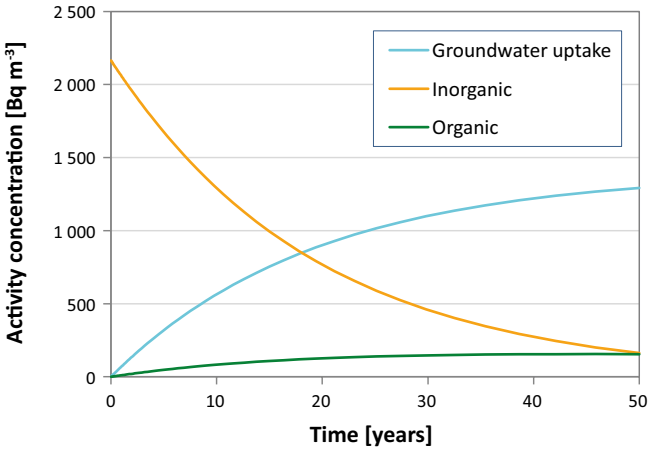

Figure 11-8. *The contribution by different sources to the Cl-36 pore water concentration in the cultivated soil during the first 50 years (a) of cultivation of the drained mire (at the time of maximum dose ~ 10 000 AD).*

To conclude, human exposure from Cl-36 in the drained mire case is primarily caused by ingestion of food that in turn depends on the pore water activity concentration in the cultivated soil. This pore water activity concentration primarily originates from the accumulated inventory of Cl-36 in the upper regolith layers before draining and the pore water concentration in the postglacial clay-gyttja (RegoPG) through groundwater uptake. Beside those two environmental concentrations, the pore water activity concentration in the till has a direct effect on exposure through drinking from a dug well.

11.5 Comparison between radionuclides

The size of the radionuclide release in combination with its half-life and sorption are important properties that influence the risk for human exposure to different radionuclides. C-14 and Mo-93 are released early from the repository, they are mobile in the bedrock and have half-life of a few thousand years resulting in a relatively early maximum release from the geosphere, around 3500 and 5000 AD, respectively (from BHA releases). The radioactive decay of Cl-36 is slower and the maximum release occurs later and continues for a much longer period before it ceases. Tc-99 is a highly sorbing radionuclide with a long half-life and its peak release from the bedrock does not happen until after 100 000 AD and stays relatively high for several hundred thousand years (Figure 11-9).

The sorption in the regolith largely determines the retention of radionuclides after the release from the geosphere. Weakly sorbing radionuclides, like Cl-36 and, in particular, non-sorbing C-14 (K_d values in Table 11-1), are mobile and quickly transported up through the regolith layers with the groundwater and are exported from the system with the surface water. The export of C-14 from the uppermost regolith layer is even faster than for Cl-36 and this is mainly caused by degassing. On average, the transport through biosphere object 206 (i.e. residence time[28]) takes approximately 15 years for C-14 and about 60 years for Cl-36 and the proportion that decays within the biosphere object before export is minimal (Figure 11-9).

Mo-93 is more strongly sorbing, in particular to the organic-rich upper regolith layers (Table 11-1). This results in considerable retention in the postglacial clay-gyttja layer (RegoPG) and in the peat (RegoPeat), and the transport through the biosphere object (residence time) would take on average about 6700 years for stable molybdenum. The retention, in combination with a relatively short half-life (4000 years), makes radioactive decay of Mo-93 within the biosphere a more important removal mechanism (about 60 %) than export from the system (about 40 %, see Figure 11-9). Due to the retention, the maximum inventory of Mo-93 in the upper regolith (just before 10 000 AD) is delayed by about 5000 years after the maximum geosphere release peak. The combination of export from and decay within the biosphere decrease the inventory, and after 30 000 AD practically no Mo-93 is left in the regolith.

[28] The residence time was estimated as the total inventory in the regolith divided by the annual unit release, assuming no decay, using a steady state solution of the radionuclide transport model for the biosphere.

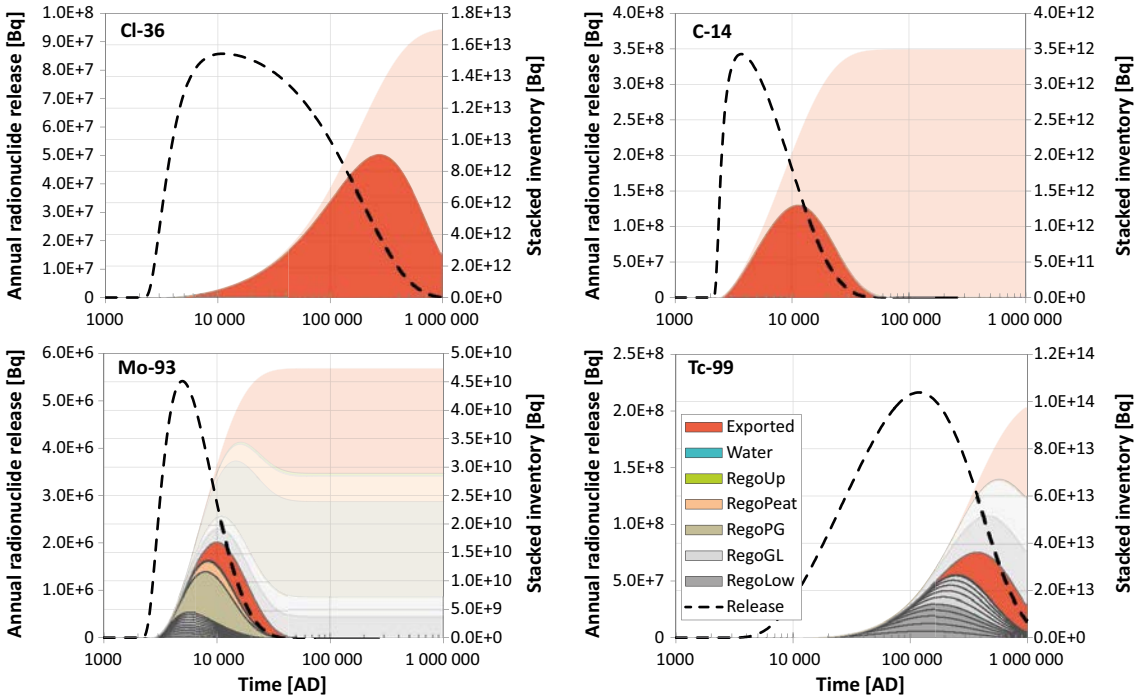

Figure 11-9. *The panels show the modelled annual geosphere release of Cl-36, C-14, Mo-93 and Tc-99 over time (dashed black line, left vertical axis) and the amount (inventory) of the released radionuclides stored per regolith layer or downstream (exported) from the biosphere object (coloured areas, right vertical axis). Semi-transparent colours show the amount decayed within each layer or after export from the object. Observe that scale on both the left and right vertical axes differs between panels (radionuclides) and therefore the panels are primarily suitable for comparing general pattern of the radionuclide behaviour rather than the activities between radionuclides.*

Tc-99 is strongly sorbing, in particular to the deeper inorganic regolith layers (RegoLow and RegoGL) and is, on average, retained for a couple of hundred thousand years before it is exported from the biosphere object. Due to the long retention time in the lower regolith layers, radioactive decay is, despite the long half-life (211 100 years), a removal mechanism of the inventory as important as export through surface runoff (Figure 11-9).

Transport, retention and decay, and accumulation of radionuclides in the mire largely determine the environmental activity concentrations and resulting doses from the cultivated drained mire. The pore water activity concentration in the regolith of the mire decreases towards the surface, as the dilution with shallow groundwater and meteoric water increase towards the surface. For mobile (and relatively long-lived) radionuclides, like Cl-36, this dilution largely determines activity concentrations in the upper layers. In the uppermost regolith layer, the pore water concentration of C-14 decreases to a much greater degree than for Cl-36, mainly due to degassing (compare C-14 and Cl-36 water activity concentrations in Figure 11-10). The gradient of the decrease in the pore water concentration towards the surface can be even steeper for radionuclides with fast radioactive decay in relation to the retention time in the regolith. This is illustrated by the larger relative difference in Mo-93 pore water concentration between the uppermost and deeper layers than for e.g. Cl-36, or the steep concentration gradient within the strongly sorbing inorganic regolith layers (RegoLow and RegoGL) for Tc-99 (Figure 11-10).

The low sorption of Cl-36 and C-14 results in a small regolith inventory in relation to the geosphere release and a large proportion exported from the system. Nevertheless, the resulting environmental concentrations are large enough to contribute significantly to the total annual doses during a longer (Cl-36) or shorter (C-14) period of the assessed time frame. In contrast to most radionuclides, including Cl-36, C-14 is completely non-sorbing ($K_d = 0$) and the inventory in the lower regolith layers is completely dissolved in the pore water. For sorbing radionuclides (Mo-93 and Tc-99) the inventory is completely dominated by the fraction sorbed to the solid fraction of the soil.

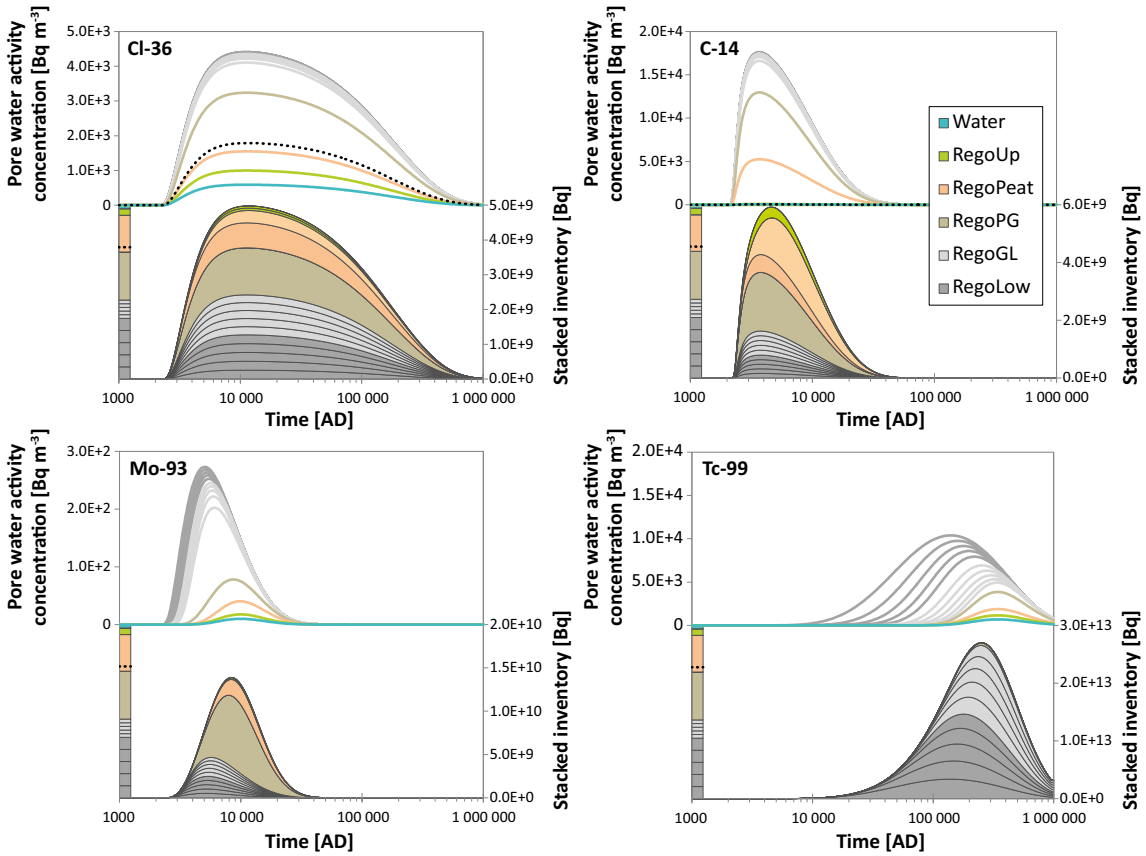

Figure 11-10. *Pore water concentration (upper sub-panels) and inventory (lower sub-panels) of four radionuclides in mire regolith layers as a function of time. The dotted black line in the upper panel for the two radionuclides with specific activity plant uptake (Cl-36 and C-14) is the average pore water activity concentration in the cultivated soil (RegoUp) during the first 50 years after draining. The lighter shades of RegoPeat and RegoUp in the lower panels indicate the inventory in the organic fraction. The bars to the left in the lower sub-panels show the relative regolith layer thickness and the dotted black line within the peat layer (RegoPeat) in this bar is the lower depth of the cultivated soil after draining the mire.*

Different exposure routes are linked to radionuclide concentrations in different regolith layers and environmental media. The most important exposure route, in the drained mire land use variant, is through ingestion of food (Figure 11-11). Exposure through food ingestion is linked directly (cereals and potatoes) or indirectly (meat and milk) to plant radionuclide uptake. Plant uptake, in turn, is proportional to the pore water activity concentrations (specific activity uptake, e.g. C-14 and Cl-36) or to the total activity concentrations (*CR* modelled uptake, e.g. Mo-93 and Tc-99) in the cultivated soil. The source of the radionuclides available for plant uptake in the drained mire varies between radionuclides. Plant uptake of C-14 originates mainly from the upward groundwater flow, whereas the uptake of Mo-93 and Tc-99 almost exclusively originates from radionuclides which have accumulated in the peat (by sorption) before cultivation (Figure 11-12). For Cl-36 the source is, as mentioned in Section 11.4 above, both the accumulated inventory before draining and the groundwater from below. The contribution from mineralisation of organic matter is generally limited. Furthermore, about half of the C-14 plant uptake occurs through the leaves (foliar uptake) and thus the atmospheric activity concentration in the canopy layer is also relevant for uptake of radioactive carbon.

For some radionuclides, drinking water from a dug well, and thus the pore water concentration in the till, makes a significant contribution to the dose in relation to ingestion of food. The relative importance of the dug well increases for radionuclides with a limited transport from the till to the upper regolith layers due to strong sorption in the layers in between. For example, the dose from Tc-99 is dominated by drinking well water until 150 000 AD due to the strong retention in the glacial clay (Figure 11-11). This effect is further strengthened in combination with a short half-life (e.g. short-lived decay products in the U-238 decay chain discussed in Section 11.6).

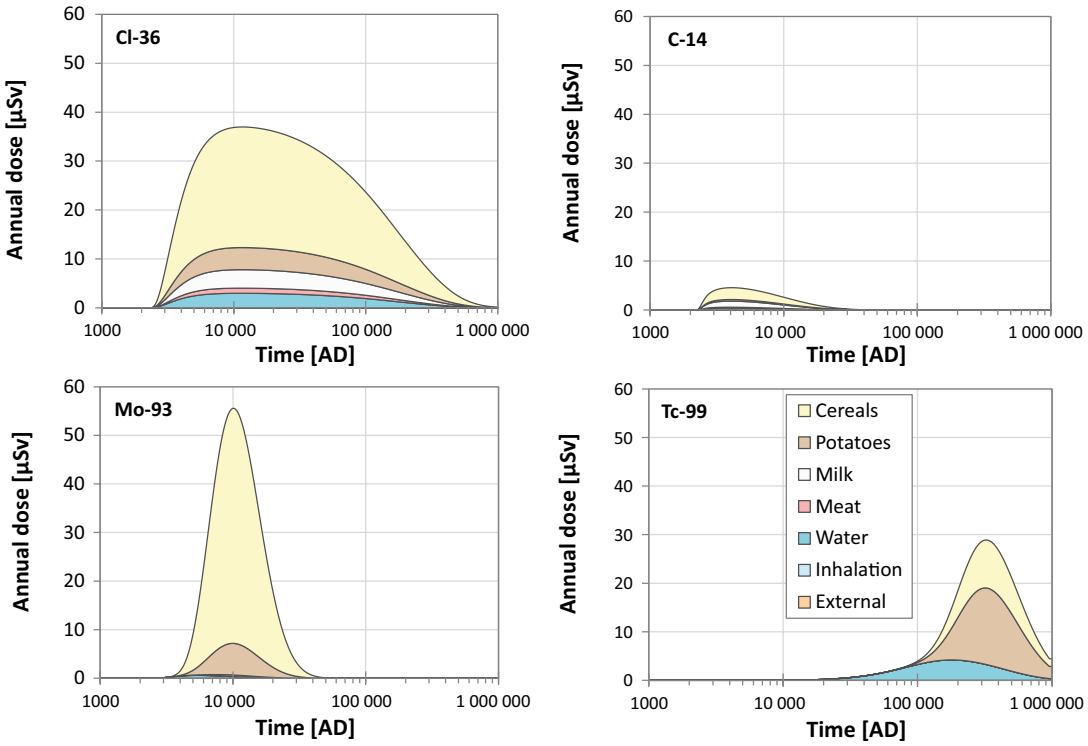

Figure 11-11. *Exposure routes for four different radionuclides in the drained mire (DM) land use variant. Ingestion of various food items is the most important routes but drinking of water from a dug well contributes significantly or even dominates the dose for some radionuclides (e.g. Tc-99 before 150 000 AD). The contribution from inhalation and external radiation is insignificant for all four example radionuclides (not visible from the line widths).*

The radionuclide-specific dose from ingestion of food thus depends on the environmental concentration as well as plant uptake and the radiotoxicity of the radionuclide (analysed further in Section 11.7). For example, the combination of higher accumulation (sorption) in the peat, higher plant uptake and higher radiotoxicity explain why the maximum Mo-93 dose is higher than those of C-14, Cl-36 and Tc-99, despite a substantially lower geosphere release of Mo-93 (Figure 11-3). The importance of specific food items is related to the activity concentration in the edible parts and to the amounts consumed. For example, the relatively large contribution of potatoes to the dose from Tc-99 (Figure 11-11) is partly caused by the larger uptake in this particular crop type (high *CR* value, Table 11-1).

The effects of plant uptake and radiotoxicity on the dose are specific to the radionuclide but independent of the characteristics of the biosphere object. The environmental concentrations, however, are determined by the interactions between radionuclide-specific properties (sorption and half-life) and object-specific properties (groundwater flows and regolith layer thicknesses). Thus, the doses from specific radionuclides and their relative importance will differ between biosphere objects in response to their half-life and sorption properties, and extrapolation from object 206 results and conclusions to other biosphere objects is not straightforward. The effects of the interaction between radionuclide- and object-specific properties are explored in *the discharge area evaluation case* (Section 12.2).

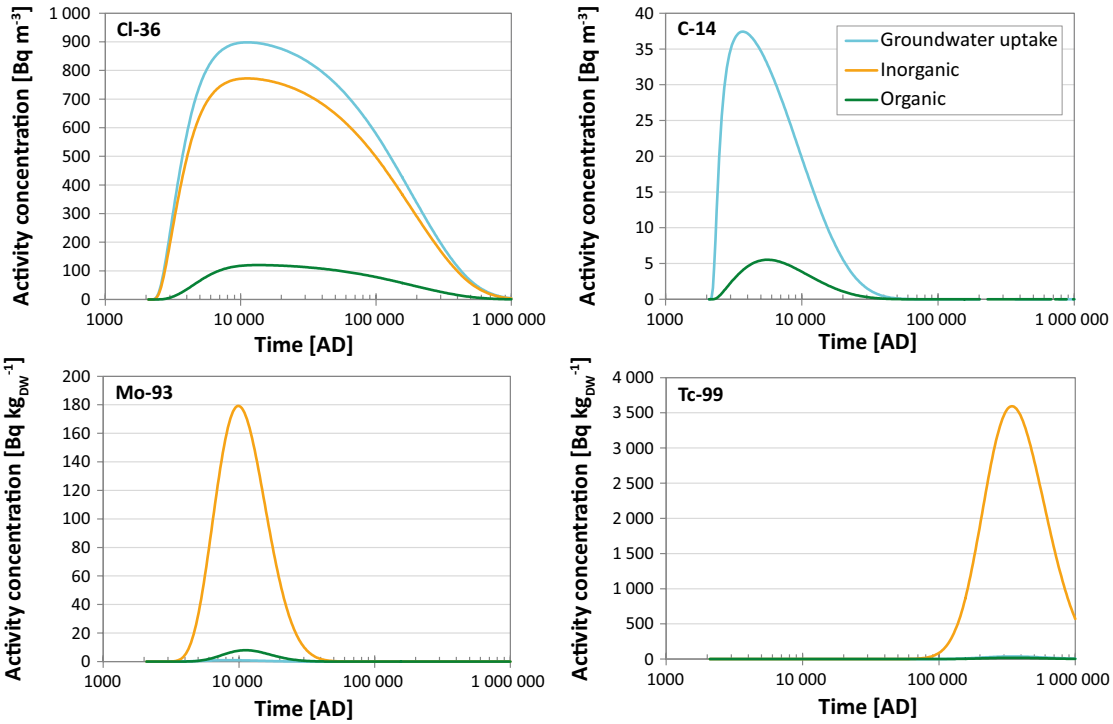

Figure 11-12. *Contribution from different source terms to the average radionuclide activity concentration in pore water (Cl-36 and C-14) or in the soil (Mo-93 and Tc-99) of the upper cultivated regolith layer during the first 50 years of cultivation of the drained mire as a function of time. Groundwater uptake during the growing season is important for weakly sorbing radionuclides (C-14, and Cl-36), whereas the accumulated initial inventory at the time of draining is the dominating source for more strongly sorption radionuclides (Mo-93 and Tc-99). Note that panel for Cl-36 is identical with Figure 11-7.*

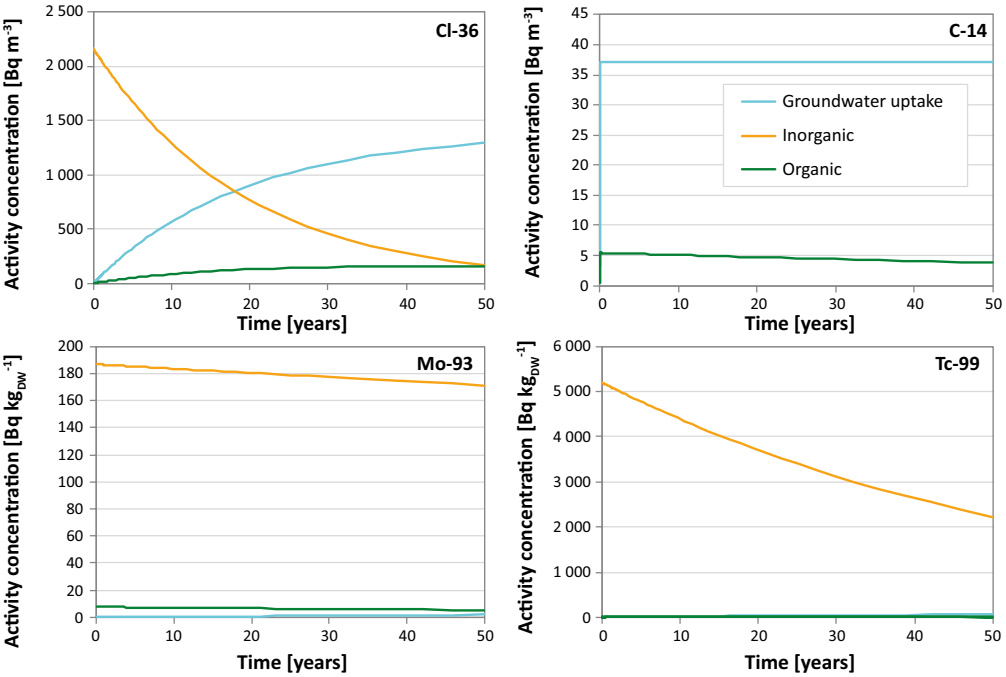

Figure 11-13. *The contribution from different sources to the activity concentration in the pore water (Cl-36 and C-14, upper panels) or in the soil (Mo-93 and Tc-99, lower panels) during the first 50 years (a) of cultivation of the drained mire (at the time of maximum dose). The initial contribution from the accumulated inventory sorbed to the soil (inorganic) is a function of sorption in the mire (K_d in RegoPeat) and declines as this storage successively leaches out as a function of K_d in the cultivated soil (low K_d means fast leaching). The contribution with the groundwater uptake is a function of the activity concentration in the source regolith layer below the cultivated soil. The contribution from the organic fraction is relatively small for all radionuclides. Note that panel for Cl-36 is identical with Figure 11-8.*

11.6 The U-238 decay chain

The geosphere releases, transport, accumulation and resulting doses of decay chains are more difficult to understand due to ingrowth of decay products with properties different from their parents. The annual effective dose from U-238 released from BHA, including the dose from all radionuclides in the U-238 decay chain, increases over time (apart from a temporal minimum around 15 000 AD) and dominates the total dose at the end of the simulation period at a level close to the dose corresponding to the regulatory risk criterion (U238+ in Figure 11-3). The radionuclides in the U-238 decay chain that are explicitly included in the BioTEx model are U-238 → U-234 → Th-230 → Ra-226 → Pb-210 → Po210, and their half-lives decrease along the decay chain, from very long for U-238 (4.5 billion years) to less than half a year for Po-210 (Table 11-2). Several radionuclides in this decay chain exist only for a very short time in relation to the time periods relevant for radionuclide transport and accumulation (i.e. residence times in regolith layers) and they are therefore not included explicitly in the radionuclide transport modelling. However, the effect on the dose of these short-lived radionuclides is included by incorporating their radiotoxicity in the radiotoxicity of their longer-lived parents (dose coefficients, *DC*, in Table 11-2 and Figure 11-14).

Table 11-2. Half-life, K_d, *CR* and dose coefficient (*DC*) for ingestion of the radionuclides in the U-238 decay chain explicitly included in the radionuclide transport model.

Parameter	Unit	Specification	U-238	U-234	Th-230	Ra-226	Pb-210	Po-210
Half-life	years		4 468 000 000	245 500	75 380	1 600	22	0.38
K_d	$m^3\ kg_{DW}^{-1}$	RegoUp (mire)	10	10	2.8	2.1	18	12
		RegoPeat	13	13	3.2	2.1	14	15
		RegoPG	3.8	3.8	13	2.6	7.7	37
		RegoGL	0.43	0.43	93	10	211	130
		RegoLow	0.022	0.022	24	1.4	17	15
CR	$m^3\ kg_{DW}^{-1}$	cereals	0.0039	0.0039	0.0082	0.038	0.0065	0.0065
		tubers (potatoes)	0.012	0.012	0.00049	0.027	0.0036	0.0066
DC	$Sv\ Bq^{-1}$	ingestion	4.5E−08	4.9E−08	2.1E−07	2.8E−07	6.9E−07	1.2E−06

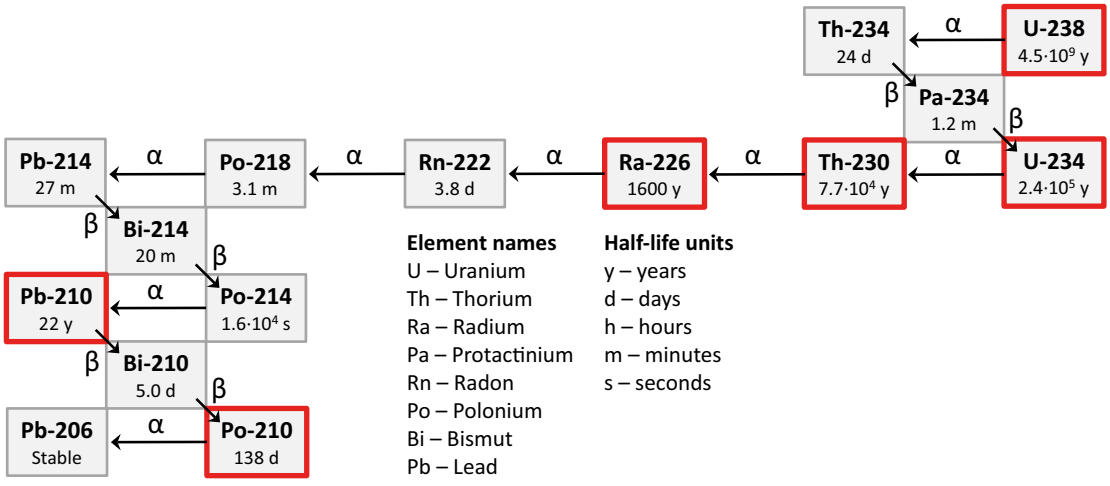

Figure 11-14. *The U-238 decay chain, including type of decay and half-life of the radionuclides in the chain (only the main decays are shown and gamma emissions are not indicated). The more long-lived radionuclides are explicitly included in the radionuclide transport model (marked by thicker red frames). Exposures from short-lived radionuclides (thinner grey frames) are included in the dose coefficients of their parent radionuclides.*

The annual dose from individual radionuclides in the U-238 decay chain in the drained mire depends on the pore water concentration in the till (exposure from drinking well water) and the activity concentration in the cultivated soil (exposure from ingestion of food). Those environmental concentrations in turn change over time as a function of geosphere release, decay rate (half-life) and mobility (K_d) of the individual radionuclides, including ingrowth from decay of parent radionuclides (with potentially different properties) in the regolith (Table 11-2). The resulting dose is further related to the radiotoxicity (*DC*) of the individual radionuclides and, for exposure through crops, to soil-to-plant uptake (*CR*).

An early geosphere release of Ra-226 (Figure 11-15, left panel), originating from Ra-226 in the waste at repository closure, results in a temporary dose maximum from Ra-226 and its decay products Pb-210 and Po-210 around 6000 AD (Ra-226+ in Figure 11-15, right panel). The sorption of Ra-226, Pb-210 and Po-210 is high in deeper regolith layers (in particular in glacial clay) and practically nothing reaches the upper regolith layers (Table 11-2 and Figure 11-16). Thus, the exposure pathway for the Ra-226 release is through drinking water from the dug well and not from ingestion of food from the cultivated soil in the drained mire (Figure 11-17, lower right panel). The Ra-226+ dose is dominated by the contribution of Po-210, followed by Pb-210 (results not shown) due to the combination of their higher radiotoxicity (*DC*) than for Ra-226 and their lower sorption in the till (K_d) resulting in a higher till pore water concentration than for Ra-226 (Table 11-2).

Geosphere releases of U-238 and U-234 increase throughout the simulation and approach maximum levels at the end of the simulation period. These uranium releases are the dominating source of the U-238 decay chain annual doses between 15 000 AD and 300 000 AD, followed by a period when geosphere releases of Th-230 and Ra-226 becomes increasingly dominant until the end of the simulation (Figure 11-15, left panel).

Uranium is relatively mobile in the lower regolith layers but more strongly sorbing in the upper layers which are rich in organic content (Table 11-2). The release of U-238 from the geosphere is thus transported to, and partly retained, in the upper layers (RegoPeat and RegoUp, Figure 11-16) and results in dose mainly from ingestion of food derived directly (plants) or indirectly (milk) from the cultivated soil (Figure 11-17). The half-life of its decay product, U-234, is however long enough (245 500 years) to prevent any further exposure by U-234 or other decay products from the geosphere release of U-238 before it is exported from the biosphere object. Consequently, the dose curves from the U-238 geosphere release and from U-238 exposure are practically identical, Figure 11-15).

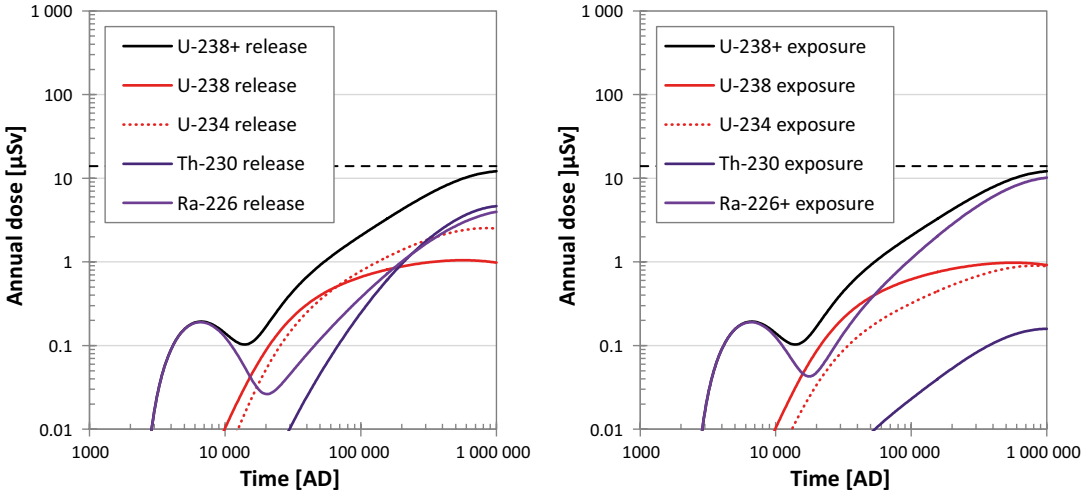

Figure 11-15. *The annual dose in the drained mire (DM) land use variant from U-238 including all of its decay products (U-238+). The left panel shows the dose originating from geosphere releases of individual radionuclides (including the dose contribution from decay products of that specific radionuclide release) and the right panel shows the dose by radionuclide (independently if the geosphere release was from that particular radionuclide or a parent radionuclide).*

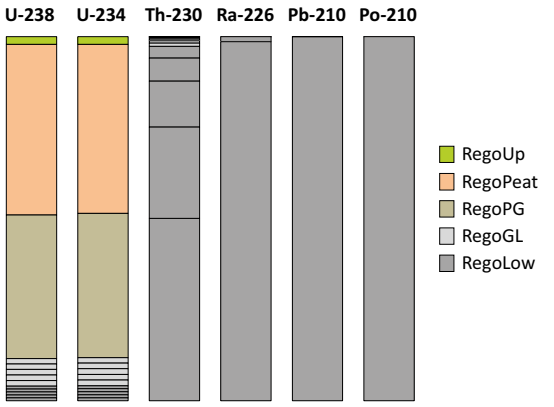

Figure 11-16. *The bars show the relative distribution of the radionuclide inventory between individual regolith layers at steady state[29] from a constant rate of bedrock release of each radionuclide (ignoring ingrowth). Uranium accumulates mainly in the organic rich post-glacial clay (RegoPG) and the peat (RegoPeat) layers. The inventory of Th-230 is mainly retained in the till (RegoLow). For Ra-226, and in particular for Pb-210 and Po-210, the combination of high sorption and fast decay (Table 11-2) prevents them from being transported from even the deepest till layer (i.e. first sub-compartment of RegoLow).*

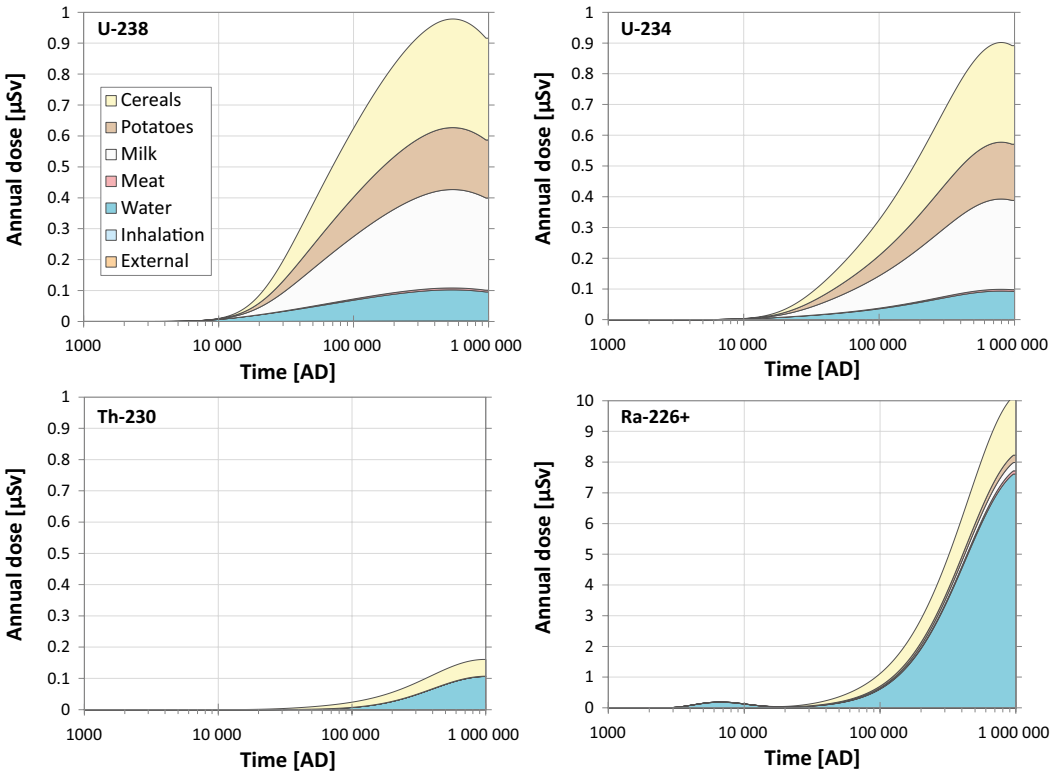

Figure 11-17. *Exposure routes for the dose from U-238, U-234, Th-230 and Ra-226+ (+ indicating inclusion of all decay products) in the drained mire land use variant with a dug well. Exposure from U-238 and U-234 is mainly through ingestion of food derived directly (cereals and potatoes) or indirectly (milk) from the cultivated soil and a smaller contribution from drinking water from the dug well. The first smaller dose peak of Ra-226+ around 6000 AD is mainly caused by drinking water from the dug well, whereas the second and larger dose peak also includes exposure from ingestion of food from the cultivated drained mire. The dose from Th-230 is much smaller than for Ra-226+ (observe that Ra-226 has ten times higher values on the vertical axis) but has a similar relation between exposure from ingestion of food and drinking water. The sum of the dose from all exposure routes in all four panels adds up to the total dose from the U-238 decay chain (U238+), but observe that the scale on the vertical axes (doses) in this figure is not logarithmic as for the dose curves in e.g. Figure 11-3 and Figure 11-15.*

[29] The distribution of the radionuclide inventory among regolith layers was estimated using a steady state solution of the radionuclide transport model for the biosphere.

As with U-238, most of the geosphere release of U-234 is transported to the upper regolith layers (Figure 11-16), resulting in a dose from ingestion of food (left panel in Figure 11-15 and upper right panel in Figure 11-17). However, the shorter half-lives of its decay products (Th-230, Ra-226, Pb-210 and Po-210), in relation to their residence times in the upper regolith, result in ingrowth and a significant contribution from those radionuclides to the dose from the drained mire (Figure 11-17). The higher plant uptake and higher combined radiotoxicity of Ra-226, Pb-210 and Po-210 than those for Th-230 (Table 11-2) explain why the Ra-226+ dose is almost two orders of magnitude larger than the Th-230 dose (Figure 11-15, right panel and Figure 11-17, lower panels). The high annual doses from Ra-226+ at the end of the simulation period thus partly originate from the bedrock release of U-234 resulting in dose from ingestion of food from the cultivated soil, but mainly from well water exposure from the increasing geosphere releases of Th-230 and Ra-226 (Figure 11-17).

To summarise, the exposure from the U-238 decay chain in the base case follow two major routes in the biosphere. One originates from the bedrock release of U-238 and U-234 that is mainly transported through the deeper regolith layers, get partly retained in the upper layers (see Figure 11-16) and results in exposure from U-238 and U-234, including its decay products through ingestion of food (Figure 11-18, left panel). The other exposure route originates from releases of mainly Th-230 and Ra-226 from the bedrock that get retained in the lower regolith layers (see Figure 11-16) and results in exposure through drinking water from the dug well (Figure 11-18, right panel), mainly from Ra-226 and its decay products Pb-210 and Po-210. Finally, it is worth noting that not only the bedrock release of U-238, but also most of the geosphere release of U-234, Th-230 and Ra-226 that contribute to the dose maximum from the U-238 decay chain at the end of the modelled period, originate from U-238 in the waste.

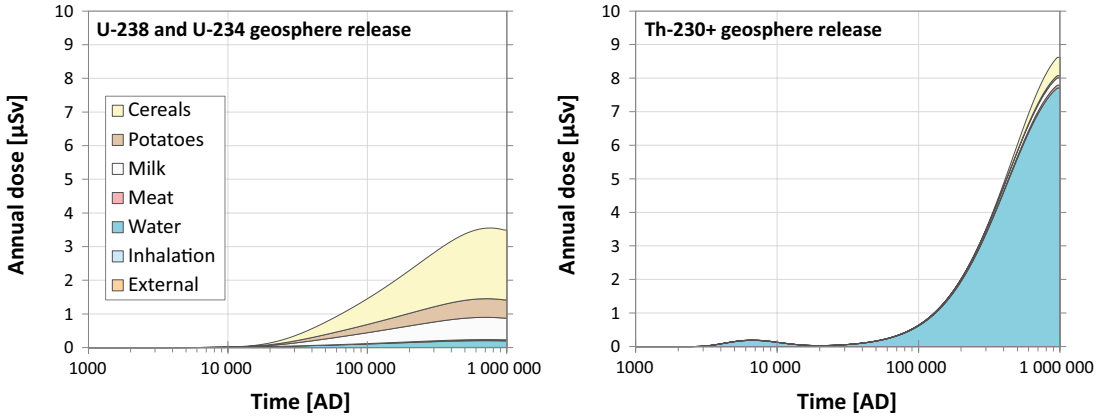

Figure 11-18. *Exposure routes for the dose from the geosphere release of U-238 and U-234 (including the dose from all decay products originating from this release, left panel), and the geosphere release of Th-230+ (including all of its decay products, in particular Ra-226, right panel). The exposure from the uranium release is through ingestion of food originating from plant uptake in the cultivated soil, and the exposure from the Th-230+ release is through ingestion of drinking water from the dug well.*

11.7 Synthesis of radionuclide property effects on doses

Some radionuclides contribute marginally (Ca-41 and Ni-59) or practically not at all (Ag-108m) to the total dose despite their relatively high annual release from the geosphere (Section 5.2.10 in the **Radionuclide transport report**). Moreover, among the radionuclides that contribute most to dose (e.g. C-14, Mo-93, Cl-36 and Tc-99 for BHA), the dose consequences for a given activity release rate vary by almost three orders of magnitude (compare the relative height of releases and doses in Figure 11-3). The ratio between annual dose and a constant geosphere release rate is referred to as the landscape dose factor (LDF). The main biosphere processes that influence the variation in LDF between radionuclides include retention and decay in lower regolith layers (K_d and half-life), accumulation in peat (K_d in peat), retardation in cultivated soil (K_d in the cultivated soil, RegoUp Agri), plant uptake (*CR*), and radiotoxicity (*DC*, Table 11-2 and Grolander and Jaeschke 2019). To synthesise and illustrate the importance of these processes, five indicators are used here. The value of each indicator corresponds to a multiplier on the dose; thus, the multiplicative effect of the indicators gives a reasonable approximation of the total release-to-dose relationship in the base case (r^2=0.95 for the crop ingestion pathway on a logarithmic scale; data not shown).

The first indicator quantifies the effect of retention and radioactive decay in deeper regolith layers. Thus, the fraction of the geosphere release that reaches the deep peat was used as an indicator for radionuclides that accumulate in the terrestrial surface environment and primarily expose through ingestion of crops (upper set of radionuclides in Figure 11-19). For many of the radionuclides that contribute significantly to the dose, almost all geosphere release reaches the deep peat layer (> 0.9 for C-14, Cl-36, Ca-41 and U-238). However, for radionuclides which have a residence time in the deeper regolith that is similar to the radioactive half-life, the release reaching the peat was approximately halved (~ 0.5 for Mo-93, Tc-99 and Ni-59).

For radionuclides with a short half-life, compared with the residence time in the lowest regolith layers, only small amounts of activity will reach the peat layer. Thus, well water is the only relevant exposure pathway and the fraction of the geosphere release that reaches the peat is not a relevant indicator. For this type of radionuclide, the activity concentration in the till pore water, in relation to the concentration of a non-sorbing species with long half-life, was used as the indicator of retention and radioactive decay in deeper regolith layers. The value of this indicator spanned an order of magnitude between the two examined radionuclides Ag-108m (0.02) and Th-230 (0.2).

For potential accumulation in layers exposed by cultivation, the sum of the K_d value and the pore volume (divided by the soil density) in the deep peat layer was used as an indicator[30]. For sorbing elements, the capacity for retention is proportional to the K_d value, whereas the pore volume also contributes to the retention capacity for mobile and non-sorbing elements. The variation of this indicator spanned almost three orders of magnitude, from 0.01 (corresponding to the pore volume) to above 10 $m^3\ kg_{dw}^{-1}$ for uranium.

The third indicator quantifies the potential for retardation of radionuclides in the cultivated soil. With the exception of C-14, the indicator describes the effects of leaching the soil by percolation with atmospheric water (i.e. runoff). This indicator is primarily a function of the soil distribution coefficient of cultivated soil. However, the response is non-linear[31]. Thus, for elements with a small distribution coefficient the potential retardation is roughly proportional to the K_d value, whereas almost all activity of radionuclides with a distribution coefficient near (or above) one is retained during a 50-year cultivation period. C-14 is primarily lost by degassing, and this process exports radionuclides from the soil much more efficiently than leaching. Thus, whereas the variation in retardation between non-volatile radionuclides is limited (to a factor of three), the total variation of this indicator spans more than three orders of magnitude.

[30] This indicator is directly proportional to the retardation factor (R_f) but has the same units as K_d ($m^3\ kg_{dw}^{-1}$): $K_d + \frac{\theta}{\rho} = \frac{\theta}{\rho}\left(1 + \frac{K_d \rho}{\theta}\right) = \frac{\theta}{\rho} R_f$, where θ is porosity (-) and ρ is density ($kg_{dw}\ m^{-3}$).

[31] The potential for retardation in cultivated soil was estimated as the average fraction remaining in soil, assuming that leaching was the primary process for the loss over 50 year of cultivation (t_{50}): $f_{regoUp,aver} \approx (1 - e^{-k_{leach}\, t_{50}})/(k_{leach}\, t_{50})$, where k_{leach} is a function of K_d and other soil properties (see Equations 7-13 and 7-41 and in Saetre et al. 2013)

The fourth indicator quantifies plant root uptake of radionuclides. For most radionuclides this indicator equals the concentration ratio (*CR*) between the plant and soil activity concentrations. For plant uptake of carbon and macro nutrients (i.e. C-14, Cl-36 and Ca-41) the equivalent to the *CR* has been calculated from plant and soil pore water elemental concentrations[32]. As cereals and potatoes are assumed to be cultivated on soil from the drained mire (and directly consumed by humans), the indicator represents the weighted average of concentration ratios for these two crops (using the dietary fractions of 0.6 and 0.1 for weights). The empirical *CR* values vary widely, and span more than four orders of magnitude, reflecting differences in plant requirements and in the availability for plant uptake of different elements.

The fifth indicator quantifies the radiotoxicity from ingestion. For radionuclides where ingestion of crops is the primary exposure pathway the indicator includes the ingrowth of decay products during 50 years of cultivation (Grolander 2013). However, in practice, the indicator corresponds to the dose coefficients for ingestion for the parent radionuclides, as listed by the ICRP (1996) (as the contribution from ingrowth of examined radionuclides is marginal). The dose coefficients correspond to the lifetime committed effective dose and take into account accumulation in the human body, tissue and organ susceptibility, and the contributions of decay products. The radiotoxicity varies by more than three orders of magnitude, primarily due to the type of radiation emitted and its energy. Thus, the alpha emitter Th-230 is more than 3000 times as radiotoxic by ingestion than is Ni-59 which decays due to electron capture (and emits radiation in form of K-shell X rays and Auger emissions).

The relative influence of these processes is shown for radionuclides with an annual geosphere release exceeding 10 000 Bq from SFL (Figure 11-19). For example, whereas the proportion of the release that decays during the transport through the regolith layers is similar for Ca-41 and Mo-93, molybdenum accumulates much more effectively in peat. The leaching rate from the cultivated soil is similar for the two radionuclides, but Ca is taken up by plants to a larger extent. Finally, the radiotoxicity of Mo-93 is significantly higher than for Ca-41. Together these factors result in the dose being about two orders of magnitude larger for Mo-93 than Ca-41, given an identical geosphere release (Figure 11-19).

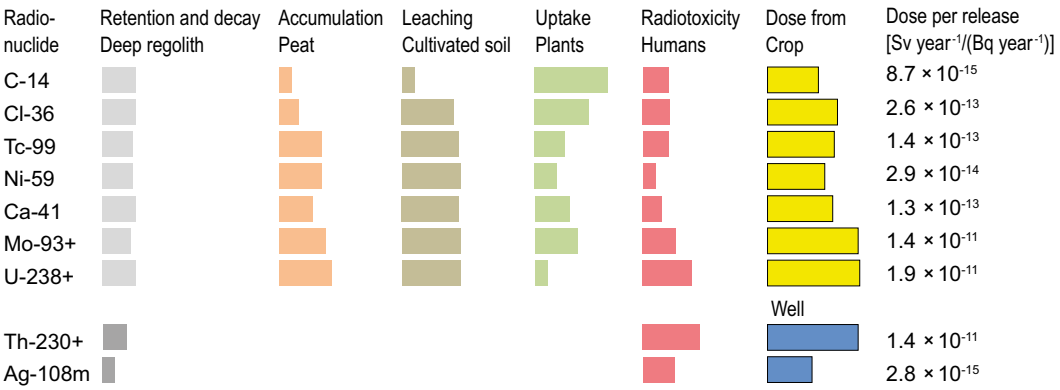

Figure 11-19. *The influence of radionuclide properties on the dose for the dominating exposure pathway from a unit release. Coloured bars without contours represent the relative importance on dose of various processes: retention and decay in deep regolith (longer bar means less decay), accumulation in peat, leaching in cultivated soil (longer bar means less leaching), plant uptake, and radiotoxicity in humans. Properties are scaled so that the length of the bars corresponds to an additive positive dose response (on a logarithmic scale). Radionuclides are organised according to the major pathway of exposure; ingestion of crops (yellow, upper) and ingestion of drinking water from a dug well (blue, lower). Note that the effects of the first two processes: retention and decay and accumulation, result from the interaction between radionuclide-specific properties and object-specific properties, whereas the three remaining properties are primarily driven by radionuclide-specific properties. Plus sign (+) indicates that the dose includes the contribution of decay products. The figure corresponds to Figure 5-22 in the* ***Radionuclide transport report****.*

[32] For C-14, 2 % of the total plant carbon was assumed to originate from the soil (100 % from the soil for all other radionuclides). The equivalent *CR* was calculated from fixed elemental plant concentrations (e.g. C, Ca and Cl) and total soil concentrations that were back-calculated from elemental pore water concentrations (accounting for soil density, porosity, soil saturation and the distribution coefficient).

Retardation and decay in the lower regolith layers have a strong effect on the release-to-dose relationship as radionuclides that are strongly sorbing (relative to their half-life) may never reach the surface of the biosphere. Thus, less than a few percent of the geosphere release of Th-230 and Ag-108m escapes the lowest regolith layer, and consequently exposure from well water is the only significant exposure pathway. However, the combined effect of smaller losses due to radioactive decay, higher toxicity, and the contribution of radiotoxic decay products (Ra-226, Pb-210 and Po-210), makes the dose from Th-230 almost four orders of magnitude higher than that from Ag-108m given an equal geosphere release rate.

Although all five processes contribute to the dose-release response to some extent, accumulation in peat (K_d), plant uptake (*CR* or equivalent) and radiotoxicity are the three factors that explain most of the variation of the relation between release and dose between the radionuclides that reach the peat layer in biosphere object 206. Excluding C-14, which differs from the other radionuclides both in transport properties and uptake mechanisms, the effects of peat accumulation, plant uptake and toxicity all vary by approximately three orders of magnitude. However, plant uptake tends to be negatively correlated with the strength of sorption, and the total variation in the release-to-dose response (again excluding C-14) in the examined radionuclides is below three orders of magnitude.

Retardation and decay depend on the properties of the object (regolith layer thickness and groundwater flows), and in objects with a thin peat layer, accumulation in post-glacial sediments (and occasionally even in glacial clay) may be relevant to the initial activity in the cultivated soil. Thus, the differences between radionuclides with respect to these two properties are specific to biosphere object 206. The sensitivities of retention, decay and accumulation in layers exposed by drainage and resulting doses, in relation to object properties are examined in the *discharge area evaluation case* (Section 12.2), and the sensitivities to radionuclide-specific sorption and plant uptake are analysed in the alternative K_d and *CR* sensitivity case (Section #13.3).

11.8 Summary and conclusions

The total annual dose from each waste vault in the *present-day evaluation case* is within an order of magnitude of the dose corresponding to the regulatory risk criterion of 14 μSv**.** Draining and cultivation of a mire in the discharge area (DM) is the land use variant that causes the highest dose. This is primarily because radionuclides can accumulate in peat over a long period of time prior to exposure, and because the dose-contributing radionuclides predominantly yield dose through ingestion of food. The dominating radionuclides are C-14 and Mo-93 for both waste vaults and Tc-99, Cl-36 and the U-238 decay chain series for BHA. The temporal dynamics of nuclide-specific doses is driven by the release from the geosphere (reflected by similarly shaped curves of releases and doses in Figure 11-3), but the individual radionuclide properties influence the environmental concentrations and exposure pathways as well as the timing and magnitude of resulting doses.

A general pattern is that non- and weakly sorbing radionuclides, like C-14 and Cl-36, mainly follow the groundwater flow. These radionuclides will reach the surface environment relatively quickly and are eventually mainly exported from the system. Except for very short-lived radionuclides, the pore water activity concentration of poorly sorbing radionuclides is determined by the rate of the radionuclide release from the geosphere and the dilution by the groundwater and meteoric water flow through the regolith. Thus, the temporal dynamics of the dose from non- and weakly sorbing radionuclides closely follows that of the release. Relevant exposure pathways are mainly through ingestion of food (based on plant uptake from cultivated soil) and ingestion of water (based on the pore water activity concentration in the till).

Strongly sorbing radionuclides are retained in the regolith, and the residence time in the regolith is positively correlated to the sorption. If the transport time through the regolith is short relative to the half-life, a larger proportion of the radionuclides will reach the upper regolith layers and become exported by surface water run-off and vice versa. Short-lived strongly sorbing radionuclides will however be prevented from reaching the upper regolith layers. Exposure through drinking water from the till can occur, but a substantial exposure through ingestion of food from the cultivated upper soil is unlikely. Strongly sorbing radionuclides that are long-lived enough, like Tc-99, can contribute to exposure both through drinking water and ingestion of food, but the time windows

for exposure differ between the pathways. Whereas exposure from a well can occur immediately after a release to the biosphere, it will take a considerable amount of time (hundreds of thousands of years) before radionuclide releases will have reached and accumulated in the upper regolith, which, after drainage and cultivation, results in exposure through ingestion of food. Sorption in the regolith delays the maximum dose of Mo-93 by approximately 5000 years and that of Tc-99 (BHA only) by more than 200 000 years in relation to the timing of the maximum geosphere release rate. Exposure through ingestion of food can be particularly important for radionuclides like Mo-93 that have a much stronger sorption to the upper organic rich regolith layers than to the deeper inorganic regolith layers.

For decay chains, ingrowth of decay products that have different properties from their parents makes the relationships between radionuclide properties and resulting doses more complex. Given the assumptions in the *present day evaluation case*, the maximum doses from the U-238 decay chain at the end of the simulation period are dominated by exposure mainly from Ra-226 and its decay products Pb-210 and Po-210 in well water, resulting from geosphere releases of Th-230 and Ra-226 (originally from U-238 BHA releases). Exposure from U-238 including its decay products through ingestion of food also contributes and results from geosphere releases of relatively mobile U-238 and U-234 transported to the upper layers.

Even though the temporal dynamics of nuclide-specific doses is largely driven by the geosphere release, the variation in annual dose for a given release spans more than three orders of magnitude for nuclides that are released in substantial amounts to the surface. For example, Mo-93 gives large doses relative to its activity release compared with e.g. Ni-59 (Figure 11-3). The mechanisms behind the nuclide-specific behaviour in the biosphere system and the dose response can be synthesised by dividing them into five factors; retention and decay, accumulation in peat, leaching from cultivated soil, plant uptake, and radiotoxicity.

Radionuclide retention (sorption) and decay in the regolith largely determine the fraction of the geosphere release that reaches the upper part of the regolith profile and thus whether exposure can occur primarily through food consumption or well water usage, or be generally restricted. Accumulation in peat (K_d) and plant uptake (*CR* or equivalent) both explain part of the variation of the relation between release and dose between the radionuclides that reach the peat layer in biosphere object 206, however, plant uptake tends to be negatively correlated with the strength of sorption. Finally, the dose that is caused by a given intake of activity is determined by how a radionuclide is metabolised and by the type and energy of its ionising radiation, both contributing to its radiotoxicity.

All these factors vary by several orders of magnitude among radionuclides that have a substantial geosphere release (Figure 11-19). In the biosphere modelling, leaching from cultivated soil, plant uptake, and toxicity are properties that are assumed to be marginally affected by conditions in the discharge area, and patterns from *present-day evaluation case* calculations can in this sense be viewed as valid for a broad range of environmental conditions. Conversely, retention and decay in the lower regolith and accumulation in peat depends on the combination of properties of the discharge area, e.g. size of object, soil depth and groundwater discharge and sorption properties of specific radionuclides. Furthermore, in objects with a thin peat layer, radionuclides accumulated not only in peat, but also in post-glacial sediments (and occasionally even in glacial clay) might contribute to the inventory in the cultivated soil. Thus, the observed differences between radionuclides with respect to these two properties are specific to biosphere object 206. The sensitivity of retention and decay in the regolith and accumulation in layers exposed by drainage to variation in object properties are examined in the *discharge area evaluation case* (Section 12.2). Similarly, the sensitivity of doses to variation in radionuclide specific sorption and plant uptake properties are explored in the alternative K_d and *CR* sensitivity case (Section 13.3).

12 Analysis of other evaluation cases

12.1 Introduction

Six evaluation cases involved changes of the biosphere system as compared with the present-day evaluation case (analysed in Chapter 11). The results with respect to annual doses for these evaluation cases are summarised in this chapter, and the analyses for the full model chain are reported in the **Radionuclide transport report**. This chapter starts with an analysis of the *alternative discharge area evaluation case*. This case examined how annual doses were affected by properties of the discharge area, and to what extent the simplifications made in the base case (including the selection of a single object, 206) influenced the projected doses. The evaluation of the effects of temporal development and habitat succession are examined in a separate section (Section 12.3, *discharge area with landscape development).*

The next four evaluation cases are organised so that the degree of complexity, with respect to the alternative biosphere assumptions, successively increases with each case. Thus, the assumptions in the first two cases (the *increased greenhouse effec*t and *alternative regional climate*) were identical to the present-day cases in all aspects except for the values for ecosystem and hydrological parameters (and in the former, long-term irrigation was also introduced). In the *initially submerged* evaluation case radionuclides were assumed to be discharged to the same object as in the base case, but the repository was assumed to be located under the sea, and thus both the geosphere release and the properties of the object responded to shoreline regression. In the *simplified glacial cycle* evaluation case, an additional level of complexity was added, as the geosphere release, the discharge area and the properties of this area changed in response to large-scale climatic change and the passage of an ice front. The last evaluation case, *drilled well*, examined the potential dose resulting from extracting water from a well located in the geosphere. No alternative biosphere assumptions were made in this case.

12.2 Alternative discharge area

Earlier safety assessments have highlighted the importance of relationships between doses and biosphere properties. In SR-PSU (Section 10.8 and 11.2 in SKB 2014d), alternative object delineations that varied the object area, regolith thickness and groundwater and surface-water flows were explored. The effects of object properties were further analysed with an analytical solution of a stylised model describing the radionuclide activity concentration in a regolith layer as a function of the radionuclide inflow and losses through advective groundwater flow and radioactive decay (Saetre and Ekström 2017b).

The *alternative discharge area evaluation case* examined how annual doses were affected by the land-use and ecosystem type, and other properties of the discharge area. Radionuclide releases from the geosphere into a range of sea basins, lakes, mires and agricultural systems were simulated. In this section, the effects of releases into time-independent objects without temporal development were explored. As in the base case, the ongoing shoreline migration and landscape development was not considered in this variant. That is, the geometry and stratigraphy of the discharge area did not change, no biological succession was accounted for, and present-day conditions were assumed for the entire assessment period of 1 million years (Sections 7.2 and 7.3, and Grolander and Jaeschke 2019 for details). The effects of landscape development on annual doses are explored separately in Section 12.3.

Nine potential discharge areas of deep groundwater (i.e. biosphere objects) in Laxemar and six areas in Forsmark were used in the analysis. The selected biosphere objects vary with respect to geometrical properties (object and watershed surface area), the depths of water, the regolith stratigraphy, and associated groundwater flows. All objects were described as the mire ecosystems that could have developed or will develop in the absence of human intervention. Five of the Laxemar objects were also described as time-independent continous agricultural systems and three other Laxemar objects as lake systems, whereof two also were considered as sea basins (Sections 7.2 and 7.3, and Grolander and Jaeschke 2019 for details).

12.2.1 Landscape geometries and regolith properties

Object areas and regolith layer thicknesses of the fully developed static mires were used in the analysis of relationships between doses and object properties below (Section 12.2.5). The object areas of the nine Laxemar and six Forsmark mire objects ranged between 8 and 150 ha, with object 206 being the smallest. Both large and small objects were represented in the Laxemar and Forsmark object sets (Figure 12-1). The total regolith thickness ranged between 3 and 15 m and the thickness of the till layer was less variable than that of the upper layers (Figure 12-1). The upper regolith layers were on average more variable and thinner in Forsmark than in Laxemar, with particularly thin peat (RegoPeat) and post-glacial sediments (RegoPG) in object 157_2 and 121_2. There was a positive correlation between the till and glacial clay layer thicknesses over objects as well as between the post-glacial sediment and the peat layer thickness, but no correlation between the lower and the upper layers (Appendix C). In relation to other biosphere objects, object 206 was a small object with intermediate regolith layer thicknesses.

12.2.2 Surface hydrology

Upward annual groundwater fluxes (q) in the nine Laxemar and six Forsmark mire objects are used in the analysis of relationships between doses and object properties in Section 12.2.5 below. The groundwater flux increased towards the surface (Figure 12-1). The variation among objects ranged from a factor of 10 (upward flow from peat) to 20 (from till). Laxemar objects had, in general, higher groundwater flows than Forsmark objects, except for the relatively high flows in Forsmark object 157_2. Groundwater flows were positively correlated between regolith layers, so that objects with high flows from the till layer (RegoLow) also had high flows in the peat layer. Correlations between regolith thicknesses and groundwater flows were generally weak and so were correlations between object area and most other object properties, except that large objects tended to also have thick glacial clay layers (Appendix C). Object 206 had a relatively high upward groundwater flux, in particular, in comparison with most Forsmark objects.

12.2.3 Total annual doses by land use variant and ecosystem type

Doses from mire ecosystems were evaluated for several land-use variants (DM – draining and cultivating a mire; IO – infield-outland farming; GP – garden plot households; HG – hunting and gathering), while time-independent agricultural and aquatic ecosystems were evaluated for traditional farming, and hunting and gathering land-use, respectively (Section 6.3 for details).

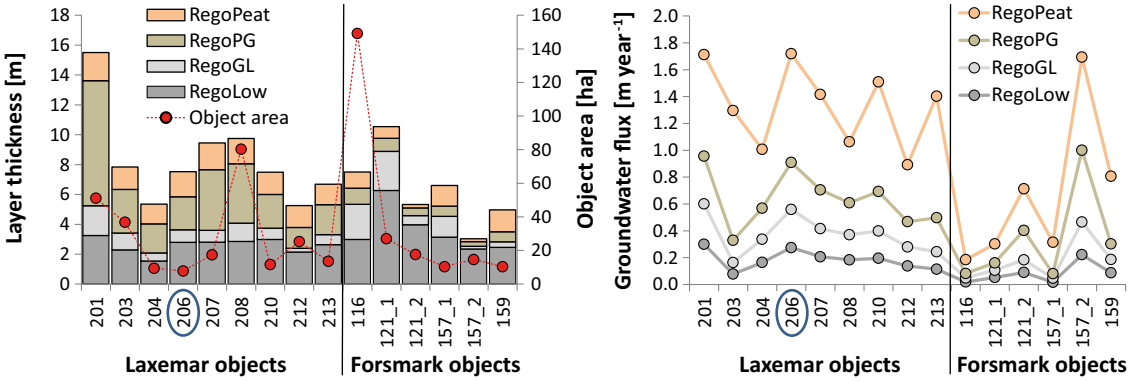

Figure 12-1. *Thicknesses of regolith layers (left vertical scale) and areas of mire objects (right vertical scale) in Laxemar and Forsmark (left panel), and upward annual groundwater flux (right panel) from the till (RegoLow), glacial clay (RegoGL), post-glacial deposits (RegoPG) and peat (RegoPeat). The Forsmark objects were in general more variable than the Laxemar objects regarding upper regolith layer thicknesses and groundwater flows. Object 206 (blue oval), upon which the base case is focused, is a small object with intermediate regolith layer thicknesses and high groundwater flow.*

Doses by different land use of mires

Doses from draining and cultivating a mire (DM) always exceeded doses from other mire land-use variants (Figure 12-2) and doses from static agricultural systems (Figure 12-3), and these findings were consistent with the base case results (Section 11.2.1). This is explained by the additional contribution from the accumulated inventory of radionuclides in the upper mire layers that becomes available for uptake by crops after draining. Doses from hunting and gathering (HG) were generally about two orders of magnitude lower than from draining the mire, while doses for garden plot households (GP) and infield-outland farmers (IO) were in between (Figure 12-2). Furthermore, the maximum annual doses from the drained mire were always higher with water supply from a dug well than from surface water (Figure 12-2). For simplicity and since doses in terrestrial ecosystems were highest for drained mires (including the dug well), this land use variant only was adopted to analyse the relationship between doses and object properties, as described in Section 12.2.5.

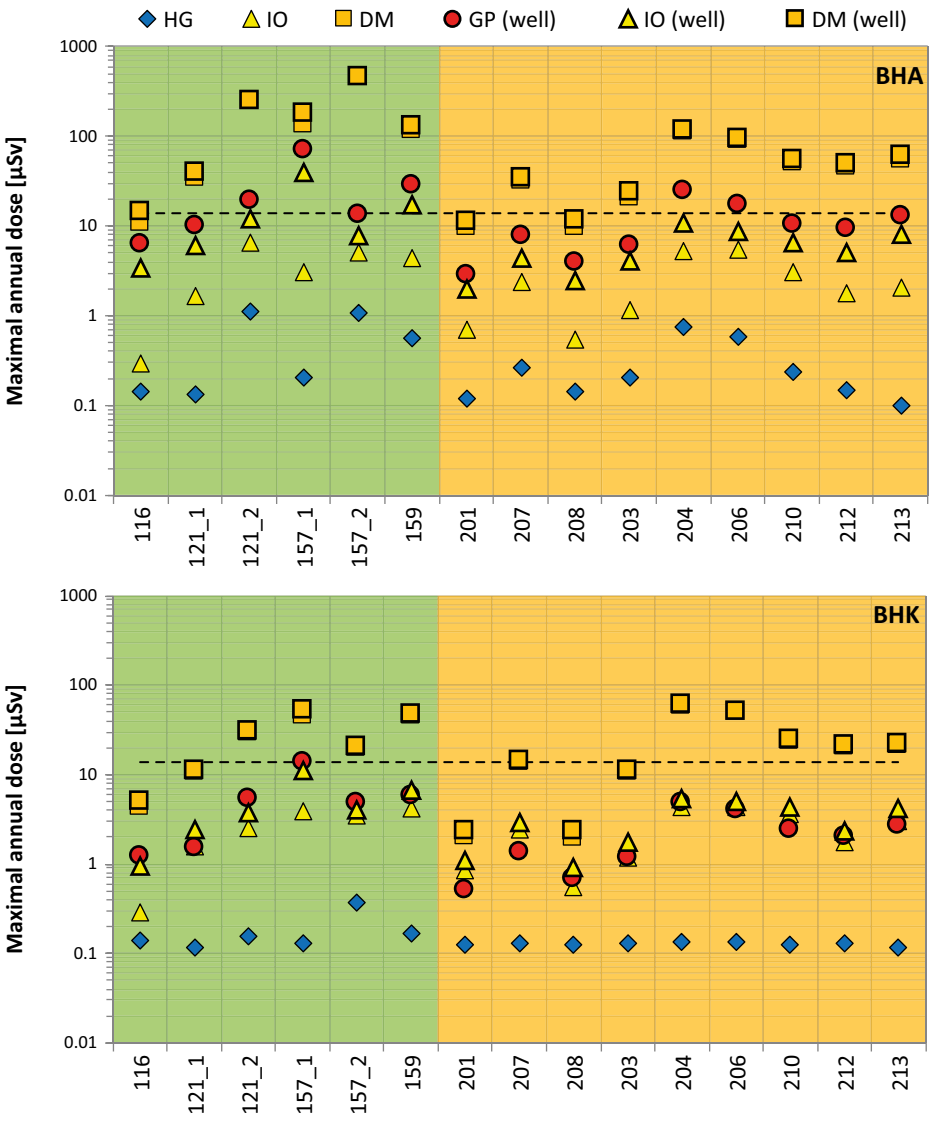

Figure 12-2. *Maximum annual doses for a release from BHA and BHK to a time-independent mire ecosystem, as a function of biosphere object and land-use variant: HG – hunting and gathering, IO – infield/outland farming, DM – drained mire agriculture, GP – garden plot. Note that for the DM and IO variants doses are displayed assuming that water was extracted either from a dug well (bold-outlined symbols) or from a stream. Observe that DM doses always exceed doses from other land-use variants on mires. The dashed horizontal black line shows the dose corresponding to the regulatory risk criterion (14 µSv).*

Doses by ecosystem types in Laxemar

Due to the lower water turnover rate, the maximum annual doses from lakes were typically higher than the corresponding doses from the open sea stage (Figure 12-3, see also *the initially submerged evaluation case*, Section 12.6). Doses from hunting and gathering in lakes could be smaller (BHA releases into object 207), similar (BHA releases in 201 and 208, BHK releases in 207) or larger (BHK release in 201 and 208) than the drained mire dose from the corresponding object (Figure 12-3). This is determined by the combination of radionuclide release composition and biosphere object properties and is further explored in Section 12.2.5. However, doses from lakes were relatively stable between objects (Figure 12-3) and, in contrast to mires, a specific analysis of relationships between doses and object properties in lakes is, therefore, of limited interest. Nevertheless, these results show that draining and cultivating a mire, as well as hunting and gathering in a lake, could potentially result in maximum doses and should therefore be explored, unless any of those ecosystems could be ruled out as a future potential area of radionuclide releases.

12.2.4 Total and radionuclide-specific annual doses

The radionuclide composition of releases from the geosphere, in combination with biosphere object properties, determines the radionuclide-specific doses and their contributions to the total doses. The maximum total mire dose (from BHA and BHK) in object 206 was, together with object 204, higher than the doses from other mire objects modelled in Laxemar. However, there was more variation in total doses from BHA releases among the Forsmark mire objects, with higher estimated doses in some objects (121_2, 157_1, 157_2 and 159) than in object 206. For BHK releases, doses in Forsmark objects were lower than in object 206 (Figure 12-4).

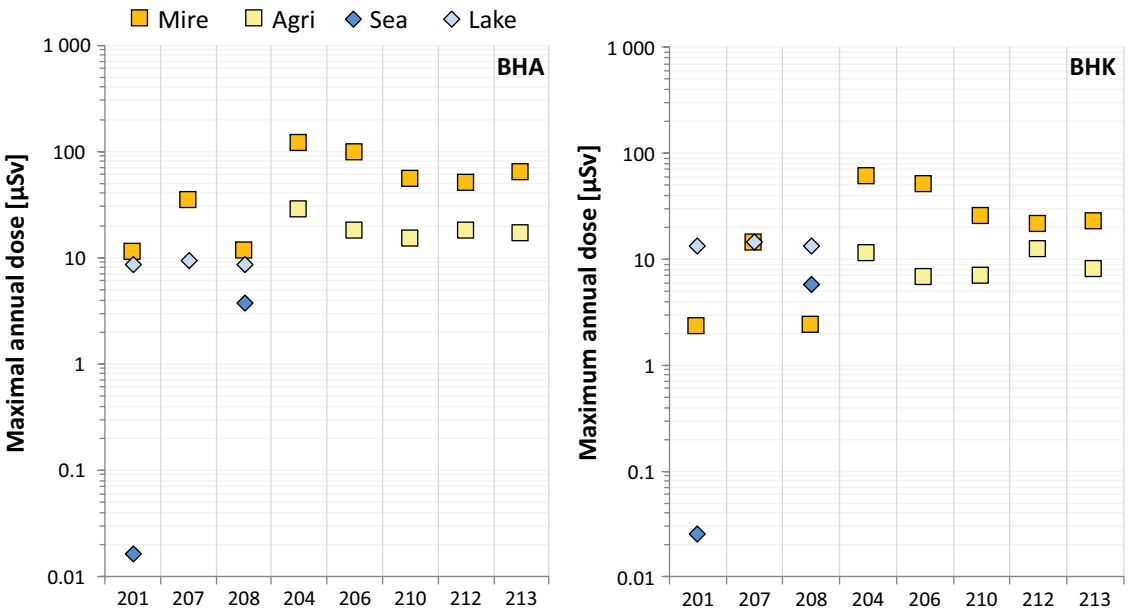

Figure 12-3. *Maximum total annual doses from BHA (left panel) and BHK (rigth panel) radionuclide releases into biosphere objects in Laxemar modelled as time-independent exposed (201) or sheltered (208) sea bays, lakes (201, 207, 208), mires (all objects) and agricultural ecosystems (204, 206, 210, 212, 213). Mire ecosystems are represented by the land use variant resulting in highest doses, e.g. drained mires with a dug well. Aquatic ecosystem doses are from hunters and gatherers and doses from agricultural ecosystems include exposure from a dug well.*

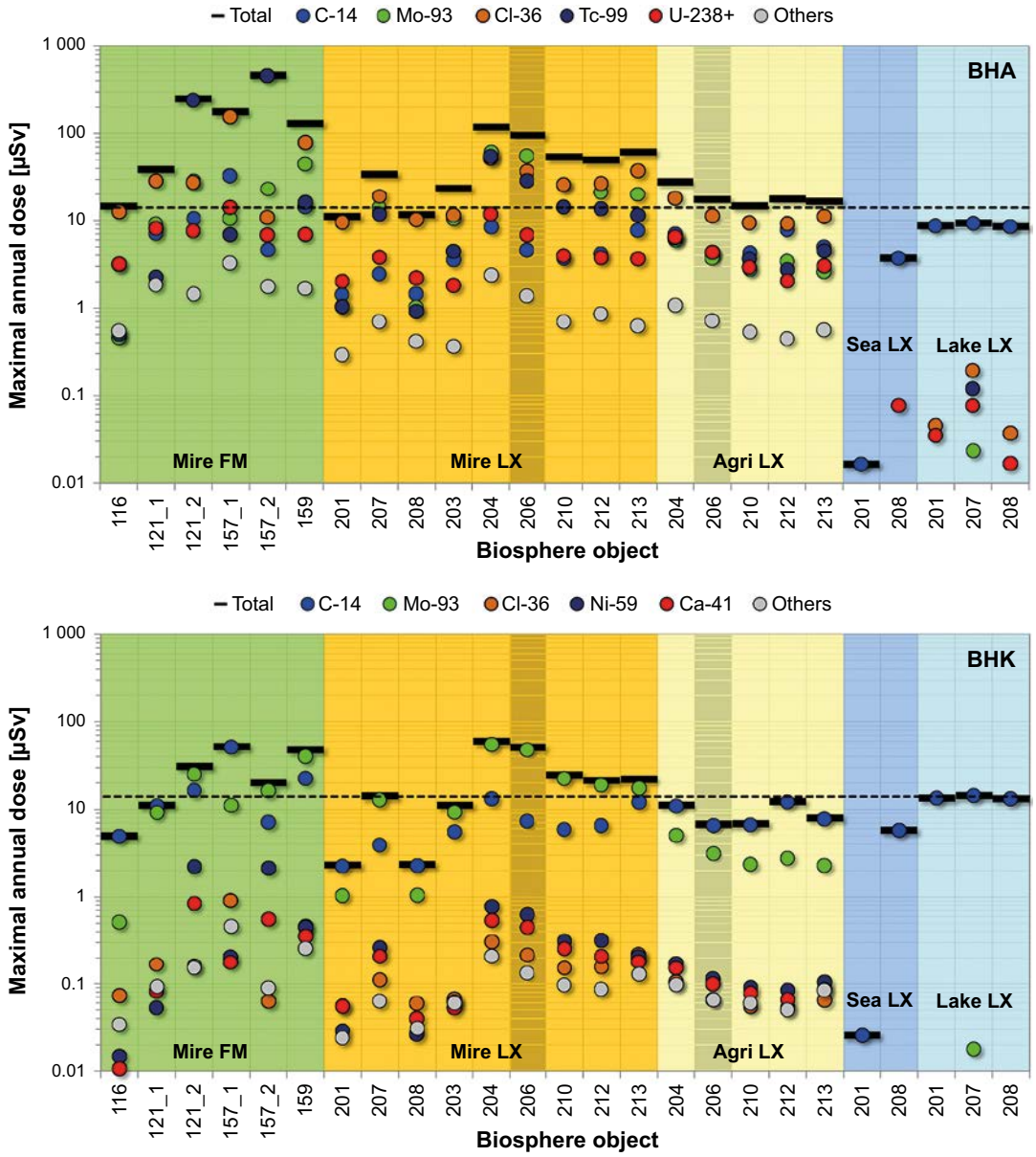

Figure 12-4. *Maximum annual doses from the most important radionuclides in Forsmark objects (green background) and Laxemar objects (all other background colours) from BHA (upper panel) and BHK (lower panel) radionuclide releases. The base case object 206 is indicated in darker shade. Time-independent mire objects in Forsmark (FM, green background) and Laxemar (LX, orange) are represented by drained mire doses including exposure from a dug well, time-independent agricultural objects (yellow) include exposure from a dug well and time-independent sea (blue) and lake (light blue) objects are represented by doses to hunters and gatherers. The dose corresponding to the regulatory risk criterion is shown with a dashed horizontal black line (14 µSv). Observe that the sum of the radionuclide-specific maximum doses can be larger than the maximum of the total dose, since the doses from individual radionuclides reach their maximum levels at different times.*

The dose-dominating radionuclides from BHA releases were Cl-36, Mo-93, Tc-99, C-14 and radionuclides in the U-238 decay chain (Figure 12-4). Cl-36 dominated the dose in most drained mires and all stationary agricultural objects. In several Laxemar mire objects, the Mo-93 dose was almost as high as the Cl-36 dose and even slightly higher in objects 204 and 206. Tc-99 was the third most important radionuclide in several Laxemar mire objects, but clearly dominated in two Forsmark mire objects (121_2 and 157_2). In static agricultural objects, Cl-36 was generally more dominant than in the mires. In aquatic objects, the dose contribution from C-14 was more than one order of magnitude larger than that from the second-most important radionuclide. The explanation is that C-14 gives a high dose from fish consumption and similar patterns were observed in the SR-PSU safety assessment (Saetre and Ekström 2016).

Drained mire doses from BHK releases were dominated by Mo-93 and C-14, and the doses from the next most important radionuclides (Cl-36, Ni-59 or Ca-41) never contributed more than 10 % to the total dose. In static agricultural systems, C-14 was the most important dose contributor followed by Mo-93, and in aquatic systems C-14 totally dominated.

12.2.5 Relationship between doses and object properties

Radionuclide classification

Radionuclides behave and respond differently to biosphere object properties due to their differences in decay and sorption properties. Non- and weakly sorbing (i.e. mobile) radionuclides with relatively slow decay rates are transported with the groundwater flow (e.g. C-14 and Cl-36), whereas sorbing radionuclides with relatively fast decay are retarded in and decay in the regolith (e.g. Ag-108m and Po-210). The lower the decay rate, the higher the sorption that is needed for a radionuclide to decay in the regolith instead of being transported through the regolith. There is an approximate sigmoidal relationship between the proportion of decay in the regolith of biosphere objects and the product of the decay rate (λ) and the distribution coefficient in the glacial clay (K_{d_GL}, i.e. in the most strongly sorbing regolith layer) as illustrated in Figure 12-5 (see Saetre and Ekström 2017b for theoretical background). Several dose-contributing radionuclides, such as Mo-93, Tc-99 and U-234, are within an intermediate group that is regulated by transport or decay, depending on the properties of the biosphere objects (indicated by the long whiskers in Figure 12-5).

Exposure pathways

Total drained-mire doses were dominated by exposure from food ingestion (77–99 % of the dose from all exposure pathways, Figure 12-6) followed by well-water exposure, whereas external exposure and inhalation contributed less than 1 % (data not shown). The doses depend on radionuclide-specific environmental activity concentrations in different media. Doses from drinking and using well water are assumed proportional to the pore water concentration in the till layer. Doses from ingestion of food, obtained through plant uptake from the drained mire, are proportional to the activity concentration in the cultivated soil. The relative doses from well water and from the cultivated soil respectively, differ between radionuclides (Figure 12-6) and are strongly influenced by their decay rates and sorption to specific regolith layers. To simplify understanding and interpretation of the relationships between doses and biosphere object properties, exposure from well water and cultivated soil respectively, are initially analysed separately for specific radionuclide groups below. The analysis of relationships between doses and object properties below was based on dose results from BHA geosphere releases, but the radionuclide specific results are general and therefore valid also for BHK releases.

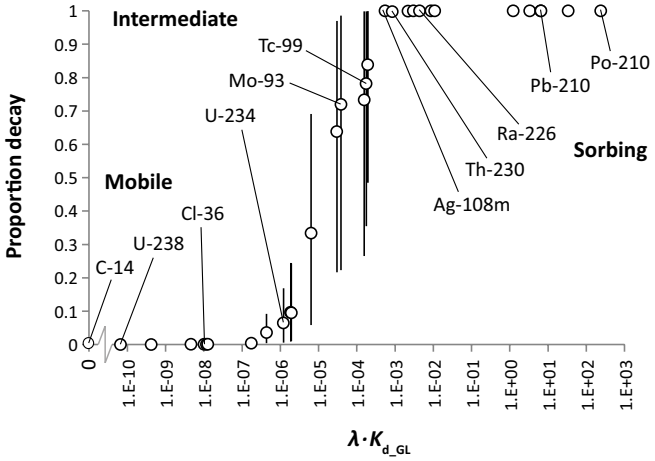

Figure 12-5. *The proportion of radioactive decay presented as a fraction of the total losses (sum of decay and transport) from biosphere objects, in relation to the product of the rate of decay (λ) and the distribution coefficient in glacial clay (K_{d_GL}). The proportion of decay was estimated from a steady state solution with a constant release rate from the geosphere into reference object 206 and the Forsmark objects for 31 radionuclides available in the release from the SFL repository. The circles are the mean proportions of decay for each radionuclide over the biosphere objects and the bars show the range between the objects with the smallest and largest proportion of decay.*

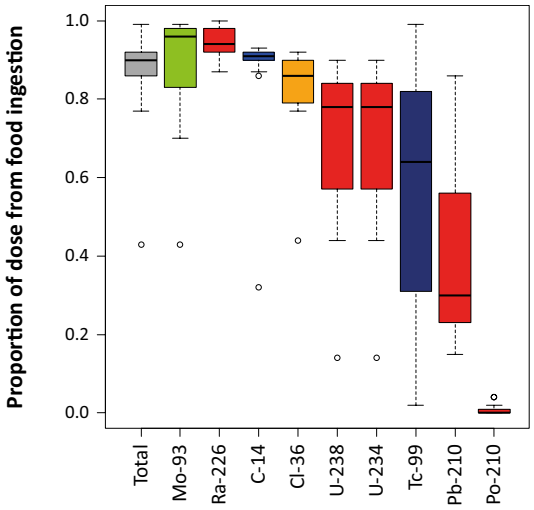

Figure 12-6. *The proportion of the total and radionuclide-specific doses from food ingestion in respect of the dose from all exposure pathways in a drained mire for BHA release. The horizontal black line shows the median, the box defines the lower and upper quartiles, and the whiskers show the minimum and maximum values over all objects analysed, except for outliers (circles).*

Well dose

A stylised model for a one-layer system (Saetre and Ekström 2017b) projects that doses from mobile radionuclides (e.g. Cl-36 and C-14) should be proportional to the inverse of the groundwater flow (volumetric flow Q [m^3 $year^{-1}$], i.e. high groundwater flows dilute mobile radionuclides resulting in lower doses. The SE-SFL BioTEx results show a strong relationship between the inverse of the upward flow of groundwater [m^3 $year^{-1}$] and the well dose from C-14 and Cl-36, explaining about 98 % of the variation (Figure 12-7). The stylised model further projects that activities and well doses of strongly sorbing radionuclides that will be retained and decay in the till will be proportional to the inverse of the volume of the till layer. That is because the radionuclide inventory gets distributed over a larger regolith volume and the BioTEx modelled variation in well doses for strongly sorbing and long-lived radionuclides such as Ra-226, Po-210 and Pb-210 between objects was almost completely explained by the inverse of the regolith volume (Figure 12-7).

The volumetric groundwater flow and the regolith volume are both functions of the object area. Therefore, the doses from both non-sorbing and more strongly sorbing radionuclides are in fact related to the inverse of the object area $1/A$ [m^{-2}]. For mobile radionuclides the remaining effect of dilution was explained by the inverse of the groundwater flux $1/q$ [year m^{-1}] and for more strongly sorbing radionuclides the dose was related to the inverse of till thickness $1/z$ [m^{-1}] (Figure 12-7).

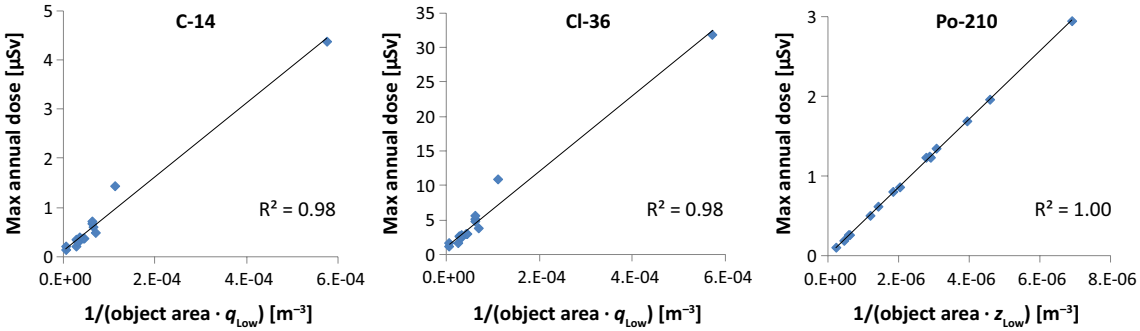

Figure 12-7. *Maximum annual doses from ingestion of well water as a function of object properties. The doses from mobile radionuclides (C-14 and Cl-36) are strongly related to the inverse of the product between the object area and the annual groundwater flux through the till (1/(object area · q_{Low}) which equals the inverse of the volumetric flow of water through till ($1/q_{Low}$). Doses from the strongly sorbing radionuclides (Po-210) are related to the inverse of the product of the object area and the till layer thickness (1/(object area · z_{Low})), which equals the inverse of the volume (or mass) of the till layer ($1/V_{Low}$).*

Dose from cultivated soil

Mobile and long-lived radionuclides are transported up through the regolith without significant losses by decay. Consequently, the activity concentrations in the upper regolith layers, from where the dose from cultivated soils originates, is regulated only by the diluting groundwater flow, as for the well dose discussed right above. C-14 is assumed not to accumulate by sorption ($K_d = 0$) in the upper regolith layers in the mire, and groundwater uptake from the saturated layer dominates the contribution to the activity concentration in the cultivated soil. There was a strong relationship between modelled C-14 doses and the inverse of the upward flow from the layer from which the groundwater uptake occurred (Figure 12-8). Cl-36 displayed a similar pattern, but in addition to the groundwater uptake from the saturated layer, the initial inventory in the drained soil also contributes to the activity in the cultivated soil ($K_d > 0$). The Cl-36 dose is thus regulated by a combination of the diluting flows in different layers so the correlation between doses and the flow in one specific layer was not as clear as for C-14 (Figure 12-8).

Strongly sorbing and short-lived radionuclides never reach the cultivated soil, except as decay products of more mobile parents in decay chains. However, radionuclides in the moderately sorbing group can contribute significantly to the total dose from cultivated soil. One example is Mo-93, for which the proportion of the geosphere release that decays in the regolith varied from 22 % to 99 % among mire objects (Figure 12-5).

Faster transport through the regolith means that a lower proportion of moderately sorbing radionuclides decays. The proportions of such radionuclides that reach the next layer are thus positively related to the upward groundwater flux (q) and negatively related to the regolith layer thickness (z) and sorption (K_d) in the layer. These relationships get stronger with higher decay rates (i.e. shorter half-lives). The proportion that reaches the uppermost layer is the product of the proportions transported through each of the underlying layers, which makes it hard to find strong correlations between activity concentrations (or doses) and object properties in one specific layer. Once released into the upper regolith, the concentrations of Mo-93 and other radionuclides in the moderately sorbing group are, within that compartment, regulated in agreement with the stylised model for one layer (Appendix C and Saetre and Ekström 2017b). That is, the activity concentration of all radionuclides should be proportional to the inverse of the object area, and while mobile radionuclides are inversely correlated to the groundwater flux in the upper layer due to dilution (comparable to the regulation of Cl-36 in the till pore water described above), the concentrations of sorbing radionuclides are correlated to the inverse of the regolith layer thickness (comparable to the regulation of Po-210 in the till discussed above). Increased deeper upward groundwater fluxes have an increasing positive effect on dose, by faster transport, whereas increased groundwater fluxes in surface layers have a decreasing negative effect on doses by dilution. Since groundwater fluxes (or flows) are correlated between layers (Appendix C), the effects of differences in groundwater fluxes could, at least partly, cancel each other out. This could be the reason why Mo-93 doses were more strongly correlated to the inverse of the product between object area and thickness of e.g. the glacial clay layer (Figure 12-8) than to relationships that include groundwater flux.

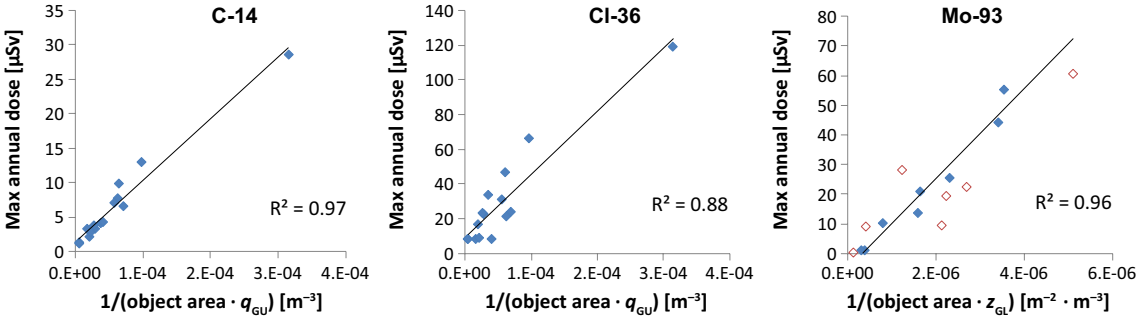

Figure 12-8. *Maximum annual doses from BHA for specific radionuclides as a linear function of object-specific properties. The doses from C-14 and Cl-36 were correlated with the inverse of the product between the object area and the annual groundwater flux in the undisturbed layer below cultivated soil (1/(object area · q_{GU})), where GU = layer of groundwater uptake), which equals the inverse of the volumetric flow through the layer (q_{GU}). The maximum annual doses from Mo-93 were correlated with the inverse of the product between the object area and the thickness of the glacial clay layer (z_{GL}), which equals the inverse of the glacial clay layer volume ($1/V_{GL}$). The unfilled red squares represent objects where accumulation in regolith layers below the peat contributed to the activity of the cultivated soil (these observations were excluded from the estimated fit).*

The activity concentration in the cultivated soil is, in turn, a function of both the accumulated initial inventory (from the preceding mire stage) in one or more of the uppermost regolith layers, depending on their thicknesses, and of the groundwater uptake from the saturated layer below the cultivated soil. Thin upper regolith layers imply groundwater uptake from a deeper and generally less diluted regolith layer, but regolith layer thickness, in combination with radionuclide-specific sorption properties in different layers, has a potentially even higher effect on doses. For example, Mo-93 sorbs strongly to peat and post-glacial sediments containing organic matter and less to minerogenic matter in deeper layers. Thin upper layers mean that the initial inventory of Mo-93 in the cultivated soil after draining could be both higher, if post-glacial sediments rich in Mo-93 are included, or lower, if glacial clay poor in Mo-93 also contribute to the cultivated soil. Therefore, the correlation was stronger between Mo-93 doses and properties in objects where only peat was included in the cultivated soils (Figure 12-8). Tc-99, on the other hand, is strongly sorbing to the glacial clay layer. Thin peat and post-glacial sediment layers mean cultivation of the glacial clay layer (Figure 12-1) and in objects 121_2 and 157_2 this results in a high initial inventory of Tc-99 in the cultivated soil after draining, and in high doses (Figure 12-4).

To summarise, there were no simple general relationships between doses from the cultivated soil and a few object properties for moderately sorbing radionuclides. This motivates the use of a relatively elaborate process-orientated radionuclide transport models, and that becomes even more important when considering decay chains. Alternatively, this behavioural uncertainty needs to be investigated and quantified, e.g. by supportive models, and then be convincingly captured by bounding cases in more simple assessment models.

For total annual doses, no simple relationships between doses and object properties are expected either, since they are a sum of exposures from the well and cultivated soil for different radionuclides that all have different responses to biosphere object properties. Nevertheless, there were some general relationships. There was a relatively strong relationship between maximum annual doses and the inverse of the object area (Figure 12-9, $R^2 = 0.67$), except for the two objects with thin upper regolith layers (121_2 and 157_2). If groundwater fluxes are not highly negatively correlated with the object area, it makes sense and it could even be argued as trivial that releases into large biosphere objects result in lower average concentrations and doses from those objects, due to higher dilution. Perhaps more surprisingly, there was an even stronger relationship between total doses and the inverse of the total regolith depth (Figure 12-9, $R^2 = 0.77$). This relationship has at least two different possible explanations. First, the thin layers in objects 121_2 and 157_2 resulted in high doses from Tc-99 due to cultivation of the glacial clay. Second, transport through thin layers is faster and concentrations and doses from the cultivated soil for radionuclides regulated by decay should therefore be higher. Although the upward groundwater flux influences the activity concentrations, the response is different for mobile and sorbing radionuclides respectively and the effect on total doses, therefore, is not obvious (Figure 12-9, R2 = 0.10). In a multiple linear regression model of the logarithms of the total doses versus the logarithms of the object properties, object area and thickness of the glacial clay layer, but not groundwater flow, were highly significant predictors, and the model explained 86 % of the variation in total doses (91 % if objects 121_2 and 157_2 were excluded).

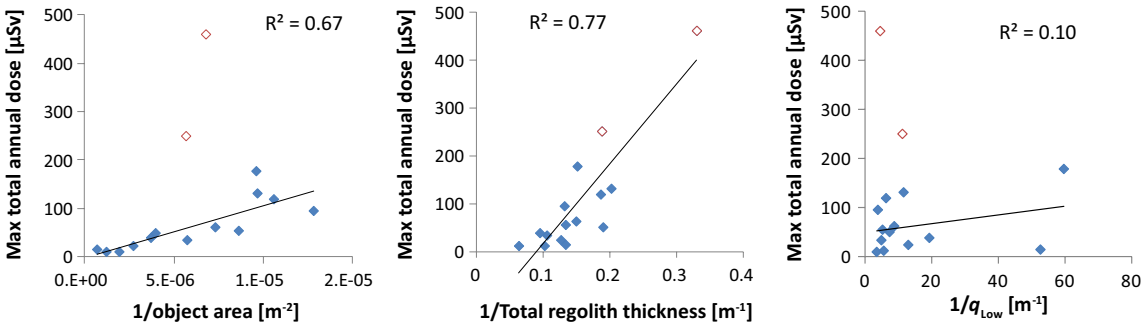

Figure 12-9. *Correlations between maximum total annual doses and the inverse of the object area, total regolith layer thickness and the upward annual groundwater flux from the till (q_{Low}). The red unfilled symbols are the total doses in object 121_2 and 157_2 with thin upper regolith layers and they are included only in the linear regression between doses and the inverse of total regolith thickness.*

12.2.6 Site selection and object characteristics

Better characterisation of the waste, well-designed repository barriers and selecting an appropriate site for SFL are all possible measures to enhance the long-term safety of the future repository. Site-selection processes have earlier focussed on finding suitable bedrock with low groundwater flows through and from the repository that provides favourable (or at least predictable) conditions for the engineered barriers and waste packages.

As shown and discussed above, the site surface characteristics in terms of ecosystem type (sea basin, lake, mire, agricultural land) and biosphere object properties (e.g. biosphere object sizes, groundwater fluxes and regolith thicknesses) influence the dose estimates. *In theory*, a repository location at a site with surface characteristics that would result in lower doses would be preferable. Doses from releases into open sea basins can be several orders of magnitude lower than corresponding releases into lakes and terrestrial ecosystems (Figures 12-3 and 12-4). Doses from drained mire systems (or from lakes if C-14 is a dominant radionuclide) are generally highest. Dose variation among drained mire objects in Laxemar and Forsmark is about 1.5 orders of magnitude (Figure 12-4), with the lowest doses in large objects with thick deep-regolith layers (e.g. thick till and glacial clay, Figures 12-7 to 12-9). Thus, sites where the geosphere release would be restricted to open sea basins or, at terrestrial sites, to large biosphere objects with thick regolith layers, would be preferable.

In practice, however, the predictability of terrestrial biosphere object characteristics at a specific site might be limited. The uncertainty with respect to the projected release area that results from flow pathways through several hundred metres of bedrock is large and hard to quantify. Besides, if doses from long-lived radionuclides in the far future could become significant, the predictability of object properties for very long time periods, including the passage of an inland ice sheet, becomes important.

Nevertheless, the large potential consequences that primarily the ecosystem type and secondarily the object properties have on doses, need to be considered in the subsequent steps of the SFL programme, i.e. site selection and safety analysis. Possible measures include cautions assumptions with respect to the properties of the discharge area, demonstration of a substantial margin to the risk-related regulatory dose limit, carefully studying current and potential future discharge areas to decrease the uncertainties, and/or actively pursuing areas with low dose consequences in the site-selection process.

12.2.7 Summary and conclusions

Since the location of the repository and the areas where groundwater from the repository will reach the surface are unknown, the *alternative discharge area evaluation case* was designed to study how total and nuclide-specific annual doses are affected by properties of the discharge area.

The maximum annual doses typically result from accumulation of radionuclides in a mire, which are subsequently exposed and mobilised by drainage and cultivation, i.e. a scenario evaluated in the base case. On the other hand, release to an open sea basin can result in doses that are several orders of magnitude lower, partly due to a reduction of the activity during slower transport through the regolith (e.g. Tc-99 and Mo-93), and partly due to dilution in the open water (all radionuclides). The doses from most radionuclides in lake ecosystems are typically lower than from terrestrial ecosystems, but the C-14 doses from lake fish consumption, in general, exceed C-14 doses from terrestrial systems. If the proportion of C-14 in the geosphere release is large enough (e.g. BHK), the exposure from a medium- and large-size relatively autotrophic lake (or a water reservoir) can yield higher total doses than from draining a mire that could have developed in the lake basin.

The total maximum annual dose from both BHA and BHK, respectively, varied by more than an order of magnitude among the drained mire objects. For BHK, the doses from C-14 and Mo-93 always contributed 90 % of the total dose or more. However, for releases from BHA, the relative contribution of individual radionuclides (e.g. Tc-99) may vary substantially from a specific object to another. In general, doses from all radionuclides were lower in large objects (c.f. object 116, 201, 208). This is because large objects typically have greater groundwater flows that result in dilution of all radionuclides, and this was especially evident for mobile radionuclides such as C-14 and Cl-36. The activity of sorbing radionuclides (e.g. Mo-93 and Tc-99) is also affected by radioactive decay, and parameters that decrease transport rates reduce the activity from the geosphere release along the upward flow pathway. Thus, there was a general trend of decreasing dose with the total depth of regolith deposits. As the groundwater flux (e.g. the area-specific discharge) affects both transport

rates and the volumetric dilution of radionuclides in the regolith, there was no coherent relationship between this quantity and the total dose. That is, whereas an increase in the groundwater flux from the bedrock may increase the activity of Mo-93 and Tc-99 that reaches regolith layers exposed by cultivation, it also dilutes radionuclides in these layers (and this is the only effect on mobile radionuclides). These general conclusions are largely in agreement with the results from the sensitivity analysis of the hydrological system (see Section 13.4), and the differences are mainly explained by correlations between properties of the objects that were not considered in the sensitivity analysis (Appendix C).

The terrestrial biosphere object (206) that was used in the base case is a mire that has developed in a small (but relatively deep) lake basin, which has a comparatively high specific discharge of groundwater from the bedrock. This configuration resulted in relatively high annual doses that were either due to exposure from Cl-36 (BHA only) and Mo-93 (first 100 000 years in BHA and BHK) or due to exposure from Tc-99 (BHA after 100 000) years. The dose from C-14 in this terrestrial object was considerably lower than in discharge areas with open lakes, but the doses from lakes were still smaller than estimated total drained-mire doses from object 206. Thus, the results indicate that using a stationary representation of the mire ecosystem in object 206 (as was done in the base case and most other evaluation cases) is a reasonable simplification of the biosphere for discharge areas in Laxemar, given the radionuclide composition and the geosphere release rates from BHA and BHK. However, with a higher proportion of C-14 in the geosphere release, doses from lake ecosystems could exceed doses from a drained mire in object 206 and should therefore be explored in future safety assessments. Furthermore, the thick layer of peat in object 206 prevented activity in the glacial clay from being exposed by drainage and cultivation. Thus, if the postulated release from BHA were to be discharged in an area with relatively thin layers of peat and post-glacial sediments overlying glacial clay, then the resulting dose from Tc-99 alone could be a factor of five larger than the total dose projected from object 206.

12.3 Alternative discharge areas with landscape development

Potentially the SFL repository could be located close to the Baltic Sea coast in an area that is influenced by shoreline displacement, resulting in landscape development from open sea basins, into coastal bays, and formation of lakes and mires. To assess the doses from SFL in such a developing landscape, three Laxemar and six Forsmark objects with landscape development were used (Figure 7-2, Section 7.3.3, Grolander and Jaeschke 2019 and Chapter 4 for details). The potential effects of shoreline migration and ecosystem succession was evaluated by comparing the resulting doses from the developing objects with doses from the corresponding time-independent biosphere objects in the *alternative discharge area case*.

The analysis of the time-independent sea bays, lakes and mires (Section 12.2) showed that the dose from C-14 releases is highest in aquatic ecosystems and results from exposure through fish consumption. Doses from other important radionuclides are highest in the drained mire, mainly through plant uptake and ingestion of food. Thus, the resulting doses during landscape development are, to a large extent, a matter of timing of the release of specific radionuclides in relation to what type of successional stage or ecosystem exists in the biosphere object.

The BHA and BHK geosphere releases of C-14 reach maximum levels relatively early during the simulation period (a few hundred years after closure and around 6000 AD, respectively; Section 11.3, Figure 11-3). In objects where the C-14 releases coincide with a sheltered sea bay or a lake stage, the doses should become close to doses from a simulated time-independent lake, but releases into exposed sea basins or mire stages should result in lower doses.

Biosphere object 201 in Laxemar was used to illustrate the temporal development of doses for an object with landscape development in relation to doses from a time-independent lake or mire object (Figure 12-10). This object has the longest aquatic state duration of all analysed objects and the maximum release of C-14 from both repositories occurs during the aquatic state. In the initial sea bay doses are slightly lower, but close to doses in the stationary lake. The minor differences are mainly explained by more dilution due to the faster water turnover in the sea basin. The slightly higher doses from the late sea stage than doses from the time-independent lake are explained by higher fish production in the sea than in the lake and a correspondingly higher consumption of fish by the most exposed group of people.

Over time, the lake area and the production of the lake decrease due to ingrowth of mire vegetation. At some point, draining and cultivating the mire will result in higher total doses than the fish consumption from the lake, and other radionuclides than only C-14 contribute to doses through plant uptake and food ingestion from cultivation. With respect to release from BHA, this point in time is when it is first possible to drain the mire. The dose increases during the early mire phase as the area of the mire expands into the lake. The relatively thin peat layers during this phase leads to cultivation of deeper soil layers, and groundwater uptake from a deeper layer with higher activity concentration results in a short period of slightly elevated doses. This explains why Cl-36 doses from BHA releases in the early developing mire initially increases and are slightly higher than the corresponding doses from the stationary mire (Figure 12-10). After the initial phase in the developing mire the doses will approach doses from the stationary mire.

With the radionuclide releases from the SFL repository, the maximum doses from biosphere objects modelled with landscape development are in general close to the doses from time-independent representations (mire or lake) of the same objects (Figure 12-11). On average, the maximum drained mire doses with landscape development were 10 % (at maximum 50 %) and 20 % (at maximum 80 %) larger than the corresponding dose from BHA and BHK releases respectively into time-independent mires. Doses to hunters and gatherers were in general lower with landscape development than in time-independent lakes, due to the mismatch of the timing between C-14 releases and a relatively enclosed aquatic system. The results indicate that using a stationary representation of the mire ecosystems (as is done in the *present day* and most *other evaluation cases*) is a reasonable and sound simplification for radionuclides for which accumulation in the mire is a primary source of exposure. However, as previously pointed out, it is important to evaluate all relevant stages of a discharge area. Excluding the possibility that the release reaches a lake (or a water reservoir) may underestimate the dose significantly at times when the contribution of C-14 dominates. If the position of the repository (or the discharge area) is influenced by shoreline displacement, the development of the object in relation to the timing of the release may influence the projected dose and shifts in the hydrological fluxes may cause transient periods of accumulation and release. Thus, irrespective of the assumptions used in the main body of calculations, it is important to evaluate the potential effects of landscape development associated with the ongoing shoreline displacement, succession of lakes and mires, as well as possible landscape development following future glaciation cycles. In *this evaluation case* the sensitivity of the results with respect to, and restricted to, the succession of biosphere objects in response to shoreline migration was examined. The effects of landscape development and long-term climate changes, including changes in bedrock groundwater flows and transient events, are explored in e.g. the *initially submerged evaluation case* (Section #12.6) and the *simplified glaciation evaluation case* (Section #12.7).

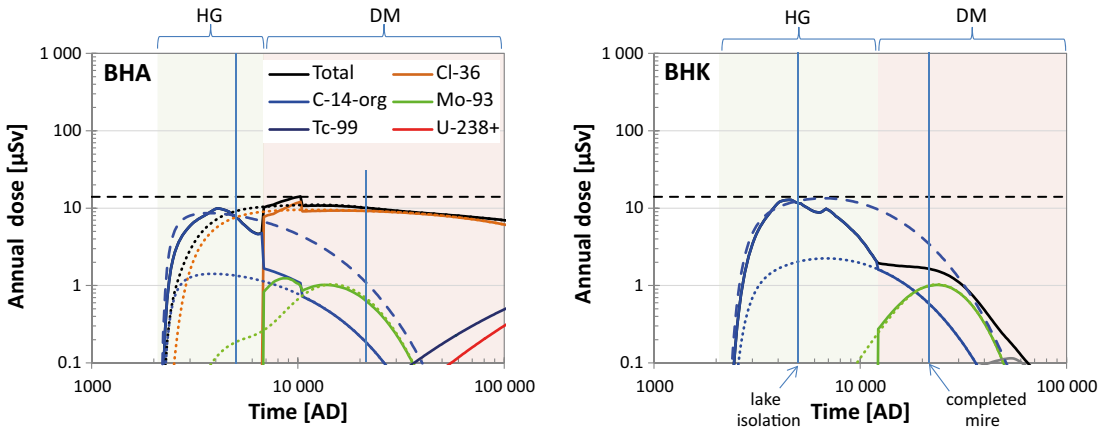

Figure 12-10. *Maximum annual total and radionuclide-specific doses from BHA and BHK releases, respectively, into biosphere object 201 with landscape development. Shoreline displacement results in a succession from a sea basin, isolation of a lake (5100 AD) and eventually development into a mire which covers the lake basin (21 100 AD). During the aquatic phase the exposure is mainly from fish consumption by hunters and gathers (HG), but as the mire expand into the lake, doses from cultivation of a drained mire (DM) becomes larger. For comparison the doses for the dominating radionuclides from a time-independent lake (dashed lines) and a time-independent mire ecosystem (dotted lines) in object 201 are shown. The black horizontal dashed line shows the dose corresponding to the regulatory risk criterion (14 µSv).*

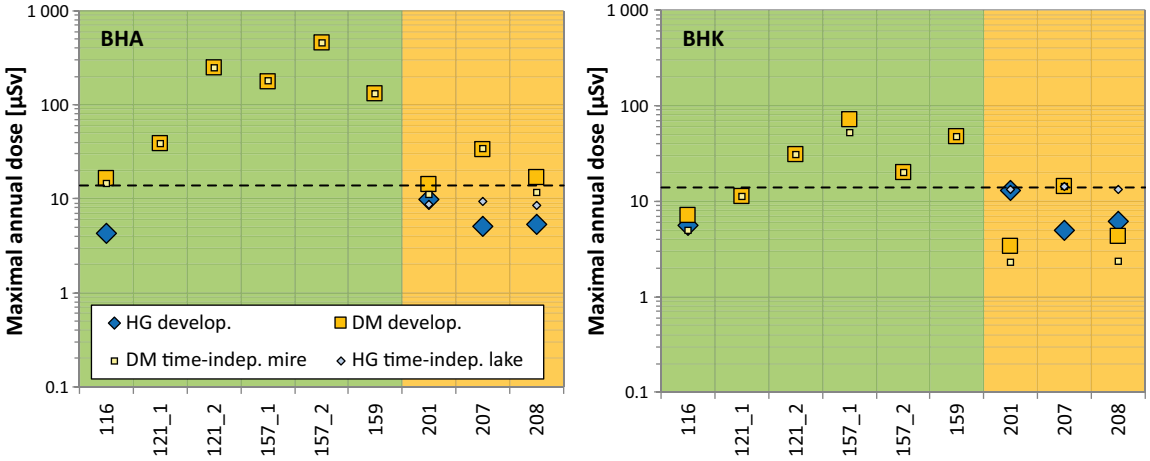

Figure 12-11. *Maximum annual doses over the entire assessment period from BHA and BHK releases, respectively, into biosphere objects in Forsmark (green background colour) and Laxemar (orange) with landscape development ("develop.", large symbols) and time-independent ("time-indep.") lake and mire objects (small symbols). The aquatic stage was short in all Forsmark objects, except in 116, resulting in low doses to hunters and gatherers (HG) and those doses are excluded from the plot. Time-independent lakes were modelled in the three Laxemar objects only. DM denotes the drained mire variant. The black horizontal dashed line shows the dose corresponding to the regulatory risk criterion (14 µSv).*

12.4 Increased greenhouse effect

The *increased greenhouse effect evaluation case* was designed to illustrate the effects of changed external conditions on post-closure safety (**Main report**). External conditions due to an increased greenhouse effect were derived from temperature and precipitation changes expected according to the IPCC's intermediate emissions scenario RCP4.5. Dose consequences of a warmer climate were evaluated in biosphere object 206, by adjusting the atmospheric concentrations of CO_2 and by modifying the discharge rates of ground and surface water. Two variants were evaluated; in the first, crop water deficit was covered by an increased uptake of groundwater through capillary rise (variant A), whereas in the second variant it was covered by irrigation with surface water (variant B, see Sections 7.4 and Grolander and Jaeschke 2019 for details).

Increased greenhouse conditions result in an increase of the maximum dose both from BHA (24 % as compared to the base case) and from BHK (11 %), when the crop-water deficit is covered by groundwater uptake. In this case as in the present-day case, the dose resulting from draining and cultivating the mire (DM) is considerably higher than that which results from continuous cultivation of the biosphere object (Agri, Figure 12-12) and, than that from all other land-use variants (data not shown). In the DM variant, cultivation is preceded by a mire stage with lower groundwater flows. If the crop water deficit during the vegetation season is covered by irrigation with surface water rather than groundwater uptake, the resulting dose is generally lower, and the lowest doses result from continuous irrigation on the continuously cultivated land (Agri). The annual dose returns to the level of the *present-day evaluation case* when the external conditions returns to those of the present day in all examined calculation variants.

The elevated maximum dose in the *increased greenhouse effect case* is primarily due to an increased accumulation of Cl-36 in peat (prior to cultivation) in combination with an increased groundwater uptake of Cl-36 during cultivation of the drained mire. For both mechanisms, it is the lower discharge in the warmer climate that leads to less groundwater dilution of Cl-36, which in turn leads to increased radionuclide concentrations in groundwater. The accumulation of Mo-93 is marginally affected by changes in groundwater flows, < 10 % increase of the annual dose. The primary source for Mo-93 in the cultivated soil is the activity accumulated in mire peat. However, the groundwater activity of Mo-93 is reduced by radioactive decay, and the reduction becomes greater with decreasing groundwater flow due to an extended transit time. Thus, the effect of a decreased dilution is partly counteracted by a decrease in the amount of the activity that reaches the peat. Consequently, the effects of a warmer climate decrease when Mo-93 contributes to the annual dose, and when Mo-93 is the dominating species, the maximum dose from increased greenhouse conditions differs little from that in present-day conditions (the DM variant for BHK in Figure 12-12).

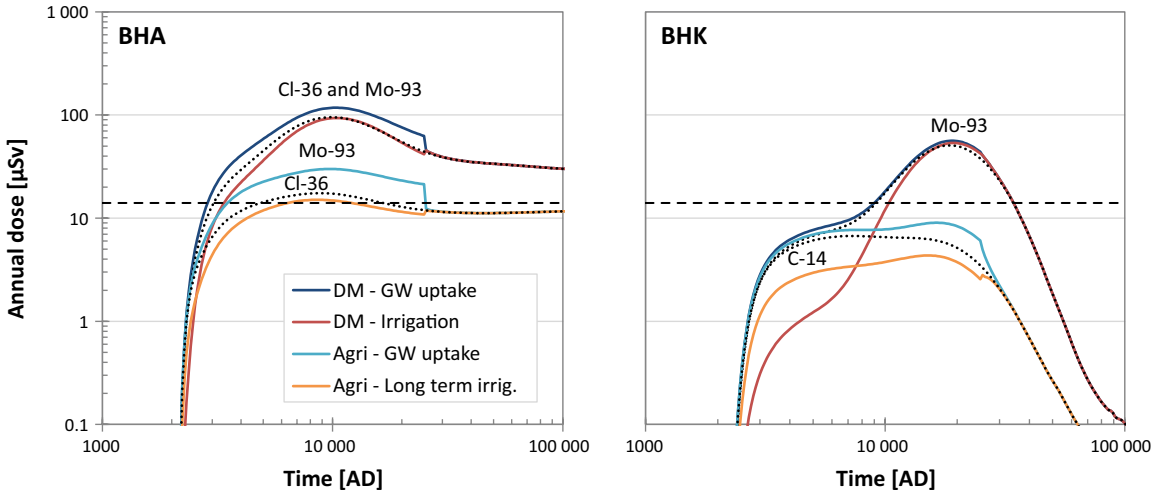

Figure 12-12. *Annual dose for release from BHA (left) and BHK (right) in the increased greenhouse effect evaluation case. Two land-use variants are examined: draining and cultivating a mire (DM) and continuous cultivation (Agri). The crop water deficit is either covered by groundwater (GW, variant A) or by irrigation (variant B). Dose in the present-day evaluation case is shown for reference (black dotted lines). Note that external conditions return to present day characteristics at 26 000 years after repository closure, and that the time axis has been truncated at 100 000 AD. Dashed horizontal black lines show the effective dose corresponding to the regulatory risk criterion (14 µSv).*

The effect of irrigation is evaluated using stream water to cover the crop water deficit. This is reasonable because stream water is generated locally and readily available in the discharge area. As stream water is diluted with the runoff generated in the catchment, the dilution is more than a factor three larger than in groundwater available for plant uptake, i.e. pore water in the saturated regolith layer below the drained soil. The effect of surface water dilution can clearly be seen when calculation variants of continuous cultivation are compared (light blue and orange lines for Agri in Figure 12-12), as accumulation in peat does not influence the results. Thus, when the plant water deficit is covered by irrigation water the annual dose is consistently clearly lower than when the deficit is covered by groundwater uptake, irrespective of which radionuclides are contributing to the dose. However, the observed dose difference is smaller than the concentration difference between surface- and groundwater because irrigation water reaches the biologically active layer directly whereas a fraction of radionuclides taken up through capillary rise will be lost through percolation and drainage before reaching the uppermost soil layer.

In SE-SFL, leaf interception also contributes to the radionuclide concentration of the irrigated crop. Approximately 6 % of radionuclides intercepted on cereal and potato leaves are translocated to edible parts, and most of the intercepted radionuclides on fodder are harvested. However, the storage capacity of leaves is limited to 1–2 mm of 45 mm irrigation water per event, and the contribution of intercepted radionuclides is negligible (< 1 %) or marginal (< 5 %) for plant concentrations of Cl-36 and Mo-93, as compared with the contribution of root uptake. For C-14 the contribution from interception is also negligible, as CO_2 in a thin water film will equilibrate with the atmosphere within minutes and the intercepted C-14 will be lost to the atmosphere (Saetre et al. 2013b).

The *increased greenhouse effect evaluation case* shows that the combination of a decrease in groundwater discharge and an increase in plant water demand may increase the annual dose from some radionuclides. However, the changes in external conditions are unlikely to result in an annual dose that is substantially higher than that calculated for present-day conditions. The largest effects may be expected for weakly sorbing radionuclides; for example, the dose from Cl-36 may be increased by 50 %. However, this is not true for C-14, since dilution caused by increased atmospheric concentrations of stable CO_2 will counteract the effect from an increased groundwater concentration. The effects of a warmer climate on radionuclides for which transport and accumulation are quantitatively affected by radioactive decay, such as Mo-93 is also expected to be less pronounced. This is because a decrease in groundwater flow will decrease the release of radionuclides discharged to upper regolith layers.

The effects of a warmer climate on radionuclide accumulation may be reversed if irrigation is assumed to cover the crop water deficit, since irrigation causes smaller crop activities compared with those resulting from plant root uptake, at least for the most dose-contributing radionuclides examined here.

12.5 Alternative regional climate

The *alternative regional climate evaluation case* illustrates to what extent the external conditions driven by the regional climate at the repository site may affect the calculated dose. External conditions are derived from temperature and precipitation regimes at three additional locations along the Swedish coast. The groundwater recharge and discharge at the surface is expected to respond to changes in climate. Thus, post-closure safety for alternative regional climates is evaluated by adjusting the groundwater flow in biosphere object 206 (Section 7.5 and Grolander and Jaeschke 2019 for details).

The *alternative regional climate evaluation case* shows that regional climate may have a limited effect on the annual dose, and that the conditions in Laxemar (low precipitation and fairly high temperature) result in slightly higher doses than wetter regional climate variants. A colder regional climate with higher precipitation is likely to result in more dilution and less accumulation of radionuclides and consequently a decrease of the maximum dose from both waste vaults is to be expected (~ 50 % reduction in dose from BHA and ~ 40 % reduction from BHK). A warmer and wetter climate (Southwest) and a somewhat colder and wetter climate (Central), are also likely to result in a reduction of the annual dose, but the reduction is more modest, i.e. approximately half of that in the Northern climate (Figure 12-13).

In all cases, the highest dose results from the land use where long-term accumulation in the mire is followed by cultivation (DM; further data not shown here), and the primary cause of the reduction in dose is an increased discharge in the mire ecosystem (Figure 12-14), which dilutes radionuclide concentrations in all regolith layers. Surface runoff (and bedrock discharge) increase with precipitation and decrease with temperature. Thus, in the Northern and Central climate variants, the changes in precipitation and temperature work in the same direction, whereas in the Southwest climate a higher annual temperature increases the evapotranspiration, which cancels out part of the effect from the increased precipitation.

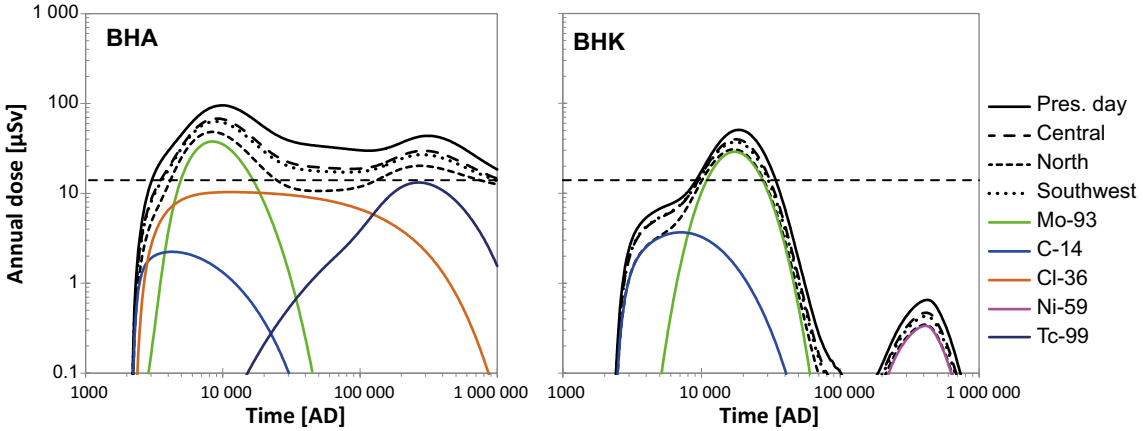

Figure 12-13. *Annual dose for release from BHA (left) and BHK (right) in the alternative regional climate evaluation case. Coloured lines represent the dose contribution from individual radionuclides for the North regional climate. The dose in the base case is shown for reference (black solid lines). Dashed horizontal black lines show the effective dose corresponding to the regulatory risk criterion (14 µSv).*

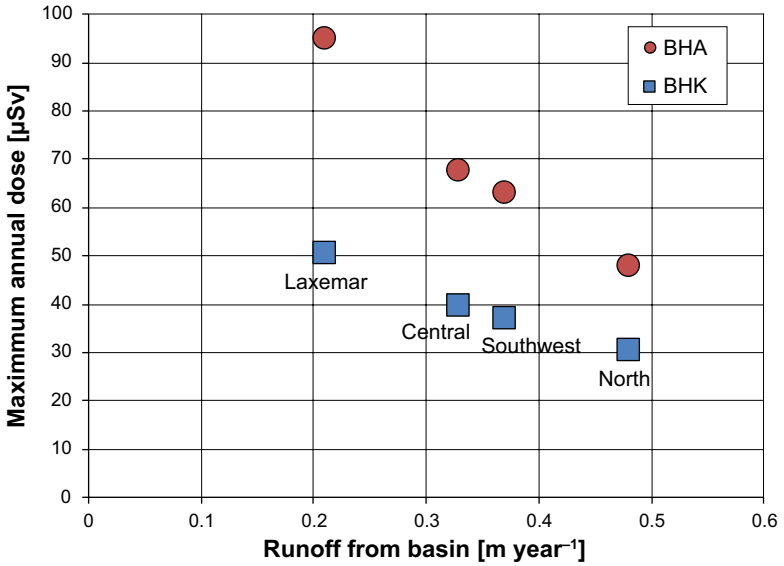

Figure 12-14. *Annual dose as a function of the runoff from the local basin for four regional climate variants. The runoff from the basin is the primary driver of the discharge in the upper part of the regolith profile (RegoPeat and RegoUp).*

Even though the relative importance of pathways and processes may vary among the climate variants, there is a tendency for a proportional reduction of the annual dose from both waste vaults with increasing discharge. Thus, on average, a doubling of the surface runoff corresponds to a 40 % reduction of the dose from BHA, and a 30 % reduction of the dose from BHK. The variation in response between the two waste vaults primarily reflects the difference in the composition of the release causing the maximum dose. The variation in response in the dose from BHA reflects the combined response of Cl-36 and Mo-93, whereas the response in dose from BHK primarily reflects variation in the accumulation of Mo-93 in peat. In the northern climate, Cl-36 doses are reduced by nearly 70 % (BHA), and both an increased dilution and a reduced groundwater uptake during cultivation contribute to the reduction. However, the reduction of the dose from Mo-93 with the northern climate is significantly weaker (30–40 %), as the effects of increased groundwater dilution are partly counterbalanced by an increased load of Mo-93 to the peat, as less activity is lost through radioactive decay when the transport rate is increased.

In this evaluation case, the extent to which variations in the regional climate have a potential to influence the annual dose from SFL has been examined. The results suggest that a climate associated with higher rates of groundwater recharge and discharge (i.e. a climate with higher precipitation and/or lower annual temperature) is likely to result in a lower annual dose than in the base case. Thus, representing the climate of a future repository with the conditions in Laxemar is a cautious assumption for present conditions compared with sites located in other parts of Sweden. However, the response to variations in regional climate is modest, but also depends on the combined effect of radionuclide composition of the release and biosphere object properties (see the *alternative discharge area evaluation case,* Section 13.2). It is unlikely that selection of a location with a favourable climate within the borders of Sweden would relevantly reduce the annual dose from SFL compared with Laxemar (the base case). Moreover, if the contribution from Mo-93 (or other radionuclides influenced by decay in the regolith) to the total dose is important, the dose reduction will be even smaller.

12.6 Initially submerged conditions

The *initially submerged conditions evaluation case* analyses the effect of locating the SFL vaults below the seabed. The groundwater flow rate is assumed to be initially lower than at present, but shoreline migration causes a transition to the present state. Low groundwater flow leads to decreased near-field and geosphere releases. Three variants are included in this evaluation case, reflecting different durations between repository closure and when the area above the repository and the discharge area

start to emerge from the sea. In the three variants, the groundwater flow starts to be influenced by the surface environment at the start of the simulations, after 5000, and after 10 000 years, respectively (see Section 7.6 and Grolander and Jaeschke 2019 for details). As in the *alternative discharge area with landscape development* (Section 12.3), the reconstructed shoreline migration is used to describe the development of the landscape. However, in this case, the geosphere release is also a function of the groundwater flow rate in the bedrock, which responds to the position of the shoreline (Section 7.3 in the **Radionuclide transport report**)

The maximum annual doses in all three variants of the *initially submerged conditions evaluation case* are lower than in the base case, and the reduction in the dose is similar for the two waste vaults (BHA, BHK). Compared with the base case, the maximum dose is approximately halved when the repository is submerged for 10 000 years (47 %, 54 %), reduced by approximately one third (37 %, 29 %) when submerged for 5000 years, and only reduced marginally (12 %, 6 %) when the discharge area is covered by 6 m water at the start of the simulations. The annual dose after 20 000 years is not noticeably affected by the length of the submerged period, and for BHA, the second maximum (at about 350 000 AD due to Tc-99) is almost as high as the first maximum in the 10 000 years submerged variant (data not shown). In the base case, the maximum dose from both waste vaults is caused to a large extent by exposure to Mo-93 (after ingestion of crops cultivated on the drained mire). This is also true for BHK in all variants of the *initially submerged conditions evaluation case*, and for BHA when submerged conditions end at repository closure. However, when BHA is submerged for 5000 years or more, the largest dose is caused by exposure to Cl-36 in the drained mire (Figure 12-15). The variations in the maximum annual dose therefore primarily reflect the reduced release of Mo-93 and C-14 from the geosphere. In BHA, this relationship is partly masked by exposure to Cl-36.

The first maximum in the annual dose curves of all variants of the *initially submerged conditions evaluation case* (Figure 12-15) reflects release to a sea basin. For BHA, the maximum is low compared with the base case, reflecting a significant reduction in the Mo-93 and C-14 releases from the geosphere, and low exposure to Cl-36 and Mo-93 from aquatic foods (due to a relatively high rate of dilution and low productivity in sea ecosystems, as compared with terrestrial cultivated ecosystems). In comparison, the first maximum from BHK in the three variants is relatively high. This reflects that the early dose from BHK is dominated by exposure to C-14. The maximum BHK release of C-14 from the geosphere is slightly higher than in the base case (data not shown), and the uptake of C-14 is more effective in aquatic than terrestrial ecosystems. Thus, the doses resulting from a C-14 release from BHK during a transitional stage exceed the C-14 dose in the base case (Figure 12-15).

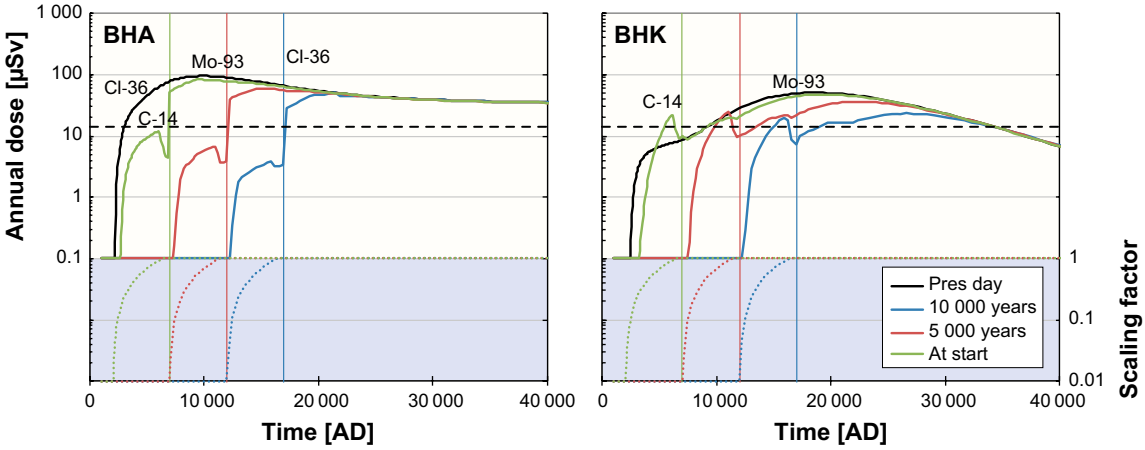

Figure 12-15. *Annual dose from BHA (left) and BHK (right) in the three variants of the initially submerged conditions evaluation case. The terrestrial landscape starts to influence flow-conditions in the waste vaults and the bedrock at the start of the simulation (green), after 5000 years (red), or after 10 000 years (blue). The annual dose in the base case is shown for reference (black line). The most dose-contributing radionuclides are indicated above the curves (early dose due to Cl-36 from BHA occurs in the base case only). Vertical lines indicate when the biosphere object is 1 m above sea level, allowing cultivation of the drained mire. Lower sub-panels show the hydrological scaling factor for the near-field and the geosphere release. Dashed horizontal black lines show the effective dose corresponding to the regulatory risk criterion (14 µSv).*

The influence of landscape development on the annual dose is evident in the shape of the dose curve. For BHA, the first maximum occurs just before lake isolation, when the water exchange rate is approaching that of the lake and the cover of mire vegetation is negligible. The decline in this initial dose maximum is primarily driven by the ingrowth of the mire. The annual dose increases by an order of magnitude when the mire can be drained. At this point, the mire area is only a few hectares, and therefore the dose continues to increase with mire ingrowth, until the mire is large enough to support the most exposed group (after a few hundred years). The influence of biosphere object development is discussed further in the *alternative discharge area case with landscape development* (Section 12.3). Over the rest of the terrestrial phase, the dynamics in dose largely reflects the dynamics in the geosphere release.

The *initially submerged conditions evaluation case* analyses the effect of locating SFL at a position that is currently below the seabed. A prolonged period of submerged conditions is likely to retard the advective transport from the repository due to low groundwater flow. The evaluation shows that the maximum release rates to the biosphere may be delayed by the duration of the submerged period, and that decay of relativiely short-lived radionuclides may reduce the maximum dose that generally occur in the terrestrial period following the sea period. As Mo-93 is a major dose-contributing radionuclide with a relatively short half-life, the maximum dose from SFL is reduced by an initially submerged period, and the size of the reduction increases with the length of the sea-covered period. However, the effect of an initially submerged period is not dramatic; the maximum dose from a repository that is submerged for 10 000 years is reduced by a factor two, as compared with release to a land location (described in the base case). It can also be noted that the reduction in dose from a near-coastal, submerged location (where the hydrology is influenced by the terrestrial landscape) is expected to be marginal (~ 10 % or less). Moreover, the C-14 dose resulting from such a repository position may even be significantly higher than from a land location, as the uptake of C-14 (per unit mass of stable carbon) is higher in aquatic plants (and food webs) than in terrestrial ecosystems.

12.7 Simplified glacial cycle

The *simplified glacial cycle evaluation case* is designed to analyse post-closure safety for the *simplified glacial cycle variant* of the SE-SFL reference evolution. This variant is included in the analysis with the aim of covering the colder end of the range within which future climate may vary. Moreover, it facilitates evaluation of the importance for post-closure safety of periglacial, glacial, and submerged conditions, and the transitions between these states. As in the *initially submerged case* (Section 12.6), the reconstructed shoreline migration is used to describe the development of the landscape and the groundwater flow rate in the bedrock (which in turn affects the geosphere release). However, in this case the geosphere release is also affected by the advance and retreat of an ice-sheet (Section 5.4 in the **Radionuclide transport report**), and the location and properties of the discharge area are a function of the climate development (see Chapter 4, Section 7.7 and Grolander and Jaeschke for details).

The annual dose in the *simplified glacial cycle evaluation case* varies as a function of the release from the geosphere, the conditions at the surface and the properties of the biosphere objects receiving the release. During temperate periods, the geosphere release and surface conditions are similar to those postulated in *the present-day evaluation case*, and conditions and doses are thus identical in the initial temperate period. Thus, during subsequent temperate periods, the annual doses to the most exposed group are similar in the two evaluation cases. For mobile radionuclides, the annual dose to the most exposed group in the simplified glacial cycle case never exceeds that resulting from constant present-day conditions (Figure 12-16). Meanwhile, the doses from sorbing and long-lived radionuclides, whose dose maxima tend to occur later in time (e.g. Tc-99 from BHA), are effectively reduced at later times in the *simplified glacial cycle evaluation case*. This is due to the re-initiation of the radionuclide inventories in the regolith layers at the end of each interglacial-glacial cycle driven by glacial erosion and flushing by glacial meltwater.

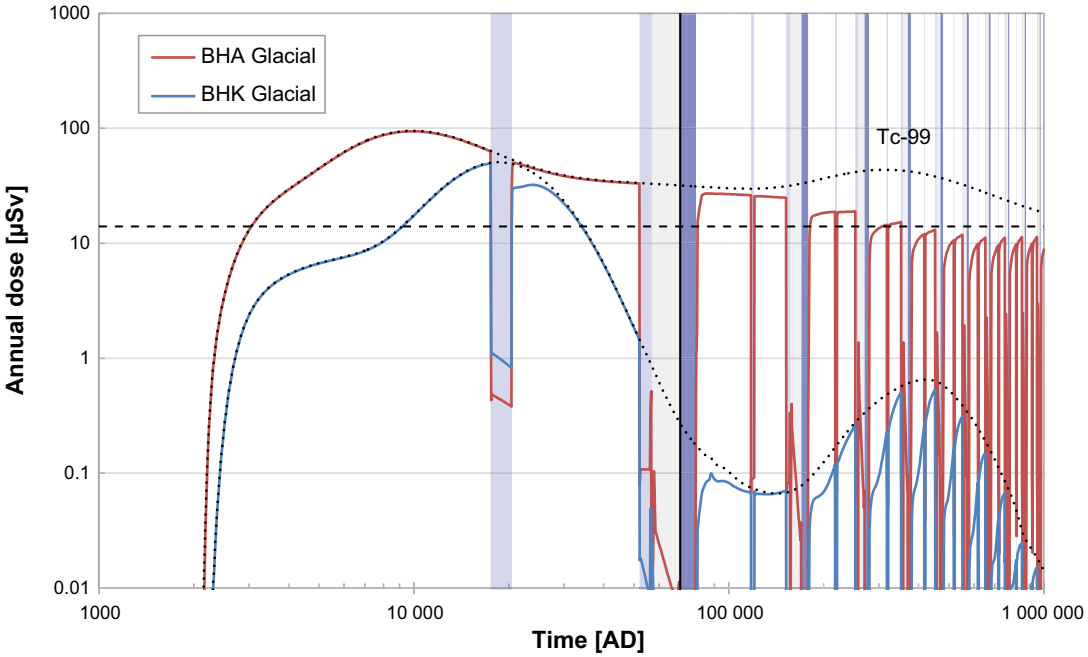

Figure 12-16. *Annual dose for release from BHA (red line) and BHK (blue line) in the simplified glacial cycle evaluation case. Doses in the present-day evaluation case are shown for reference (black dotted lines), where exposure from Tc-99 dominates the dose from BHA during the second half of the simulation time (Figure 11-3). Background colour represents climate domains, i.e. surface condition where lavender = periglacial, grey = glacial, blue=submerged, and white = temperate. The vertical black line indicates the start of the second interglacial-glacial cycle. The dashed horizontal black line shows the effective dose corresponding to the regulatory risk criterion (14 µSv).*

In the periglacial period, permafrost prevents discharge of deep groundwater and thus any release of radionuclides to the mire in object 206. The annual dose resulting from foraging the mire in cold conditions is significantly lower than in temperate conditions when the mire can be drained and cultivated, and the annual dose from the mire decreases with time, as radionuclides in the active layer are leached out (Figure 12-17). In the permafrost landscape, the release from the geosphere is instead discharged to the lake in object 207 through a talik. When permafrost conditions coincide with substantial annual releases of C-14, such as from BHK in in the first periglacial period, the dose from the lake talik may be significantly higher than the dose from foraging the mire. However, the annual dose under periglacial conditions is still an order of magnitude below that from the drained mire during temperate conditions in the first interglacial-glacial cycle, and several orders of magnitude lower in subsequent cycles.

In the glacial period, there is no exposure in the biosphere objects above the repository, as the area is covered by an inland ice sheet. Instead, consequences of a release in this period are evaluated in a semi-enclosed sea bay located somewhere in front of the ice sheet (with properties from object 208). The releases of Cl-36, Tc-99 (BHA) and Ni-59 (BHK) from the geosphere reach their maxima when the ice front is approaching and passing the repository (Figure 5-29 in the **Radionuclide transport report**). Moreover, radionuclides with a residence time in the regolith of the same order as their half-life (e.g. Mo-93) will be transported faster when groundwater flows are enhanced. This will have a dose-increasing effect to the most exposed group at the end of the second periglacial period, i.e. at the beginning of the glacial period. However, this effect is by far overshadowed by the dose-decreasing effects from elimination of exposure pathways at the surface caused by permafrost and submerged conditions, i.e. inhibition of cultivation and extraction of well water (Figures 12-16 and 12-17).

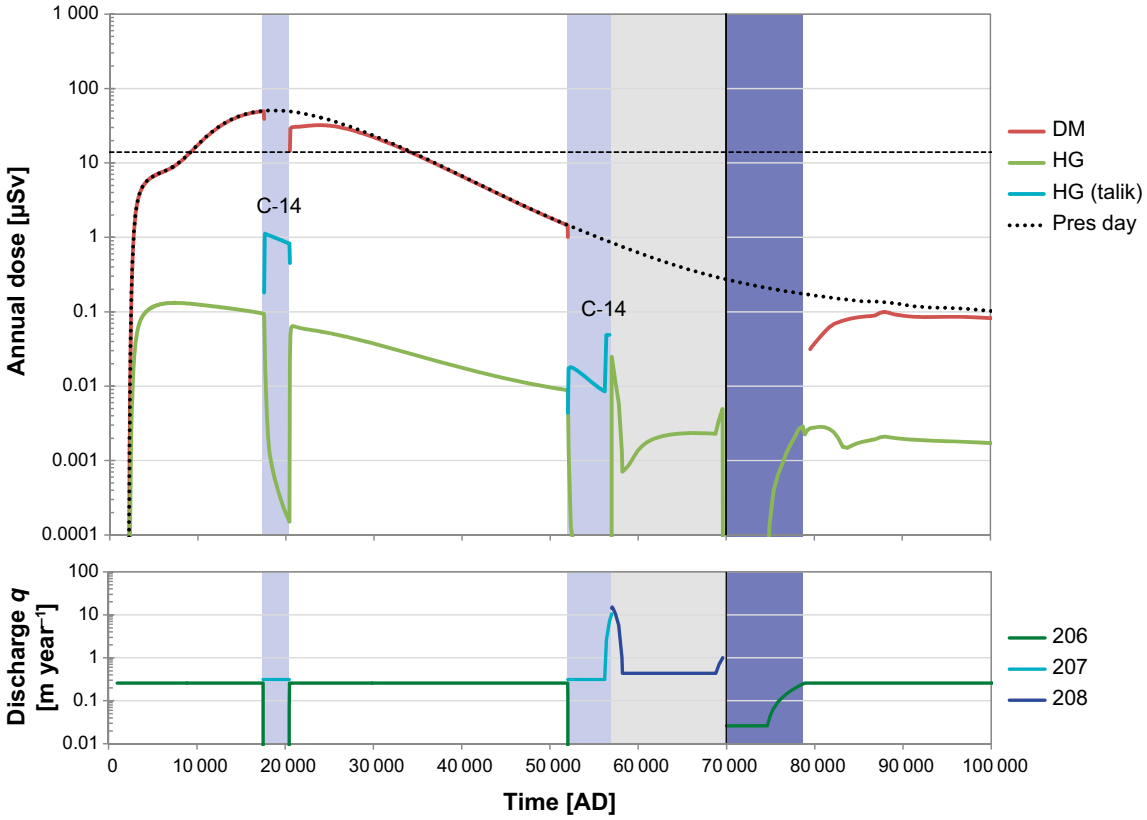

Figure 12-17. *Annual dose for release from BHK in the first interglacial-glacial cycle as a function of exposed group and biosphere object. Lines in upper panel represent the annual dose to different exposed groups; red = drained-mire farmers, olive green = hunter-gatherers, cyan = hunter-gatherers at the lake talik. The black dashed line represents the annual dose in the present-day evaluation case (drained mire farmers). Lines in the lower panel represent the groundwater flow from the bedrock to different biosphere objects; green = 206, cyan = 207 and dark blue = 208. Background colour represents climate domains, i.e. surface conditions, where lavender = periglacial, grey = glacial, blue=submerged, and white = temperate. The dashed horizontal black line shows the effective dose corresponding to the regulatory risk criterion (14 µSv). The black vertical line indicates the start of the second interglacial-glacial cycle. Note that the time scale is not logarithmic as in Figure 12-16.*

After the ice retreat, the landscape above the repository is submerged, and the regolith above the repository is assumed to have been depleted of radionuclides by glacial erosion and flushing with large volumes of glacial meltwater. In the submerged period, as in the temperate period, radionuclides are assumed to be discharged to object 206, which develops from an open sea bay towards becoming a semi-enclosed bay. The annual dose from this period increases over time as radionuclides successively build up in the regolith layers and the exchange of water with the Baltic Sea decreases because of shoreline regression. However, even at the end of this period when the bay is isolated from the sea, the annual dose from consumption of aquatic food (HG in Figure 12-17) is at least an order of magnitude below that resulting from draining and cultivating a mire ecosystem in the base case.

In the *simplified glacial cycle evaluation case*, a detailed and cyclically repeated chain of events is adopted to illustrate the release of radionuclides and dose consequences due to the passage of an inland ice sheet and to shoreline migration. Groundwater flow is changed in synchrony along the model chain and the conditions and properties of the surface system are modified according to climatic conditions and the succession of discharge areas. Although the maximum annual release of several dose-contributing radionuclides increases when the ice front passes the repository, the annual dose never exceeds the maximum levels recorded in the initial temperate period. This is because dose-contributing radionuclides like Mo-93 and C-14 have decayed significantly by the time that the ice approaches, and because the surface conditions associated with the maximum release, i.e. permafrost or submerged conditions, prevent both exposure through cultivation of mire peat, with a continuous history of radionuclide accumulation, and extraction of well water.

The results from the more detailed, and to some extent more realistic, calculations in the *simplified glacial cycle evaluation case* suggest that doses estimated with the simplifying assumptions of constant external conditions (as applied in the *present-day evaluation case*) may overestimate doses in periods with a cold climate or a submerged landscape. This is also the case for the doses from radionuclides that requires several hundreds of thousands of years to reach maximum dose rates, as repeated glaciations are expected to interrupt their accumulation in the regolith layers.

12.8 Drilled well

In this evaluation case the effect of using drinking water from a well drilled into the bedrock is analysed. Five hypothetical, 60 m deep, wells are positioned in the areas north and east of the repository, where discharge from the repository occurs. With the postulated water abstraction rate, only one of these five wells would receive radionuclides from the repository at the example site. The properties from this single well are used to assess the potential dose in this evaluation case (see Section 7.8 and **Radionuclide transport report**, Section 7.8 for more details).

The maximum annual dose from a drilled well is above 100 µSv for release from BHA (Figure 12-18). This dose level is reached about 200 000 years after the start of the assessment and the dose keeps rising continuously throughout the assessment period. Decay products from the U-238 decay chain are the main contributors to the dose from consumption of this drinking water. Of these, Ra-226 (including its two shorter-lived decay products Pb-210 and Po-210) is particularly important (Figure 12-19). After 200 000 years of the assessment, there is no activity left of the initial inventory of Ra-226 in BHA (the half-life of Ra-226 is 1600 years), and the primary source of Ra-226 is thus decay of uranium (U-238 and U-234) and thorium (Th-230) isotopes in the bentonite backfill and the bedrock matrix. In the latter half of the assessment period, almost all Ra-226 originates from U-238 deposited in the repository. In addition, Cl-36 and Tc-99 give a significant dose contribution of 10 µSv after 5000 and 100 000 years, respectively (Figure 12-18). However, as the number of people exposed to water extracted from a single drilled well is limited, the dose from Cl-36, Tc-99 and other radionuclides from BHA is at least an order of magnitude below the dose corresponding to the risk criterion for a small group (140 µSv), and the total dose from BHK is almost two orders of magnitude below this level at all times of the assessment (Figure 12-18).

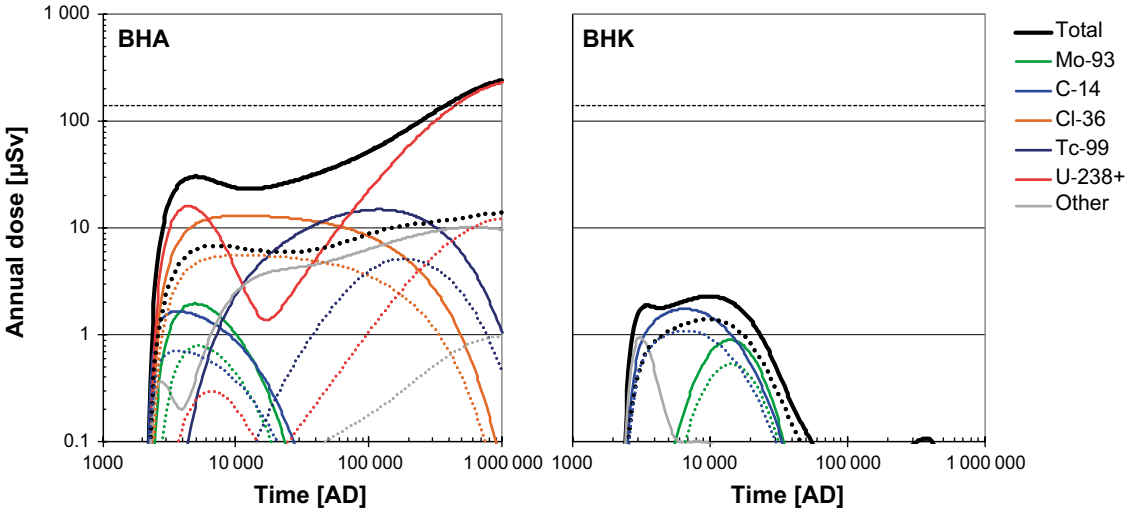

Figure 12-18. *Annual dose from BHA and BHK to a garden plot household in the drilled well evaluation case. Colours represent doses from individual radionuclides. Dotted lines represent the dose in the base case (for a garden plot household without exposure through fertilisation with ash). The dose corresponding to the regulatory risk criterion for a small group (140 µSv) is shown with a horizontal dashed black line.*

Well water is the primary environmental medium that contributes to dose in this evaluation case. Thus, a comparison of the concentrations in well water illustrates the processes that underlie the elevated dose in the drilled well, as compared with the water in a dug well used in the base cases. The dilution of the radionuclide release in the drilled well, ~ 2–3 % of the daily geosphere release in the base case diluted in 700 L of water (see Section 7.8), is about half of the dilution that occurs by discharging groundwater in the till (approximately all geosphere release diluted in the groundwater discharge from the bedrock into biosphere object 206). Thus, for radionuclides that are marginally affected by radioactive decay when transported through the till, e.g. C-14, Cl-36, and Mo-93, the concentration in water from the drilled well is twice as high as that from a dug well (horizontal line in the right-hand panel of Figure 12-19). On the other hand, the dissolved concentration of radionuclides with a relatively short half-life in relation to their times in the till (due to high decay rates and/or strong sorption), is even more reduced in the till (sloping line in Figure 12-19). This is because the water in the regolith well is assumed to be extracted from the entire till layer, and short-lived radionuclides decay before they reach the upper sections of the well.

Sorption properties (K_d values) in the regolith are typically two orders of magnitude larger than in the rock matrix, and accumulation of parent radionuclides may lead to an additional load of activity in the till. For example, Ra-226 exhibits almost five orders of magnitude greater sorption in the regolith than in the rock matrix, and consequently the concentrations of its decay products Pb-210 and Po-210 are considerably higher in the water from the dug well than expected from the geosphere release (radionuclides below the sloping line in Figure 12-19). However, despite the additional ingrowth of activity in the regolith, the water concentrations of decay products in the dug well are more than an order of magnitude below those in the drilled well. This is primarily due to stronger sorption in till than in bedrock of the decay products (about two orders of magnitude) which limits their concentrations in the lower section of the well and prevents the radionuclides from being transported to the upper sections of the well.

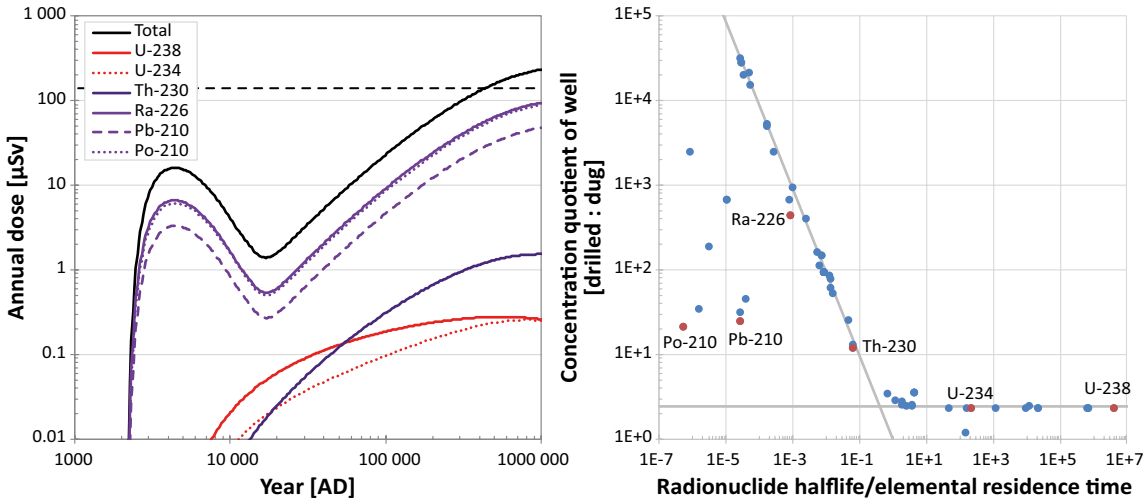

Figure 12-19. *Annual dose and relative activity concentration of well water from BHA. Left: Dose from U-238 including decay products (black line), and contributions from individual radionuclides (coloured lines, observe that Po-210 is largely covered by the Ra-226 line). Right: Quotient of activity concentration in well water extracted from a drilled (numerator) and dug (denominator) well, as a function of the ratio between half-life and transit time in till (RegoLow). Red symbols correspond to U-238 and its decay products. Note that the dose is calculated for a household utilising the well for drinking water and irrigation (GP).*

The dose from the drilled well is evaluated with a garden plot household of five members as the most exposed group. Since there are no a-priori assumptions on where the well is located apart from its feasibility to provide sufficient amounts of water, this land-use variant is not combined with exposure associated with the use of natural resources from the mire, e.g. through foraging on or draining and cultivating the mire. To assess mire land-use and drilled well doses separately is also a reasonable simplification from a radiation protection perspective in terms of the regulations. That is, if the dose assessed from the drilled well is close to the dose corresponding to the regulatory risk criteria for a small group (140 μSv), then the additional contribution from potential mire land-use will be marginal (≤ 10 %) as long as dose from this land use meets the dose level corresponding to the regular risk criterion (14 μSv). Moreover, in the present safety evaluation, ingestion of crops from the garden plot accounts for 36 % of the dose when Ra-226 and its decay products dominate the dose. This means that the contribution from garden-plot crops to dose (~ 35 μSv) is close to or even above that from ingestion of food from the drained mire in the latter part of the assessment period. It would be double counting to assume that food requirements are obtained from both these sources, so only the larger contribution should be included if these two exposure pathways were to be combined.

The annual effective dose that results from extracting water from a drilled well is above 100 μSv for release from BHA after 200 000 years of the assessment period, and the annual dose keeps rising. Ra-226 and its decay products are the main contributors to dose, and the geosphere release of Ra-226 at times beyond 20 000 AD originates from U-238 in the waste (and accumulation of uranium and thorium isotopes in the near-field and the geosphere). The primary reason for a significantly higher activity of Ra-226 in the drilled well, when compared with a dug well, is the stronger sorption and resulting reduction by radioactive decay along the transport pathway in the till (from where the dug well water is extracted). Although the annual effective dose from the drilled well is significantly higher than that from a drained mire, the number of people exposed to water extracted from a single well is limited, and the dose from BHA is in the same order of magnitude as the dose corresponding to the risk criterion for a small group (140 μSv). The dose from BHK is almost two orders of magnitude below this level.

13 Analysis of sensitivity cases

13.1 Introduction

This chapter describes results from three sensitivity cases that examine how uncertainties in the biosphere assumptions may affect environmental concentrations and potential doses. In the first section, *aged soil*, the effects of changed soil conditions (due to long-term cultivation) are examined. In the second section, the effects of *alternative K_d and CR values* are evaluated by benchmarking against a generic data set. In the last section the sensitivity to changes in landscape geometry, regolith thickness and other parameters driving *the groundwater flow* are examined. The three sensitivity cases are only evaluated in the biosphere assessment (i.e. they are not propagated to the safety evaluation). To broaden the scope of the analysis, and to simplify interpretations of results, a unit release rate was used in parallel with the reference geosphere release.

13.2 Aged soil

Cultivated soils along the valleys of Laxemar presently have a high organic content. The regolith stratigraphy suggests that these areas have gone through both a sea bay and a lake phase, before developing into mires, which were then drained. That is, remnants of peat are found in the cultivated soil, and below the drained soil there are thick layers of clay gyttja, typically with a high organic content (Sohlenius and Hedenström 2008). If cultivation were to prevail for a long period, then the organic content in these soils would be expected to decrease due to oxidation (Sohlenius et al. 2013), until most of the organic carbon content was lost. This means that the properties of the regolith profile are expected to change under the regime of continuous cultivation. In this sensitivity case, an examination is made as to what extent the potential dose to future farmers is affected by regolith conditions expected as a result of long-term cultivation.

13.2.1 Method

In the sensitivity case, the release from the geosphere is discharged into biosphere object 206, which is assumed to be drained and continuously cultivated by self-sufficient farmers (Agri). For simplicity, the thickness of the drained (and unsaturated) layer (represented by the compartments RegoUp, where root uptake occurs, and RegoSub, below root uptake) is assumed to be the same as in the present-day calculations. However, this soil layer is assumed to be depleted in organic matter. Thus, the porosity, density and degree of water saturation in the unsaturated soil layers are adjusted to reflect a cultivated soil with a low organic content (~ 6.5 %) (Table 13-1; Tables 5-9 and 5-11 in Grolander 2013) and the soil respiration is reduced (assuming no further decomposition of peat and gyttja). The sorption properties of the organic-depleted cultivated peat and clay-gyttja layer are adjusted to reflect conditions in cultivated glacial clay (Table 3-3 in Sheppard et al. 2011). The concentrations of Cl, Ca and K in the soil pore water are derived from the same soil samples as were used to characterise sorption properties (Sheppard et al. 2011). For elements that could not be detected, element analogues are used to assign K_d values (following recommendations in Tröjbom et al. 2013). Moreover, the clay-gyttja layer (RegoPG) is assumed to have been completely depleted by oxidation, and the total soil profile has subsided by 1.4 m. The thicknesses of the glacial clay and till layers are assumed to be unaffected by oxidation and compaction, but the groundwater flows in these layers are adjusted by the hydrological sub-routine to reflect the reduced regolith thickness on top of these layers. Doses (and environmental concentrations) are calculated for time-dependent releases from BHA and BHK, as well as for a unit release rate (1 Bq year^{-1}) during the assessment period.

Table 13-1. Parameter values that are changed in the aged soil calculations. The relationship between parameter values in aged and present-day soils is illustrated as ratio differences (on a logarithmic scale, ratio A:P), with orange indicating a larger value in aged soils. * = K_d values for unsaturated soil layers are changed for all elements except carbon (full data not shown).

Parameter	Unit	Aged Soils	Present day	Ratio A:P (log scale)
z_regoPG	m	0	1,4	NA
dens_regoUp	$kg_{DW}\ m^{-3}$	1564	771	
poro_regoUp	m^3	0,38	0,63	
SoilResp	$kgC\ m^{-2}\ y^{-1}$	0,59	1,46	
Conc regoUp disolv.				
Ca	$gCa\ m^{-3}$	109	46	
Cl	$gCl\ m^{-3}$	6,5	5,3	
K	$gK\ m^{-3}$	6,1	1,7	
K_d regoUp/Sub*				
Cl-36	$m^3\ kg_{DW}^{-1}$	0,007	0,021	
Mo-93	$m^3\ kg_{DW}^{-1}$	0,18	0,74	
Ni-59	$m^3\ kg_{DW}^{-1}$	1,5	0,83	
Tc-99	$m^3\ kg_{DW}^{-1}$	0,068	0,067	

13.2.2 Results

The *aged soil case* evaluates the sensitivity of calculated doses to long-term effects of cultivation of organic soils, and thus the dose is evaluated with the biosphere model for continuous cultivation (Agri). The shift in soil properties leads to a marginal decrease in the maximum dose from BHA (~ 10 %). However, the dose from BHK increases by 50 %, as compared with the dose from the corresponding land-use under present-day conditions. The higher dose from BHK reflects an increased specific activity of C-14 in soil and crop, whereas the response in dose from BHA primarily reflects a decreased dose from Cl-36 (which is partly off-set by an increased dose from C-14). However, since cultivation in the early period after draining (DM) yields an order of magnitude higher dose than continuous cultivation, the doses from the aged soils are still significantly lower than those in the present-day case (Figure 13-1).

In the calculation case, several soil properties have been adjusted to reflect expected changes in environmental conditions due to soil subsidence and the loss of soil organic matter (Table 13-1). Some of the changes in parameter values have clear effects on transport and accumulation of radionuclides. However, for C-14, which contributes most to the elevated dose observed for BHK, effects on the stable carbon cycle have a greater impact on the results. That is, although a reduced rate of degassing (due to a low porosity) leads to elevated levels of C-14 in aged soils, the concentration of stable carbon is affected in a similar way (and thus the change in degassing rate does not affect the specific activity of C-14)[33]. However, the reduced rate of soil respiration (associated with depletion of organic matter) causes a specific activity of C-14 that is more than twice as high in the pore water of aged soils as compared with the base case. This shift is propagated to an elevated C-14 concentration also in crop biomass, originating from root uptake of carbon. However, as a substantial portion of C-14 assimilation originates from fixation of atmospheric C-14 (and the specific activity in the canopy atmosphere is marginally affected by soil processes), the dose response (increase by 50 %) is less pronounced than the change in soil respiration.

Other environmental factors that influence the accumulation of radionuclides in soil, and are affected by soil ageing, include; changed sorption and a reduced regolith depth. A shift in K_d value of the unsaturated soil can explain most of the variation in the response of soil concentrations for radionuclides that contributes to dose (Figure 13-2). This is because the rate of radioactive decay is slow

[33] The specific activity is the activity concentration, in soil pore water, in canopy atmosphere or in plant tissue, divided by the concentration of the stable element in the same environmental medium. It has the unit of $Bq\ kg^{-1}$ (or mole) of the stable element.

compared with the residence time in the sub-soil for these radionuclides, and thus the soil concentration primarily becomes a function of the K_d value in the uppermost regolith layer. Two radionuclides deviate noticeably from this pattern; Cs-135 which requires more time than the assessment period to come to equilibrium in the cultivated soil, and Mo-93 which has a half-life that is relatively short compared with its residence time in several soil layers (see below).

In SE-SFL, the plant concentrations of macronutrients (i.e. Cl, Ca and K) are assumed to be regulated, and thus the concentrations of the corresponding radionuclides are calculated from the specific activity of the corresponding radionuclides in soil pore water (see Chapter 8). Thus, elevated levels of stable chloride in aged soils (Table 13-1) lead to a reduction of crop activity concentrations, and consequently the dose from Cl-36 is decreased, but just with 15 % as compared with the dose with present-day continuous cultivation of organic soils (Figures 13-1 and 13-2). The pore water concentrations of K and Ca (and the doses from ingestion of K-40 and Ca-41) appear to be more sensitive to depletion of organic matter, but the contribution of these radionuclides to the annual dose from both BHA and BHK is negligible. Due to lack of data, plant-soil concentration ratios (*CR* values) have not been differentiated between present and aged soils. Thus, changes in crop concentration (and dose from ingestion) of radionuclides which are not plant regulated simply follow the changes in soil concentrations. This approach is likely to have overestimated the sensitivity of doses to the postulated shifts in sorption, as a negative relationship between plant availability and soil retention has been observed in the measurements underlying SKB's plant and soil parameters (Sheppard et. al. 2011).

The dose from Mo-93 that results from cultivating aged soils is approximately half of that resulting from continuous cultivation in the base case (Figures 13-1 and 13-2). The difference is primarily due to a lower sorption in the aged soils (i.e. the K_d value is reduced by a factor of four). However, the activity of Mo-93 is noticeably reduced by radioactive decay along the transport pathway from the till to the unsaturated cultivated soil layer (see Section 11.5, e.g. Figure 11-9). A reduction in the regolith depth of the biosphere object shortens the transport time through the regolith profile and the absence of a clay gyttja layer decreases the accumulation and decay in the saturated regolith layers by almost two thirds, as compared with present-day conditions. Moreover, the reduced K_d value in the unsaturated soil also decreases the decay in the subsoil (RegoSub). Taken together, this leads to approximately twice as much release of Mo-93 to the upper cultivated soil layer (RegoUp), compared with present-day conditions. This explains why the Mo-93 concentrations in the upper soil layer differ less between aged and present-day soil conditions than the corresponding difference in sorption (righthand panel in Figure 13-2).

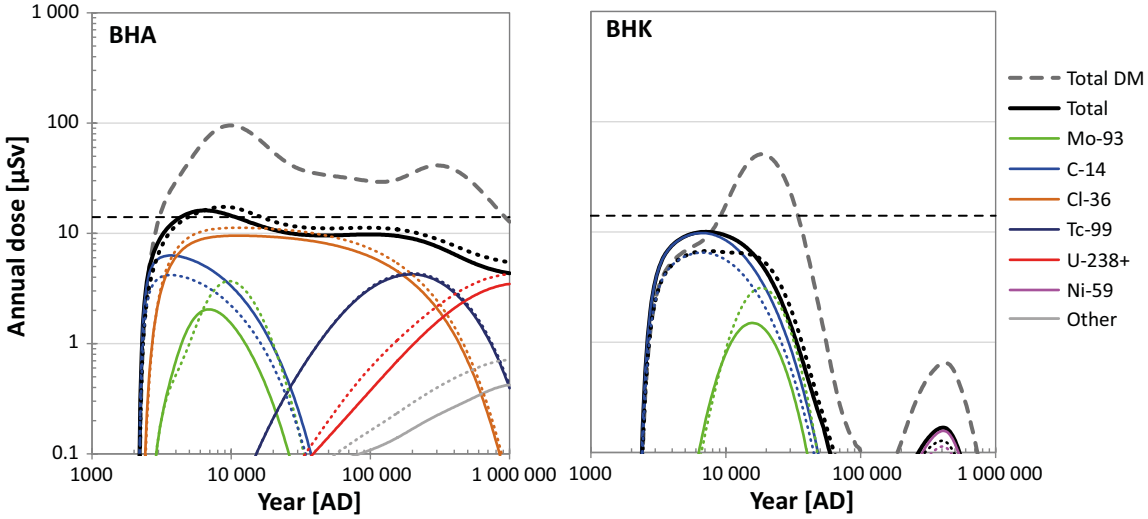

Figure 13-1. *Annual dose from BHA (left) and BHK (right) in the aged soils sensitivity case. Total dose (black lines), and doses from individual radionuclides (coloured lines), are calculated for continuous cultivation of object 206. The corresponding doses given present-day conditions are shown with dotted lines, and the total annual dose from draining and cultivating the mire is given for reference (DM, grey dashed line). The dose corresponding to the regulatory risk criteria is shown with a black dashed line (14 µSv).*

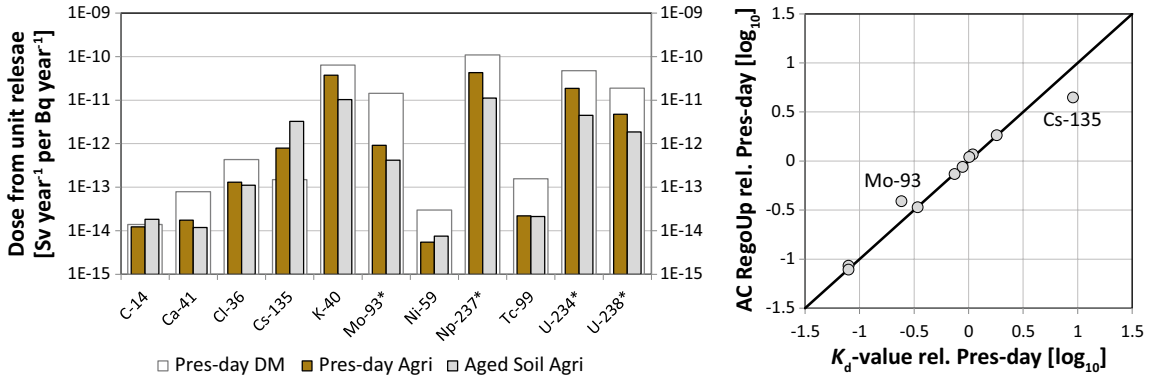

Figure 13-2. *Annual doses from, and radionuclide concentrations in, aged soils given a constant release rate of 1 Bq year^{-1} to object 206. Left) Maximum annual doses for eleven radionuclides from cultivation of aged soils (grey), as compared with doses from continuous cultivation in present-day conditions (brown). Doses from draining and cultivating a mire (DM) are given for reference (white broader bars in the background). Right) Relative radionuclide activity concentration (AC, Bq kg$_{dw}^{-1}$) in the upper cultivated regolith (RegoUp) layer (at the time of maximum dose) as a function of the relative K_d value (m^3 kg$_{dw}^{-1}$) of the unsaturated soil layers. A value of one indicates that the soil concentration (or the K_d value) is an order of magnitude larger in aged soils than in soils under present-day conditions. * = the dose includes contribution from decay products.*

13.2.3 Conclusions

Several soil properties that are expected to change in response to long-term cultivation have the potential to influence transport, accumulation and doses in the biosphere object that receives discharge from the SFL waste vaults. For example, the loss of soil organic matter is expected to decrease soil respiration, which may result in increased dose from C-14. Increased concentrations of plant macronutrients (e.g. Cl) in pore water may, on the other hand, result in decreased doses from the corresponding radionuclides. Loss of organic matter is also expected to decrease the accumulation in the upper regolith layers of most radionuclides, due to weaker sorption. Taken together, ageing of organic soils is expected to have only a limited effect on the dose from continuously cultivated soils, and no influence on the evaluation of the safety, as the dose from other land use variants considered (i.e. draining and cultivating a mire) yield significantly higher doses.

13.3 Alternative K_d and *CR* values

K_d and *CR* values are, as described in Tröjbom et al. (2013), dependent on site-specific properties. US EPA (1999) states that measured K_d values are only valid for the conditions at the sampling site. IAEA (2010) also states that K_d values derived using data from different studies should be used in screening studies only and not in specific safety assessments. For the SFL safety evaluation, the site has not been selected, but Laxemar is used as an illustrative model site. To be internally consistent, site specific K_d and *CR* values from Laxemar are used as far as possible for the base case, but SR-PSU parameter values (from Forsmark) are used if Laxemar data are missing (Grolander and Jaeschke 2019, Chapter 6).

In the *Alternative K_d and CR values sensitivity calculation case*, generic K_d and *CR* data are used instead. The generic K_d and *CR* values are based on a compilation of data from the available literature made by IAEA (2010). These IAEA data were previously used by SSM as a benchmark for the site-specific K_d and *CR* data used in SR-Site (SSM 2014) and SR-PSU (SSM 2017). The full range of the K_d values in the IAEA data set represents a wide range of geochemical conditions and can be applied to a wide variety of sites, including different climate and chemical conditions in the far future. The full ranges of the parameter distributions are too broad to be applicable at any one site, and consequently the central values (means) of the generic data set have been used. This data set is not considered to give a better representation of an unknown site in Sweden than site-specific data from e.g. Laxemar or Forsmark, but is simply an alternative representation of an unknown site. The sensitivity case is

evaluated for a drained mire and it provides a benchmark for the Laxemar (and Forsmark) specific K_d and *CR* parameters used in the base case. The results highlight some general effects of uncertainty and variation in K_d and *CR* values on resulting doses.

13.3.1 Method

Selected K_d values based on literature data

In Technical Report 472 published by IAEA (2010), K_d data from available literature studies have been compiled for many elements and characterised as applicable to various soil types. These types included three texture types for mineral soil (sand, loam, clay) and one organic soil type. When data points were few, when properties of the soil samples were not specified in the original study, or when parameter values did not differ between soil categories, K_d values were presented for aggregated soil groups only (e.g. loam+clay, mineral soil and all soils).

The regolith layers used in the radionuclide transport model in this sensitivity case were till (RegoLow), glacial clay (RegoGL), post-glacial clay-gyttja (RegoPG), reduced and oxidised peat (RegoPeat, RegoUp_ter), and the upper cultivated drained mire layer (RegoUp). These layers did not match the soil types described by IAEA, and thus the IAEA soil group that was assumed to best represent the modelled regolith layer was selected based on the organic matter and soil texture (Table 13-2). For simplicity (and lack of data) the same K_d value was used for till and glacial clay, which have little or no organic content, and for the preferred choice from the IAEA data was the K_d value for mineral soil. For post-glacial clay-gyttja K_d values for loam were used. The same K_d value was used for the three organic soils, for which the preferred choice was the value for organic soils. Element analogues were used when IAEA data were missing (Table 13-2), and these were selected according to Tröjbom et al. (2013).

Table 13-2. Choice of the IAEA soil group for the selection of K_d values for the modelled regolith layers.

	IAEA soil group used to select K_d value			
Regolith layer in the model	**First choice**	**Second choice**	**Third choice**	**Fourth choice**
RegoLow (till) RegoGL (glacial clay)	Mineral soil[1]	Clay[2]	Sand[3]	All soils[4]
RegoPG (clay gyttja)	Loam (+Clay)[5]	Loam (+Sand)[6]	All soils[7]	
RegoPeat (peat) RegoUp_ter (oxidised upper peat) RegoUp (cultivated drained peat soil)	Organic[8]	Organic (+Loam+Clay) or Organic (+Clay)[9]	All soils[10]	

[1] For Cm, Eu, Gd, La, Tb, *Ho* was used as *element analogue*, and Tc was used for Re.
[2] For Co and Ra data for *clay* were used.
[3] For Am, Cs, K, Nb, Pb, Pu, Se, Sr, and Zr data for *Sand* were used, and for Ti, *Zr* was used.
[4] For Ba, Cl, Mo, and Ni data for *All soils* were used.
[5] For Ac, Cm, Eu, Gd, Ho, La, Pa, Pd, Sm and Tb, *Am* was used as the *element analogue,* and for Ti, *Zr* was used.
[6] For Co, Ni and Re, data for *Loam* (+*Sand*) were used, and for Sr, data for *Loam+Clay+Organic* were used.
[7] For Ag, Ba, Be, Ca, Cd, Cl, I, Mo, Np, Po, Si, Sn, Tc, Th and U, data for *All soils* were used and for Re, *Tc* was used as *element analogue*.
[8] For Cm, Eu, Gd, La, Tb and Zr, *Am* was used as *element analogue, and Tc* and *Zr*, were used for Re and Ti, respectively.
[9] For Sr, data for *Organic+Loam+Clay* soils were used and for Ni data for *Organic+Clay* were used.
[10] For Ba, Cl and Mo data for *All soils* were used.

Selected CR values based on literature data

Literature values, presented in IAEA (2010), were used also for *CR* values for cereals and fodder cultivated on the drained mire in the *alternative K_d and CR sensitivity case*. IAEA presents data for various plant groups (e.g. cereals, pastures, leguminous fodder), divided into plant compartments (e.g. grains, stems and shoots, leaves, and roots) and soil types (sand, loam, clay, organic and all soils). In this study, *CR* values corresponding to *grain* were used for cereals, and values for the *stem* and *root* (of pasture) were used for fodder. In both cases, data from all soil types were used. The literature values were converted from the unit kg_{DW}per kg to kg_{DW} kg_C^{-1} by using carbon content conversion factors of 0.44 (kg_C kg_{DW}^{-1}) for cereals and 0.42 for pasture (IAEA 2010, Tröjbom et al. 2013). There were no *CR* data for Mo in fodder, and the values for leguminous fodder were used

instead (as a parameter analogue). In all other cases where IAEA data were missing, element analogues were used. Thus, the *CR* values for Ac, Eu, Gd, Ho, La, Pa, Sm and Tb were represented by the *CR* values for Am from IAEA (2010), and Ag, Pd, Re, Se and Sn were represented by Zn, Ni, Tc, Te and Th, respectively. For cereals, the *CR* value for Be was represented by the *CR* value for Sr. For fodder, Cd was represented by the *CR* value for Zn, and Th was used as an analogue for Si and Ti. Since SKB has not measured *CR* values for tubers, literature data (from IAEA 2010) were used also in the base case.

Plant uptake of C, Ca, Cl and K are not described by *CR* values in SE-SFL, and consequently plant uptake of these elements was not changed in the sensitivity calculations.

13.3.2 Results

Comparison of literature data and site-specific data

There were some general differences between the generic literature K_d and *CR* data used in this sensitivity case and the parameter values used in the base case (Table 13-3). The K_d values based on literature data were typically lower than or equal to the site-specific values (negative values in Table 13-3). The tendency for lower K_d values was particularly evident for the two mineral regolith layers; literature values in the till layer were on average more than ten times smaller than the site specific values (exceptions were Ra, U, Mo and Co) and on average more than 100 times smaller in the glacial clay. This indicates that using literature K_d values would result in less retention in the lower mineral soil compartments. The K_d values in post-glacial clay-gyttja and the organic soils (reduced, oxidised and cultivated peat) show a similar, but somewhat weaker pattern (indicated by blue colour in Table 13-3). Methodological issues may explain part of the systematic difference between literature and site-specific data. That is, SKB has used a standardised method to measure the K_d value on field samples (Sheppard et al. 2011)[34], whereas the IAEA literature compilation has been derived from both field measurements and laboratory experiments with various methods for sampling and analysis. Moreover, the pronounced difference in glacial clay is most likely due to a lack of literature data with respect to clay soils, and the literature values used for glacial clay typically reflected a larger grain size (sand, mineral soils, all soils) with significantly less surface for sorption. There was no clear general tendency in the difference between literature and site-specific *CR* values.

Doses

Total annual effective doses as well as annual doses from several radionuclides estimated with the literature based K_d and *CR* values differed from the base case (Figure 13-3). For BHA, the total annual dose peak around 10 000 AD decreased to half as an effect of substantially decreased Mo-93 doses, and instead Cl-36 became dose dominating. Similarly, the maximum total annual dose from BHK decreased by about five times due to the decrease in Mo-93 dose and became dominated by C-14. For BHA, the annual dose from Ra-226+ (i.e. including dose from its decay products Pb-210 and Po-210) dominates the total dose from about 200 000 years to the end of the simulation, and increases by approximately an order of magnitude at one million years which produces a maximum total annual effective dose larger than the maximum total effective dose in the base case.

[34] SKBs methodology is based on measurements of the indigenously sorbed elements on laboratory incubations of field samples restored to operational field capacity. Elemental concentrations of the aqueous phase are determined after one week of equilibration, followed by centrifugation to separate the liquid and solid phases, and the element concentration in the solid phase is determined after extraction with a relatively strong solvent (*aqua regia*). The method is described in Sheppard et al. (2011), and the uncertainties are estimated using the methodology discussed in Tröjbom et al. (2013). In contrast, many sorption studies, although not all, reported in the literature pertain to sorption-desorption experiments with added (radio) tracers, results of which typically depend on the equilibration time of the model system. It remains unclear which types of studies are covered by the pooled data in IAEA (2010).

Table 13-3. Comparison between the literature and site-specific K_d and *CR* values. The base-10 logarithm of the ratio between the geometric mean of the literature data and the site data shows the order of magnitude of the differences. Thus e.g. −1 or 1 means that the literature data is ten times smaller or larger respectively than the site-specific values. The intensity of the colours indicates the size of the difference between the literature data and the site-specific data, where blue symbolises a smaller literature value and yellow is a larger literature value compared to the site data. K_{d_RegoUp} and CR_{Fodder} are not shown due to their limited effect on drained mire doses. The average (last row of the table) is the arithmetic mean of the logged K_d ratios for all radionuclides in the table (i.e. the geometric mean of the non-logged K_d ratios).

	K_d				CR		K_d				CR		K_d				CR
Element	RegoLow	RegoGL	RegoPG	RegoPeat	Cereal	Element	RegoLow	RegoGL	RegoPG	RegoPeat	Cereal	Element	RegoLow	RegoGL	RegoPG	RegoPeat	Cereal
Ac	-0.9	-1.9	0.1	-0.6	-2.0	H						Ra	1.4	0.6	-0.1	-0.2	0.0
Ag	-0.9	-0.4	-1.0	0.6	2.0	Ho	-1.0	-2.1	0.2	-0.6	-1.9	Re	-4.8	-5.9	-4.2	-2.9	1.7
Am	-1.0	-2.0	0.1	-0.6	-2.0	I	-0.3	-1.5	-1.8	-1.4	-1.3	Se	-0.4	-1.2	-0.8	0.4	0.6
Ba	-2.7	-4.0	-3.7	-3.1	-2.1	K	-1.0	-2.8	-1.5	-0.5	1.8	Si	-1.6	-2.8	-1.5	-0.8	-1.5
Be	-1.1	-1.2	-0.2	0.7	1.4	La	-1.2	-2.2	0.1	-0.6	-2.0	Sm	-1.2	-2.2	0.1	-0.5	-1.9
C						Mo	0.3	-0.7	-1.9	-2.0	0.2	Sn	-1.6	-1.7	-1.2	-0.8	-0.9
Ca	-1.6	-2.1	-0.7	-0.5		Nb	-2.3	-2.9	-1.1	-0.8	0.5	Sr	-0.7	-1.5	0.1	-0.8	0.0
Cd	-1.0	-2.2	0.3	-1.4	0.9	Ni	-0.5	-1.8	-0.9	-0.4	0.6	Tb	-1.2	-2.2	0.1	-0.6	-2.0
Cl	-0.3	-1.2	-1.4	-1.9		Np	-3.1	-3.7	-2.6	-0.6	0.1	Tc	-4.8	-5.9	-4.2	-2.9	1.7
Cm	-1.2	-2.2	0.1	-0.6	-2.0	Pa	-0.9	-1.9	0.1	-0.2	-2.0	Th	-1.0	-1.6	-0.8	-0.6	-0.2
Co	0.2	-1.3	-0.3	-1.5	0.2	Pb	-1.9	-3.0	0.2	-0.8	0.6	Ti	-2.0	-3.2	0.1	0.2	-1.5
Cs	-1.4	-2.8	-2.1	-0.2	0.4	Pd	-0.8	-2.1	0.6	-0.8	0.6	U	0.9	-0.4	-1.3	-1.0	0.6
Eu	-1.2	-2.2	0.1	-0.7	-2.1	Po	-1.9	-2.8	-2.2	-0.4	-1.1	Zr	-2.0	-3.2	0.1	0.2	-1.5
Gd	-1.2	-2.2	0.1	-0.6	-2.0	Pu	-1.4	-2.4	-0.5	-1.1	-2.3	Average	-1.3	-2.2	-0.9	-0.8	-0.5

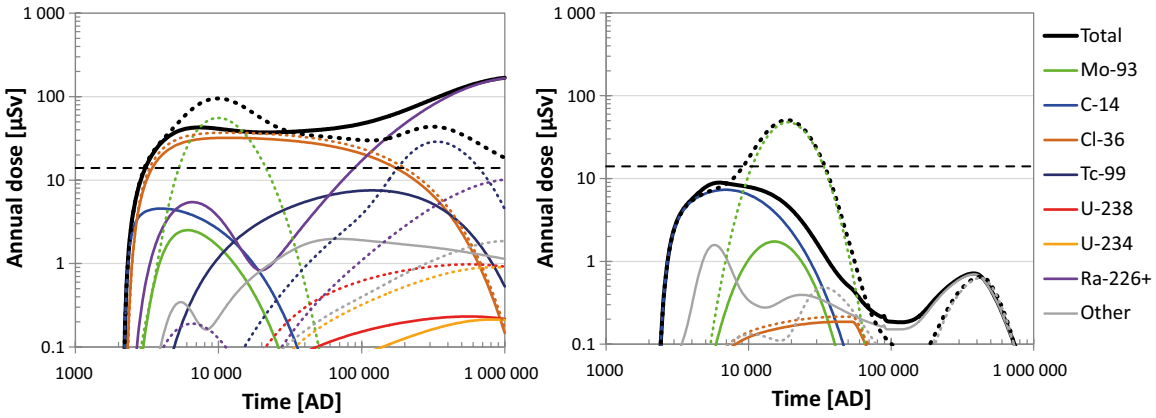

Figure 13-3. Total and the most important radionuclide specific doses (solid lines) from BHA (left panel) and BHK (right panel) estimated with the literature based K_d and CR values. Dotted lines show the corresponding doses in the base case for comparison (i.e. calculated by using site-specific K_d and CR values). Note that dose from C-14 is identical with that in the base case (as C is non-sorbing and plant uptake is not described by a CR). The black horizontal dashed lines show the dose corresponding to the regulatory risk criterion (14 µSv).

However, given the relatively strong reductions in sorption (one and two orders of magnitude on average) in the mineral regolith layers (till and glacial clay) the change in total dose to the potentially exposed group was moderate. This was partly due to the relatively high dose contribution of mobile radionuclides (C-14 and Cl-36) for which retention properties had little effect on transport (and for which *CR* values were not used to describe plant uptake). Moreover, the activities of most radionuclides that are substantially affected by retention in regolith (i.e. the ones with short half-life in relation to their residence time) are strongly reduced by decay in the near-field barriers and during the transport through the geosphere, and do not contribute significantly to the dose. Thus, the calculations indicate that uncertainties with respect to the K_d and *CR* values used in SE-SFL, in general, have a limited effect on the estimated dose from SFL. There were however, two exceptions that are discussed in the next paragraphs.

The maximum dose for Mo-93 was considerably lower with K_d values from the literature as compared with the dose in the base case. For Mo-93 the main exposure pathway was ingestion of food cultivated on the drained mire. Thus, the lower dose with generic values primarily reflected a decreased accumulation of Mo-93 in peat. The low accumulation that occurred was due to the generic K_d value assigned to peat being two orders of magnitude lower than the site-specific value. The reduced sorption in peat was partly offset by increased release of Mo-93 to peat (caused by a similar decrease of the K_d value in clay-gyttja). However, as the reduction of Mo-93 activity by radioactive decay was limited in the base case (approximately a factor of two, see Figure 11-9 in *the present-day evaluation case*) the dose reduction in the generic case was on the same order of magnitude as the reduction of the K_d value in the peat.

The dose response of Ra-226 and its decay products (Ra-226+) from drinking well water appeared to meet expectations from a general shift in K_d in the till (decrease by a factor of 10), as the dose from Ra-226+ increased by approximately a factor of 10 (Figure 13-4). However, this was a coincidence as the shifts in till K_d values of Ra-226 and its decay products did not follow the general trend. Instead the K_d value of Ra-226 in till was 30 times larger in the generic data than in the base case which resulted in significantly lower pore water concentrations of Ra-226. However, as almost no activity of Ra-226 escaped the lowest regolith layer in either of the cases, Ra-226 from the geosphere acted as a similar source for Pb-210 and Po-210 in the till layer in the base and the sensitivity case. Thus, as the till K_d values of these two decay products was a factor of 100 lower in the generic data, the water concentration and the radionuclide-specific doses increased by the same factor (Figure 13-4). Thus, it was the combined effect of these concentration shifts (weighted by the radiotoxicity of the radionuclides) that resulted in an overall increase in the maximum dose from Ra-226+ by approximately an order of magnitude.

At first appearance, the results for Mo-93 and Ra-226+ signal that there may be considerable uncertainties with respect to the dose from these radionuclides. However, a closer examination of the data reveals that a substantial part of this apparent uncertainty may in fact reflect the different nature of the two data sources. That is, SKB has empirical measurements from a wide array of relevant environmental conditions, which support strong sorption of Mo-93 in organic-rich environments. On the other hand, the generic K_d value for Mo-93 represents a small number of samples (9) from unspecified conditions ("all soils"), and the range of the IAEA data did not even nearly cover the K_d values which SKB has measured in clay-gyttja and peat samples[35]. Furthermore, SKB has also sampled till at a considerable depth, with conditions that are relevant for saturated and anoxic conditions expected for a dug well. The K_d value for Pb measured in such conditions was almost two orders of magnitude larger than the K_d value assigned from the IAEA data (representing sand, presumably in oxidised topsoil conditions). However, the reported K_d values for Pb are highly variable and the range of the IAEA data ("all soils") included the site-selected data with a broad margin. Thus, these two examples emphasise the importance of selecting parameter values reflecting the relevant environmental conditions.

[35] The maximum IAEA (2010) value is 0.13 $m^3\ kg^{-1}$ (n=9) as compared with the median values measured in clay-gyttja 3.4 (n=6), deep peat 3.9 (n=6) and surface peat 3.4 (n=5) $m^3\ kg^{-1}$ (Tröjbom et al. 2013).

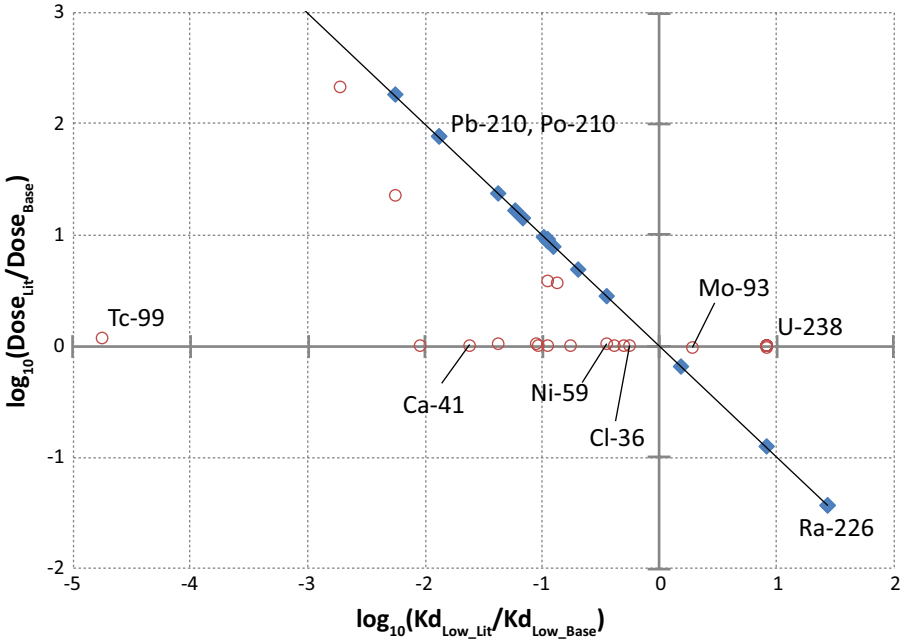

Figure 13-4. *Radionuclide-specific doses from drinking well water in response to changes in K_d values. The panel show the logarithm of the relative change in drinking well water doses as a function of the logarithm of the relative change in K_d values in the till between the alternative K_d and CR sensitivity case and the base case, respectively. The doses from drinking well water are determined by the pore water concentrations in the till (RegoLow). For a radionuclide with a long residence time in the till in relation to its half-life (due to strong sorption and/or short half-life, i.e. decay constant $\lambda \times K_d > 0.0001$, indicated by blue squares), resulting in a substantial proportion of decay in the till, the pore water concentration is inversely proportional to the K_d value. Thus, a lower K_d by a factor of ten (the $\log_{10} K_d$ ratio on the vertical axis = −1) results in a ten times higher pore water concentration and drinking water dose (the $\log_{10}$ dose ratio on the horizontal axis = 1). The results are based on unit releases from the geosphere (excluding dose contribution from decay products). Radionuclides with atomic numbers larger than uranium were excluded for clarity of presentation.*

13.3.3 Conclusions

The comparison showed that the mean values of the generic K_d values, with a few exceptions, tended to be lower than the site-specific values, and this was most pronounced in mineral regolith layers. This has been noted also in previous regulatory reviews of SKB's distribution coefficients (SSM 2014). However, the total dose to the potentially exposed group was relatively insensitive to a decreased retention in mineral regolith layers. This was partly due to the relatively high dose contribution of mobile radionuclides (C-14 and Cl-36) for which uncertainty in retention properties has little effect on transport. Besides, *CR* values were not used to describe plant uptake of those two radionuclides and therefore their doses were unaffected by the alternative dataset also in that sense. Moreover, the activity of most radionuclides that are substantially affected by retention in regolith has already been strongly reduced by decay in the near-field barriers and during transport through the geosphere due to retention also there.

However, changes or uncertainty in K_d values could be important for radionuclides that are regulated by decay in the regolith and contribute significantly to the total dose (or would contribute with lowered K_d values). Mo-93 and Ra-226 (including decay products) were identified as two such examples, but the detailed analysis revealed limitations in the generic data (in this context). That is, the IAEA data do not always span sorption properties under conditions that are relevant here (e.g. with respect to grain size, redox conditions and organic matter content). Moreover, the literature values typically reflect a wide range of frequently unspecified conditions and measurements derived with various methods. Taken together this highlights the importance of measuring not only typical parameter values for relevant conditions, but also to quantify the uncertainty in the methods used to derive these parameters from the measurements, as well as the natural variation associated with these parameters at the selected site in respect of the present and future conditions.

13.4 Alternative object geometries and groundwater flows

In SE-SFL, a new method for extracting hydrological fluxes from MIKE SHE water balances was developed (briefly mentioned in Section 8.4.2 and described in detail in Chapter 5 in Grolander and Jaeschke 2019). The method explicitly uses net precipitation from the atmosphere and discharge from the geosphere, together with object and catchment characteristics, to calculate groundwater flows, maintaining the water balance in each model compartment. In this section, the sensitivity of activity concentrations and doses to variations in parameters that drive or modify groundwater flows and to variations in regolith layer thicknesses that influence retention and decay are examined.

13.4.1 Method

The system for calculating hydrological fluxes was implemented as a subroutine within the transport model for the time-independent mire model. All parameter values were kept constant in each iteration of the sensitivity analysis, representing conditions associated with the fen stage of the mire. Excluding early successional stages (i.e. the sea and lake stages) was a reasonable model simplification, as long-term accumulation in mire ecosystems (except for C-14) resulted in the highest potential exposures of future human inhabitants (Chapter 11). Constant biosphere conditions also matched the biosphere representation of object 206 in *the present-day evaluation case*.

In the analysis, properties that influence groundwater flows were varied independently of each other in a range that spanned temperate conditions and properties of discharge areas in a broad range of locations (see below). For simplicity, uniform distributions between minimum and maximum values of parameters were used in the analysis. Thus, the net precipitation varied between 130 (increased greenhouse effects in Laxemar) and 370 mm year^{-1} (present conditions at a Northern coastal location). The dependency between net precipitation in the object and runoff from the basin was preserved by assuming a complete correlation between the two parameters. The value of runoff was thus calculated by scaling the value of the net precipitation with a fixed constant. The area-specific discharge from the bedrock was viewed as a site-specific property and its value was varied between 70 mm and 300 mm year^{-1}, representing variations between objects in Laxemar (as quantified with MIKE-SHE water balances, Chapter 5 in Grolander and Jaeschke 2019).

The area of the object, the area of the basin (excluding the area of the object), and the thicknesses of regolith layers were varied over approximately one order of magnitude (Figure 13-5). This variation was larger than found among the potential discharge areas identified in Laxemar and spanned properties of objects in the future landscape of Forsmark (SKB 2014d); including a larger mire (object 116), mires with thicker clay layers (objects 116 and 121_1) and mires with thinner regolith layers (objects 121_2 and 157_2).

The parameters for properties that describe the vertical distribution of the discharge from the catchment were derived from catchments in Laxemar (Table 5-2 in Grolander and Jaeschke 2019). The variation in these quantities was typically limited to a factor of two. As the landscape along the streams in Laxemar (where deep groundwater discharge is expected) is presently cultivated, the parameters describing percolation in mires were derived from water-balances modelled for future mires as described in SR-PSU (Section 5.6 and Table 5-3 in Grolander and Jaeschke 2019). The values of these parameters typically spanned less than a factor of two. The parameter describing how the percolation at reference depth decreases with the thickness of the glacial clay layer was an exception; this parameter was common to all examined objects, and the span of the values was nominally set to ± 10 %.

The model used in the sensitivity analysis was implemented in Ecolego. For each of the five radionuclides Cl-36, C-14, Mo-93, Ni-59 and Tc-99 the results from 1000 Monte-Carlo simulations were used in a sensitivity analysis. In each simulation, a unit release rate from the geosphere was used as the source term, and simulations were run for 10^6 years. The primary endpoints of the analysis were the pore water activity concentrations in regolith layers at the end of the simulation, approximating steady-state conditions. The results from the simulations were analysed with a multiple regression analysis approach. As most of the underlying relationships are multiplicative, the analysis was carried out on logarithms of the data[36]. The regression coefficient from the analysis is used as a sensitivity index, indicating the percentage of

[36] This means that $\log Y = \alpha + \sum \beta_i \log X_i$, where i indicates the parameters varied in the sensitivity analysis (Figure 13-5).

Parameter	Unit	Range Min	Range Max	Description
Boundary fluxes				
NetPrec	m year^{-1}	0.13	0.37	Area specific precipitation less evapotranspiration. Range from *regional climate* and *increased greenhouse effect*.
q_bedrock	m year^{-1}	0.07	0.3	Area specific discharge from bedrock. Range from Laxemar (Lx).
Surface extension				
area_obj	10^4 m^2	9	149	Size of biosphere object. Range from Lx and SR-PSU.
area_basin_c	10^4 m^2	25	868	Size of the basin, excluding the biosphere object. Range from Lx and SR-PSU.
Regolith thickness				
z_regoPeat	m	0.14	1.89	Thickness of peat at equilibrium. Range from Lx and SR-PSU.
z_regoPG	m	0.32	8.37	Thickness of post glacial sediments. Range from Lx and SR-PSU.
z_regoGL	m	0.17	3.98	Thickness of glacial cay. Range from Lx and SR-PSU.
z_regoLow	m	1.98	6.34	Thickness of till. Range from Lx and SR-PSU.
Catchent dischrage				
f_disch_stream	unitless	0	0.53	The fraction of basin runoff that is discharged directly into the stream. Range from Lx.
f_disch_surf	unitless	0.45	0.93	The fraction of the discharge from the local catchment that reaches the surface peat in the object . Range from Lx.
delta_disch	m^{-1}	0.9	1.6	The rate of changed with depth for groundwater discharge from the local catchment. Range from Lx.
Percolation				
f_surfperc_LC	unitless	0	0.5	Part of surface discharge that contribute to percolation. Range from SR-PSU mires.
f_surfperc_obj	unitless	0.45	1	Fraction of net precipitataion that infiltrates from the surface. Range from SR-PSU mires.
b_percol	m^{-1}	0.9	1.1	The rate of decrease for percolation at reference depth with thickness of the glacial clay layer. +/- 10% of common estimate from SR-PSU mires.
m_percol	m^{-1}	0.17	0.49	The rate of changed of percolation with depth below the reference level. Range from SR-PSU mires.

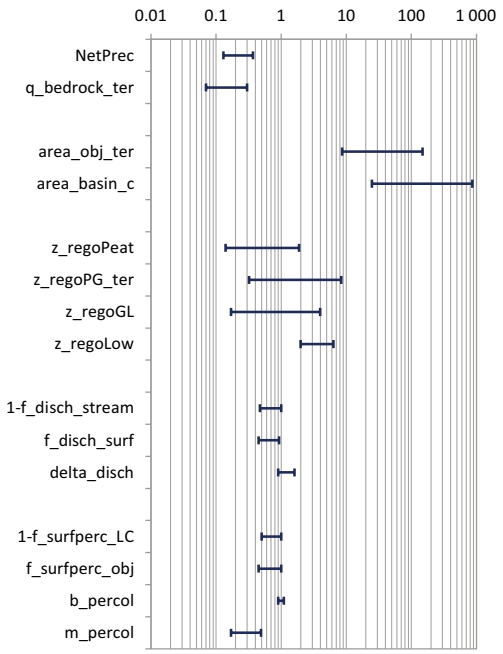

Figure 13-5. *Parameters affecting the groundwater discharge in regolith layers. Left) Description of the parameter and the range of values used in the sensitivity analysis. Right) Relative ranges of selected parameter values. Note that the scale is logarithmic, and for variables that can take a value of 0, the displayed range represents 1 less the parameter values.*

response to the percentage of change in the parameter values. To quantify the overall importance of each parameter in the context of the prescribed parameter variation, the fraction of the total variation of the response explained by variation in each parameter was also examined. In addition, the response of the annual dose to variations in net precipitation, bedrock discharge and object properties was briefly examined in a separate analysis. In this analysis the time-dependent geosphere release from BHA was used as a time-dependent source term, and sensitivity analyses were carried out for multiple points in time.

13.4.2 Results

The results section starts with a detailed analysis of the sensitivity of activity concentrations to variation in parameters that drive or modify groundwater flows and influence retention and decay. Focus is on the mechanistic understanding and the analyses of radionuclides with relatively simple behaviour (Cl-36, C-14) are followed by analyses for radionuclides with more complex behaviours, including radioactive decay (Ni-59, Tc-99 and Mo-93). At the end, the effects of the parameter variation on annual radionuclide specific doses from BHA are presented and changes in the effects of parameters on total annual doses during the simulation period in response to shifts in dose dominating radionuclides are discussed.

Chlorine sorbs weakly in regolith ($K_d < 0.03$ m^3 kg$_{DW}^{-1}$ for all layers) and Cl-36 has a long half-life compared with its residence time in the regolith (with respect to solute transport). This means that only a tiny fraction of the geosphere release (< 0.1 %) was typically lost through radioactive decay in the regolith. Consequently, the concentration gradient in the pore water (from the bedrock to the surface) primarily reflected dilution with groundwater. In the deepest regolith layers (RegoLow and RegoGL) the contribution of groundwater from the local catchment (and from precipitation) was typically insignificant, and the geosphere release was almost exclusively diluted with the groundwater from the bedrock. The rate of dilution (m^3 year^{-1}) is the product of the area of the object (area_obj, m^2) and the area-specific flux of deep groundwater (q_bedrock, m^3 m^{-2} year^{-1}, or m year^{-1}). Thus, the pore water concentration of Cl-36 in these two layers decreased in proportion to an increase in either of these two variables (as indicated by a regression coefficient of approximately −1, Figure 13-6).

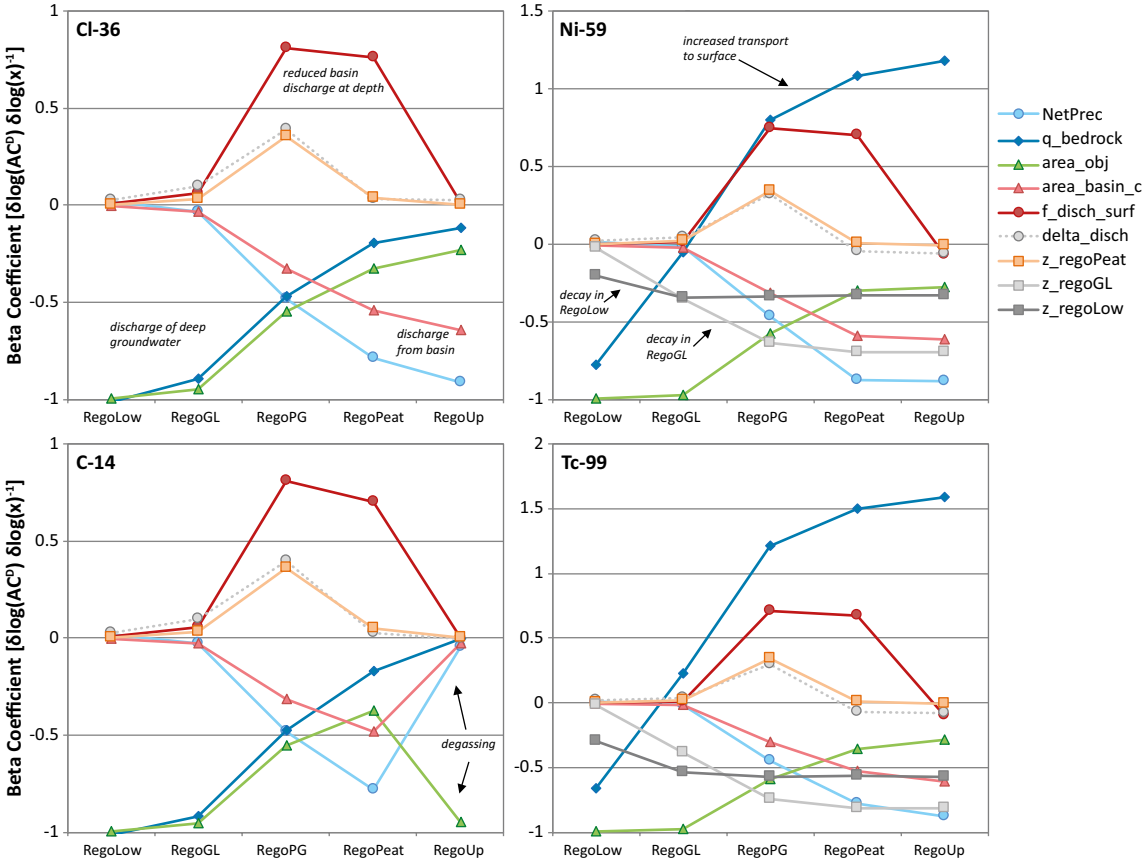

Figure 13-6. *Sensitivity of response in pore water concentration (AC^D) along a regolith profile to changes in parameter values (x). Regression (or beta) coefficients from a multiple linear regression on logarithmic scales were used as sensitivity indices. The mechanisms associated with the response are indicated with text in the figures. Dilution is the only process influencing the activity concentration of Cl-36. Degassing influences the concentration of C-14 in the surface peat (RegoUp), and radioactive decay affects the concentration of Ni-59 and Tc-99 in all layers. Beta coefficients with small influence have been excluded from the figure for clarity.*

The discharge from the local catchment (m^3 $year^{-1}$) was proportional to the area of the basin (area_basin_c, m^2), and the net precipitation (NetPrec, m $year^{-1}$), and it decreased with depth. Thus, the relative importance of deep groundwater was reduced in the upper parts of the regolith profile, whereas the opposite was true for groundwater from the local catchment (Figure 13-6). The groundwater discharge to the intermediate section of the regolith profile (i.e. to RegoPG and RegoPeat) decreased when the fraction of surface runoff increased (f_disch_surf, m^{-1}). For RegoPG, discharge was also significantly reduced with increasing steepness of the decline of discharge with depth (delta_disch, m^{-1}), and with thickness of the layer on top (z_RegoPeat, m), which buries the post-glacial sediments deeper down in the regolith profile. Consequently, the pore water concentration in RegoPG increased with the values of these parameters (Figure 13-6). The response was less than proportional, as deep groundwater and percolating meteoric water also contribute to dilution at intermediate depths. It was also noted that parameters that drive the vertical distribution of the discharge from the local catchment (light grey in Figure 13-6) do not affect the concentration in the surface peat (RegoUp). This was expected as all groundwater, irrespective of flow path, passes through the surface peat before it is discharged to the stream in the water balance model.

C-14 from the repository was assumed to reach the biosphere in the form of non-sorbing species (K_d = 0), and when it reached the surface peat it was assumed to be in the form of dissolved CO_2. As with Cl-36, only a small fraction of the geosphere release (< 1 %) was typically lost through radioactive decay in the regolith. Thus, the effects of changes in parameter values on pore water concentration of C-14 were almost identical to those of Cl-36 in all but the uppermost regolith layers (Figure 13-6). In the saturated surface peat, degassing of C-14 was a much faster process than transport with water discharging to the stream. The area of the object was the only parameter included in the analysis that affects the rate of degassing, and consequently it was the only parameter that affects the concentration of C-14 in the surface peat (RegoUp in Figure 13-6).

Ni-59 and Tc-99 both adsorb relatively strongly in most regolith layers ($K_d \sim 1$ m^3 kg$_{DW}^{-1}$), and particularly strongly in glacial clay ($K_d > 15$ m^3 kg$_{DW}^{-1}$). The elemental residence times in the lower section of the regolith profile (i.e. RegoLow and RegoGL) were typically larger than the half-life of both Ni-59 (7.6×10^4 years) and Tc-99 (2.1×10^5 years). This means that in addition to the effect of dilution, the regolith concentration of these radionuclides also depended on radioactive decay. For objects with a limited (area-specific) discharge, and/or with thick regolith layers, only small amounts of activity reached the upper part of the regolith profile. As the discharge from the bedrock (q_bedrock, m year^{-1}) drove the groundwater flux through the lower section of the regolith profile, and as the effects of radioactive decay accumulated along the flow pathway, the response to a change in this parameter was strong. From RegoGL for Tc-99 and from RegoPG for Ni-59 and upward the increased amount of activity out-weighed the effect of dilution, and the positive effect on activity concentration increased towards the surface (Figure 13-6). Thus, although the bedrock discharge contributes to dilution in the peat layer (see Cl-36 in Figure 13-6), the concentration of Ni-59 in peat increases more than proportionally with an increase in the bedrock discharge, and the response was even stronger for the concentration of Tc-99 (Figure 13-6).

The removal by radioactive decay increases with the residence time in the regolith layers, and consequently the average activity concentrations of Ni-59 and Tc-99 in RegoLow and RegoGL decreased with the thickness of the layer (Figure 13-6). Both RegoLow and RegoGL are discretised into five stacked compartments (Figure 8-1) and the effect of radioactive decay increased cumulatively along the upward flow path through these sub-layers. Thus, the effect of the till layer was preserved in the regolith profile above glacial clay (RegoPG to RegoUp). Finally, an increase of the thickness of the glacial clay layer resulted in a larger reduction of the activity concentration than a corresponding increase of the till layer. This was expected as the transport in glacial clay is more strongly retarded by sorption, and consequently the quantitative effect of radioactive decay is more important (i.e. rate limiting) in glacial clay than in till.

Mo-93 sorbed weakly in the lowest regolith layer. However, the sorption of this element increased towards the surface, and the sorption was strong ($K_d > 3$ m^3 kg$_{DW}^{-1}$) in the upper organic-rich layers (RegoPG, RegoPeat and RegoUp). The residence time associated with a regolith layer increased with sorption, bulk density and the thickness of the layer, and decreased with the (area-specific) groundwater discharge rate. Mo-93 has a relatively short half-life of 4 000 years (as compared with Ni-59 and Tc-99) and it may be affected by radioactive decay in all regolith layers with the exception of the surface peat (RegoUp). However, with the selected range of parameter values the effect of radioactive decay was typically marginal in the till (RegoLow) and glacial clay layers (RegoGL), but relatively large in both the post-glacial sediments (RegoPG) and the peat layer (RegoPeat). Thus, as with Ni-59 and Tc-99, the discharge rate from the bedrock (q_bedrock, m year^{-1}) had a clear effect on the amount of activity that reaches the upper part of the regolith profile (Figure 13-7). However, the effect of q_bedrock was considerably weaker for Mo-93 than for Ni-59 and Tc-99. This was because the contribution of the discharge from the local catchment increased and the relative contribution of bedrock discharge decreased towards the surface where the decay of Mo-93 primarily occurred.

Similarly, the importance of radioactive decay for transport and accumulation of Mo-93, can also be seen in the response of the activity concentration to changes in regolith thickness. That is, the concentration was reduced with increasing thickness of the RegoPG and RegoPeat layers, and the reduction was inherited by overlying layers (Figure 13-7). Moreover, the effect of basin discharge on dilution was partly counteracted by its effect on transport. This was evident in the reduced positive response of the Mo-93 concentration in RegoPG to increased values of parameters that reduce the discharge from the catchment to RegoPG (f_disch_surf , delta_disch and z_regoPeat) as compared with corresponding responses for other radionuclides (Figures 13-6 and 13-7).

The importance of a parameter for the uncertainty in results was determined by two factors; how strongly the parameter affects the response variable (as discussed above), and the amount of natural variation (or uncertainty) that was assigned to the parameter value. Thus, in the context of between object variability, the importance of parameters was shifted towards those that showed a large span of natural variation. This means that the area of the object, the area of the local catchment, and the thickness of regolith layers became even more important for the variations in activity concentrations (Figure 13-7, righthand panel). On the other hand, the importance of less variable parameters, such as net precipitation and bedrock discharge was downscaled, and the variation in activity concentration even became insensitive to parameters that showed limited variation between discharge areas in Laxemar, such as those describing the vertical distribution of the discharge from the basin (i.e. f_disch_surf, f_disch_stream and delta_discharge).

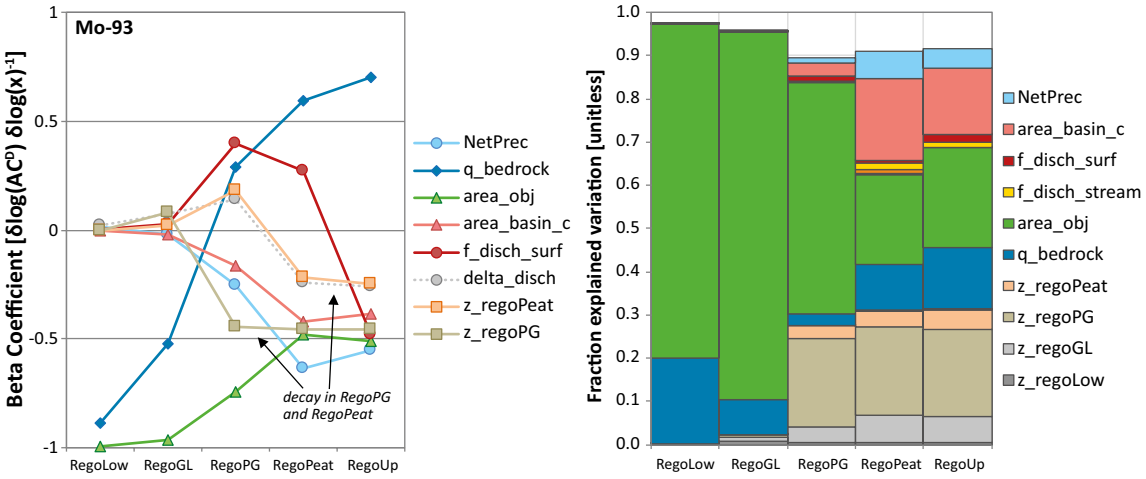

Figure 13-7. *Sensitivity of response in pore water concentration (AC^D) of Mo-93 to changes in parameter values (x) along a regolith profile. Left) Beta coefficients from a multiple linear regression on logarithmic scales were used as sensitivity indices. Mechanisms associated with the response (and not already listed in Figure 13-6) are indicated with text in the figure. Right) Fraction of response explained by the variation in individual parameters. In both figures parameters with small influence have been omitted for clarity.*

In a final step the effects of parameter variation on annual dose from BHA was examined. As in the *present-day evaluation case*, C-14 contributed to the average total dose during the first millennium of the assessment period, Cl-36 contributed significantly between 3000 and 200 000 AD, Mo-93 contributed during the time for the maximum dose (~ 10 000 AD), and the contribution from Tc-99 was most important in the period after 200 000 AD. Variation in the size of the biosphere object drove most (60–80 %) of the dose variation (or uncertainty) during the first 100 000 years of the assessment period. Object size was also important for the latter part of the assessment period, but the proportion of explained variation was reduced with time, and occasionally it accounted for less than 40 % of the dose variation. The discharge from the bedrock, the area of the basin, and the thickness of several regolith layers (RegoGL, RegoPG and RegoPeat) each accounted for a maximum of between 8 and 15 % of the variation in dose. None of the other parameters explained more than 4 % of dose variation at any time. The timing of the importance of parameters for dose was primarily driven by the geosphere release rate, and the properties of, individual radionuclides.

During the initial period of the assessment, the two mobile radionuclides C-14 and Cl-36 contributed significantly to the dose. For mobile radionuclides, uptake of groundwater from the saturated zone was an important source of activity in the cultivated soil. The drained layer typically included the peat and parts of the post-glacial sediments. The groundwater uptake was assumed to originate from the undisturbed saturated layer (typically RegoGL). In this layer, discharge of deep groundwater determined the degree of dilution. Thus, the area of the object (area_obj) and the area-specific rate of discharge (q_bedrock) explained much of the variation in dose. As the area of the object varied more than the discharge rate (Figure 13-5), the object area was the most important source of variation for dose during the first 2000 years of the assessment period (Figure 13-8). Chlorine sorbed weakly in peat and post-glacial sediments, and the importance of accumulation in these layers prior to drainage increased when Cl-36 was the main contributor to the total dose. The accumulation of Cl-36 in RegoPG and RegoPeat depended on several parameters affecting dilution (Figure 13-6). Of these, the area of the basin (area_basin_c) explained the largest amount of dose variation (Figure 13-8). This was because a large discharge from the local catchment decreased the pore water concentration in both RegoPG and RegoPeat, and because the basin area varied by more than an order of magnitude between biosphere objects (Figures 13-5 and 13-6).

Accumulation of activity in mire peat and clay gyttja was by far the most important exposure pathway from Mo-93. The amount of activity that reached regolith layers that are exposed by drainage was strongly dependent on how much of the release was lost by decay along the transport pathway. Thus, the thickness of RegoPG explained a significant part of the dose variation when Mo-93

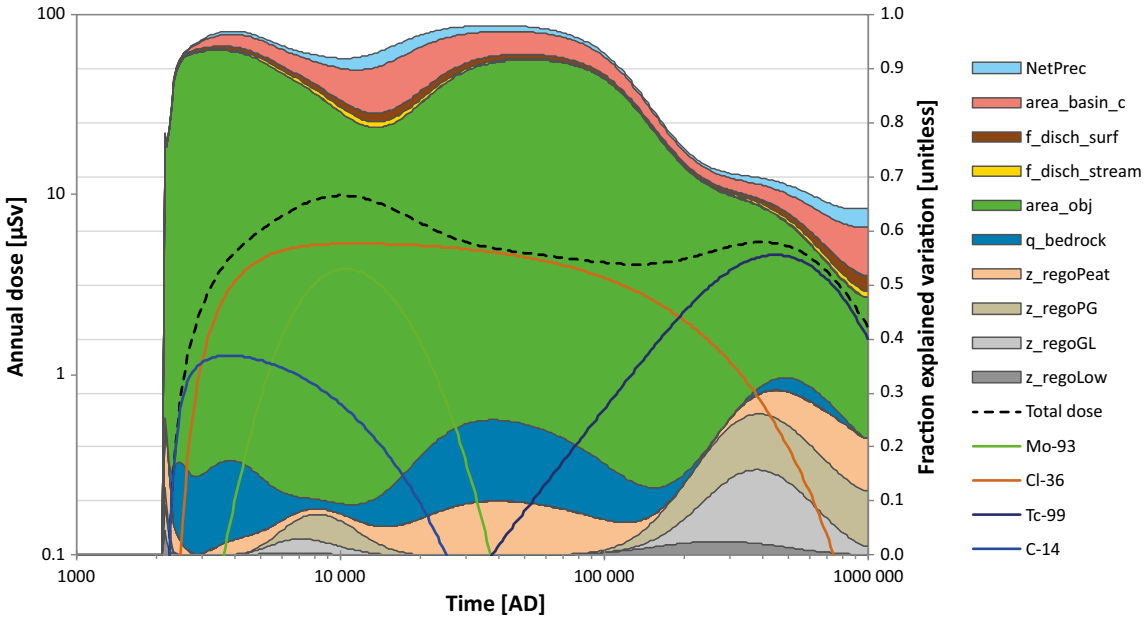

Figure 13-8. *Effects of parameter variations on annual dose resulting from a release from BHA to a mire ecosystem. The most exposed group was self-sufficient farmers draining the mire. Parameters explaining most of the dose variation are shown as coloured areas (fraction of explained variation; right axis). The mean annual dose from 1000 simulations (dashed line, left axis) is shown together with the doses from four individual radionuclides C-14 (blue), Cl-36 (orange), Mo-93 (green), and Tc-99 (dark blue).*

contributed to dose (Figure 13-7). This was because the activity in all drained regolith layers was affected by decay in RegoPG (Figure 13-7), and because the thickness of the post-glacial sediments varied considerably between objects (Figure 13-5). The importance of variables that contribute to dilution in post-glacial sediments and peat (e.g. area_basin_c, f_disch_surf) was strengthened when Mo-93 contributed to dose. However, as the bedrock discharge had opposite effects on the dose from Cl-36 (from dilution in RegoGL) and Mo-93 (increased transport to the intermediate and upper layers), the effects of differences in bedrock discharge on total dose were cancelled out (Figure-13-8). The depth of the peat layer (z_regoPeat) also affected accumulation of Mo-93 and Cl-36 in different ways (Figures 13-6 and 13-7) and thus the amount of dose variation explained by this parameter was limited when both radionuclides contribute to dose (Figure 13-8).

Accumulation in peat was also the main exposure pathway for Tc-99, at least when the activity concentration has reached steady-state levels in the upper part of the regolith profile. The steady-state activity concentration in the regolith layers that were drained and cultivated was heavily influenced by radioactive decay in the lower part of the soil horizon (Figure 13-6). Thus, the thickness of glacial clay explained a significant part of the dose variation when Tc-99 contributed to dose (Figure 13-8). This was because the activity in all drained regolith layers was affected by decay in RegoGL (Figure 13-6), and because the thickness of the glacial clay varied considerably between objects (Figure 13-5).

The amount of dose variation that could be explained by common (multiplicative) relationships decreased as the contribution of Tc-99 started to be significant, i.e. the cumulative variation explained falls below 90 %. One reason for this was that the dose-dominating pathway for Tc-99 (at a specific point in time) may vary between simulations and drinking water from a well may be the most important pathway in simulations that have not approached steady-state. As increased discharge from the bedrock dilutes the well water at the same time as it enhances release to the above regolith layers, there is no common dose response to changes in the bedrock discharge. Another reason for loss of explanatory power towards the end of the assessment period was the substantial variation in the time for peak dose from Tc-99 between the simulations.

13.4.3 Summary and conclusions

Probabilistic simulation was used to examine the sensitivity of environmental concentrations and doses to variations in parameters driving (or modifying) groundwater fluxes. In the analysis, a subroutine of the BioTEx model was used to calculate hydrological fluxes for each parameter realisation separately (n=1000) maintaining water balance in each model compartment. The results were similar to those of *the discharge area evaluation case* (Section 12.2). However, by varying object properties independently this exercise could disentangle individual effects of properties that are typically correlated in the landscape (e.g. object and basin area, and thickness of individual regolith layers).

All radionuclides were affected by dilution in a similar way. This means that the activity concentrations in the lower regolith layers decreased with object area and bedrock discharge, whereas the concentrations in the upper profile decreased with the area of the basin and the net precipitation. Sorbing radionuclides (Mo-93, Ni-59 and Tc-99) were also affected by radioactive decay, and parameters that decrease transport rates (e.g. decreased bedrock discharge and thicker regolith layers) reduced the activity from the geosphere release along the upward flow pathway. When between-object variation was accounted for, the area of the object was the property that explained most of the variation of the concentration in the lower regolith profile (RegoLow and RegoGL). The object area also explained a significant part of the variation in regolith layers closer to the surface, as did the area of the basin (for mobile radionuclides), and the thickness of the first strongly sorbing regolith layer for less mobile radionuclides (e.g. RegoGL for Tc-99 and RegoPG for Mo-93). Cultivation of mire peat was a major pathway for exposure, and consequently parameters that affected the activity concentration in the upper part of the regolith profile explained most of the variation in dose. As the relative contributions of individual radionuclides changed over time (primarily as a function of the geosphere release), so did the amount of variation explained by individual parameters. Despite these shifts, the area of the object explained a significant part of the variation of the dose from BHA at all times. It is noted that the model results were insensitive to parameters describing the percolation through the regolith profile. Parameters that control the vertical distribution of the discharge from the basin had a significant effect on environmental concentrations, but as they varied little between objects their combined effect on concentrations and doses was limited to less than 10 percent of the total variation.

14 Review of the potentially important elements Cl, Mo, Ni

One of the objectives of SE-SFL is to provide SKB with a basis for prioritizing areas in which the level of knowledge and adequacy of methods must be improved in order to perform a full safety assessment for SFL (Section 1.2). In support of this objective, two review studies were performed in parallel with the safety evaluation. These studies examine the environmental properties of three potentially important elements, namely chlorine (as chloride), molybdenum and nickel. This chapter summarizes the findings from reviews of the most recent literature, and the full versions of reviews are in progress as a part of SKBs RD&D program. If Cl-36, Mo-93 and Ni-59 are of high relevance for the radiation safety of SFL also in the next steps of the assessment cycle, the adequacy of methods used to the represent the fate of these radionuclides will be evaluated in the light of the presented process understanding (Section 17.7).

14.1 Chlorine

14.1.1 Introduction

Chlorine (Cl) is one of the 20 most common elements on earth. The inorganic form of chlorine, chloride (Cl^-), is the most common chemical species present in the environment. The anion is easily dissolved in water and is present in minerals. Chlorine in the environment has been observed not only in its inorganic form but also in organic forms (Cl_{org}); more than 5000 chlorinated organic substances have been identified (Gribble 2015). Naturally produced Cl_{org} is a diverse group, which contains simple alkane compounds, such as chloromethane (Gribble 2010), but also more complex forms as a result of, for instance, plant decay (Myneni 2002). Many of these have known anti-competitor functions, used by organisms to secure resources and as antibiotics (Winterton 2000, Öberg 2002). However, for most of the compounds, the ecological function is not known. In addition, the concentrations of observed Cl_{org} in most soils are typically as large as, or exceed, the levels of Cl^-, which indicates the likelihood of additional ecological functions for Cl_{org}. Researchers have also established that volatile chlorinated organic compounds (VOCls) are formed in soil and terrestrial ecosystems and, in particular, coastal areas, wetlands and boreal forest soils seem to produce significant amounts of chloroform (see Svensson 2019).

Work on understanding the fate of Cl compounds in the environment has mostly been concentrated on anthropogenic compounds, despite the fact that organochlorine compounds are also produced and mineralised in soils through natural processes. Studies in terrestrial environments in recent decades have revealed that chlorine is very *reactive*, contradictory to the prior view that Cl^- deposited on soil has a short residence time in soil (i.e. no interaction with soil minerals, microorganisms or vegetation), and is quickly flushed to groundwater and eventually into the oceans. It is now evident that there is ubiquitous and extensive natural chlorination of organic matter in terrestrial ecosystems. Recent experimental work with radioactive Cl-36 as a tracer has confirmed extensive natural chlorination rates corresponding to as much as 50–300 % of the annual wet deposition of Cl in several types of soils (Bastviken et al. 2009, Gustavsson et al. 2012). Moreover, natural chlorination has been experimentally confirmed at the ecosystem level in different types of forests with rapid increases in chlorinated soil organic matter (Cl_{org}) over a period of 30 years (Montelius et al. 2015). The new views of chlorine have implications for studies on Cl storage and dynamics in terrestrial ecosystems and landscapes, raising issues as to what is driving the processes and what ecological functions are involved.

In nature, Cl occurs primarily as the two stable isotopes Cl-35 (~ 76 %) and Cl-37 (~ 24 %). In addition, seven radioactive isotopes exist, of which six have half-lives of less than one hour and are of little interest with respect to Cl cycling in the environment. In contrast, Cl-36 has a half-life of 3.01×10^5 years. Cl-36 is produced by natural nuclear reactions; in the atmosphere by the spallation of argon with cosmic ray protons, and in soil and rock by neutron activation of potassium (K), calcium (Ca) and Cl (White and Broadley 2001). Cl-36 was produced in large amounts by neutron activation of seawater due to nuclear weapons testing between 1952 and 1958 (Peterson et al. 2007). These inputs of Cl-36 have been used for dating groundwater (White and Broadley 2001, Campbell et al. 2003).

Cl-36 is also produced during nuclear power reactor operation due to neutron capture by stable Cl-35 that may be present at trace levels in core materials, graphite, coolant water, and construction materials such as steel and concrete (Fréchou and Degros 2005, Hou et al. 2007). In addition, Cl-36 can be produced in considerable amounts via spallation reactions of other concrete constituents, such as K and Ca, primarily in fast reactors where high-energy particles such as fast neutrons are present (Aze et al. 2007). Although ambient Cl-36 levels typically are low, the active uptake of Cl by organisms leads to higher concentrations in plants than in the soils on which they grow (White and Broadley 2001, Kashparov et al. 2007a, b). Therefore, information about Cl cycling in soils and sediments, including bioavailability and residence times is necessary for long-term risk assessments related to handling and storage of radioactive waste (Limer et al. 2009).

Two reports have been published in SKB specifically focusing on chlorine cycling in terrestrial environments as well as volatilisation of chlorine in terrestrial ecosystems (Bastviken et al. 2013, Svensson 2019). This synthesis aims to compile the current knowledge of chlorine in terrestrial ecosystems, potentially important in the assessment of radioactive waste including Cl-36.

14.1.2 The terrestrial ecosystem

Chlorine in vegetation

Chlorine is ubiquitous in plant biomass, but the concentrations vary greatly within and between different parts of plants, among species, and between ecosystems (Table 14-1). The inorganic form of chlorine, Cl^-, is essential for plants and has a direct role in photosynthesis, is important in osmotic adjustment of the plant, and plays an essential role in stomatal regulation (White and Broadley 2001). The need, indicated by that the plant does not show deficiency symptoms, has been estimated to 100 μg g_{DW}^{-1} (Marschner 2012). Although Cl^- dominates in plants, over 130 chlorinated organic compounds have been isolated from higher plants (Engvild 1986, Gribble 2010). For example, a Cl_{org}-containing plant growth hormone is produced in plants such as peas, lentils, vetch, and fava beans (Gribble 1998), and the Japanese lily produces several Cl_{org} fungicides to protect itself from pathogenic fungi (Monde et al. 1998).

There is considerable variation in the ability of plants to accumulate Cl^- depending on the type of plant and where it grows (White and Broadley 2001). Plants can take up nutrients by active (metabolic) or passive processes (non-metabolic). Specific inorganic ion uptake by means of electrochemical gradients, ion pumping, and uptake through ion channels are examples of such active uptake. Active uptake by roots is assumed to predominate at low Cl^- concentrations, in contrast to saline conditions where passive uptake is thought to dominate (White and Broadley 2001). Ions can be absorbed over the whole plant for submerged plants and non-vascular plants (bryophytes). For most vascular plants, ion uptake is largely by the roots, where ions are absorbed from the soil solution. Cl uptake from soil is generally considered to be of the inorganic form. Some uptake can be through foliage, where Cl^- in rainwater is absorbed. This route has been suggested for Cl in some agricultural plants (Henner et al. 2013, Hurtevent et al. 2013). However, the major part of vegetation uptake is by moving Cl^- through the root and into the xylem and further to the shoot, where it accumulates or is redistributed throughout the plant via the phloem (Atwell et al. 1999, MacAdam 2009). Movement of chlorine within the plant (translocation) has been shown to be very efficient for Cl^-, being more rapid than for iodine and selenite (Henner et al. 2013).

In radioecology, the most common method to model transfer of elements from soil into plants is the use of empirical transfer factors, under the assumption that there is a linear relationship between plant and soil concentrations (e.g. Sheppard and Evenden 1988, 1990, Vera Tome et al. 2003, IAEA 2010). The relationship between Cl in plant and soil (i.e. the organic layer) was examined and the highest biomass Cl concentrations were found in the field layer (Table 14.2), suggesting a large accumulation of Cl in field layer annual (i.e. non-perennial) biomass. The high Cl concentrations are most pronounced at wet and moist sites and seem to be species related (rather than related to the soil Cl concentration). Neither the total soil concentration nor the chloride concentration (Cl_{tot} or Cl^-) is clearly related to the foliar concentration.

The distribution of Cl can also vary greatly within the plant. In trees, more Cl^- is found in leaves and needles than in bark and branches (Montelius et al. 2015). Higher concentrations can also be measured in older leaves than in seeds, fruits and floral parts of smaller plants (White and Broadley 2001). Among trees the reported total Cl concentrations vary between 6–820 μg g_{DW}^{-1} (Holmes

and Baker 1966, Edwards et al. 1981, Flodin et al. 1997, Lovett et al. 2005, Hannu and Karlsson 2006, Montelius et al. 2015, Gielen et al. 2016). Despite the large variation in trees, it seems likely that the highest concentrations are found in foliage and roots, followed by bark and branches. The lowest total Cl concentrations, < 30 µg g_{DW}^{-1}, are found in wood. Based on the data available on the distribution of Cl forms in trees, Cl^- is more abundant than Cl_{org} in trees, both deciduous and coniferous. The proportion of Cl_{org} relative to total chlorine is approximately 10 % in foliage, but could be higher in wood, though still < 30 %.

Table 14-1. Reported average (minimum-maximum) concentrations of Cl in different types of vegetation. (DW = dry weight). Data in bold originates from the Forsmark area. The last row shows the parameter value that was used to describe the plant concentration of chlorine for the Laxemar example site in the SFL evaluation. n.d. = not detected.

	Vegetation		TotCl (µg g_{DW}^{-1})	Cl^-(µg g_{DW}^{-1})	Cl_{org} (µg g_{DW}^{-1})	Reference
Tree layer	Foliage	Norway spruce Alder	**657 (405–989)** **1 255 (365–2 117)**		**14 (4–23)** **n.d.**	*Unpublished*
		Norway spruce	**10 367 (6 100–15 000)**			*1*
		*	1 214 (183–14 264)	266 (110–590)	37 (10–150)	*2, 3, 4, 5, 6, 10*
	Wood	Norway spruce Alder	**96 (25–197)** **179 (59–362)**		**15 (3–64)** **13 (7–24)**	*Unpublished*
		Norway spruce	**3 700 (1 900–5 600)**			*1*
		**	80 (6–530)	74 (9–380)	26 (3–150)	*3, 5, 6*
	Branches	**	66 (26–133)	55 (13–121)	8 (6–12)	*5, 6*
	Bark	***	98 (26–296)	87 (19–281)	9 (2–15)	*5, 6*
	Roots		**3 150 (2 000–4 200)**			*1*
Field layer	Above-ground plant		**6 871 (504–14 073)** **31 360 (12 000–68 000)** 1 237 (116–4 420)	 1 131 (28–4 241)	**21 (3–39)** 107 (10–243)	*Unpublished* *1* *3, 7, 8, 9*
Bottom layer			**637 (191–1 344)** **5 063 (890–9 600)** 757 (541–1 030)	 575 (285–800)	**50 (24–90)** 154 (60–265)	*Unpublished* *1* *3, 7, 9*
Parameter value	Green plant parts	Laxemar	4 200			*11, 12*

[1.] (Hannu and Karlsson 2006)
[2.] (Holmes and Baker 1966)
[3.] (Flodin et al. 1997)
[4.] (Lovett et al. 2005)
[5.] (Montelius et al. 2015)
[6.] (Gielen et al. 2016)
[7.] (Asplund et al. 1994)
[8.] (Nkusi and Müller 1995)
[9.] (Zlamal et al. 2017)
[10.] (Edwards et al. 1981)
[11.] (Grolander 2013)
[12.] (Engdahl et al. 2006)

* Birch, oak, European beech, sugar maple, Norway spruce, black pine, Douglas-fir, Scots pine, *Fraxinus pennsylvanica, Betula pendula, Caragana arborescens, Prunus virginiana, Cornus stolonifera, Ulmus americana, Ulmus pumila, Lonicera tatarica, Acer negundo, Quercus macrocarpa, Elaeagnus angustifolia, Pinus contorta, Pinus resinosa, Populus balsamifera, Populus tremuloides, Populus* sp.*, Picea pungens, Picea glauca, Salix pentandra*
** Oak, European beech, black pine, Douglas fir, Norway spruce
*** Oak, European beech, black pine, Douglas fir, Norway spruce, Scots pine

Unpublished: The unpublished data cover data gathered by SKB from a field study in Forsmark conducted in 2017 along ecosystem gradients from upland dry coniferous forest, via moist coniferous forest to wet alder forest wetlands.

Chlorine in soil

Cl^- in soils originates from sea salt deposition ('sea spray') but also from internal sources like weathering of bedrock or of marine deposits left by the regressing Baltic Sea (Schlesinger 1997, Tröjbom and Grolander 2010). Cl_{org} is found in all soil layers and Cl_{org} is 29–100 % of total Cl in soil, even in deeper mineral soils, i.e. it frequently exceeds the level of Cl^- (previously assumed to dominate the Cl pool) (Figure 14-1). The DW fraction of organically bound Cl in surface soils (0.01–0.5 %) is comparable to naturally occurring levels of several important nutrients, including phosphorous (0.03–0.2 %), nitrogen (1–5 %) and sulphur (0.1–1.5 %) (Öberg 1998, Keppler and Biester 2003). The total storage of Cl_{org} is usually largest in the mineral soil layer because of its greater thickness compared with the organic surface layer which typically has higher concentrations (Redon et al. 2011), but few data separate organic and mineral soil layers. Data indicate that Cl_{org} levels are higher in soils with more organic matter (Redon et al. 2011).

A consistent pattern where the concentration of Cl_{org} was higher in soils covered by coniferous forest than soils covered by deciduous forest has been observed (Johansson et al. 2003, Redon et al. 2011). This pattern was confirmed by Redon et al. (2011) in a study of more than 50 forested sites in France. In addition, Montelius et al. (2015) found that plots with Norway spruce had the highest net accumulation of Cl^- and Cl_{org} over the experimental period and showed 7- and 9-times higher storage of Cl^- and Cl_{org}, respectively, in the soil humus layer as compared with plots with oak. Thus, it seems likely that vegetation characteristics can explain local soil chlorine levels and why the occurrence is frequently independent of atmospheric deposition. Tröjbom and Grolander (2010) estimated that the terrestrial biomass pool of Cl in Forsmark (Sweden) was in the order of 60 % of the total catchment pool. The high enrichment of Cl in biomass, much higher than in biomass from a similar area (Laxemar, Sweden; see also in Table 14-1), calls for further studies to confirm the results. It is known that Cl is an essential element, but this level of enrichment indicates that the roles of Cl for organisms may not be fully understood, and that a large part of potential contaminant Cl-36 reaching terrestrial parts of the landscape will be taken up by biota.

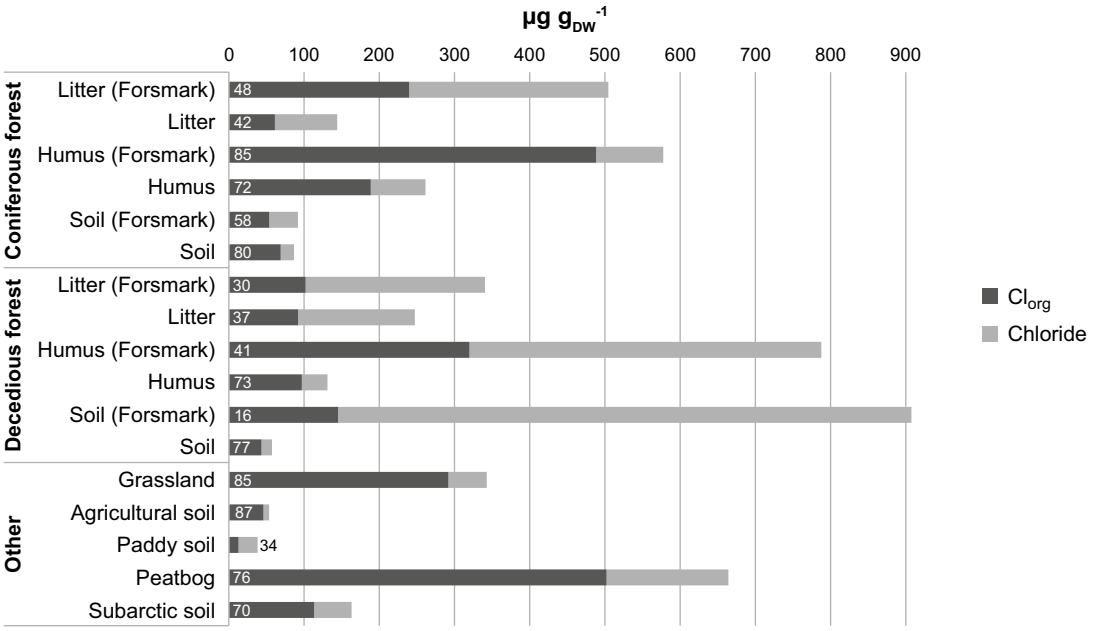

Figure 14-1. *Chloride and Cl_{org} per gram dry weight (DW) in various investigated soils. The numbers in the bars denote the percentage of Cl_{org} in the total chlorine contents, the sum of Chloride and Cl_{org}. The figure is based on Table 4-1 in Bastviken et al. (2013) and unpublished data from a field study conducted in Forsmark gathered by SKB in 2017 (based on ecosystem gradients ranging from upland dry coniferous forest, via moist coniferous forest and wet alder forest wetlands).*

Multiple Cl-36-tracer chlorination experiments have shown that more than 90 % of recently formed soil organic-matter bound (SOM bound) chlorine is non-leachable (see references in Bastviken et al. 2013). Data also indicate that Cl_{org} levels are higher in soils with more organic matter (Redon et al. 2011). Hence Cl_{org} seems to be strongly associated to soil particles and this can have larger effects on the stability of the Cl_{org} pool than the Cl:C ratio per se. The relative mobility of Cl_{org} versus other SOM is not clear. Even if a large amount of organic matter is chlorinated it is not clear if the chlorinated organic matter is stable and resistant to degradation or labile and more easily degraded by organisms. Leri and Myneni (2010) investigated degradation of leaves and found very stable material. Thus, this indicates that a large fraction of the chlorinated organic matter could remain for a long time in soils.

Chlorine sources

The major fluxes of chlorine into and out of ecosystems are dominated by Cl^-, where the input consists of both wet and dry deposition (see references in Bastviken et al. 2013). An estimate of total wet and dry deposition from Forsmark, based on the mean of two years, was 0.45 g m^{-2} $year^{-1}$ (Berg 2007, Qvarfordt et al. 2008). The deposition is relatively similar at Laxemar, as both sites are coastal locations (Löfgren 2008, Appendix 9). Another source of chlorine is weathering. Cl^- has long been believed to participate in geochemical processes only, i.e. transported from oceans via soil and back to the oceans again, being negligibly affected by biological cycling. Therefore, riverine Cl^- has in the past been considered to originate from the atmosphere only, and potential weathering processes during the pathway through the soil have been ignored (Eriksson 1960, Schlesinger 1997). Cl is present in most igneous rocks at low concentrations, e.g. about 0.02 % (Kuroda and Sandell 1953). However, Cl is not a part of the geochemical mapping in Sweden. Approximately 2 % of the Cl^- stream output was estimated to originate from weathering in a small stream at Hubbard Brook experimental forest (NY, USA) with bedrock consisting of mainly granite, which can be considered as small compared with the atmospheric contribution (Lovett et al. 2005). Montelius et al. (2015) measured the mineral-bound Cl in soil developed from granite, collected in Breuil-Chenue (Bourgogne France), to be less than 12 % of the total soil Cl. Land rise in previously glaciated regions can result in soils that originated as marine sediments and therefore are rich in Cl^-. Release of Cl^- from such marine deposits constitutes a special case with a significant subsurface contribution of Cl^- to soils, water and organisms, and is difficult to separate from weathering. In the Forsmark area, in central East Sweden, investigated thoroughly by SKB, leaching from marine deposits (and weathering) could have contributed up to 25 % of the Cl^- exported from the area (Tröjbom and Grolander 2010).

Soil leaching

Within ecosystems, many processes are ongoing that affect the internal cycling and leaching of Cl. These processes are primarily driven by vegetation, gaseous emission from the soil, and biochemical transformation in the soil. It is generally assumed that most of the deposited Cl^- is transported through soil unaltered, with only a minor influence of Cl^- soil adsorption by e.g. ion-exchange processes (Brady and Weil 2002). Traditionally Cl^- is thought to only be bound electrostatically and therefore the binding is easily reversible, which results in rapid equilibration with the soil solution. As previously mentioned, Cl^- is easily dissolved in water and could percolate to groundwater and surface waters, but Cl_{org} is also present in soil pore water. Soil pore water has been observed to contain generally from 0.9–3.6 mg TotCl l^{-1}, with an average of 1.8 mg TotCl l^{-1} (Svensson et al. 2013). High Cl_{org} concentrations, 400–4000 µg l^{-1}, corresponding to 16–54 % of the total Cl leaching from top-soil, were observed in a laboratory topsoil lysimeter study (Öberg and Sandén 2005). Chlorine is thus transported to a significant degree as organically bound, at least in topsoil. However, on a catchment scale the annual transport of Cl^- is approximately 30 times smaller than the total storage (Cl_{org} + Cl^-) of chlorine in the soil and the transport of Cl_{org} is negligible in relation to the transport of Cl^- (Svensson et al. 2007).

Table 14-2. Pool estimates of Cl in soil and biomass. Tree biomass divided into above-ground (AG) and below-ground (BG) biomass.

	Tree (AG) g m^{-2} TotCl (Cl^-+Cl_{org})	Tree (BG) g m^{-2} TotCl (Cl^-+Cl_{org})	Understory g m^{-2} TotCl (Cl^-+Cl_{org})	Soil (Org) g m^{-2} TotCl (Cl^-+Cl_{org})	Soil (Mineral) g m^{-2} TotCl (Cl^-+Cl_{org})	Ref
Coniferous forest						
Norway spruce (Dry)	**3.6** (1.7+6.5)		**0.19** (0.04+0.31)	**4.8** (3+5.8)	**21.8** (15.1+28.4)	*Unpublished*
Norway spruce (Moist)	**6.0** (2.1+10.4)		**0.65** (0.37+0.87)	**4.8** (1.9+9.9)	**14.6** (6.9+23.2)	*Unpublished*
Norway spruce	**2.45** (2.19+0.26)			**1.98** (0.72+1.26)	**40.5** (17.0+23.5)	*Montelius et al. 2015*
Spruce				**1.80** (0.23+1.57)	**18.7** (4.7+13.1)	*Redon et al. 2011*[4]
Douglas fir	**0.95** (0.8+0.15)			**0.95** (0.25+0.7)	**41.7** (15.9+25.8)	*Montelius et al. 2015*
Douglas fir				**0.58** (0.1+0.49)	**28.1** (3.29+23.7)	*Redon et al. 2011*[4]
Scots pine	**0.55**	**0.47**		**3.45** (0.81+2.64)[1]	**55.6** (15.5+40.1)[2]	*Van den Hoof and Thiry 2012*
Pine				**2.92** (0.78+2.14)	**22.5** (3.8+18.5)	*Redon et al. 2011*[4]
Black pine	**0.57** (0.49+0.08)			**0.52** (0.18+0.34)	**37.7** (15.5+22.2)	*Montelius et al. 2015*
Silver fir				**0.24** (0.07+0.13)	**17.5** (3.3+14.2)	*Redon et al. 2011*[4]
Pine + Norway spruce	**2.2** (2.1+0.1)				**20.0** (7.0+13.0)[3]	*Öberg et al. 2005*
Deciduous forest						
Alder	**10.4** ***(2.3+25.1)***		**1.13** (0.7+1.51)	**21.2** (7.6+43.0)		*Unpublished*
Oak	**0.27** (0.21+0.06)			**0.25** (0.11+0.14)	**39.8** (8.8+31.0)	*Montelius et al. 2015*
European beech	**0.33** (0.24+0.09)			**0.37** (0.12+0.25)	**45.5** (16.8+28.7)	*Montelius et al. 2015*
Oak				**0.36** (0.13+0.24)	**24.7** (5.14+19.6)	*Redon et al. 2011*[4]
Beech				**0.37** (0.11+0.24)	**22.6** (5.0+16.5)	*Redon et al. 2011*[4]

[1.] Forest floor.
[2.] Soil
[3.] Soil samples collected to 0–40 cm depth including humus.
[4.] Humus

Unpublished: The unpublished data cover data gathered by SKB from a field study in Forsmark conducted in 2017 based on ecosystem gradients ranging from upland dry coniferous forest, via moist coniferous forest and wet alder forest wetlands.

Preliminary evidence of large soil loss of VOCls

High fluxes of chloromethane of 0.6 g Cl m^{-2} $year^{-1}$ from coastal areas and > 0.1 g Cl m^{-2} $year^{-1}$ from wetlands, but also significant chloroform formation and release from terrestrial sources specially forested ecosystems have been found (see Svensson 2019). A Cl-36 radiotracer study indirectly indicated substantial release of Cl to the atmosphere corresponding to 0.2 g Cl m^{-2} $year^{-1}$ or 44 % of the annual wet deposition of Cl^- in a coniferous forest in southeast Sweden (Bastviken et al. 2009). This is a high rate that needs validation, but interestingly it includes an estimate of total VOCls in contrast to other estimates that measure specific VOCl compounds only. Despite the potential importance of VOCl formation for atmospheric emission and chlorine cycling, it is not at all clear what mechanisms control these relationships (see further discussion in Svensson 2019).

Chlorination and dechlorination

The origin of Cl_{org} in soil is not clear (Lovett et al. 2005, Öberg et al. 2005, Svensson et al. 2012). The input of Cl_{org} by deposition, 0.007 g m^{-2} $year^{-1}$, is significantly smaller than the deposited Cl^-, 0.4 g m^{-2} $year^{-1}$, and cannot explain the large storage of Cl_{org} in soil (Svensson et al. 2007). Previous studies imply that a considerable turnover of Cl^- to Cl_{org} takes place in soil, i.e. Cl^- is deposited on soil and subjected to a transformation to Cl_{org}. The underlying processes of formation of Cl_{org} in soil are still a matter for discussion. In time, Cl^- transformation will lead to a build-up of Cl_{org} in soil (Bastviken et al. 2006). Bastviken et al. (2007) suggest that biotic processes are responsible for the incorporation and there is evidence that several types of soil organism can form Cl_{org} (see Bastviken et al. 2013). Abiotic formation of Cl_{org} also takes place in soil (Keppler et al. 2000, Fahimi et al. 2003, Hamilton et al. 2003), but biotic processes dominate.

There are several proposed mechanisms behind the chlorination, such as intracellular chlorination regulated by enzymatic processes and alternatively extracellular chlorination. The extracellular chlorination is thought to be driven by formation of reactive Cl (e.g. hypochlorous acid, HOCl), from reactions between hydrogen peroxide and Cl^-, where the reactive Cl reacts with surrounding organic matter leading to an unspecific chlorination of various organic compounds in the large and complex pool of soil organic matter. In a recent experimental study, an increased availability of labile organic matter increased the Cl_{org} formation rates and thus linked those rates to general microbial activity (Svensson et al. 2017).

The first estimates of the chlorination rate (i.e. the mass of the standing-stock Cl^- that become organically bound per day) ranged from 1.4–89.8 ng Cl^- g_{DW}^{-1} day^{-1} (Gustavsson et al. 2012). There are few studies on how chlorination is regulated and how environmental variables influence the rates. Studies investigating the effects of nitrogen levels have yielded ambiguous results (Bastviken et al. 2006 , Montelius et al. 2019), and local variability seems large. In addition, a factorial study has showed that total chlorination was hampered by addition of nitrate or by nitrate in combination with water, but enhanced by addition of chloride as well as labile organic matter (glucose and maltose) (Svensson et al. 2017). A few studies have found that rates are slower under anoxic conditions (Bastviken et al. 2009), which is reasonable given that chlorination of organic matter is an oxidative process. The estimates are based on bulk soil excluding roots, which likely has underestimated the chlorination potential as it has more recently been shown that the majority of chlorination occur in the rhizosphere (Montelius et al. 2019).

Dechlorination processes (transformation from Cl_{org} to Cl^- by either organic matter decomposition or by selective removal of Cl atoms from organic molecules) have been extensively studied in relation to organochlorine pollution and bioremediation (van Pée and Unversucht 2003). The first study reporting directly measured dechlorination rates for bulk Cl_{org} in terrestrial environments indicated that soil Cl_{org} levels result from a dynamic equilibrium between the chlorination and rapid dechlorination of some Cl_{org} compounds, whereas another Cl_{org} pool is dechlorinated more slowly (Montelius et al. 2016). Hence both chlorination and dechlorination processes are important for understanding the behaviour of Cl^- in soils and it has even been suggested that the balance between chlorination and dechlorination is more important for soils Cl^- levels than Cl^- deposition (Gustavsson et al. 2012, Montelius et al. 2015).

Microbial exchange of Cl^- with surrounding soil has rarely been studied. However, data from a Cl-36 radiotracer study showed that 20 % of the Cl-36 added was taken up by microbial cells over a 5-day period (Bastviken et al. 2007). This indicates that soil microbes can rapidly take up Cl^- under periods of rapid growth, and that such mechanisms can cause considerable short-term variability in soil Cl^- levels driven by environmental variables affecting microbial activity.

14.1.3 Aquatic environments

Cl^- is a standard variable in aquatic monitoring, and has been regarded as inert, with no or negligible reactions in any processes. However, more in-depth budgets for transport of Cl^- from river basins to rivers have shown that Cl^- is reactive in soils and sediments (Lovett et al. 2005, Svensson et al. 2012, Kopáček et al. 2014, Robinson et al. 2017). Cl^- dominates Cl_{org} in aqueous phases (the former in levels of mg l^{-1} compared to µg l^{-1} typical to the latter), although there are trends in Cl_{org} and Cl-reduction, when comparing groundwater with surface water (lakes and streams; see Table 4-2 in Bastviken

et al. 2013). While groundwater has the highest Cl^- concentrations in comparison with precipitation and surface waters, Clorg concentrations can be highest in surface waters. A study of runoff from forests and marshes in Finland also showed that the Cl_{org} content increased four times from precipitation to surface water (from 6 to 24 µg L^{-1}) (Manninen and Lauren 1995). A similar study from Stubbetorp, a coniferous forested catchment in Östergötland, showed Cl and Cl_{org} values corresponding to 1.2 mg Cl^- l^{-1} and 6 µg Cl_{org} l^{-1} in precipitation and 2.5 mg Cl^- l^{-1} and 39 µg Cl_{org} l^{-1} in runoff (Svensson et al. 2007). This has been interpreted as the formation of Cl_{org} in soils but could also partly be due to formation in the aquatic environment. The apparently large pool of Cl in soils may have possible effects on Cl transport in aquatic systems, previously not taken into consideration.

Most of the studies in aquatic systems have focussed on anthropogenic impacts and especially on chlorinated pollutants such as DDT, PCB, dioxins, chlorobenzene or chlorinated acetic acids A few have reported bulk estimated AOX (absorbable organic halogens; the letter 'X' in the abbreviations AOX, EOX and TOX stands for the halogens chlorine, bromine and iodine) or EOX (extractable organic halogens). There are several studies that have focused on specific chlorinated pollutants, but only one study on bulk estimates in sediments (Maatela et al. 1990). In that study, Cl_{org} data from two lakes suggest that Cl_{org} in sediment can be formed or broken down naturally, but the dynamics are not known. Despite the few data available, it seems likely that the amount of Cl_{org} in sediments exceeds the amount of Cl^-, as in soils. This may indicate that the same processes occur in sediments as in soils, suggesting that Cl_{org} is also primarily bound to particulate phases in aquatic environments, but this needs further confirmation. Analyses using a similar methodology as for soils (TOX; total organic halogens in solid samples) appear to be largely missing and therefore Cl^- and Cl_{org} levels in sediments as well as in organisms and vegetation are presently not well determined.

The current knowledge of Cl turnover in aquatic environments is very limited. Previous research focused mainly on chloride or chlorinated pollutants without considering Cl_{org}.Thus, there is currently insufficient information to draw conclusions about the total chlorine turnover or its interactions with organisms which applies both to terrestrial and aquatic environments. The flow of dissolved Cl through aquatic systems can be expected to occur at similar rates as the water flow. However, interactions with sediment and organisms can be extensive and lead to a different residence time for Cl compared with water. Just as in soils, Cl_{org} levels appear to exceed the levels of chloride in sediment in the few systems studied. This can be of importance whether it is due to formation of Cl_{org} in the sediment or accumulation of Cl_{org} produced in other environments.

14.2 Nickel

14.2.1 Introduction

Nickel (Ni) is a transition metal (Z=28) that occurs as a divalent ion, Ni^{2+}, in natural waters. As such it has much in common with other divalent ions of transition metals, e.g. Fe^{2+}, Co^{2+}, Mn^{2+}, Cu^{2+} and Zn^{2+}, but it also has an ionic radius close to that of Mg^{2+}. Important processes for the mobility of Ni in the surface environment include complexation with organic matter and Fe oxides. These complexes tend to become stronger at high pH so generally Ni can be expected to be more mobile at lower pH and more strongly sorbed to soils and particles at higher pH (Alloway 2012).

Ni is a key constituent of certain enzymes and is therefore essential to plants and microorganisms (Zamble et al. 2017). For example, nickel is needed in urease, which is involved in the decomposition of urea. The required amounts of nickel are, however, low, and Ni limitation is therefore rare, although it has been observed in certain hyperaccumulators (Küpper et al. 2001). Instead, environmental problems with Ni are more commonly associated with its toxicity at higher concentrations (Chen et al. 2009, Tóth et al. 2016).

From a radioecological perspective, there are two important Ni isotopes: the more long-lived Ni-59 (half-life = 75 000 years) and the more short-lived Ni-63 (half-life = 96 years). In radioactive waste, both isotopes are activation products from neutron radiation in nuclear power plants (where Ni is a part of many alloys in metallic components), but in the case of Ni-59 there is also a cosmogenic source in nature. Both radionuclides decay to stable progeny – Co-59 in the case of Ni-59 (mainly by electron capture) and Cu-63 in the case of Ni-63 (by β^- decay) – so there is no decay chain dynamics involved in the radiation doses caused by these radionuclides.

14.2.2 Sources of natural nickel

A major source of natural Ni in the site investigation areas is weathering of local soils. In analysed till samples from Forsmark (n=59), the Ni concentrations mostly varied between 2.9 µg g^{-1} and 18 µg g^{-1} (Figure 14-2). This means that the Ni concentrations in Forsmark are somewhat on the low side compared with the estimated average Ni concentration of upper continental crust (~ 19 µg g^{-1}), but Swedish soils generally have relatively low Ni concentrations (Wedepohl 1995, Tóth et al. 2016). Two deep (5.7–7 m) till samples from the east side of Eckarfjärden (SFM0016) have been observed to contain up to 32 µg g^{-1} of Ni. These samples were also characterised by high concentrations of Co, Cr, Fe, Mg and Zn, which most likely is associated with a slightly different mineralogy compared to the rest of the Forsmark area. Geochemically, Ni can substitute for several different cations in minerals, but it is often associated with Fe (Alloway 2012). In Forsmark, Ni in soils correlates most strongly with Cr ($r=0.89$, $p < 0.01$) and Fe ($r=0.87$, $p < 0.01$) (Figure 14-2). In the Simpevarp area, Ni concentrations between 8.1 µg g^{-1} and 33 µg g^{-1} have been observed in mineral soils (n=18). Ni was positively correlated to the same group of elements as in Forsmark, e.g. Fe ($r=0.91$), Co ($r=0.92$) and Cr ($r=0.86$). Therefore, it is likely that Ni mostly occurs in some Fe-bearing minerals at both sites.

The other important source of Ni is atmospheric deposition, which has increased considerably in modern times, the main source being oil combustion (Krachler et al. 2003, Nieminen et al. 2007, Augustsson et al. 2010). It is estimated that the atmospheric deposition of Ni in Forsmark currently is on par with the stream water export and the situation is probably similar in Simpevarp (Tröjbom and Grolander 2010). Judging from the landscape patterns in other boreal catchments, however, most of the deposited Ni is believed to accumulate in topsoil, so that surface water concentrations and fluxes are dominated by geogenic Ni (Lidman et al. 2014).

14.2.3 Nickel in near-surface groundwater and surface water

In near-surface groundwater (i.e. groundwater in Quaternary deposits) the observed Ni concentrations ranged over two orders of magnitude, from 0.15–24 µg l^{-1} in the Forsmark area (n=135). Most groundwater samples had, however, Ni concentrations < 1 µg l^{-1} with a median concentration of 0.89 µg l^{-1}. In Simpevarp, the Ni concentrations were higher, ranging from 0.26–40 µg l^{-1} with a median concentration of 3.3 µg l^{-1} (n=101). At both sites, Ni was generally correlated to the same type of elements as in the soils, e.g. Co, which occurs as Co^{2+} in natural waters (Figure 14-3). This suggests that Ni broadly is affected by the same processes as other divalent transition metals, albeit to different degrees. For instance, fractionation between Ni and Co could be expected in connection with oxidation of Mn.

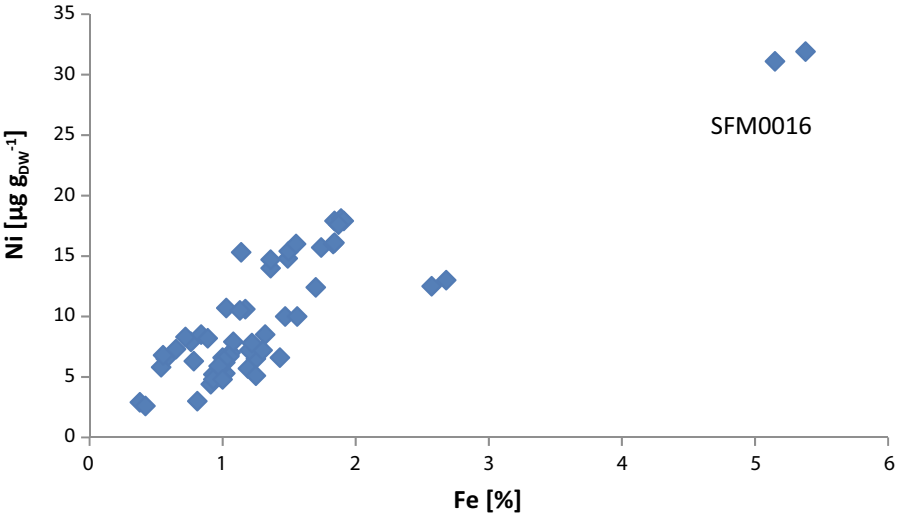

Figure 14-2. *Concentration of Ni and Fe in till samples from Forsmark. Two deep till samples are marked with SFM0016.*

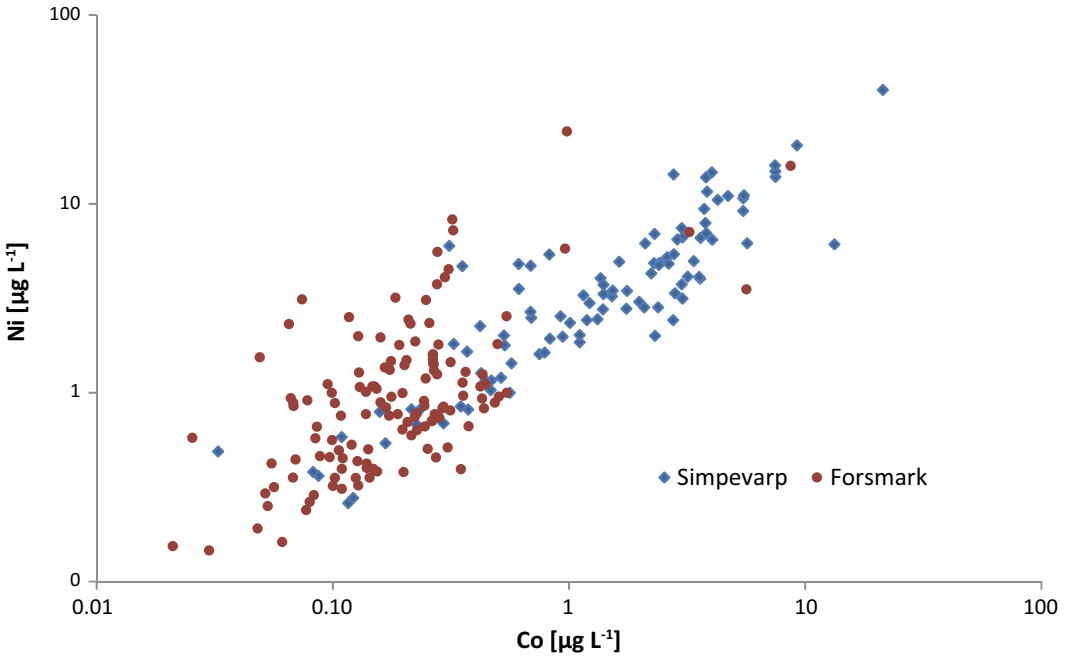

Figure 14-3. *Ni and Co concentrations in near-surface groundwater from Simpevarp and Forsmark.*

In lake water in the Forsmark area, Ni concentrations ranging from 0.14 µg l^{-1} to 2.8 µg l^{-1} have been observed (n=83 representing eight lakes). The median Ni concentration was 0.41 µg l^{-1}, and except for two outliers all observations exhibited Ni concentrations < 1 µg l^{-1}. Sampling of eight streams in the Forsmark area (n=83) showed Ni concentrations between 0.18 µg l^{-1} and 1.5 µg l^{-1} with a median of 0.48 µg l^{-1}. Overall, the Ni concentrations in surface waters were generally somewhat lower than in the groundwater (Figure 14-4). The main reason for this is most likely that the surface water is more influence by water that has been in contact with mineral soil for a shorter time than most sampled groundwaters, which often are sampled at depths of several metres.

In the Simpevarp area, there are fewer lakes and the only sampled lake, Frisksjön, had Ni concentrations in the range 1.2–1.9 µg l^{-1} (n=10). In stream water, the Ni concentrations ranged between 0.79 µg l^{-1} in a stream near Plittorp (PSM002071) and 15 µg l^{-1} in a stream near Basteböla (PSM002086), south of Laxemar (n=27, altogether). The generally higher Ni concentrations in the surface waters of the Simpevarp area, as compared with the Forsmark area, probably reflect the higher abundance of Ni in the local soils and higher weathering rates of Ni-bearing minerals in the Simpevarp area, rather than differences in mobility (Section 14.2.2; Figure 14-4).

The sampling of lakes and streams was conducted on a seasonal basis, which revealed clear trends in some, but not all, of the objects. In lakes with a seasonal variation, the concentrations were higher during the winter, suggesting a greater influence from deeper groundwater, and lower during the growing season (Figure 14-5). In the Forsmark area, the summers are characterised by high pH and precipitation of $CaCO_3$ from the lake water, which may contribute to the scavenging of Ni (Zachara et al. 1991). This would be consistent with the accumulation of Ni in calcareous lake sediments described below (Section 14.2.5)

14.2.4 Speciation of Ni(II)

Based on thermodynamic modelling, the speciation of Ni(II) in near-surface groundwater and surface water at both sites is believed to be dominated by free Ni^{2+} ions, particularly at lower pH, and organically bound Ni, mainly at higher pH. This is consistent with observations from other boreal waters, where organic colloids have been identified as the major carrier of Ni (Dahlqvist et al. 2007, Ilina et al. 2016). Many waters in Forsmark have high carbonate concentrations due to the presence of calcite in the local till, but even when pH is high, as in the lakes during the summers, the speciation is expected to be dominated by free Ni^{2+} and organically bound Ni rather than Ni-carbonate complexes (Figure 14-6).

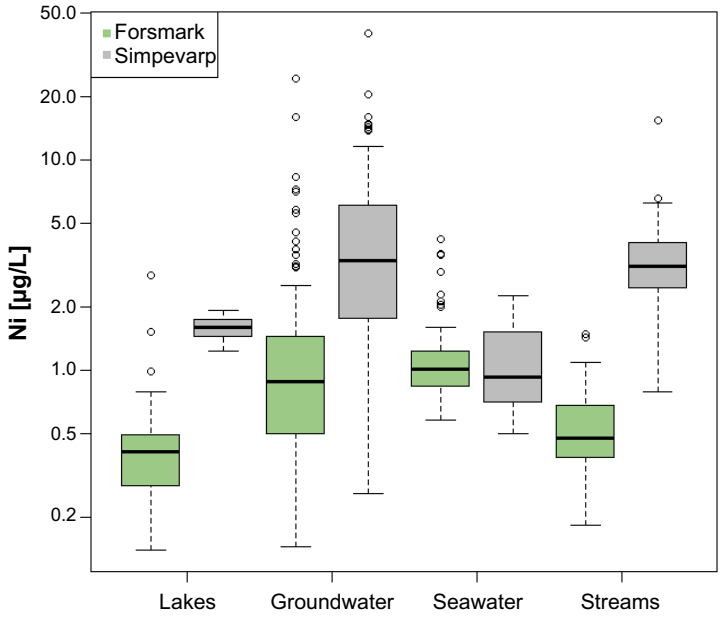

Figure 14-4. *Ni concentrations in different types of water in the Forsmark (green) and Simpevarp (grey) areas, respectively. The bottom, centre and top of the boxes represent the 25th, 50th and 75th percentiles of the data. The whiskers include all observationations within a distance of 1.5 times the interpercentile range.*

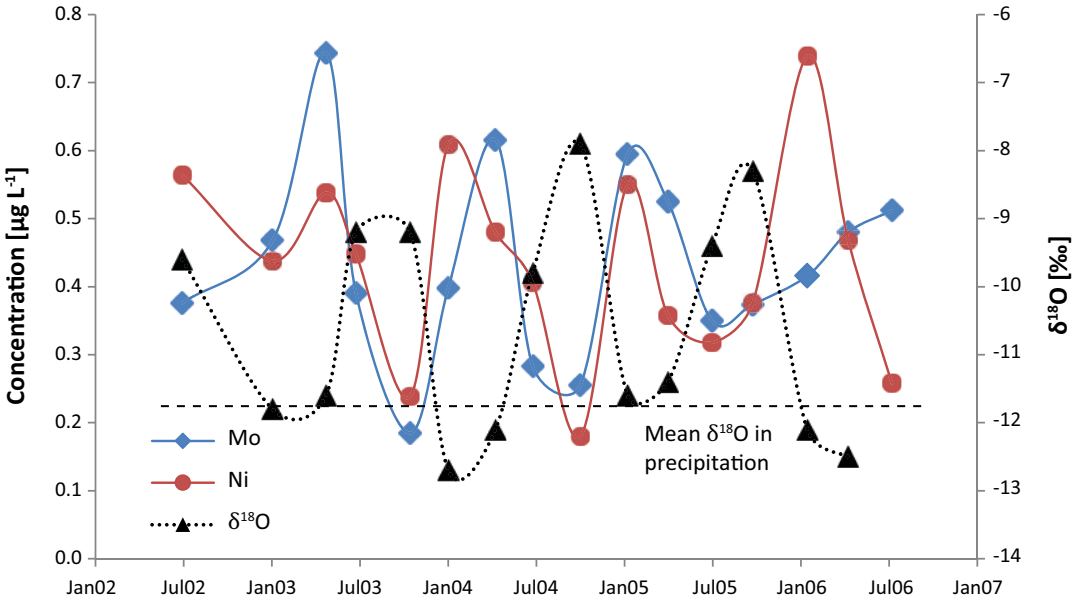

Figure 14-5. *Temporal variation in $\delta^{18}O$ (right-hand axis) and concentrations (left-hand axis) of Mo and Ni in Labboträsket, Forsmark, 2002–2006. The deviation of the $\delta^{18}O$ signal from the meteoric isotope composition during the summers reflects evaporation of lake water.*

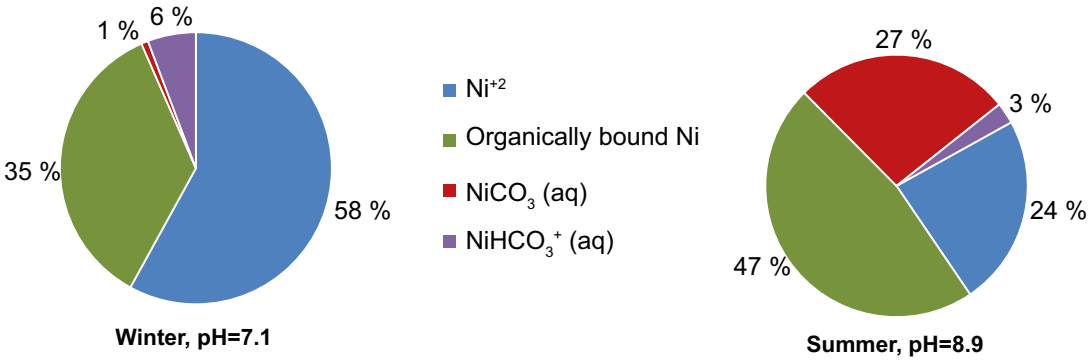

Figure 14-6. *Two examples of modelled Ni speciation in Bolundsfjärden, Forsmark, during winter conditions (left) with relatively low pH (17 January 2003) and summer conditions (right) with high pH (7 July 2005). Association to Fe colloids was not considered, but Ni has been observed to bind preferentially to organic matter in boreal waters (Dahlqvist et al. 2007). Generally, the proportion of free Ni^{2+} ions decreases with increasing pH, whereas the proportion organically bound Ni increases.*

14.2.5 Nickel in sediments

One potentially important mechanism for retention of Ni in the landscape is accumulation in sediments. Concentrations of up to 72 µg g^{-1} and 67 µg g^{-1} have been observed in sediments from Frisksjön (Simpevarp) and clayey marine sediments in Forsmark (PSM006062), respectively, which in both cases is higher than in the local till (Section 14.2.2). The highest concentrations were generally found in more inorganic sediments, as illustrated by sediments from Eckarfjärden in Forsmark in Figure 14-7. From a radioecological perspective, however, it is important to distinguish between sedimentation of Ni in primary minerals and accumulation of Ni that at some point has been in the aqueous phase, since only processes affecting the latter fraction will be important for radionuclides from a deep repository.

One common method to estimate the sedimentation of elements from the dissolved phase is to normalise against elements like Zr or Ti, which are believed to occur mainly in primary minerals (Boes et al. 2011). In the deeper clay sediments in Eckarfjärden the Ni/Ti × 1 000 ratios were around 10, which is a typical value for the till in the Forsmark area (Figure 14-7). This suggests that most of the Ni at these depths may occur in primary minerals. As the sediments became more organic above ~ 1 m, the Ni/Ti × 1000 ratio increased to a maximum of 70, indicating that there also has been sorption of dissolved Ni onto the sediment particles found at these depths.

Given the relatively strong affinity of Ni for organic matter it is likely that much of the sorbed Ni found in the sediments was brought there by sedimentation of organic matter or sorption directly to the sediments. Since organic sediments tend to become strongly reducing, there is also a possibility that the accumulation of Ni is enhanced by the precipitation of sulphides. Ni can potentially precipitate directly as millerite (NiS), but more likely is coprecipitation with or adsorption onto Fe sulphides (Morse and Arakaki 1993, Huang et al. 2010). When such sediments are exposed to air, e.g. by land uplift and ditching, the sulphides will be oxidised, which can lead to high concentrations of Ni and other associated elements in the runoff (Nordmyr et al. 2008).

In the Forsmark area, the lakes are characterised by precipitation and sedimentation of $CaCO_3$ during the growing season (Jaremalm et al. 2013). This is the reason for the calcareous gyttja sediments in Eckarfjärden (and elsewhere), which contain up to 46 % $CaCO_3$ (Figure 14-7). This was also the section of the sediment core with the highest Ni/Ti ratio, i.e. the highest accumulation of Ni from the dissolved phase (Figure 14-7). It is known that there can be an appreciable adsorption and coprecipitation of Ni with calcite when the pH is as high as in the lakes in Forsmark (Zachara et al. 1991, Hoffmann and Stipp 2001, Andersson et al. 2014). The adsorption and coprecipitation of Ni and other related metals is dependent on which polymorph of $CaCO_3$ is being formed in the lakes, but high Sr concentrations in the calcareous gyttja suggest that it might be aragonite or amorphous $CaCO_3$ rather than calcite, since Sr^{2+} ions are too large to fit very well into the crystal structure of calcite (Curti 1999). The lakes are also affected by seasonal changes in the redox conditions, which causes precipitation of Fe and Mn during the summers and dissolution thereof during the winters, which can also affect Ni and other transition elements.

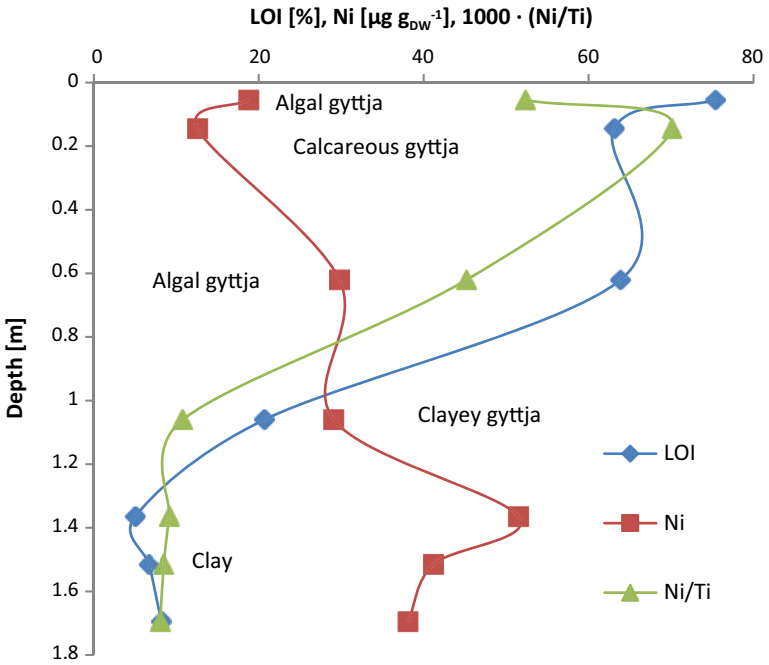

Figure 14-7. *Ni concentrations, LOI (loss on ignition) and Ni/Ti ratios in sediments from Eckarfjärden, Forsmark.*

14.2.6 Nickel on the landscape scale

Further insights into the processes that govern the fate of Ni can be gained by studying the occurrence of Ni from a landscape perspective. The relatively high affinity of Ni for organic matter suggests that wetlands and other organic soils are locations where accumulation of Ni could be expected. Catchments in the Forsmark area typically consist of ~ 10–20 % wetlands, but the landscape composition is too complex to discern any clear effects on the Ni concentrations. In the Krycklan catchment in northern Sweden, however, Ni concentrations in different sub-catchments followed a clear gradient from forest- to wetland-dominated catchments (Figure 14-8). The decrease in Ni with increasing wetland coverage was partly due to dilution due to low weathering in wetlands, but there was also a clear accumulation of Ni in the peat, which can be expected to be representative also for wetlands in the site investigation areas (Lidman et al. 2014).

In Forsmark there was a trend with lower Ni concentrations in lakes with longer residence times, particularly during the winters. Similar trends could be observed for a range of other elements, for example, Ca, Fe, Cr, Mo, U, Si, rare earth elements and sulfate, suggesting that it might reflect scavenging from the water column. The number of lakes is, however, small (n=6), and more work is needed to determine whether there are other factors that could be responsible for this.

14.2.7 K_d values for Ni

Ni was included in the site-specific K_d measurements from the site investigations presented by Sheppard et al. (2011). The K_d values for Ni were, in relative terms, low in clay gyttja (0.13–1.0 m^3 kg^{-1}), which probably was related to the high DOC concentrations observed during the analyses (Figure 14-9). The cultivated peat and the wetland peat had intermediate K_d values, ranging from 1.5–17 m^3 kg^{-1}. The mobility of Ni in these soils is likely to be enhanced by the high DOC concentrations, as predicted by the Ni speciation (Figure 14-6), and the K_d values are also consistent with the accumulation of Ni that has been observed in wetlands (Figure 14-8).

The highest – but also the most variable – K_d values were observed in the glacial clay, which displayed K_d values between 1.5 m^3 kg^{-1} and 33 m^3 kg^{-1}. These soils were characterised by large differences between shallow (20–25 cm) and deep samples (50–55 cm), approximately an order of magnitude.

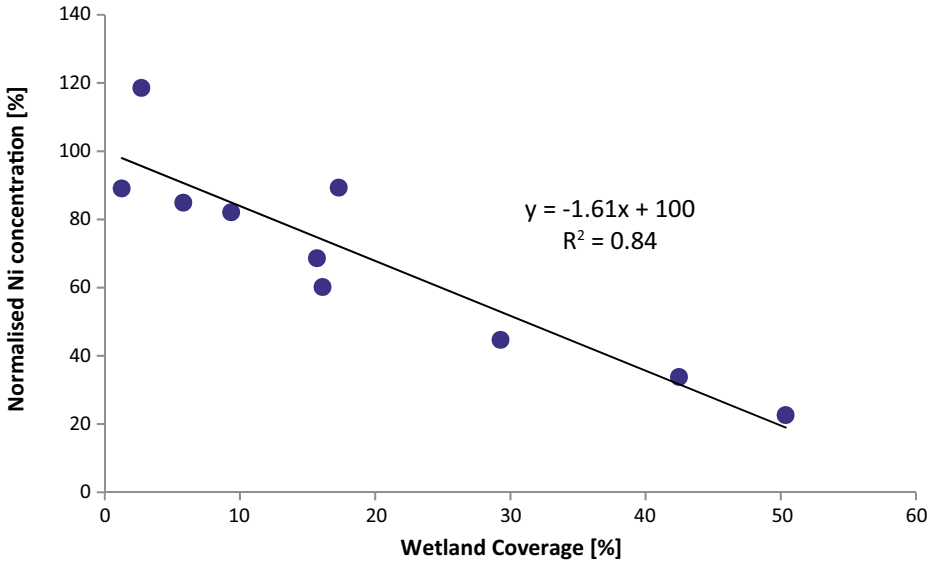

Figure 14-8. *Normalised Ni concentrations in ten streams in the Krycklan catchment in northern Sweden as a function of the wetland coverage in each catchment (data from Lidman et al. 2014).*

Similar or even larger differences were observed for several other elements, e.g. Co, Mn and Zn, and these are most likely related to differences in both particle-size distribution and mineralogy. The shallow soils had lower clay content than the deeper soils (on average 37 % and 55 %, respectively), but a higher sand content (34 % and 5.8 %, respectively), both of which would favour higher K_d values in the deeper soils. The shallow soils also contained less carbon (1.3 %) than the deeper soils (7.7 %), suggesting a larger proportion of calcite in the deeper soil horizons.

The K_d values for Ni followed the same trends as other comparable elements. The similarities between the K_d values for Ni and other transition metals such as Co and Zn are consistent with the results from the site investigations as outlined above (Figure 14-9). This indicates that the behaviour of Ni in the surface environment is governed by the same type and range of processes as other comparable elements and that there are no special mechanisms involving Ni that need to be considered in modelling of the element.

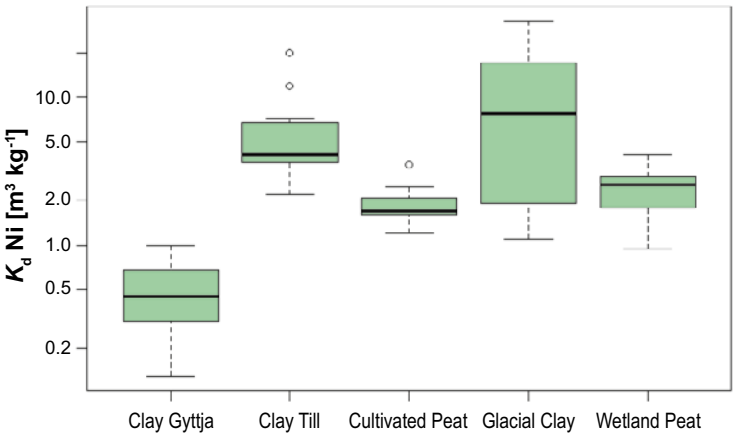

Figure 14-9. *Site-specific K_d values for Ni from the study of Sheppard et al. (2011). Notataion as in Figure 14-4.*

14.2.8 Ni in biota

The bioavailability and toxicity of nickel has been shown to depend on the presence of free Ni^{2+} ions, which in turn is largely dictated by pH and organic matter (Martino et al. 2003, Weng et al. 2004). The biological uptake of Ni is also affected by competition from similar elements (also, see above). For example, Mg is known to decrease the uptake of Ni in hard waters (Deleebeeck et al. 2009).

In primary producers in the site investigation areas, observed Ni concentrations range from < 0.035 µg g_{DW}^{-1} in wood from Norway spruce (*Picea abies*) to 199 µg g_{DW}^{-1} in marine microphytobenthos (Hannu and Karlsson 2006, Kumblad and Bradshaw 2008). Some samples with high Ni concentrations, for instance the above-mentioned microphytobenthos, also had conspicuously high concentrations of metals such as Al, Hf and Zr, which are known to have generally low solubility and low biological uptake. It is therefore likely that these samples include minerogenic matter and that the actual uptake of Ni may be lower than indicated by these measurements. Apart from these anomalies, however, the observed Ni concentrations agreed with Ni concentrations in plants reported in general literature for non-contaminated areas, ~ 0.1–5 µg g^{-1} (Alloway 2012, and references therein). The Ni concentrations in primary producers broadly followed the same pattern as Co and other similar elements, suggesting that there is no specific process involved in the uptake of Ni (Figure 14-11).

In animal samples from the site investigation areas, Ni concentrations ranging from < 0.02 µg g_{DW}^{-1} in elk meat (*Alces alces*) to 3.24 µg g_{DW}^{-1} in mussels (*Cerastoderma glaucum*) were observed. Some of the variability is, however, related to differences in the analytical procedures, e.g. whole-body samples vs. muscle tissue and dissolution vs. total extraction (Hannu and Karlsson 2006, Kumblad and Bradshaw 2008). As in the primary producers, there was a tendency for samples with high Ni concentrations, particularly benthic fauna, also to contain high concentrations of typically minerogenic elements like Al and Hf, suggesting that there may be a contribution from mineral particles also in some of the animal samples. No signs of biomagnification were observed for Ni, which is consistent with literature (Nieminen et al. 2007).

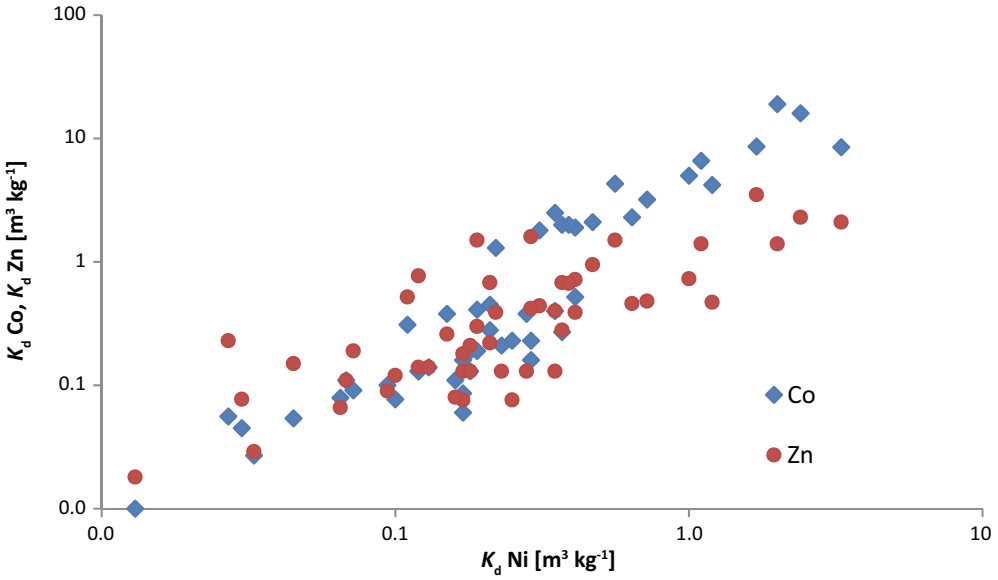

Figure 14-10. *Measured K_d values for Ni plotted against the corresponding K_d values for Co and Zn, respectively. All data are taken from Sheppard et al. (2011).*

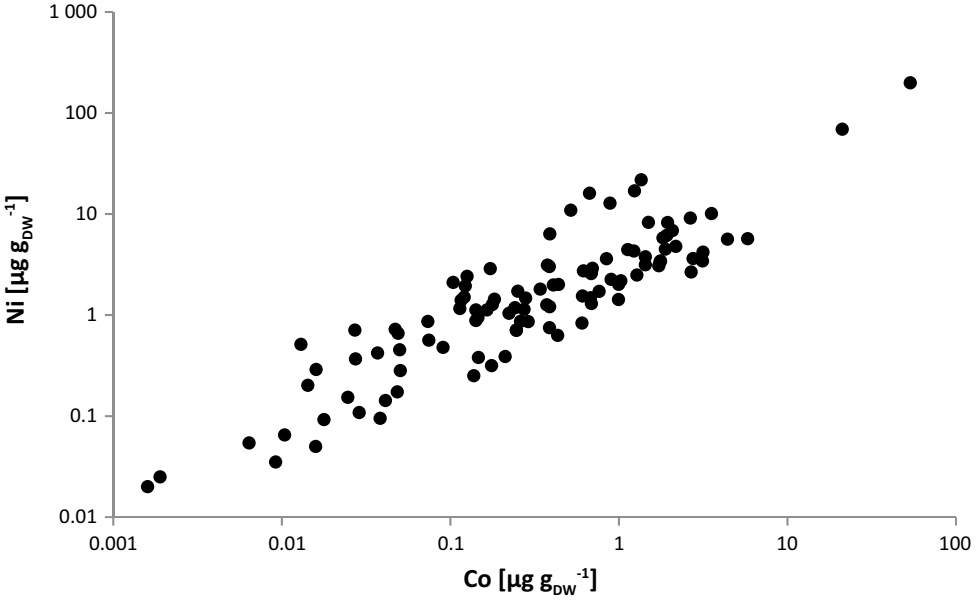

Figure 14-11. *Ni and Co concentrations in primary producers from the site investigations (data from Engdahl et al. 2006, Hannu and Karlsson 2006, Roos et al. 2007, Kumbland and Bradshaw 2008, Sheppard et al. 2011).*

14.3 Molybdenum

14.3.1 Introduction

Molybdenum (Mo) is a transition metal (Z=42) that can occur in different oxidation states in nature. The dominating oxidation state in surface water and groundwater is Mo(VI), which occurs as the oxyanion molybdate, MoO_4^{2-}. This tendency of high-valence states to form an oxyanion is a property that Mo shares with many of its closest neighbours in the periodic table of the elements, e.g. V, Cr, Tc, Re and W. Molybdate is stable over a wide range of chemical conditions, and as an anion Mo tends to be more mobile at high pH. Important retention processes for molybdate includes sorption onto Al and Fe oxyhydroxides, especially at low pH. Recently, it has also been demonstrated that molybdate can bind strongly to organic matter (Gustafsson and Tiberg 2015).

Under strongly reducing (approximately sulfidic) conditions Mo(VI) can be reduced, predominately to Mo(IV) (Crusius et al. 1996, Smedley and Kinniburgh 2017). This has far-reaching consequences for the mobility of Mo, since it implies that Mo is transformed from a relatively mobile oxyanion to a high-valence cation with low solubility. As a consequence, there can be appreciable accumulation of Mo in strongly reducing environments such as organic sediments (Crusius and Thomson 2000, Dahl et al. 2013, Wirth et al. 2013, Chappaz et al. 2014).

Mo is an essential nutrient that plays an important role in enzymes involved in N_2 fixation and reduction of nitrate (Cole et al. 1993). It has been observed that asymbiotic N_2 fixation by feather mosses can account for as much as two thirds of the N input to boreal forests, and that this fixation during the middle of the growing season sometimes can be limited by Mo (Jean et al. 2013). There is also evidence that Mo can limit the primary production in certain oligotrophic lakes (Glass et al. 2013). Therefore, there are reasons to expect a considerable uptake of Mo, and certain bacteria are known to release ligands that can mobilise Mo from organic matter (Wichard et al. 2009). In high concentrations, however, Mo is toxic, which appears to be because it inhibits the uptake of Cu (Vunkova-Radeva et al. 1988).

In a radioecological context, Mo is a concern because of the artificial radionuclide Mo-93 (half-life = 4000 years). Mo-93 is produced mainly by neutron irradiation of stable Mo-92 in nuclear power plants. Mo is present as impurities in many types of reactor materials, but higher Mo concentrations can occur in certain alloys, e.g. some types of Inconel and stainless steel, which have been used above all in certain light-water reactors. It decays by electron capture to stable Nb-93 so it is not involved in any decay chains.

14.3.2 Sources of natural Mo

The average Mo concentration in the upper continental crust has been estimated to 1.4 µg g^{-1} (Wedepohl 1995). Most of this is believed to reside in feldspars and plagioclase, although it may also occur in minerals such quartz and biotite (Ahrens et al. 2013). In till from the Forsmark area, Mo concentrations between 0.060 µg g^{-1} and 1.4 µg g^{-1} have been observed (n = 59). Mo correlated most strongly with sodium ($r = 0.62$, $p < 0.05$) so it possible that weathering of albite (a Na-rich type of plagioclase) could be a major source of Mo. In the Simpevarp area, Mo concentrations between 0.35 µg g^{-1} and 2.0 µg g^{-1} have been observed in mineral soils (n = 18). As in Forsmark, there was a weak correlation to Na ($r = 0.49$, $p < 0.05$).

In addition to weathering of local soils, there may also be a significant atmospheric deposition of Mo, especially in the Forsmark area due to pollution from steel works in the Sandviken area ~ 80 km northwest. On larger scales, it has been observed that the atmospheric deposition of Mo has increased significantly since the onset of the Industrial Revolution (Krachler and Shotyk 2004).

14.3.3 Mo in near-surface groundwater and surface water

In near-surface groundwater in Forsmark, Mo concentrations between 0.063 µg l^{-1} and 31 µg l^{-1} have been observed (n=135). The Mo concentration tended to be higher in groundwater with high pH, which can be explained by a generally weaker sorption and higher mobility of anions in more alkaline waters (Figure 14-12). Particularly low Mo concentrations were encountered in a groundwater well with high concentrations of sulphide (SFM0049). This was consistent with the expected reduction and immobilisation of Mo in sulphate-reducing environments (Section 14.3.1). In the Simpevarp area, the Mo concentrations showed a similarly high variability, ranging from < 0.05 µg l^{-1} to 14 µg l^{-1} (n=101).

In the Forsmark area, the surface waters, as a rule, had notably lower Mo concentrations than the near-surface groundwater, ranging from 0.19–1.1 µg l^{-1} in lake water (n=83) and from 0.082–1.9 µg l^{-1} in stream water (n=48). In the Simpevarp area, the differences between near-surface groundwater and surface water were smaller with Mo concentrations between 0.92 µg l^{-1} and 1.3 µg l^{-1} in Lake Frisksjön (n=10) and between 0.069 µg l^{-1} and 6.8 µg l^{-1} in stream water (n=27). These data are displayed in Figure 14-13).

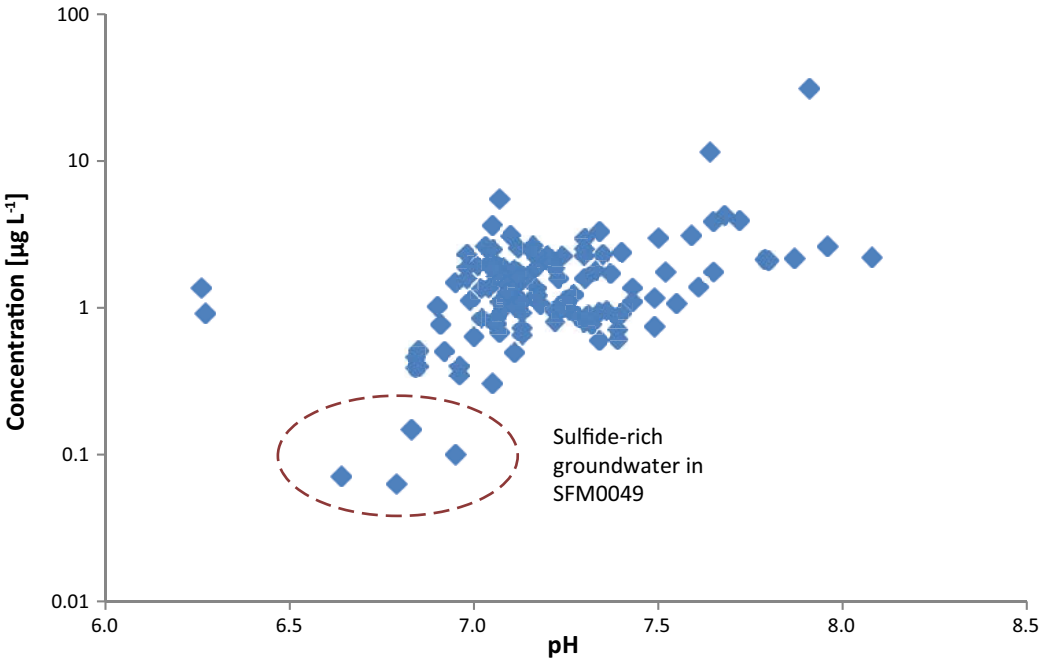

Figure 14-12. *Mo concentrations in groundwater from Forsmark as a function of pH. The lowest concentrations were encountered in SFM0049, which is a sulfide-rich groundwater well.*

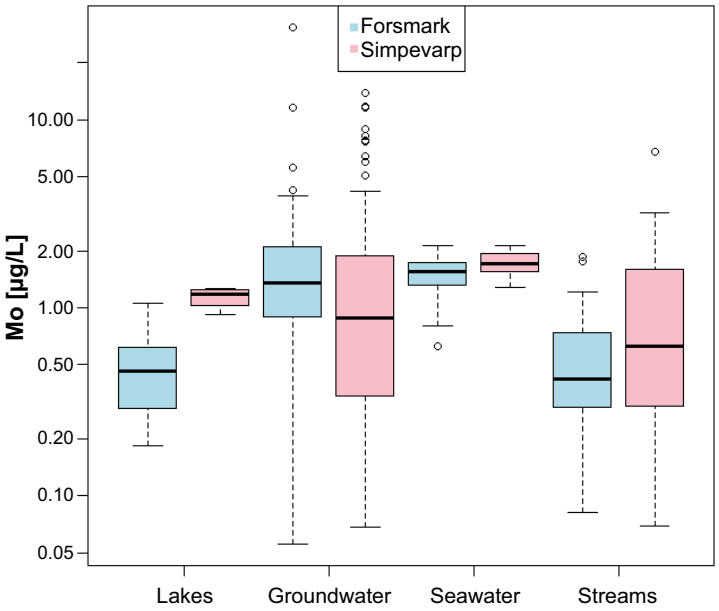

Figure 14-13. *Mo concentrations in different types of waters in the Forsmark (blue) and Simpevarp (pink) areas, respectively.*

Many of the sampled streams and lakes displayed seasonal variations in the Mo concentrations, e.g. Labboträsket in Forsmark (Figure 14-5). Unlike Ni, however, which tended to peak during the winter, the highest Mo concentrations in lake water were often observed during the summer, particularly in Bolundsfjärden and Norra bassängen in Forsmark. Evidently, Mo was not affected in the same way as Ni by the increasing pH and precipitation of $CaCO_3$ during the summers. Instead, Mo was, for example, positively correlated to V ($r=0.85$, $p < 0.05$), which also tends to occur as an oxyanion, as well as to pH ($r=0.81$, $p < 0.05$) in Bolundsfjärden, Forsmark. This behaviour is consistent with the occurrence of Mo as molybdate (Goldberg et al. 1996).

Based on thermodynamic modelling of groundwater and surface water in the site investigation areas, the speciation of Mo is believed to be dominated by molybdate and its complexes with Mg and Ca, as exemplified by lake water from Labboträsket (Forsmark) in Figure 14-14 (Gustafsson 2012).

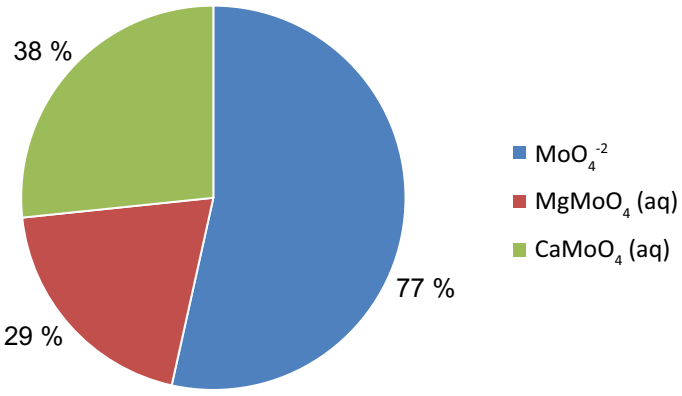

Figure 14-14. *Example of modelled Mo speciation in Bolundsfjärden during a period of high pH (pH=9.1) 17 July 2006. The speciation does not appear to vary appreciably throughout the year.*

14.3.4 Mo in sediments

Mo is expected to remain relatively mobile if it is present as molybdate, but, as outlined above, its mobility is expected to decrease considerably if it is reduced. It is well-established that reduction of molybdate can cause significant accumulation of Mo in both marine and freshwater sediments (Dahl et al. 2010, Helz et al. 2011, Chappaz et al. 2014).

In Stocksjön in Forsmark, Mo concentrations of up to 73 µg g^{-1} have been recorded, which was more than 50 times higher than the highest observations from the local till (Figure 14-15). Furthermore, the Mo/Ti ratios were ~ 100 times higher than in the local till, which a strong indication that there has been a substantial accumulation of Mo. The enrichment of Mo coincided with high concentrations of S (up to 3.5 %), which suggests the sediments are sulfidic. This was further supported by the accumulation of U, which is expected to be reduced from U(VI), occurring as comparatively mobile uranyl-carbonate complexes, to immobile U(IV) under similar conditions as Mo (Figure 14-15). High Mo concentrations have also been encountered at certain depths in sediment cores from other sites in the Forsmark area, e.g. 14 µg g^{-1} in gyttja from a wetland near Bolundsfjärden (PFM006023), 8.0 µg g^{-1} in gyttja sediments from Eckarfjärden and up to 18 µg g^{-1} in marine sediments (PFM002560) (Hannu and Karlsson 2006). In the Simpevarp area, Mo concentrations of up to 24 µg g^{-1} in were found in Frisksjön, coinciding with high concentrations of S, and up to 7.1 µg g^{-1} in gyttja sediments under a wetland (Klarebäcksmossen). Hence, if the redox conditions are reducing enough, there are strong reasons to expect a considerable accumulation of Mo in sediments even in lakes as shallow as those in the Forsmark area. This accumulation of Mo in strongly reducing environments is likely to be a major retention mechanism for Mo in the surface environment.

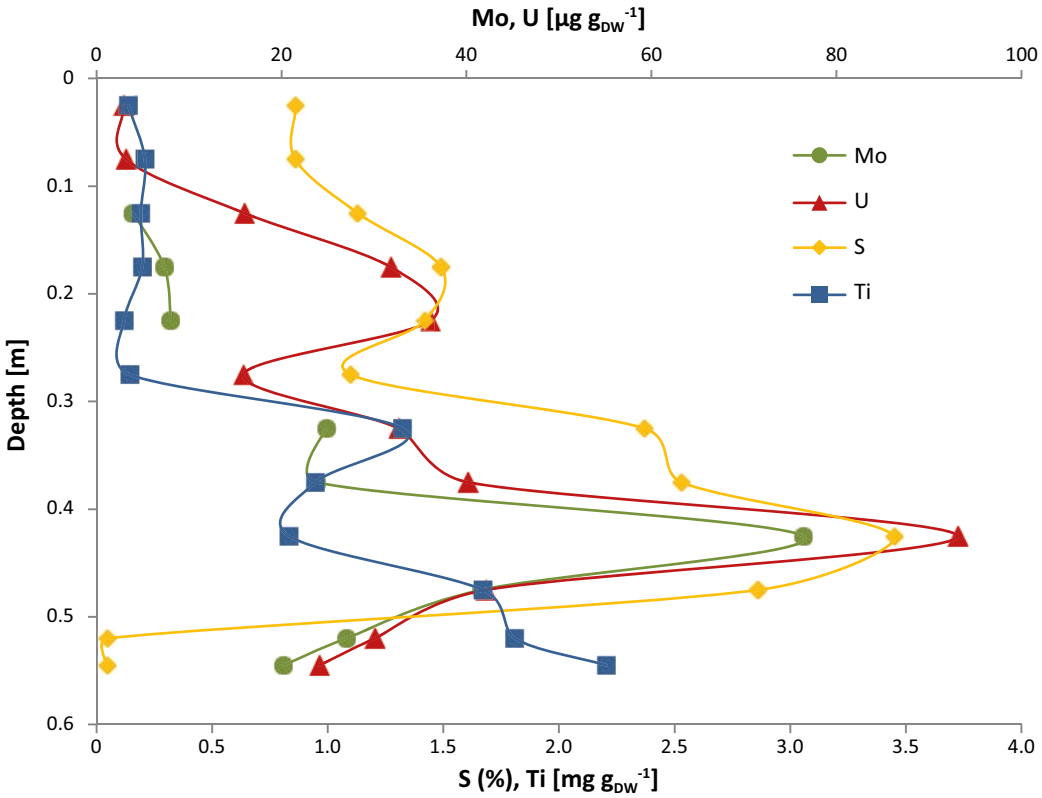

Figure 14-15. *Concentrations of Mo, U, S and Ti in sediments from Stocksjön, Forsmark.*

14.3.5 Mo on the landscape scale

When comparing the lakes in the Forsmark area there was a clear relationship between Mo concentrations and the lake elevation (Figure 14-16). Given the on-going land rise, the elevation is in this case also directly related to the age of the lakes. High Mo concentrations in the Forsmark area are typically associated with either groundwater or seawater, so one possible explanation would be that this gradient represents gradual loss of marine Mo from the soils (Figure 14-16). A similar trend was observed for Sr (and a range of other elements), which also occurs in higher concentrations in sea water (Figure 14-16)However, the isotopic signature of the Sr indicated that although there was more marine Sr in the situated lakes lower, most of the Sr was of geogenic origin. Hence, it would suggest that the observed trend is more likely to be related to an influence from weathering. The explanation could therefore be that lower-lying lakes are fed by groundwater with longer transit times in the soils.

When sampling Mo in two adjacent streams in the Krycklan catchment in Northern Sweden – one draining a completely forested catchment and one draining a mire covering nearly 50 % of the catchment area – the Mo concentrations were on average nearly 50 times higher in the forest-dominated stream than at the outlet of the mire (Bauer 2018). However, there was no significant difference when comparing tungsten (W) concentrations between the two streams. Just like Mo, tungsten tends to occur as an oxyanion, tungstate, but it is more difficult to reduce. This suggests that the low Mo concentrations in the mire-dominated stream were caused by reduction of molybdate and accumulation of Mo in the peat. Similar patterns are not discernible in the site investigation areas due the heterogeneity of the landscape, but the accumulation of Mo that has been observed suggests that there should be a similar retention of Mo in wetlands in the site investigation areas (Section 14.3.4).

14.3.6 K_d values for Mo

Mo was included in the site-specific K_d measurements reported by Sheppard et al. (2011). The frequency distribution of Mo K_d values displayed a clearly bimodal tendency, which is likely to be connected to the redox properties of Mo (Figure 14-17). The general pattern was that Mo exhibited low K_d values in inorganic soils such as clay till and glacial clay, mostly in the range 0.06–0.26 $m^3\ kg^{-1}$, whereas higher K_d values were found in more organic soil matrices such as clay gyttja and peat (up to 26 $m^3\ kg^{-1}$). The accumulation of organic matter in these soil types is related to lower redox potential so these differences are consistent with the general understanding of the biogeochemistry of Mo and the accumulation of Mo that has been observed in such environments in the site investigations (Section 14.3.4). The low K_d values in the till and glacial clay would support the view that Mo mainly is present as molybdate in these soils, whereas there is a preferential accumulation – and quite possibly reduction – of Mo in more organic layers, i.e. in lake sediments and wetlands. The measured K_d values therefore seem to reflect the redox behaviour of Mo, which is central to predicting the fate of Mo in the surface environment.

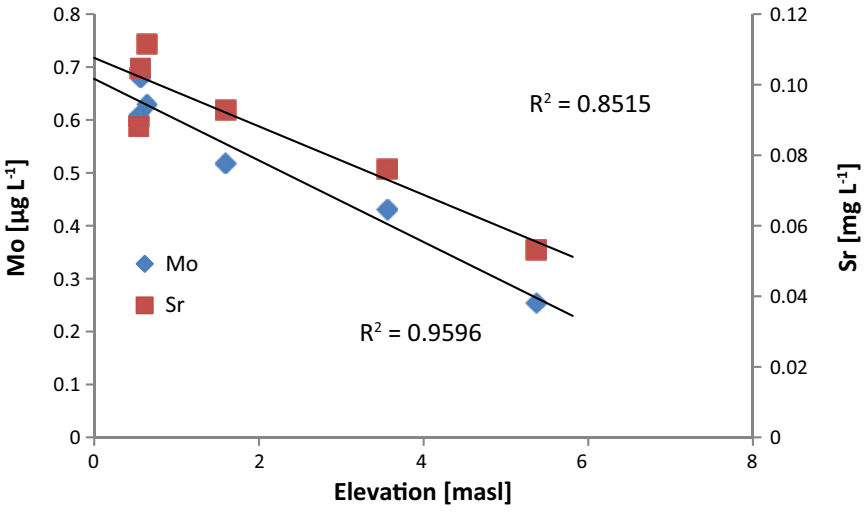

Figure 14-16. *Average concentration of Mo and Sr in lakes in the Forsmark area as a function of the lake elevation (metres above current sea level). The elevation is related to the age of the lakes.*

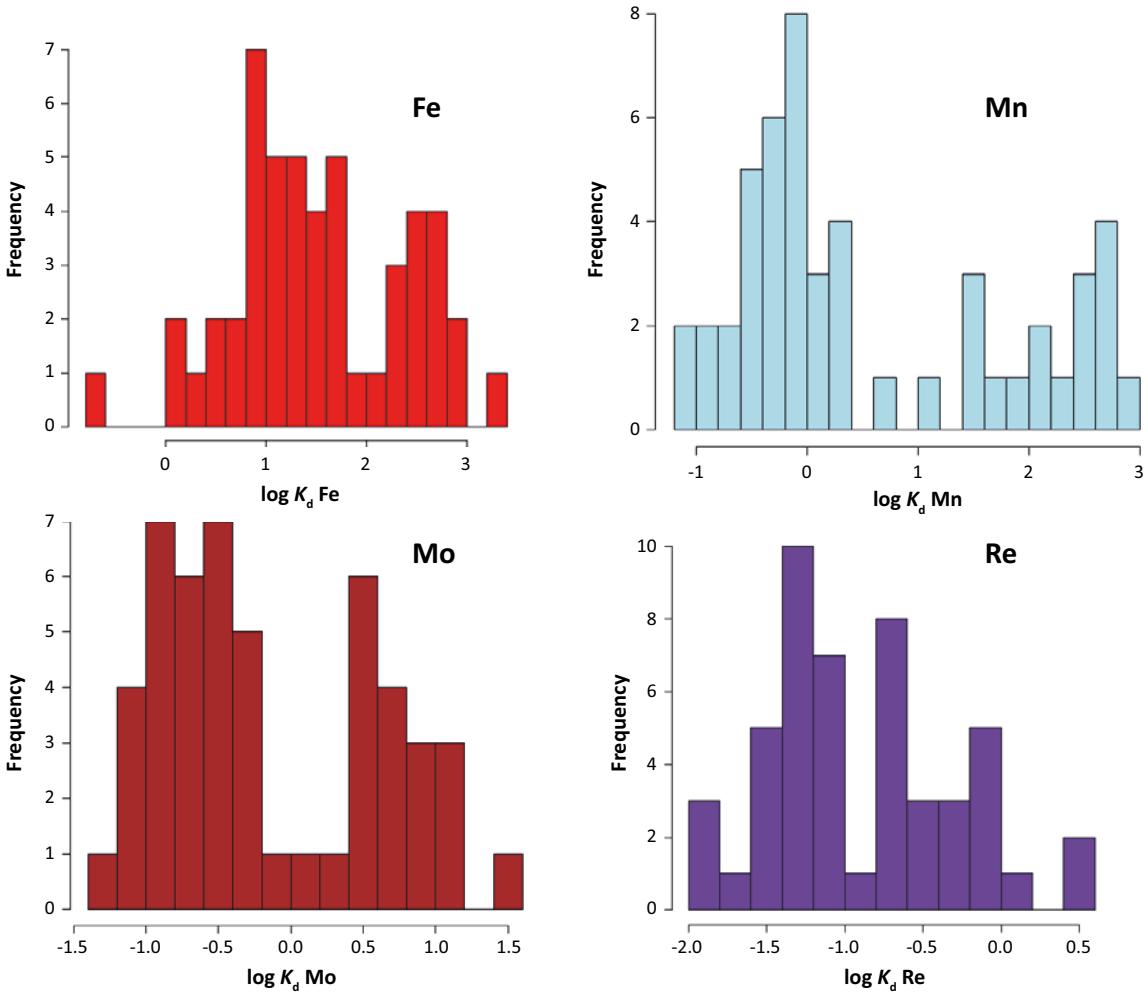

Figure 14-17. *The log K_d values for Mo exhibit a bimodal distribution, which probably is related to its redox properties (data from Sheppard et al. 2011).*

The variation in the K_d values for Mo did not closely resemble that of any other analysed element, which may be explained by it special redox properties, but the bimodal distribution was a tendency Mo shared with several other redox-sensitive elements with large expected differences between the dominating oxidation states, e.g. Fe, Mn and Re (Figure 14-17).

14.3.7 Mo in biota

In animals from terrestrial, marine and freshwater environments, Mo concentrations ranging from < 0.01 µg g_{DW}^{-1} to 1.34 µg g_{DW}^{-1}, have been reported from the site investigations. The variability partly reflects different analytical procedures, for instance analyses of whole bodies vs. just muscles or shells, or total digestion vs. dissolution. The highest concentrations were observed in mussels (*Anodonta* sp. and *Mytilus edulis*) (Hannu and Karlsson 2006, Engdahl et al. 2006). Mo in animals broadly followed the same trend as W, which also tends to occur as an oxyanion (Figure 14-18).

In primary producers, Mo concentrations ranging from 0.01 µg g_{DW}^{-1} in wood samples from Norway spruce (*Picea abies*) to 18 µg g_{DW}^{-1} in an algal mat in a lake have been reported (n=106; Hannu and Karlsson 2006, Kumblad and Bradshaw 2008, Sheppard et al. 2011). The latter represents an environment not unlike the sediments in Stocksjön, so it is uncertain whether this really represents biological uptake (Figure 14-15). High Mo concentrations have also been reported for marine macrophytobenthos (10.7 µg g_{DW}^{-1}), roots from trees (5.7 µg g_{DW}^{-1}) and waterlilies (*Nymphaeaceae* sp.; 4.6 µg g_{DW}^{-1}). As was noted for Ni, these samples are characterised by high concentrations of metals like Ti, Zr and Al, which makes it likely that there were mineral particles present in the samples. As in the animal samples, there was a correlation between Mo and W, which also occurs as an oxyanion ($r=0.90$, $p < 0.01$).

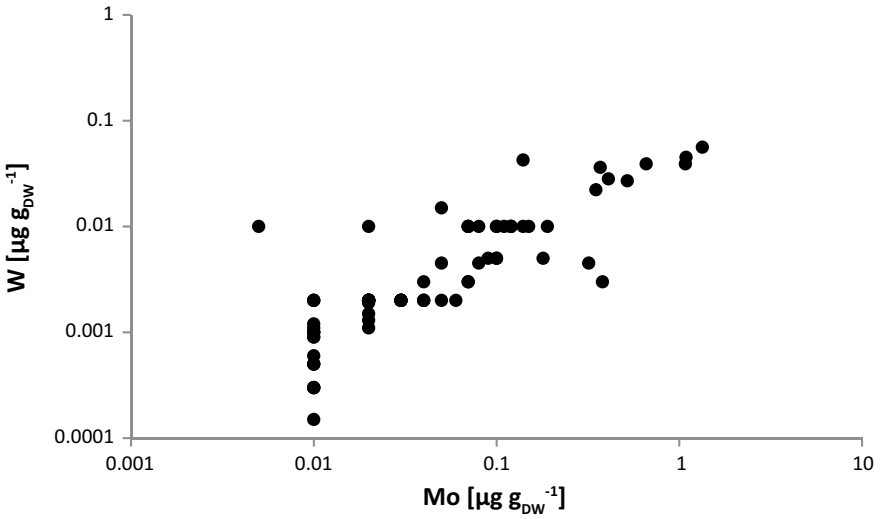

Figure 14-18. *Mo and tungsten (W) concentrations in animal samples from Forsmark and Simpevarp. The assemblages of observations at certain levels reflect the analytical difficulties of measuring Mo and W in these matrices. Observations below the reporting limits are plotted at half the value of the reporting limit.*

15 3D modelling of radionuclide transport in regolith

15.1 Introduction

The safety evaluation of potential radionuclide migration from the SFL repository relies on computationally efficient compartment models where the spatial heterogeneity of the regolith system is greatly simplified. Distributed numerical models with a higher spatial resolution and a more detailed representation of transport and chemical processes are computationally very expensive but can provide qualitative and quantitative understanding of retention and transport in heterogeneous systems. Insights from this kind of detailed modelling can be used to inform structural improvements, to justify process simplifications and to extract and select reasonable parameters for the compartment models used for safety assessments.

In the next section, results from ongoing studies of transport pathways and patterns of radionuclide accumulation are summarised. The results were derived from two different distributed transport model approaches. Both approaches were based on distributed three dimensional (3D) models that were implemented in COMSOL Multiphysics (COMSOL 2015). In the first approach chemical reactivity was simulated based on linear sorption (i.e., K_d-based sorption) and radioactive decay. This *distributed K_d model* involved a moderate computational cost and could therefore be run at the basin scale to gain a better understanding of object-specific patterns of radionuclide transport and accumulation. In the second approach, retention was broken down into individual processes (including cation exchange, surface complexation or precipitation of solid solutions) which were explicitly modelled by linking Comsol to the PHREEQC chemical toolbox (Nardi et al. 2014). This *distributed reactive model* involved a high computational cost and was therefore run only for a smaller domain. Model results from the distributed reactive model were used to assess the importance of individual retention processes as well as to evaluate in how far the mechanistically modelled retention resembled empirical estimates of retention.

The later section examines to what extent a stylised *compartment model* can capture spatially averaged values of accumulated activity and environmental activity concentrations simulated by the distributed K_d model. Chemical reactivity in the compartment model was simulated as in the distributed K_d model (i.e., based on linear sorption and radioactive decay). In the example presented, features from detailed spatial modelling of a heterogeneous system were used to inform the structures of the stylised compartment model and to derive aggregated parameters. Adjustments to the compartment model were made iteratively by comparisons with the results from the distributed K_d model.

The results suggest that compartment models can be used to calculate average concentrations at the scale of a biosphere object with reasonable accuracy, and that patterns of radionuclide accumulation can be improved if parameters are derived from the primary area of radionuclide discharge. This chapter describes the key results with respect to transport and accumulation of a few radionuclides in the regolith profile.

15.2 Distributed models of radionuclide transport

The main characteristics, assumptions and results of the two distributed models of radionuclide transport and retention in the near-surface environment are presented in this section. The two models that were implemented in COMSOL were:

1) a basin-scale model using a K_d approach to evaluate the retention of the radionuclides, hereafter described as the *distributed K_d model*; and
2) a more detailed smaller-scale reactive transport model, hereafter termed the *distributed reactive model*.

The formulation of distributed 3D models requires the implementation of the most relevant features and processes for solute transport. Data from previous SKB projects from Laxemar were used for this purpose (SKB 2008).

The Quaternary deposits in the studied area are formed by till, glacial clay, post-glacial sand, clay gyttja, and peat (Nyman et al. 2008). The top regolith surface was derived from the digital elevation model (DEM) (Strömgren and Brydsten 2008). The geometry and extent of individual regolith layers were derived from the soil depth model (Sohlenius and Hedenström 2008). Hydrological conditions were derived from Johansson and Sassner (2019). However, the chemical system used for the implementation of the regolith retention capacity was based on the geochemical model described in Sena et al. (2008) and Piqué et al. (2010, 2013) using site-specific data for the Forsmark site (Andersson et al. 2003, Tröjbom and Söderbäck 2006b, Sheppard et al. 2009, 2011).

The locations of radionuclide releases at the bottom boundary of the domains were qualitatively based on the results of particle transport simulations carried out with the regional hydrogeological model in ConnectFlow (Joyce et al. 2019).

15.2.1 Distributed K_d model

Groundwater flow and radionuclide mobility (migration, retardation and decay) were modelled for the adjoining basins of biosphere objects 206 and 210 (Figure 15-1). The processes represented in the distributed K_d (transport) model were:

- The groundwater flow under complex three-dimensional hydrogeological conditions in saturated and unsaturated conditions.
- The transport of Cl-36, Cs-135, Ni-59, Ra-226 and Mo-93 radionuclides due to advection, diffusion and dispersion.
- The retention of radionuclides in the regolith by means of linear sorption (i.e. the K_d approach).
- Radioactive decay (Mo-93 and Ra-226 only).

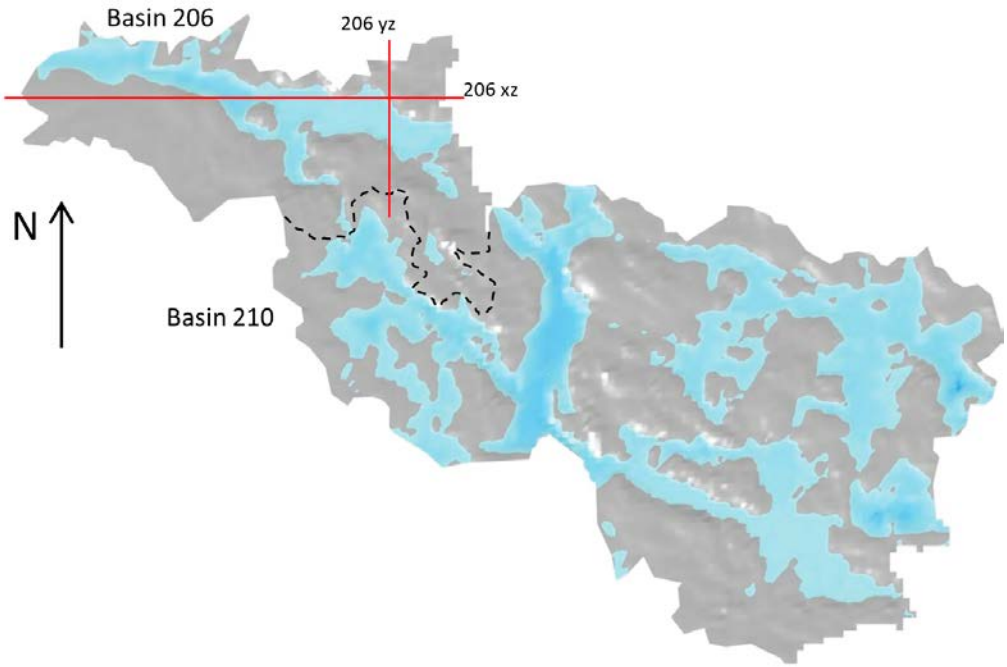

Figure 15-1. *Areas with water discharge at the ground surface of the regolith (light blue). The outside borders of the displayed domain correspond to the watershed boundaries that surround the adjoining basins 206 and 209. The dashed black line indicates the watershed divide that separates basin 206 from 210. The red lines indicate the location of the vertical 2D cross-sections (206xz and 206yz) for which more detailed graphical results are presented.*

In the simulations, a continuous flux of radionuclide-rich groundwater was supplied from the bedrock to the regolith. A flux of 1 Bq year^{-1} over 10 000 years was assumed for each radionuclide in each basin. The exit points of the repository-derived particles at the bedrock-regolith interface calculated by Joyce et al. (2019) were used to specify the locations of radionuclide inflows at the bedrock-regolith interface. The locations coincided with inflow areas associated with the presence of deformation zones in the bedrock which were in many cases below the arable land in each basin.

The K_d distribution coefficient linearly relates the mass retained in the solid phase (sorbed) to that in the liquid phase (pore water). The differences in the retention capacity within the regolith depend on the material properties and background chemical conditions (e.g. pH, Eh, and ionic composition). The K_d integrates a variety of processes and is commonly used in highly heterogeneous systems where a comprehensive characterisation of materials is lacking. The K_d values implemented in the distributed K_d model (Table 15-1) were obtained from a dataset from the Forsmark area (Sheppard et al. 2009, 2011). A comparison with Laxemar K_d values in the same regolith materials demonstrated a reasonable agreement between the two sites (Tröjbom et al. 2013).

Table 15-1. K_d (m^3 kg^{-1}) values for selected radionuclide in the different regolith materials. The values were selected from Sheppard et al. (2009, 2011).

Element	Peat	Clay-gyttja	Post-glacial sediments	Glacial clay	Till
Mo	0.4	5.06	0.045	0.2125	0.014
Cl	0.038	0.0114	0.0005	0.0048	0.0008
Ni	1.8	0.4551	0.13	5.0792	0.75
Ra	2	2.6	3.1	5.5	1.3
Cs	4.5	30	0.53	170	11

Groundwater flow within the regolith system was found to be complex and heterogeneous, largely depending on the topography of the basins and on the distribution and hydraulic properties of the different regolith materials. For example, the spatial distribution of highly permeable post-glacial sand and low-permeable glacial clay determined the water pathways and the region where deep groundwater mixes with surface water. The glacial clay acted as an aquitard between the top and bottom regolith layers due to its low permeability and, thus, reduced the vertical connectivity. In areas with a thick glacial clay layer (i.e. at the centre of the arable lands), the main flow component in the till and post-glacial sand was horizontal from west to east. Where the clay materials thinned out (i.e. at the basins' borders), the distributed K_d model predicted high mixing between deep groundwater and groundwater from the catchment. Mixing affects the dilution and circulation of radionuclide activities through the highly permeable post-glacial sand. The predicted water pathways, therefore, strongly depend on the assumed spatial configuration of glacial clay. An example of the groundwater flow field in a cross-section is shown in Figure 15-2.

Water discharge areas were located at topographic depressions, for example at the east of basin 206 and at the south-eastern part of basin 210 (Figure 15-1). Most of the water streamlines ended at the arable lands of basins 206 and 210 (i.e. the biosphere objects). Around 10 % of the water inflow into the domain occurred through the bottom surface (i.e. the regolith-bedrock interface) where radionuclides entered the domain (Table 15-2). The remaining 90 % of the water entered the domain through the ground surface, leading to a substantial dilution of the radionuclide-rich water in the regolith. The amount of water that exits the domain through the regolith-bedrock interface is twice as large as the amount of water entering through it. Thus, the bottom boundary acts as a net sink on the basin scale.

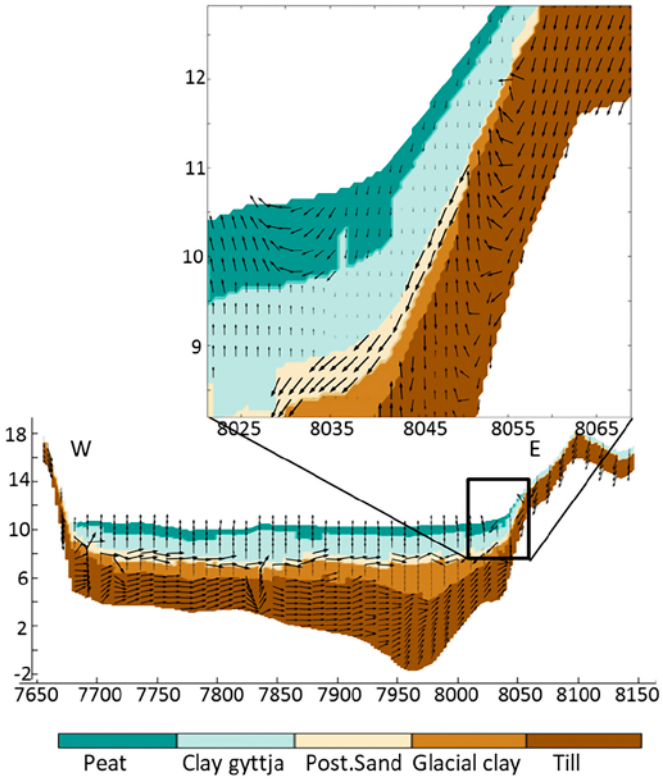

Figure 15-2. *Detail of the cross-section 206 xz (see location on Figure 15-1) showing the groundwater velocity vectors. The size of the vector is proportional to the Darcy velocity magnitude. Colours illustrate the materials. The vertical axis is exaggerated 5 times. The coordinate system of the figure and all data presented is RT90 with local references as described in figure 15-3.*

Table 15-2. Water balance of the distributed K_d model with water flows given in thousand cubic meters per year (10^3 m^3 $year^{-1}$). The outflows through the ground surface and the lateral boundaries are model outputs.

	Bottom surface		Ground surface		Lateral boundaries	
	Inflow	Outflow	Inflow	Outflow	Inflow	Outflow
Total	54.8	102	380.6	331.1		0.42
Basin 206	32.6	20.4	79.8	98.7	1.2	8.4
Basin 210	22.2	81.6	300.7	232.4	8	1.2
Object 206	18.1	0.0	11.2	82.1	66.7	13.5

Radionuclide dilution occurred when radionuclide-rich water from the bedrock was mixed with radionuclide-free water percolating from the surface or, to a limited extent, flowing from the parts of the basin that were unaffected by the release. This dilution was most pronounced in the highly permeable post-glacial sand that conveyed a substantial part of the horizontal groundwater flow. The dilution contributed to a lower activity concentration in the upper layers of the regolith (clay gyttja and peat), compared with the layers below the post-glacial sand (till and glacial clay) where water mixing and dilution was less pronounced.

The outcome of transport and accumulation processes in the regolith materials is exemplified by the distribution of Ni-59 activity (Figure 15-3). After 10 000 simulation years, the highest concentrations of dissolved radionuclides were found at the bedrock-till interface in the area where radionuclides were discharged to the till. High activity concentrations occurred in the till and glacial clay. Low activity concentrations were found in the upper layers of the regolith.

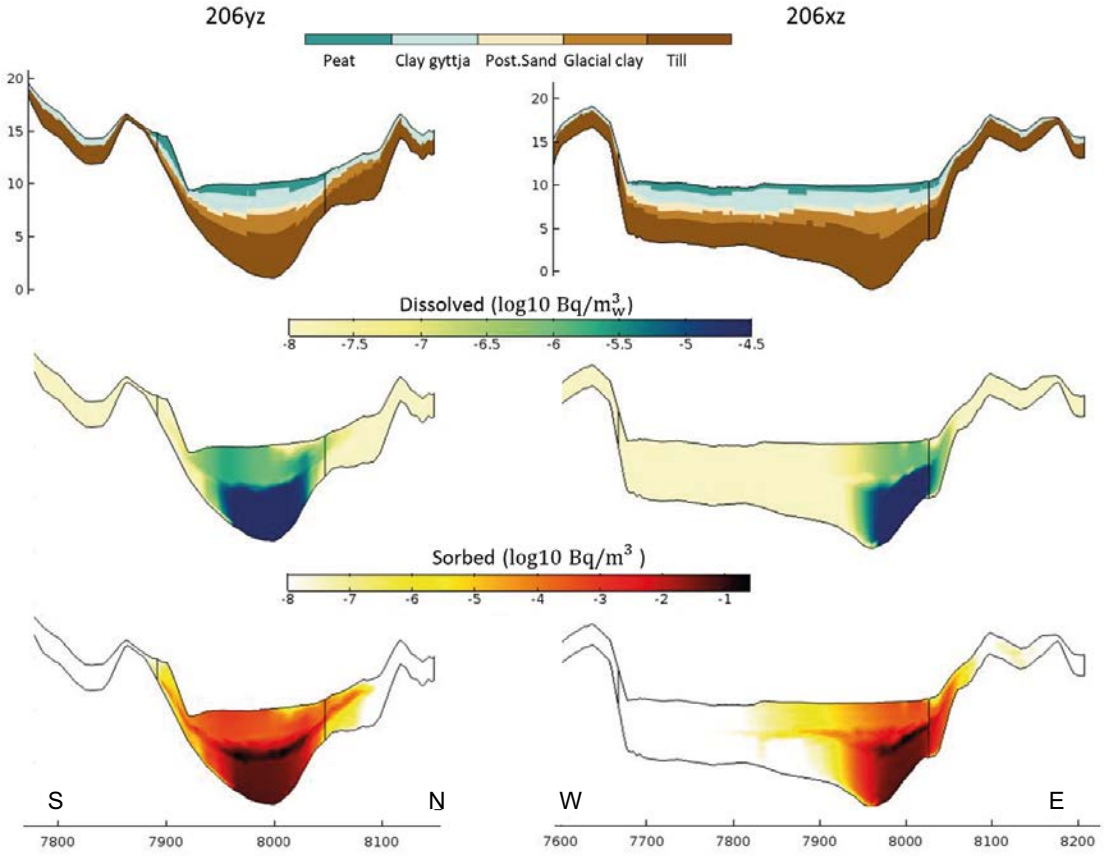

Figure 15-3. *Nickel-59 activity concentration in pore water (log_{10} Bq m^{-3}water) and sorbed (log_{10} Bq m^{-3}) at 206 yz (left) and 206 xz (right) vertical profiles in basin 206 at 10 000 years. The location of the cross-section is shown in Figure 15-1. Regolith materials are shown in the topmost panel. The vertical axis is exaggerated 5 times. Note that the concentrations are displayed in a logarithmic scale. A local reference system is used with X = XRT90−X0 and Y = YRT90−Y0, where X0 = 1 539 000 m and Y0 = 6 360 000 m.*

The glacial clay (located above the till) acted as a natural barrier and slowed down the advective migration of radionuclide in the biosphere. For all studied radionuclides except for Mo-93, glacial clay was the regolith layer with the highest potential for sorption (Table 15-1). For Ni-59 the distribution coefficient was almost forty times higher in glacial clay than in till, and at the end of the simulation the total accumulation in glacial clay was similar to the total accumulation in the till in basin 206 (Figure 15-4). As the pore water activity concentration in the glacial clay was significantly higher than in sand (Figure 15-3), the accumulation in the clay most likely reflected vertical transport from the till (mostly by diffusion). Moreover, the large amount of Ni-59 absorbed in the glacial clay together with the mixing with uncontaminated water in the post-glacial sand, led to low nickel-59 activity concentrations and low overall accumulation (< 2 %) in the three uppermost regolith layers (post-glacial sand, clay gyttja and peat) (Figure 15-4). Although Ni-59 simulations did not reach steady state conditions in the glacial clay after 10 000 simulation years, Ni-59 concentrations in the remaining layers showed almost no variation between 5000 and 10 000 years. It can therefore be expected that a Ni-59 pattern at steady-state conditions would resemble o the pattern seen after 10 000 simulation years.

Biologically-driven incorporation into soil organic matter was not modelled in any of the three model approaches and, thus, simulated retention of chlorine was negligible. Since radioactive decay of Cl-36 was not modelled (due to its half-life greatly exceeding the simulation period) chlorine essentially acted like a transport tracer in the distributed K_d model (as well as in the compartment model): After 10 000 simulation years practically the same flow of released chlorine entering the model domain exited it again through either the surface or bottom boundary (Figure 15-4). Compared with chlorine, nickel was strongly sorbing (especially in the till and glacial clay), and thus more than 50 % of the release had accumulated in the regolith materials at the end of the simulation. Radioactive decay was not modelled for Ni but given the long half-life of this radionuclide (7.6×10^4 years) not more than 4.4 % of the release would have decayed during the simulation time even if the nickel had all accumulated in the regolith.

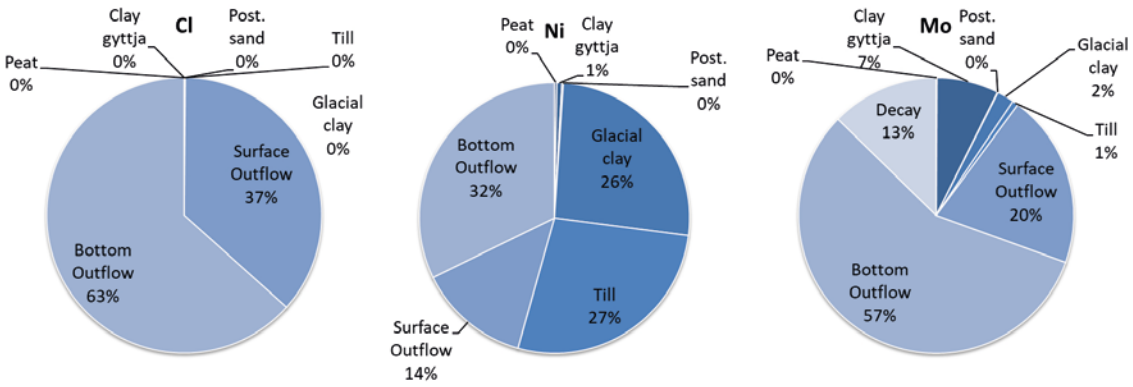

Figure 15-4. *Distribution of the total activity of Cl-36, Ni-59 and Mo-93 in the regolith materials (till, glacial clay, post-glacial sand, clay gyttja and peat) and accumulated activity that left the model domain through the ground surface (surface outflow) and the bottom (bottom outflow) at 10 000 years for basin 206.*

Molybdenum is a relatively mobile element that adsorbs in regolith layers which are rich in organic matter. The released radionuclides equilibrated relatively fast in the lower regolith layers (~ 2 000 years), and only 10 % of the released radionuclides accumulated in regolith (primarily in clay gyttja). However, as Mo-93 has a relatively short half-life (4 000 years), the retardation in regolith layers still caused 13 % of the released activity to decay along the transport pathways.

15.2.2 Distributed reactive model

The distributed reactive (transport) model of the retention processes affecting radionuclides was implemented in a smaller domain of the regolith. The model contains the part of basin 206 that concentrates most of the groundwater discharge to the biosphere (Figure 15-5).

The following retention processes (or chemical reactions, Table 15-3) are included in the distributed reactive model:

- Equilibrium reactions with siderite, pyrite and ferrihydrite.
- Precipitation/dissolution reactions with calcite and/or barite.
- Surface complexation of several ionic species into the surface of illite and ferrihydrite.
- Cation exchange reactions on illite surfaces.

Table 15-3. Initial mineralogical and aqueous compositions of the regolith materials.

Materials	Minerals in equilibrium	Solid-solutions	Exchanger	Surface complexation
Clay gyttja-peat	Siderite/Pyrite	Calcite/Barite	Illite	Illite
Post-glacial sand	Siderite/Pyrite	Calcite/Barite	-	-
Glacial clay	Siderite/Pyrite	Calcite/Barite	Illite	Illite
Till	Siderite/Ferrihydrite	Calcite/Barite	Illite	Illite/Ferrihydrite

Reactive transport models require well substantiated conceptual models of the chemical reactions affecting the mobility of a given radionuclide supported by thermodynamic data and by a good description of the geochemical background conditions. For Sr and Ni these criteria were judged to be reasonably fulfilled with respect to conditions in the bedrock and some geological materials. However, interactions with organic matter were not explicitly represented at this early-stage model, and thus the simulations of the mobility of Sr and Ni in the upper regolith profile (clay-gyttja and peat) are not meant to be realistic.

In the simulations, a flow of radionuclide-rich groundwater was considered to enter the model through more than half of the bottom boundary (bedrock/regolith interface) (Figure 15-5). The concentrations of repository-derived strontium and nickel in deep groundwater were calculated by assuming equilibrium with solubility limiting phases of a reference water (Duro et al. 2006).

Following the groundwater flow paths, radionuclides reach the surface in the southern and south-eastern parts of the domain roughly corresponding to two thirds of the area where radionuclide-rich water was released (Figure 15-6). However, the amount of the release that reaches the surface and the locations of the maximum radionuclide concentrations depend on the properties of the radionuclides.

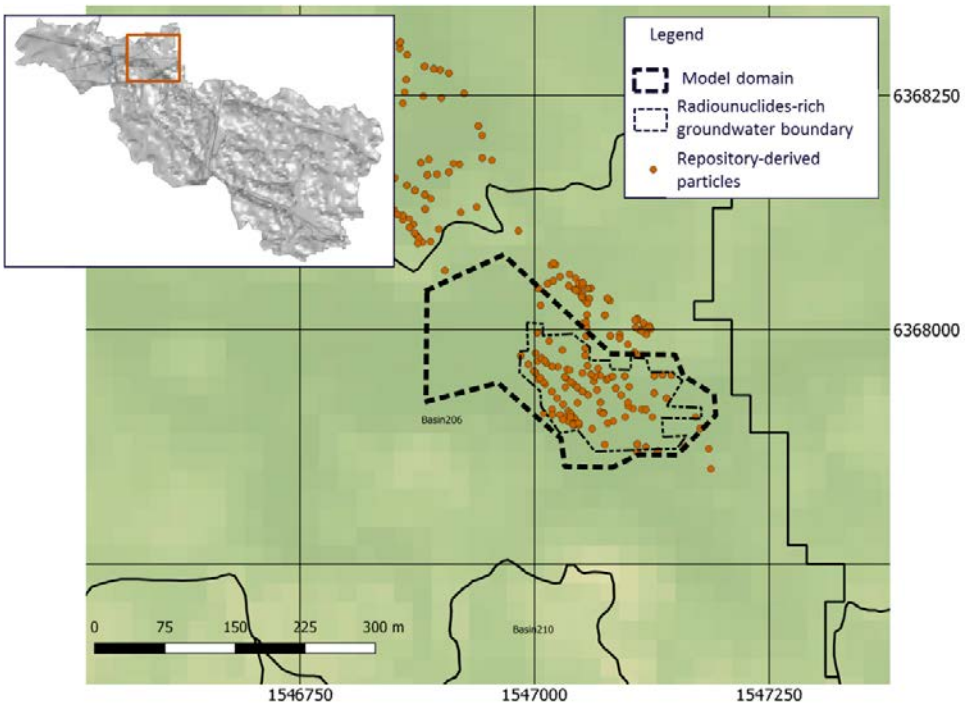

Figure 15-5. *Area where radionuclide-rich groundwater enters the distributed reactive model at the regolith/bedrock interface. The boundary of the model domain and exit points of repository-derived particles (from ConnectFlow model, Joyce et al. 2019) are shown for reference.*

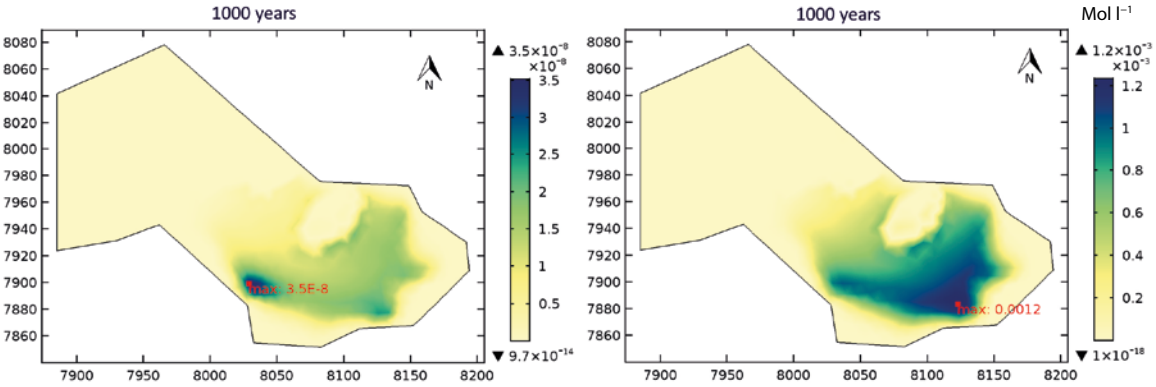

Figure 15-6. *Dissolved repository-derived (RD) nickel (left) and strontium (right) at the ground surface of the model after 1 000 year. The maximum concentration location and value is plotted in red. The concentrations of repository-derived Ni and Sr in the deep groundwater entering the bottom boundary were* 4.16×10^{-7} *mol* l^{-1} *and* 1.56×10^{-3} *mol* l^{-1}*, respectively.*

Most of the repository-derived Ni was strongly retained in the regolith, and less than 8.5 % of the Ni entering the domain reached the surface. On the contrary, (repository-derived) Sr migrated relatively fast through the regolith and 77 % of the released radionuclide reached the surface. Surface complexation within and onto illite was the most effective mechanisms for the retention of Ni, whereas exchange onto illite was the dominant process for retention of Sr. Thus, both radionuclides were primarily retained in layers postulated to have high contents of illite (glacial clay and clay gyttja-peat).

In this study, it has not been possible to simulate retention onto or into organic matter with the distributed reactive modelling approach. Thus, layers in the lower regolith profile (containing little or no soil organic matter) are better suited for a comparison between modelled and empirical estimates of retention than the surface layers. For Ni, the mechanistically calculated relationship between solid and solute concentrations (i.e. the apparent K_d) resembled that of the measured K_d, with the highest degree of sorption in the glacial clay (Table 15-4). For the glacial clay layer, the best-estimate for the measured K_d value fell between the maximum and average values of the reactive modelling approach. However, in case of till the measured K_d value exceeded the maximum value simulated by the distributed reactive model. The results suggest that the importance of some retention processes in the till has been underestimated in the reactive model. This could, for example, be due to important retention mechanism being missing in the prescribed geochemistry of the system and/or that the assumed amount of illite and ferrihydrite does not match the characteristics of the soil samples used for the K_d measurements. The spatial variation of the apparent K_d was noticeable (Table 15-4). However, for Ni the apparent K_d was similar to the average in most of the model domain, and deviations were constrained to the interphase between regolith layers and to the boundary of the model, suggesting local disequilibrium with the inflowing water. The overall results suggest that a systematic conceptual and numerical calibration between empirical K_d values and mechanistically calculated values (under relevant geochemical conditions) should be undertaken prior to mechanistic reactive model simulations in future work. Such a calibration would facilitate the interpretation of results, allowing a separation of the effects of reactive transport from those emerging from differences in the description and representation of retention processes.

Table 15-4. Calculated and measured K_d values (m^3 kg^{-1}) for Ni. The value calculated with the distributed reactive model (apparent K_d) corresponds to the final simulation time.

Regolith layer	Apparent K_d		Measured K_d
	Avg.	Max.	
Clay gyttja/peat	1.5	4.3	0.46/1.8
Post-glacial sand	-	-	0.13
Glacial clay	0.49	11.9	5.08
Till	0.07	0.12	0.75

15.3 Capturing average results with a stylised compartment model

In SE-SFL, compartment models were used to calculate environmental concentrations that result from transport and accumulation of radionuclides in potential discharge areas (Chapter 8). In these compartment-based models, each regolith layer was represented by one (or a few) homogenous compartments. As biosphere objects typically located in a discharge area, and the horizontal extent of the area is orders of magnitude larger than the regolith depth, transport within the object was assumed to be sufficiently described by its vertical component (Werner et al. 2013). The models were parameterised primarily with data from the Laxemar area, and regolith depth and groundwater flows were summarised as averages across the discharge areas (i.e. biosphere objects).

In this section, we examine to what extent a compartment model can capture the result of transport and accumulation processes in a heterogeneous area. This is done by comparing results from a stylised compartment model with those from the distributed K_d model simulating the same area. The structure of the stylised compartment model, the selection of parameters and the spatial extent of the modelled area, all have the potential to influence the results. Thus, an iterative approach (two such iterations are used below) appears to be reasonable for making informed simplifications and to derive a suitable structure and parameterisation of the stylised compartment model . However, it is also recognised

that distribution of the geosphere release, the physical configuration of the examined area, and the properties of the studied radionuclides may all influence to what degree simplifications in a stylised compartment model are justifiable. Thus, the exercise should primarily be seen as an example of a methodology under development.

The first step taken in this example was to deduce a structure for a stylised compartment model from the regolith stratigraphy in object 206 (outlined in green in Figure 15-7). Next, vertical groundwater flows across regolith boundaries within the object were extracted from the distributed K_d model (Section 15.1.2.1). Transport and accumulation of radionuclides were then simulated with the stylised compartment model, and results were compared with those from the distributed K_d model. However, the postulated geosphere release was localised in an area (blue area in Figure 15-7) that is substantially smaller than biosphere object. Thus, in a second iteration the above steps were repeated for a smaller area (outlined in red in Figure 15-7), for which the derived parameters for regolith depth and groundwater flow presumably gave a better (geographic) representation of the flow pathways and accumulation of discharged radionuclides.

In the stylised compartment model, solute transport by advection and diffusion was implemented as in BioTEx model (Chapter 8) and in previous SKB safety assessments, described by Saetre et al. (2013b). Parameter values for linear sorption (Table 15-1), bulk density, porosity and effective diffusivity (Table 15-5) were, however, chosen to be identical to those in the distributed K_d model to make the model results more comparable. For the same reason, and contrary to the BioTEx compartment model (Chapter 8), organic matter reactions were not modelled in the stylised compartment model in this section. The average regolith depth (Table 15-6) and the gross groundwater flux parameters for the stylised compartment model were directly extracted from the distributed K_d model (see below). One Becquerel per year was released to the till (RegoLow) in the stylised compartment model and the released radionuclides were not allowed to leave the model through the till/bedrock boundary. The simulations were run for 10 000 years, and the results compared to those from the distributed K_d model. The presentation below is focused on accumulation patterns of Mo-93, but similar calculations were also performed for Ni-59.

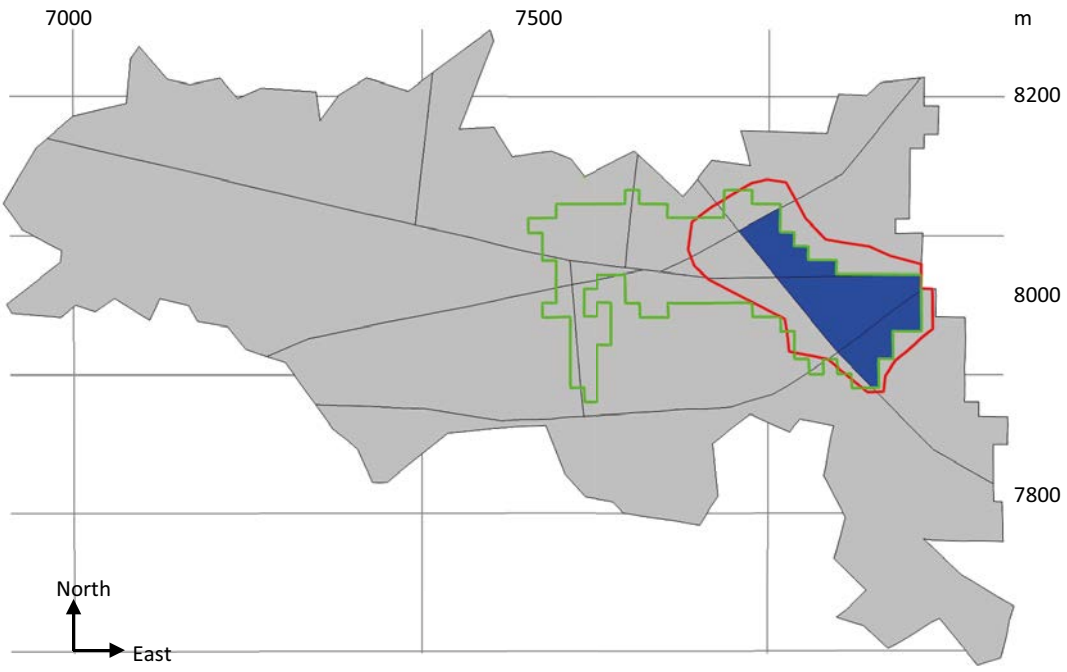

Figure 15-7. *Areal extent of landscape features of interest for comparing the results from a stylised compartment model with that of a distributed model. The extent of the Basin 206 (approximately the local watershed of object 206) is shown in grey and the footprint of the area where radionuclides enter the regolith (at the bedrock interface) is shown in blue. The area of object 206 (presently cultivated land) is outlined in green, and the identified area affected by radionuclides is outlined in red (i.e. the discharge area). The dark grey lines represent the deformation zones in the underlying bedrock.*

Table 15-5. Material properties for regolith layers.

	Effective Porosity	Bulk density (kg_{pw} m^{-3})	Effective diffusivity for Mo (m^2 $year^{-1}$)
Peat	0.24	240	7.63×10^{-3}
Clay gyttja	0.03	670	9.5×10^{-4}
Post-glacial sand	0.25	1400	7.9×10^{-3}
Glacial clay	0.25	1300	7.9×10^{-3}
Till	0.05	1400	1.6×10^{-3}

15.3.1 Object 206

Object 206 has a surface extent of 8×10^4 m^2 and an (area-weighted) average regolith depth of 5.9 m (Table 15-6). It represents an area that is presently under agricultural use. The stratigraphy of the object suggest that the area has been a mire (formed in a lake basin), which has been drained and cultivated in the past. In the distributed K_d model, the regolith layers in this area are fully saturated (Figure 15-1) and in the simulations the object thus represents a wetland area with a pronounced discharge of groundwater (Figure 15-3). This kind of ecosystem is highly relevant in the context of radiation protection, as exposure from cultivation after long-term accumulation is expected to be substantially higher than from other evaluated land-use types.

In a compartment modelling approach, radionuclides are assumed to by homogenously distributed in each compartment. This is a reasonable assumption when the release occurs more or less homogenously throughout the object. However, in the distributed K_d model the release was localised to the eastern part of object 206 (Figure 15-7), and large parts of the object received very small fractions of the geosphere release (Figure 15-3). Thus, a model comparison at the scale of a biosphere object is not expected to yield environmental concentrations that are representative of the area with the highest activity. However, the present agricultural land, located on top of a former lake basin, represents an easily recognisable feature in the landscape (that can be identified without information on the postulated geosphere release), and the mire is a well characterised ecosystem. Consequently, the outlined biosphere object represents the unit that SKB traditionally has used to assess the long-term safety after repository closure (and which applies also to SE-SFL). Equally important, the size of object 206 (~ 8 ha) is also reasonable with respect to plausible land-use that results in a relatively high exposure. That is, the object is a unit that can be (and has been) drained and cultivated, and the resulting land has the potential to support a few self-sufficient families practicing traditional small-scale agriculture (Saetre et. al. 2013a). Thus, the average radionuclide concentrations in regolith layers in the former lake basin are highly relevant and meaningful in the context of the safety assessment.

The stratigraphy in object 206 is composed of five regolith layers with variable thickness and geometry (Figure 15-2). Maps of the regolith thickness show that three of five layers do not cover the outlined object fully (i.e. the glacial clay, the post-glacial sand and the peat layers are missing in the south east part of the object, Figure 15-8). Consequently, flow pathways that short-circuit the typical stratigraphy (e.g. discharge from till to clay gyttja) have been implemented in parallel with the main flow pathway in the stylised compartment model. Nevertheless, the main flow pathway was discharge of groundwater from till towards the surface through the typical regolith layers sequence (till → glacial clay → sand → clay gyttja → peat)[37] which was primarily driven by vertical (26 %) and horizontal (45 %) discharge into the till, from the bedrock and the surrounding basin, respectively.

[37] In the BioTEx model there are no short-cuts in the flow pathway, and transport follows the typical flow pathway (Figure 8-1).

Table 15-6. Geometrical parameters transferred from the distributed K_d model to the stylised compartment model.

	Object 206		Radionuclide discharge area	
	Area (m²)	Average thickness (m)	Area (m²)	Average thickness (m)
Peat	47 660	0.66	32 872	0.71
Clay gyttja	79 547	1.21	54 632	1.12
Post-glacial sand	65 278	0.57	40 477	0.56
Glacial clay	68 435	0.95	43 661	0.97
Till	79 547	2.99	54 632	2.79

The spatial distribution of aqueous activity concentration of Mo-93 after 10 000 years of simulation with the distributed K_d model is given in Figure 15-9 (left panel). Seen from above, the aqueous concentration is reduced towards the surface, presumably due to an increasing dilution with uncontaminated groundwater with the largest shift between the glacial clay and the sand layer. Moreover, the size of the area with above-average concentration is noticeably reduced in the post-glacial sand layer. This was due to a significant fraction of the transport following flow pathways outside the object (i.e. from the till directly to the clay gyttja), and thereby bypassing the glacial clay and post-glacial sand layers (i.e. in the eastern and north-eastern part of the object 206 in Figure 15-8).

As the radionuclide concentration in the solid state was assumed to be linearly related to the aqueous concentration (with the K_d value), the spatial pattern of the solid activity concentration (Bq kg_{DW}^{-1}) is directly proportional to that of the solute phase within each layer. The inventory/sorbed activity concentration (right-hand panel in Figure 15-9) is also proportional to the product of the aqueous concentration and the K_d value, but it additionally scales directly with the thickness and the density of the regolith layer. In spite of the increasing dilution towards the surface (and a relatively low bulk density), most of the accumulated Mo-93 activity was located in the relatively thick clay gyttja layer, primarily reflecting its strong sorption properties for Mo (Table 15-1).

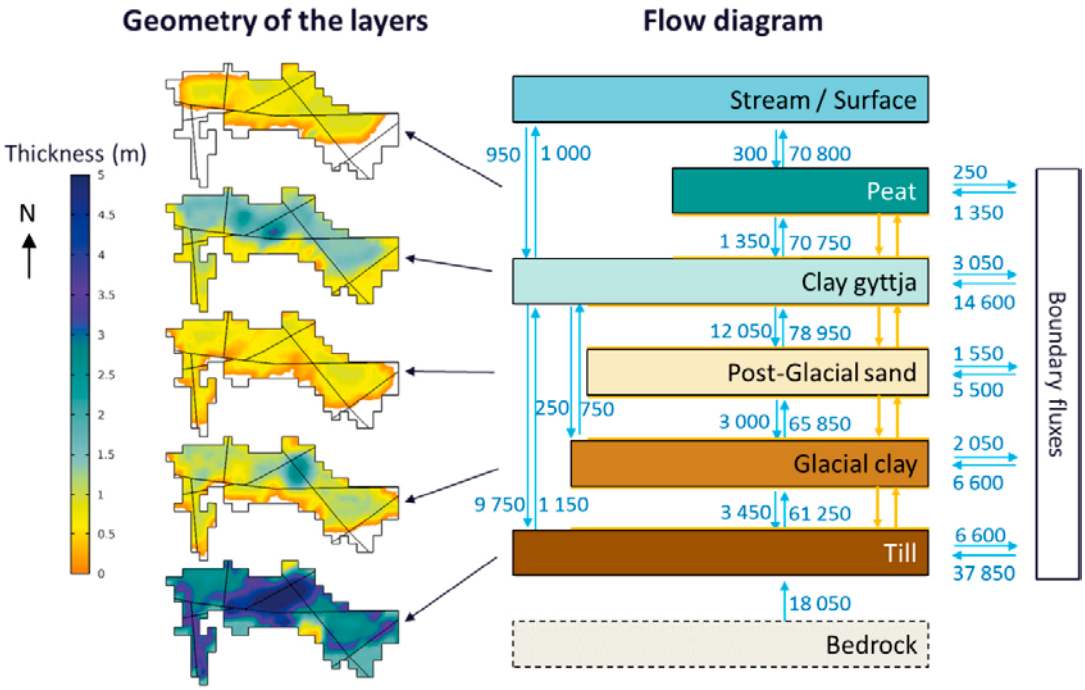

Figure 15-8. *Thickness of the regolith layers in object 206 (left) and gross groundwater flow (m^3 $year^{-1}$) between the layers. The structure of the flow diagrams corresponds to that of the stylised compartment model. That is, each regolith layer was represented by one compartment, and advective transport between the layers was proportional to groundwater flow (vertical blue arrows). However, in the stylised model horizontal exchange of groundwater across the boundary (i.e. the horizontal blue lines) was excluded, and diffusion (yellow arrows) was limited to the major contact areas between adjacent regolith layers (yellow lines) only.*

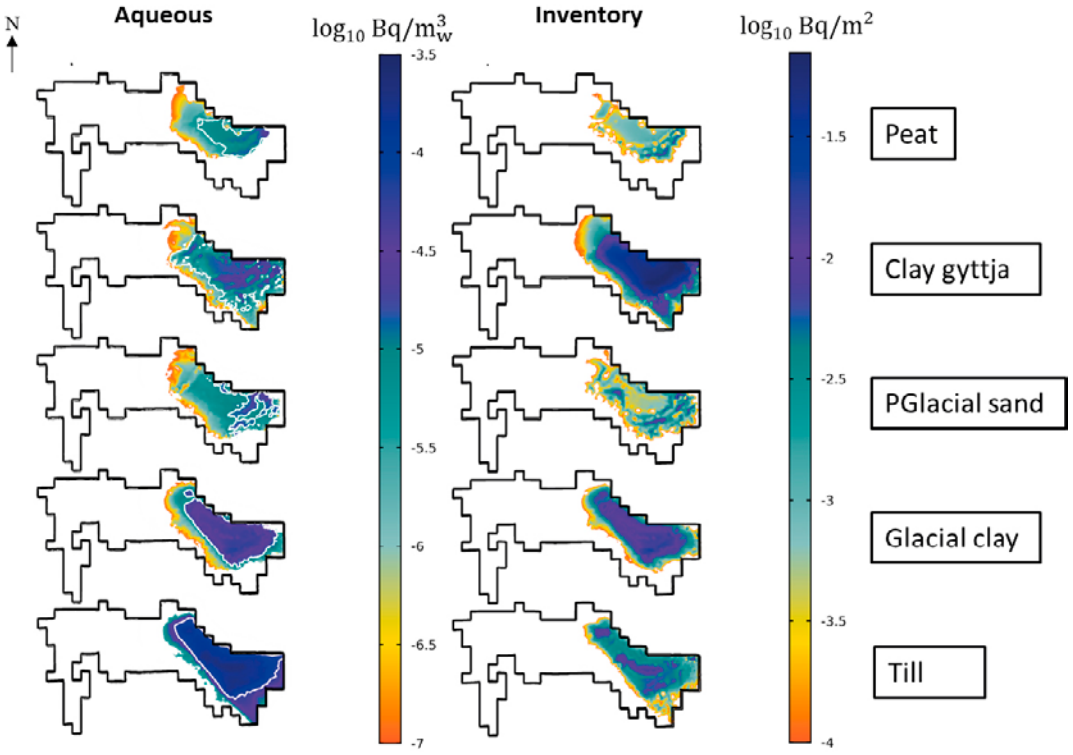

Figure 15-9. *Spatial distribution of Mo-93 aqueous activity concentration (Bq m_w^{-3}) (left) and sorbed activity concentration per unit area (Bq m^{-2}) (right) in the regolith materials after 10 000 years in object 206. The aqueous concentration is the average concentration of the regolith layers. Note that aqueous values below 1×10^{-7} (Bq m^{-3}) and sorbed values below 1×10^{-4} (Bq m^{-2}) are not plotted in the figure. The white lines in aqueous Mo-93 show the average concentration of Mo. Note that concentrations are displayed on a logarithmic scale.*

The overall patterns of increasing dilution towards the surface and of preferential accumulation in clay gyttja, and to a less degree also in glacial clay, are captured by the compartment model (Figure 15-10). However, the time that it takes to approach steady-state conditions appears to be accelerated in the stylised compartment model, partly reflecting an unrealistic numerical dispersion introduced by the assumption of spatial homogeneity within compartments. It is also noticeable that the compartment model (parameterised with average properties of the object) over-estimates the pore water concentration in sand and the accumulation in the clay gyttja predicted to occur in the distributed model.

Quantitative comparisons are hampered by the fact that a fraction of the radionuclides that are released to the till in the distributed K_d model are subsequently lost through the lower boundary of the model domain primarily through dispersion. Over the entire simulation period, 57 % of the geosphere release is lost back to the geosphere close to the area of the release, and therefore the concentrations and the inventory predicted in the distributed model are scaled by division with the remaining release (~ 0.43 Bq $year^{-1}$) to provide a less biased comparison[38].

The inventories (and the concentrations) in the two lowermost layers appear to be under-estimated by approximately a factor of two in the stylised compartment model. Although the cause for this difference has not been examined in detail, there are several factors that may contribute to the lower accumulation in the compartment model: i) the implementation of advective transport in the compartment model may systematically overestimate dilution[39], ii) the transport time through the regolith compartment is not explicitly accounted for, iii) differences in groundwater fluxes between the area where

[38] A global scaling factor does not capture temporal and spatial variations with respect to the loss of activity and may thus introduce some systematic errors. Nevertheless, the scaling was considered appropriate for model comparisons at this stage.

[39] In the stylized compartment model the flows at the regolith boundaries are used to characterize the flow through the whole layer. This approach will overestimate dilution in the lower sections of the layer when the upward flux increases towards the surface (see Chapter 9).

radionuclides are discharged and the rest of the object[40] may overestimate dilution, and iv) average characteristics may yield an insufficient representation of transport and decay in a heterogeneous discharge area[41].

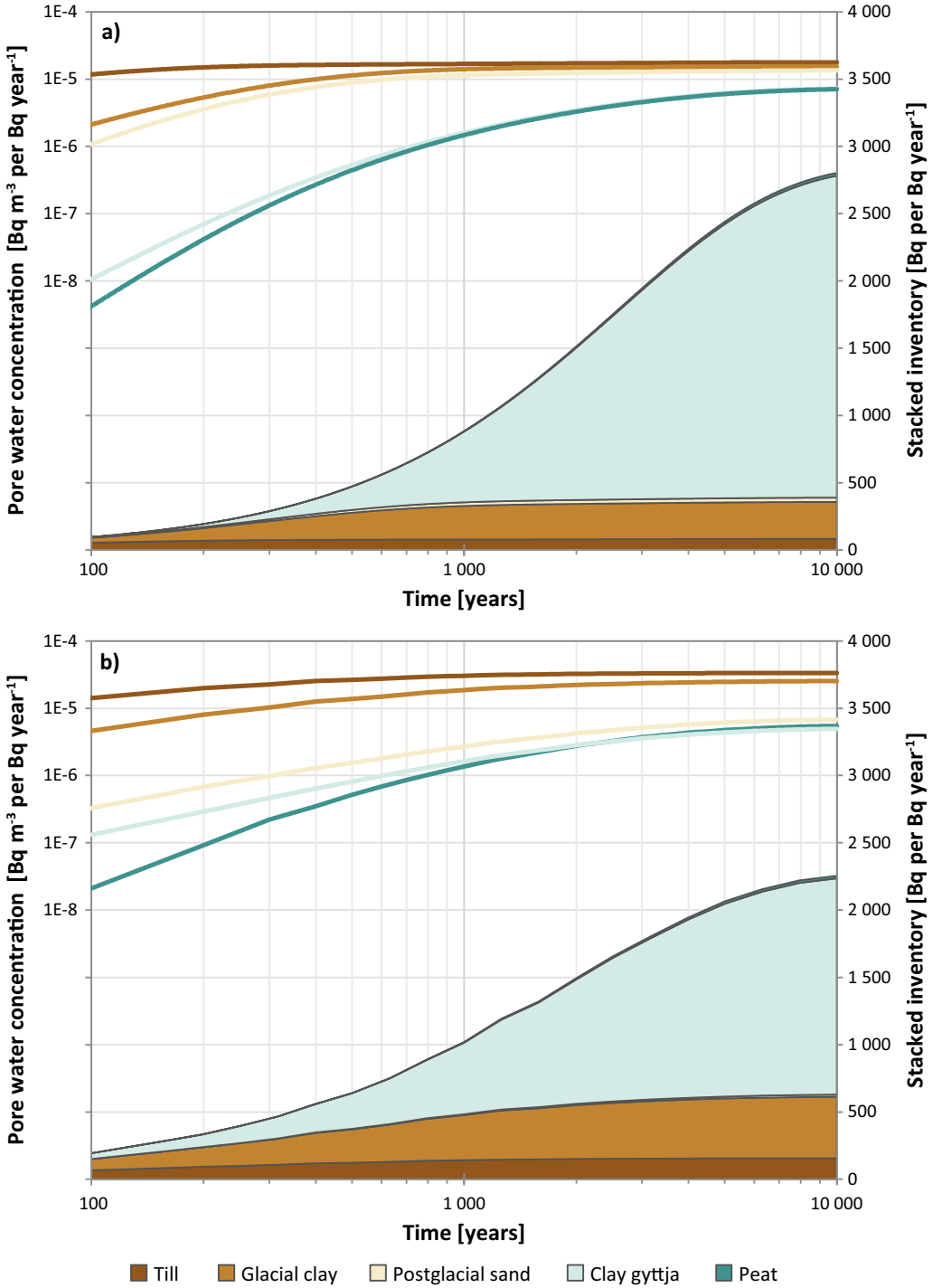

Figure 15-10. *Inventory and pore water concentration of Mo-93 in the regolith layers as a function of time for the stylised compartment model (a) and the scaled distributed K_d model (b) for object 206. Note that the pore water concentration is expressed on a logarithmic scale (left axis) while the inventory is expressed on the original (untransformed) scale (right axis).*

[40] Groundwater flux (m³ per m² and per year) is on average somewhat higher in the parts of the object where there is no transport of radionuclides and thus the properties at the object level will overestimate dilution.

[41] When the transport of radionuclides is not evenly distributed across flow pathways, average flow characteristics can either over- or under-estimate the effects of dilution and radioactive decay.

The concentrations of the two uppermost regolith layers were more similar between the two models, and the inventories (and concentrations) of the clay-gyttja and the peat layers were approximately 40 % higher in the compartment model as compared with the distributed K_d model. However, the compartment model could not capture the relatively low concentrations of radionuclides in the sand layer that were apparent in the distributed K_d model, and the estimated concentration in the compartment model was more similar to that of the lower regolith layers than to that of the upper regolith profile.

At first sight, the comparison of model results above can be seen as a relevant example of how assumptions of a fairly homogenous release of radionuclides into an easily identified landscape feature may bias estimates of radionuclide accumulation in a heterogeneous object where the radionuclide release is localised to a part of the object. However, since the results are derived from two very different models, the effects of the assumption that radionuclides are homogenously released to the object (iii) are confounded with the effects of other factors (i, ii and iv). Thus, to better understand the drivers of observed differences at the object scale, model comparisons were repeated at the scale of the discharge area (see next section).

15.3.2 Radionuclide discharge area

The results from the distributed K_d model simulations showed that radionuclide accumulation was not restricted to object 206, nor was the accumulation homogenous within the boundaries of the object. For example, almost half of the biosphere object had very low pore water concentrations of Mo-93 (below 1×10^{-7} Bq m^{-3}, white areas in Figure 15-9) and relatively high concentrations were expected north-east outside the object boundary. To better capture the average characteristics of the primary area for accumulation, a discharge area was outlined. In practice, this area was a modest expansion of the bedrock release area (Figure 15-7). The surface extent of the discharge area was approximately 70 % of the original biosphere object size (~ 5.5×10^4 m^2) with an average regolith thickness which was slightly reduced (6 %) as compared with that of the original object 206 (~ 5.5 m).

According to the simulations with the distributed K_d model (Section 15.2.1), the accumulation of radionuclides outside this area was limited. This was expected as the discharge area fully covered the bedrock release area and little groundwater left the discharge area horizontally (Figures 15-7 and 15-11). The inclusion of the area north-east of the original object resulted in a small increase in the accumulation of radionuclides in the discharge area (5-18 %) as compared with that in the original object 206 (right-hand axis on lower panels in Figures 15-10 and 15-12). However, as the area (and volume) was 30 % smaller, the average activity concentrations increased accordingly. Taken together, this resulted in a 60 % higher average activity concentration of Mo-93 in till, glacial-clay and peat. In clay-gyttja and sand, where the area of the regolith layers were more reduced in the discharge area (Table 15-6), the differences in activity concentrations were somewhat larger (i.e. it was 70–85 % larger in the discharge area than in object 206).

The overall flow pattern of groundwater in the discharge area was similar to that of object 206 (as evident from Figures 15-8 and 15-11), but the flows of water were almost halved in the discharge area. The reduced flow was partly due to the smaller area (see above) and partly due to a lower area-specific flow (i.e. the net groundwater flux was reduced by approximately 30 % in the discharge area, as compared with the original object). However, the inclusion of the north-east area increased the flow from till to clay-gyttja and led to a larger exchange of water between the three lowermost layers, probably driven by thin or absent glacial clay and sand layers in the area. As parameters describing the flow of groundwater in the compartment model were directly derived from the water balance, these differences have a potential to affect the accumulation of radionuclides in the compartment model.

We first noted that a shift of regolith and groundwater parameters in the compartment model only caused a relatively small change in the accumulation of Mo-93. That is, the inventory of Mo-93 in the discharge area increased between 4 % and 19 % as compared with the object (right-hand axis on the upper panels in Figures 15-10 and 15-12). This change predicted by the compartment model was similar to the change in predicted the distributed K_d model although the underlying common cause (i.e., reduced groundwater dilution) was represented differently in the two different model approaches. Essentially, differences in release capture and bypass effects were explicitly modelled by the distributed K_d model whereas these differences translated into a change of the lumped parameter values used in the compartment model. That is, in the distributed K_d model, the discharge area

captured a larger fraction of the release, whereas the increased accumulation in the compartment model was caused by a shift in postulated properties of the modelled area. Thus, the increased inventory in the compartment model primarily reflected a lower area-specific groundwater flow (leading to less dilution) in the discharge area (see above). This effect was, however, partly offset by thinner regolith thicknesses, and the consideration that ~ 10 % of the discharge bypassed the glacial clay and sand layers. As in the distributed K_d model, the activity concentration in the discharge area increased between 60 and 85 % in the compartment model, and the primary reason for this was decreased dilution with groundwater discharging in the model area (see above).

As noted above, the compartment model has the capability of capturing the patterns of increasing dilution towards the surface and of a preferential accumulation of Mo-93 in clay gyttja (Figure 15-12). With the groundwater flows from the discharge area, the time to approach steady-state conditions was more similar to that of the distributed K_d model, reflecting circulation of groundwater in the lower section of the regolith profile, Figure 15-11. It was also noticeable that the compartment model for the discharge area has a better capability to capture the relatively low average activity concentration of the sand layer predicted by the distributed K_d model (as compared with the model for object 206). This was due to an increased contribution of less contaminated groundwater to the sand layer in the discharge area. That is, the contribution of groundwater from above (or from outside) was 20 % of the flow through the sand layer for object 206 as a whole, whereas this fraction was 40 % in the discharge area (Figures 15-8 and 15-11).

As previously mentioned, a quantitative comparison of results between the two models (compartment vs distributed) was hampered by the loss of activity to the bedrock in the distributed K_d model. Nevertheless, after correcting the results from the distributed model for the lost activity (see above), the compartment model still under-estimated the activity concentrations in the lower regolith layers. However, the deviation in steady-state concentrations was reduced from a factor of two to 60 % and 40 % in the till and glacial clay layers, respectively. For the upper part of the regolith horizon, the compartment model over-predicted the accumulated concentration by 30 % also for the discharge area case.

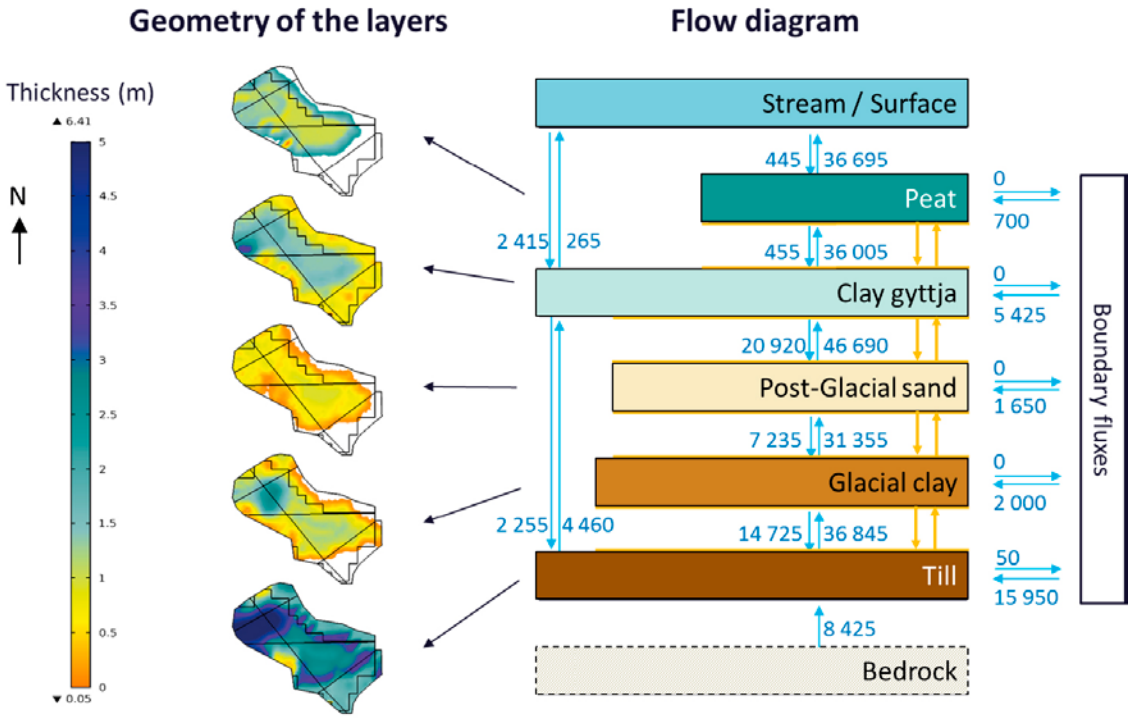

Figure 15-11. *Areas and thicknesses of the material layers in the radionuclides discharge area in object 206 (left) and total groundwater flow (m^3 $year^{-1}$) between the layers (right). The same symbols are used as in Figure 15-8.*

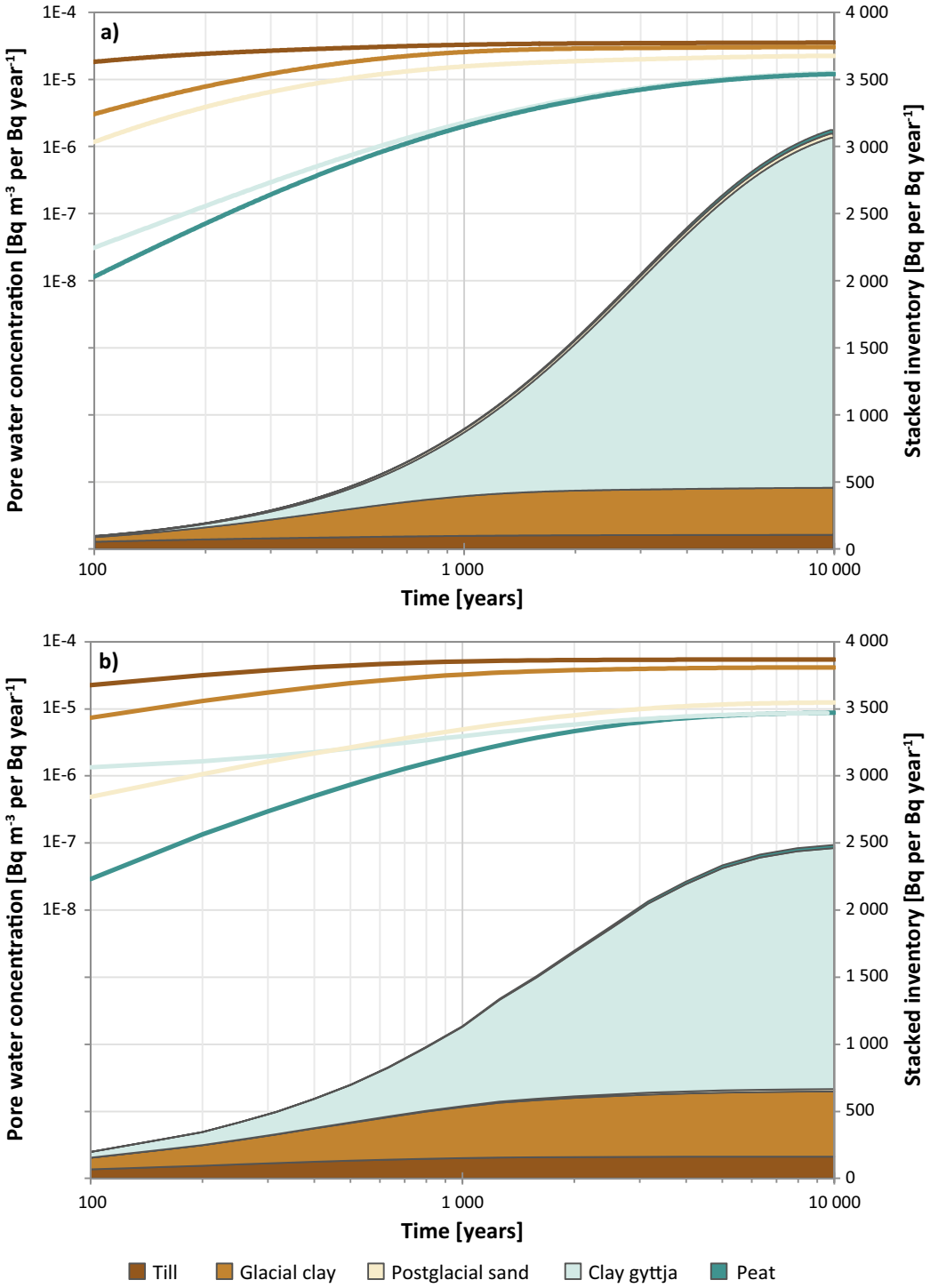

Figure 15-12. *Temporal distribution of the molybdenum-93 in the regolith materials for the stylised compartment model (a) and the scaled distributed K_d model (b) in the radionuclide discharge area in object 206. Note that pore water concentration is expressed on a logarithmic scale (left axis) whereas the inventory is expressed on the original (untransformed) scale (right axis).*

15.3.3 Discussion and conclusions

The comparative analysis presented in this section demonstrates how insights from a distributed 3D model can be used to inform the selection of the structure of a stylised compartment model and the selection of parameters for that model. It is suggested that alternative model structures and parameter choices are evaluated iteratively, by comparisons with the results from distributed models. In the presented example, two iterations (with a focus on the delineation of the model area) were performed to demonstrate the approach. However, for a safety evaluation, a broader evaluation of plausible model structures and simplifications is needed.

The two model comparisons (for object 206 and for the discharge area) demonstrate that compartment models have the capability to capture the overall patterns of dilution and accumulation of Mo-93 in the regolith profile. At the same time distributed model simulations can help to ensure that potential radionuclide discharge areas located close to object boundaries are properly accounted for. As expected, results from a compartment model are more similar to those from a distributed model if parameters are derived from (and if comparisons made at the level of) the area where radionuclides accumulate. This is true with respect to (i) the accumulation in lower regolith layers, to (ii) the dilution in the permeable sand layer, as well as with respect to (iii) the time it takes to approach equilibrium concentrations.

Although the average accumulation at the end of the simulation calculated with the compartment models was within a factor of two from the results of the distributed model, there is clearly room for further iterations to improve the performance of the compartment model. For example, an increased discretisation of lower regolith layers (Chapter 8 and 9), and the considerations of preferential flow paths are issues that could be explored in further iterations of compartment models. In such evaluations, additional endpoints, such as average flow-path lengths and residence times for particle transport could be helpful for model and parameter selection. For future iterations it is also important to avoid conceptual discrepancies between the compartment and distributed model, such as sinks at the bedrock-regolith boundary, and to be clear on how dispersion in a heterogeneous system is represented in a highly discretised and distributed model.

16 Discussion

16.1 Introduction

There are two main objectives for SE-SFL. The first is to evaluate conditions under which the repository concept has the potential to fulfil the regulatory requirements for post-closure safety (Chapter 1). Such an evaluation depends on calculations describing dispersion of radionuclides in the environment, and the purpose of the biosphere analysis of the SE-SFL assessment is thus to allow a quantitative evaluation of potential adverse effects from projected releases from SFL. The intention is not to simulate conditions that will necessarily be present in the future, but to capture the main features of transport, accumulation and exposure for a suite of possible future conditions. The level of detail and most assumptions underlying the biosphere model used in SE-SFL are based on the previous biosphere assessment SR-PSU. This model has proven to be useful through experience (SKB 2014d) and has been judged to give a good description of the biosphere system and to yield reasonable results (e.g. SSM 2019). Thus, the SE-SFL model is considered to give an adequate representation of dose consequences for a coastal site in Sweden.

Nevertheless, an evaluation of potential radiological consequences far into the future is inevitability associated with large uncertainties. Handling of uncertainties is thus an integral part of a safety assessment (SSMF 2008:37), and this chapter therefore discusses uncertainties and their potential impact on the results of the performed calculations. Following Galson and Khursheed (2007), uncertainties can be categorised into three types: model uncertainties, scenario (or system) uncertainties and parameter uncertainties (see Sections 16.2 to 16.4, below). The categories broadly correspond to those described in SSM's guidelines in SSMF 2008:21 (SSM 2008b). All three categories of uncertainty contain elements of epistemic (i.e. knowledge-based and reducible) and aleatory (i.e. random in nature and irreducible) uncertainty, and a particular piece of uncertainty could fall within more than one of the categories. Thus, the classification should primarily be seen as a systematic way to facilitate the reporting and discussion of uncertainties identified.

The second main objective of SE-SFL is to provide SKB with a basis for prioritising areas in which the level of knowledge and adequacy of methods must be improved in order to perform a full safety assessment for SFL. Several areas of the biosphere methodology have been evaluated in SE-SFL, for example, the use of water balances to estimate flow path length, the use of a homogenous biosphere object to calculate accumulation of a localised discharge in a heterogeneous environment, and the representativeness of K_d values used given relevant environmental conditions and understanding of underlying biogeochemical processes. The discussion of the first two evaluations can be found in the section of model uncertainties, whereas the third is discussed in the section on parameter uncertainties.

No site has yet been selected for SFL. In order to have a realistic and consistent description of a site for geological disposal of radioactive waste, data from the Laxemar site in Oskarshamn municipality, have been used (Section 1.2). In addition, data from Forsmark have been utilised to broaden the range of landscape and ecosystem features. The effects of the regional climate have been examined by utilising conditions from two additional coastal sites. Moreover, the potential effects of geochemical conditions other than those captured by SKB's site investigation programmes have briefly been addressed by using generic values for K_d and *CR* parameters. Thus, taken together the biosphere approach used in SE-SFL has been aimed at giving a broader picture of possible outcomes than a site-specific safety analysis. In the final section of this chapter, the potential implications of the biosphere analysis for the future site selection are briefly discussed.

16.2 Model uncertainties

Model uncertainties refer to uncertainties arising from an incomplete knowledge or lack of understanding of ecosystems and the processes important for radionuclide transport and accumulation. It includes uncertainties that arise from assumptions associated with a stylised representation of complex systems and from assumptions associated with the mathematical description.

In the BioTEx model, complex ecosystems are represented by compartments that are considered internally homogeneous. With the modelling approach used, radionuclides entering a regolith layer are assumed to be homogeneously distributed within the relevant time scales. The soundness of such an assumption is dependent on many factors, such as spatial heterogeneity, the transport time in a regolith layer, the radioactive half-life and the horizontal distribution of the source. Therefore, the vertical discretisation of regolith layers in the BioTEx and supporting models is discussed below. The consistency between two different approaches to describing groundwater flows (i.e. using water-balances or flow-pathways) is also examined.

Transport, retention and biological uptake of radionuclides are complex processes. In radioecology, retention and plant uptake are traditionally represented by simple equilibrium parameters. However, for elements that are biologically important and have limited sorption, the primary mechanism of retention can be biological fixation and storage in organic matter. Two examples of such radionuclides are C-14 and Cl-36, for which the plant uptake is only weakly related to the total soil concentration. Thus, a process-orientated specific activity approach was used to model the fate of C-14 and Cl-36, and evaluated in the last part of this section.

16.2.1 Vertical discretisation of regolith layers

In previous assessments, all regolith layers have been represented by single compartments in the biosphere model. However, in the lower section of the regolith profile the groundwater flow may be relatively low leading to long residence times in these layers of the regolith. With such conditions, the numerical dispersion within one compartment is likely to exceed the physical dispersion rate, and thus a one-compartment representation may underestimate the solute transport time through the layer. To get a more reasonable representation of the break-through time and the effects of radioactive decay, the discretisation of the two lowermost regolith layers was increased to yield a numerical dispersion similar to the physical dispersion expected under field-scale conditions (see Chapter 8).

Comparison of models showed that effects of an increased vertical discretisation on transport and accumulation of radionuclides strongly depended on the properties of the considered biosphere object and the radionuclide type (Chapter 9). That is, in an area with a high bedrock discharge, where the contribution of discharge from the local catchment to upward flow is limited, the increased discretisation had marginal or no effect on steady-state groundwater concentrations. On the other hand, in an area with a limited discharge from the bedrock, the release and accumulation of sorbing radionuclides in surface layers may be noticeably reduced with a more realistic representation of dispersion. In the presented examples, an increased discretisation resulted in a reduction of the release of Mo-93 to, and accumulation in, the upper regolith profile (where plant uptake occurs) by a factor of two, whereas the release of Ni-59 was reduced by an order of magnitude.

In SE-SFL, a model describing continuous cultivation in the discharge area was also introduced. The description of the unsaturated layer in this model was more detailed than that in the model used to assess dose consequences from early cultivation of a mire (Chapter 7 in Saetre et al. 2013b). A comparison of activity concentrations of Cl-36, C-14 and Mo-93 in the upper soil layer (where plant uptake occurs) showed that the two models gave similar results. The environmental concentrations of Ni-59 that were calculated with the more stylised model turned out to be somewhat high but were within a factor of two of the results from the more detailed model. Thus, the more detailed model of an agricultural ecosystem introduced in SE-SFL confirms that the outputs from the stylised model (used to assess for example consequences after drainage) are reasonable and fit for purpose.

16.2.2 Detailed hydrological modelling – effects of discretisation and flow-path analysis

Following the SR-PSU methodology, groundwater flows were described with detailed hydrological modelling, and parameters for transport calculations were derived from water balances obtained with the MIKE SHE tool (Werner et al. 2013). In the MIKE SHE models of the Laxemar area, the regolith stratigraphy was described by two calculation layers. Thus, the extraction of parameters for individual regolith layers in the BioTEx model required interpolation from derived water balances (Werner et al. 2013) or side calculations with the help of a stylised water balance model (Chapter 5

in Grolander and Jaeschke 2019). For transport calculations, it is desirable that the regolith description used for groundwater flow calculations captures the physical properties (and boundaries) of individual layers. Therefore, Johansson and Sassner (2019) examined if the number of calculation layers could be increased in the detailed hydrological model, while maintaining a good overall model performance. The analysis included a detailed flow-path analysis describing the travel time and path length of particles from the bedrock to the surface. The authors also suggested a method for outlining an area within the biosphere object where most of the released particles passed (i.e. the discharge area for the geosphere release). The results are briefly summarised, synthesised and discussed below.

The model study showed that a discretisation of the lower regolith profile into separate layers of till, glacial clay and sand is feasible and yielded similar results as the original site descriptive model (SDM) with respect to the regional water balance and stream discharge. Moreover, an increased discretisation improved the overall performance of the model with respect to forecasting the hydraulic head and the location of the groundwater table in soil and bedrock (Table 3-1 in Johansson and Sassner 2019). However due to limitations in the MIKE SHE tool with respect to the representation of evapotranspiration, a separation of the upper regolith layers would require a recalibration of the model. As such a calibration was outside the scope of the study, a simple separation of the upper regolith profile (into clay-gyttja and peat) was evaluated and found to result in an underestimation of the evapotranspiration (~ 10 %) and consequently a systematic overestimation of runoff and stream discharge. Thus, an intermediate level of discretisation into four calculation layers (till, glacial clay, sand and an upper layer combining all geological layers on top ofthe sand) was used for the detailed flow-path analysis described in the following.

The effect of the discretisation on the water-balance of two biosphere objects (207 and 212) was also examined. The effects on the upward groundwater flow in the lower half of the regolith, where the flow is primarily driven by bedrock discharge, was limited, and the difference between discretisation alternatives was in the order of 25 % to 30 %. However, in the upper parts of the regolith profile the effects were stronger. For example, in the lake object (207), the exchange across the water-sediment boundary was consistently smaller in the more discretised alternatives than in the coarse SDM model, and discretisation alternatives spanned a factor of four. The opposite was true for the unsaturated soil under a deciduous forest, where percolation increased with increasing discretisation, and alternatives spanned a factor of two (object 212). Thus, it appears that the groundwater flow profile in the upper regolith cannot be captured by lumping together regolith layers. This suggests there is room for additional development to provide robust predictions of flow patterns in the upper part of the regolith.

Particle tracking from a localised release was used to derive transport relevant flow-path characteristics for three separate regolith layers (till, glacial clay and sand) and the upper part of the regolith horizon (~ 2m). The median travel time through the till was approximately 190 days, whereas the corresponding numbers for glacial clay and sand were 270 days and 95 days, respectively. Although the median flow path length was significantly longer than the depth of the till and sand layers (~ 10–20 m vs. 0.5–2 m), the median path length was on the horizontal scale of a single model cell (10×10 m²) rather than on the scale of the discharge area (259 cells). This means that a typical particle is unlikely to leave the object sub-horizontally. The primary travel direction in glacial clay was vertical. The travel distance in the upper regolith horizon was much shorter than the average thickness of the layer (0.4 vs. 2 m), primarily reflecting that particles were drained to the stream system before reaching the surface (or that particles reached the unsaturated zone where tracking was aborted).

The analysis within the discharge area (which covered approximately a third of the biosphere object) allowed for a direct comparison of the travel time of particles with the corresponding time calculated from water-balance flows. The upward advective travel times for till, glacial clay and sand were calculated by dividing the flow at the upper boundary of the regolith layers with the average thickness of the layer, adjusting for the soil porosity. The calculated travel times were 155 days, 255 days and 80 days, respectively. Thus, it seems that the groundwater fluxes from the water balance approach (that are propagated to assessment transport calculations) give reasonable travel times. The advective travel times were somewhat shorter than those for an average particle (6–2 %), which seems reasonable as particles do not travel along vertical streamlines. Moreover, in terms of radionuclide transport, an underestimation of the travel time should in most cases be cautious, as there is less time for radioactive decay.

16.2.3 Distributed transport modelling – effects of spatial heterogeneity

Safety evaluation of potential radionuclide migration from geological repositories relies on compartment models where the spatial heterogeneity of the regolith system is strongly simplified (Chapter 8). Distributed numerical models with a greater spatial resolution can provide qualitative and quantitative understanding of transport in heterogeneous systems. Therefore, transport pathways and patterns of radionuclide accumulation were studied within SE-SFL with a distributed three-dimensional (3D) model implemented in COMSOL Multiphysics (COMSOL 2015) coupled with the PHREEQC code through the iCP interface (Nardi et al. 2014) (Chapter 15).

Patterns from the distributed model highlighted the control of groundwater flow paths and dilution on radionuclide accumulation. Results from the modelling indicated, for example, that the spatial distribution of highly permeable post-glacial sand and low-permeable glacial clay layers determined the water pathways and the areas where deep groundwater mix with surface waters. The glacial clay (located above the till) acted as a natural barrier and slowed down the vertical migration of radionuclides in the regolith profile. Although slow, vertical transport seemed to be a primary driver for accumulation patterns of adsorbing radionuclides in the lower regolith layers. In addition, preferential flow paths seemed to have potential to influence accumulation patterns in the upper regolith, as by-passing of the clay and sand layers favoured accumulation of Mo-93 in the clay-gyttja layer.

It was also examined to what extent average results, with respect to accumulated activity and environmental activity concentrations, could be captured by a stylised compartment model. The two model comparisons (for object 206 and for the discharge area within object 206) demonstrated that stylised models have the capability to capture the overall patterns of dilution and accumulation of Mo-93 in the regolith profile. As expected, results from the stylised model were more similar to those from a distributed model when parameters were derived from, and comparisons made at the level of, the area where radionuclides are transported and accumulate. This was true with respect to the accumulation in lower regolith layers, the dilution in the permeable sand layer, as well as the time to approach steady-state concentrations in all regolith layers, although the improvements were not dramatic.

In summary, the results from these model exercises show that distributed models can be used to extract and select reasonable parameters for assessment models, and it is clear that insights from distributed modelling in future work can be used to inform structural model improvements and to justify process simplifications for stylised modelling. Moreover, model comparisons for object 206 suggest that the heterogeneity within the object was not a major source of uncertainty, and that a stylised model parameterised to reflect the whole biosphere object performed reasonably well as compared to the distributed model (i.e. average concentrations were within a factor of two at the end of the simulation). Thus, uncertainties that arise from heterogeneities within the biosphere object (with respect to object properties) were deemed to have a limited effect on the calculated accumulations of radionuclides in object 206, and this uncertainty is unlikely to have any significant influence on the evaluation of post-closure safety for the proposed repository concept for SFL.

16.2.4 Representation of carbon and chloride cycling

As in previous safety assessments, a specific activity approach has been used to model plant uptake of C-14, and in SE-SFL this approach was expanded to uptake of Cl-36 of all terrestrial plants (Chapter 8). In this approach, it is assumed that the rate of plant uptake is proportional to the concentration of the radionuclide relative to the concentration of the stable element (i.e. the isotopic fraction) in relevant environmental media. The cycling and fate of common elements is better known than the cycling of trace elements. Therefore, this approach has a potential to reduce uncertainties for common elements as compared with a general approach, where only the fate of the radionuclides is modelled, and allow for evaluation of part of the model against empirical data. However, in this approach it is important to couple the calculations of the radionuclide and the stable element. If this is not done properly there is a risk of introducing systematic errors (and increased variation) in the calculations.

In SE-SFL, several updates were introduced in the terrestrial C-14 model to make sure that C-14 and stable carbon are described consistently in deterministic and probabilistic simulations (see Chapter 8). The updates of the C-14 model primarily affected the concentration of carbon in the uppermost regolith layer in saturated and unsaturated soils. Thus, the calculations of root uptake were directly affected, but the model updates had practically no effect on the atmospheric concentration and foliar uptake (as almost all C-14 was released to the canopy atmosphere irrespective of model assumptions). In the updated model, transport of stable and radioactive carbon are affected by the same processes, and thus the specific activity in the soil pore water was in practice reduced to the ratio between the release of C-14 (through advective transport and mineralisation) and the release of stable carbon by soil respiration. Though not explicitly studied in SE-SFL, the model updates are expected to reduce the model uncertainties considerably (as the results become independent of uncertainties in the rate of degassing). Moreover, soil respiration, which is a new key parameter in the updated model, is a well-studied soil biological property. The SE-SFL implementation of the specific activity approach thus ensures that the model robustly captures the effects of environmental changes that affect biological properties (such as primary production, soil quality, temperature and/or moisture).

As release to water may result in a specific activity of C-14 (in surface water) that is much higher than in the atmosphere, doses from the aquatic foodchain can be important in a safety assessment despite the relatively low productivity of these ecosystems. In SE-SFL, the concentration of dissolved inorganic carbon (DIC) in lake water was treated as a constant parameter (based on empirical measurements in Lake Frisksjön). If C-14 turns out to be a main contributor to the dose also in future assessments, the concentration of stable carbon in lake water will be an important source of uncertainty. This uncertainty can be reduced if systematic spatial and temporal variation can be accounted for (due to e.g. primary production, upwelling and the load of carbon from the catchment, Natchimuthu et al. 2017). Moreover, if the calculations of stable and radioactive carbon concentrations are not explicitly coupled in future assessments, it will be important to make sure that stable carbon concentrations are still reasonable given the assumptions used for the C-14 calculations also in probabilistic simulations (e.g. through correlations of the DIC values with parameters affecting the degassing rate).

In SE-SFL, the current knowledge of chlorine cycling in terrestrial ecosystems has been synthesised and summarised (Section 14.1). Immobilisation in soil organic matter, and plant uptake and release are key processes for cycling and retention of chlorine in terrestrial ecosystems. In a traditional radioecological approach, plant elemental uptake and concentration are assumed to be proportional to total soil elemental concentration (as described by the plant to soil concentration ratio *CR*). However, ongoing SKB studies show that the link between plant and soil chlorine concentrations is weak, and that models where plant uptake is based on a *CR* approach cannot reproduce empirical patterns of chlorine distribution in a coniferous forest ecosystem. The reason is probably that Cl plays such an important biological role, for example for maintaining the osmotic balance, so that its uptake and concentration are strongly regulated by the plants (Section 14.1.2).

The weak link between soil and plant chlorine concentrations was the rationale for a systematic change of how plant uptake (and content) was modelled in terrestrial ecosystems. Thus, in the SE-SFL version of the BioTEx model, the traditional *CR* approach for plant uptake was replaced by a representation based on the assumption that plant uptake is independent of soil concentration. Plant uptake of Cl-36 was instead modelled as being proportional to the plant concentration of chlorine and the ratio of Cl-36 to stable chlorine in soil pore water. However, before the specific activity approach can be propagated to a full safety assessment it needs to be ensured that key processes for transport and retention will affect concentrations of stable and radioactive chlorine in a consistent manner (for example with respect to the effects of immobilisation) and that this consistency is maintained also in probabilistic calculations. Moreover, it is noted that the bound fraction of chlorine found in boreal soils is typically similar to the proportion of organic chlorine (e.g. 35–90 % in surface peat, Sheppard et al. 2011, Section 14.1). This means that the K_d value for organic soil is likely to be determined mainly by the contribution from chlorine immobilised in organic matter. Thus, a future revision of an assessment model for Cl-36 needs to consider both plant uptake and soil immobilisation consistently, accounting for the different forms of chlorine (i.e. organic and inorganic) and in a way that treats Cl-36 and stable chlorine uniformly.

16.3 System uncertainties

System (or scenario) uncertainties typically refer to uncertainties associated with significant changes over time with respect to external and internal biosphere conditions. This includes uncertainties with respect to development of ecosystems during temperate conditions, the response to large-scale climate change, and long-term changes in soil conditions. In general, system uncertainties contain a larger element of aleatory (i.e. irreducible) uncertainty. Uncertainty associated with the future human utilisation of natural resources is not associated with temporal changes, but as it is irreducible by nature, it has also been included in this section.

16.3.1 Development of the biosphere

The main features of the Laxemar landscape are determined by bedrock topography, which is expected to change only marginally over the next one million years. However, passage of an inland ice sheet, relative sea-level change, wave erosion, sedimentation, and mire formation will affect the regolith stratigraphy overlying the bedrock and its dynamics. In SE-SFL, as in previous safety assessments, the expected development of regolith layers and the associated ecosystem succession has been described with the regolith-lake development model (Section 5.3).

The importance of explicitly including development was evaluated by comparing results from developing discharge areas with those from time-independent ecosystems (i.e. sea, lake and mire ecosystems). The comparison utilised three biosphere objects from the Laxemar area and six objects from the Forsmark area. The doses in the developing objects were similar to those from time-independent representations of the same ecosystems and the difference was typically not larger than 10 % to 20 %. Thus, the results indicate that using a time-independent representation of lake and mire ecosystems (as done in the base case) is a reasonable and sound simplification to representing developing ecosystems in a discharge area.

However, it is important to evaluate all relevant stages of a discharge area. If the conditions at the position of repository, or the discharge area, are influenced by shoreline displacement, the development of the object in relation to the timing of the release may also influence the projected dose. In addition, changes in the hydrological fluxes may cause transient periods of accumulation and release. Thus, irrespective of the assumptions used in the main body of calculations, it is important to evaluate the potential effects of landscape development and to address uncertainties with respect to this development. In SE-SFL, potential effects of shoreline displacement, ecosystem succession (within temperate conditions) and projected changes in the groundwater flow (at repository depth and in the surface system) were accounted for in the submerged condition and the simplified glacial cycle cases (Sections 12-6 and 12-7).

Despite the persistence of the large-scale topography, the outcomes from landscape development models are intrinsically uncertain. This is true, for example, with respect to the projected regolith stratigraphy of specific discharge areas (Section 5.6 in SKB 2014d). As a time-independent representation of a biosphere object was found to be a reasonable simplification for dose calculations, a wide array of time-independent biosphere objects (as presented in the discharge area case) was considered to also cover the uncertainty with respect to the outcomes of development for a specific discharge area. How landscape properties (e.g. area of object and regolith thickness) affect environmental concentrations of radionuclides and how these properties interact with the local hydrology is further discussed in Section 16.4.4.

16.3.2 Climate conditions

In SE-SFL, the uncertainty of future climates was handled by using three different evaluation cases, namely: the present-day (or base) case, the increased greenhouse effect case and the simplified glacial cycle case. The present-day case was the reference point for all calculations. In this case, temperate climatic conditions (similar to those at the present day) were assumed to prevail for the full assessment period, and radionuclides were released to a terrestrial ecosystem (see Section 9.2).

In the increased greenhouse effect evaluation case, an intermediate CO_2 emissions case was assumed to cause a mean annual temperature and an annual precipitation that are 2.6 °C and 12 % higher than the present conditions (IPCC's scenario RCP4.5, Section 9.3). These changes were expected to

reduce runoff and groundwater discharge and to increase the water deficit for cultivated crops. It was shown that if the water deficit was covered by groundwater uptake, then the annual dose from some radionuclides may increase, but the opposite was true if large-scale irrigation with surface water was practiced. However, the dose was not substantially higher than calculated for present-day conditions. Although a limited number of parameters were adjusted in the calculations (Section 7.4), the case is deemed to adequately address the effects of a warmer climate, including potential effects of large-scale irrigation and plant translocation[42]. The results are reasonable and in line with previous SKB assessments, concluding that modest changes in a temperate climate are expected to have limited effects on plant and soil biological properties (Chapter 11, Löfgren 2010 and Section 10.6 in SKB 2014d).

Covering crop water deficit with groundwater uptake (as an alternative to irrigation) is a somewhat cautious simplification, as plant water uptake can be expected to be restricted if the groundwater table is depressed due to extended summer droughts. However, the simplification is deemed as a reasonable way to handle uncertainty for moderate changes in climate. If emissions of greenhouse gases are accelerated in the future, more extreme changes in the climate are to be expected, with potential implications for both the groundwater system and the feasibility of specific agricultural practices. The evaluation of more pessimistic emission scenarios can also be informative. However, when less likely scenarios are evaluated, it is important to balance consequences with the likelihood of the postulated (or worse) conditions, so that extreme cases are not given an undue weight in the assessment.

In the simplified glacial cycle evaluation case, a cyclically repeated chain of events was adopted to illustrate dose consequences given the passage of an inland ice sheet. In the calculations, the conditions and properties of the surface system were modified according to climatic conditions and the succession of discharge areas. For example, in periglacial periods groundwater flows in the mire were halted, due to permafrost, and radionuclides were instead discharged through a talik to a lake. When glacial conditions persisted, the groundwater discharge was cautiously assumed to reach a semi-enclosed bay in front of the ice sheet, and after the retreat of the ice sheet, the area went through a continuous development from a sea basin to a mire.

Although the peak release rate of several dose-contributing radionuclides was expected to increase when the inland ice passes the repository, the maximum annual dose over the assessment period is unlikely to exceed that of the base case in these situations. This is partly because the main dose-contributing radionuclides like Mo-93 and C-14 have decayed significantly by the time of the first ice approach, and because the surface condition associated with the peak release (permafrost or submerged conditions) occurs in low-productivity ecosystems with no wells. The overall conclusion from these stylised calculations was deemed to rely on reasonable and robust assumptions, and the results were in line with those from the previous SKB assessment for the final repository for spent nuclear fuel (Section 13.5.6 in SKB 2011a). Thus, it is concluded that uncertainties with respect to future glaciation cycles have been handled in an adequate way in SE-SFL and that they remain modest.

16.3.3 Development of soil conditions

Cultivated soils along the valleys of the Laxemar area presently have a high organic content. Remnants of peat are found in the soil, and below the drained soil there are thick layers of clay-gyttja with a high organic content as well (Sohlenius and Hedenström 2008). If cultivation were to prevail for a long period, the organic content in these soils is expected to decrease due to oxidation (Sohlenius et al. 2013), until most of the organic carbon content is lost. This means that the properties of the regolith profile are expected to change under the regime of continuous cultivation. To examine to what extent the potential dose to future farmers is affected by regolith conditions expected as a result of long-term cultivation, the aged soil sensitivity case was designed (Section 13.2).

Soil properties that have the potential to influence transport and accumulation and are affected by the loss of organic matter include: decreased soil respiration (which increases root uptake of C-14), increased concentrations of plant macro-elements (e.g. Cl) in soil pore water (which decreases plant uptake), and decreased sorption in the regolith profile (which decreases decay of Mo-93 in the

[42] Translocation refers to the transport of radionuclides within a plant, for example the transport of radionuclides intercepted on leaves to edible below ground structures like tubers.

saturated layers and decreases the retention of many radionuclides in the cultivated soil). However, the quantitative effects of the individual processes were limited, typically below a factor of two, and the response in terms of plant concentrations of individual radionuclides went in different directions (Section 13.2). Thus, taken together, ageing of organic soils is expected to have only a limited effect on the dose from continuously cultivated soils, and no influence on the evaluation of the safety, as the doses from another land-use variant considered (i.e. draining and cultivating a mire) yields significantly higher doses.

16.3.4 Land use and exposure of future human inhabitants

The uncertainties with respect to the degree to which future humans will inhabit and/or utilise natural resources in the biosphere object have been handled according to Swedish regulations (SSM 2008a) and in line with U.S. and international standards and guidance (e.g. ATSDR 2005, ICRP 2006) That is, the potentially exposed groups used in the evaluation represent credible bounding cases with respect to identified exposure pathways. The assigned characteristics and habits of the potentially exposed group are reasonable and sustainable with respect to physical constraints of the landscape, to human needs for nutrients and energy, and to present and/or historical land use (Saetre et al. 2013a). As cautious assumptions have been made in selecting the exposure pathways, land uses and diets adopted for assessment purposes, the relatively large doses that have been estimated provide a cautious, rather than a realistic, estimate of the health risks to humans in the far future.

The exposure pathways covered by the four potentially exposed groups include ingestion, inhalation and direct exposure from inhabiting or using natural resources. Use of natural and agricultural ecosystems is covered by the groups, as is the exposure from ingestion of radionuclides with surface and well water. In addition, potential exposures resulting from irrigation, from burning of biomass fuel (peat or wood) and from fertilisation with ash or seaweed, are included on the scale of a household garden plot. By evaluating a variety of potentially exposed groups, all with habits that lead to relatively large exposures, uncertainties in the effects of the use of natural resources by humans are judged to be adequately covered.

Draining and cultivation of a mire in the discharge area is the land use that causes the highest dose. This is primarily because radionuclides can accumulate in peat over a long period prior to exposure, and because the dose-contributing radionuclides predominantly yield dose through ingestion of food. The handling of this land use in the biosphere evaluation is cautious, as the present land-use is predominantly agriculture at the example site (and only one mire remains). Moreover, the effect of cultivation is evaluated at all possible times without accounting for the probability that the mire has already been drained (which would decrease the potential for long-term accumulation)[43].

However, given the timescale of the evaluation and the fact that the location of the repository is yet to be decided upon, this simplifying assumption is not unreasonable. For Mo-93, the time to reach equilibrium in the environment is similar to its half-life, and thus accumulation in a period of approximately four thousand years would be sufficient to yield environmental concentrations similar to those from continuous accumulation. Moreover, for other dose-contributing radionuclides, the exposure through other land-uses may yield similar (C-14 from lakes, U-238 chain from small-scale horticulture) or only moderately lower doses (within a factor of two to five). Thus, the consequences of the assumed long-term accumulation do not lead to substantially different dose estimates than those from other plausible land-uses.

16.4 Parameter uncertainties and sensitivity analyses

Uncertainties associated with the values of the parameters that are used in the implemented models are termed parameter (or data) uncertainties. These uncertainties partly arise because the biosphere model uses single spatially averaged values for parameters (derived from measurements at discrete

[43] Doses from the drained mire can only persist over a few generations. Thus, the expectation value of dose to an individual living in the vicinity of the mire at a predefined time in the future is less than the expectation value of dose to an individual living at the unknown time at which the mire has just been drained.

locations), whereas in reality there is continuous variation in parameter values over space and time. Parameter uncertainty may also stem from difficulties in obtaining precise measurements, lack of measurements from relevant conditions, or because aggregated parameters represent the outcome of multiple processes.

In SE-SFL, site-specific data, generic data, and expert judgement were used to assign reasonable values to model parameters (Chapter 8). The representativeness of the assigned values for a future site is unknown for many parameters. At this stage, it was deemed premature to quantify the effects of uncertainty arising from individual parameters as described with probability density functions. A comprehensive evaluation of the effects of parameter uncertainties on dose estimates, and a comprehensive sensitivity analysis, are thus outside the scope of the biosphere analysis in SE-SFL. However, the potential influence of overall parameter uncertainties is discussed in Section 16.5.2.

To cast some light on how sensitive the biosphere calculations are to the selected discharge area and the choice of values of key parameters, sensitivity calculations with respect to the discharge area properties and K_d and *CR* values were performed. The results from these calculations are discussed in Sections 16.4.1 and 16.4.2 below. Next SKB's pilot study on distributed reactive transport in regolith layers is discussed in Section 16.4.3. This section on parameter uncertainties ends with a discussion of *the alternative groundwater sensitivity case* (Section 16.4.4). The influence of landscape geometry and regolith thickness on groundwater flow is summarised, and potential effects on environmental concentrations and dose are discussed and related to the results from Section 16.4.1.

16.4.1 Dispersion of geosphere release and discharge area properties

In the biosphere calculations, it is assumed that all geosphere releases occur in a single biosphere object (or discharge area). This is a cautious simplification, since the hydrogeological analysis suggested that the geosphere releases will typically be dispersed among two or three objects (Figures 5-3 and 5-4). However, this assumption is not overly cautious as 60 % (or more) of test particles released from the postulated repository location end up underneath (or close to) one of the biosphere objects (Figure 5-4). Thus, explicitly accounting for dispersal between biosphere objects is not likely to have any significant effect on the assessed dose, and thus the handling of dispersion is deemed to be reasonable and adequate.

Since the location of the repository and the areas where groundwater from the repository will reach the surface are unknown, the effects of alternative discharge areas have been evaluated (Section 7.6). In the evaluation case, the effects of a geosphere release to a large number of different biosphere objects (fifteen) and ecosystem states (mire, agriculture, lake and sea) were examined.

The calculations showed that the highest annual effective doses typically result from accumulation of radionuclides in a mire (which is then drained and cultivated). Release to an open sea basin could, on the other hand, result in doses that are several orders of magnitude lower. The doses from lake ecosystems were also typically lower than from terrestrial ecosystems, but aquatic exposure pathways could yield a higher dose from C-14 than terrestrial pathways.

In general, doses were lower in large objects, as these tended to have a large local catchment and a greater discharge of groundwater which will dilute a given geosphere release. Doses from sorbing radionuclides were lower in objects with thick regolith layers, where a prolonged residence time increased the effects of radioactive decay. Thus, the effects of uncertainties with respect to the properties of the discharge area differ between radionuclides. For example, the annual dose from mobile radionuclides (C-14 and Cl-36) varied by a factor of five between mire objects, whereas the dose from moderately sorbing radionuclides (Mo-93 and Ni-59) spanned more than an order of magnitude (Figure 12-4). It was also noted that dose variation increased notably by including objects from an area with a flatter topography (i.e. Forsmark), where groundwater also discharges in hill-slope wetlands with relatively thin regolith layers.

In summary, the discharge area evaluation case captured a broad array of features for a potential discharge area in terms of geometry, regolith stratigraphy, hydrology and ecosystem states. Uncertainties with respect to object properties are thus deemed to have been thoroughly handled in SE-SFL. In addition, the evaluation cases cast light on which conditions in the discharge area are of importance for accumulation of and exposure to radionuclides. This issue is further discussed in Section 16.4.4 below.

16.4.2 Regolith sorption properties

In the *alternative K_d and CR values* sensitivity case, generic data based on a compilation of literature by IAEA (2010) were used as a benchmark for the site-selected data (Section 13.2). The generic data were derived from various geochemical conditions and, through various methods, and within the comparison, values for best matching soil types based on soil texture/organic matter content were used. The comparison showed that the geometric mean value of the generic K_d values tended to be lower than the site-specific values, and this was most pronounced in mineral regolith layers (Section 13.3.2). However, the dose to the potentially exposed group was relatively insensitive to the differences in the retention in these soil layers. This was partly due to the relatively high dose contribution of mobile radionuclides (C-14 and Cl-36) for which uncertainties in retention properties have little effect on the transport and for which plant uptake was not modified in the alternative calculations (since the *CR* approach was not used for these nuclides). Moreover, the activities of radionuclides that are substantially affected by retention in regolith tended to already have been strongly reduced by the radioactive decay in the near-field and geosphere barriers. Thus, the *alternative K_d and CR values* sensitivity case indicated that uncertainties with respect to the K_d and *CR* values used in SE-SFL, in general, had a limited effect on the estimated dose.

There were, however, two notable examples where the radionuclide-specific dose appeared to be considerably affected by the K_d value, with potential significance for the overall dose. Firstly, the dose from Mo-93 was considerably reduced when generic data were used, primarily due to reduced sorption in peat. Secondly, the dose from well water was more than an order of magnitude higher when IAEA data were used as compared with the base case, primarily due to lower K_d values of the Ra-226 decay products Pb-210 and Po-210 in till. At first sight, this signals that there may be substantial uncertainties with respect to the dose from Mo-93 and Ra-226+[44]. However, a closer examination of the data reveals that a substantial part of this apparent uncertainty may in fact reflect limitations of the generic data set.

That is, SKB has empirical measurements from a wide array of relevant environmental conditions, which supports strong sorption of Mo-93 in organic-rich environments. Strong sorption of Mo in reducing environments is also consistent with the general understanding of Mo biogeochemistry. The generic K_d value for Mo-93 represents a small number of samples (9) from unspecified conditions (all soils), and the range of the IAEA data did not cover the K_d values which SKB has measured in clay-gyttja and peat samples[45]. Hence, the IAEA dataset is likely to only represent environments where Mo is present in its mobile oxidised form (molybdate), not organic soils where Mo can be immobilised by reduction. Furthermore, SKB has sampled till at a considerable depth, with conditions that are relevant for saturated and anoxic conditions expected for a well. The K_d value for Pb in such conditions was almost two orders of magnitude larger than the K_d value selected from the IAEA data (representing sand). However, the reported K_d values for Pb are highly variable and the range of the IAEA data (pooled for all soils) included the site-s data with a broad margin. These two examples clearly emphasise the potential importance of understanding and quantifying the key retention processes, and selecting parameter values to adequately reflect relevant environmental conditions.

In Chapter 14, the environmental properties of three potentially important elements are examined, namely for chlorine, molybdenum and nickel. The review of chlorine (entering the biosphere as chloride) was used to update of the assessment model in SE-SFL and points towards key aspects of chlorine cycling that need to be considered in transport modelling (see Section 16.2.4). Molybdenum is of specific interest, as Mo-93 contributes significantly to the dose from both SFL waste vaults and because generic data are so sparse for this element. The mobility of Mo is primarily determined by its chemical form in combination with environmental conditions (Section 14.3). Mo is typically found in the form molybdate (MoO_4^{2-}) in surface waters and groundwaters and it tends to be more mobile at high pH. Important retention processes for molybdate include sorption onto Al and Fe oxyhydroxides (at low pH) and binding to organic matter. The low K_d values of Mo in till and glacial clay that SKB has measured are consistent with the properties of molybdate, and high K_d values in clay-gyttja and peat are consistent with their high content of organic matter. In strongly reducing environments, such as organic-rich lake sediments and wetlands, the reduction of the relatively

[44] Ra-226+ indicates the dose from Ra-226 including its decay products Po-210 and Pb-210.

[45] The maximum IAEA (2010) value is 0.13 $m^3\ kg^{-1}$ (n=9) as compared to the median values measured in clay-gyttja 3.4 (n=6), deep peat 3.9 (n=6) and surface peat 3.4 (n=5) $m^3\ kg^{-1}$ (Tröjbom et al. 2013)

mobile oxyanion Mo(VI) to a high-valence cation Mo(IV) with a low solubility is expected to further accentuate the accumulation of Mo. Thus , it can be concluded that the K_d values used in SE-SFL capture a significant part of environmental variation in the mobility of Mo, and that this variation is consistent with the understanding of underlying biogeochemical processes. Although not discussed in detail here, the same conclusion can be drawn for the K_d values used for the mobility of nickel (see Section 14.2.7).

These examples illustrate that a significant part of the uncertainty that is inherent in compilations of data can be explained by systematic variations attributed to environmental conditions. However, in some cases it is hard to measure the retention of an element of interest (e.g. Po). In such cases SKB has used element analogues from well-characterised samples to approximate element mobility. By the analogue method, the uncertainty in K_d values can potentially be significantly reduced as compared to the alternative of using parameters derived from data compilations reflecting variable and often insufficiently described environmental conditions. Nevertheless, for elements that have the potential to contribute to dose, it is essential that the selection of element analogues is clearly justified from biogeochemical understanding and, if possible, that the choice is supported by empirical measurements in relevant environmental media and conditions. The outcome of more recent IAEA programmes as well as compilations of surface chemistry data from Finland may provide valuable sources for future comparisons and validations of distribution coefficients[46].

16.4.3 Distributed transport modelling – effects of reactive transport

The transport calculations underpinning safety evaluations typically rely on calculating retention using a linear sorption approach, where distribution coefficients are based on empirical measurements, as exemplified for Mo in the previous section. As sorption processes can be complex and depend on local conditions along preferential transport pathways, an attempt to identify the most important chemical reactions for accumulation under flow-through conditions was carried out in SE-SFL. In this *reactive transport model*, the retention processes were described with a reactive transport model, where a thermodynamic chemical reaction model (PHREEQC) was coupled to a distributed hydrological model (implemented using COMSOL) (Chapter 15). The included geochemical mechanisms were chemical equilibrium reactions such as precipitation/dissolution, surface complexation and cation exchange. Due to its high computational cost, the reactive transport simulations could only be applied to a relatively small domain (a part of object 206) and a relatively short timescale (1000 years).

In the present work, no retention mechanism was described in the sand layer, and the retention due to complexation with solid or dissolved organic matter was not included in the model. Thus, the results from the lower regolith profile are of primary interest here. For Ni, the calculated relationship between solid and solute concentrations (i.e. the apparent K_d) resembled the measured K_d value in the lower part of the regolith profile, with high sorption in the glacial clay (Table 15-4).

However, the variability in the apparent K_d between regolith layers was large. For the glacial clay layer, the best-estimate for the measured K_d value fell between the maximum and average values of the mechanistic approach, but for the till the measured K_d value was above the maximum value calculated with the reactive transport model. Thus, the importance of some retention processes appeared to have been underestimated in the calculations. Plausible explanations could be related to the role of organic matter, underestimation of the clay fraction, or conceptual differences in the mobile fraction between chemical extractions of the samples and the modelled chemical equilibria. The results suggest that a systematic conceptual and numerical calibration between empirical K_d values and mechanistically calculated values (under relevant geochemical conditions) should be undertaken prior to mechanistic calculations in future work. Such a calibration would facilitate the interpretation of results, allowing a separation of the effects of reactive transport from those emerging from differences in the description and representation of retention processes.

[46] SKB has participated in the IAEA programs EMRAS II and MODARIA I, II, where K_d and CR data have been compiled. Part of this data have been published in Wood et al. (2013) and IAEA (2014, 2016). Several compilations of data from Finnish surface ecosystems have been published by Posiva (e.g. Haavisto and Toivola 2017, Kuusisto 2017, Lahdenperä 2017).

16.4.4 Alternative object geometries and groundwater flows

In SE-SFL, a new method for extracting hydrological fluxes from MIKE SHE water balances was developed (Chapter 5 in Grolander and Jaeschke 2019) and the method was implemented in the time-independent models of terrestrial ecosystems. The method explicitly used hydrological input from the atmosphere and the geosphere, together with object and catchment characteristics, to calculate groundwater fluxes, maintaining the water balance in each model compartment. In *the alternative object geometries and groundwater flow case* (Section 13.4) the sensitivity of activity concentrations and doses to variations in parameters driving or modifying groundwater flows was examined.

In the analysis, properties that influence groundwater flows were varied independently of each other in a range that spanned temperate conditions and properties of discharge areas in a broad range of locations. For each parameter realisation, hydrological flows were calculated (n=1000), maintaining water balance in each model compartment.

All radionuclides were affected by dilution in a similar way. This means that the activity concentrations (from a given geosphere release) in the lower regolith layers decreased with object area and bedrock groundwater discharge, whereas the concentrations in the upper profile decreased with the area of the basin and the net precipitation. Sorbing radionuclides (Mo-93, Ni-59 and Tc-99) were also affected by radioactive decay, and parameters that decrease transport rates (e.g. decreased area-specific discharge and thicker regolith layers) reduce the activity from the geosphere along the upward flow pathway.

Among object properties, the area of the object was the property that explained most of the concentration variation in the lower regolith profile (i.e. in the till and glacial clay layers). The object area also explained a significant part of the variation in regolith layers closer to the surface, as did the area of the basin (for mobile radionuclides), and the thickness of the lowermost strongly sorbing regolith layer (for less mobile radionuclides, e.g. glacial clay for Tc-99 and clay-gyttja for Mo-93).

Cultivation of mire peat was a major pathway for exposure, and consequently parameters that affected the activity concentration in the upper part of the regolith profile explained most of the variation in dose. As the contribution of individual radionuclides shifted over time primarily as a function of the geosphere release, so did the fraction of the variation that was explained by individual parameters. Despite these shifts, the area of the object always explained a significant part of the variation of the dose from BHA.

Finally, it was noted that the downward flux of water decreased rapidly with regolith depth and that model results were insensitive to parameters describing this percolation. The horizontal discharge of water from the local catchment was typically much larger than the percolation, and parameters that controlled the vertical distribution of the horizontal discharge had a significant effect on environmental concentrations. However, as theses parameters varied little between objects, their combined effect on concentration and dose was limited to less than 10 percent of the total variation.

In the *discharge area calculation case*, differences between objects were studied with sets of properties that are consistent with geographic areas in Laxemar (Section 12.2). The general conclusions from the sensitivity analysis are largely in agreement with the results from the analysis of different objects in *the discharge area case*. However, in *the discharge area case* dependencies in the landscape made it hard to detect effects of correlated properties in objects. For example, the area of the object and the area of the local catchment both affect environmental concentrations, but in analysis of biosphere objects, the two effects could not be separated, since large objects also tend to have large local catchments. Similarly, the thicknesses of individual regolith layers were not independent of other characteristics of the biosphere objects (Appendix C). The sensitivity analysis was based on probabilistic realisations with few constraints of how landscape geometries and regolith thicknesses were combined in individual iterations, and thus the analysis provided a basis for dissecting the effects of confounded factors. However, the unconstrained variation of parameters may bias the variation attributed to individual parameters, and thus the explained variation for parameters that would in reality be correlated with others should be interpreted with some caution. Thus, the analyses of *the alternative groundwater flow case* and *the discharge area case* complement each other.

16.5 Validity of the base case and discussion of overall uncertainty

The terrestrial object that was used to evaluate dose consequences in the base case, and most other evaluation cases, is a specific geographic area, referred to as biosphere object 206. The object represents the most likely area for discharge of groundwater from the repository, as determined by particle tracking from the assumed repository position to the present surface landscape (Figures 5-4 and 5-5). The area was selected to achieve a detailed and consistent description of the transport of radionuclides from the repository to the surface. However, as the repository location is yet to be determined, the area can only provide a relevant example. Thus, doses calculated for a release to this area need to be interpreted in the context of the large uncertainties associated with the properties of the potential discharge area. This is the focus of Section 16.5.1.

The effects of landscape development have been incorporated in several evaluation cases (Table 7-1). However, uncertainties in the time-pattern of releases of radionuclides from the geosphere relative to shifts in surface hydrology makes it difficult to single out the effects of biosphere characteristics and assumptions on the resulting doses. As discussed in Section 16.3.1, using a time-independent representation of the biosphere for a discharge area is a reasonable and sound simplification. Accordingly, most of the biosphere calculations considered transport and accumulation under constant biosphere conditions, with the same time-dependent release rate from the geosphere. This setup allows for simple and unbiased evaluation of the effects from addressed uncertainties, and a systematic comparison of these calculation cases is the focus of Section 16.5.2.

16.5.1 Validity of base case results in relation to uncertainty of the discharge area

The location of biosphere object 206 appears to be sound given SKB's prior knowledge of deep groundwater discharge. That is, the object is in a topographically low-lying cultivated area that is likely to have developed from lake and mire stages (Chapter 5). Moreover, hydrological modelling suggests that the object has a relatively high rate of specific deep groundwater discharge (Chapter 5 in Grolander and Jaeschke 2019), reflecting an increased likelihood of receiving radionuclides from repository depth. Furthermore, the selected area is geographically limited and has a relatively small local catchment that results in a relatively low degree of dilution in the upper parts of the regolith profile.

When comparing object 206 with other potential discharge areas in Laxemar, it was found to be representative for relatively small terrestrial discharge areas in the locality. It was therefore concluded that it can constitute a reasonable and sound simplification of a potential discharge area in Laxemar. However, it was also noted that the response to object properties differs between radionuclides. Thus, whereas the estimated dose from Mo-93 and Ni-59 in object 206 was high even for a small object (about five and three times above the geometric mean), the opposite was true for C-14 (two times below the geometric mean in the Forsmark area, Figure 12-1). The comparatively high doses from moderately sorbing radionuclides are due to a high rate of groundwater discharge from bedrock, resulting in fast transport to the upper soil layers. The relatively low C-14 dose is due systematic differences between the two sites. That is, the pronounced topographical relief in Laxemar results in enhanced groundwater discharge in valleys. This, in turn, leads to a relatively low concentration of C-14 in the pore water of intermediate regolith layers (which provide plants with water during dry periods). Thus, whereas a high rate of bedrock discharge may have increased the importance of Mo-93 in object 206, this effect was partly counter-balanced by more dilution of C-14.

It was also noted that a release into a lake could result in an elevated dose from C-14, as compared with the base case (about a factor two in object 206). However, if C-14 is not a main contributor to dose in the drained mire land-use variant, then exposure from an aquatic recipient is unlikely to yield a substantially higher total annual dose than exposure from a mire. This is because the dose from radionuclides other than C-14 typically is considerably lower (about three orders of magnitude lower) from a lake than from a mire (e.g. BHA in Figure 12-3).

16.5.2 Comparison of effects of evaluated uncertainties

The uncertainties in doses caused by other properties (the most influential being K_d, *CR* and other transfer factors) than discharge area characteristics (i.e. ecosystem type, geometry, regolith stratification and hydrology) and climate were not quantified in SE-SFL, except for the benchmark to generic mean parameter values in the *alternative K_d and CR sensitivity case*. However, as the biosphere model is essentially the same as the one used in SR-PSU, and as the variation around typical values could be expected to be similar among potential sites, previous quantification of the effects of parameter uncertainties (Section 10.9 in SKB 2014d) was considered a relevant point of reference.

To allow for a straightforward comparison between variations quantified in SE-SFL and random variations expected in parameter values, the maximum annual dose from a unit release rate (1 Bq year^{-1}) to object 206 was first calculated. The upper and lower confidence limits[47] of the SR-PSU results (which were also based on a unit release rate) were then normalised by the unit release rate dose from object 206. The derived dose span caused by parameter uncertainty should be interpreted with some care, as the importance of some parameters may depend on the properties of the object used in the base case (and these differed between SE-SFL and SR-PSU).

The comparison with the SR-PSU results showed that the uncertainty in doses caused by variations in discharge area properties was comparable with that expected from variations in other biosphere parameters (Figure 16-1). An exception to this was Cl-36, for which object properties appeared to have a smaller influence on dose variation than other parameter uncertainties. For Cl-36, Mo-93 and Ni-59, the properties that drove most of the uncertainties were distribution coefficients for regolith layers and biological transfer factors (including *CR* and transfer from fodder to milk and meat, SKB 2014d). In future safety assessments, the numerical representation of these parameters should be sufficiently large to cover natural variation and a relevant span of possible future conditions. However, the central values also need to be firmly anchored in the conditions of the selected site. This is especially important for elements for which the local chemical environment is expected to have a significant influence on transport properties, and for biological uptake in agricultural systems, since most of the SKB data underpinning these parameters have been collected from one specific site (i.e. Forsmark).

The uncertainty of the C-14 dose was primarily driven by variables that determine the release and uptake of stable carbon in and from cultivated soil. The model updates introduced in SE-SFL are expected to have reduced these uncertainties noticeably. The reduction is expected, since the primary driver of dose uncertainties in SR-PSU was the gas diffusivity of CO_2 in cultivated soil (~ 50 % of uncertainty, Figure 10-34 in SKB 2014d). In the updated biosphere model, degassing of stable carbon and of C-14 is described by the same processes, and thus the C-14 dose calculations in the SE-SFL model are expected to be insensitive to the diffusivity of CO_2 (Saetre and Ekström 2017a). Nevertheless, soil respiration and groundwater uptake are key parameters for calculations of C-14 dose that need careful consideration once a site has been selected. In SE-SFL, C-14 exposure from lakes was more important than exposure from the drained mire. Thus, if C-14 turns out to be a major dose-contributing radionuclide in future SFL assessments, then site-specific consideration of aquatic parameters (e.g. the concentration of CO_2 in lake water) will also be required.

[47] The span between the 5th and 95th percentiles of the radionuclide-specific dose from (1 000) realisations was used as an indicator of the expected effects of parameter uncertainties.

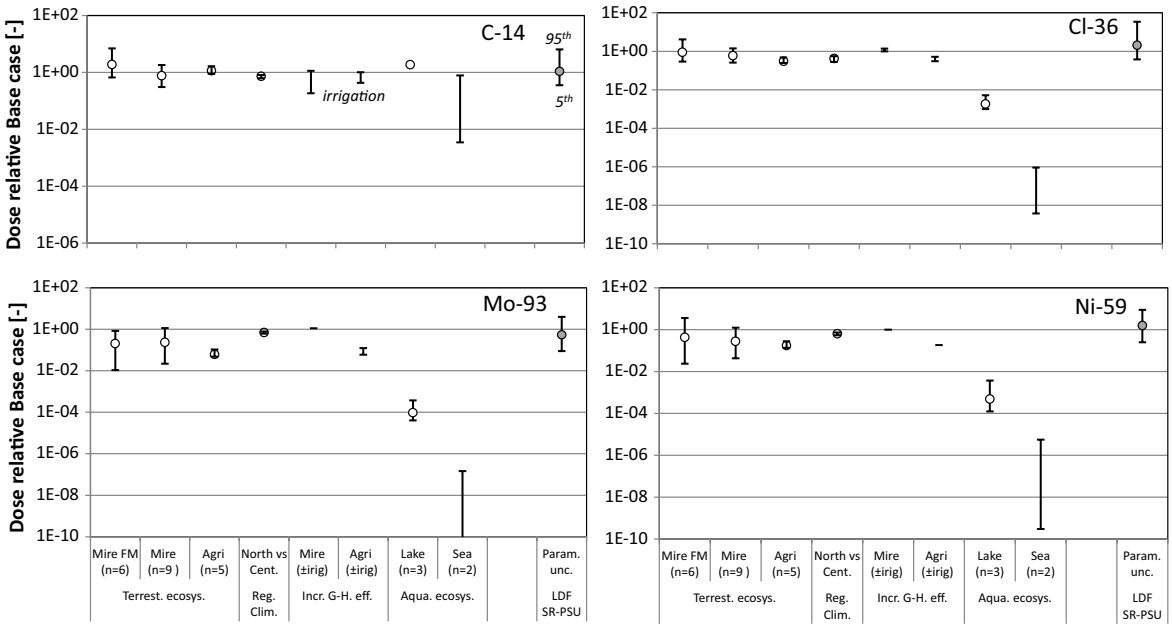

Figure 16-1. *Variation in annual doses from four key radionuclides as a function of the location of the release (Lx, Laxemar; Fm, Forsmark), ecosystem type (Mire, Agri, Lake, Sea), variation in temperate climate (alternative regional climate abbreviated as Reg. Clim.) and increased greenhouse effect (Incr. G-H eff.) evaluation case, and parameter uncertainty (including K_d and CR). Geometric means (white circles) and ranges (minimum and maximum values) of object-specific doses are given for calculations from this report. When just two observations are available, only minimum and maximum values are given. Parameter uncertainties at the right-hand side of each panel are taken from SR-PSU (SKB 2014d). These are characterised by the median value (grey circle) and the 5th and 95th percentiles from 1000 Monte-Carlo simulations. All values have been normalised by the corresponding annual dose in object 206.*

16.6 Implications of results for site selection

The potential effect on annual doses from the regional climate as reflected in variation along the Swedish coasts is clearly limited as compared with the variation caused by uncertainty in object properties (Figure 16-1). Climates associated with high rates of groundwater recharge and discharge (i.e. a climate with high precipitation and/or low annual temperature) are likely to result in a lower annual dose than in the base case (Section 12.5). However, it is unlikely that a location with a favourable climate within the borders of Sweden will reduce the annual dose from SFL by more than a factor of two as compared with the regional climate used in the base case. Thus, there are no indications of regional climate being a factor of significant importance for site selection.

The results from the initially submerged conditions (Section 12.6) and the discharge area cases (Sections 12-3 and 12-4) suggest that locating SFL at a position below the seabed will cause significantly lower doses during the submerged period. This is partly due to significantly reduced advective transport (that results in an increased radioactive decay) and partly due to a relatively high rate of dilution and low productivity in sea ecosystems as compared with terrestrial arable land. Submerged conditions are likely to delay the maximum release to the biosphere, and if the period is sufficiently long, it may also reduce the maximum dose from C-14 and Mo-93 substantially in the terrestrial period that follows due to shoreline migration). However, decay of very long-lived radionuclides (half-life $> 2 \times 10^5$ years) will be limited even during prolonged periods of submerged conditions. Thus, the benefits of a submerged location will depend on the length of the submerged period and on the inventory of very long-lived radionuclides.

The analyses of biosphere object properties clearly indicate that features of the discharge area have significant effects on environmental concentrations and on the potential dose from SFL. *In theory*, a repository location that would result in discharge to relatively large and deep basins in lower terrain would be preferable as such a location is expected to be associated with thick regolith layers and substantial groundwater discharge from the landscape. However, *in practice*, the uncertainty with respect to the projected release area that results from flow pathways through several hundred metres of bedrock is large and hard to quantify. Thus, it is of key importance that the uncertainties with respect to the characteristics of potential recipient locations at potential sites for SFL are handled properly in future safety assessments.

17 Summary of development and considerations regarding future work on assessments

17.1 Introduction

Progress has been made with respect to several areas in the biosphere analysis of SE-SFL. These areas include: formulation of evaluation and sensitivity cases, extraction of parameter values from supportive modelling, transport modelling, and presentation and interpretation of results. The development has partly been motivated by reviews undertaken by SSM (and their external experts) of previous safety assessments. In addition, developments to increase the consistency in analyses and to facilitate the understanding of the results have been introduced. The most import developments are summarised below, and the potential benefits from the development in future safety analyses are highlighted. Integration with the overall safety evaluation has been a lead motive in the biosphere analysis, and the interdisciplinary work has been facilitated by a fully integrated calculation chain and holistic analyses from the near field to the surface. The next stage of the SFL programme will involve an evaluation of the repository performance at one or more geographical locations. In the last section of this chapter, conclusions for the next stage are drawn, and areas in which improved methodology may benefit the full safety assessment are identified.

17.2 Formulation of evaluation and sensitivity cases

In SE-SFL, potential consequences of the location of the discharge area, and its properties, have been examined in terms of the regional climate and discharge the area evaluation cases. For the latter, the sensitivity of doses to several object properties was explicitly examined, and the importance of object size and soil depth was demonstrated. Moreover, it was shown that landscape development had a limited effect on the dose at late successional stages, and it was suggested that time-independent ecosystem models give robust estimates of potential exposure. The approach and the findings should be applicable also to future safety analyses, in which the uncertainties with respect to the location and the properties of potential discharge areas are large due to, for example, significant releases to the biosphere being projected to occur in the far future. Time-independent models also have a potential to more clearly address some of the uncertainties that arise from combining a time-dependent geosphere release with a developing biosphere.

In the increased greenhouse effect evaluation case, the potential effects of a seasonal water deficit in arable land were examined. The consequences of covering the deficit by irrigation, and the importance of translocation of radionuclides within plants (from leaf interception to root storage), were evaluated. The evaluation of long-term irrigation utilised a new (multi-compartmental) model describing continuous cultivation. The approach and conclusions from these calculations should be relevant to future safety analyses in which potential effects of a warmer climate are evaluated. In the simplified glaciation cycle evaluation case, the discharge area and the groundwater flow conditions were changed in response to the approach and withdrawal of an inland ice sheet. The changes in flow conditions in the biosphere were closely co-ordinated with those in the geosphere. The approach has ensured a consistent handling of the groundwater response across the geosphere-biosphere interface, and it may be worthwhile to consider similar approaches also in future analyses.

17.3 Model development

The core challenge for the development of assessment level models is to capture the main features of transport, accumulation and exposure within the biosphere with highly stylised models. SKB's safety assessment models have traditionally been dependent on detailed process-orientated models (describing e.g. groundwater flow and landscape development) to provide aggregated input parameters on the scale of individual discharge areas. However, these models have typically been run deterministically, and the results do not reflect any variation (or uncertainty) in external and internal conditions.

Thus, to facilitate flexibility and scalability of input parameters, well-defined interfaces between stylised and complex models would be beneficial. In SE-SFL, two different approaches to such interfaces were developed: a simplified model of lake ingrowth and a stylised model of the water balance in mires and agricultural areas. Both approaches were used to generate model parameters, and the second approach was also integrated into versions of the BioTEx model itself.

The introduction of stylised water balance models may well be the model development with the widest implications for the biosphere analysis in SE-SFL. The stylised models were used to interpret and summarise the water balances from MIKE SHE in terms of the driving hydrological flows, vertical distribution functions and a limited number of empirically derived parameters. Thus, percolation and discharge in the biosphere object could be described from net precipitation, bedrock discharge, the size of the object (and its local catchment) and the average regolith stratigraphy. In SE-SFL, the approach was primarily used to extrapolate groundwater flows to climate and ecosystem stages where data from detailed modelling were not available. As the method was scalable with respect to object size and regolith stratigraphy, it was implemented as an integrated part of the BioTEx model and used to examine the sensitivity of environmental activity concentrations to object properties and hydrological drivers. This type of analysis has been requested by SSM and should be valuable to build understanding of model results in future safety analyses.

In addition, the BioTEx model has been modified as a result of SSM's reviews of the SR-Site and SR-PSU assessments. The most important update, in terms of potential effects on modelling results, is the increased discretisation of the lower regolith layers (i.e. till and glacial clay layers). In previous assessments, a single compartment representation of these layers has been used. For radionuclides that have a residence time that is similar to, or longer than, the radioactive half-life, a single lower regolith layer may overestimate the activity released to the surface (due to numeric dispersion). In SE-SFL, the discretisation has been increased so that the numerical dispersion mimics the expected field-scale dispersion. As the update is considered to increase the realism of the modelling (for example with respect to the timing of radionuclide breakthrough at the surface), SKB intends to use this modified model also in future safety analyses.

In addition to the developments mentioned above, the transparency, consistency and realism of the biosphere model have been increased in several areas. For example, previous parameters for stable carbon (such as the rate of peat growth and pore water concentrations in saturated and unsaturated soil) are calculated as functions within the SE-SFL model. These updates increase consistency in the handling of C-12 and C-14 in the model. As this consistency is maintained in probabilistic simulations, it is also expected to reduce the uncertainty in estimates of plant uptake of C-14. The C-14 model development has been driven by SSM's reviews and requests for complementary information. SKB intends to use these modifications also in future safety analyses. From model comparisons, other model updates are expected to have a minor influence on model results. Nevertheless, the benefits from increased consistency and realism (as well as from justified model simplifications) will also be realised in future safety analyses.

17.4 Supporting modelling

Process understanding and appropriate conceptual models are key elements for a successful reduction of ecosystem complexity, but supportive calculations with detailed transport models, and comparisons between alternative model formulations, are also important elements for model evaluation.

Detailed hydrological modelling has typically been used by SKB to derive groundwater flows for stylised transport modelling in surface ecosystems. In SE-SFL, distributed models were used for supporting characterisation of groundwater flow pathways and radionuclide accumulation in a heterogeneous discharge area. Particle tracking in 3D with MIKE SHE confirmed that, on the scale of a discharge area, groundwater flow paths are primarily directed upwards. It was also shown that the advective travel times associated with aggregate parameters (of water flow and regolith depth) were similar to the travel times of particles. Using a similar approach in COMSOL, it was shown how insights from distributed transport modelling can be used to inform structural improvements, to justify process simplifications and to extract reasonable parameters for stylised modelling. Results

from model comparisons (on the scale of a discharge area), suggested that the heterogeneity within the object was not a major source of uncertainty for radionuclide accumulation, and that a stylised model parameterised with average characteristics can predict radionuclide concentrations with a reasonable accuracy (i.e. within a factor of two, relative to the distributed model). Taken together, the model comparisons confirm that the stylised assessment-level modelling used by SKB is based on sound assumptions and yields reasonable results. Similar approaches can be useful also in future development to gain insights into transport pathways, to inform structural modifications and simplifications of assessment models, and to address questions of discretisation in relation to field-scale transport and dispersion.

The mobility of two transitional metals, Ni and Mo, were examined in detail in SE-SFL. The mobility of these two elements is primarily determined by their chemical form in combination with environmental conditions. It was concluded that the applied K_d values capture a significant part of natural variation in the mobility of the two examined elements, and that this variation is consistent with the understanding of the underlying biogeochemical processes. In a separate exercise, geochemical modelling was combined with transport calculations. The results from such reactive transport modelling have the potential to provide a detailed description of retention that is conditioned on the transport of radionuclides and on the local chemical conditions. However, the calculations require that the primary retention processes are well characterised, and that detailed descriptions of the soil chemistry for individual regolith layers are available. The present work demonstrates that the computational capability and capacity for reactive transport calculations in 3D, at the level of a discharge area, is readily available. However, a mechanistic process description in organic soils and detailed chemical characteristics along the full transport pathways are still insufficiently described. Thus, it is suggested that a systematic conceptual and numerical calibration between empirical K_d values and mechanistically calculated retention should be undertaken prior to future reactive transport calculations. Such a calibration would clearly facilitate model comparisons and evaluation of results from reactive transport calculations.

17.5 Presentation and evaluation of results

The analysis and means of presentation have been refined in SE-SFL. For example, in the analysis of the base case, the accumulation and decay of radionuclides in regolith layers are visualised in holistic graphs, an overview of the influence of radionuclide properties on the release to dose relationship is presented, and the origin and fate of individual radionuclides in the U-238 decay chain are explicitly depicted. In addition, improvements have been made with respect to the analyses and presentation of the effects of object properties on modelling results, both in the discharge area evaluation cases and in sensitivity analyses. Graphs that display important parameters and/or illustrate individual mechanisms that are of importance for transport and exposure have also been tailored to the individual evaluation and sensitivity cases. Taken together, the improvements in analysis and presentation of results have been significant in SE-SFL, and the developments that have been implemented will be used in future assessments to facilitate the understanding of modelling results.

17.6 Integration with overall assessment

Good communication amongst modellers and empiricists increases the likelihood of coherent use of data from field and experimental studies and supporting models in assessment models, and thus also enables correct interpretations and conclusions from model results. In projects that assess post-closure safety for geological repositories for radioactive waste, communication is vital both within groups that work in a specific discipline and between groups in different disciplines.

In SE-SFL, members of the biosphere team have worked with experts from other disciplines as a part of the radionuclide transport team. The integration has been facilitated by, for example, a clear and consistent description of the transport pathway from the repository to the discharge area (Figure 1-5) and a fully integrated calculation chain from waste releases to dose calculations (Figure 2-4). A presentation of the results, focusing on mechanistic understanding (Section 17.5), that can be communicated

appropriately across disciplines and potentially reach a broader target audience, has contributed to the increased integration. Furthermore, holistic analyses across model domains (see **Radionuclide transport report**, Chapters 5 to 8) have allowed for a comprehensive and insightful interpretation of results, from the waste vaults to the surface ecosystems.

The interdisciplinary work has been particularly fruitful in the identification and definition of the evaluation cases, in combination with the interpretation of results. Discussions and iterations between these two steps have resulted in stylised evaluation cases that are internally consistent and have allowed for straightforward comparisons that address the features of overall interest. For example, in the *simplified glaciation evaluation case*, temporal changes in hydrological forcing as a response to the existence of an ice sheet and relative sea-level changes, are consistent across the near-field, geosphere and biosphere.

Despite the obvious advantages of the integrated approach in the SE-SFL projects, the benefits are expected to be even greater in a full safety assessment with a broader coverage of uncertainties. That is, a holistic approach is likely to promote a consistent treatment of uncertainties, and a proper balance of simplifications, across the different model domains (e.g. climate, near-field, geosphere and biosphere), as well as formulations of coherent scenarios that address the uncertainties most relevant to system understanding and the overall assessment results.

17.7 Conclusions for future work

The SFL safety evaluation shows that the repository concept for SFL has potential to fulfil regulatory requirements under suitable conditions (**Main report**). The results of the radionuclide transport and dose calculations indicate that the conditions assumed in the base case yield doses that are too high to comply with the risk criterion. However, the full set of evaluation cases indicates that conditions and further efforts could improve the performance of the repository. These include obtaining suitable site conditions, such as low groundwater flow rates, and reducing uncertainties in the radionuclide inventory. Technical developments and optimisation of the repository design and components can also be used to improve repository performance.

The biosphere model is an integrated part of the transport and dose calculation chain, which underpins the safety evaluation. The level of detail and most assumptions underlying the biosphere model are based on the previous biosphere assessment SR-PSU. The evaluation deals with consequences far into the future, and thus a balanced handling of sometimes large uncertainties have been an integral part of the assessment. However, the effects of quantified uncertainties were found to be modest and are therefore not expected to have a significant influence on the interpretation of results. Taken together, this report builds confidence that the biosphere analysis in SE-SFL yields robust estimates of annual effective dose, which reflect process understanding and a relevant description of an example site. Thus, the results from the analysis are considered to give an adequate representation of dose consequences for this step of the safety analysis process.

The next stage of the process will involve evaluation of the repository performance at one or more geographical locations. From the analysis in this safety evaluation it is clear that there are some benefits from locating SFL at a position below the seabed. However the benefits of a submerged location will depend on the length of the submerged period and on the inventory of very long-lived radionuclides (Section 16.6). Moreover, there were no indications of regional climate being a factor of significant importance for site selection. However, features of the discharge area can have significant effects on environmental concentrations and on the potential dose from SFL. Thus, it is of key importance that the uncertainties with respect to the characteristics of potential recipient locations at a considered site for SFL are handled properly also in future safety assessments.

If Mo-93, C-14 and Cl-36 remains the main dose contributing radionuclides in the next steps of the safety assessment cycle, these radionuclides should be given specific attention also in future assessments. This includes both site measurements (see below) and further process-orientated modelling. Molybdenum occurs in many forms in the environment, and its mobility is a key property for exposure and dose calculations (Section 16.4.2). Thus, it will be important to ensure that K_d values for molybdenum capture a significant part of this environmental variation, and that selected

properties are consistent with the understanding of underlying biogeochemical processes at the selected site. For C-14, the dose from the aquatic food-chain is expected to be important. It may thus be desirable to reduce the uncertainty of C-14 uptake by describing the processes that governs spatial and temporal patterns of aquatic DIC concentrations (Section 16.2.4). Similarly, a process based ecosystem model for chlorine (in accordance with current knowledge, Chapter 14) would be a reasonable starting point for reducing uncertainties with respect to the fate of Cl-36 in terrestrial ecosystems. Future revision of the assessment model should account for the relevant forms of carbon and chlorine in the environment and treat the fate of the radionuclides and their stable isotopes consistently (Section 16.2.4).

For the next step, a detailed description of the biosphere at the site will be needed. Such a description includes the estimation of the geometric properties of potential discharge areas, associated groundwater flows, key ecosystem parameters (describing e.g. soil retention, plant uptake and background concentrations of stable isotopes) under relevant conditions, and associated natural variation and uncertainties. Given the timescales considered, the development of the landscape and the response of ecosystems to large scale climatic changes (and the sea-level development) also need to be described at the site, and the understanding handled on a scale of individual discharge areas. This includes describing the annual and seasonal water balances and groundwater flows under considerably warmer conditions. Moreover, the large uncertainties inherent in such projections need to be described so that they can be adequately addressed in the safety assessment. Finally, it is acknowledged that empirical data also can offer an opportunity for partial model validation, which can strengthen the confidence that can be put into the results from safety assessment models.

References

SKB's (Svensk Kärnbränslehantering AB) publications can be found at www.skb.com/publications. SKBdoc documents will be submitted upon request to document@skb.se.

References with abbreviated names

Main report, 2019. Post-closure safety for a proposed repository concept for SFL. Main report for the safety evaluation SE-SFL. SKB TR-19-01, Svensk Kärnbränslehantering AB.

Biosphere synthesis, 2019. Biosphere synthesis for the safety evaluation SE-SFL. SKB TR-19-05, Svensk Kärnbränslehantering AB.

Climate report, 2019. Climate and climate-related issues for the safety evaluation SE-SFL. SKB TR-19-04, Svensk Kärnbränslehantering AB.

FEP report, 2019. Features, events and processes for the safety evaluation SE-SFL. SKB TR-19-02, Svensk Kärnbränslehantering AB.

Initial state report, 2019. Initial state for the repository for the safety evaluation SE-SFL. SKB TR-19-03, Svensk Kärnbränslehantering AB.

Radionuclide transport report, 2019. Radionuclide transport and dose calculations for the safety evaluation SE-SFL. SKB TR-19-06, Svensk Kärnbränslehantering AB.

Other references

Adrian R, O'Reilly C M, Zagarese H, Baines S B, Hessen D O, Keller W, Livingstone D M, Sommaruga R, Straile D, van Donk E, Weyhenmeyer G A, Winder M, 2009. Lakes as sentinels of cli-mate change. Limnology and Oceanography 54, 2283–2297.

Ahrens L H, Press F, Runcorn S K (eds), 2013. Physics and chemistry of the Earth: Progress series. Elsevier.

Alexandersson H, Eggertsson Karlström C, 2001. Temperaturen och nederbörden i Sverige 1961–1990. Referensnormaler – utgåva 2. Norrköping: SMHI. (Meteorologi 99) (In Swedish.)

Alloway B J (ed), 2012. Heavy metals in soils: trace metals and metalloids in soils and their bioavailability. Springer Science & Business Media.

Andersson E, 2010. The limnic ecosystems at Forsmark and Laxemar-Simpevarp. SKB TR-10-02, Svensk Kärnbränslehantering AB.

Andersson E, Tudorancea M-M, Tudorancea C, Brunberg A-K, Blomqvist P, 2003. Water chemistry, biomass and production of biota in Lake Eckarfjärden during 2002. SKB R-03-27, Svensk Kärnbränslehantering AB.

Andersson M P, Sakuma H, Stipp S L S, 2014. Strontium, Nickel, Cadmium, and Lead Substitution into Calcite, Studied by Density Functional Theory. Langmuir 30, 6129–6133.

Aquilonius K (ed), 2010. The marine ecosystems at Forsmark and Laxemar-Simpevarp. SR-Site Biosphere. SKB TR-10-03, Svensk Kärnbränslehantering AB.

Asplund G, Grimvall A, Jonsson S, 1994. Determination of the total and leachable amounts of organohalogens in soil. Chemosphere 28, 1467–1475.

ATSDR, 2005. Public health assessment guidance manual (Update). U.S. Department of Health and Human Services, Public Health Service Agency for Toxic Substances and Disease Registry (ATSDR), Atlanta, Georgia.

Atwell B J, Kriedemann P E, Turnbull C G N, 1999. Plants in action: adaption in nature, performance in cultivation. MacMillan Education Australia.

Augustsson A, Peltola P, Bergback B, Saarinen T, Haltia-Hovi E, 2010. Trace metal and geochemical variability during 5,500 years in the sediment of Lake Lehmilampi, Finland. Journal of Paleolimnology 44, 1025–1038.

Avila R, Moberg L, 1999. A systematic approach to the migration of ^{137}Cs in forest ecosystems using interaction matrices. Journal of Environmental Radioactivity 45, 271–282.

Aze T, Fujimura M, Matsumura H, Masumoto K, Nakao N, Matsuzaki H, Nagai H, Kawai M, 2007. Measurement of the production rates of ^{36}Cl from Cl, K, and Ca in concrete at the 500 MeV neutron irradiation facility at KENS. Journal of Radioanalytical and Nuclear Chemistry 272, 491–494.

Bastviken D, Sandén P, Svensson T, Ståhlberg C, Magounakis M, Öberg G, 2006. Chloride retention and release in a boreal forest soil: effects of soil water residence time and nitrogen and chloride loads. Environmental Science and Technology 40, 2977–2982.

Bastviken, D, Thomsen F, Svensson T, Karlsson S, Sandén P, Shaw G, Matucha M, Öberg G, 2007. Chloride retention in forest soil by microbial uptake and by natural chlorination of organic matter. Geochimica et Cosmochimica Acta 71, 3182–3192.

Bastviken, D, Svensson T, Karlsson S, Sandén P, Öberg G, 2009. Temperature sensitivity indicates that chlorination of organic matter in forest soil is primarily biotic. Environmental Science & Technology 43, 3569–3573.

Bastviken, D, Svensson T, Sandén P, Kylin H, 2013. Chlorine cycling and fates of ^{36}Cl in terrestrial environments. SKB TR-13-26, Svensk Kärnbränslehantering AB.

Bauer S, 2018. Dissolved and suspended transport of tungsten, molybdenum, and vanadium in natural waters. Available from: http://urn.kb.se/resolve?urn=urn:nbn:se:ltu:diva-66852 [23 April 2018].

Berg C, 2007. Forsmark site investigation. Sampling and analysis of precipitation, September 2005 to June 2007. SKB P-07-170, Svensk Kärnbränslehantering AB.

Boes X, Rydberg J, Martinez-Cortizas A, Bindler R, Renberg I, 2011. Evaluation of conservative lithogenic elements (Ti, Zr, Al, and Rb) to study anthropogenic element enrichments in lake sediments. Journal of Paleolimnology 46, 75–87.

Bosson E, Sassner M, Gustafsson L-G, 2009. Numerical modelling of surface hydrology and near-surface hydrogeology at Laxemar-Simpevarp. Site descriptive modelling, SDM-Site Laxemar. SKB R-08-72, Svensk Kärnbränslehantering AB.

Bosson E, Sassner M, Sabel U, Gustafsson L-G, 2010. Modelling of present and future hydrology and solute transport at Forsmark. SR-Site Biosphere. SKB R-10-02, Svensk Kärnbränslehantering AB.

Bosson E, Sabel U, Gustafsson L G, Sassner M, Destouni G, 2012. Influences of shifts in climate, landscape, and permafrost on terrestrial hydrology. Journal of Geophysical Research Atmospheres 117, D05120. doi:10.1029/2011JD016429

Brady N C, Weil R R, 2002. The nature and properties of soils. 13th ed. Upper Saddle River, NJ : Prentice Hall.

Brunberg A-K, Carlsson T, Brydsten L, Strömgren M, 2004. Oskarshamn site investigation. Identification of catchments, lake-related drainage parameters and lake habitats. SKB P-04-242, Svensk Kärnbränslehantering AB.

Brydsten L, 2004. A mathematical model for lake ontogeny in terms of filling with sediments and macrophyte vegetation. SKB TR-04-09, Svensk Kärnbränslehantering AB.

Brydsten L, 2009. Sediment dynamics in the coastal areas of Forsmark and Laxemar during an interglacial. SKB TR-09-07, Svensk Kärnbränslehantering AB.

Brydsten L, Strömgren M, 2010. A coupled regolith-lake development model applied to the Forsmark site. SKB TR-10-56, Svensk Kärnbränslehantering AB.

Brydsten L, Strömgren M, 2013. Landscape development in the Forsmark area from the past into the future (8500 BC – 40,000 AD). SKB R-13-27, Svensk Kärnbränslehantering AB.

Campbell K, Wolfsberg A, Fabryka-Martin J, Sweetkind D, 2003. Chlorine-36 data at Yucca Mountain: Statistical tests of conceptual models for unsaturated-zone flow. Journal of Contaminant Hydrology 62–63, 43–61.

Chapin F S, Matson P A, Mooney H A, 2002. Principles of terrestrial ecosystem ecology. New York: Springer.

Chappaz A, Lyons T W, Gregory D D, Reinhard C T, Gill B C, Li C, Large R R, 2014. Does pyrite act as an important host for molybdenum in modern and ancient euxinic sediments? Geochimica et Cosmochimica Acta 126, 112–122.

Chen C, Huang D, Liu J, 2009. Functions and toxicity of nickel in plants: Recent advances and future prospects. Clean-Soil Air Water 37, 304–313.

Claesson Liljedahl L, Kontula A, Harper J, Näslund J-O, Selroos J-O, Pitkänen P, Puigdomenech I, Hobbs M, Follin S, Hirschorn S, Jansson P, Kennell L, Marcos N, Ruskeeniemi T, Tullborg E-L, Vidstrand P, 2016. The Greenland Analogue Project: Final report. SKB TR-14-13, Svensk Kärnbränslehantering AB.

Clarhäll A, 2011. SKB studies of the periglacial environment – report from field studies in Kangerlussuaq, Greenland 2008 and 2010. SKB P-11-05, Svensk Kärnbränslehantering AB.

Cole J J, Lane J M, Marino R, Howarth R W, 1993. Molybdenum assimilation by cyanobacteria and phytoplankton in freshwater and salt water. Limnology and Oceanography 38, 25–35.

COMSOL, 2015. COMSOL Multiphysics. Reference Manual. Version 5.1. Burlington, MA: COMSOL Inc.

Crusius J, Thomson J, 2000. Comparative behavior of authigenic Re, U, and Mo during reoxidation and subsequent long-term burial in marine sediments. Geochimica et Cosmochimica Acta 64, 2233–2242.

Crusius J, Calvert S, Pedersen T, Sage D, 1996. Rhenium and molybdenum enrichments in sediments as indicators of oxic, suboxic and sulfidic conditions of deposition. Earth and Planetary Science Letters 145, 65–78.

Curti E, 1999. Coprecipitation of radionuclides with calcite: estimation of partition coefficients based on a review of laboratory investigations and geochemical data. Applied Geochemistry 14, 433–445.

Dahl T W, Anbar A D, Gordon G W, Rosing M T, Frei R, Canfield D E, 2010. The behavior of molybdenum and its isotopes across the chemocline and in the sediments of sulfidic Lake Cadagno, Switzerland. Geochimica et Cosmochimica Acta 74, 144–163.

Dahl T W, Ruhl M, Hammarlund E U, Canfield D E, Rosing M T, Bjerrum C J, 2013. Tracing euxinia by molybdenum concentrations in sediments using handheld X-ray fluorescence spectroscopy (HHXRF). Chemical Geology 360–361, 241–251.

Dahlqvist R, Andersson K, Ingri J, Larsson T, Stolpe B, Turner D, 2007. Temporal variations of colloidal carrier phases and associated trace elements in a boreal river. Geochimica et Cosmochimica Acta 71, 5339–5354.

Deleebeeck N M E, De Laender F, Chepurnov V A, Vyverman W, Janssen C R, De Schamphelaere K A C, 2009. A single bioavailability model can accurately predict Ni toxicity to green microalgae in soft and hard surface waters. Water Research 43, 1935–1947.

Duro L, Grivé M, Cera E, Domènech C, Bruno J, 2006. Update of a thermodynamic database for radionuclides to assist solubility limits calculation for performance assessment. SKB TR-06-17, Svensk Kärnbränslehantering AB.

EC, 2002. Guidance on the realistic assessment of radiation doses to members of the public due to the operation of nuclear installations under normal conditions. European Commission. (Radiation Protection 129)

Edwards I K, Kalra Y P, Radford F G, 1981. Chloride determination and levels in the soil-plant environment, Environmental Pollution. Environmental Pollution Series B, Chemical and Physical 2, 109–117.

Eliasson P, 1992. "Genom helvetes port, men…" – skogsdikning som mål och medel. Aktuellt om historia 3–4, 46–60. (In Swedish.)

Elfwing M, Evins L Z, Gontier M, Grahm P, Mårtensson P, Tunbrant S, 2013. SFL concept study. Main report. SKB TR-13-14, Svensk Kärnbränslehantering AB.

Eng T, Hudson J, Stephansson O, Skagius K, Wiborgh M, 1994. Scenario development methodologies. SKB TR 94-28, Svensk Kärnbränslehantering AB.

Engdahl A, Ternsell A, Hannu S, 2006. Oskarshamn site investigation. Chemical characterisation of deposits and biota. SKB P-06-320, Svensk Kärnbränslehantering AB.

Engqvist A, 2010. Estimation of residence times of coastal basins in the Laxemar-Simpevarp area between 3000 BC and 9000 AD. SKB R-10-57, Svensk Kärnbränslehantering AB.

Engvild K C, 1986. Chlorine-containing natural compounds in higher-plants. Phytochemistry 25, 781–91.

Eriksson E, 1960. The yearly circulation of chloride and sulfur in nature; meteorological, geochemical and pedological implications, Part II. Tellus 12, 63–109.

Evins L, 2013. Progress report on evaluation of long term safety of proposed SFL concepts. SKB R-13-41, Svensk Kärnbränslehantering AB.

Fahimi I J, Keppler F, Schöler H F, 2003. Formation of chloroacetic acids from soil, humic acid and phenolic moieties. Chemosphere 52, 513–520.

Flodin C, Johansson E, Borén H, Grimvall A, Dahlman O, Mörck R, 1997. Chlorinated structures in high molecular weight organic matter isolated from fresh and decaying plant material and soil. Environmental science and technology 31, 2464–2468.

Fréchou C, Degros J-P, 2005. Measurement of ^{36}Cl in nuclear wastes and effluents: Validation of a radiochemical protocol with an in-house reference sample. Journal of Radioanalytical and Nuclear Chemistry 263, 333–339.

French H M, 2007. The periglacial environment. 3rd ed. Chichester: Wiley.

Galson D A, Khursheed A, 2007. The treatment of uncertainty in performance assessment and safety case development: state-of-the art overview. PAMINA Milestone Report M1.2.1, European Commission.

Gelhar L W, Welty C, Rehfeldt K R, 1992. A critical-review of data on field-scale dispersion in aquifers. Water Resources Research 28, 1955–1974.

Gielen S, Vives i Batlle J, Vincke C, Van Hees M, Vandenhove H, 2016. Concentrations and distributions of Al, Ca, Cl, K, Mg and Mn in a Scots pine forest in Belgium. Ecological Modelling 324, 1–10.

Glass J B, Chappaz A, Eustis B, Heyvaert A C, Waetjen D P, Hartnett H E, Anbar A D, 2013. Molybdenum geochemistry in a seasonally dysoxic Mo-limited lacustrine ecosystem. Geochimica et Cosmochimica Acta 114, 204–219.

Goldberg S, Forster H S, Godfrey C L, 1996. Molybdenum adsorption on oxides, clay minerals, and soils. Soil Science Society of America Journal 60, 425–432.

Gribble G W, 1998. Naturally occurring organohalogen compounds. Accounts of Chemical Research 31, 141–152.

Gribble G W, 2010. Naturally occurring organohalogen compounds: a comprehensive update. Wien: Springer.

Gribble G W, 2015. A recent survey of naturally occurring organohalogen compounds. Environmental Chemistry 12, 396–405.

Grolander S, 2013. Biosphere parameters used in radionuclide transport modelling and dose calculations in SR-PSU. SKB R-13-18, Svensk Kärnbränslehantering AB.

Grolander S, Jaeschke B, 2019. Biosphere parameters used in radionuclide transport modelling and dose calculations in SE-SFL. SKB R-19-18, Svensk Kärnbränslehantering AB.

Gustafsson J P, 2012. Visual MINTEQ 3.0. Available at: https://vminteq.lwr.kth.se/download/

Gustafsson J P, Tiberg C, 2015. Molybdenum binding to soil constituents in acid soils: An XAS and modelling study. Chemical Geology 417, 279–288.

Gustavsson M, Karlsson S, Öberg G, Sanden P, Svensson T, Valinia S, Thiry Y, Bastviken D, 2012. Organic matter chlorination rates in different boreal soils: The role of soil organic matter content. Environmental Science & Technology 46, 1504–1510.

Haavisto F, Toivola M, 2017. Studies on the aquatic environment at Olkiluoto and reference area: 6. Poosjoki River in 2014–2015. Posiva Working Report 2017-13, Posiva Oy, Finland.

Hamilton J T G, McRoberts W C, Keppler F, Kalin R B, Harper D B, 2003. Chloride methylation by plant pectin: an efficient environmentally significant process. Science 301, 206–209.

Hannu S, Karlsson S, 2006. Forsmark site investigation. Chemical characterisation of deposits and biota. SKB P-06-220, Svensk Kärnbränslehantering AB.

Harrison J P, Hudson J A, 2006. Comprehensive hazard identification in rock engineering using interaction matrix mechanism pathways. In: Golden Rocks 2006: the 41st U.S. Symposium on Rock Mechanics (USRMS), Golden, CO, 17–21 June 2006. Golden, CO: Colorado School of Mines.

Hartikainen J, Kouhia R, Wallroth T, 2010. Permafrost simulations at Forsmark using a numerical 2D thermo-hydro-chemical model. SKB TR-09-17, Svensk Kärnbränslehantering AB.

Helz G R, Bura-Nakic E, Mikac N, Ciglenecki I, 2011. New model for molybdenum behavior in euxinic waters. Chemical Geology 284, 323–332.

Henner P, Hurtevent P, Thiry Y, Levchuk S, Yoschenko V, Kashparov V, 2013. Translocation of ^{125}I, ^{75}Se and ^{36}Cl to edible parts of radish, potato and green bean following wet foliar contamination under field conditions. Journal of Environmental Radioactivity 124, 171–184.

Hoffmann U, Stipp S L S, 2001. The behavior of Ni^{2+} on calcite surfaces. Geochimica et Cosmochimica Acta 65, 4131–4139.

Holmes F W, Baker L A, 1966. Salt injury to trees. II. Sodium and chloride in roadside sugar maples in Massachusetts. Phytopathology 56, 633–636.

Hou X L, Østergaard L F, Nielsen S P, 2007. Determination of ^{36}Cl in nuclear waste from reactor decommissioning. Analytical Chemistry 79, 3126–3134.

Huang S, Lopez-Capel E, Manning D A C, Rickard D, 2010. The composition of nanoparticulate nickel sulphide. Chemical Geology 277, 207–213.

Hurtevent P, Thiry Y, Levchuk S, Yoschenko V, Henner P, Madoz-Escande C, Leclerc E, Colle C, Kashparov V, 2013. Translocation of ^{125}I, ^{75}Se and ^{36}Cl to wheat edible parts following wet foliar contamination under field conditions. Journal of Environmental Radioactivity 121, 43–54.

IAEA, 2003. "Reference Biospheres" for solid radioactive waste disposal. Report of BIOMASS Theme 1 of the BIOsphere Modelling and ASSessment (BIOMASS) Programme. Part of the IAEA Co-ordinated Research Project on Biosphere Modelling and Assessment (BIOMASS). IAEA-BIOMASS-6, International Atomic Energy Agency.

IAEA, 2004. Safety assessment methodologies for near surface disposal facilities. Vienna: International Atomic Energy Agency.

IAEA, 2010. Handbook of parameter values for the prediction of radionuclide transfer to humans in terrestrial and freshwater environments. Vienna: International Atomic Energy Agency. (IAEA Technical Reports Series 472)

IAEA, 2014. Modelling of biota dose effects. Report of working group 6 biota dose effects modelling of EMRAS II Topical heading reference approaches for biota dose assessment Environmental Modelling for RAdiation Safety (EMRAS II) programme. IAEA TECDOC -1737, International Atomic Energy Agency, Vienna.

IAEA, 2016. Environmental change in post-closure safety assessment of solid radioactive waste repositories. IAEA TECDOC-1799, International Atomic Energy Agency, Vienna.

ICRP, 1996. International Commission on Radiological Protection. Age-dependent doses to members of the public from intake of radionuclides: Part 5, compilation of ingestion and inhalation dose coefficients. Oxford: Pergamon. (ICRP Publication 72; Annals of the ICRP 26)

ICRP, 2000. Radiation protection recommendations as applied to the disposal of long-lived solid radioactive waste. Oxford: Pergamon Press. (ICRP Publication 81; Annals of the ICRP 28)

ICRP, 2006. Assessing dose of the representative person for the purpose of radiation protection of the public and the optimisation of radiological protection: broadening the process. Oxford: Pergamon. (ICRP Publication 101; Annals of the ICRP 36)

ICRP, 2008. Nuclear decay data for dosimetric calculations. Oxford: Pergamon. (ICRP Publication 107; Annals of the ICRP 38 (3))

ICRP, 2012. Compendium of dose coefficients based on ICRP Publication 60. Oxford: Pergamon. (ICRP Publication 119; Annals of the ICRP 41)

Ilina S M, Lapitskiy S A, Alekhin Y V, Viers J, Benedetti M Pokrovsky O S, 2016. Speciation, size fractionation and transport of trace elements in the continuum soil water–mire–humic lake–river–large oligotrophic lake of a subarctic watershed. Aquatic Geochemistry 22, 65–95.

Jaremalm M, Köhler S Lidman F, 2013. Precipitation of barite in the biosphere and its consequences for the mobility of Ra in Forsmark and Simpevarp. SKB TR-13-28, Svensk Kärnbränslehantering AB.

Jean M-E, Phalyvong K, Forest-Drolet J, Bellenger J-P, 2013. Molybdenum and phosphorus limitation of asymbiotic nitrogen fixation in forests of Eastern Canada: Influence of vegetative cover and seasonal variability. Soil Biology and Biochemistry 67, 140–146.

Johansson P-O, 2008. Description of surface hydrology and near-surface hydrogeology at Forsmark. Site descriptive modelling, SDM-Site Forsmark. SKB R-08-08, Svensk Kärnbränslehantering AB.

Johansson E, 2016. The influence of climate and permafrost on catchment hydrology. PhD thesis. Stockholm University.

Johansson E, Sassner M, 2019. Development of methodology for flow path analysis in the surface system – Numerical modelling in MIKE SHE for Laxemar. A report for the safety evaluation SE-SFL. SKB R-19-04, Svensk Kärnbränslehantering AB.

Johansson E, Sandén P, Öberg G, 2003. Organic chlorine in deciduous and coniferous forest soil in southern Sweden. Soil Science 168, 347–355.

Joyce S, Appleyard P, Hartley L, Tsitsopoulos V, Woollard H, Marsic N, Sidborn M, Crawford J, 2019. Groundwater flow and reactive transport modelling of temperate conditions. Report for the safety evaluation SE-SFL. SKB R-19-02. Svensk Kärnbränslehantering AB.

Kashparov V, Colle C, Levchuk S, Yoschenko V, Svydynuk N, 2007a. Transfer of chlorine from the environment to agricultural foodstuffs. Journal of Environmental Radioactivity 94, 1–15.

Kashparov V, Colle C, Levchuk S, Yoschenko V, Zvarich S, 2007b. Radiochlorine concentration ratios for agricultural plants in various soil conditions. Journal of Environmental Radioactivity 95, 10–22.

Kautsky U (ed), 2001. The biosphere today and tomorrow in the SFR area. SKB R-01-27, Svensk Kärnbränslehantering AB.

Kellner E, 2003. Wetlands – different types, their properties and functions. SKB TR-04-08, Svensk Kärnbränslehantering AB.

Keppler F, Biester H, 2003. Peatlands: a major sink of naturally formed organic chlorine. Chemosphere 52, 451–453.

Keppler F, Eiden R, Niedan V, Pracht J, Schöler H F, 2000. Halocarbons produced by natural oxidation processes during degradation of organic matte. Nature 403, 298–301.

Kjellström E, Strandberg G, Brandefelt J, Näslund J-O, Smith B, Wohlfarth B, 2009. Climate conditions in Sweden in a 100,000-year time perspective. SKB TR-09-04, Svensk Kärnbränslehantering AB.

Kopáček J, Hejzlar J, Porcal P, Posch M, 2014. A mass-balance study on chloride fluxes in a large central European catchment during 1900–2010. Biogeochemistry 120, 319–335.

Krachler M, Shotyk, W, 2004. Natural and anthropogenic enrichments of molybdenum, thorium, and uranium in a complete peat bog profile, Jura Mountains, Switzerland. Journal of Environmental Monitoring 6, 418–426.

Krachler M, Mohl C, Emons H, Shotyk W, 2003. Atmospheric deposition of V, Cr, and Ni since the Late Glacial: Effects of climatic cycles, human impacts, and comparison with crustal abundances. Environmental Science & Technology 37, 2658–2667.

Kumblad L, Bradshaw C, 2008. Element composition of biota, water and sediment in the Forsmark area, Baltic Sea. Concentrations, bioconcentration factors and partitioning coefficients (K_d) of 48 elements. SKB TR-08-09, Svensk Kärnbränslehantering AB.

Kuroda P K, Sandell E B, 1953. Chlorine in igneous rocks: Some aspects of the geochemistry of chlorine. Bulletin of the Geological Society of America 64, 879–896.

Kuusisto J, 2017. Geochemical and physical properties and in situ distribution coefficients of the deep soil pits OL-KK25 and OL-KK26 at Olkiluoto. Posiva Working Report 2017-2, Posiva Oy, Finland.

Küpper H, Lombi E, Zhao F-J, Wieshammer G, McGrath, S P, 2001. Cellular compartmentation of nickel in the hyperaccumulators *Alyssum lesbiacum*, *Alyssum bertolonii* and *Thlaspi goesingense*. Journal of Experimental Botany 52, 2291–2300.

Lahdenperä A M, 2017. Reference lake sediments, geochemistry and in situ distribution coefficients, K_d values, Southwestern Finland. Posiva Working Report 2017-16, Posiva Oy, Finland.

Larsson-McCann S, Karlsson A, Nord M, Sjögren J, Johansson L, Ivarsson M, Kindell S, 2002. Meteorological, hydrological and oceanographical information and data for the site investigation program in the community of Oskarshamn. SKB TR-02-03, Svensk Kärnbränslehantering AB.

Leri A C, Myneni S C B, 2010. Organochlorine turnover in forest ecosystems: the missing link in the terrestrial chlorine cycle. Global Biogeochemical Cycles 24, GB0241. doi:10.1029/2010GB003882

Lidman F, Köhler S J, Mörth C-M, Laudon H. 2014. Metal transport in the boreal landscape – the role of wetlands and the affinity for organic matter. Environmental Science & Technology 48, 3783–3790.

Limer L, Albrecht A, Bytwerk D, Marang L, Smith G, Thorne M, 2009. Cl-36 Phase 2: dose assessment uncertainties and variability. Version 2.0 (Final). A report prepared within the BIOPROTA international cooperation programme and published by Andra: D.RP.CSTR.09.0026. Available from http://www.bioprota.org.

Lindborg T (ed), 2008. Surface system Forsmark. Site descriptive modelling SDM-Site Forsmark. SKB R-08-11, Svensk Kärnbränslehantering AB.

Lindborg T (ed), 2010. Landscape Forsmark – data, methodology and results for SR-Site. SKB TR-10-05, Svensk Kärnbränslehantering AB.

Lindborg T (ed), 2018. BIOPROTA. BIOMASS 2020: Interim report. BIOPROTA report, produced in association with IAEA MODARIA II working group 6. SKB R-18-02, Svensk Kärnbränslehantering AB.

Lindborg T, Brydsten L, Sohlenius G, Strömgren M, Andersson E, Löfgren A, 2013. Landscape development during a glacial cycle: Modeling ecosystems from the past into the future. Ambio 42, 402–413.

Losjö K, Johansson B, Bringefelt B, Oleskog I, Bergström S, 1999. Groundwater recharge – climatic and vegetation induced variations. Simulations in the Emån and Äspö areas in southern Sweden. SKB TR-99-01, Svensk Kärnbränslehantering AB.

Lovett G M, Likens G E, Buso D C, Driscoll C T, Bailey S W, 2005. The biogeochemistry of chlorine at Hubbard Brook, New Hampshire, USA. Biogeochemistry 72, 191–232**.**

Lundin L, Lode E, Stendahl J, Björkvald L, Hansson J, 2005. Oskarshamn site investigation. Soils and site types in the Oskarshamn area. SKB R-05-15, Svensk Kärnbränslehantering AB.

Lundqvist L, 2006. Inledande kulturhistoriska studier i Simpevarpsområdet: Småland, Misterhults socken, Oskarshamn kommun. SKB R-06-65, Svensk Kärnbränslehantering AB. (In Swedish.)

Löfgren A (ed), 2008. The terrestrial ecosystems at Forsmark and Laxemar-Simpevarp. Site descriptive modelling SDM site. SKB R-08-01, Svensk Kärnbränslehantering AB.

Löfgren A (ed), 2010. The terrestrial ecosystems at Forsmark and Laxemar-Simpevarp. SR-Site Biosphere. SKB TR-10-01, Svensk Kärnbränslehantering AB.

Maatela P, Paasivirta J, Särkkä J, Paukku R, 1990. Organic chlorine compounds in lake-sediments. II Organically bound chlorine. Chemosphere 21, 1343–1354.

MacAdam J, 2009. Structure and function of plants. Ames, IA: Wiley-Blackwell.

Manninen P K G, Lauren M, 1995. Naturally produced organic chlorine in the Finnish aquatic environment. In Grimvall A, de Leer E W B (eds). Naturally-produced organohalogens. Dordrecht: Kluwer Academic Publishers. (Environment & Chemistry 1), 131–137.

Marschner P (ed), 2012. Marschner‘s mineral nutrition of higher plants. 3rd ed. London: Elsevier/ Academic Press.

Martino M, Turner A, Millward G E, 2003. Influence of organic complexation on the adsorption kinetics of nickel in river waters. Environmental Science & Technology 37, 2383–2388.

Meinshausen M, Smith S J, Calvin K, Daniel J S, Kainuma M L T, Lamarque J-F, Matsumoto K, Montzka S A, Raper S C B, Riahi K, Thomson A, Velders G J M, van Vuuren D P P, 2011. The RCP greenhouse gas concentrations and their extensions from 1765 to 2300. Climatic Change 109, 213–241.

Monde K, Satoh H, Nakamura M, Tamura M, Takasugi M, 1998. Organochlorine compounds from a terrestrial higher plant: Structures and origin of chlorinated orcinol derivatives from diseased bulbs of *Lilium maximowiczii*. Journal of Natural Products 61, 913–921.

Montelius M, Thiry Y, Marang L, Ranger J, Cornelis J-T, Svensson T, Bastviken D, 2015. Experimental evidence of large changes in terrestrial chlorine cycling following altered tree species composition. Environmental Science &Technology 49, 4921–4928

Montelius M, Svensson T, Lourino-Cabana B, Thiry Y, Bastviken D, 2016. Chlorination and dechlorination rates in a forest soil – A combined modelling and experimental approach. Science of the Total Environment 554–555, 203–210.

Montelius M, Svensson T , Lourino-Cabana B, Thiry Y, Bastviken D, 2019. Radiotracer evidence that the rhizosphere is a hot-spot for chlorination of soil organic matter. Plant and Soil 443, 245–257.

Morosini M, Hultgren H, 2003. Inventering av privata brunnar i Simpevarpsområdet, 2001-2002. SKB P-03-05, Svensk Kärnbränslehantering AB.

Morosini M, Jenkins C, Simson S, Albrecht J, Zetterlund M, 2007. Oskarshamn site investigation. Hydrogeological characterization of deepest valley soil aquifers and soil-rock transition zone at Laxemar, 2006 Subarea Laxemar. SKB P-07-91, Svensk Kärnbränslehantering AB.

Morse J W, Arakaki T, 1993. Adsorption and coprecipitation of divalent metals with mackinawite (FeS). Geochimica et Cosmochimica Acta 57, 3635–3640.

Myneni S C B, 2002. Formation of stable chlorinated hydrocarbons in weathering plant material. Science 295, 1039–1041.

Nardi A, Idiart A, Trinchero P, de Vries L M, Molinero J, 2014. Interface COMSOL-PHREEQC (iCP), an efficient numerical framework for the solution of coupled multiphysics and geochemistry. Computers & Geosciences 69, 10–21.

Natchimuthu S, Sundgren I, Gålfalk M, Klemedtsson L, Bastviken D, 2017. Spatiotemporal variability of lake pCO_2 and CO_2 fluxes in a hemiboreal catchment. Journal of Geophysical Reseasrch: Biogeosciences 122, 30–49.

Nieminen T M, Ukonmaanaho L, Rausch N, Shotyk W, 2007. Biogeochemistry of nickel and its release into the environment. In Sigel A, Sigel H, Sigel R K (eds). Nickel and its surprising impact in nature. Chichester: Wiley, 1–29.

Nilsson G, 2004. Oskarshamn site investigation. Investigation of sediments, peat lands and wetlands. Stratigraphical and analytical data. SKB P-04-273, Svensk Kärnbränslehantering AB.

Nkusi G, Müller G, 1995. Naturally produced organohalogens: AOX-monitoring in plants and sediments. In Grimvall A, de Leer E W B (eds). Naturally-produced organohalogens. Dordrecht: Kluwer Academic Publishers. (Environment & Chemistry 1), 261–268.

Nordmyr L, Åström M, Peltola P, 2008. Metal pollution of estuarine sediments caused by leaching of acid sulphate soils. Estuarine Coastal and Shelf Science 76, 141–152.

Nyman H, Sohlenius G, Strömgren M, Brydsten L, 2008. Depth and stratigraphy of regolith. Site descriptive modelling SDM-Site Laxemar. SKB R-08-06, Svensk Kärnbränslehantering AB.

Odén M, Follin S, Öhman J, Vidstrand P, 2014. SR-PSU Bedrock hydrogeology. Groundwater flow modelling methodology, setup and results. SKB R-13-25, Svensk Kärnbränslehantering AB.

Ottosson P, 2006. Nulägesbeskrivning av rekreation och friluftsliv i Oskarshamn. SKB P-06-114, Svensk Kärnbränslehantering AB. (In Swedish.)

Pers K, Skagius K, Södergren S, Wiborgh M, Hedin A, Morén L, Sellin P, Ström A, Pusch R, Bruno J, 1999. SR 97 – Identification and structuring of process. SKB TR-99-20, Svensk Kärnbränslehantering AB.

Peterson J, MacDonell M, Haroun L, Monette F, Hildebrand R, Taboas A, 2007. Radiological and chemical fact sheets to support health risk analyses for contaminated areas. Lemont, IL: Argonne National Laboratory Environmental Science Division.

Piqué À, Grandia F, Sena C, Arcos D, Molinero J, Duro L, Bruno J, 2010. Conceptual and numerical modelling of radionuclide transport in near-surface systems at Forsmark. SR-Site Biosphere. SKB R-10-30, Svensk Kärnbränslehantering AB.

Piqué À, Arcos D, Grandia F, Molinero J, Duro L, Berglund S, 2013. Conceptual and numerical modeling of radionuclide transport and retention in near-surface systems Ambio 42, 476–487.

Påsse T, 2001. An empirical model of glacio-isostatic movements and shore-level displacement in Fennoscandia. SKB R-01-41, Svensk Kärnbränslehantering AB.

Qvarfordt S, Borgiel M, Berg C, Nilsson A-C, 2008. Forsmark site investigation. Hydrochemical monitoring of near surface groundwater, surface waters and precipitation. Results from sampling in the Forsmark area, August 2007 – December 2007. SKB P-08-55, Svensk Kärnbränslehantering.

Redon P O, Abdelouas A, Bastviken D, Cecchini S, Nicolas M, Thiry Y, 2011. Chloride and organic chlorine in forest soils: storage, residence times, and influence of ecological conditions. Environmental Science & Technology 45, 7202–7208.

Robinson H K, Hasenmueller E A, Chambers L G, 2017. Soil as a reservoir for road salt retention leading to its gradual release to groundwater. Applied Geochemistry 83, 72–85.

Roos P, Engdahl A, Karlsson S, 2007. Oskarshamn and Forsmark site investigations. Analysis of radioisotopes in environmental samples. SKB P-07-32, Svensk Kärnbränslehantering AB.

Saetre P, Ekström P-A, 2016. Drainage of runoff water from 157_2 into 157_1 via a stream – Biosphere complementary information for SR-PSU. SKBdoc 1554499, ver 1.0, Svensk Kärnbränslehantering AB.

Saetre P, Ekström P-A, 2017a. Kompletterande beräkningar för gasavgång. SKBdoc 1610560, ver 1.0, Svensk Kärnbränslehantering AB.

Saetre P, Ekström P-A, 2017b. Kompletterande beräkningar om biosfärsobjekt. SKBdoc 1571087 ver 1.0, Svensk Kärnbränslehantering AB.

Saetre P, Valentin J, Lagerås P, Avila R, Kautsky U, 2013a. Land use and food intake of future inhabitants: outlining a representative individual of the most exposed group for dose assessment. Ambio 42: 488–496.

Saetre P, Nordén S, Keesman S, Ekström P-A, 2013b. The biosphere model for radionuclide transport and dose assessment in SR-PSU. SKB R-13-46, Svensk Kärnbränslehantering AB.

Sassner M, Sabel U, Bosson E, Berglund S, 2011. Numerical modelling of present and future hydrology at Laxemar-Simpevarp. SKB R-11-05, Svensk Kärnbränslehantering AB.

Schlesinger W H, 1997. Biogeochemistry: an analysis of global change. 2nd ed. San Diego, CA: Academic Press.

Sena C, Grandia F, Arcos D, Molinero J, Duro L, 2008. Complementary modelling of radionuclide retention in the near-surface system at Forsmark. Development of a reactive transport model using Forsmark 1.2 data. SKB R-08-107, Svensk Kärnbränslehantering AB.

Shahkarami P, 2019. Input data report for near-field and geosphere radionuclide transport modelling. Report for the safety evaluation SE-SFL. SKB R-19-09, Svensk Kärnbränslehantering AB.

Sheppard S C, Evenden W G, 1988. The assumption of linearity in soil and plant concentration ratios: An experimental evaluation. Journal of Environmental Radioactivity 7, 221–247.

Sheppard S C, Evenden WG, 1990. Characteristics of plant concentration ratios assessed in a 64-site field survey of 23 elements. Journal of Environmental Radioactivity 11, 15–36.

Sheppard S, Long J, Sanipelli B, Sohlenius G, 2009. Solid/liquid partition coefficients (K_d) for selected soils and sediments at Forsmark and Laxemar-Simpevarp. SKB R-09-27, Svensk Kärnbränslehantering AB.

Sheppard S, Sohlenius G, Omberg L-G, Borgiel M, Grolander S, Nordén S, 2011. Solid/liquid partition coefficients (K_d) and plant/soil concentration ratios (CR) for selected soils, tills and sediments at Forsmark. SKB R-11-24, Svensk Kärnbränslehantering AB.

Sitch S, Smith B, Prentice I C, Arneth A, Bondeau A, Cramer W, Kaplan J O, Levis S, Lucht W, Sykes M T, Thonicke K, Venevsky S, 2003. Evaluation of ecosystem dynamics, plant geography and terrestrial carbon cycling in the LPJ dynamic global vegetation model. Global Change Biology 9, 161–185.

Skagius K, Ström A, Wiborgh M, 1995. The use of interaction matrices for identification, structuring and ranking of FEPs in a repository system. Application on the far-field of a deep geological repository for spent fuel. SKB TR 95-22, Svensk Kärnbränslehantering AB.

SKB, 1999. Deep repository for long-lived low- and intermediate-level waste. Preliminary safety assessment. SKB TR-99-28, Svensk Kärnbränslehantering AB.

SKB, 2001. Project SAFE. Scenario and system analysis. SKB R-01-13, Svensk Kärnbränslehantering AB.

SKB, 2008. Site description of Forsmark at completion of the site investigation phase. SDM-Site Forsmark. SKB TR-08-05, Svensk Kärnbränslehantering AB.

SKB, 2009. Site description of Laxemar at completion of the site investigation phase. SKB TR-09-01, Svensk Kärnbränslehantering AB.

SKB, 2010a. Geosphere process report for the safety assessment SR-Site. SKB TR-10-48, Svensk Kärnbränslehantering AB.

SKB, 2010b. Biosphere analyses for the safety assessment SR-Site – synthesis and summary of results. SKB TR-10-09, Svensk Kärnbränslehantering AB.

SKB, 2010c. Climate and climate-related issues for the safety assessment SR-Site. SKB TR-10-49, Svensk Kärnbränslehantering AB.

SKB, 2010d. Comparative analysis of safety related site characteristics. SKB TR-10-54, Svensk Kärnbränslehantering AB.

SKB, 2011a. Long-term safety for the final repository for spent fuel at Forsmark. Main report of the SR-Site project. SKB TR-11-01, Svensk Kärnbränslehantering AB.

SKB, 2011b. Site selection – siting of the final repository for spent nuclear fuel. SKB R-11-07, Svensk Kärnbränslehantering AB.

SKB, 2013a. Components, features, processes and interactions in the biosphere. SKB R-13-43, Svensk Kärnbränslehantering AB.

SKB, 2013b. RD&D Programme 2013. Programme for research, development and demonstration of methods for the management and disposal of nuclear waste. SKB TR-13-18, Svensk Kärnbränslehantering AB.

SKB, 2013c. Site description of the SFR area at Forsmark at completion of the site investigation phase. SDM-PSU Forsmark. SKB TR-11-04, Svensk Kärnbränslehantering AB.

SKB, 2014a. Waste form and packaging process report for the safety assessment SR-PSU. SKB TR-14-03, Svensk Kärnbränslehantering AB.

SKB, 2014b. Engineered barrier process report for the safety assessment SR-PSU. SKB TR-14-04, Svensk Kärnbränslehantering AB.

SKB, 2014c. Geosphere process report for the safety assessment SR-PSU. SKB TR-14-05, Svensk Kärnbränslehantering AB.

SKB, 2014d. Biosphere synthesis report for the safety assessment SR-PSU. SKB TR-14-06, Svensk Kärnbränslehantering AB.

SKB, 2014e. Climate and climate-related issues for the safety assessment SR-PSU. SKB TR-13-05, Svensk Kärnbränslehantering AB

SKB, 2014f. FEP report for the safety assessment SR-PSU. SKB TR-14-07, Svensk Kärnbränslehantering AB.

SKB, 2015a. Safety analysis for SFR. Long-term safety. Main report for the safety assessment SR-PSU. Revised edition. SKB TR-14-01, Svensk Kärnbränslehantering AB.

SKB, 2015b. Handling of biosphere FEPs and recommendations for model development in SR-PSU. SKB R-14-02, Svensk Kärnbränslehantering AB.

SKB, 2019. Fud-program 2019. Program för forskning, utveckling och demonstration av metoder för hantering och slutförvaring av kärnavfall SKB. Svensk Kärnbränslehantering AB. (In Swedish.)

SKI/SSI, 2001. SKI:s och SSI:s gemensamma granskning av SKB:s preliminära säkerhetsanalys för slutförvar av långlivat låg- och medelaktivt avfall. Granskningsrapport. SKI Rapport 01:14, Statens kärnkraftsinspektion (Swedish Nuclear Power Inspectorate), SSI-rapport 2001:10, Statens strålskyddsinstitut (Swedish Radiation Protection Institute). (In Swedish.)

Smedley P L, Kinniburgh D G, 2017. Molybdenum in natural waters: A review of occurrence, distributions and controls. Applied Geochemistry 84: 387–432.

Sohlenius G, Hedenström A, 2008. Description of regolith at Laxemar-Simpevarp. Site descriptive modelling SDM-Site Laxemar. SKB R-08-05, Svensk Kärnbränslehantering AB.

Sohlenius G, Schoning K, Baumgartner A, 2013. Development, carbon balance and agricultural use of peatlands – overview and examples from Uppland Sweden. SKB TR-13-20, Svensk Kärnbränslehantering AB.

Soininen A M, 1959. Burn-beating as the technical basis of colonisation in Finland in the 16th and 17th centuries. Scandinavian Economic History Review 7, 150–166.

Spitz K, Moreno J, 1996. A practical guide to groundwater and solute transport modeling. New York: Wiley.

SSM, 2008a. The Swedish Radiation Safety Authority's regulations and general advice concerning the protection of human health and the environment in connection with the final management of spent nuclear fuel and nuclear waste. Stockholm: Swedish Radiation Safety Authority. (SSMFS 2008:37) .

SSM, 2008b. The Swedish Radiation Safety Authority's regulations and general advice concerning safety in connection with the disposal of nuclear material and nuclear waste. Stockholm: Swedish Radiation Safety Authority. (SSMFS 2008:21).

SSM, 2014. Assessment of the derivation and use of distribution coefficients and concentration ratios – Main Review Phase. SSM Technical Note 2014:32, Swedish Radiation Safety Authority.

SSM, 2017. SSM's external experts' review of SKB's safety assessment SR-PSU – dose assessment, K_d-values, and safety analysis methodology. SSM Report 2017:33, Swedish Radiation Safety Authority.

SSM, 2018. Strålsäkerhet efter slutförvarets förslutning. Beredning inför regeringens prövning Slutförvaring av använt kärnbränsle. SSM Rapport 2018:07, Swedish Radiation Safety Authority. (In Swedish.)

SSM, 2019. Granskningsrapport – Utbyggnad och fortsatt drift av SFR. Del III Långsiktig strålsäkerhet. SSM Granskningsrapport SSM2017-5969-2, Swedish Radiation Safety Authority. (In Swedish.)

Stenberg K, Rensfeldt V, 2015. Estimating doses from exposure to contaminated air when burning peat or wood. SKB R-14-33, Svensk Kärnbränslehantering AB.

Strack M, Waddington J M, Turetsky M, Roulet N T, Byrne K A, 2008. Northern peatlands, green-house gas exchange and climate change. In Strack M (ed). Peatlands and climate change. Jyväskylä: International Peat Society, 44–69.

Strömgren M, Brydsten L, 2008. Digital elevation models of Laxemar-Simpevarp. SDM-Site Laxemar SKB R-08-63, Svensk Kärnbränslehantering AB.

Svensson G, 1988. Bog development and environmental conditions as shown by the stratigraphy of Store Mosse mire in southern Sweden. Boreas 17, 89–111.

Svensson T, 2019. Measurements and fluxes of volatile chlorinated organic compounds (VOCl) from natural terrestrial sources. Measurement techniques and spatio-temporal variability of flux estimates. SKB TR-18-09, Svensk Kärnbränslehantering AB.

Svensson T, Sandén P, Bastviken D, Öberg G, 2007. Chlorine transport in a small catchment in southeast Sweden during two years. Biogeochemistry 82, 181–199.

Svensson T, Lovett G M, Likens G E, 2012. Is chloride a conservative ion in forested ecosystems? Biogeochemistry 107, 125–134.

Svensson T, Högbom L, Johansson K, Sandén P, Ring E, 2013. Effects of previous nitrogen addition on chlorine in forest soil, soil solution and biomass. Biogeochemistry 116, 3–13.

Svensson T, Montelius M, Andersson M, Lindberg C, Reyier H, Rietz K, Danielsson Å, Bastviken D, 2017. Influence of multiple environmental factors on organic matter chlorination in podsol soil. Environmental Science & Technology 51, 14114–14123.

Söderbäck B (ed), 2008. Geological evolution, palaeoclimate and historical development of the Forsmark and Laxemar-Simpevarp areas. Site descriptive modelling. SDM-Site SKB R-08-19, Svensk Kärnbränslehantering AB.

Söderbäck B, Lindborg T, 2009. Surface system Laxemar-Simpevarp. Site descriptive modelling SDM-Site Laxemar. SKB R-09-01, Svensk Kärnbränslehantering AB.

The BACC Author Team, 2008. Assessment of climate change for the Baltic Sea basin. Berlin: Springer.

Tóth G, Hermann T, Szatmári G, Pásztor L, 2016. Maps of heavy metals in the soils of the European Union and proposed priority areas for detailed assessment. Science of The Total Environment 565, 1054–1062.

Tröjbom M, Grolander S, 2010. Chemical conditions in present and future ecosystems in Forsmark – implications for selected radionuclides in the safety assessment SR-Site. SKB R-10-27, Svensk Kärnbränslehantering AB.

Tröjbom M, Söderbäck B, 2006a. Chemical characteristics of surface systems in the Simpevarp area. Visualisation and statistical evaluation of data from surface water, shallow groundwater, precipitation and regolith. SKB R-06-18, Svensk Kärnbränslehantering AB.

Tröjbom M, Söderbäck B, 2006b. Chemical characteristics of surface systems in the Forsmark area. Visualisation and statistical evaluation of data from shallow groundwater, precipitation, and regolith. SKB R-06-19, Svensk Kärnbränslehantering AB.

Tröjbom M, Söderbäck B, Kalinowski B, 2008. Hydrochemistry of surface water and shallow groundwater, Site descriptive modelling, SDM-Site Laxemar. SKB R-08-46, Svensk Kärnbränslehantering AB.

Tröjbom M, Grolander S, Rensfeldt V, Nordén S, 2013. K_d and CR used for transport calculations in the biosphere in SR-PSU. SKB R-13-01, Svensk Kärnbränslehantering AB.

Tuovinen T S, Roivainen P, Makkonen S, Kolehmainen M, Holopainen T, Juutilainen J, 2011. Soil-to-plant transfer of elements is not linear. Results for five elements relevant to radioactive waste in five boreal forest species. Science of the Total Environment 410–411, 191–197.

Tuovinen T S, Kolehmainen M, Roivainen P, Kumlin T, Makkonen S, Holopainen T, Juutilainen J, 2016. Nonlinear transfer of elements from soil to plants: impact on radioecological modeling. Radiation and Environmental Biophysics 55, 393–400.

US EPA, 1999. Understanding variation in partition coefficient, Kd values. Volume I: The Kd model, methods of measurements, and application of chemical reaction codes. EPA 402-R-04-002C, U.S. Environmental Protection Agency, Washington, DC.

Van den Hoof C, Thiry Y, 2012. Modelling of the natural chlorine cycling in a coniferous stand: implications for chlorine-36 behaviour in a contaminated forest environment. Journal of Environmental Radioactivity 107, 56–67.

van Pée K-H, Unversucht S, 2003. Biological dehalogenation and halogenation reactions. Chemosphere 52, 299–312.

Velasco H R, Ayub J J, Belli M, Sansone U, 2006. Interaction matrices as a first step toward a general model of radionuclide cycling: application to the ^{137}Cs behavior in a grassland ecosystem. Journal of Radioanalytical and Nuclear Chemistry 268, 503–509.

Vera Tome F, Blanco Rodríguez M, Lozano J, 2003. Soil-to-plant transfer factors for natural radionuclides and stable elements in a Mediterranean area. Journal of Environmental Radioactivity 65, 161–175.

Vunkova-Radeva R, Schiemann J, Mendel R-R, Salcheva G, Georgieva D, 1988. Stress and activity of molybdenum-containing complex (molybdenum cofactor) in winter wheat seeds. Plant Physiology 87, 533–535.

Walke R, Limer L, Shaw G, 2017. In-depth review of key issues regarding biosphere models for specific radionuclides in SR-PSU. In SSM's external expert's review of SKB's safety assessment SR-PSU – dose assessment, Kd-values and safety analysis methodology. Main review phase. SSM Report 2017-33, Part 2, Swedish Radiation Safety Authority.

Wedepohl K H, 1995. The composition of the continental crust. Geochimica et Cosmochimica Acta 59, 1217–1232.

Weng L P, Wolthoorn A, Lexmond T M, Temminghoff E J M, Van Riemsdijk W H, 2004. Understanding the effects of soil characteristics on phytotoxicity and bioavailability of nickel using speciation models. Environmental Science & Technology 38, 156–162.

Werner K, 2009. Description of surface hydrology and near-surface hydrogeology at Laxemar-Simpevarp. Site descriptive modelling, SDM-Site Laxemar. SKB R-08-71, Svensk Kärnbränslehantering AB.

Werner K, Bosson E, Berglund S, 2006. Description of climate, surface hydrology, and near-surface hydrogeology. Preliminary site description Laxemar subarea – version 1.2. SKB R-05-61, Svensk Kärnbränslehantering AB.

Werner K, Öhman J, Holgersson B, Rönnback K, Marelius F, 2008. Meteorological, hydrological and near-surface hydrogeological monitoring data and near-surface hydrogeological properties data from Laxemar-Simpevarp. Site descriptive modelling, SDM-Site Laxemar. SKB R-08-73, Svensk Kärnbränslehantering AB.

Werner K, Sassner M, Johansson E, 2013. Hydrology and near-surface hydrogeology at Forsmark – synthesis for the SR-PSU project. SR-PSU Biosphere. SKB R-13-19, Svensk Kärnbränslehantering AB.

White P J , Broadley M R, 2001. Chloride in soils and its uptake and movement within the plant: A review. Annals of Botany 88, 967–988.

Wichard T, Mishra B, Myneni S C B, Bellenger J-P, Kraepiel A M L, 2009. Storage and bio-availability of molybdenum in soils increased by organic matter complexation, Nature Geoscience 2, 625–629.

Wirth S B, Gilli A, Niemann H, Dahl T W, Ravasi D, Sax N, Hamann Y, Peduzzi R, Peduzzi S, Tonolla M, Lehmann M F, Anselmetti F S, 2013. Combining sedimentological, trace metal (Mn, Mo) and molecular evidence for reconstructing past water-column redox conditions: The example of meromictic Lake Cadagno (Swiss Alps). Geochimica et Cosmochimica Acta120, 220–238.

Winterton N, 2000. Chlorine: the only green element – towards a wider acceptance of its role in natural cycles, Green Chemistry 2, 173–225.

Wood M D, Beresford N A, Howard B J, Copplestone D, 2013. Evaluating summarised radionuclide concentration ratio datasets for wildlife. Journal of Environmental Radioactivity 126, 314–325.

Zachara J M, Cowan C E, Resch C T, 1991. Sorption of divalent metals on calcite. Geochimica et Cosmochimica Acta 55, 1549–1562.

Zamble D, Rowińska-Żyrek M, Kozlowski H (eds), 2017. The biological chemistry of nickel. London: Royal Society of Chemistry.

Zlamal J E, Raab T K, Little M, Edwards R A, Lipson D A, 2017. Biological chlorine cycling in the Arctic Coastal Plain. Biogeochemistry 134, 243–260.

Öberg G, 1998. Chloride and organic chlorine in soil. Acta Hydrochimica et Hydrobiologica, 26, 137–144.

Öberg G, 2002. The natural chlorine cycle – fitting the scattered pieces. Applied Microbiology and Biotechnology 58, 565–581.

Öberg G, Sandén P, 2005. Retention of chloride in soil and cycling of organic matter-bound chlorine. Hydrological Processes 19, 2123–2136.

Öberg, G, Holm M, Sandén P, Svensson T, Parikka M, 2005. The role of organic-matter-bound chlorine in the chlorine cycle: a case study of the Stubbetorp catchment, Sweden. Biogeochemistry 75, 241–269.

Appendix A

Glossary – Terms and acronyms in SE-SFL Biosphere

Table A-1. Terms and acronyms used is the SE-SFL biosphere assessment.

Term/acronym	Definition/description
Abiotic	Non-living physical or chemical component or process.
Autotroph	Organism that utilises photosynthesis or chemosynthesis to build up organic carbon.
Basin	In the SE-SFL terminology, a basin is the drainage area of a biosphere object (cf. below) minus the drainage area of any upstream object. When the basin is below sea level, the basin equals the biosphere object.
Biosphere	The part of the environment normally inhabited by living organisms. In the context of safety assessments usually more constrained to the surface (see *surface ecosystem*).
BIOMASS	Biosphere Modelling and Assessment (IAEA co-ordinated research programme)
Biosphere object	A part of the landscape that potentially will receive radionuclides released from a repository.
BioTEx	The Biosphere Transport Exposure model calculates transport and concentration of radionuclides in different environmental media, and human exposure to radionuclides in the biosphere.
Biotic	Living ecosystem component or process involving living organisms.
Climate case	SE-SFL describes a set of climate cases, which are possible future climate developments at Forsmark.
Climate domain	A climatically determined environment with a specific set of characteristic processes of importance for repository safety.
CR	Concentration ratio. *CR* values are used to calculate uptake of radionuclides by biota and are defined as the element-specific concentration ratios between the concentrations in biota and in the surrounding medium (soil or surface water).
Conceptual model	A qualitative description of important components and their interactions.
DEM	Digital elevation model. The DEM describes the topography and bathymetry of the modelled area. It is a central data source for the site characterisation and is used as input to most of the descriptions and models produced for the surface system.
Deterministic analysis	Analysis using single numerical values for each of the parameters (taken to have a probability of one), which leads to a single value for the result.
Discharge points/locations	Locations/areas where groundwater reaches the ground surface. In the safety assessment context, these terms refer to discharge of groundwater that has passed though the repository volume in the bedrock and hence could carry radionuclides to the surface.
DM	Drained-mire farmers. DM refers to a self-sustained industrial agriculture in which wetlands are drained and used for agriculture (both crop and fodder production). It is one of four land use variants considered in SE-SFL for assessment of the most exposed group.
Dose	Dose, as used in SE-SFL, refers to the mean annual effective dose to a representative individual from the most exposed group. The calculated dose accounts for retention of radionuclides in the human body and exposure from radionuclide progeny, as well as radiation sensitivities of different tissues and organs.
Dose rate to biota	Dose rate to biota represents mean absorbed dose rates in the whole body of a given radionuclide and is expressed in μGy h^{-1}.
DW	Dry weight
Ecolego tool	Computer software used to model radionuclide transport.
Ecosystem model	Conceptual or mathematical representation of an ecosystem, divided into compartments, and its included processes.
Effective dose	Effective dose or effective dose equivalent is a measure of dose designed to reflect the risk associated with the dose. It is calculated as the weighted sum of the dose equivalents in the different tissues of the body.
ERICA tool	Computer software used to determine dose-rates and radiological effects for different types of non-human biota.
Exposure	The act or condition of being subject to irradiation. (Exposure should not be used as a synonym for *dose,* which is a measure of the effects of exposure.)
	External exposure. Exposure to radiation from a source outside the body.
	Internal exposure. Exposure to radiation from a source within the body.
FEPs	Features, Events and Processes

Term/acronym	Definition/description
Functional group	A group of organisms with a common function in the ecosystem, e.g. primary producers and filter feeders.
GP	Garden-plot households. GP refers to a type of household that is self-sustained with respect to vegetables and root crops produced through small-scale horticulture. It is one of four land use variants considered in SE-SFL for assessment of the most exposed group.
Geosphere	Those parts of the lithosphere not considered to be part of the *biosphere*. In safety assessments usually used to distinguish the subsoil and bedrock below the depth affected by normal human activities, in particular agriculture, from the soil that is part of the *biosphere*.
Glacial cycle	Used in climate descriptions to denote a period of ~ 120 000 years that includes both a glacial, e.g. the Weichselian, and an interglacial.
Heterotroph	Organism that uses organic compounds produced by autotrophs.
HG	Hunter-gatherers. HG refers to a community that uses the undisturbed surface ecosystems as living space and to obtain food. It is one of four land use variants considered in SE-SFL for assessment of the most exposed group.
Hydrodynamic model	In SE-SFL, the hydrodynamic model is the flow model of the sea part of the considered model area and gives outputs of annual mean flows between adjacent marine basins and water retention times for each individual basin.
Hydrological model	The SE-SFL hydrological modelling includes conceptual and mathematical modelling of surface, near-surface and bedrock water flows. The SE-SFL hydrological modelling utilises GIS, as well as the MIKE SHE and DarcyTools numerical modelling tools.
IM	Interaction matrix. The IM is a tool used to ensure that all relevant processes affecting transport and accumulation of radionuclides in the biosphere are considered in the assessment.
Infilling	Infilling describes the combined process of sedimentation and organogenic deposition, which turns lakes into wetlands.
IO	Infield-outland farmers. IO refers to a self-sustained agriculture in which infield farming of crops is dependent on nutrients from wetlands for haymaking (outland). It is one of four land use variants considered in SE-SFL for assessment of the most exposed group.
K_d	Element-specific soil/liquid partition coefficient defined as the ratio between the elemental concentrations in the solid and liquid phases.
LDF	Landscape dose conversion factor. The LDF is a radionuclide-specific dose conversion factor, expressed in Sv year^{-1} (Bq year^{-1})$^{-1}$, which represents the mean annual effective dose to a representative individual from the most exposed group, resulting from a unit constant release rate to the biosphere of a specific radionuclide. This means that the LDF relates a unit release rate to annual dose.
LDM	Landscape development model. The LDM is a model at landscape level that describes the long-term development of a landscape. The model is used to describe time-dependent properties of the biosphere objects that are input parameters to the *Radionuclide model*.
Mass balance model	The mass balance model calculates the total sum of major sources and removal mechanisms for individual chemical elements in the landscape.
Most exposed group	In SE-SFL, the most exposed group refers to the group of individuals subjected to the highest exposure during any time period.
NHB	Non-human biota.
NPP	Net primary production. The balance between gross primary production and plant respiration.
Probabilistic analysis	Mathematical analysis of stochastic (random) events or processes and their consequences. Since the input is described in stochastic terms, also the output is stochastic (e.g. in the form of probabilities or distributions).
Radionuclide model	Model used to calculate radionuclide inventories in different compartments of the biosphere, radionuclide fluxes between the compartments and radionuclide concentrations in environmental media (soil, water, air and biota). The radionuclide model utilises the Ecolego modelling tool.
Regolith	All matter overlying the bedrock is collectively denominated regolith. This includes both minerogenic and organogenic deposits, as well as anthropogenic landfills.
RDM	Regolith depth and stratigraphy model. The RDM interpolates observation points of the analysed vertical distribution of regolith into a three-dimensional model of the regolith extent.
Relative sea-level change	The vertical height difference between the sea surface at a specific time and the present height of the sea surface relative to land. The relative sea-level is defined to be zero at 2000 AD (RH2000).
Regression Regression	Withdrawal of the coastline from the land as the average sea-level decreases, which in turn increases the extent of the land area with time.
RLDM	Coupled Regolith-Lake Development Model. The RLDM is divided into a marine module that predicts the sediment dynamics caused by waves, and a lake module that predicts infilling of lakes. The model output is the regolith distribution and thickness of different strata at the studied time steps.

Term/acronym	Definition/description
SDM	Site descriptive model. The SDM is a multi-disciplinary description of the studied site, including both qualitative and quantitative information, which is based on both direct observations and modelling studies.
SFR	The existing final repository for short-lived radioactive waste.
Shoreline migration	The movement of the shoreline, due to relative sea-level change.
SR-PSU	The safety assessment of the existing SFR facility (SFR 1) and its planned extension (SFR 3).
Sub-catchment	In the present context defined the drainage area of a biosphere object minus the drainage area of the surface water inputs to the object.
Surface ecosystem	In the safety assessment context, surface ecosystem refers to the part of the analysed system that is above the bedrock, with all its abiotic and biotic processes and features.
Terrestrialisation	The transformation of an aquatic ecosystem (marine or limnic) to a terrestrial ecosystem.
Transgression	The relative sea-level is increasing, and thus the extent of the land area decreases with time.
Watershed	In the present context defined as the drainage area of a biosphere object.

Appendix B

Other exposure pathways

This section evaluates residual exposure pathways that were identified during a screening analysis of multiple pathways of exposure (Section 6.3). The SFL safety evaluation (SE-SFL) adopts the same screening methodology as used in SR-PSU safety assessment (SKB 2014d) and does in this case end up with the same potential residual exposure pathways as for SR-PSU (Table 6.1). The identified residual exposure pathways that not are included in the calculation cases presented in the section referred to above are:

- Exposure from inadvertent ingestion of inorganic and organic soil.
- External exposure from the vegetation.
- External exposure from aquatic sediment.

The analysis of these exposure pathways in SR-PSU (SKB 2014b) showed that the majority of the 55 radionuclides contributed with far less than 1 % of the max dose if included. Below are the residual exposure pathways described and result discussed in relation to the most dose contributing radionuclides in SE-SFL.

B1 Exposure from inadvertent ingestion of inorganic and organic soil

Inadvertent ingestion of soil and dust may result from activities such as eating vegetables, and hand to mouth contact following gardening, gathering of food items or other activities leading to soil/dust contact. Some exposure from inadvertent soil ingestion is already accounted for in the land use variants that are part of the biosphere calculation cases. For example, as the *CR* values for vegetables and root crops are empirically derived parameters, the calculated concentration in food items includes a contribution from the small amounts of soil left after washing. Moreover, the dose contribution from inhalation of soil dust (see below) was included in all land use variants (see Section 6.3). The two land use variants were chosen because they represent two different soil types (with potential for accumulation of different radionuclides). The garden plot soil originated from gyttja clay and was richer in minerals, whereas the soil resulting from draining a mire primarily originated from organic sediments (peat and clay-gyttja). In addition, the garden plot was irrigated with well water (containing short-lived radionuclides) and fertilised with seaweeds or biofuel ash (see Section 7.2). For a brief description of the two land use variants and their exposure pathways, see Section 6.3. The screening calculation for soil ingestion was based on the principles used to calculate dose from intake of food. That is, the dose was calculated from the amount of soil ingested and the radionuclide concentration in the ingested soil.

Inadvertent soil ingestion typically resulted in far less than 1 % of the combined dose from ingestion of food and water, inhalation and direct external exposure. However, for uranium isotopes (U-234, U-238 and U-235) inadvertent soil ingestion resulted in 2–3 % of the maximum landscape dose factor (LDF) for the garden plot. Similarly, inadvertent ingestion of organic soil resulted in a residual dose of U-238 that was approximately 1 % of the maximum LDF in the drained mire scenario. Based on this it was concluded that exposure from inadvertent ingestion of soil and peat could be disregarded as significant sources to dose in Forsmark. In the results for *present-day evaluation case* in SE-SFL (Section 7.2) uranium isotopes are among the most dose contributing radionuclides in the drained mire of 206 and the results from SR-PSU would therefore suggest an increase of the total maximal dose by 3 %. However, preliminary results calculated on the data from Laxemar showed that these results instead were 0.04 % of the maximal dose found in the *present-day evaluation case*. Thus, it can be concluded that exposure from inadvertent ingestion of cultivated clay-gyttja and peat can be disregarded as significant sources to dose in SE-SFL.

B2 External exposure from the vegetation

External exposure from vegetation could potentially contribute to the dose from radionuclides that accumulate in biomass of primary producers and emit gamma (or high energy beta) radiation. No shielding from vegetation biomass, snow or any other material was accounted for. Thus, the

radionuclide content in vegetation (expressed as Bq m^{-2}) was converted to an external dose using dose coefficients for external exposure from a surface source (Sv h^{-1} (Bq m^{-2})$^{-1}$) in the SR-PSU assessment (Grolander 2013, Chapter 3). Moreover, it was cautiously assumed that inhabitants were exposed to radiation from vegetation 24 hours a day. These calculations could be thought of as the maximum exposure for a hunter-gatherer group setting up a camp in one biosphere object and being in close contact with vegetation all year around. Radiation from Sn-126 and Ag-108m caused the largest external exposure relative to that of the base case, and the dose was 8 % and 3 % of the maximum LDF, respectively. The external dose from the highly bioaccumulating radionuclide Cl-36 was only 0.2 % of the maximum LDF, reflecting that Cl-36 is a pure beta emitter. In the SE-SFL *present-day evaluation case* neither of the radionuclides Sn-126 or Ag-108m is among the most dose-contributing radionuclides. However, Cl-36 is, but based on the small contribution from this exposure pathway demonstrated earlier, it can be concluded that external exposure from vegetation can be disregarded as a significant source of dose in SE-SFL.

B3 External exposure from sediment

External irradiation from gamma-emitting radionuclides on beaches or in sediments normally needs to be considered (EC 2002). In the present biosphere assessment radionuclides will reach aquatic surface sediments in areas where groundwater from the repository is discharged, during the submerged period. In other areas, radionuclides may reach marine sediments with surface water during the submerged period and lake sediments during the land period. Human exposure to aquatic sediments could primarily be expected in shallow coastal areas or near lake shores. Exposure could occur during activities such as bathing, fishing or gathering seaweed in ice-free periods.

In SR-PSU, it was assumed that the dose from being in contact with aquatic sediments could be sufficiently approximated with the method used for direct exposure from the ground and no shielding from water was accounted for. Thus, the radionuclide content in the two uppermost regolith layers, representing the thin layer of surface sediments and the underlying clay-gyttja, was used to calculate the radionuclide concentration (Bq m^{-3}). The annual dose was then calculated using the dose coefficient for external exposure (Sv h^{-1} (Bq m^{-3})$^{-1}$) ("dosCoef_ext", Grolander 2013) and assuming that inhabitants spent one hour a day during the three summer months in this environment (i.e. 90 hours or 0.01 y^{-1}). These calculations could be thought of as the exposure for a hunter-gatherer group catching fish with nets in near-shore environments, or foraging lake shores for crayfish.

The maximum dose from external exposure from aquatic sediments over the full simulation time was generally several orders of magnitude lower than the maximum LDF from the base calculation case. As with exposure from vegetation, gamma radiation from Sn-126 and Ag-108m caused the largest external exposure relative to that of the base case, and the dose was 3 % of the maximum LDF. In the SFL *present-day evaluation case* neither of the radionuclides Sn-126 or Ag-108m is among the most dose contributing radionuclides. Based on these results, it can be concluded that external exposure from aquatic sediments can be disregarded as a significant source to dose in SE-SFL.

Appendix C

Correlations between object properties

Relationships between radionuclide-specific drained mire doses and object properties were explored in the *alternative discharge area evaluation case* (Section 12.2). Object area, upward groundwater flux and regolith layer thicknesses influence radionuclides to various extents, depending on radionuclide properties (half-life and sorption) and exposure pathway (well water or food). The general conclusions were largely in agreement with the results from the *alternative groundwater flow sensitivity analysis* of the hydrological system (Section 13.4). In this sensitivity case, object properties that influence groundwater flows, sorption and the resulting radionuclide specific doses, were varied independently of each other. In reality, object properties are not completely independent and correlations between properties in the biosphere objects used in the alternative discharge area case, mainly explained the differences between the two analyses. Upward groundwater fluxes (q) are correlated between adjacent, but also distant regolith layers (Figure C-1). This means that the expected positive effect on e.g. Mo-93 doses by increasing deeper upward groundwater fluxes and the negative effect on doses due to increased groundwater flows in surface layers could, at least partly, cancel each other out and therefore become difficult to disentangle (discussed in 12.2.5). Furthermore, there is a weaker correlation between the thicknesses of two deeper regolith layers (till and glacial clay) as well as between the two shallower layers (post-glacial sediments and peat), and there is a tendency that the glacial clay layer is thicker in larger objects.

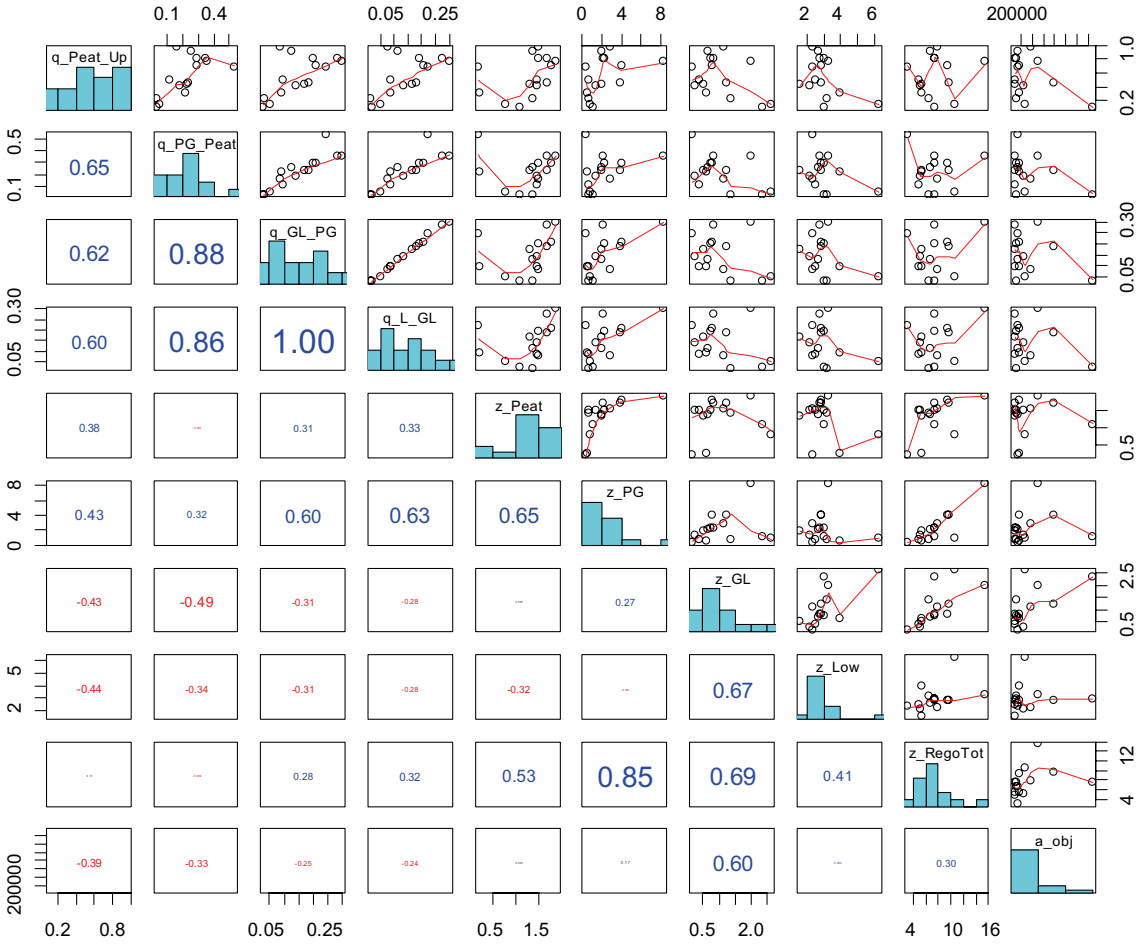

Figure C-1. *Pair plot of the correlations among object properties (upward groundwater flux = q, regolith layer thickness = z, object area = a_obj) included in the analysis of the relationship between doses and object properties in the alternative discharge area evaluation case. The diagonal shows the frequency distribution of the object properties and the upper panel shows the scatterplots between object properties. The lower panel shows correlation coefficients, with positive correlations in blue and negative in red, and the font size is proportional to the absolute value. Regolith layers are till (Low), glacial clay (GL), post-glacial sediments (PG), peat and the uppermost oxidised layer (Up). For example, q_Low_GL means the upward groundwater flux from the till to the glacial clay layer.*

Arkitektkopia AB, Bromma, 2020

SKB is responsible for managing spent nuclear fuel and radioactive waste produced by the Swedish nuclear power plants such that man and the environment are protected in the near and distant future.

skb.se